CONF

AEC-660904

Volume 1

# PROCEEDINGS
# of the
# NINTH AEC AIR CLEANING CONFERENCE

held in

Boston, Massachusetts

13-16 September 1966

Nuclear Consulting Services Inc.

Sponsors: The Harvard Air Cleaning Laboratory
Harvard University

and

Division of Reactor Development and Technology
U. S. Atomic Energy Commission

Editors

James M. Morgan, Jr.
Melvin W. First

January 1967

# FOREWORD

During 1966, commercial nuclear power became a major atomic energy activity, with many utilities announcing their plans for the design and construction of large water reactor, central station electric generating facilities. The use and effectiveness of high-efficiency air-cleaning systems, for assuring reactor safety under normal operating and accident conditions, received major attention during the Ninth Air Cleaning Conference held at the Sheraton-Boston Hotel, Boston, Massachusetts, from September 13-16, 1966. Approximately 240 people, including representatives from the United Kingdom, France, Canada, Mexico, Switzerland, Denmark, Germany, and Italy participated in the four-day meeting.

The conference was sponsored through the radioactive effluent control research and development program of the Environmental and Sanitary Engineering Branch of the Division of Reactor Development and Technology, U. S. Atomic Energy Commission. Major credit for development of the technical program and arrangements for the conference is given to Dr. M. First and Mr. F. Viles and other members of their staff at the Harvard Air Cleaning Laboratory.

Approximately 55 technical papers were presented during the meeting on all phases of the air cleaning field including source term characterization, high-efficiency filter performance and evaluation, in-place testing, iodine removal, confinement and containment, incineration, noble gas studies, sodium and plutonium aerosols, and off-gas monitoring and analysis. An opportunity was also provided for the participants to visit the research facilities of the Harvard Air Cleaning Laboratory.

The conference was saddened by the absence of Dr. Leslie Silverman, who passed away during the early part of 1966. As a founder and leader of these air cleaning conferences since their inception in 1951, his presence was sorely missed. We in the AEC are especially grateful for the 17 years of personal effort and extensive research which he devoted to our air cleaning problems and nuclear safety program. An expression of this appreciation was made at the beginning of the conference, in the form of a commendation to the Harvard Air Cleaning Laboratory in the name of Dr. Silverman.

Walter G. Belter

Walter G. Belter, Chief
Environmental & Sanitary Engineering Branch
Division of Reactor Development & Technology
U. S. Atomic Energy Commission

# Dedication

The Proceedings of the Ninth U. S. Atomic Energy Commission Air Cleaning Conference are dedicated to the memory of Leslie Silverman, Director of the Harvard Air Cleaning Laboratory, Consultant to the Atomic Energy Commission, originator and guiding spirit of the First to Ninth USAEC Air Cleaning Conferences.

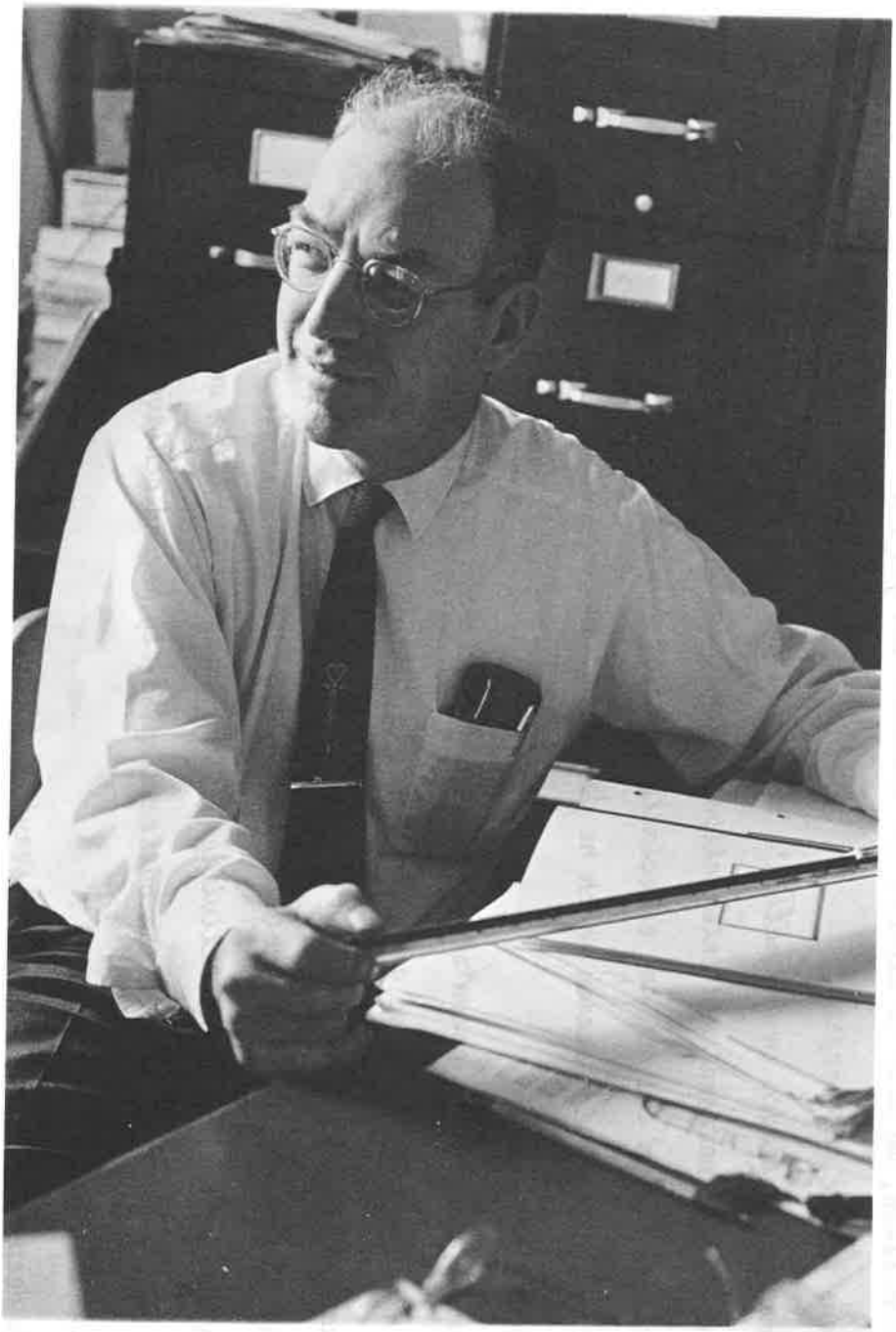

# LESLIE SILVERMAN
## 1914 – 1966

Professor of Engineering in Environmental Hygiene, Head of the Department of Industrial Hygiene, Harvard University, School of Public Health, Member and former Chairman of the Statutory Advisory Committee on Reactor Safeguards.

September 13, 1966

On this occasion of the 9th AEC Air Cleaning Conference, and on behalf of the Atomic Energy Commission, we wish to express our appreciation for Dr. Leslie Silverman's many contributions to the AEC program.

Dr. Silverman was a leader in our nation's air pollution control programs. His contributions to the national and international atomic energy programs are too numerous to mention. We in the AEC are especially grateful for the 17 years of personal effort and extensive research which he devoted to our air cleaning problems and nuclear safety program.

A wide segment of the Commission's operational and research programs have benefited from his overall knowledge and guidance. In this regard, many of the air cleaning applications which we now find in everyday use in the nuclear energy industry are the direct result of his untiring efforts. In a similar way, Dr. Silverman's participation in the activities of the Advisory Committee on Reactor Safeguards has been a major factor in the outstanding safety record achieved by the nuclear energy industry.

It is with deep appreciation of these services to the Atomic Energy Commission, that we offer this commendation to the Harvard Air Cleaning Laboratory in the name of Dr. Leslie Silverman.

UNITED STATES ATOMIC ENERGY COMMISSION

# Certificate of Appreciation

*awarded to*

THE HARVARD AIR CLEANING LABORATORY
in the name of DR. LESLIE SILVERMAN

*for* Outstanding Services Rendered to the Atomic Energy Commission
in the Fields of Air Cleaning and Nuclear Safety

September 13, 1966
*Date*

Glenn T. Seaborg

# TABLE OF CONTENTS

## Volume I


Foreword . . . . . iii

Dedication to Dr. Leslie Silverman . . . . . iv

Certificate of Appreciation, United States Atomic Energy Commission . . . . . vi

WELCOME by Dr. J. Snyder, Dean, Harvard School of Public Health . . . . . 1

OPENING REMARKS by Dr. J. A. Lieberman, Assistant Director for Nuclear Safety, U. S. Atomic Energy Commission . . . . . 1


### Fission Product Characterization

Session 1A - Tuesday, 13 September 1966
Chairman: J. A. Lieberman, USAEC


ANALYTICAL DESCRIPTION OF THE DISTRIBUTION OF FISSION PRODUCTS DURING NUCLEAR REACTOR ACCIDENTS FOR WATER AND GAS COOLED REACTORS by David L. Morrison, James A. Gieseke and Robert L. Ritzman . . . . . 4

Discussion . . . . . 27

CHARACTERIZATION OF SOURCE TERMS FOR AEROSOL TRANSPORT DURING SODIUM FIRES by G. N. Lauben and C. L. Larson. . . . . 28

Discussion . . . . . 49

IN PILE STUDIES OF CONTAMINATION RELEASED IN $CO_2$ GAS COOLED REACTORS by J. Dadillon . . . . . 52


### High Efficiency Filters

Session 1B - Tuesday, 13 September 1966
Chairman: J. A. Young, Naval Research Laboratory


REQUIREMENTS FOR FIRE RESISTANT HIGH EFFICIENCY PARTICULATE AIR FILTERS by C. A. Burchsted . . . . . 62

SUGGESTIONS ON SPECIFICATION WRITING FOR ABSOLUTE FILTERS by A. R. Allan, Jr. . . . . 75

Discussion . . . . . 77

EFFECT OF SHOCK OVERPRESSURE ON HIGH EFFICIENCY UNITS by W. L. Anderson and T. Anderson . . . . . 79

EFFECT OF FIRE INTRUSION AND HEAT ON HEPA FILTER UNITS by Jack L. Murrow . . . . . 96

Discussion . . . . . 106

PROGRESS REPORT - FACTORS INFLUENCING HIGH-EFFICIENCY GASKET LEAKAGE by F. E. Adley . . . . . 109

DEVELOPMENTS IN CONTAMINATED FILTER REMOVAL EQUIPMENT by C. A. Hahs . . . . . 149

Discussion . . . . . 158

Iodine and Iodide Removal
Session 2 - Wednesday, 14 September 1966
Chairman: George Parker, ORNL

DEVELOPMENT OF IMPREGNATED CHARCOALS FOR TRAPPING METHYL IODIDE AT HIGH HUMIDITY by D. A. Collins, L. R. Taylor and R. Taylor . . . . . 159

RETENTION OF METHYL IODIDE BY IMPREGNATED CARBONS UNDER AMBIENT CONDITIONS by G. W. Parker, G. E. Cheek, and A. Ferreli . . 199

MECHANISMS THAT AFFECT THE ADSORPTION OF METHYL IODIDE ON CHARCOAL UNDER HUMID CONDITIONS by Frank J. Ackerman and John Z. Grens . . . . . 230

Discussion . . . . . 271

REMOVAL OF IODIDE AND METHYL IODIDE BY AEROSOL FORMATION WITH HYDRAZINES by F. J. Viles, Jr. and L. Silverman. . . . . 273

REMOVAL OF METHYL IODIDE FROM SIMULATED REACTOR CONTAINMENT ATMOSPHERES WITH HYDRAZINE by J. Mishima, L. C. Schwendiman, L. L. Burger and R. A. Hasty . . . . . 298

Discussion . . . . . 317

Luncheon - 14 September 1966

Introduction of Guest Speaker by Professor Theos Thompson, MIT . . . . . 319

Address by Professor Manson Benedict, Head, Department of Nuclear Engineering, Massachusetts Institute of Technology . . . . . 320

Confinement and Containment
Session 3A - Wednesday, 14 September 1966
Chairman: A. H. Peters, Savannah River Laboratory

REMOVAL OF RADIOACTIVE METHYL IODIDE FROM STEAM-AIR SYSTEMS by R. D. Ackley, R. E. Adams, and W. E. Browning, Jr. . . . . 331

Discussion . . . . . 346

PERFORMANCE OF AIRBORNE ACTIVITY CONFINEMENT SYSTEMS IN SAVANNAH RIVER PLANT REACTOR BUILDINGS by W. S. Durant . . . 348

Discussion . . . . . 370

FLOATING ROOF CONTAINMENT VESSELS by Melvin W. First, Leslie Silverman, Daniel Pender and Stanley Dawson . . . . . 371

Discussion . . . . . 388

CONFINEMENT SYSTEMS TESTS PERFORMED DURING DEACTIVATION OF THE 100 F REACTOR by M. L. Smith . . . . . 389

AIR CLEANING FOR REACTORS WITH VENTED CONTAINMENT by R. D. Collins, J. J. Hillary and J. C. Taylor . . . . . 419

EFFECTS OF CONTAINMENT SYSTEM SIZE ON FISSION PRODUCT BEHAVIOR by G. M. Watson, R. B. Perez and M. H. Fontana . . . . . 454

VENT GAS TREATMENT PLANT by J. Ackerman, R. Bundrick, J. Cowles, V. DuVal, J. Grens, R. Holzman, C. Hannon, J. Harrar, C. Morris, L. Rigdon, R. Heckman and D. Snoeberger . . . . . 496

Radioactive Waste and Incineration
Session 3B - Wednesday, 14 September 1966
Chairman: R. Dennis, G. C. A. Corporation

AN ENGINEERING EVALUATION OF A RADIOACTIVE-WASTE INCINERATOR by David G. Lachapelle . . . . . 509

DISPOSAL OF LOW LEVEL RADIOACTIVE WASTE IN COMMERCIAL INCINERATORS by M. W. First, F. Zilles and J. Walkley . . . . . 570

RECENT ADVANCES IN MONITORING OF RADIOACTIVE GASEOUS WASTE AT ORNL by J. F. Manneschmidt . . . . . 586

Discussion . . . . . 612

Volume II

Filtration and Filter Performance Evaluation
Session 4 - Thursday, 15 September 1966
Chairman: M. D. Thaxter, Lawrence Radioation Laboratory

SERIES DISTRIBUTION SAMPLING ERRORS INTRODUCED BY THE POINT-PLANE ELECTROSTATIC PRECIPITATOR SAMPLING DEVICE by Parker C. Reist . . . . . 613

Discussion . . . . . 625

EVALUATION OF THE EQUATION THAT GOVERNS THE COAGULATION OF AN AEROSOL by P. Spiegler, J. G. Morgan, M. A. Greenfield and R. L. Koontz . . . . . 626

Discussion . . . . . 646

MECHANICS OF COLLECTION OF PARTICLES BY INERTIA AND INTERCEPTION IN A FIBROUS AIR FILTER by Stanley V. Dawson . . . . . 647

EFFECTS OF PARTICLE ACCUMULATION ON AEROSOL FILTER LIFE by Charles E. Billings . . . . . 656

Discussion . . . . . 676

CHARACTERIZATION OF RADIOACTIVE PARTICULATE AEROSOLS BY THE FIBROUS FILTER ANALYZER by M. D. Silverman, J. Truitt, W. E. Browning, Jr., L. F. Franzen and R. E. Adams . . . . . 680

Discussion . . . . . 700

PENETRATION OF SUBMICRON TI BACTERIOPHAGE AEROSOLS AND BACTERIAL AEROSOLS THROUGH COMMERCIAL AIR FILTERS by J. B. Harstad, Herbert M. Decker, Lee M. Buchanan and Melvin E. Filler . . . . . 701

Discussion . . . . . 714

PERFORMANCE OF FILTER SYSTEMS UNDER ACCIDENT CONDITIONS by R. E. Adams, J. S. Gill, W. D. Yuille, W. E. Browning, Jr., L. F. Parsley and C. E. Guthrie . . . . . 715

Discussion . . . . . 738

REMOVAL OF PLUTONIUM HEXAFLUORIDE FROM CELL EXHAUST AIR BY HYDROLYSIS AND FILTRATION by Robert W. Kessie . . . . . 741

Discussion . . . . . 762

AN EVALUATION OF TWO PORTABLE THERMAL AEROSOL GENERATORS FOR IN-PLACE FILTER TESTING by R. H. Knuth . . . . . 763

Noble Gas Studies
Session 5A - Thursday, 15 September 1966
Chairman: F. J. Viles, Jr., Harvard Air Cleaning Laboratory

INCREASED DETECTION SENSITIVITY FOR KRYPTON-85 by D. G. Smith, P. C. Reist and L. Silverman . . . . . 781

Discussion . . . . . 799

PRELIMINARY RESULTS OF DIFFUSION MEMBRANE STUDIES FOR THE SEPARATION OF NOBLE GASES FROM REACTOR ACCIDENT ATMOSPHERES by S. Blumkin, H. Briggs, A. Dounoucos, E. Von Halle, J. M. Holmes and R. H. Rainey. . . . . 801

MASS TRANSFER OF KRYPTON-85 IN CHARCOAL ADSORPTION BEDS by Dwight Underhill . . . . . 824

Discussion . . . . . 847

Aerosols from Burning Reactor Components
Session 5B - Thursday, 15 September 1966
Chairman: M. A. Greenfield, University of California

STANDARDIZED GENERATION OF VAPOR-PRODUCED SODIUM AEROSOLS AND THEIR BEHAVIOR by R. L. Koontz, C. T. Nelson and L. Baurmash . . . . . 848

TECHNIQUES FOR SAMPLING SODIUM SMOKE AND FISSION PRODUCTS by C. T. Nelson, L. Baurmash and C. T. Nelson . . . . . 860

SODIUM AEROSOL AND ITS FILTRATION by P. Himot, F. J. Viles, Jr., J. Sullivan and M. W. First . . . . . 877

CHARACTERISTICS OF THE AEROSOL PRODUCED FROM BURNING PLUTONIUM by H. J. Ettinger, W. D. Moss and H. Busey . . . . . 905

Discussion . . . . . 927

Analysis and Monitoring of Contamination
Session 5C - Thursday, 15 September 1966
Chairman: J. Ege, Argonne National Laboratory

PORTABLE SMOKE PHOTOMETER by H. H. Hunter and R. I. Mitchell . . . . 928

Discussion . . . . . 941

ZPPR ROOF SAND FILTRATION OF URANIUM, PLUTONIUM AND URANINE AEROSOLS by C. L. Cheever, D. R. McFee, J. Sedlet and T. L. Duffy . . . . . 942

THE DESIGN, TEST AND USE OF THE BROOKHAVEN NATIONAL LABORATORY (BNL) REACTOR BYPASS FILTER FACILITY by R. O. McClintock . . . . . 965

CONTINUOUS SAMPLER-MONITOR FOR FISSION PRODUCTS IN CONTAMINATED ATMOSPHERES by R. E. Schindler . . . . . 974

Discussion . . . . . 977

In-Place Testing
Session 6 - Friday, 16 September 1966
Chairman: J. Thomas, New York Operations

FILTER TESTING PROGRAM, ATOMIC ENERGY OF CANADA LIMITED by F. Panchuk and W. Rachuck . . . . . 979

Discussion . . . . . 1020

TESTING OF AIR CLEANING SYSTEMS - TESTING OF THE COMPONENTS - IN-PLACE TESTS by F. Billard and J. Brion . . . . . 1021

Discussion . . . . . 1031

ON-SITE TESTING OF FILTERS WITH SPECIAL REFERENCE TO SOLID AEROSOLS by Hans Flyger and H. C. Rosenbaum . . . . . 1032

IN-PLACE TESTING OF CHARCOAL FILTER BANKS AT AMES LABORATORY RESEARCH REACTOR by G. A. Gukeisen and K. L. Malaby . . . . . 1063

Discussion . . . . . 1069

IN-PLACE NONDESTRUCTIVE LEAK TEST FOR IODINE ADSORBERS by D. R. Muhlbaier . . . . . 1071

IN-PLACE IODINE FILTER TESTING by J. H. Swanks . . . . . 1092

Discussion . . . . . 1105

IN-PLACE IODINE REMOVAL EFFICIENCY TEST by F. J. Viles, Jr. and L. Silverman . . . . . 1108

Discussion . . . . . 1132

IN-PLACE TESTING FOR IODINE REMOVAL EFFICIENCY USING AN ELECTRONIC DETECTOR by W. G. Thomson and R. E. Grossman . . . . 1134

Discussion . . . . . 1150

Open End Discussion
Session 7 - Friday, 16 September 1966
Chairman: M. W. First, Harvard University

Discussion . . . . . 1154

Formal Statement by Mr. B. Fish on Retention and Removal . . . . . 1154

PROTECTION OF HEPA FILTER SYSTEMS AGAINST HIGH EXPANSION FOAM PLUGGING by C. L. Lindenken and R. D. Taylor . . . . . 1159

Discussion . . . . . 1167

THE COMPARATIVE ENVIRONMENTAL HAZARDS FROM A RELEASE OF METHYL IODIDE OR ELEMENTAL IODINE by D. R. Bunch. . . . . 1169

Discussion . . . . . 1175

Formal Statement by Mr. D. J. Keigher on Fire Protection Considerations in Clean Rooms . . . . . 1177

Discussion . . . . . 1180

CLOSING REMARKS by Mr. W. G. Belter, Division of Reactor Development and Technology, U. S. Atomic Energy Commission . . . . . 1194

Statement Submitted After Conclusion of Conference: Moisture Separator Study For Iodine Removal Systems for Connecticut Yankee Reactor Containment by R. D. Rivers . . . . . 1196

List of Attendees . . . . . 1197

## WELCOME

Dr. J. Snyder, Dean
Harvard School of Public Health

On behalf of the Faculty of Public Health, I welcome the members of the Conference to this 9th meeting.

I regret that the Harvard School of Public Health does not have facilities to accommodate a meeting of this size. Our only room approaching this in its cubic content is the Air Cleaning Laboratory at 665 Huntington Avenue. It is now filled with instruments of one sort or another, and a major commotion would ensue if we were to reconvert it to an assembly hall today.

The proper person to address you on behalf of our School would be Dr. James L. Whittenberger, Professor of Physiology and Director of the Kresge Center for Environmental Health, which comprises the three departments of the School of Public Health most concerned with environmental problems, namely, Physiology, Industrial Hygiene, and Sanitary Engineering. Dr. Whittenberger was unable to be here today. Particularly on his behalf, and that of the other members of the faculty, I wish you success in your forthcoming conferences. I hope the opportunity to exchange ideas with our faculty members and former students will be profitable. Thank you.

## OPENING REMARKS

Dr. J. A. Lieberman
Assistant Director for Nuclear Safety, USAEC

Dean Snyder, before we get into this conference and before any words of welcome, I am sure there are many of you here that will join me in recognition of a man who perhaps has done more for the whole business of air cleaning in the atomic energy industry and who was certainly a well-known person in all of the air cleaning conferences, namely, Dr. Leslie Silverman.

As a result of Les' work, which I won't go into in detail here because it is familiar to many of you participating in this Air Cleaning Conference and the ones we have had in the past, there has been awarded a Certificate of Appreciation in the name of Dr. Leslie Silverman to the Harvard Air Cleaning Laboratory, signed by Dr. Glen Seaborg as Chairman of the Atomic Energy Commission, and if you will permit me, Dean Snyder, I would like to read the Citation.

I am sure that all of you here join me in presenting this to Dr. Snyder for the Harvard Air Cleaning Laboratory.

DR. SNYDER: I am very grateful for this Certificate and statement which will be mounted, suitably-framed, in the Air Cleaning Laboratory in the School of Public Health.

DR. LIEBERMAN: Thank you very much. (Applause.)

On behalf of the Atomic Energy Commission, obviously we welcome all of you to this 9th AEC Air Cleaning Conference. I would particularly like to welcome our friends from overseas and to the North and South of our borders to this meeting.

The Air Cleaning Conference has just about become an institution in the AEC. The first one was also at Harvard; and, as I recall, it was back in the early '50s. So, as the industry goes, there is a relatively long history of attention and research and development effort and the relating of operational experiences in the air cleaning and the nuclear energy business.

I would like to point out that at this time, particularly in the United States, although I know it is true in other countries also, the tremendously increased interest not only on the part of the public but on the part of our scientific and technological community on problems relating to the impac of human endeavor on our environment and the control of that impact. I think that the group here can well take pride in the contributions that have been made in this area by their work in the past, and it seems to me that this is something we can look forward to in the future.

In glancing through the titles of the papers, there are very good reflections of the level of accomplishment and, perhaps, even the level of sophistication achieved in this aspect of the nuclear energy activities. At the same time, I think one can also recognize the applications that have been made as a result of this work to our technology on an almost across-the-board basis. As you glance through the titles, you perhaps will see those that do not seem very much different than they were several years ago, and this is perhaps something that should be understood, because some of these problems are still with us.

At the same time, I think there is also an indication of new problems that will face us with the onset of liquid metal, fast breeder reactor, new fuels, and so on.

We have a long and, I might even say, arduous schedule in front of us. I would hope that the formality of this opening is not something that prevails throughout the meeting; while it is one of the largest conferences that we have had, and the agenda is perhaps one of the longest, I would hope, if it is not in violation of any other ground rules, that there will still be opportunity for questions, discussion, and maybe even a good argument or two.

In the absence of any particular ground rules and in the presence of, as I understand it, almost all the preprints, I would hope that the participants who are going to present their papers, at least in the session for which I have responsibility, will attempt to summarize the highlights of their conclusions so that there will be time for questions after the sessions.

Mr. Walter Belter remarked last night that if Mr. Morrison's is a first-rate paper, as I expect it will be, a good part of this conference might have already been taken care of, but I think it will serve as a useful introduction. He is here and it looks like he's ready to present the paper. Are there any questions before we begin? If not we will get underway.

# ANALYTICAL DESCRIPTION OF THE DISTRIBUTION OF FISSION PRODUCTS DURING NUCLEAR REACTOR ACCIDENTS FOR WATER AND GAS COOLED REACTORS*

David L. Morrison, James A. Gieseke, and Robert L. Ritzman
Battelle Memorial Institute
Columbus Laboratories

A mathematical model has been developed to describe fission product release during water-reactor accidents. The input parameters for the equations for the release from the fuel are based upon experimental data, and the temperature input to the model is supplied from an independent heat transfer analysis. The transport and deposition of the fission products in the core and primary vessel are calculated to provide the source term for the transport and deposition analysis within the containment vessel. Two simple models, transport within a well-mixed gas or diffusion in a stagnant gas, are considered for this region. An analytical description of the time-space distribution of fission products in an accident can be obtained by the proper combination of these mathematical models.

## INTRODUCTION

A general description of the temporal and spatial distribution of fission products in a reactor accident involves the consideration of the complex interrelationships among several processes. The lines of direct interaction which must be considered for a loss-of-coolant accident in a water cooled and moderated reactor are illustrated in Figure 1. In an analytical sense, the fission product distribution is described by the fission product release and the fission product transport and deposition models but these models in turn require input from the description of the solid and fluid temperature distributions, the heat-generation-rate distribution, the geometry flow in the system, and the fluid flow during and following the blowdown. Each of these processes must be described by specific models covering the individual physical and chemical changes which occur during the accident. In a gas-cooled reactor accident, the specific chemical and physical processes would differ from those considered in the water reactor accident, but in this case also, the time-space distribution of the fission products would be the primary concern.

The complex processes which must be considered in the development of the fission product release and the fission product transport and deposition models include the preaccident distribution of the fission products on a core-wide and individual fuel pin basis, determination of the kinetics of the release as a function of temperature, chemical and physical identity of the released

* Work performed under AEC Contract No. W-7405-eng-92.

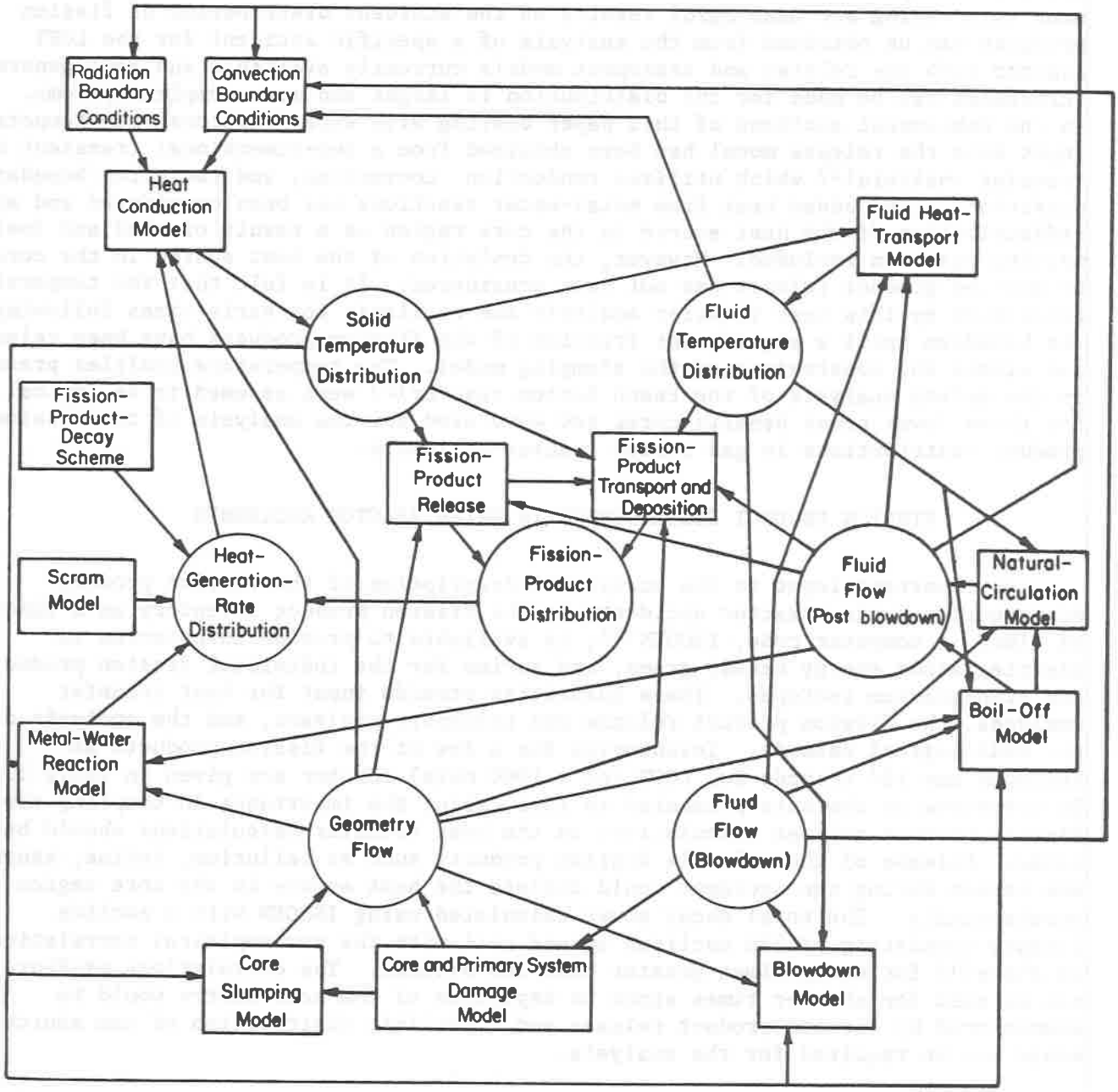


Figure 1. Flow Diagram Showing Lines of Direct Interaction in a Loss-of-Coolant Accident Analysis

fission products, particle formation and growth mechanisms, transport within the primary and containment systems, and deposition and removal mechanisms from the gas phase to the walls and condensate. Existing experimental data have been employed to develop an analytical description of the processes and to formulate the fission product release and the fission product transport and deposition models required for the analytical description of the fission product distribution during a reactor accident. However, the complete description of this distribution would require the time dependent and spatial dependent analysis of the reactor as a whole considering the proper interrelation of the factors noted above. To date, this complete analysis is not available and even if it were, the distribution of fission products would have to be based upon the assumption of a specific system and an accident model which would include the size and location of the rupture in the primary system. Although all of the interrelationships have not been considered, some interesting and meaningful results on the accident distribution of fission products can be obtained from the analysis of a specific accident for the LOFT reactor with the release and transport models currently available and some general inferences can be made for the distribution in larger and more complex systems. In the subsequent sections of this paper dealing with water reactors, the temperature input into the release model has been obtained from a two-dimensional transient heat transfer analysis[1] which utilizes conduction, convection, and radiation boundary conditions. The added heat from metal-water reactions has been considered and some redistribution of the heat source in the core region as a result of clad and fuel melting has been included. However, the depletion of the heat source in the core by fission product release has not been considered. It is felt that the temperatures calculated by this heat transfer analysis are realistic for early times following the blowdown until a significant fraction of the fission products have been released and within the constraints of the slumping model. The temperature profiles presented in the safety analysis of the Peach Bottom reactor[2] were assumed to be typical for these lower power density cores and were used for the analysis of the fission product distributions in gas cooled reactor accidents.

## FISSION PRODUCT DISTRIBUTION IN WATER REACTOR ACCIDENTS

An important input to the analytical description of the fission product distribution during reactor accidents is the fission product inventory as a function of time. A computer code, ISOGEN[3], is available to provide inventories in disintegration energy rates, grams, and curies for the individual fission products and transuranium isotopes. These quantities provide input for heat transfer analyses, the fission product release and transport analyses, and the analysis of the radiological hazards. Inventories for a few of the fission products at shutdown and $10^3$ seconds for LOFT and a 1000 MW(e) reactor are given in Table 1. In reference to the data presented in this table, the importance in coupling the fission product release calculations to the heat transfer calculations should be noted. Release of the volatile fission products such as tellurium, iodine, xenon, and cesium during the accident could deplete the heat source in the core region substantially. The total decay power calculated using ISOGEN with a nuclide library consisting of 333 nuclides agreed well with the semiempirical correlation of Shure[4] for decay times greater than 100 seconds. The correlations of Shure can be used for shorter times since no depletion of the heat source would be encountered by fission product release and a nuclidic distribution of the source would not be required for the analysis.

The analytical treatment of fission-product release also requires detailed input relating to the distribution of fission products on both a macro- and microscale within the reactor core prior to the accident. The general core-wide distribution specifies the relative heat generation rates at various points which is a primary input factor for the heat-transfer analysis and also identifies the regions of high fission product concentrations. Most pressurized water and boiling

TABLE 1: FISSION PRODUCT INVENTORIES AT END-OF-CORE LIFETIME

| Element or Isotope | At Shutdown | | | |
|---|---|---|---|---|
| | LOFT | | BWR(5)* 1000 MW(e) Design | |
| | Grams | Percent of Total Decay Power | Grams | Percent of Total Decay Power |
| Tellurium | 31.7 | 2.0 | $3.0 \times 10^4$ | 2.0 |
| Iodine | 19.5 | 6.6 | $1.2 \times 10^4$ | 6.4 |
| Xenon | 260 | 3.6 | $3.2 \times 10^5$ | 3.5 |
| Cesium | 130 | 7.4 | $1.9 \times 10^5$ | 7.2 |
| Ruthenium | 103 | 0.2 | $1.1 \times 10^5$ | 0.3 |
| Strontium | 88.3 | 4.4 | $8.2 \times 10^4$ | 4.4 |
| | Curies | | Curies | |
| Te-132 | $1.85 \times 10^6$ | | $8.7 \times 10^7$ | |
| I-131 | $1.19 \times 10^6$ | | $6.0 \times 10^7$ | |
| Cs-137 | $5.46 \times 10^3$ | | $6.8 \times 10^6$ | |
| Ru-106 | $9.73 \times 10^3$ | | $5.7 \times 10^6$ | |
| Sr-90 | $5.49 \times 10^3$ | | $6.8 \times 10^6$ | |
| | Decay Time = $10^3$ sec | | | |
| Tellurium | 31.6 | 3.3 | $3.0 \times 10^4$ | 2.9 |
| Iodine | 19.5 | 13.7 | $1.2 \times 10^4$ | 12.0 |
| Xenon | 260 | 2.7 | $3.2 \times 10^5$ | 2.4 |
| Cesium | 130 | 6.4 | $1.9 \times 10^5$ | 5.6 |
| Ruthenium | 103 | 0.5 | $1.1 \times 10^5$ | 0.7 |
| Strontium | 88.3 | 6.3 | $8.2 \times 10^4$ | 6.0 |
| | Curies | | Curies | |
| Te-132 | $1.85 \times 10^6$ | | $8.7 \times 10^7$ | |
| I-131 | $1.19 \times 10^6$ | | $6.0 \times 10^7$ | |
| Cs-137 | $5.46 \times 10^3$ | | $6.8 \times 10^6$ | |
| Ru-106 | $9.73 \times 10^3$ | | $5.7 \times 10^6$ | |
| Sr-90 | $5.49 \times 10^3$ | | $6.8 \times 10^6$ | |

* Based upon 520,000 lbs $UO_2$ and a U-235 enrichment of 2.0 percent.

1400 to 2500 C in helium atmospheres. The release behavior of the fission products studied appeared to follow the kinetics of a diffusion process and Arrhenius parameter values for iodine, tellurium, strontium, ruthenium, cesium, cerium, lanthanum, zirconium-niobium, molybdenum, and xenon were presented. The lower temperature range covered in these studies overlaps the range over which Parker, et al., made measurements, so a comparison of the results was made. At all temperatures, the data of Oi and Takagi indicated a higher release rate of fission products than the data of Parker, with cesium exhibiting the most pronounced disagreement. The values for the release rate of a given fission product did tend to converge when extrapolated to the melting point of $UO_2$. At temperatures above 1700 C, evaporation of $UO_2$ may have a significant effect on the release of fission products and may contribute to the discrepancies in the results reported by the two groups of experimenters. Since the data of Parker, et al., were selected for use in the lower and higher temperature ranges, they were also selected for input for calculations of release at temperatures between 1500 and 2800 C. Calculations performed for identical core temperature histories indicate that use of the Parker data in this temperature region may lead to release fractions which are a factor of five lower than those which would have been calculated from the Oi and Takagi data. The fission product release parameter coefficients which have been derived from the experimental data and applied in the present analysis are summarized in Table 2.

The analytical description of the fission product release by diffusion in the two lower temperature regions is based upon the equivalent sphere concept It is convenient to assume this representation for the fuel since the results are only mildly sensitive to geometry effects. The sequence of computations to obtain the release as a function of time during the accident is equivalent to performing successive heatings at increasing temperature levels, so accurate description of release in any time interval requires that the previous release history be considered. This can be done by proper modification of the release parameters. The analytical system for describing fission product release during the loss-of-coolant accident analysis is coded for machine computation and the computer program FRACREL (FRACtional RELease) supplies cumulative fractional release values for up to 12 elements or isotopes from each of 120 reactor core regions at specified time increments during the accident. Cumulative fractional release per element or isotope for the entire core is also included in the output. The generalized equations for calculation of fission product release from any core region up to the fuel melting point then are:

$$F_{i,k,l,n} = \frac{6}{\sqrt{\pi}}\left(\sum_{n=1}^{n} \tau_{i,k,l,n}\right)^{1/2} - 3\left(\sum_{n=1}^{n} \tau_{i,l,l,n}\right) \quad (4)$$

for $F < 0.9$, and

$$F_{i,k,l,n} = 1 - \frac{6}{\pi^2} \exp\left[ - \pi^2 \left(\sum_{n=1}^{n} \tau_{i,k,l,n}\right)\right] \quad (5)$$

for $0.9 \leq F \leq 1.0$, where

$F_{i,k,l,n}$ = the cumulative fractional release of isotope i from axial section k of radial core zone l after n time intervals

$\tau_{i,k,l,n}$ = the release parameter for isotope i located in axial section k of radial core zone l for the n-th time interval.

The release parameter $\tau_{i,k,l,n}$ is further defined as

$$\tau_{i,k,l,n} = \frac{D_{i,k,l} \cdot \Delta tn}{a^2} \quad (6)$$

where

TABLE 2. FISSION PRODUCT RELEASE PARAMETER COEFFICIENTS SELECTED FROM EXPERIMENTAL DATA FOR FRACREL COMPUTATIONS

| Fission Product Species | Applicable Temperature Range: 300 C ≤ T < 1500 C | | 1500 C ≤ T < 2800 C | | T ≥ 2800 C | |
|---|---|---|---|---|---|---|
| | $D_o$ $cm^2/sec$ | Q Kcal/g-atom | $D_o$ $cm^2/sec$ | Q Kcal/g-atom | A $sec^{-1/2}$ | B |
| Xe, Kr | $4.3 \times 10^{-4}$ | 72 | $1.6 \times 10^{-4}$ | 67 | 0.1162 | 0 |
| I, Br | $1.9 \times 10^{-3}$ | 68 | $1.5 \times 10^{-5}$ | 53.5 | 0.1162 | 0 |
| Te | $5.6 \times 10^{-1}$ | 84 | $4.2 \times 10^{-5}$ | 58 | 0.0298 | 0.60 |
| Cs, Rb | $4.5 \times 10^{-7}$ | 40 | $1.9 \times 10^{-5}$ | 52 | 0.0828 | 0 |
| Sr, Ba | $8.6 \times 10^{1}$ | 140 | $8.6 \times 10^{1}$ | 140 | 0.00272 | 0 |

$D_{i,k,l}$ = the diffusion coefficient for isotope i located in axial section k of radial core zone l, $cm^2/sec$

$\Delta t_n$ = the n-th time interval, sec

a = the equivalent-sphere radius, cm

and the diffusion coefficient values are obtained from the Arrhenius equation,

$$D_{i,k,l} = D_{o_i} \exp\left(- Q_i/RT_{k,l}\right) \quad , \tag{7}$$

where

$D_{o_i}$ = the limiting value of the diffusion coefficient, $cm^2/sec$

$Q_i$ = the Arrhenius activation energy, cal/mole

R = the universal gas constant, cal/mole-deg K

T = the absolute temperature, deg K .

The total cumulative fractional release from any core region in the reactor is given by:

$$(F_T)_{i,k,l,n} = F_{i,k,l,n} + f_{i,k,l} \quad , \tag{8}$$

where

$f_{i,k,l}$ = the fraction of isotope i released to the cladd fuel gap of axial section of radial core zone l during operation .

The initial release of the quantity f does not occur until the temperature of any axial section of a radial zone exceeds a specified cladding rupture temperature which may be arbitrarily designated for the computation. The total cumulative fractional release from each core region can be multiplied by the fractional fission product inventory for the region to obtain the cumulative fractional inventory release values region by region or,

$$(F_T^*)_{i,k,l,n} = (F_T)_{i,k,l,n} \cdot V_{k,l} \quad . \tag{9}$$

The cumulative fractional release of an isotope or element from the entire core at any time then is the sum of the cumulative fractional inventory release values for all regions up to that time or,

$$F_{CORE_i} = \sum_{l=1}^{1} \sum_{k=1}^{k} (F_T^*)_{i,k,l,n} \quad . \tag{10}$$

The release from the molten fuel is treated by the linear square root of time relationship mentioned previously and is given by,

$$F_{i,k,l,n} = F_{i,k,l,n-1} + A\,(\Delta t_n)^{1/2} + B \tag{11}$$

where

$F_{i,k,l,n-1}$ = the cumulative fractional release of isotopic from axial section k of radial core zone l after n-1 time intervals

A = slope of linear F vs $\sqrt{t}$ fit to experimental release data, $sec^{-1/2}$

B = F - axis intercept value .

Computations of fission product release from the LOFT core during loss-of-coolant accident conditions have been performed. The initial rupture point of the Zircaloy cladding was designated to occur at a temperature of 1200 C. Gaseous fission products introduced to the pellet-cladding gap both during reactor operation and during core heatup following the loss-of-coolant were assumed to be quantatively

released at this point. Only the rare gases and the halogens were designated as being gaseous at this point in the computations. The event of cladding rupture was assumed to eliminate physical restrictions for subsequent release of any fission product from the $UO_2$ fuel, i.e., the possible effects of the size of the fissure in the cladding and of fission product transport to the fissure were not considered. Total core fractional release values were calculated at 20 second time intervals ($\Delta t_n$ = 20) from the beginning of core heatup to about 400 seconds. The temperature information for each core region at each time step was used directly as generated by the NURLOC heat-transfer analysis code. The five fission product elements treated in the computation included the rare gases, the halogens, tellurium, the alkali metals, and the alkaline earth metals. The set of Arrhenius release parameters used for these species are given in Table 2 along with the coefficients used for each to describe release from molten $UO_2$ (M.P. = 2800 C). The simple diffusion model requires specification of an equivalent sphere radius value; and for all computations here, a value of $4 \times 10^{-3}$ cm was used, which is characteristic of 93-94 percent dense $UO_2$. The results of these computations are given in Figures 2 and 3.

A release calculation was also performed for a 600 MW(t) boiling-water reactor using the same release parameters. The heat transfer results for this case showed that 280 seconds were required to reach cladding failure temperature (1200 C) in the hottest core pin. Only three of the ten radial core pins reached rupture temperature when the calculation was terminated at 260 seconds. Diffusional release is relatively minor in this low temperature range so that even for the gaseous species (rare gases and halogens) the total core fractional release at the 360 second time point was found to be less than $2.5 \times 10^{-3}$ and consisted of about equal amounts of gas released during reactor operation and of gas released during the time span of the accident analysis. Comparison of these results to results for the LOFT reactor case shows that in the BWR case where cladding rupture required nearly 3 times longer to occur, the fractional release values for the more volatile fission products were about one order of magnitude lower at the end of the calculation, 360 seconds.

These fission product release calculations can be used as an input to the fission product transport and deposition model to obtain the description of the fission product distribution during a reactor accident. However, the analytical description of transport and deposition of fission products during a loss-of-coolant accident also depends upon a number of assumptions, a choice of geometries, and input information from the blowdown, heat transfer, and fluid flow analyses. The other analyses generally set the variable conditions, the system geometry affects the number of models possible, and the assumptions provide input parameters and also specify other conditions.

In general, the process of fission product transport and deposition can be followed in a step-wise fashion from the point of fission product release from the fuel to the point of release from the containment. Using this basis there are four primary areas of concern which can be specified separately for the case of an accident resulting from severance of a primary coolant pipe. Following the order in which they are exposed to fission products, these regions are (1) the core section between fuel pins, (2) the upper plenum chamber of the pressure vessel, (3) the blowdown line, and (4) the containment vessel. Before considering each of these regions separately, some general observations should be made concerning information needed in the description of all regions.

An analytical description of fission product transport and deposition can be divided into small models describing the various mechanisms determining fission product behavior. The primary mechanisms are (1) transport of fission products to the neighborhood of a surface, (2) transfer of fission-product material across a boundary layer to the surface-air interface, and (3) interactions between the

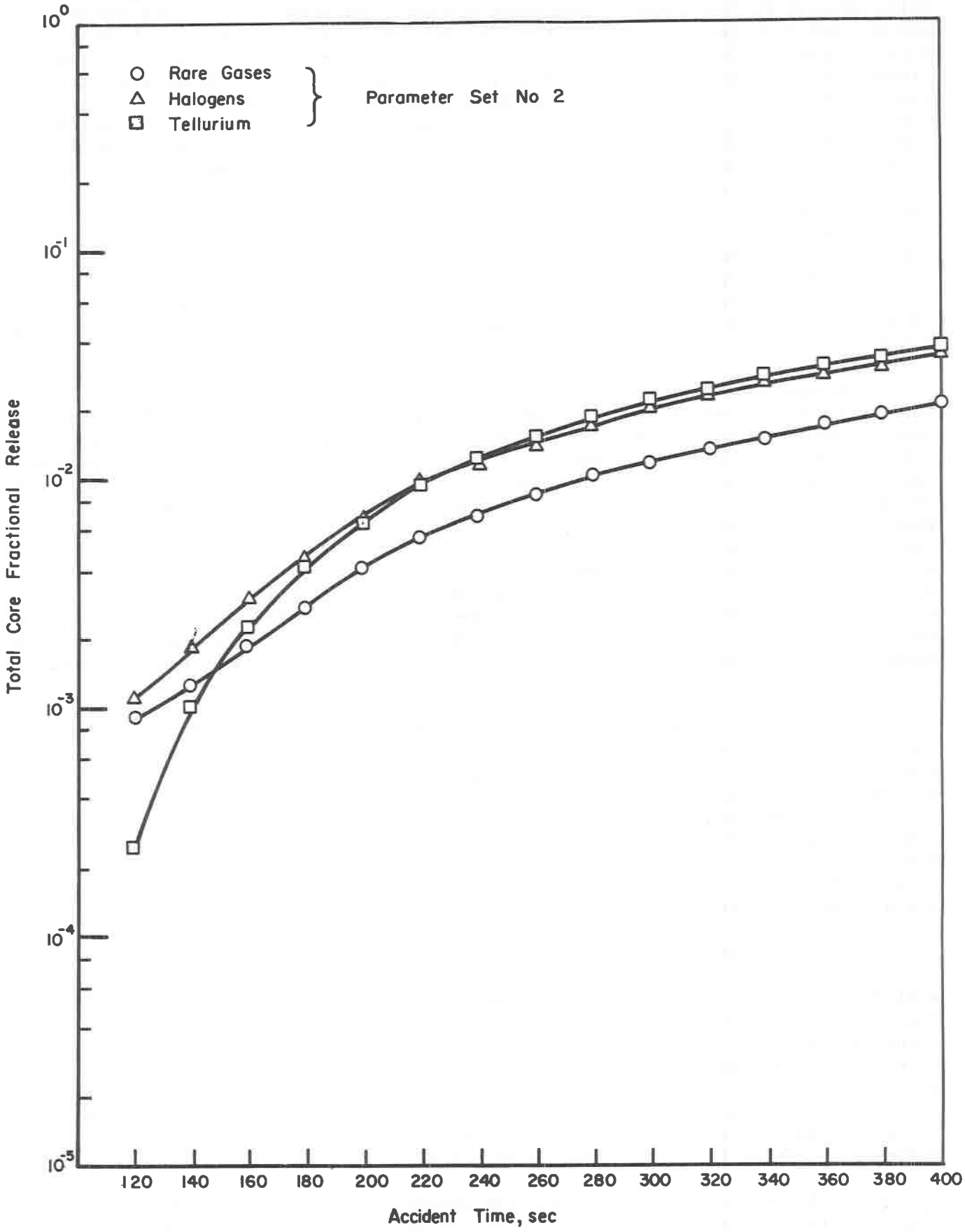


Figure 2. Release of Rare Gases, Halogens, and Tellurium from Loft Reactor Fuel

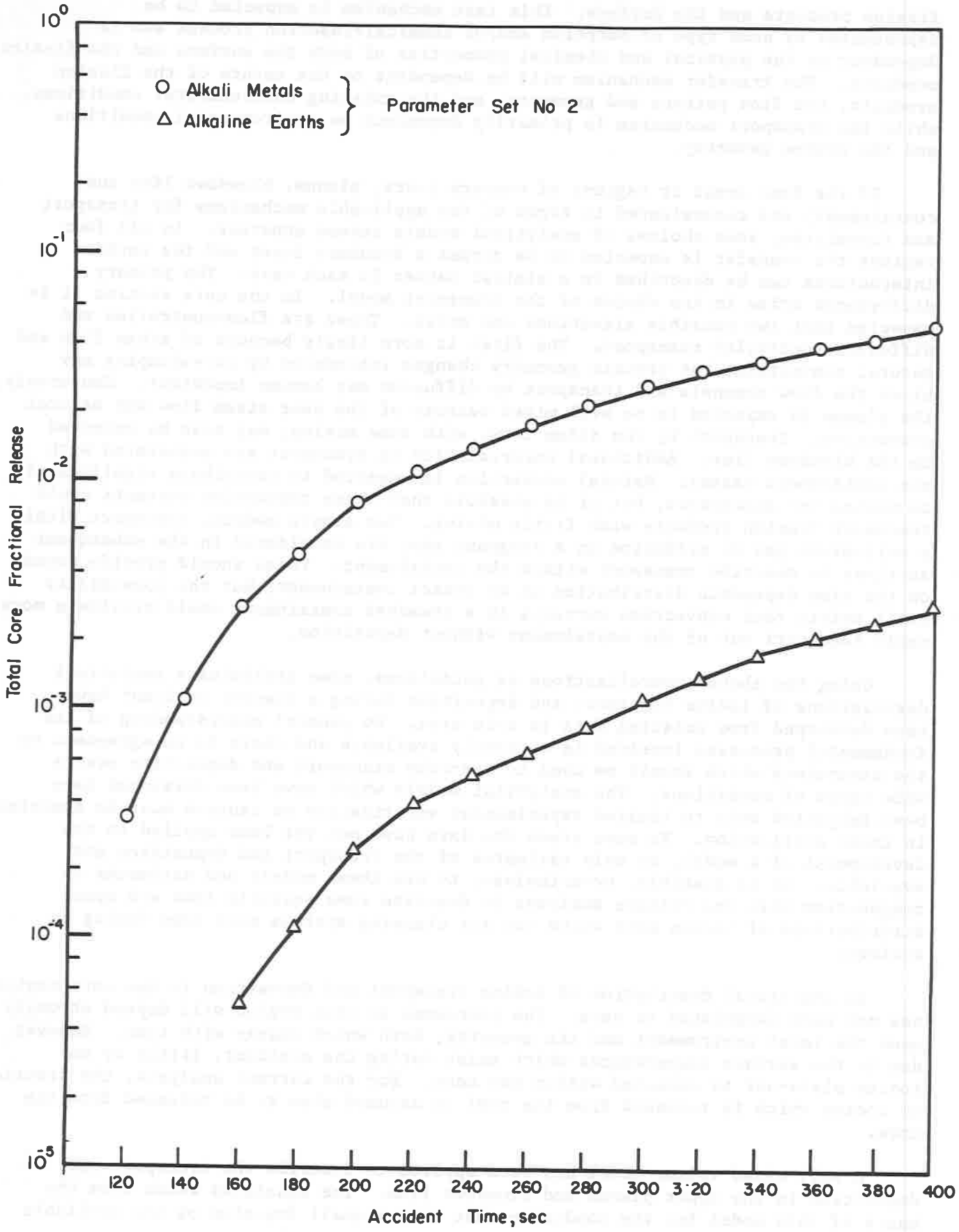


Figure 3. Release of Alkali Metals and Alkaline Earths from Loft Reactor Fuel

fission products and the surface. This last mechanism is expected to be represented by some type of sorption and/or chemical-reaction process and is dependent on the physical and chemical properties of both the surface and the fission products. The transfer mechanism will be dependent on the nature of the fission products, the flow pattern and geometry, and the existing environmental conditions, while the transport mechanism is primarily dependent on environmental conditions and the system geometry.

If the four areas or regions of concern (core, plenum, blowdown line and containment) are reconsidered in terms of the applicable mechanisms for transport and deposition, some choices of analytical models become apparent. In all four regions the transfer is expected to be across a boundary layer and the surface interactions can be described in a similar manner in each case. The primary differences arise in the choice of the transport model. In the core section it is expected that two possible situations can exist. These are flow-controlled and diffusion-controlled transport. The first is more likely because of steam flow and natural convection, but certain geometry changes introduced by core slumping may block the flow channels and transport by diffusion may become important. Conversely, the plenum is expected to be well mixed because of the same steam flow and natural convection. Transport by the steam flow, with some mixing, may also be expected in the blowdown line. Additional uncertainties in transport are associated with the containment vessel. Natural convection is expected to contribute significantly to mixing the atmosphere, but it is possible that these convection currents could transport fission products with little mixing. Two simple models, transport within a well-mixed gas or diffusion in a stagnant gas, are considered in the subsequent sections to describe transport within the containment. These should provide bounds on the time dependent distribution in an intact containment, but the possibility still exists that convection currents in a breached containment could provide a more rapid transport out of the containment without deposition.

Using the above generalizations as guidelines, some preliminary analytical descriptions of iodine transport and deposition during a reactor accident have been developed from existing data in this area. No general understanding of the fundamental processes involved is currently available and there is no agreement on the parameters which should be used to describe transport and deposition over a wide range of conditions. The analytical models which have been developed have been subjected only to limited experimental verification so caution must be exercised in their application. In some areas the data have not yet been applied to the development of a model, so only estimates of the transport and deposition are available. It is possible, nevertheless, to use these models and estimates in conjunction with the release analyses to describe some possible time and space distributions of iodine with which the air cleaning systems must cope during an accident.

An analytical description of iodine transport and deposition in the core region has not been formulated to date. The processes in this region will depend strongly upon the local environment and the geometry, both which change with time. However, due to the surface temperatures which exist during the accident, little or no iodine plate-out is expected within the core. For the current analysis, the fraction of iodine which is released from the fuel is assumed also to be released from the core.

A well-mixed volume model has been applied to describe the transport and deposition in the upper plenum and blowdown line. The equations which form the basis of this model for the condition that only a small fraction of the available surface is covered by fission products are:

$$\frac{dC}{dt} + \frac{Q}{V}(C - C_o) + \frac{A}{V}\frac{dS}{dt} = 0 \qquad (12)$$

$$\frac{dS}{dt} = \frac{k_G RT}{M} (C - C^*) \qquad (13)$$

$$\frac{dS}{dt} = k_A C^* - k_D S \quad , \qquad (14)$$

where

$C$ = airborne concentration, gm/cm$^3$
$S$ = surface concentration, gm/cm$^2$
$C^*$ = airborne concentration at surface, gm/cm$^3$
$C_o$ = inlet airborne concentration, gm/cm$^3$
$A$ = surface area, cm$^2$
$V$ = volume, cm$^3$
$Q$ = inlet and outlet flow rate, cm$^3$/sec
$k_G$ = mass transfer coefficient, gm/cm$^2$ sec atm
$k_A$ = sorption coefficient, cm/sec
$k_D$ = desorption coefficient, sec$^{-1}$ .

For the conditions at $t = 0$ of $S = S_i$, $C = C_i$, and $(dS/dt)_{t=0} = F$, the solution for the surface concentration as a function of time is:

$$S = \frac{\left(\frac{k_7}{k_6} + S_i\right)}{(r_1 - r_2)} \left[r_1 e^{r_2 t} - r_2 e^{r_1 t}\right] - \frac{k_7}{k_6} + \frac{F}{(r_1 - r_2)} \left[e^{r_1 t} - e^{r_2 t}\right] \qquad (15)$$

where

$S_i$ = initial surface concentration
$F$ = initial adsorption rate
$C_i$ = initial concentration

$$r_1 = \frac{-k_5 + \sqrt{k_5^2 + 4k_6}}{2}$$

$$r_2 = \frac{-k_5 - \sqrt{k_5^2 + 4\,k_6}}{2}$$

$$k_5 = \frac{k_A}{V}\left(\frac{k_G RTA - Vk_D M}{k_G RT + k_A M}\right) + k_D + \frac{Q}{V}$$

$$k_6 = \frac{Q}{V}\left[k_A\left(\frac{k_D M}{k_G RT + k_A M}\right) - k_D\right]$$

$$k_7 = \frac{k_A Q C_o}{V}\left(\frac{k_G RT}{k_G RT + k_A M}\right) \quad .$$

This transport and deposition model has been applied to compute the airborne concentration of iodine emanating from the blowdown nozzle for LOFT. In order to simplify the calculations, it was assumed that the surfaces of the plenum and the blowdown line remain at a constant temperature of 300 C, that the surface loading was far from saturation, and that the iodine was in the gas phase as $I_2$. The surface reaction coefficients were obtained from the iodine sorption and desorption data of Kress and Neill[17], Morris and Nicholls[18], Barton, et al.[19], and

Chamberlain, et al.[20]. The results of these calculations using as input the data from FRACREL (extrapolated to 700 seconds) are given in Figure 4. The results of these preliminary analyses indicate that a large fraction of the iodine released from the core will escape from the plenum and blowdown line during the first 700 seconds. The fraction which is released is a strong function of the volumetric steam flow rate which in turn depends upon the amount of water remaining in primary vessel following blowdown and the boil-off rate. Additional results of blowdown tests will be required to establish if the values used in this analysis are realistic. The fraction of iodine calculated to deposit on the walls is 6.3 percent of the amount entering for a sorption coefficient, $k_A$, of $2.5 \times 10^{-2}$ cm per sec and a desorption coefficient, $k_D$, of $7 \times 10^{-4}$ $sec^{-1}$. These values probably give higher deposition than one might expect but there is only a limited amount of data for iodine sorption on stainless steel at 300 C and it is therefore difficult to predict accurately deposition at these conditions. Since the present calculations are only possible for times up to 700 seconds, the source term for the containment is not yet completely defined.

As mentioned previously, models for two extreme conditions have been considered to date to describe transport and deposition of fission products within containment vessels. Neither of the models ultimately may be found to be applicable to the analysis of these processes during an accident, but they have been invaluable for interpretation of experimental results from the ADF and NSPP and in evaluation of system parameters. It is likely that the natural convection currents in the containment vessel during an accident will cause some mixing of the atmosphere but possibly not as much as assumed in the well-mixed model. The actual situation may be somewhere between the extremes. For illustrative purposes in the succeeding sections, it is assumed that all of the iodine that is released from the blowdown nozzle is released to the containment instantaneously (the time for iodine input is short with respect to the time for significant occurrances in the containment). Some estimates of its behavior in the containment vessel are made by applying these models to yield an appreciation of the air cleaning problems which may be encountered.

Wantland[21] has developed a model for describing diffusion from a spherical shell to a perfectly absorbing wall. This model can be applied to estimate the time required for an instantaneous release as a point source at the center of the sphere to be reduced by fifty percent. For the LOFT containment with a radius of $1 \times 10^3$ cm and assuming a value of 0.08 $cm^2$ per sec for the iodine diffusion coefficient, the time is calculated to be $3.2 \times 10^4$ min. A similar calculation performed for a larger containment vessel with a radius of $2.9 \times 10^3$ cm which is typical of a 600 MW(t) BWR yields $2.4 \times 10^5$ minutes for the time required to reduce the airborne concentration by one-half. Another diffusion model has been developed which assumes that the iodine is initially uniformly distributed within the containment volume. Long airborne residence times are also estimated with this model. It is evident from these calculations that if stagnant conditions exist in the containment during an accident, iodine and the other fission products would be expected to remain airborne for long periods of time due to the combination of small diffusion coefficients and large vessel sizes.

Estimates of the time-dependent behavior of accident released iodine in a containment vessel can also be based upon a wet-wall, well-mixed volume model which has been applied to the evaluation of data from experiments in the Aerosol Development Facility. In this model, it is assumed that the iodine is released instantaneously into the containment volume and is uniformly distributed within it. The airborne concentration is maintained uniform by mixing. Condensation of steam is occuring at the wall and a film of water is assumed to wet the surface. Equilibrium between the iodine in the gas phase at the interface and the liquid film is maintained in the accordance with Henry's law and irreversible reaction of iodine in the liquid with the wall is assumed. Calculations were performed for the LOFT and the larger containment vessel previously described using input parameters

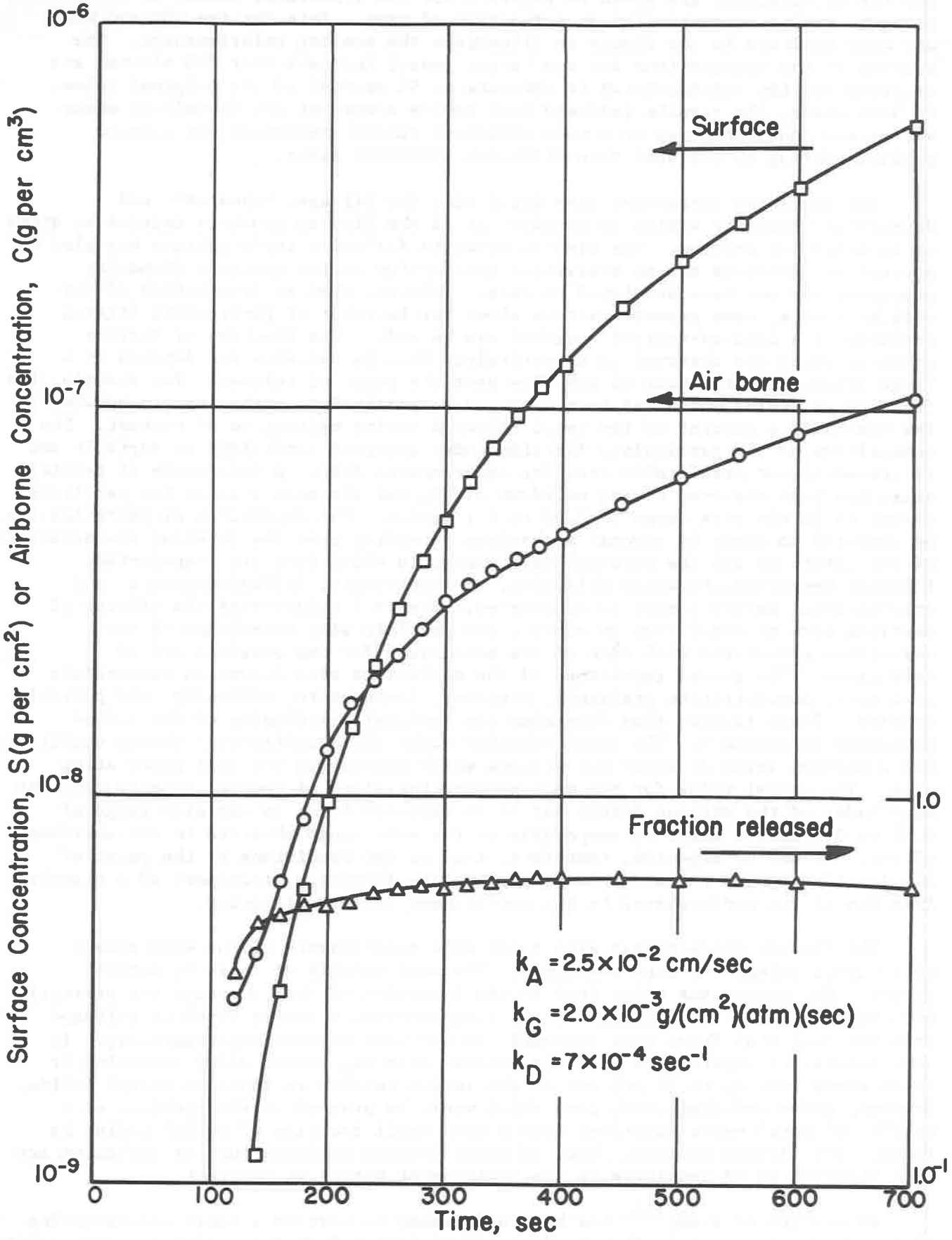


Figure 4. Iodine Distribution in Primary Vessel Plenum for Loft

for the model determined from analysis of ADF experimental results. The results for the calculations are given in Figure 5 for the fractional amount of the initial airborne iodine concentration as a function of time. Data for the ADF and NSPP are also included in the figure to illustrate the scaling relationships. The results of the calculations for the larger vessel indicate that 350 minutes are required for the concentration to decrease to 50 percent of its original value. In both cases, the results indicate that iodine transport and deposition under well-mixed conditions may be a more effective removal mechanism for fission products during an accident than diffusion processes alone.

The preceding paragraphs have dealt with the release, transport, and deposition processes during an accident as if the fission products existed as atoms or as molecular species. The fission products following their release may also be present as particles but an analytical description of the particle formation processes has not been developed to date. However, from an examination of the available data, some generalizations about the behavior of particulate fission products in a loss-of-coolant accident can be made. The fraction of fission products which are observed in a particulate form is variable and depends to a large extent upon the rate of gas flow past the point of release. For example, the fraction of iodine which has been observed as particulate matter ranges between a few tenths of a percent of the total released during melting to 50 percent. The composition of the particulate fraction under accident conditions is variable and is presently not predictable from the experimental data. A wide range of particle sizes has been observed during meltdown of $UO_2$ but the mean size of the particles formed is in the size range of 0.02 to 0.1 micron. The deposition of particles can be expected to occur by several mechanisms depending upon the physical characteristics of the particles and the physical environment in which they are transported. Inertial impaction, Brownian diffusion, thermophoresis, diffusiophoresis, and gravitational settling must be considered. Figure 6 illustrates the effects of particle size on deposition by showing the particle size dependence of the velocities associated with each of the mechanisms for one possible set of conditions. The actual importance of the mechanisms will depend on temperature gradients, concentration gradients, pressure, temperature, viscosity, and particle density. These factors then determine the vertical positioning of the curves presented in Figure 6. The total velocity under these arbitrarily chosen conditions has a minimum value at about 0.4 microns which represents the most penetrating size. The actual value for the most penetrating size, of course, depends upon the magnitudes of the various forces but it is expected to be in the size range of 0.05 to 0.5 micron which is comparable to the size range observed in the meltdown of $UO_2$. It may be expected, therefore, that if the conditions at the point of the fission product release promote particulate formation, transport of a sizable fraction of the particulates to the containment vessel will occur.

The fission products may also react with constituents of the environment after their release to form compounds. The most notable of these is methyl iodide. The mechanisms which lead to the formation of this compound are presently not understood and the fraction of the fission-product iodine which is released from the fuel that forms this compound is not well defined experimentally. In some laboratory experiments when the release from $UO_2$ occurs under oxidizing or inert conditions up to 10 percent of the iodine release is found as methyl iodide. However, under reducing conditions which would be present in the accident as a result of metal-water reactions only a very small fraction of methyl iodide is found. The various chemical forms of other fission products such as ruthenium are also expected to be sensitive to the environment during an accident.

An analytical study[22] has been undertaken to develop a basic understanding of the chemical processes that lead to methyl iodide formation under reactor accident conditions using thermodynamic and kinetic considerations. Typical iodine concentrations in reactor-accident environments were assumed to lie in the range

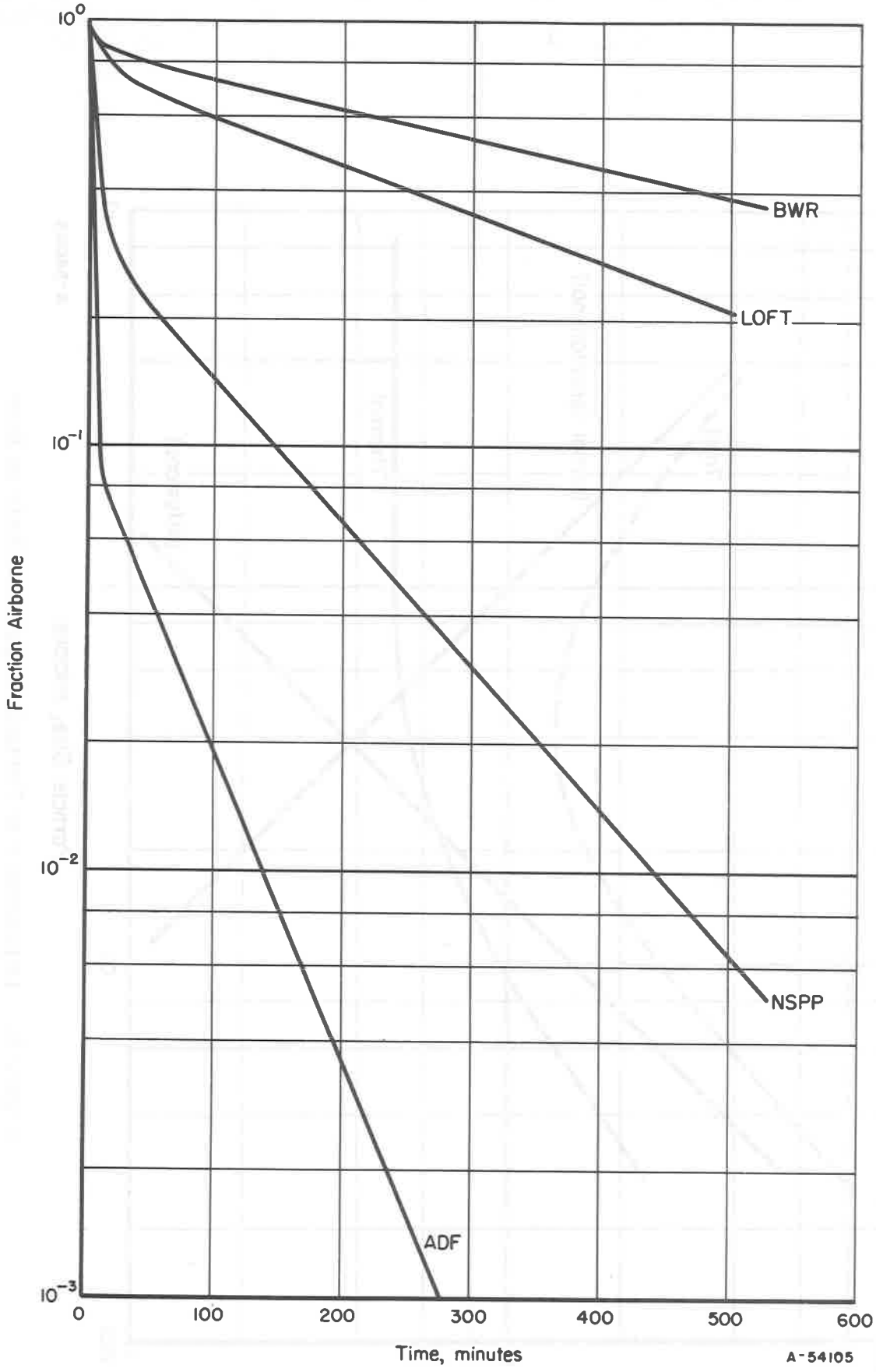


Figure 5. Iodine Distribution in Containment Vessels Based Upon a Wet-Wall, Well-Mixed Volume Model

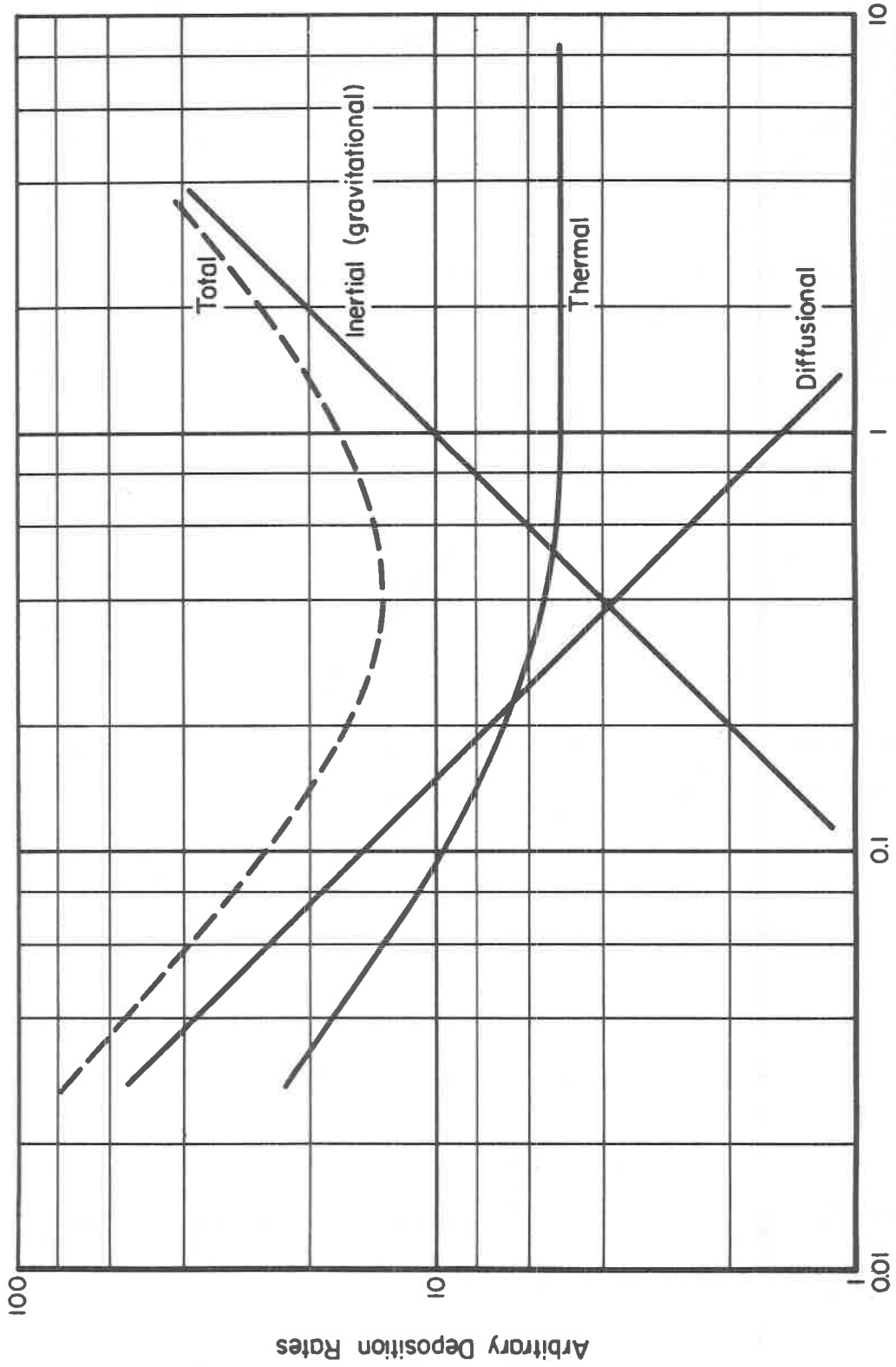


Figure 6. Dependence of Particle Deposition Rate on Size

of $10^{-4}$ to $10^{-9}$ g-moles/liter with as much as several percent of the iodine, in some cases, being in the form of $CH_3I$. For the thermodynamic studies, two different chemical equilibrium systems, one involving water-saturated air and the other steam with both systems containing small amounts of carbon and iodine, were considered. The species present were assumed to be CO, $H_2O$, $H_2$, $CO_2$, HI, $CH_4$, $CH_2O$, $CH_3OH$, $I_2$, $CH_3I$, and in some cases, solid carbon and their equilibrium concentrations were calculated at temperatures ranging from 300 to 1000 K at a pressure of 1 atm. The results show that if thermodynamic equilibrium exists, the $CH_3I$ concentration should be several orders of magnitude lower than actually observed, indicating that the kinetic aspects of $CH_3I$ formation are important. Only by suppressing the presence of certain species in the equilibrium system is it possible to reproduce the observed $CH_3I$ concentrations. It is apparent that further analytical studies of this nature corroborated by experimental results will be required to provide a description of the distribution of iodine and other fission products among non-elemental forms.

The current efforts to provide an overall analytical description of the distribution of fission products during a loss-of-coolant accident in a water-cooled reactor have yielded considerable insight into this complex area. Although a complete description of the distribution has not been developed to date, some of the areas which contribute to the overall analysis have been found to be amenable to analytical description and the necessary input parameters can be based upon existing experimental information. In other areas, there is a dearth of experimental data and an analytical description of the processes has not been formulated. This is especially true for the transport and deposition characteristics of fission products other than iodine in all parts of the reactor system and for iodine in the core and primary vessel plenum regions. Current experimental studies at various laboratories will be providing the additional data needed as input to the model and as data become available from the large scale engineering tests, a validation of the analytical approaches can be obtained.

## GAS COOLED REACTORS

The situation regarding the release and transport of fission products following a loss-of-coolant accident in a gas-cooled reactor is significantly different from that in a water-cooled reactor. The current design concepts for gas-cooled reactors in the United States employ coated uranium-thorium carbide particles dispersed in graphite as fuel. In the event of an accident the fission products are to a large extent retained by the particle coatings and the graphite. The coatings are high temperature materials and present a barrier to the release even under accident conditions. Not only do the intact coatings reduce the amount of fission product release but the mechanism of release from coated-particle fuel elements is different than the mechanism of release from metal-clad $UO_2$. The combination of these factors in a gas-cooled reactor accident produces a fission product release which has a chemical composition different than that for accidents in water-cooled reactors.

The analytical description for the distribution of fission products in these accidents requires the same type of information on the preaccident inventory of the fission products as required in the water-reactor description. This information could be supplied from the ISOGEN code previously described with the appropriate modifications to the nuclide library and the proper treatment of neutron energy spectrum effects on nuclear reaction rates. Input from an analysis of the loss-of-coolant transient in terms of blowdown forces on the core during blowdown, and from a heat transfer analysis following blowdown, is also needed. The former is not as essential as the latter since the operating pressure of the system and

the stored enthalpy in the coolant are not as great as they are in water reactors. However, since the major driving force for fission product release is the temperature rise in the system due to limited cooling, input from a detailed heat transfer analysis must be obtained. The NURLOC code could be used to generate these temperature data for a typical gas-cooled reactor. This analysis has not been performed, but temperature data during an accident for a gas-cooled reactor are available from the hazards analysis of the Peach Bottom Reactor[2]. The maximum temperature which is obtained in this core following the loss-of-coolant accident is 2300 C. Only 3 percent of the core exceeds 2200 C and the average temperature in the core for a period of 20 hours to 100 hours following the accident is 1540 C. The temperature distributions in a larger reactor would center around a higher value than in Peach Bottom but gross changes would not be expected since the volumetric power density in all similar gas-cooled reactors is low. Although the quantitative description of the distribution of fission products during an accident will vary with the temperature, some qualitative description can be formulated which will give an insight into the air cleaning problems which may be encountered.

Several processes must be considered in the description of the release, transport, and deposition of fission products in a gas-cooled reactor accident once the inventory and temperature inputs have been obtained. The release rates of the various fission products from the coated fuel particles must be known. Since the coated particles are dispersed in graphite to form the fuel elements, the transport rates of the fission products through graphite must also be considered. Some of the fission products will be sorbed on the graphite so adsorption in addition to diffusion through the matrix will control the release of the fission products from the fuel elements. From this point much of the description of the transport and deposition of fission products during an accident in a gas-cooled system is similar to a water-cooled reactor. Transport and removal mechanisms in the core and primary vessel must be considered. These processes are dependent upon the form and composition of the released fission products, the types of surfaces encountered, the temperatures in the system, and upon the gas flows available for transport. Within the containment building, transport and deposition will occur in a dry atmosphere so it will not be necessary to consider the effects of steam condensation and wet surfaces upon these processes.

A considerable amount of experimental data is available on the postirradiation release of fission products from pyrolytic carbon-coated fuel particles typical of those considered for gas-cooled reactor applications. The mechanisms governing the release are not completely understood but the process generally appears to be diffusion through the intact coating. The initial release rates (fraction released per hour) obtained by General Atomic for the BISO pyrolytic carbon-coated particles are illustrative of the releases as a function of temperature. Some of these data are given in Figure 7 for the BISO pyrolytic carbon-coated $(Th,U)O_2$ particles (Lot GA-2813-49E-4)[23,24] and the BISO pyrolytic carbon-coated $UC_2$ particles (Lot GA-2813-141E)[24]. Some of the differences in the release rates can be attributed to the differences in the fuel. It has also been observed at ORNL[25] that fission product release rates are lower for pyrolytic carbon-coated $UC_2$ and $(Th,U)C_2$ particles. Examination of these data reveals that the chemical composition of the fission products released from the fuels in gas-cooled reactor accidents is significantly different than the composition of the release products in water-cooled reactor accidents. The alkaline earths have the highest release rates from coated particles followed by the alkali metals. At the temperatures where comparative data are available, the release rates of iodine are a factor of $10^2$ to $10^3$ lower than the alkaline earths and the release rates for the rare gases are even lower. Thus, most of the hazards to be encountered in a gas-cooled reactor accident will be due to the alkaline earths and the alkali metals rather than the halogens and rare gases if release from the fuel particles alone is considered.

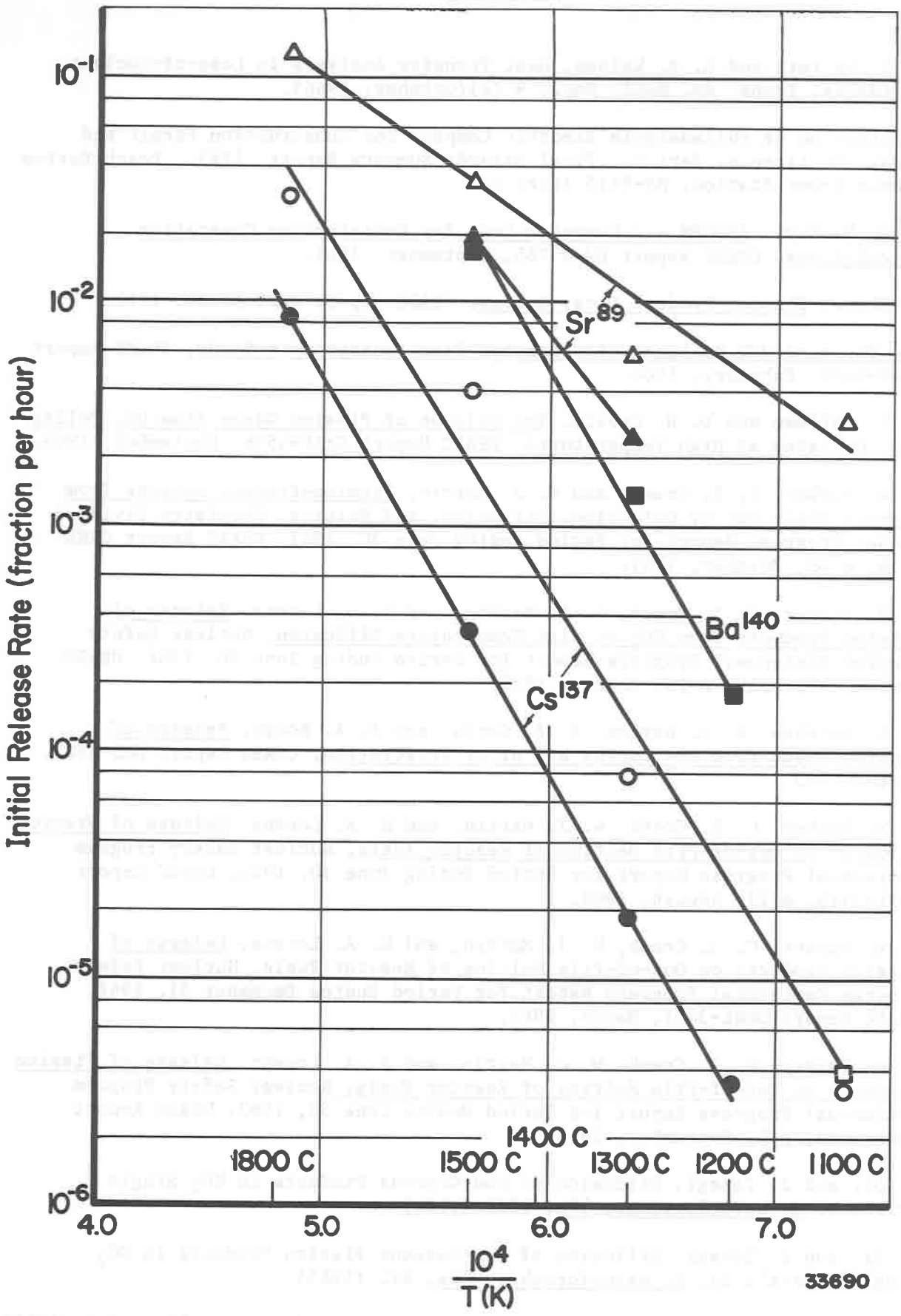


Figure 7. Release of Fission Products from Pyrolytic-Carbon-Coated Fuel Particles

## REFERENCES


1. C. T. Walters and G. E. Raines, Heat Transfer Analysis in Loss-of-Coolant Accidents, Trans. Am. Nucl. Soc., 9 (2)(October, 1966).

2. Application of Philadelphia Electric Company for Construction Permit and Class 104 License, Part C, Final Hazards Summary Report, 1963. Peach Bottom Atomic Power Station, NP-9115 (Part C).

3. H. H. VanTuyl, ISOGEN - A Computer Code for Radioisotope Generation Calculations, USAEC Report HW-83785, September, 1964.

4. K. Shure, Fission Product Decay Energy, USAEC Report WAPD-BT-24, 1961.

5. One Thousand MWE Boiling-Water Reactor Plant Feasibility Study, USAEC Report GEAP-4476, February, 1964.

6. J. P. Hoffman and D. H. Coplin, The Release of Fission Gases from $UO_2$ Pellet Fuel Operated at High Temperatures, USAEC Report GEAP-4596, September, 1964.

7. G. W. Parker, G. E. Creek, and W. J. Martin, Fission-Product Release from Reactor-Grade $UO_2$ by Oxidation, Diffusion, and Melting, Chemistry Division Annual Progress Report for Period Ending June 30, 1961, USAEC Report ORNL 3176, p 68, October, 1961.

8. G. W. Parker, G. E. Creek, W. J. Martin, and R. A. Lorenz, Release of Fission Products from $UO_2$ by High Temperature Diffusion, Nuclear Safety Program Semiannual Progress Report for Period Ending June 30, 1962, USAEC Report ORNL-3319, p 13, August, 1962.

9. J. B. Melehan, R. H. Barnes, J. E. Gates, and F. A. Rough, Release of Fission Gases from $UO_2$ During and After Irradiation, USAEC Report BMI-1623, March, 1963.

10. G. W. Parker, G. E. Creek, W. J. Martin, and R. A. Lorenz, Release of Fission Products on Out-of-Pile Melting of Reactor Fuels, Nuclear Safety Program Semiannual Progress Report for Period Ending June 30, 1962, USAEC Report ORNL-3319, p 11, August, 1962.

11. G. W. Parker, G. E. Creek, W. J. Martin, and R. A. Lorenz, Release of Fission Products on Out-of-Pile Melting of Reactor Fuels, Nuclear Safety Program Semiannual Progress Report for Period Ending December 31, 1962, USAEC Report ORNL-3401, March, 1963.

12. G. W. Parker, G. E. Creek, W. J. Martin, and R. A. Lorenz, Release of Fission Products on Out-of-Pile Melting of Reactor Fuels, Nuclear Safety Program Semiannual Progress Report for Period Ending June 30, 1963, USAEC Report ORNL-3483, p 9, September, 1963.

13. N. Oi, and J. Takagi, Diffusion of Non-Gaseous Products in $UO_2$ Single Crystals, Z. Naturforschg., 19a, 1331 (1964).

14. N. Oi, and J. Takagi, Diffusion of Non-Gaseous Fission Products in $UO_2$ Single Crystals II, Z. Naturforschg., 20a, 673 (1965).

15. N. Oi, Xe Diffusion in $UO_2$ Single Crystals, Z. Naturforschg., 20a, 1566 (1965).

16. J. Takagi, Evaporation Behavior of Non-Gaseous Fission Products from $UO_2$, Z. Naturforschg., 20a, 1566 (1965).

17. T. S. Kress and F. H. Neill, A Model for Fission Product Transport and Deposition Under Isothermal Conditions, USAEC Report ORNL-TM-1274, October, 1965.

18. J. B. Morris and B. Nicholls, The Deposition of Iodine Vapor on Surfaces, British Report AERE-R-4502, March, 1965.

19. C. J. Barton, G. E. Creek, R. A. Lorenz, W. J. Martin, and G. W. Parker, Behavior of Fission Products Released from High-Burnup $UO_2$ in the Containment Mockup Facility, Nuclear Safety Program Semiannual Progress Report for Period Ending Decamber 31, 1965, USAEC Report ORNL-3915, pp 27-37, March, 1966.

20. A. C. Chamberlain, A. E. J. Eggleton, W. J. Megaw, and J. B. Morris, Physical Chemistry of Iodine and Removal of Iodine from Gas Streams, Reactor Science and Technology (Journal of Nuclear Energy Parts A/B), 17, 519 (1963).

21. J. L. Wantland, Theoretical Diffusion Studies, Nuclear Safety Progress Report for Period Ending June 30, 1965, USAEC Report ORNL-3843, pp 117-123, Sept., 1965.

22. R. H. Barnes, J. F. Kircher, and C. W. Townley, Thermodynamic and Kinetic Studies of Methyl Iodide Formation in Nuclear Reactor Accident Environments, Paper presented at the 152nd Meeting of the American Chemical Society, September, 1966.

23. W. V. Goeddel, J. C. Bokras, H. K. Lonsdale, C. S. Luby, and L. R. Zumwalt, Coated-Particle Fuels Research at General Atomic from October 30, 1964 through April 30, 1965, USAEC Report GAMD-6344, April, 1965.

24. W. V. Goeddel, C. S. Luby, and L. R. Zumwalt, Coated-Particle Fuels Research at General Atomic From April 30, 1965 through October 30, 1965, USAEC Report GAMD-6817, Part I, November, 1965.

25. Gas-Cooled Reactor Program Semiannual Progress Report for Period Ending March 31, 1965, USAEC Report ORNL-3807, June, 1965.

26. Public Service Company of Colorado 330-MW(E) High-Temperature Gas-Cooled Reactor Research and Development Program, Quarterly Progress Report for the Period Ending December 31, 1965, March, 1966.

27. E. E. Anderson, and L. R. Zumwalt, Trans. ANS, 7, 451 (1964).

28. TARGET, A Program for a 1000-MW(E) High-Temperature Gas-Cooled Reactor, Quarterly Progress Report for the Period Ending May 31, 1965, USAEC Report GA-6418, June, 1965.

## DISCUSSION

LIEBERMAN: That was a very good introduction to this conference in addition to being a rather well-developed analytical approach to this whole problem of an understanding of the nature and behavior of fission products relating from a nuclear accident. I would emphasize that we are talking here, now, at least in terms of the presentation, to the consequences of an accident if it should occur, and this is something we want to keep in mind during the course of the conference with the developments in the application of nuclear energy to central station electrical generation.

# CHARACTERIZATION OF SOURCE TERMS FOR AEROSOL TRANSPORT DURING SODIUM FIRES*

by

G. N. Lauben
C. L. Larson

Atomics International
A Division of North American Aviation, Inc.

## ABSTRACT

The sources, consequences and radiological considerations resulting from a postulated spill in a reactor system are studied as they relate to aerosol transport. The heat and mass transfer processes and system variables are discussed. Analytical approaches are discussed with an example involving a semi-empirical accident model which includes gas buoyancy considerations. The current experimental systems and recent early results are described.

## INTRODUCTION

Vaporization from the liquid sodium pool, which would result from a postulated primary coolant spill in a sodium-cooled, nuclear power plant, provides the material source term for aerosol transport. The vapor may react in the gas phase or simply condense forming aerosols of sodium and sodium oxides, and possibly fission products in combination with or separate from the sodium product aerosols. The energy sources are supplied by the gas phase sodium combustion reaction and condensation, by possible heterogeneous surface oxidation, and from the sensible heat of the hot liquid.

As a consequence of the mass and energy release, the system may become pressurized by heating of the atmosphere. Heating and thermal stresses in the structure may also occur. Generation of convective currents needed for aerosol transport and the actual transport of radioactivity associated with the aerosols constitute the major consequence. Possible compromise of the containment must also be considered.

In a sodium-cooled, fast breeder reactor, sodium-24 (from neutron activation), plutonium-bearing fuel material, and associated fission products which may be present during certain primary coolant accidents are a potential radiological safety problem. In a core using vented fuel elements, volatile fission products such as iodine may enter the coolant and be available for release from a sodium spill. Several AEC-sponsored projects have investigated the release of fission products into sodium coolant.[1,2] Previous investigations have shown that iodine combines chemically with the coolant to form sodium iodide.

* Work performed for the U. S. Atomic Energy Commission under Contract AT(11-1)-GEN-8.

The distribution of volatile fission products such as iodine and cesium (a product of noble gas decay) between liquid sodium and an inert cover gas is currently under study on another project.[3] The release of iodine during sodium vaporization and combustion has been measured during a large sodium fire experiment and some of these results are presented later. Detailed characterization of the sodium aerosols and iodine released from a sodium fire is being investigated[4] under the overall sodium fires program at Atomics International.

Although there have been several earlier investigations of sodium fires, the results have shown wide scatter. This is at least partly due to the different conditions under which tests were conducted. The present program at Atomics International is directed toward identifying the important variables in the sodium vaporization and combustion processes and quantitatively determining the effect of these variables on burning rate and aerosol release rate.

## COMBUSTION CONSIDERATIONS

Several alternate paths exist for energy transfer from a pool of spilled sodium. These, together with the possible heat sources and sinks, are shown in Figure 1. The sensible heat of gas always acts as a sink whereas the gas phase reaction, surface reaction, and condensation are always heat sources. Since heat is always required for vaporization, it is a sink. The sensible heat of the liquid could act as source or sink depending on the thermal gradient near the surface. The four curves adjacent to the diagram represent temperature profiles from just below the sodium surface to the gas-particle cloud above the gas phase reaction zone. The profile representing the case under consideration depends upon the relative intensity of the sources and sinks. The numbers associated with each transport path correspond to the temperature profiles. Heat transfer to and from walls and containers has been neglected for simplicity. Under certain cases of low oxygen concentration or high surface temperature the surface reaction may be absent or negligible. This is the case with most non-metallic liquids.[5] In such instances the temperature distribution is like curve 4 and heat transfer parts are A, B, E, and F. Figure 2 depicts the paths for sodium transfer from the pool. In an evnironment with any appreciable oxygen (21%). Path A has not been observed and oxidation of Na vapor will occur exclusively. Path B will not occur in zero oxygen environments, but significant sodium fume is generated. In such a case the energy paths in Figure 1 are B, D, and H.

In the study of matter and energy release from a sodium pool, an element of gas is viewed in terms of the potentials present for mass and energy transport. Heat is transferred to or from the gas volume by conduction and radiation (from particles), based on temperatures of the gas and its surroundings, and by convection or local gas flow. The high surface-to-mass ratio of airborne particles assures that they will be at nearly the same temperature as the gas. Heat is liberated within the volume by the Na-$O_2$ reaction and by condensation of Na vapor. Sodium and oxygen molecules enter and leave the volume by diffusion and gas flow, and both are removed from the gas phase by the oxidation reaction. Sodium vapor is also "removed" by condensation.

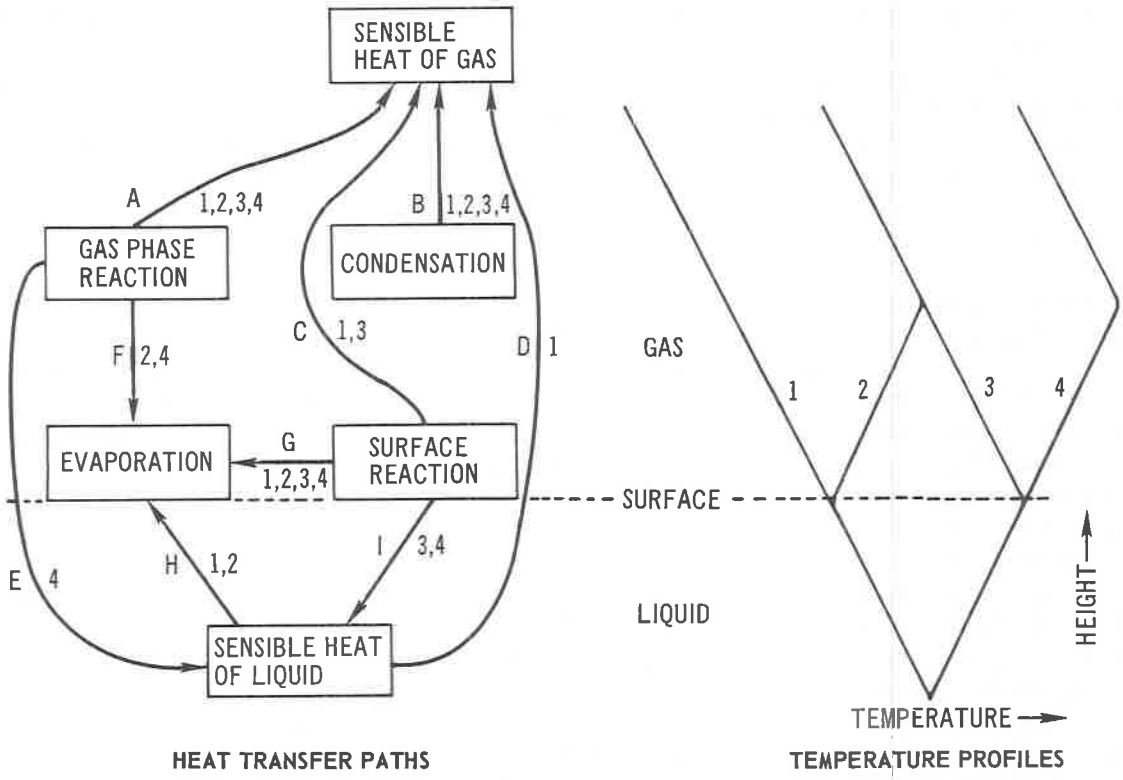


**Figure 1. Reaction Region Heat Transfer**

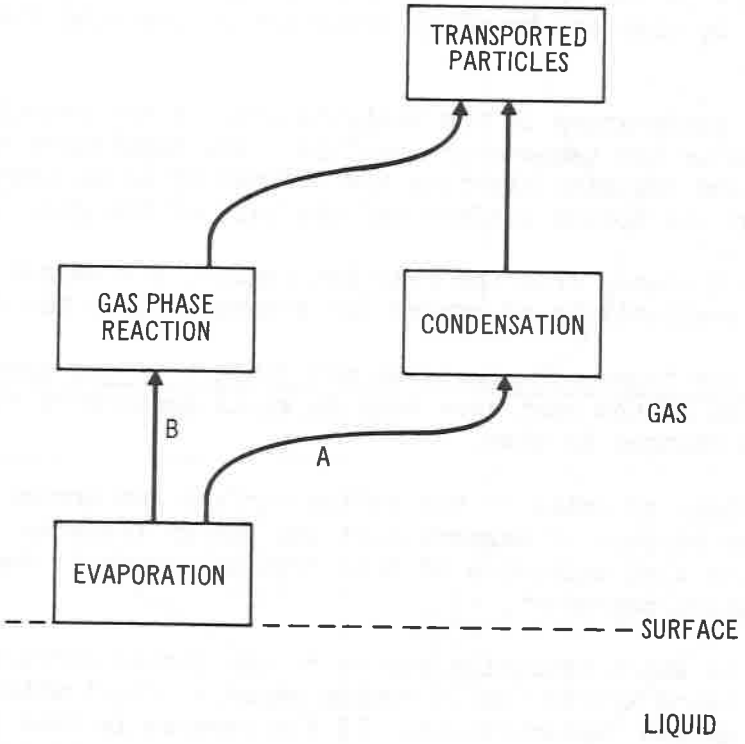


Figure 2. Reaction Region Matter Transfer

A preliminary, general analytical model was developed to describe energy transport during an accident involving a large sodium fire, using semi-empirical expressions for all processes in the reactor system. The resulting linear equations have been programmed in a SOFIRE accident code which includes the important gas bouyancy consideration for natural convection.

The low flame of the sodium pool fire tends to create a region of high temperature gas plus combustion products just above the sodium. The presence of cooler, heavier gas well above the flame establishes buoyancy forces which remove the hot gases from the flame by updrafts while cooler gases flow down toward the flame. A calculation of the vertical steady-state flow rates can be made readily for a simplified two-compartment model. Figure 4 shows the geometry under consideration, chosen to be typical of many sodium fire experiments. A volume of gas equivalent to the volume of gas in the burn pot, $V_1$, is assumed to be homogeneous in composition and temperature ($C_1$,$\rho_1$, $T_1$), and the remainder of the gas in the system is assumed to occupy volume $V_2$ with average properties $C_2$,$\rho_2$, and $T_2$.

The buoyancy pressure available to accelerate the hot gas upward from the sodium to the top of the pot is

$$\Delta P = (\rho_2 - \rho_1)Z \quad , \qquad \ldots(1)$$

where P is pressure in $lb/ft^2$, $\rho$ is density in $lb/ft^3$, and Z is height in feet. It is assumed that the pressure drop represents potential energy which is converted to gas kinetic energy by the following relation:

$$\Delta P = (\rho_2 - \rho_1)Z = \frac{\rho_1 v_1^2}{2g} \quad , \qquad \ldots(2)$$

where $v_1$ is the gas velocity in ft/hr and g is the acceleration of gravity in $ft/hr^2$.[1] Equation 2 can be solved for $v_1$ in terms of Z and gas densities:

$$v_1 = 28{,}900\sqrt{\frac{Z(\rho_2 - \rho_1)}{\rho_1}}\ \text{ft/hr} \quad . \qquad \ldots(3)$$

The problem is greatly simplified by the assumption that one-half the burnpot cross-section area is available for upflow, $F_1$ $ft^3/hr$, and one-half for downflow, $F_2$ $ft^3/hr$. Also, the heat carried away by the gas flow in a well insulated system is the net heat of combustion of liquid sodium, 3880 Btu/lb, and the system operates at a constant pressure of 1 atm with sufficient mixing so that the oxygen:nitrogen ratio is the same in $V_1$ and $V_2$. Heat and mass balances on the gas in $V_1$ result in

$$\frac{F_1}{A_o} = \frac{16{,}170\,R}{39.8\left(1 - \frac{T_2}{T_1}\right)} = 14{,}450\sqrt{Z\left(\frac{T_1}{T_2} - 1\right)} \quad , \qquad \ldots(4)$$

and

$$F_2 = F_1\rho_1/\rho_2 = F_1T_2/T_1 \quad , \qquad \ldots(5)$$

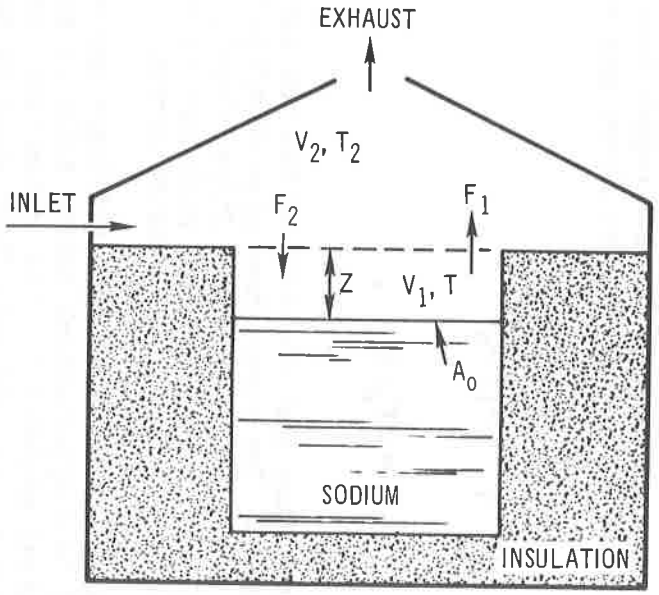


$A_0$ = FIRE AREA ($ft^2$)

$F_1$ = HOT GAS UPFLOW ($ft^3/hr$)

$F_2$ = COLD GAS DOWNFLOW ($ft^3/hr$)

T = HOT GAS TEMPERATURE ($^0R$)

$T_2$ = COLD GAS TEMPERATURE ($^0R$)

$V_1$ = HOT GAS VOLUME ($ft^3$)

$V_2$ = COLD GAS VOLUME ($ft^3$)

$Z_c$ = HEIGHT OF $V_1$ (ft)

Figure 4 Typical Sodium Fire Test Arrangement and Nomenclature

where R is the burning rate, lb Na/hr-ft$^2$, $C_p$ = 0.24 Btu/lb gas-°F, atmospheric conditions are 0.075 lb gas/ft$^3$ at 530°R, the perfect gas law is assumed, and second-order terms are neglected.

For numerical calculations, it is assumed that R is proportional to $C_1$ (or $1/T_1$) as discussed above for small fires at low oxygen concentrations, that the burning rate[6] is 6.0 lb/hr-ft$^2$ in air at 500°F, and the free height of the pot above the sodium is 0.5 ft. Equation 4 for a fire in air reduces to

$$T_1\left(1 - \frac{T_2}{T_1}\right)\sqrt{\frac{T_1}{T_2} - 1} = 229 \quad . \qquad \ldots(6)$$

From Equation 9, we can obtain $T_2$ as a function of $T_1$, and using Equations 4 and 5, obtain $F_1/A_o$ and $F_2/A_o$ vs $T_1$. Values of $F_1/A_o$ and $F_2/A_o$ are plotted vs $T_1$ in Figure 2, and it is apparent that these velocities are not very dependent upon the actual temperature level. The actual temperatures could be determined by a heat balance on the gas in $V_2$, but this is not necessary to learn the general magnitude of velocities resulting from buoyancy forces.

Similar analysis for an atmosphere of 4 vol % oxygen results in lower gas velocities which are also shown in Figure 5. The linear gas velocities will be given by

$$v_1 = 2F_1/A_o \qquad \ldots(7)$$

and

$$v_2 = 2F_2/A_o \quad , \qquad \ldots(8)$$

because of the earlier assumption that one-half of the pot surface area is for upflow, one-half for downflow. The cases shown give downflow velocities 2 ft/sec and upflow ~ 2 ft/sec (4% $O_2$) and ~ 4 ft/sec (air). Any airborne particulates, such as $Na_2O$ combustion products, will tend to rise with $F_1$ into $V_2$, and settle there, plate out, or enter the exhaust stream.

The concept of buoyancy forces creating significant gas velocities near the flame can be extended to a hypothetical sodium spill in an open reactor primary sodium cell. Typical geometry for the system under consideration is shown in Figure 6. In such a fire, the cell floor would be covered with sodium, which would burn with the air in $V_1$. After an initial rapid transient in which all gas flow was away from the fire, buoyancy forces would create a "counterflow" of gases in the cell access opening. Thus, building gases would replenish oxygen in the cell and promote the burning. A digital computer code, SOFIRE, has been developed at Atomics International for analyzing this problem. The code takes into account heat transfer rates to the cell floor and walls and to building walls. It allows for building gas inleakage ($F_3$) and exhaust ($F_4$), and can be used for constant pressure or for containment pressurization fires.

In a SOFIRE calculation of fire conditions in a fast breeder reactor plant, the gas velocities in the cell opening were on the order of 15 ft/sec upward and 12 ft/sec downward. For the geometry considered, the cell floor area was 288 $ft^2$, while the access opening was 72 $ft^2$. These velocities were high enough that the $O_2$:$N_2$ ratios in $V_1$ and $V_2$ were within 3% throughout the fire.

The influence of the above gas velocities on aerosol transport during a sodium fire has not been analyzed. It is clear, however, that gas movement will be rapid enough to allow an appreciable fraction of airborne sodium oxide to be carried from a fire in an open cell to the room above that cell.

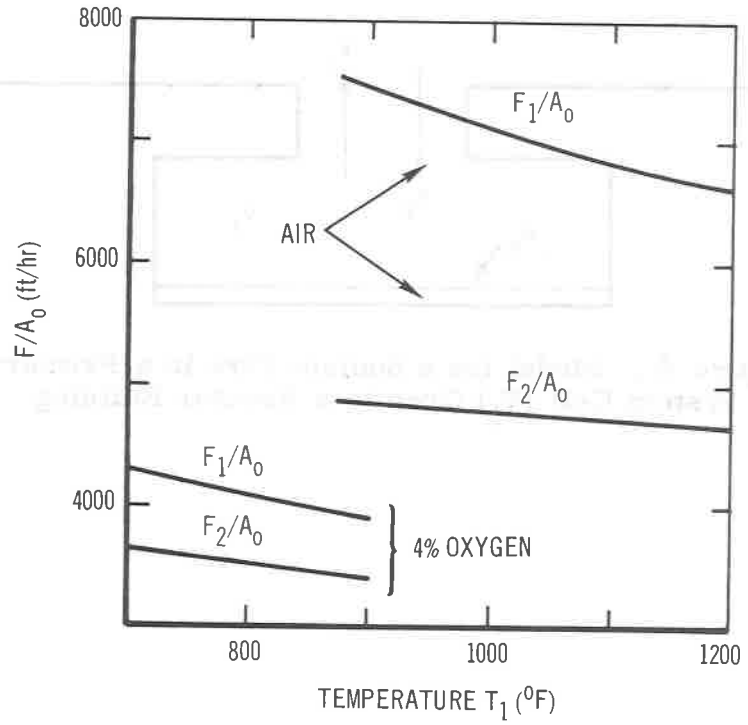


Figure 5. Calculated Gas Flow Rates for Sodium Fire Tests in Air and 4% Oxygen Atmosphere (Geometry in Figure 4)

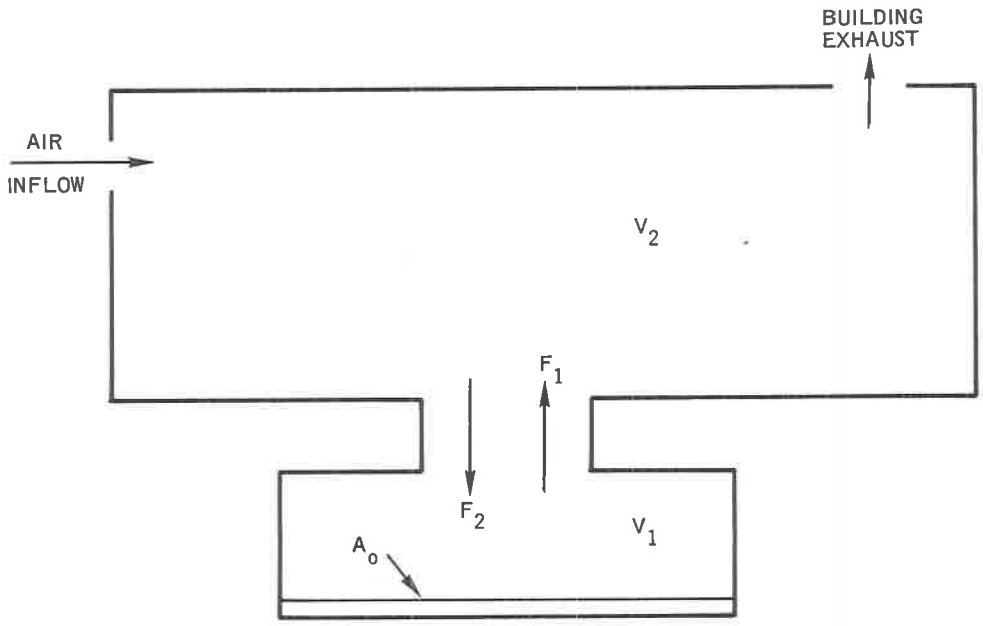


Figure 6 . Model for a Sodium Fire in a Primary System Cell ($V_1$) Open to a Reactor Building

## EXPERIMENTAL INVESTIGATIONS

A detailed experimental program is being conducted at Atomics International to assist in properly characterizing matter and energy release source terms following a sodium fire. The experimental results are integrated with analytical studies to provide the most useful model for predicting consequences of postulated accidents and modeling experiments which simulate accidental sodium spills.

In postulated accidents or accident modeling experiments, large transients may occur before any relative stability occurs. It has been observed that the most significant release of matter and energy can occur during these early transients. The "fundamental fires" experiments are designed to reach equilibrium fairly rapidly and to reflect the important conditions that might be expected throughout the duration of an accident. In order to achieve and maintain equilibrium conditions and aid in making release measurements, a forced flow of gas was maintained throughout the experiments. The influence of this artificial, induced flow and the more restrictive geometries of the fundamental experiments must always be taken into account when applying results to an actual accident.

Three similar apparatus have been used to study sodium pool combustion fundamentals. The large fires apparatus has an enclosed gas volume of 40 $ft^3$. The chamber can accommodate burn pots up to 5 ft in diameter and 4-1/2 ft high, although only 2-ft diameter pots have been used for sodium fires to date. Figures 7 and 8 show the large apparatus as recently installed in the Sodium Fires Test Installation. The initial small fires apparatus (Mark I) had a gas space of 0.1 $ft^3$ and used 4-in.-diameter by 8-in.-deep pots. A modified small fires apparatus (Mark II) has a gas volume of 12 $ft^3$ and accommodates burn pots up to 8 in. in diameter. Only 4-in. pots have been used thus far. The Mark II apparatus uses a glove box for the gas volume, and this has been very valuable to the understanding of the nature of sodium burning because it permits visual observation of fires under various conditions. A photograph and schematic flow diagram of the Mark II apparatus is shown in Figures 9 and 10. All three systems meter and mix the inlet air and nitrogen so that oxygen concentration can be varied from 0 to 21%. Flowmeters and oxygen analyzers monitor the inlet and outlet gas flow. The effluent gas is washed in wet scrubbing systems and samples are taken or solution conductivity measured to monitor the smoke release rate. Thermocouples measure temperatures throughout each system to aid in measuring energy release. Pool temperatures are maintained with controlled electric heaters. Gas temperature can be controlled in the large apparatus with an electric heater.

A large modeling experimental installation is being planned for simulating actual sodium spill accidents. It will provide large scale validation of accident models developed from equilibrium data. The gas volume here would be at least 5,000 $ft^3$. All existing auxiliary equipment, e.g. inlet and outlet gas systems and instrumentation including a 300-channel data logger are available for this facility.

Several experiments of various sizes have been conducted with induced air flow (21% oxygen).[6] In these experiments, combustion was initiated at sodium temperatures between 350 and 1000°F. During the initial periods (1/4 to 3 hr),

Figure 7. Large Fires Experiment

Figure 8. Large Fires Experiment - Outdoor Equipment

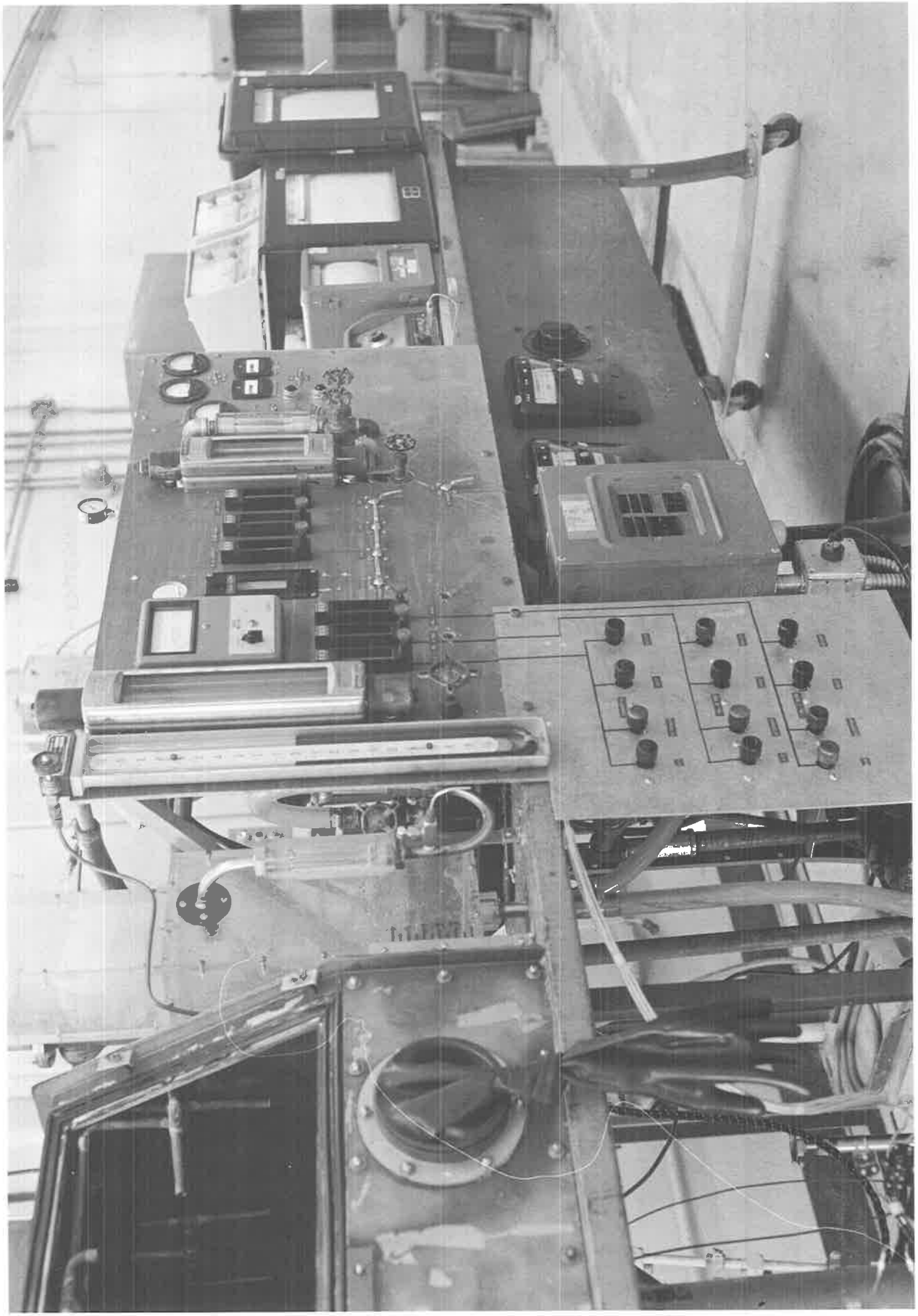

Figure 9. Mark II - Small Fires Apparatus

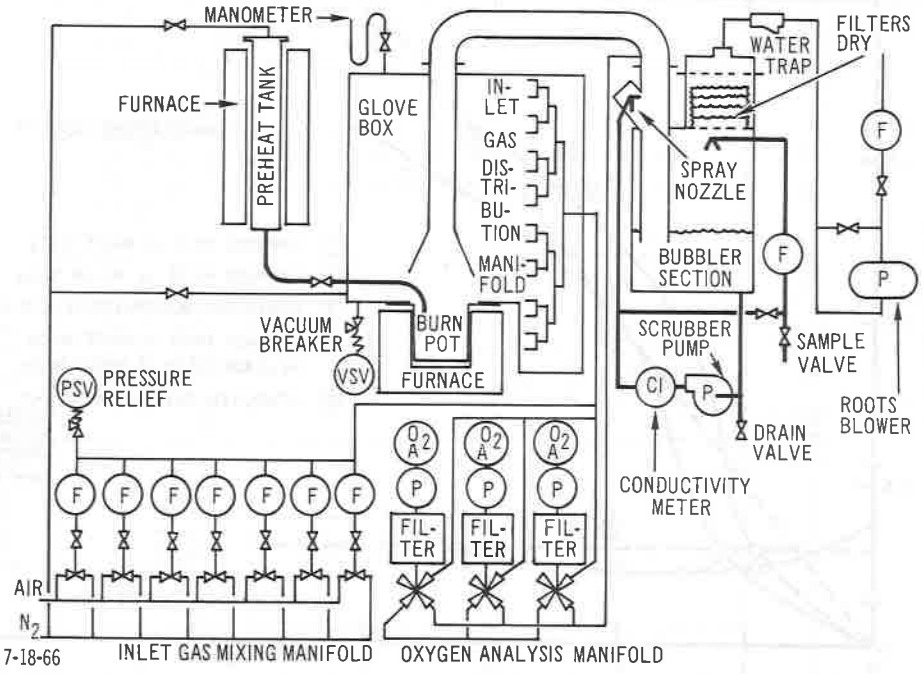


Figure 10 Schematic Flow Diagram of Mark II Small Fires Experiment

when the surface temperatures were below 1225°F, the sodium burned on the nodular, oxidized surface at the rate of about 9 lb/hr-ft$^2$. After the higher temperature was reached, the oxide buildup disappeared and the rates diminished to between 4 and 7 lb/hr-ft$^2$. The sodium release rates to the cleaning systems varied between 1.5 and 4.5 lb/hr-ft$^2$, being strongly dependent on the proximity and magnitude of the induced air velocities over the pool surface. Poorly insulated experiments were extinguished as temperatures dropped due to heat dissipation. Those with good insulation lasted until the oxide which had sunk to the pool bottom eventually built up to meet the falling liquid level. The most important experiment of all the "air" fires was the so-called first fire (LF-1) conducted in the Large Fires apparatus. The inclusion of oxygen analysis equipment, large wet scrubber and metered exhaust system allowed considerably better quantitative results than was previously possible. I-131 was seeded into the sodium and results showed that at 1300°F, the released phase iodine concentration was 1/2 that in the sodium pool. A large hole formed in the side of the pot which necessitated a series of metallurgical experiments. These results showed that sodium peroxide is the corrosive agent and that carbon steel is less susceptible than stainless steel to its effect.

A series of runs was made in the large apparatus maintaining a surface temperature at 1000°F and using inlet gas oxygen concentrations of 0, 1, 2, and 4% at low gas flows (12 to 20 scfm) and high gas flows (200 scfm).(7) Zero oxygen runs showed that a considerable amount of heat and sodium are released without combustion and that heat release must include contributions from surface radiations, convection, and evaporation. The combustion rate appeared to be nearly linear with oxygen concentration, ranging from 0.3 lb/hr-ft$^2$ at 1% oxygen to 1.6 lb/hr-ft$^2$ at 4% oxygen. The release rate to the scrubber system showed a dependence upon sodium temperature and gas flow without an apparent relationship to oxygen concentration. The burning and sodium release results are shown in Figure 11. The results, including the iodine release, are given in Table 1. The liquid pools were seeded with I-131 in both of the large fires using normal air and gas depleted in oxygen. On the basis of limited data, the iodine release fraction did not appear to depend on oxygen concentration, but apparently was a function of surface temperature. At 1300°F, the released sodium was about one-half as concentrated in iodine as was the sodium pool; at 1000°F, the released phase sodium was about one-fifth as concentrated as the pool sodium.

Several tests were performed in the Mark I small fires apparatus at sodium temperatures from 1000 to 1300°F, gas flows from 0.035 to 1.41 scfm, and oxygen concentrations from 0 to 4%. In these tests, considerable difficulty was encountered in obtaining reproducible results due to increased buildup of oxide when making several runs with the same batch. Some of the tests which were not affected too severely in this manner yielded results that were comparable with the larger experiments for burning and release rate per unit area. The sodium temperature dependence of aerosol release inferred from the large experiment (Table 1) was not as strong in the smaller size experiments.

The Mark II small fires experiment is being used to determine and utilize the proper techniques for maintaining reasonably constant pool surface areas that are free from extraneous, geometry-dependent effects. The so-called creeping of oxide and sodium on the burn pot walls which was observed contribute significantly to the release of considerable mass and energy. Since it is

a perimeter effect, it would likely be less important at larger diameters. The atmosphere into which the sodium is charged during the start of an experiment has a strong influence on the creeping rate and consequently the mass and energy release rates. Experiments have shown that buildup of this material on the pot wall can be significantly suppressed in 4-inch burn pots during the initial 30 minutes or so, to provide meaningful data, by initiating a test in the particular oxidizing atmosphere to be studied. Various techniques for extending the period of time for operation with insignificant wall buildup are being evaluated in order to extend the capability and value of the "small fires" concept.

## CONCLUSIONS

The following conclusions which are important and applicable to sodium spill accident consideration can be drawn from the studies conducted to date:

1) Combustion of sodium occurs if any oxygen is present and the rate is proportional to oxygen concentration at low concentrations for sodium temperatures near 1000°F.

2) Burning rates in air have not exceeded 10 lbs/hr-ft$^2$ over a wide range of experimental variations of geometry, temperature, and induced air flow.

3) Sodium fires can be self-extinguishing by heat dissipation in favorable environments because of high thermal conductivity and heat of vaporization, and steep thermal gradients.

4) The released phase in a sodium fire is apparently not enriched or significantly reduced in iodine concentration compared to the liquid.

5) Heat and sodium fume are released down to 0% oxygen. Heat transfer from the liquid should be considered at any oxygen concentration.

GREENFIELD: I wonder if I can address a question to Dr. Morrison similar to the prior question about the most penetrating particle. Is it really possible to characterize it without discussing the geometry of the system which, in turn, might have an effect on the lifetime particle, hence, influence its possible growth by a conglomeration or fallout or plating, that is to say, can you really characterize it without these other parameters being considered?

LIEBERMAN: I might also add to this. I don't know what useful purpose it serves to attempt to characterize it in any specific sense because it depends on the situation.

MORRISON: I think we tend to agree with the fact you can't characterize it until you talk about the specific case, but you can say that about anything that we presented here. You cannot characterize the whole accident unless you designate where the break in the primary system is and what the course of the accident is. This is the size range we are talking about. We aren't talking about real large particles or real small particles. This is the thing we should worry about here.

LAWROWSKI: Do you plan sometime in the near future to include plutonium in some of your calculations? Or have you already?

MORRISON: We haven't included it in any of our release or transport calculations to date. The equations are general enough that we can add it in the future. We do plan to do it, but we haven't as yet.

HILLIARD: I would like to address a question to Dr. Morrison. I think the answer may be similar to that given to Dr. Greenfield's question. In your slide showing the fraction of iodine released to containment, which leveled off at about one percent, you selected certain transport values. Did you repeat this calculation with other selected values and, if so, can you give us an idea of the range obtained, compared to the one percent result?

MORRISON: I can't give you an idea of the actual values we used; we can go back to the data in the calculations and find out what they were, but I think I can sum up by saying we did vary $k_A$, the adsorption coefficient, and $k_D$, the desorption coefficient, by several orders of magnitude. These are not the controlling factors in this particular calculation.

As it turns out, probably the overriding factor in this whole analysis is the steam flow rate through the system. This was calculated from the same boil-off model we used in our metal-water reaction calculations. This very low Q in the equations we had is rate controlling. The release depends more strongly on the flow rate than anything else in the calculation.

HILLIARD: I think the point I was trying to get across is that we shouldn't establish the feeling here that only about one percent gets out into the containment vessel, but that it can range from low on up, perhaps to high fractions, depending on what values are put into the transport equations.

LIEBERMAN: As I understood the answer, it was not very sensitive to the coefficient used but more sensitive to the steam flow rate.

HILLIARD: What value of Q was used?

MORRISON: We think the Q value is a realistic number to a factor of two or three. I don't think there is an order of magnitude uncertainty here. The conclusion I would like to leave is not so much the percentage released but the time scale involved. We are talking 10 minutes; we aren't talking 10 seconds. With this sort of delay time, we can do something about the accident situation.

HILLARY: When Dr. Morrison was discussing the removal of iodine and the containment, I think, he referred to the application for iodine removal. Did he take into account the deviations from Henry's Law which occur at low concentrations where the iodine tends to become ionized in the water?

MORRISON: Yes, we did. The value of Henry's Law Coefficient, I think, was something of the order of $10^{-4}$. If you don't take into consideration this hydrolysis reaction that occurs at low concentrations, you get a value of around $10^{-2}$. It was taken into consideration somewhat indirectly in that the value was allowed to vary to obtain the best fit to the ADF data. Whatever value was typical of the steam conditions in that system was carried through in the calculations for the other ones. We also made some parametric variation of Henry's Law Coefficient in our calculations.

LIEBERMAN: Can you comment on how sensitive your results would be to that kind of variation?

MORRISON: It isn't terribly sensitive to that kind of variation. With either extreme value the liquid film could take up all the iodine presented to it. There is probably more uncertainty in the volume of liquid film which we used by assuming a certain thickness.

# IN PILE STUDIES OF CONTAMINATION RELEASED IN CO 2 GAS COOLED REACTORS

by

J.DADILLON[1]

## ABSTRACT

Experiments have been made using an in-pile loop in which UO2 fuel elements with clad failure were irradiated.

In these studies, we were essentially interested in the iodine and its compounds.

The volume of the loop was 1m3 and was filled with CO2 gas at a pressure of 60 Kg/cm2.

The iodine concentration at the sampling point varied from 4 to 34 $\mu$Ci/m3 (atm.pres.).

The filter packs used for sampling were composed of an asbestos paper, a knit-mesh (silver-plated copper wool), a charcoal-impregnated paper, five 1 cm thick charcoal beds and a final 5 cm charcoal bed maintained at temperature of -40°C.

We have been able to show off the main following results :

1 - there were at least two iodine compounds in the loop with different behavior in charcoal.

2 - the efficiency of 5 cm charcoal for the compounds or the forms which have not been trapped by the impregnated paper or the knit-mesh was about 99%.

3 - the charcoal impregnated paper trapped from 3 to 13% of the total activity.

4 - only about 1% of iodine generally remained in the knit-mesh.

---

1) Commissariat a l'Energie Atomique - Service d'Etudes de Sureté Radiologique - CADARACHE - FRANCE -

## INTRODUCTION

We used different usual filtering elements, trying to show off iodine compounds which could appear inside the CO2 gas loop where UO2 fuel element was irradiated, with a clad failure.

This fuel element was an EL4 element composed of twelve sticks of natural UO2, weighing 575 Gr., with beryllium cladding.

At the time of sampling, its burn-up was about 3000 MWd/ton.

During irradiation, the clad temperature was nearly 600°C.

Our design was to obtain some information concerning the trapping of iodine and the compounds which can be released in the event of an accident occuring in CO2 gas cooled reactors.

## DESCRIPTION OF THE EXPERIMENTAL DEVICES -

The loop (fig.1) was layed in the swimming pool reactor PEGASE in CADARACHE.

The part containing the fuel could be placed at different distances from the core.

The total volume of this loop was 1m3, the pressure of the CO2 being 60 Kg/cm2.

The circulation of the CO2 was made by a compressor with oil transmission, which caused the release of oil traces inside the loop. Therefore it is likely that hydrocarboned radicals have appeared which could have formed some organic compounds whith iodine.

Near the irradiation zone, the gas was at 450°C, but a heat exchanger and the passage of the pipes in the water reduced the temperature down to about 40°C at the sampling point.

The samples were made with filter packs (fig.1) directly at initial pressure of 60 Kg/cm2.

The packs contained successively an asbestos paper, a knit-mesh, a charcoal impregnated paper, five 1cm thick charcoal beds and finally a 5cm thick bed maintained at -40°C ; the charcoal used being always a non impregnated coconut charcoal, acticarbone NC-35-8-16.

## EFFICIENCY OF CHARCOAL AND KNIT-MESH FOR IODINE AND COMPOUNDS

The experimental conditions were such that one could expect a little amount of the least volatil forms or of those which are the most easily adsorbed on materials (especially elemental iodine) ; so the

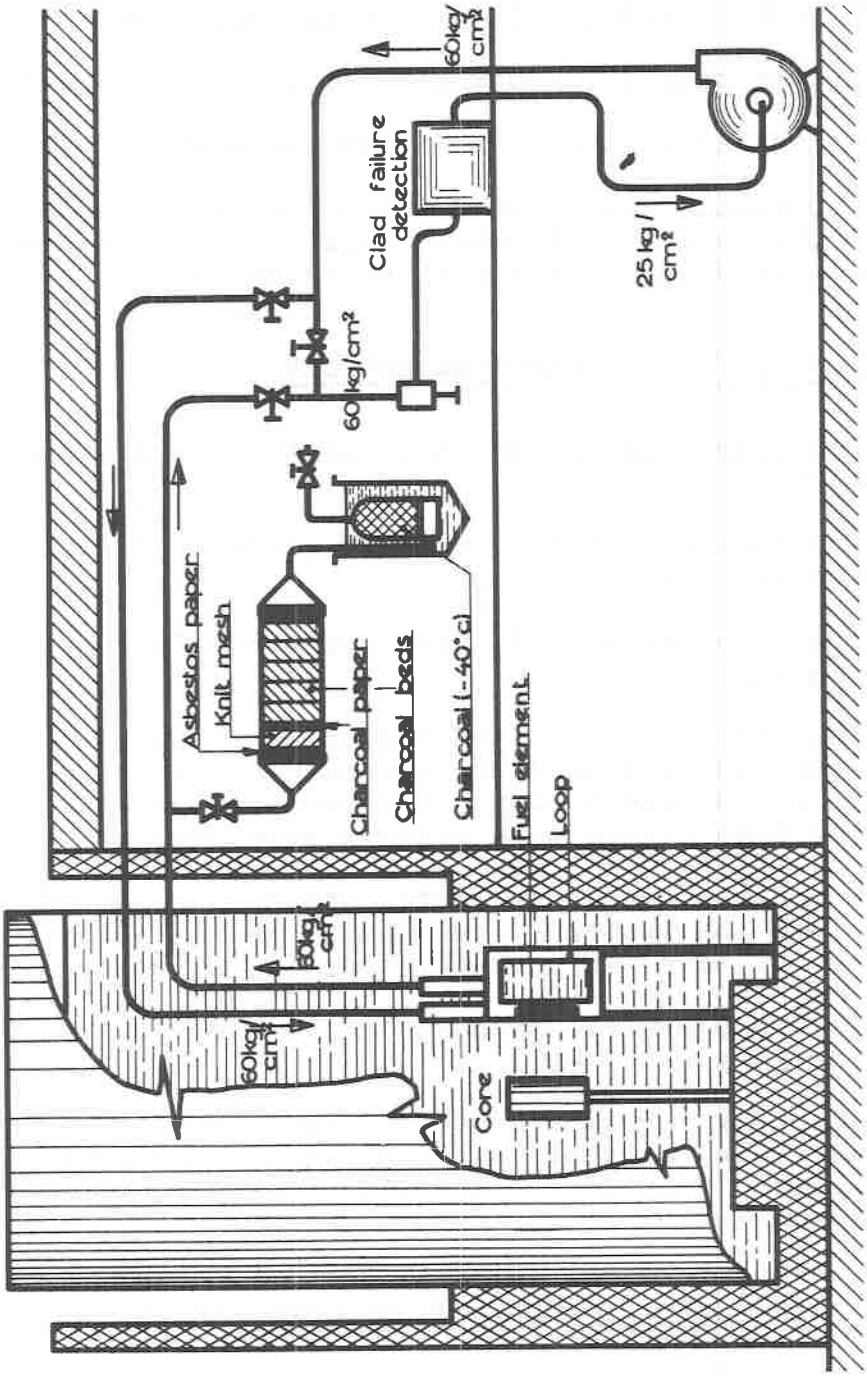


Fig 1- Schematic diagram of the $CO_2$ Loop

iodine released from UO2 fuel flowed in the loop between each run. The knit-mesh and impregnated paper activities showed clearly this fact (table 1 - fig.2).

However, the behavior of elemental iodine and of the forms easily adsorbed in filters, especially in charcoal, is on the one hand much better known and on the other hand less important owing to their less penetrating character.

Nevertheless for comparison, the efficiency of charcoal for iodine released by oxidizing of sodium iodide can be seen in fig.4.

The iodine generated by this method has been previously adsorbed on glass marbles at low temperature, then it was desorbed by heating and carried into an out-of-pile loop of 120 l, filled with CO2 at about 40°C, the pressure being 20 Kg/cm2.

The iodine concentration in the loop was 60 $\mu$Ci/m3 (Atm.pres.) at sampling point.

The CO2 gas velocity entering the filter-pack was 3cm/s.

In addition to the forms removed by knit-mesh and impregnated paper, there were at least two iodine compounds in charcoal (fig. 2 and 3) and it can be easy to determine the fraction of the least adsorbed compound.

Let us remind the behavior formulation of several forms in charcoal:

$E_1 , E_2 , \dots , E_n$ charcoal efficiency for the forms 1,2, ..., n

$\alpha_1 , \alpha_2 , \dots , \alpha_n$ 1,2, ..., n forms adsorption constant of charcoal

$p_1 , p_2 , \dots , p_n$ 1,2, ..., n forms ratio

$x$ depth of charcoal bed.

we suppose : $E_1 > E_2 > \dots > E_n$

$$\frac{1}{E} = \frac{p_1}{E_1} + \frac{p_2}{E_2} + \dots + \frac{p_n}{E_n}$$

$$= p_1 e^{-\alpha_1 x} + p_2 e^{-\alpha_2 x} + \dots + p_n e^{-\alpha_n x}$$

$$(1) \quad \text{Log } E = \alpha_n x - \text{Log} \left( p_1 e^{-(\alpha_1 - \alpha_n) x} + \dots + p_n \right)$$

$$\frac{\text{Log } E}{x} \longrightarrow \alpha_n \qquad x \longrightarrow \infty$$

TABLE I

EXPERIMENTAL CONDITIONS

| | SAMPLING TIME (mn) | VOLUME SAMPLED (m3 atm.pres.) | CO2 VELOCITY (cm/s) | IODINE CONCENTRATION IN LOOP (Sample point) µCi/m3 atm.pres. |
|---|---|---|---|---|
| run 1 | 50 | 0,28 | 5 | 4,3 |
| run 2 | 170 | 1,31 | 5 | 3,4 |
| run 3 | 120 | 1,34 | 7,5 | 68 |
| run 4 | 140 | 1,65 | 8 | 5,3 |
| run 5 | 70 | 1,09 | 10 | 33,6 |

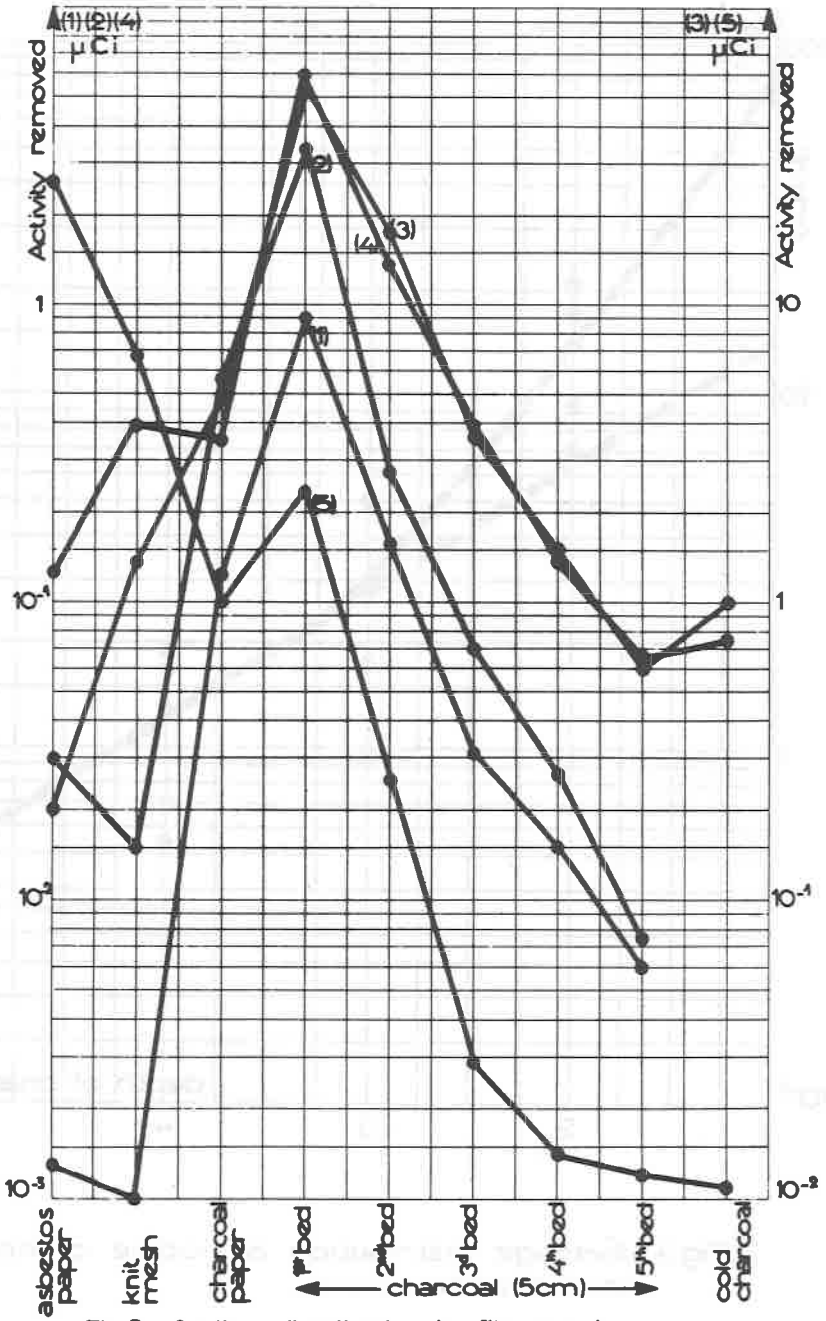


Fig 2 _ Iodine distribution in filter-pack

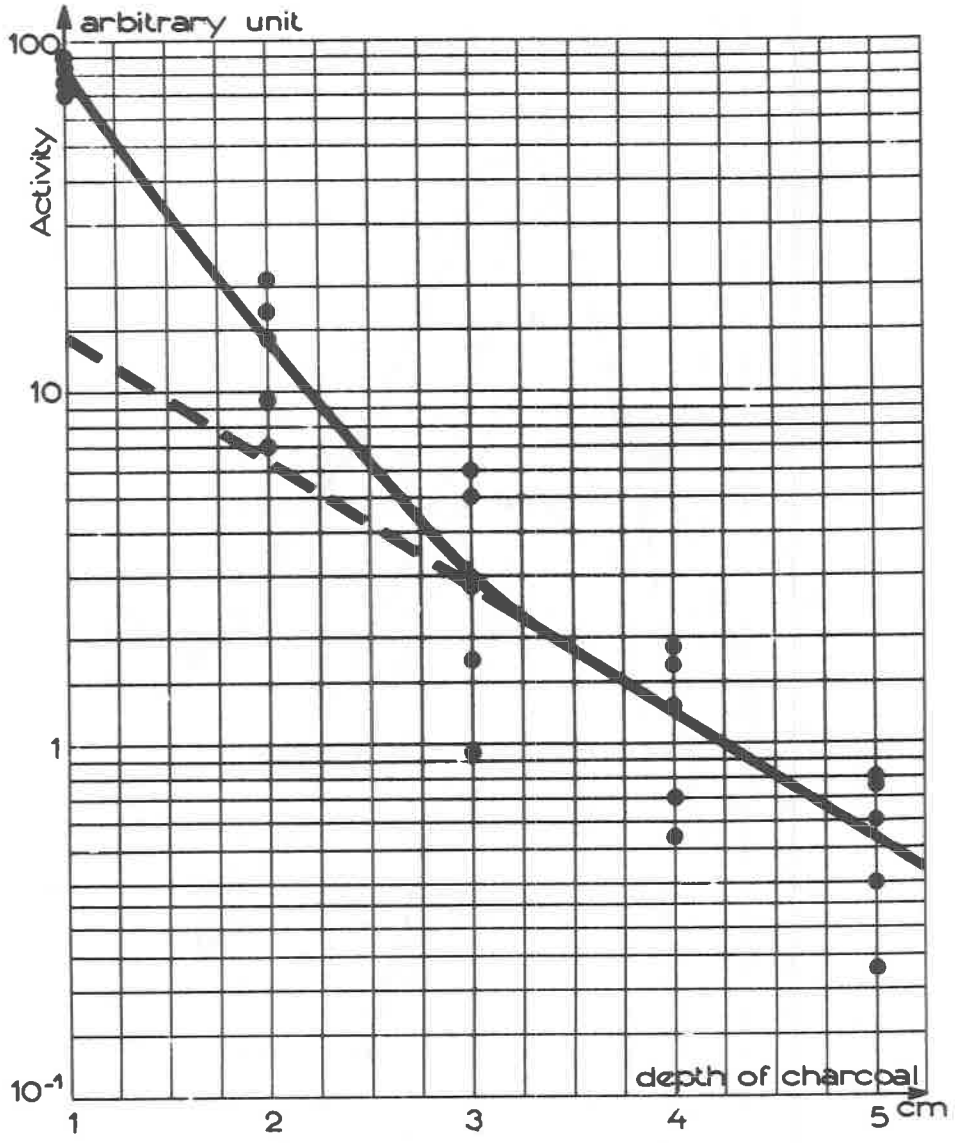


Fig.3_Average distribution of iodine compounds in charcoal

## TABLE II

### IODINE DISTRIBUTION IN FILTER-PACK

A = Activity ( $\mu$ Ci)
P = Percent of total activity trapped

| | Run 1 | | Run 2 | | Run 3 | | Run 4 | | Run 5 | |
|---|---|---|---|---|---|---|---|---|---|---|
| A ( Ci)-P(%) | A | P | A | P | A | P | A | P | A | P |
| Asbestos paper | 0,0013 | 0,1 | 0,04 | 0,9 | 0,2 | 0,3 | 0,12 | 1,3 | 26,3 ++ | 71,7 |
| Knit-Mesh | 0,00098 | 0,1 | 0,015 | 0,3 | 1,3 | 1,4 | 0,39 | 4,4 | 6,6 | 18 |
| Charcoal paper | 0,12 | 9,7 | 0,55 | 12,6 | 2,3 + 2,4 | 10,7 | 0,35 | 4 | 1 | 2,8 |
| 1st Charcoal | 0,9 | 73,1 | 3,4 | 77,9 | 55,5 | 61,1 | 5,95 | 67,6 | 2,4 | 6,6 |
| 2d Charcoal | 0,16 | 12,7 | 0,27 | 6,1 | 17,6 | 19,4 | 1,35 | 15,4 | 0,25 | 0,7 |
| 3d Charcoal | 0,031 | 2,6 | 0,069 | 1,5 | 3,6 | 3,9 | 0,39 | 4,4 | 0,029 | 0,08 |
| 4th Charcoal | 0,015 | 1,2 | 0,026 | 0,6 | 1,5 | 1,7 | 0,14 | 1,6 | 0,014 | 0,04 |
| 5th Charcoal | 0,006 | 0,5 | 0,0074 | 0,2 | 0,6 | 0,7 | 0,065 | 0,7 | 0,012 | 0,03 |
| Cold Charcoal trap | | | | | 1 | 0,8 | 0,075 | 0,6 | 0,011 | 0,02 |

+ : two charcoal-impregnated papers were placed in this pack.
++: in run 5, the pack was heated at approximatily 70°C.

$$\text{Log } E \; - \alpha_n \, x \xrightarrow[x \to \infty]{} \text{Log} \frac{1}{p_n}$$

With semi-logarithmic plots, it can be seen that the curve (1) has an asymptote : $\text{Log } E = \alpha_n \, x + \text{Log} \frac{1}{p_n}$

Its ordinate at the origin is : $\text{Log } E = \text{Log} \frac{1}{p_n}$ or $E = \frac{1}{p_n}$

Then it appears (fig.4) that the average fraction of the least adsorbed compound was about 1/5 or 20% of the forms trapped in charcoal.

The average efficiency of the five 1cm thick charcoal beds, for the iodine compounds which have not been adsorbed on the loop materials or in the knit-mesh and the impregnated paper, is about $10^2$ (fig.4). And for the least adsorbed compound, the efficiency is reduced down to 50.

In run 5, the tube, 50 cm long and 0,5 cm in diameter, which connected the sample point and the filter pack, was heated at about 70°C.

The differences are shown in table 1 and fig.2. The most important is the efficiency of the asbestos paper: its stainless steel holder itself retained 30% of the total activity, the fraction remained on paper being 40%.

In this run, the efficiency of the knit-mesh has also been relatively more important.

## CONCLUSION

It seems that in the event of an accident occurring in a $CO_2$ gas cooled reactor, the charcoal filters should trap at least 99% of the iodine and of the compounds which could appear after the iodine release.

It appears unlikely that, in case of a large accident, the most penetrating forms ratio would be more important than in the experiment, because the contamination would quickly reach the filters.

Therefore the efficiency of $10^2$ which has been found, may be considered as a pessimistic value.

However it should be suitable to identify these compounds so that they can be generated in laboratory for studying their behavior in detail.

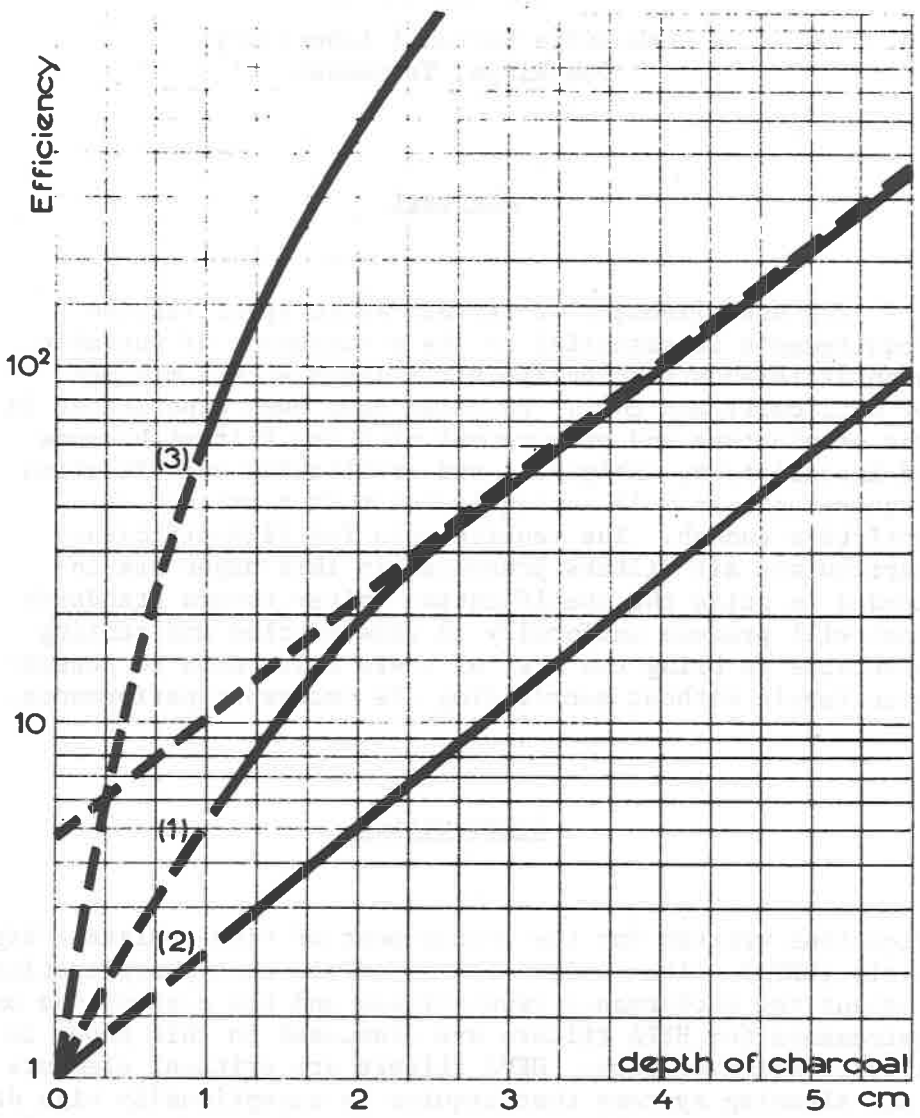


Fig. 4 – (1) Average efficiency of charcoal for iodine compounds

(2) Average efficiency of charcoal for the least adsorbed compound

(3) Efficiency of charcoal for iodine generated by oxydation of NaI

# REQUIREMENTS FOR FIRE-RESISTANT HIGH-EFFICIENCY PARTICULATE AIR FILTERS*

C. A. Burchsted

Oak Ridge National Laboratory
Oak Ridge, Tennessee

## Abstract

The establishment of certain basic specification requirements is essential to the procurement of suitable high-efficiency particulate air filters with a minimum of difficulty and cost. Problems have been experienced in the manufacture and procurement of these filters because of inconsistent, ambiguous, and conflicting specification requirements as well as requirements that are not restrictive enough. The requirements for high-efficiency particulate air filters presented in this paper are intended to guide the specification writer toward standards that will produce uniformity in construction and testing practices to bring the cost of these units down to reasonable levels without sacrificing the necessary performance.

## Introduction

Specifications written for the procurement of fire-resistant high-efficiency particulate air (HEPA) filter units used in atomic energy applications determine to a great extent the performance capabilities and the cost of the unit procured, and the requirements for HEPA filters are discussed in this paper to provide a guide for specification writers. HEPA filters are critical elements in exhaust and supply air cleaning systems that require an exceptionally high degree of particulate removal. These filters are very fragile, and many variables in their construction and handling will affect their operation under the wide range of environmental conditions to which they may be exposed. Therefore, the properly written specification will aid in the procurement of suitable filter units at minimum cost.

Problems in specification writing fall into two categories: those that impede manufacture and result in higher costs and procurement delays and those

---

*Research sponsored by the U. S. Atomic Energy Commission under contract with the Union Carbide Corporation.

that can result in inadequate protection to the user. To explore these problems in specifications and use of HEPA filters, two conferences were held recently by representatives of users, manufacturers, the Atomic Energy Commission, the AEC Quality Assurance Stations, and the Underwriters' Laboratories. The results of these meetings and of practical experience indicate the need for a standard specification for HEPA filter units to produce uniformity in construction and testing practices that will maintain costs of these units at reasonable levels without sacrificing the necessary performance required for public safety. Adoption of the requirements and values outlined in the remainder of this paper may alleviate many of the current problems in the purchase and use of commercially available HEPA filters.

## Performance

The performance of any given type HEPA filter is determined by both nondestructive and destructive testing. In general, tests of the nondestructive type should be run on all filters produced, whereas the destructive type tests are run only on prototypes of a specific filter unit to determine the suitability of the design or materials for the wide range of service conditions to which the filter may be exposed. These destructive or qualification tests are usually quite expensive and difficult to conduct, and once made, they need not be repeated in subsequent orders of filter units of the same materials and construction.

### Performance Factors Determined by Nondestructive Tests

Nondestructive tests are made on a filter unit to determine its efficiency and pressure drop, penetration, and whether or not it leaks around the frame.

Efficiency and Pressure Drop. Particle removal efficiency and the pressure drop across the filter are two of the most important properties of any HEPA filter unit; the first is a measure of its primary function and the second has a direct bearing on its operating cost. By definition, a HEPA filter is one that (1) has a minimum removal efficiency of 99.97% when tested with a thermally generated 0.3-micron-diameter particle dioctyle phthalate smoke and (2) has a maximum clean filter pressure drop of 1.0 in. $H_2O$ when operated at rated capacity. Nondestructive tests to confirm these properties are made by the manufacturer and, when specified, by the AEC Quality Assurance Station, following Edgewood Arsenal procedures.[1]

The figure of 99.97% is a reasonable compromise between necessary manufacturing tolerance and protection for the user; most of today's filters test at substantially higher values. For a given filter design, pressure drop is a direct function of flow capacity or of face velocity. The figure of 1.0 in. $H_2O$ is arbitrary, but it is specified to permit direct comparison between filter units of different manufacture or design or of tests on the same filter made at different times or places. Its use does not preclude operation of the filter at either higher or lower flows or face velocities.

Penetration. Two-flow testing is recommended by the AEC to disclose pinholes and leaks that cannot be found by full-flow testing or visual inspection.[2] Pinholing is a media defect that permits unfiltered air to pass through the filter even in units that show full-flow test efficiencies as high as 99.99%.[3] Since penetration of pinholed filters is independent of particle size,[4] particles with diameters of several microns can escape through the filter. A statistical analysis of filter test results showed a 95% probability of the existence of

The proposed requirements are grouped in three categories - performance; materials and construction; and acceptance. Performance is further broken down into features that can be confirmed by non-destructive testing of each filter unit, and features that can only be confirmed by destructive qualification testing of a prototype. Adoption of features discussed in the remainder of this paper may alleviate some of the current problems in purchase and use of commercially availably HEPA filters; the paper intended as a guide for writers of procurement specifications.

The need for comprehensive specifications cannot be overstressed; during the past year Mr. A. B. Fuller and I have visited both AEC operated and commercially operated nuclear sites throughout the country. The best filter systems we have seen are those in which the operator uses a detailed specification for buying these filters. Without fail, operators of less adequate systems are those who bought filters under a simple catalog description. I believe that an understanding of the basic requirements for these filters, and the reasons for specifying these requirements, will induce an appreciation for what is required to achieve an adequate filter installation. The consensus of the users and manufacturers who attended the conferences at Underwriters' Laboratories is that greater uniformity in specification requirements, and in the values specified for certain requirements, will benefit both the manufacturer and the user but particularly the user.

## Performance

The performance of any given type HEPA filter is determined by both nondestructive and destructive testing. In general, tests of the nondestructive type should be run on all filters produced, whereas the destructive type tests are run only on prototypes of a specific filter unit to determine the suitability of the design or materials for the wide range of service conditions to which the filter may be exposed. These destructive or qualification tests are usually quite expensive and difficult to conduct, and once made, they need not be repeated in subsequent orders of filter units of the same materials and construction.

### Performance Factors Determined by Nondestructive Tests

Nondestructive tests are made on a filter unit to determine its efficiency and pressure drop, penetration, and whether or not it leaks around the frame.

Efficiency and Pressure Drop. Particle removal efficiency and the pressure drop across the filter are two of the most important properties of any HEPA filter unit; the first is a measure of its primary function and the second has a direct bearing on its operating cost. By definition, a HEPA filter is one that (1) has a minimum removal efficiency of 99.97% when tested with a thermally generated 0.3-micron-diameter particle dioctyle phthalate smoke and (2) has a maximum clean filter pressure drop of 1.0 in. $H_2O$ when operated at rated capacity. Nondestructive tests to confirm these properties are made by the manufacturer and, when specified, by the AEC Quality Assurance Station, following Edgewood Arsenal procedures.[1]

The figure of 99.97% is a reasonable compromise between necessary manufacturing tolerance and protection for the user; most of today's filters test at substantially higher values. For a given filter design, pressure drop is a direct function of flow capacity or of face velocity. The figure of 1.0 in. $H_2O$ is arbitrary, but it is specified to permit direct comparison between filter units of different manufacture or design or of tests on the same filter made at different times or places. Its use does not preclude operation of the filter at either higher or lower flows or face velocities.

Penetration. Two-flow testing is recommended by the AEC to disclose pinholes and leaks that cannot be found by full-flow testing or visual inspection.[2] Pinholing is a media defect that permits unfiltered air to pass through the filter even in units that show full-flow test efficiencies as high as 99.99%.[3] Since penetration of pinholed filters is independent of particle size,[4] particles with diameters of several microns can escape through the filter. A statistical analysis of filter test results showed a 95% probability of the existence of

significant pinholing if the difference in penetration between the full-flow test and a 20%-flow test exceeded 0.01%;[5] this is borne out by the work of Adley[6] and Knuth.[7]

Inclusion of a requirement for two-flow testing, at full flow and at 20% flow, with a maximum permissible difference in the absolute value of penetration of 0.01% is recommended in specifications for filter units with a capacity of 500 cfm and larger. Two-flow testing of smaller units is not practical since the low flow velocities at 20%-flow testing make the results questionable.

Frame Leakage. A requirement for frame leak testing is recommended because of the significant number of "frame leakers" discovered during Quality Assurance Station testing. Frame leaks can result from improper manufacturing processes or from properties of the materials themselves. These are discussed in the section on materials and construction.

## Performance Factors Determined by Destructive Tests

Destructive or qualification tests are made on prototype filter units to determine their resistance to fire and hot air, moisture resistance, pressure loading resistance, and dust holding capacity. Qualification of a given design or set of materials by one manufacturer does not confer qualification of a similar design or materials on another manufacturer because differences in methods of construction could result in differences in performance.

Resistance to Fire and Hot Air. Qualification tests for fire and hot air are made by Underwriters' Laboratories in accordance with Standard UL-586.[8] Qualification includes a hot air test at a temperature of 700°F for five minutes while the filter is being operated at its rated capacity and a spot flame test in which the flame from a Bunsen burner is directed against the upstream face of the filter for five minutes while the filter is being operated at its rated capacity. Although the standard permits a reduction of 3% in filtration efficiency following hot air testing, the results of tests usually show a reduction of less than 0.3%.[9] The spot flame test is a test of combustibility rather than a test of the effect on filtration performance. The test will breach the filter and is successful if no sustained burning takes place on the downstream face of the filter.

When specified, Underwriters' Laboratories qualification is evidenced by the UL label on the filter unit. It is not necessary in writing specifications to go to great length in spelling out fire resistance, flame spread ratings of materials, cracking or shrinkage of adhesives, or similar details. All of these can be covered by the single requirement for UL labeling.

Underwriters' Laboratories qualification is not a certification of filter efficiency nor is it a substitute for Quality Assurance Station or other performance testing. It only certifies that the materials and construction meet the requirements of UL-586, and that materials and construction of units furnished on the order are identical to those of the unit originally tested. A valuable service of the Underwriters' Laboratories program is spot checking of manufacturers to ensure compliance of labeled filter production, and part of this check is to make sure that there has been no change in materials or construction.

Moisture Resistance. Moisture resistance has two aspects: resistance to plugging of the filter when exposed to low-quality steam or fog containing water droplets and resistance to saturation that would reduce the strength of the media or separators below some tolerable minimum. Tests for moisture resistance are still under development and will be discussed at meetings being held concurrently with this conference. The results of those meetings will be reported at a later date.

Pressure Loading. To withstand occasional overpressure and operation under high dirt loadings with a reasonable factor of safety, HEPA filters must be able

to withstand a pressure drop of 10 in. $H_2O$ across the filter while operating at full rated capacity under both dry and moist conditions without rupture or loss in filtration efficiency. As with moisture testing, no suitable test has been developed to date. Uniform specification of both moisture and pressure loading resistance is recommended as soon as suitable tests become available. This will make possible a standard qualification procedure that can perhaps be included in a later version of UL-586.

Dust Holding Capacity. Dust holding capacity is a measure of potential filter life, and it is a direct function of media area. It is not desirable to specify this property indirectly by stipulating a minimum media area, a minimum number of separators, or a maximum flow velocity through the media itself because these may conflict with other requirements. For example, the number of separators will change in accordance with the type and thickness of media and separators. A minimum separator count based on a unit with 0.0015-in.-thick aluminum separators might be impossible to meet if a unit with 0.016-in.-thick asbestos separators were specified in a purchase order. Conversely, a separator count based on asbestos separators would permit too loose a filter pack should a unit with aluminum separators be ordered.

Specification of dust holding capacity as a performance requirement is recommended. The recommended minimum loadings to produce a 2-in. $H_2O$ pressure drop while operating at rated capacity, using a National Bureau of Standards Cottrell precipitator test dust are tabulated below.

| Filter Size (scfm) | Minimum Dust Loading (grams) |
|---|---|
| 25 | 75 |
| 50 | 160 |
| 125 | 400 |
| 500 | 1650 |
| 1000 | 3000 |

Both test dusts and minimum recommended dust loadings are still under investigation. The distribution of particle sizes in the National Bureau of Standards test dust may vary considerably from batch to batch, and a more uniform dust, such as that proposed by the Air Filter Institute, may be proposed when more is known about its loading characteristics in HEPA filters. For the present, the above values are adequate.

## Materials and Construction

The commercially available open-face HEPA filters covered by this guide conform to a rather uniform design and construction. They usually consist of a filter pack, made by pleating fiber glass paper back and forth over corrugated aluminum or asbestos separators, sealed in a plywood or cadmium-plated steel frame with a suitable adhesive. This configuration provides a unit with maximum filtration area (about 230 $ft^2$ in a 1000-cfm unit) and minimum frontal area and volume (4 $ft^2$ and 4 $ft^3$, respectively, in a 1000-cfm unit). Materials and construction have a direct bearing on performance, resistance to damage and deterioration under operating conditions, and cost. Other materials may be used to meet special requirements but should be specified with care.

Frames

The strength and rigidity of the frame directly affect the ability of the filter to withstand mounting bolt loadings and racking and warping that could damage the filter pack or its seal. The usual frame materials are 3/4-in. exterior-grade A-A plywood or No. 16 U.S. gage cadmium-plated carbon steel.

Plywood should be specified to be in accordance with either Commercial Standard CS-45 or CS-122,[10, 11] which define the requirements for exterior and type grading. Lesser grades than A-A should not be specified because of the tendency of manufacturers' personnel to turn the poor side in for appearances sake, which could prevent an adequate seal between the frame and the filter pack. Wood frames should have rabbeted corners and be assembled by double nailing or double screwing (i.e., fasteners through both surfaces of the joint) using coated box nails, galvanized flat-head screws, or galvanized screw nails. Mat-formed wood-particle board has been proposed as an alternate for plywood. It offers economies in filter construction, but preliminary tests have shown sufficient porosity to cause frame leaks. This material is still under investigation, and the results of this investigation will be reported at a later date.

Cold-rolled carbon steel sheet is preferred to hot-rolled sheet because it is flatter and is held to closer dimensional and surface tolerances. Steel frames are usually made up of four panels assembled with cadmium plated rivets, bolts, or drive screws. Frame panels should be cadmium plated after completion of all shearing, forming, and welding operations to ensure proper coating of sheared edges and weld areas. Minimum coating of Type OS in accordance with ASTM A165[12] is recommended. Without this restriction, the manufacturer could legitimately furnish a plate so thin as to be almost useless. A Type OS plate is 7.6 microns thick. Frames should have double-turned flanges on both faces; single-turned flanges are too weak to withstand the bolt loads often applied to seal these filters into their mountings. Abutting sections of the flange face should have no more than a 1/32-in. gap to assure proper seating of the gasket. Gaps as large as 1/8 in. have been observed. On both wood and steel frames, the mating surfaces of corner joints should be thoroughly coated with adhesives before assembly to ensure a tight joint.

If stainless steel frames are required, the gauge and assembly requirements for carbon steel should be required for the stainless steel frames except that the fasteners should also be stainless steel. Since stainless steel is specified for its corrosion resistance, it is advisable to specify a grade and conformance to ASTM A240.[13]

Frame Dimensions. Five sizes of HEPA filters have been widely accepted as standard and these are tabulated below.

| Capacity (scfm) | Face Dimensions (in.) | Depth Less Gaskets (in.) |
|---|---|---|
| 25 | 8 by 8 | 3 1/16 |
| 50 | 8 by 8 | 5 7/8 |
| 125 | 12 by 12 | 5 7/8 |
| 500 | 24 by 24 | 5 7/8 |
| 1000 | 24 by 24 | 11 1/2 |

The use of these standard sizes is recommended for new construction because higher costs will result from using special sizes due to manufacturing inefficiencies, stocking problems, and procurement delays. It is not necessary to design a system to use filter units exactly matched to system flow. If the next larger standard size is specified, pressure drops will be lower (with resultant fan and

duct saving), longer filter life will be obtained (with resultant savings in both procurement and maintenance costs), and excess capacity will be provided for the inevitable system addition.

Special sizes may be required because of inattention to details in the design and construction of filter banks and housings. One user is burdened with the necessity of buying 23 1/2- by 23 1/2-in. filter units for one system because insufficient spacing was provided between mounting bolts. Although a standard-size unit will go into the available space, the least amount of moisture will cause swelling that jams the unit in the frame. There has been a recent trend toward the use of very large filter units in certain applications with face dimensions up to 4 by 6 ft. Unless heavily reinforced, these units are structurally weak and are subject to pinholing and cracking of the media and the seal between the filter pack and frame caused by racking and warping during shipping and handling.

Dimensional Tolerances. Specifications for face dimension tolerances range from ± 1/32 in. in 2 ft, which is beyond the accuracy of a production woodworking shop, to ± 1/8 in., which is so loose that a user could have trouble in seating the filter in a tight mounting. The recommended frame tolerances are tabulated below.

| | Size of Filter Unit | |
|---|---|---|
| | 25, 50, 125 scfm | 500, 1000 scfm |
| Face Dimensions | + 0, - 1/16 in. | + 0, - 1/8 in. |
| Depth | + 1/16 in., - 0 | + 1/16 in., - 0 |
| Diagonals | Equal within 1/16 in. | Equal within 1/8 in. |

The plus zero tolerance on the face dimension provides for interchangeability in housings or tight mountings without selective fitting. The minus zero tolerance on depth ensures a minimum gasket deflection in mountings with toggle or cam-operated clamping devices that have a fixed amount of deflection.

Because the condition of gasket surfaces is critical to proper sealing of the filter unit, faces should be flat with opposite faces parallel within 1/16 in. total indicator reading (TIR) as measured with one face resting on a truly flat surface, such as a machinist's surface plate. Gasket surfaces should be square with the sides of the frame to within ± 2°.

## Separators

The usual separator materials are asbestos (containing no more than 5% combustible material and having a basic weight of 4 lbs/100 $ft^2$) and aluminum (0.0015-in.-thick minimum, H-19 temper, preferably a solution hardening alloy since work hardening alloys anneal and soften at fairly low temperatures). However, asbestos has practically no moisture resistance, and aluminum has neither corrosion nor high-temperature resistance. Aluminum will fail nearly explosively at temperatures above 1000°F. Polyvinyl chloride and stainless steel have both been used for corrosion resistance. However, polyvinyl chloride cannot be fire rated and is too soft even at room temperature, and stainless steel is prohibitively expensive. Specially-treated asbestos papers are under development by all four HEPA filter manufacturers and several paper manufacturers. These show promise of excellent resistance to moisture after exposure to concentrated reagents, fire, and steam. Two materials have met all requirements of a tentative qualification test,[14] and should be available upon establishment of a formal qualification agency and completion of UL fire tests.

## Media

Investigations to improve media tensile and wet strength, to increase media bulk (to provide better protection against pinholing due to separator vibration during shipping and operation), and to develop a hydrogen-fluoride-resistant media are in progress. Results of these investigations will be reported at a future date.

Recognizing a number of drawbacks in the current version of Military Standard MIL-F-51079,[15] the following requirement is suggested as an interim specification.

> Glass or glass-asbestos paper at least 0.015 in. thick containing no more than 5% combustible material in accordance with MIL-F-51079 except cross machine tensile strength shall be 2.5 lbs/in. paragraph 3.2.10 (pH) shall be deleted; and paragraph 3.2.6.2 shall be changed to say that the minimum tensile strength after folding shall be no less than 50% of the original tensile strength.

Spot patching to repair holes or tears in media cause "hot spots" when the filter is exposed to hot air or fire and should not be permitted. The defect should be cut out and the media repaired by splicing. Where two pieces of media are to be joined by splicing, each piece should be coated with adhesive for 1 to 2 in. across the full width of the sheet. A limitation of one or two splices in a 500 or 1000 cfm filter unit is unreasonable because the manufacturer has no control over where he finds defects or the end of a roll. Such limitations increase costs due to the excessive waste involved, and a limit of four or five splices may be reasonable if such a requirement is considered necessary. A restriction on the number of splices in smaller units may be desirable because of flow restriction caused by splicing. Because of smaller quantities of media involved, waste would be correspondingly less and could be held to within reason.

## Adhesives

The adhesive used in a HEPA filter must retain sufficient strength and resiliency to maintain its sealing integrity under exposure to flowing hot, cold, dry, or moist air, steam and condensed moisture, some small amount of working of the frame, shear forces set up by pressure loading, and other conditions to which the filter may be exposed in service. Adhesives can therefore only be qualified by destructive tests of the entire filter. In addition to tests by Underwriters' Laboratories, tests are made by the Atomic Energy Commission. Currently available adhesives that meet the requirements of both UL-586 and AEC testing are tabulated below.

| | |
|---|---|
| Minnesota Mining & Manufacturing Company | No. EC-2155 |
| Pittsburgh Plate Glass Company | No. Z-743 |
| Goodyear Pliobond | No. HT-30-FR |
| Talon Adhesives Company | Cemen-TAC NB-38A |
| | Cemen-TAC NB-38B |
| | Cemen-TAC NB-38C |

In addition to these commercially available adhesives, a proprietary foamed-in-place polyurethane has proved very successful. Because the choice of adhesive is so critical to performance of the filter, specification of one of these materials or of an identified alternate specifically approved by the buyer is recommended.

## Workmanship

Loose packing and kinked or nonperpendicular pleats and separators can result in media damage due to separator vibration and working of the media during shipping and operation. Although not so common today, they still give enough trouble that a requirement limiting them may be desirable. Some degree of kinking and nonperpendicularity of separators must be allowed for manufacturing tolerance and has not been found to be harmful by dioctyl phthalate testing. Reasonable limits are a maximum kink of 1/4 in. from a line drawn from end to end of the separator and a maximum deviation of $\pm$ 1/4 in. from a perpendicular drawn from the opposite end of the separator. Greater deviation is evidence of poor workmanship.

Loose packing is not so easily defined. A reasonable test is to place one's hand firmly against the face of the filter and attempt to move it laterally; any motion of the separators is cause for rejection. This test is not suitable with polyvinyl chloride, however, because polyvinyl chloride is so soft that the corrugations will flatten and permit separator movement. Separators should extend at least 1/8 in. from the pleats to give adequate protection to the media.

## Gaskets

Gasket selection is the subject of a study by F. E. Adley that is to be reported at this conference. Numberous materials have been used for gaskets, including fiber glass mat, cork-rubber and several grades of neoprene. Until the results of Mr. Adley's research can be evaluated, closed-cell expanded neoprene grade SCE-43 in accordance with ASTM D1056 [16] is recommended. Fiber glass mat is too fragile and will leak from edge to edge regardless of how much it is compressed. Cork-rubber, though specified to be 20-40 durometer, is usually 60 or harder, and it requires very high clamping-bolt loads to seal the filter. Neoprene softer than SCE-43 is too soft. ASTM D1056 measures hardness in terms of compression because the hardness of sponge materials cannot be accurately determined with a durometer. Grade SCE-43 reqires a load of 11 1/2 lb/in.$^2$, $\pm$ 2 lb, to produce 25% compression.

## Face Guards

Although recommended by the AEC for several years, face guards are not required by most users. HEPA filters can be very easily damaged during handling and installation or by materials scraped across them while mounted in a bank or housing. I have recently had the privilage of visiting air cleaning facilities at a large number of atomic energy installations throughout the county, and in nearly every one where face guards were not used, some degree of face damage to installed filters was evident. The savings gained by eliminating face guards can quickly be lost in the cost of a few damaged filter units.

The least expensive face guard is 4-mesh galvanized hardware cloth conforming to Commercial Standard CS 132.[17] Edges should be firmly embedded in adhesive (the Quality Assurance Stations reported numerous loose face guards) and projecting wires at the edges must not penetrate the media or extend outwards where they could be a hazard to personnel.

Face guards are only recommended for 1000-cfm filter units or larger, and they should be specified to be on both faces. Smaller filter units are light enough and manageable enough that the probability of damage by persons handling them is relatively low.

## Acceptance, Packaging, and Shipping

Inspection and nondestructive acceptance testing of HEPA filter units for use in the U. S. atomic energy program are carried out by the AEC Quality Assurance Stations at Oak Ridge, Tennessee for sites east of the Mississippi River and Hanford in Richland, Washington. Acceptance of fire-resistant units is based on presence of the Underwriters' Laboratories label, inspection for shipping damage or obvious defects, and successful completion of performance tests. When specified in the specification or purchase order, testing includes two-flow and frame leak testing.

### Acceptance

Although in-place testing of filter systems by the user is highly recommended, it is not a suitable substitute for acceptance testing of filter units by the Quality Assurance Stations. The hot smoke (i.e., thermally generated dioctyl phthalate) used in Quality Assurance Station testing is a uniform dispersion of 0.3-micron-diameter particles that permits determination of the basic removal efficiency for small particles. QAS testing also provides a valuable check on performance tests by the manufacturers and ensures uniformity of testing procedures. Neither of these can be done with the cold smoke (air-generated dioctyl phthalate) used for in-place testing. Because cold smoke is a polydisperse mixture of particle sizes,* penetration values produced by cold smoke testing are distorted by a preponderance of large particles. Therefore, very high efficiency readings from cold smoke testing tell nothing about the removal efficiency for the very small particles against which the filter was designed to protect. Small particle removal efficiency can only be determined by hot smoke testing. Because of the high cost of hot smoke testing facilities, this service is provided through the stations at Hanford and Oak Ridge.

Title to filter units normally passes to the buyer upon successful completion of inspection and testing. This does not preclude subsequent inspection by the buyer for shipping damage or conformance to materials and construction requirements, or special performance requirements not covered by Quality Assurance Station testing.

### Packaging

Each filter unit should be legibly and permanently marked with the manufacturer's name or symbol, the filter serial number, the actual percent penetration at rated capacity (as determined by manufacturer's test), the clean filter pressure drop (as determined by manufacturer's test), the air flow capacity, and an arrow showing the direction of air flow during test. Marking should be on the top of the filter unit with separators vertical and should be used as a guide by the buyer's personnel when installing the filter. Filters should always be installed with the separators vertical.

---

*Eight percent of the particles produced by a NRL Type II aerosal generator were reported to have diameters larger than 1.88 microns, and 77% had diameters larger than 0.59 microns.[18]

The serial number should be printed with figures at least 1/2 in. high with a sequencing numbering machine to avoid duplicate numbering or mis-numbering. Other characters may be either machine or hand printed, but they should be at least 3/8 in. high for legibility. Labels, particularly typewritten, should not be permitted for marking.

Cartons used for shipping HEPA filters, in addition to meeting Interstate Commerce Commission regulations, must provide adequate shock protection and must not contain excelsior or other dusty materials that could clog the filter. Several users go to some length in specifying packaging requirements. An excellent carton is that described in U.S. Patent No. 3,057,468,[19] which is reported by the Quality Assurance Stations to be one of the most satisfactory both from the standpoint of protection and from the standpoint of safe handling and reuse. This carton has been made available to all manufacturers for government and government-contractor orders without royalty.

Tops of cartons should be sealed with tape and not glue or staples because the cartons will be reused by the QAS and in many instances by the buyer for packaging dirty filters removed from his system. The exterior of the carton should be marked with the manufacturer's name or symbol, the filter description, the buyer's purchase order number, and FRAGILE and THIS SIDE UP legends. Filters should always be packed in cartons with pleats and faces vertical, and cartons should be handled, stored, and shipped with the faces vertical. A statement in the specification outlining these requirements is recommended.

## Shipping

After leaving the Quality Assurance Station, shipping damage is the responsibility of the carrier and not the manufacturer unless inadequate packaging has been provided because the Quality Assurance Stations repack filters in the same cartons. If such damage is frequent, the buyer should look to his packaging and shipping methods rather than to elimination of Quality Assurance Station testing.

Shipment of filters by rail is not recommended because of the humping and jarring normally encountered. If shipped by truck, it is advisable to require that the filters be shipped in the same truck or trailer from the QAS to the buyer's receiving dock, with no transshipment. Personnel handling filters in the buyer's receiving department should be instructed in proper handling of HEPA filters, see USAEC report TID-7023,[20] and they should be required to unload all shipments. Cartons should be shipped and stored in a vertical position and stacked no more than three high.

## References


1. Filter Testing Penetrameter Instruction Manuals Q76, Q107, and Q117, Edgewood Arsenal, U. S. Army. These manuals replace MIL-STD-282 and will eventually be replaced by an American Standard.

2. H. Gilbert, "Panel B - Round Table Discussion," Proceedings of the Eighth Air Cleaning Conference Held at Oak Ridge National Laboratory October 22-25, 1963, USAEC Report TID-7677, p. 439.

3. F. E. Adley and D. E. Anderson, "The Effect of Holes on the Performance Characteristics of High-Efficiency Filters," Proceedings of the Eighth Air Cleaning Conference Held at Oak Ridge National Laboratory October 22-25, 1963, pp. 494-507.

4. J. W. Thomas, "Aerosol Penetration Through Pinholed Filters," Health Physics 2: 667-673, Pergamon Press, 1965.

5. C. A. Burchsted, Oak Ridge National Laboratory, unpublished data, July 1966.

6. F. E. Adley, Hanford Occupational Health Foundation, personal communication, 1966.

7. R. H. Knuth, "Performance of Defective High Efficiency Filters," Am. Ind. Hyg. Assoc. J., 26: 593-600, November-December 1965.

8. Standard UL-586, High Efficiency Air Filter Units, Underwriters' Laboratories, Chicago, Illinois, June 1964.

9. L. Horn, "Panel B - Round Table Discussion," Proceedings of the Eighth Air Cleaning Conference Held at Oak Ridge National Laboratory October 22-25, 1963, USAEC Report TID-7677, p. 443.

10. Commercial Standard CS-45-64, Standard for Douglas Fir Plywood, U. S. Department of Commerce, 1964.

11. Commercial Standard CS-122-64, Standard for Western Softwood Plywood, U. S. Department of Commerce, 1964.

12. ASTM A165-55, "Specification for Electrodeposited Coatings of Cadmium on Steel," ASTM Standards 1966, Vol. 1, American Society for Testing and Materials, 1966.

13. ASTM A240-63, "Specification for Chromium and Chromium-Nickel Stainless Steel Plate, Sheet, and Strip for Fusion Welded Unfired Pressure Vessels," ASTM Standards 1966, Vol. 3, American Society for Testing and Materials, 1966.

14. C. A. Burchsted, "Qualification Test for Moisture and Corrosion Resistant Separator Materials," Tentative ORNL Standard AR-2.01, Oak Ridge National Laboratory, June 1966.

15. Military Specification MIL-F-51079, Filter Medium, Fire Resistant, High Efficiency, U. S. Army, April 6, 1962.

16. ASTM D1056-66, "Specification for Sponge and Cellular Rubber Products," ASTM Standards 1966, Vol. 28, American Society for Testing and Materials, 1966.

17. Commercial Standard CS-132-46, Standard for Hardware Cloth, U. S. Department of Commerce, 1946.

18. W. H. Echols and J. A. Young, Studies of Portable Air-Operated Generators, U. S. Naval Research Laboratory Report No. 5929, July 26, 1963.

19. A. R. Allan, Jr., Package for Filters, U. S. Patent No. 3,057,468, October 9, 1962.

20. H. Gilbert and J. H. Palmer, High Efficiency Particulate Air Filter Units; Inspection, Storage, Handling, Installation, USAEC Report TID-7023, August 1961.

# SUGGESTIONS ON SPECIFICATION WRITING FOR ABSOLUTE FILTERS

BY A. R. ALLAN, JR.

FLANDERS FILTERS, INC., RIVERHEAD N. Y.

Some recent specifications for absolute filters have been issued that are unnecessarily burdensome to the filter manufacturers. They appear to have been written without a full knowledge of either the product or the proceedure under which they are customarily purchased. We recommend that all proposed specifications be submitted for comment to the manufacturers in order that the specification writer may have the benefit of the manufacturers opinion.

The basic aim of a specification should be to assure the acquisition of a product of the desired quality at the lowest cost. A poorly written specification adds to the cost of a product in the following ways:

1. If the specification does not describe the produce adequately for the manufacturer to determine what is wanted.

   Example: "In addition, all type "A" and type "C" filters shall be capable of passing a minimum of 80% of rated flow of 95% to 100% saturated air at 200 degrees F. and a pressure differential of 2.5" w.g. for two hours." The problem here is one of wetting. Will it occur or won't it? The manufacturer must choose which separator to use. If wetting will occur it will be an expensive separator. If not, a cheaper one can be used.

   Some manufacturers will interpret this test to mean that wetting will occur, while others will not, so that a truly competitive bid will not be received.

2. Cost is added to a product by requiring material certification which is already certified to by the U.L. Label.

3. Cost is added by ambiguity. Example: "The glue used in the filter frame joints shall be water resistant with characteristics at least equal to the bonding glue used in the plywood." As the glue used to bond the plywood is pressure setting and the glue used in the joints is a rubber base or polyurethane foam one wonders what characteristics are supposed to be equal. Water resistance? Strength? Flexibility?

Two kinds of filters constitute the major portion used by A.E.C. prime contractors. One has an aluminum separator and the other an asbestos separator, while common to both are fire retardent plywood frames, glass or glass asbestos paper medium and either a rubber base or polyurethane foam adhesive. Surely one specification could cover both of these filters for all A.E.C. contractors. Both of these filters carry the U.L. Label and much of the specification can be accomplished by reference to the label.

Other filters in order of their approximate usage are as follows:

| Medium | Separators | Frame | Adhesive |
|---|---|---|---|
| Glass or Glass asbestos | Aluminum | Cad Plated Steel | Rubber or Poly Foam |
| Glass or Glass asbestos | Asbestos | Cad Plated Steel | Rubber or Poly Foam |
| Glass or Glass asbestos | Waterproof Asbestos | Cad Plated Steel | Rubber or Poly Foam |
| Glass or Glass asbestos | Waterproof Asbestos | Cad Plated Steel | Glass Packing |
| Glass or Glass asbestos | Aluminum | Cad Plated Steel | Glass Packing |

All of these are, or can be U.L. Labeled and one simple specification referencing U.L. could be used by all A.E.C. sites.

The U.L. Label has been obtained by all manufacturers at considerable expense. Its' purpose is to guarantee not only fire retardency but also efficiency, pressure drop and quality manufacture. With the U.L. Label available we see no reason why each site must have its' own specification for each filter. The U.L. Label assures the purchaser that certain tests have been performed on the filters and that the filters are made with materials of a certain standard. Duplication of U.L. testing and certification of materials called for in some recent specifications are unnecessary.

## DISCUSSION

CHEEVER: I would like to ask Mr. Allan, what type of specifications do you think are best for clean room filters? We have had some experience where the user would try to write-up his own specifications on vacuum cleaning of the filter and polybagging.

ALLAN: There is only one standard specification for clean rooms, and practically none for the filters, that I know of. As you also mentioned, everyone makes up his own and this is very confusing. The only specification now is the cleanliness of the room.

This business of vacuuming and polybagging of a filter is absolute nonsense. The filters just cannot be kept that clean in manufacture, and the only way to purge them, as far as I can see, is in the clean room itself, when the clean room itself is purged; and I would suggest that this be done at about double the flow of the filters, if possible.

I don't know enough to tell you how clean a clean room should be, and what small edge leaks that are present in most, or whether absolute filters are allowable or not. This is a thing that we are going through in this particular business of having each specifying engineer decide whether these leaks should be plugged or not plugged. We recently did a big job in which they decided they didn't have to be plugged, so I don't know.

BURCHSTED: I think that 99 percent of the requirements that we use for AEC filters, if you want to use that term, are equally applicable to clean room filters, and also we use a fire-resistant filter. Frequently the clean rooms are not so equipped and sooner or later are going to have trouble with some rather disastrous fires.

CHEEVER: Could I expand on one point? Would you recommend scan testing to be specified, or would you simply select filters that have a low penetration of DOP?

BURCHSTED: I have not gone into that myself, but I think that a low penetration DOP test will correlate pretty well with the scan. In any event, DOP testing, based on efficiency, is at least useful to determine if or where subsequent scanning may be needed.

THOMAS: I have Burchsted's paper here and, talking about 2-flow testing for pinhole effect, he says that he thinks a requirement ought to be made, with the maximum permissible difference in absolute value of penetration at the two flows to be 0.01%. In other words, if they differ more than that, the penetration was higher by more than 0.01% at the lower flow rate, they would reject the filter. I was just wondering why the requirement isn't made that the efficiency should be 99.97 at both flow rates instead of writing it up this way. Wouldn't it be simpler?

BURCHSTED: It would certainly be simpler. We made a statistical analysis of a number of filters from the AEC quality station and rechecked at ORNL, and we found there was a very high correlation between visible pinholing if the difference in penetration was 0.01% or more than that. We find a very distinct correlation on that point.

THOMAS: Do you think if a pinhole type defect exists, it might get worse? Is that the real reason? Whether you have the correlation or not, it seems to me the efficiency of 99.97 of flow rate ought to be sufficient. Do you think those with pinholes are going to get worse with air flowing through them?

BURCHSTED: Partly. Many of these filters are operated at very low air flows and the penetration at very low flow probably, in time, will get worse.

THOMAS: I think you finally convinced me.

PHELPS: I have a question for Mr. Burchsted. I was wondering if you could tell me what document would give a detailed description of this thermally generated DOP test?

BURCHSTED: I think Mr. Young can answer that question better than I can.

YOUNG: Military Specification 282.

BURCHSTED: 282 is now being revised, just to clarify the situation.

# EFFECT OF SHOCK OVERPRESSURES ON HIGH EFFICIENCY FILTER UNITS

W. L. Anderson
Naval Research Laboratory

T. Anderson
Naval Ordnance Laboratory

## INTRODUCTION

For many years air cleaning in the atomic energy program has been dependent upon the high-efficiency particulate air filters to prevent the spread of particulate matter that is toxic or radioactive. These units are specially constructed filtration devices that remove from the air stream particles one micron and less in size with a high degree of efficiency.

Early models of the filter units were constructed over U. S. Army Chemical Corps specifications and were composed of cellulose-asbestos filter paper, Kraft paper separators, and plywood frames. This type of filter unit was extensively evaluated and proven with respect to its overall performance (1) as well as its ability to withstand rough handling and blast damage (2). Although the unit was very efficient in the collection of small particles, the combination of the various materials of construction created a unit that was highly combustible and a serious fire hazard.

In order to overcome the combustible nature of the earlier filter units, a new fire-resistive high-efficiency particulate filter unit was designed and constructed. This new unit had the same or higher degree of filtration efficiency and was constructed of glass-fiber filter paper, asbestos or metal separators, non-combustible adhesives and with either fire-retardent plywood or metal frames.

At about the same time that construction material changes were being made to make the units fire resistant, specifications and/or manufacturing techniques were modified in order to accomplish some savings in manufacturing costs. Unfortunately these latter changes resulted in a loss of the inherent ruggedness of the original unit and the filters became very susceptible to damage in handling and shipping. Once this deficiency was recognized, corrective measures were initiated, specifications were strengthened, and the trend to frailty was reversed.

The high-efficiency filter manufactured over current specifications has the strength, durability, and performance equal to or better than the original combustible units (3). It is the purpose of this investigation to determine whether the resistance of the fire-resistant units to shock overpressures is equivalent to or better than the combustible units.

### Filter Unit Construction

Since all sizes of filters common to the AEC program were to be evaluated in this study, it was decided to obtain the units for test on a single procurement

from one individual manufacturer. It was believed that by this means, the materials of construction and the techniques of manufacturing would be identical for all units and that the differences in results could be attributed to the physical configurations of the units themselves. Elaborate precautions were taken to assure that the overall units conformed to the military specification MIL-F-51068A as amended by AEC Health and Safety Information Issue No. 212, June 25, 1965.

Prior to filter unit fabrication, representative samples of the filter media to be used were obtained from the manufacturer. All of the physical and performance characteristics of the media were determined to assure that the minimal requirements of the military specification MIL-F-51079 (as amended) for filter media were satisfied. Once these requirements were achieved, the filter media was certified for fabrication into the overall unit. DOP and resistance tests on the completed units were performed by the filter manufacturer to assure that the completed unit met the performance specification.

Following manufacture, all units were shipped via public transportation to the Filter Testing Station at Oak Ridge. At the station all units were inspected for conformance of construction components specified and for workmanship and transportation damage. Penetration and resistance tests of all units were conducted at 100% flow, 20% flow, and when encapsulated. The 20% flow was required to detect pinhole leaks in the media and/or adhesive; the encapsulation test was required to detect leaks in the frame and/or gasket seal. All units passed these tests and were certified for the shock studies. The units were then re-shipped by public transportation to the Naval Ordnance Laboratory where the shock studies were conducted. Upon arrival at the Laboratory all units were visually examined for transportation damage. One unit was selected at random, and individual tests performed to reassure performance of all aspects of the purchase specification. Following these tests, the unit was disassembled and the media tested for specification conformance.

## Shock Tests

All exposures of the filter units to the overpressures from the shock wave were conducted on the 180 foot Conical Shock Tube (CST) at the Naval Ordnance Laboratory. The CST consists of a cone frustrum 180 feet long, having a uniform taper of one foot in 90 (included angle approximately 2/3 degree). Figure 1 is a view of the CST looking down the tube from the detonation chamber end. The frustrum is 6 inches in diameter at the small end, tapering to a 30-inch diameter at the large end. The small end is attached to the muzzle of a 6-inch gun used as a firing chamber for the high explosive charge which generates the blast wave. Each filter for test was mounted in the center of a 1/4-inch thick steel plate which completely covered the open end of the CST. Figure 2 is a view of the CST looking down the tube from the filter test end. A filter unit, ready for test, is mounted on the end of the tube. Only the face of the filter was exposed

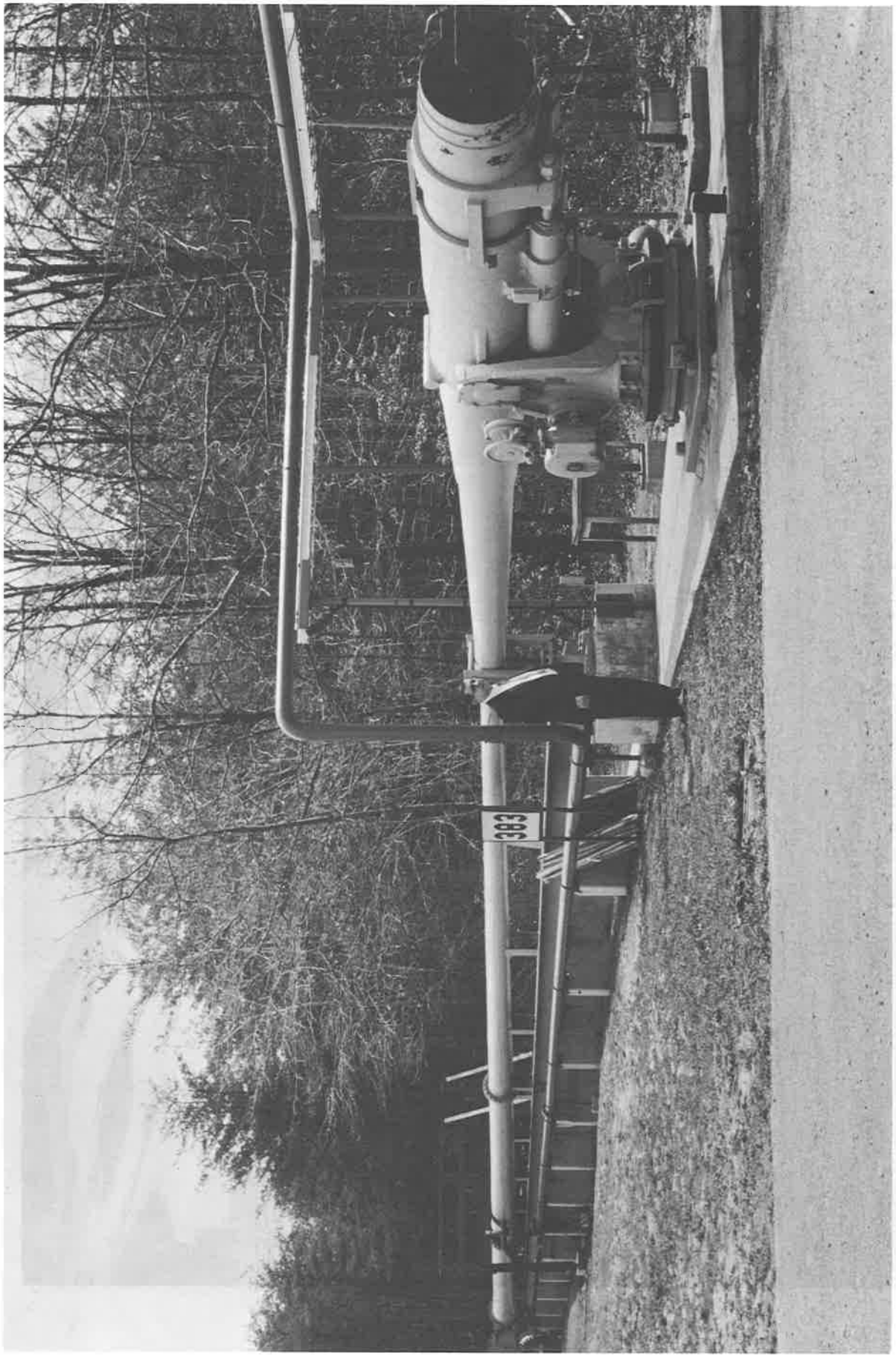


Figure 1. Conical Shock Tube from Detonator End

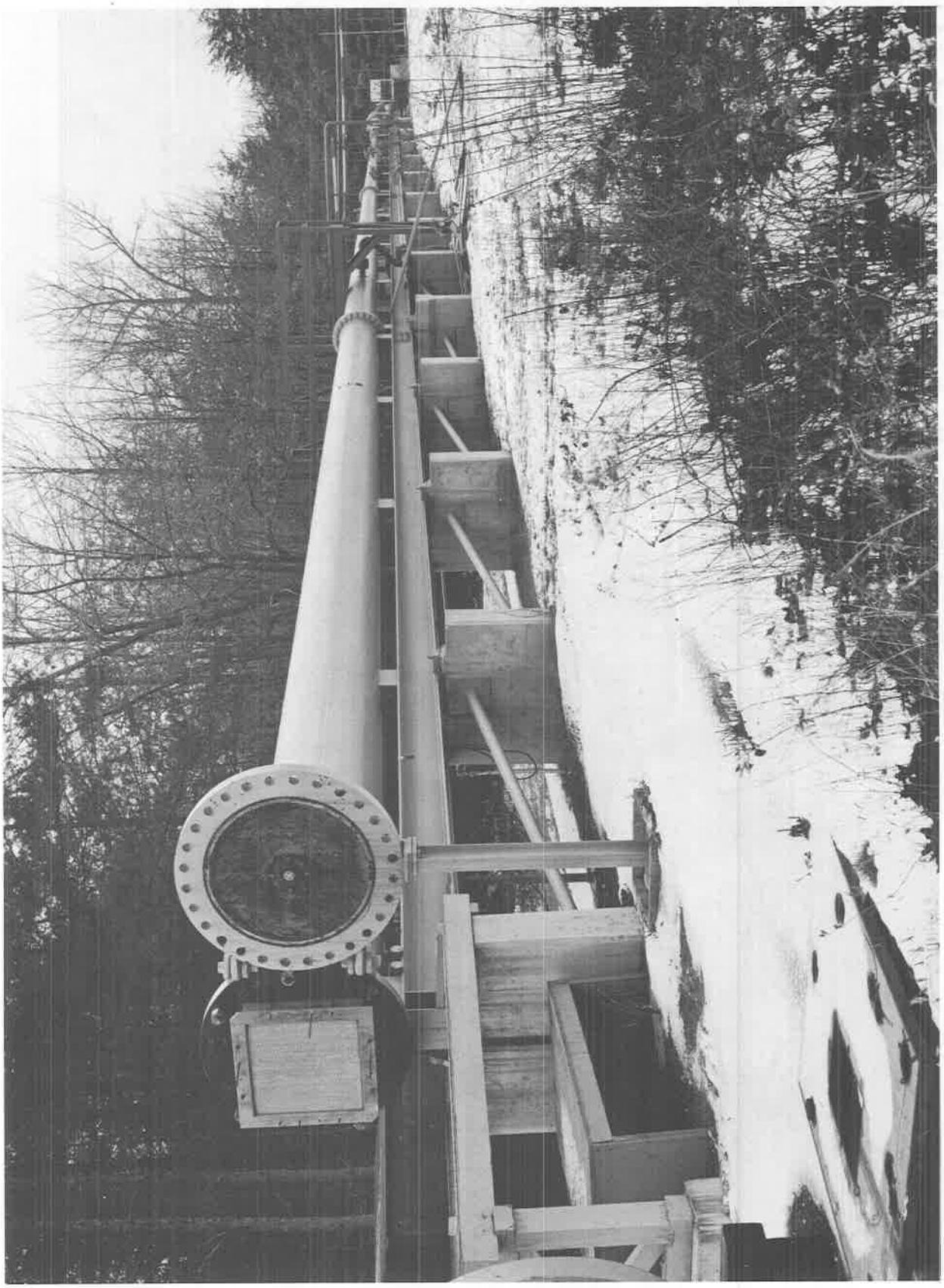

Figure 2. Conical Shock Tube from Test Plate End

to the blast; the remainder of the filter was outside the CST. The direction of motion of the blast wave was normal to the filter surface. Measurements of the pressure-time profile of the blast wave were made with piezoelectric gages mounted side-on with their faces flush with the interior of the CST. Two gages were used: one 1.5 feet and the other 3 feet from the face of the filter. Signals from the gages are fed to a Tektronix 502A dual beam oscilloscope and recorded by conventional Polaroid photography. An appropriate delay determined by the size of the explosive charge is introduced between the firing of the charge and the triggering of the scope. This permits the positive portion of the gage record to be displayed in more detail than if the charge firing and scope trigger occur simultaneously.

The explosive charges for this series of tests ranged from 0.5 to 86 grams in weight. The 0.5 gram charge consisted of an Olin-Mathieson plastic Seismo Cap. The larger charges were of cast Pentolite (50/50 mixture by weight of TNT and pent-erythritol tetranitrate). For charges 13 grams and larger, the Pentolite was in the form of one-inch diameter rods cut to length to give the desired weight. Smaller charges were made of 1/4-inch Pentolite rods. The initiator in all cases was the plastic Seismo "cap."

To fire the shock tube, a charge is taped to a Styrofoam support designed to center the charge in the chamber of the 6-inch gun. Figure 3 shows such a charge being inserted in the gun chamber. A detonator is inserted in a pre-drilled hole in the charge, the charge is placed in the gun chamber, the leads from the detonator are brought out through the primer hole in the gun breechblock, and the gun breech is closed. The detonator leads are connected to a firing line. When the instrumentation is ready, the charge is set off by a firing circuit supplying 250 volts DC to the detonator. Simultaneously, the time delay for the oscilloscope is triggered. The time required for the shock wave to get to the far end of the tube depends on the charge size used; for the tests reported here it is between 90 and 150 milliseconds (longer time corresponds to Seismo cap, the shorter for the 86-gram charge). Just before the blast wave gets to the gages, the oscilloscope is triggered by the delay, and the scope begins to record. The blast wave passes the gages, hits the filter and mounting plate and is reflected back. This stronger reflected wave passes the gage and is also recorded. Figure 4 shows typical pressure data recorded by the oscilloscope as the wave passes. Thus a record consists of a sudden sharp jump in pressure as the incident wave goes by, a slow drop in pressure as the wave continues toward the filter and returns, and a second sharp rise as the reflected wave passes. The pressure then decays slowly.

The pressures quoted in this investigation are the peak side-on (hydrostatic) pressure of the incident wave. This does not represent the full pressure that the filter sees but is indicative of the pressure that the filter would experience under use conditions. The actual pressure the test filter sees would also contain a component (the dynamic pressure) caused by the motion of the air particles behind the shock wave.

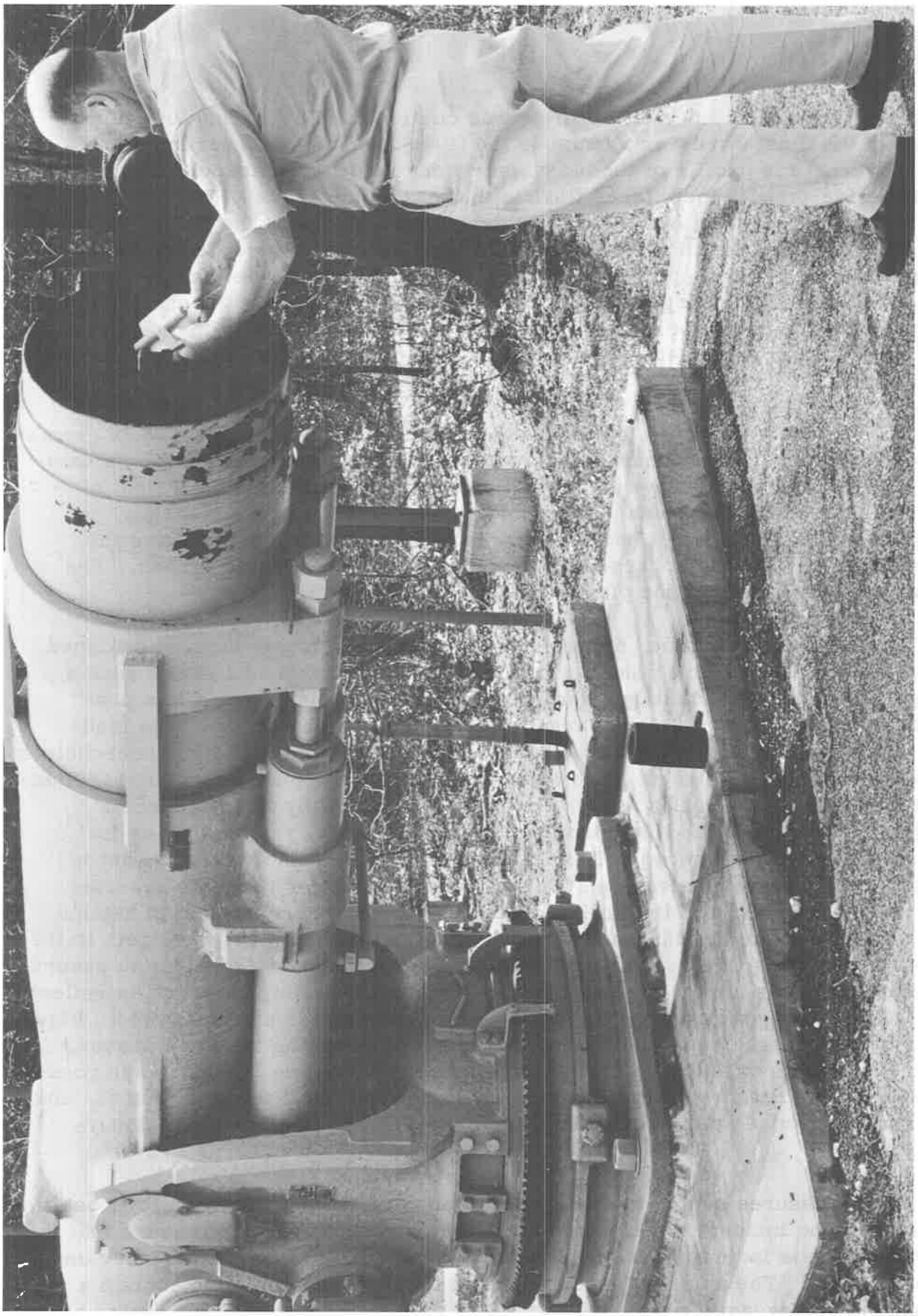

Figure 3. Insertion of Explosive Charge in Shock Tube

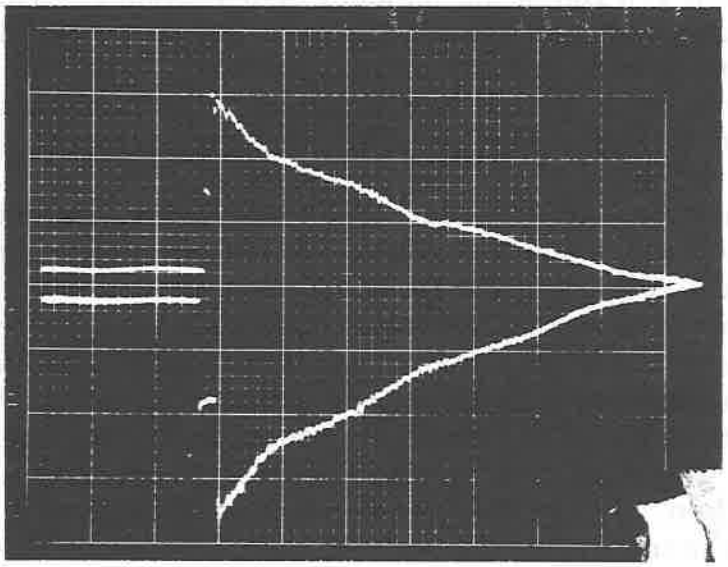

Figure 4. Pressure Shock Wave Traces

If the filter were perfectly rigid, the reflected pressure the filter sees is related to the side-on pressure at the filter face by the relation

$$P_R = 2P \left( \frac{102.9 + 4P}{102.9 + P} \right)$$

where $P_R$ = reflected pressure, psi

$P$ = side-on pressure, psi.

Since the filter is not rigid, the reflection coefficient 2 in the equation is affected. The departure from rigidity cannot be calculated, nor can the face-on (reflected) pressure at the filter face be measured directly since a gage cannot adequately follow the distortion of the filter face. However, an adjusted value of the reflection coefficient may be estimated from the test results. The peak reflected pressure observed was about 1.5 times the incident overpressure. Thus for the range $0 < P < 5$ psi used in this investigation, a reflection coefficient of 1.3 to 1.5 is indicated (as opposed to 2.0 for a rigid surface). For this investigation, the resistance of the filter is quoted as a function of the incident side-on pressure, since its resistance to an explosion is of prime importance.

A few comments about the blast wave shape (i.e. its pressure-time profile) should be made to understand the overall explosion-filter relationship. The purpose of the CST is to simulate the blast wave from very large spherical explosive charges. A spherical charge produces a blast wave characterized by a modified exponential decay of the overpressure starting immediately after the passage of the shock front. Unlike a true exponential decay, the pressure eventually decreases below the ambient pressure existing before passage of the shock wave. The time required for the overpressure to return to zero is the positive duration. Large charges produce long durations, and these long durations greatly increase the damage effects of the wave. For this reason, items which easily withstand 5 psi overpressure (small duration) from a small charge may be demolished by 5 psi waves from a nuclear explosion (long duration). The CST produces a positive duration of 50 milliseconds at its large end and this value is almost independent of charge size. The total explosive charge sizes simulated in these studies range from 33 to 5800 pounds. Thus, it should be stated that the peak overpressures which the filters will withstand as determined in these studies are conservative if one is considering the effect of a small local explosion.

## RESULTS

Each filter unit was secured to the test plate and tested individually. At the start of the program, a given unit was subjected to gradually increasing overpressures until such time as a tentative break point was established. Once an estimation of the failure pressure was determined, individual units were

evaluated at overpressures broaching the previously determined break point to clearly define the limit of resistance to the overpressure wave. After each exposure to the shock wave, the filter unit was removed from the shock tube and visually examined. If no visible damage was apparent, the filter was installed in the smoke test rig and the DOP penetration determined. The unit was said to have failed when the penetration values exceeded the specification penetration for the unit, i.e., > 0.030%.

A listing of all of the shock tests on the various sized units is given in Table 1. These units have been certified to have met the minimal specification requirements and are equivalent to those currently commercially available from various manufacturers. The values of overpressures

TABLE 1

FILTER UNIT SHOCK STUDIES

| Filter Size | Measured Peak Overpressures |
|---|---|
| 8x8x3 | 2.6, 2.99, 3.00, 3.09, 3.22, 3.27, 3.31, 3.45, 3.51, 3.68, 3.94, 4.04, 4.09, 4.41 |
| 8x8x6 | 3.1, 3.53, 3.58, 3.84, 4.08, 4.11, 4.32, 4.53, 4.54, 4.76, 4.92, 5.00 |
| 12x12x6 | 2.5, 2.52, 2.92, 3.00, 3.13, 3.47, 3.58, 3.58, 3.59, 4.19, 4.25 |
| 24x24x6 | 0.72, 1.20, 1.44, 1.94, 2.26, 2.53, 2.83, 2.84 |
| 24x24x12 | 2.68, 2.86, 2.99, 3.12, 3.25, 3.30, 3.46, 3.52, 3.65 |

that are underlined are those where the filter unit was determined to have failed during test. The absence of an underline indicates that there was no detectable change in unit performance. Table 2 shows in summary form the results of the shock tests.

TABLE 2

SUMMARY FILTER UNIT SHOCK STUDIES

| Filter Size | Overpressure at Failure (PSI) |
|---|---|
| 8x8x3 | 3.6 |
| 8x8x6 | 4.5 |
| 12x12x6 | 3.6 |
| 24x24x6 | 2.2 |
| 24x24x12 | 3.2 |

It can be seen from the data that the physical dimensions of the units are related to the ability of the units to withstand the overpressure wave. In general, the smaller the individual unit and the thicker the unit of a given size, the better its ability is to withstand the shock wave. The actual points of failure were also indicative of the pressure wave intensity. Pressures near the failure pressures resulted in adhesive cracking or small leaks at the media-adhesive bond. Pressures of 0.5 to 1.0 psi greater than the failure pressure resulted in blowout slits in the downstream ends of the filter pleats. Figure 5 shows specific areas of slit damage of one of the units tested. An enlarged view of one of the slits in this filter is shown in Figure 6. It is believed that this type of damage resulted from either weaknesses present in the media (due to creasing during pleating operations) and/or a lateral movement of the separators during the blast wave passage. Pressures of more than 2 psi greater than the ultimate failure pressures caused extensive damage to the filter unit. Figure 7 shows extensive cross pleat cracking of one of the units tested at this level. It is believed that lateral movement of the unsupported center section was the cause of this type of damage. On occasion, essentially all of the media and separators were removed from the frame during tests at the higher levels of overpressures. Figure 8 shows such a filter after test at the elevated overpressures, e.g., 8-10 psi.

Since the adhesive cracking was the initial point of failure, a small amount of effort was directed toward its solution. A polyurthane foam-type material was investigated as a possible replacement adhesive. Several units of different sizes were constructed using this type of adhesive and the units subjected to the shock tests. Table 3 shows the results of these tests.

TABLE 3

EFFECT OF FOAM ADHESIVE

| Filter Size | Adhesive | Measured Peak Overpressure |
|---|---|---|
| 8x8x3 | Regular | 2.6, 3.0, 3.2, 3.5, 3.7, 3.9, 4.0, 4.1 |
| 8x8x3 | Foam | 2.5, 3.0, 3.4, 3.5 |
| 8x8x6 | Regular | 3.1, 3.5, 3.8, 4.1, 4.3, 4.5, 4.7, 4.9 |
| | Foam | 3.1, 3.95, 4.6, 5.1 |
| 24x24x12 | Regular | 2.7, 2.9, 3.1, 3.25, 3.46, 3.52, 3.65 |
| 24x24x12 | Foam | 3.39, 3.5, 3.8 |

It can be concluded from this study that the foam-type adhesive gave very little, if any, additional resistance to overpressure shock waves. In fact, if suitable precautions were not taken to insure a good adhesive to plywood frame

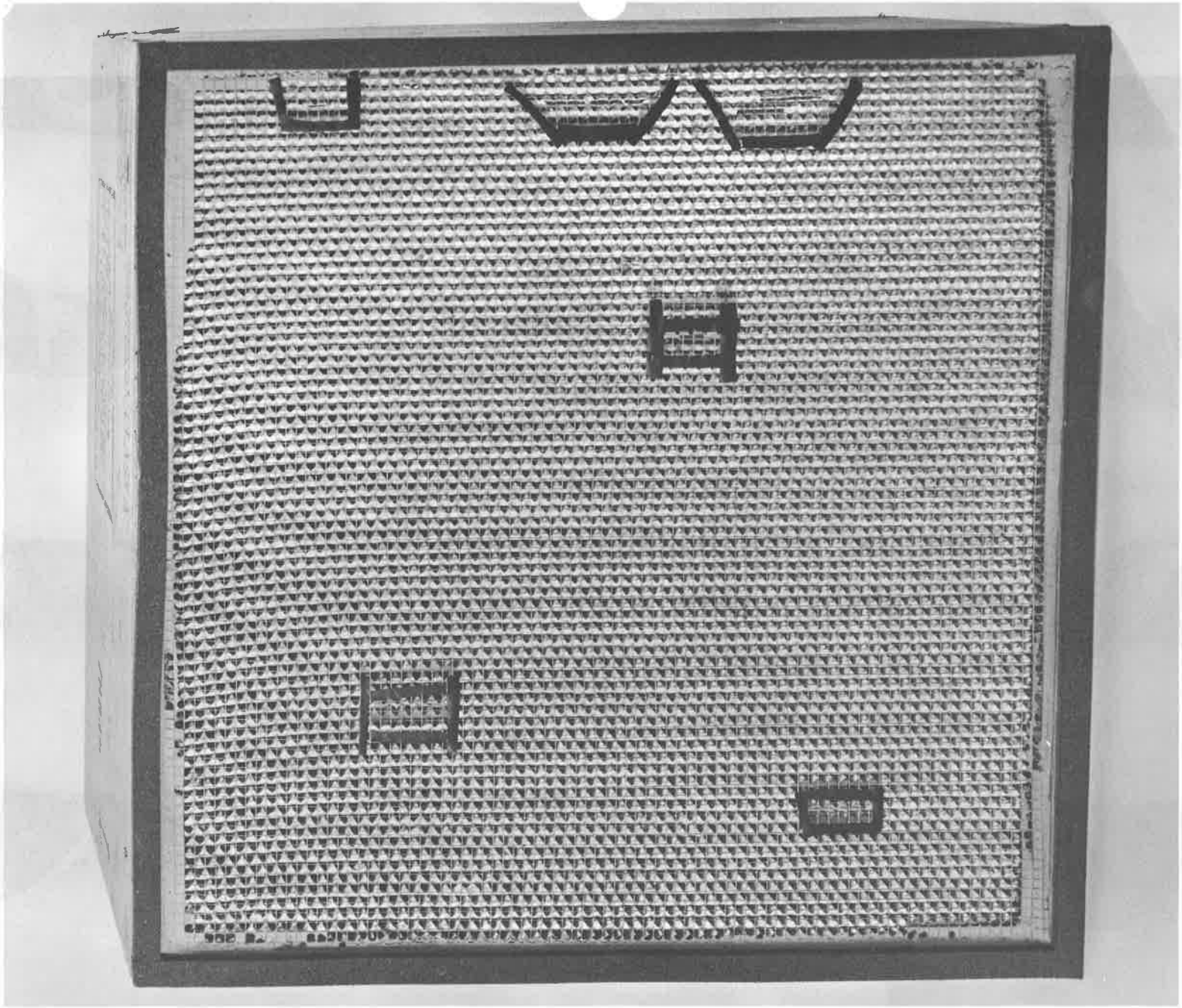

Figure 5. Typical Damage to Filter Unit (0.5 to 1.0 psi greater than failure pressures)

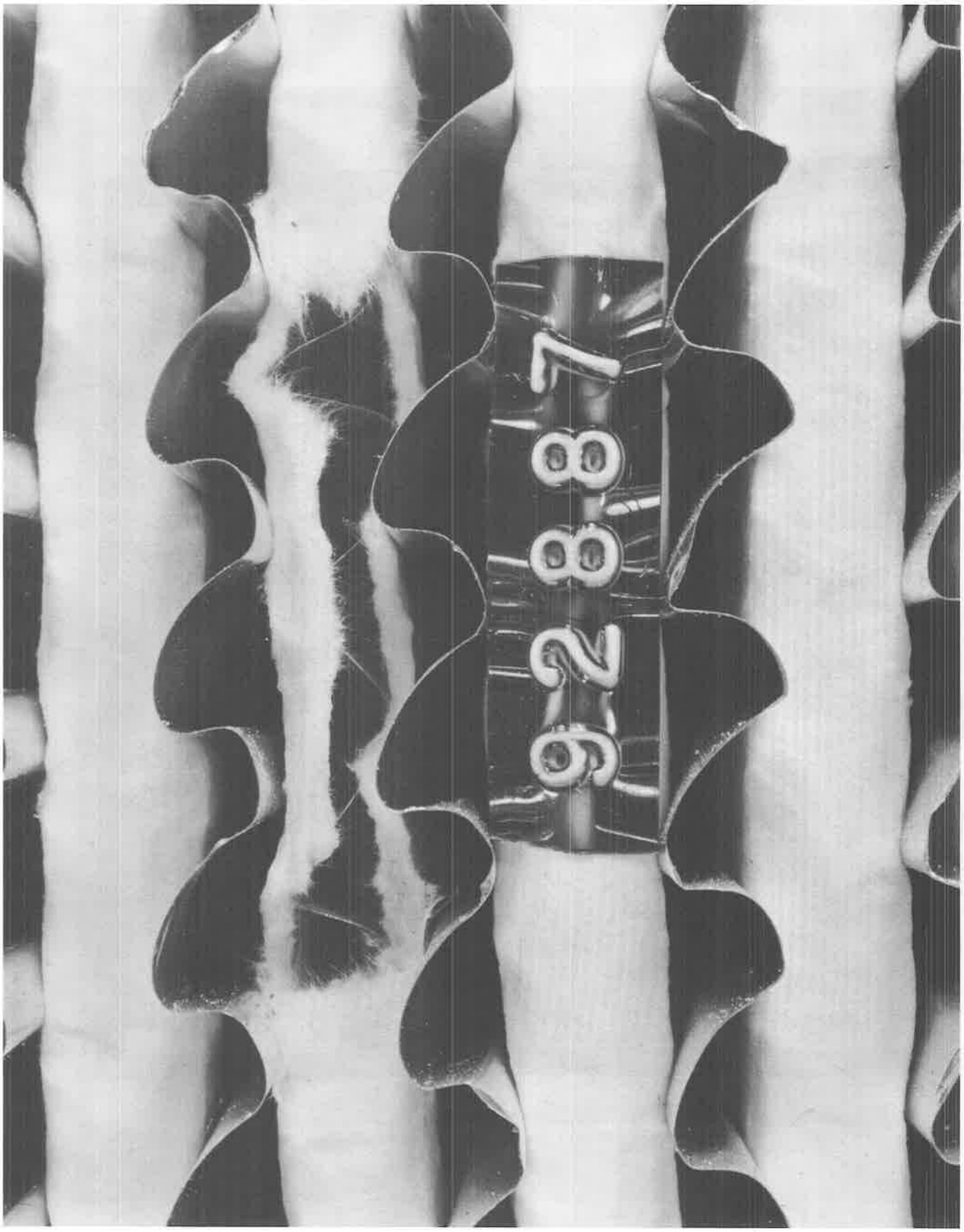


Figure 6. Enlargement of Damage Shown in Figure 5.

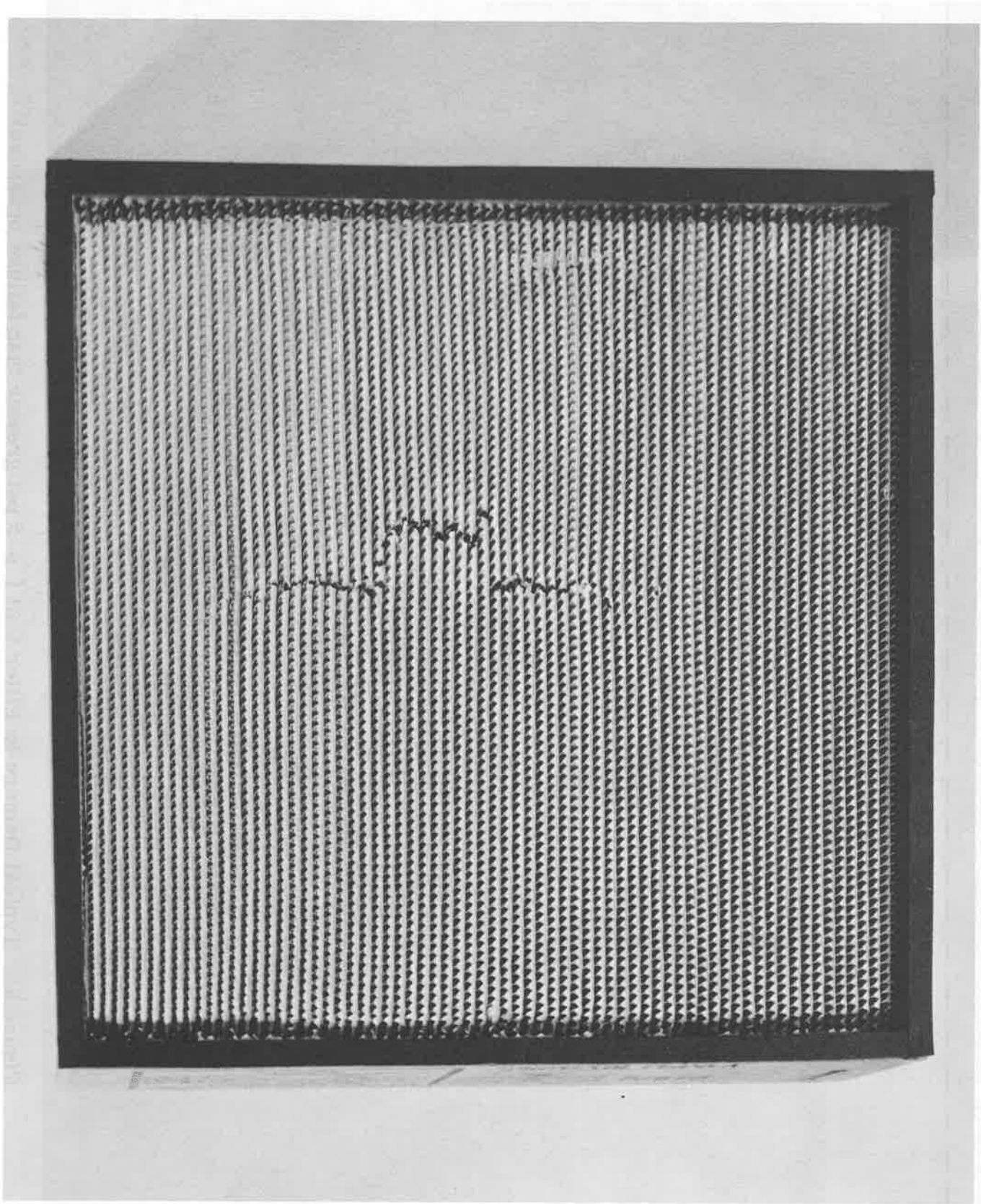

Figure 7. Typical Damage to Filter Unit (1 to 2 psi greater than failure pressure)

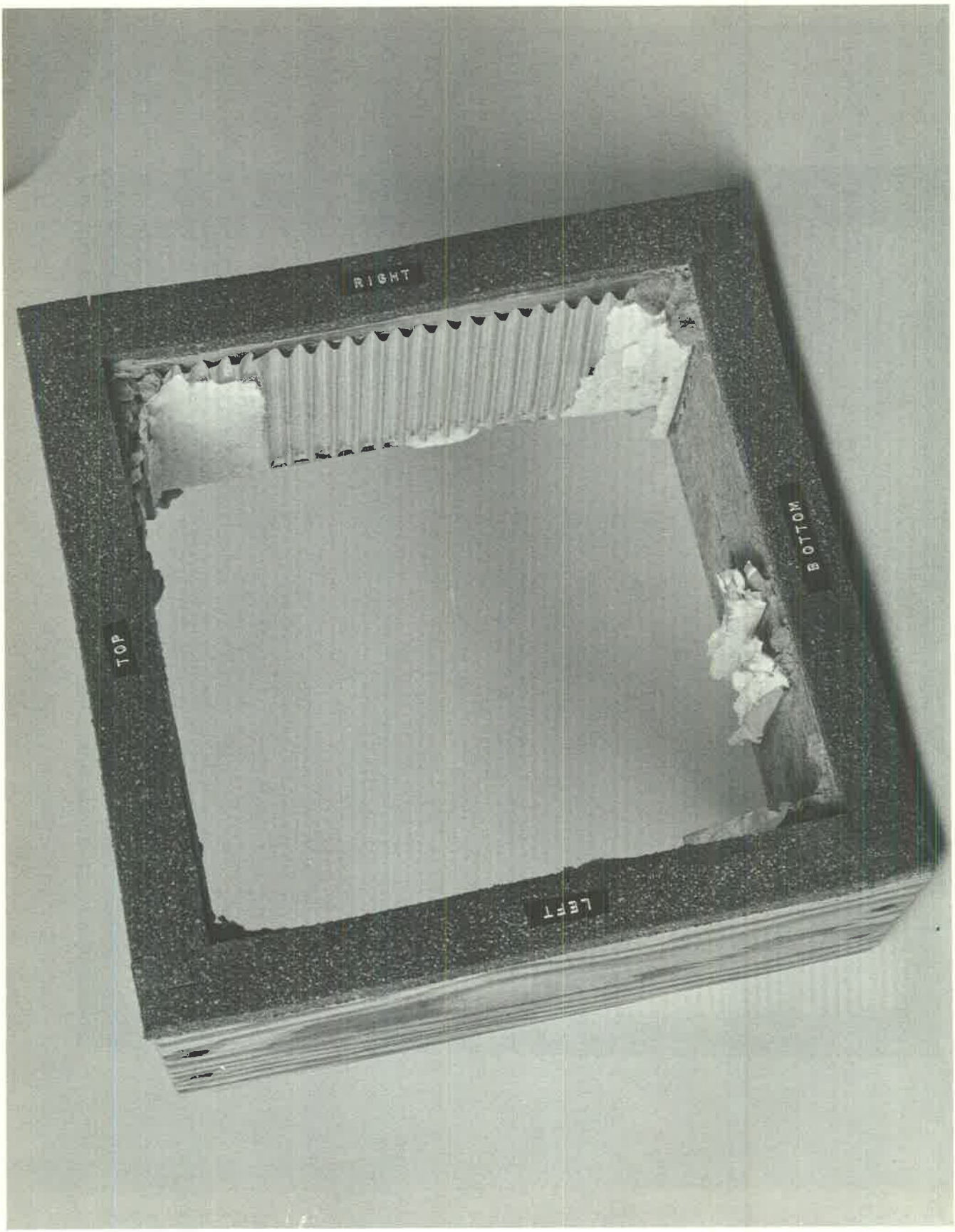


Figure 8. Typical Damage to Filter Unit ( > 5 psi greater than failure pressure)

bond, the entire filter-separator pack could be removed as one plug at lower overpressures than with the regular adhesives. Figure 9 shows the result when the adhesive does not make a good bond with the frame.

All of the above results were obtained with new filter units. Of equal concern was the shock resistance of the filter units as they were approaching the end of their useful service life. To study this problem, a number of filter units were artificially loaded with dust to simulate accumulation of natural debris as a function of time. The test dust utilized was a finely divided talc that is similar to many dusts encountered in industry and yet readily available in large quantities. Microscopic sizing showed the median number diameter to be about 0.5 microns and the mass median diameter to be about 1.8 microns. All filter units were loaded with the talc until the resistance drop of the total unit reached 4.0 in. of water at its rated flow (an increase in resistance of about 5). The loaded units were then mounted on the shock tube with the dust-laden side toward the explosive charge. Since resistance to shock overpressure was the variable to be studied, no effort was made to determine dust re-entrainment or loading loss due to the shock wave passage. Table 4 shows the results of this particular study. It can be seen from this

TABLE 4

EFFECT OF DUST LOADING

| Filter Size | Condition | Measured Peak Overpressure (PSI) |
|---|---|---|
| 8x8x6 | Regular | 3.1, 3.5, 3.8, 4.1, 4.3, 4.5, 4.7, 4.9 |
| 8x8x6 | Dust Loaded | 2.9, 3.0, 3.7, 3.9, 3.93, 4.83 |
| 24x24x12 | Regular | 2.7, 2.9, 3.1, 3.25, 3.46, 3.52, 3.65 |
| 24x24x12 | Dust Loaded | 2.39, 2.9, 3.1 |

table that the accumulation of dust on the unit lowers its resistance to the overpressure shock wave. The increase in loading equivalent to a 5-fold increase in air resistance shows about a 15% drop in the shock wave resistance capability.

It was noticed that during the shock tests of the 24x24x6 units, the hardware cloth protective screen was often loosened and sometimes partially separated from the frame. A check on the merit of this screen material for overpressure resistance was made. Several 24x24x6 filter units were obtained without the standard wire cloth facings. These units were tested on the shock tube and the results are compared with the standard units in Table 5. It can be seen from this data that

Figure 9. Poor Adhesive Bond Between Filter Media and Frame

TABLE 5

EFFECT OF WIRE CLOTH FACING

| Filter Size | Condition | Measured Peak Overpressure, PSI |
|---|---|---|
| 24x24x6 | Regular | 0.72, 1.2, 1.4, 1.9, 2.3, 2.5, 2.8, 2.9 |
| 24x24x6 | W/O Cloth Facing | 0.60, 1.2, 1.4, 1.9 |

the wire cloth facing does give some rigidity to the filter unit and that resistance (overpressure) of the unit with the wire cloth is increased by about 40%.

## CONCLUSIONS

As a result of these studies it can be concluded that the present non-combustible high-efficiency filter units have as good a resistance to blast overpressures as those reported earlier for the combustible units. It is apparent that the physical dimensions of the filter unit itself is one of the controlling factors in rupture due to shock waves. In general, the longer and thinner the unsupported span of filter media, the lower the shock wave required for failure. The simple addition of the hardware wire cloth for the protection of physical damage seems to increase materially the resistance to shock. It is believed that additional work on resilient adhesives and methods of support for the center areas of the larger filter units would result in a filter unit that would be markedly improved with respect to blast resistance.

## REFERENCES


(1) "Investigations of Stock Gas Filtering Requirements and Development of Suitable Filters," NYO-1575, Waste Disposal, June 30, 1951

(2) "Blast Effects in an Air Cleaning System," R. Dennis, C. C. Billings, and L. Silverman, W-T-1475, Dept. of Commerce

(3) "Development of a High Temperature-High Efficiency Air Filter," NYO-4527, Waste Disposal, Aug. 18, 1953

# EFFECT OF FIRE INTRUSION AND HEAT ON HEPA FILTER UNITS

Jack L. Murrow

Lawrence Radiation Laboratory, University of California

Livermore, California

## ABSTRACT

Special equipment has been developed for the dynamic testing of 1000-cfm high-efficiency particulate air filters by fire intrusion or high temperature. USNRL-type mechanical D.O.P. generator and photometer systems are used to determine "before" and "after" filter efficiencies. The degree of protection of the HEPA filter from fire is almost directly related to the heat-absorbing capacity of the prefilter. Three new sealing materials have successfully passed hot gas tests. Particle board treated for fire retardance by the pressure-soak method has been accepted as framing material. Particle board having the fire-retardant material mixed in before pressing also shows promise as framing material, and is less expensive than particle board or plywood treated by soaking.

In the early part of World War II the Chemical Warfare Service contracted with the Arthur D. Little Co. to develop high efficiency filter "paper". Their research soon led to the media known as CWS-6, a mixture of cellulose fibers and Bolivian blue asbestos. Continued work, especially with experimental batches of glass fibers, showed that mixtures of glass fibers and asbestos as well as glass fibers with binders could be used to produce high efficiency filter media.

Manhattan District engineers realizing the need for high efficiency, high volume, medium pressure drop space filters had them produced by the Chemical Warfare Service. They consisted of CWS-6 paper arranged in large pleats around heavy, serrated, cardboard separators in a wooden frame.

Upon declassification of materials and methods, the filters were produced commercially by one company, later by two more, and presently by four companies in the United States. As the Atomic Energy program increased, the incidence of fires in filters and filter banks increased. The combustible materials of construction not only allowed but encouraged the spread of fire from a single unit to an entire bank, causing extensive equipment damage and long shutdowns. As part of the program to reduce these losses, the AEC requested A. D. Little Co. to do further development on space filters to increase their capacity and to find other filter fibers which were available in the U. S. and which were more uniform. Non-combustibility would also be desirable. The result was the forerunner of the HEPA filter we use today.

As more customers requested fire resistant filters, the filter manufacturers persuaded the glass fiber manufacturers to produce the fine fibers in commercial quantities. Following the research already done by A. D. Little Co. the filter manufacturers were then able to produce fire resistant filters.

In 1956, Mr. Palmer, an engineer at General Electric Co., Hanford, began a series of tests to evaluate the durability and fire-spread characteristics of filters under fire intrustion to select the best filters for the Hanford works. The AEC, Fire & Safety Division, recognized the need for these tests and encouraged Mr. Palmer. The testing program continued at intervals until Mr. Palmer retired in 1961.

By 1963 equipment was available to LRL Livermore to carry on a modified series of fire-intrusion tests. Later Modifications permitted testing of fire-stop filters as protection for HEPA filters and for full-flow, hot-air tests. The addition of a multipoint temperature recorder and a portable DOP generator-photometer has made the results somewhat quantitative.

## FIRE INTRUSION

The first series of tests were performed on June 24 and 25, 1963, with the equipment shown in Fig. 1. The equipment was designed to test the resistance of the filter pack to fire intrusion. A dolly, carrying a cluster of five natural gas-air burners, could be positioned as close to the filter as desired. Any or all could be used. Figure 2 shows the burners, hand-supported

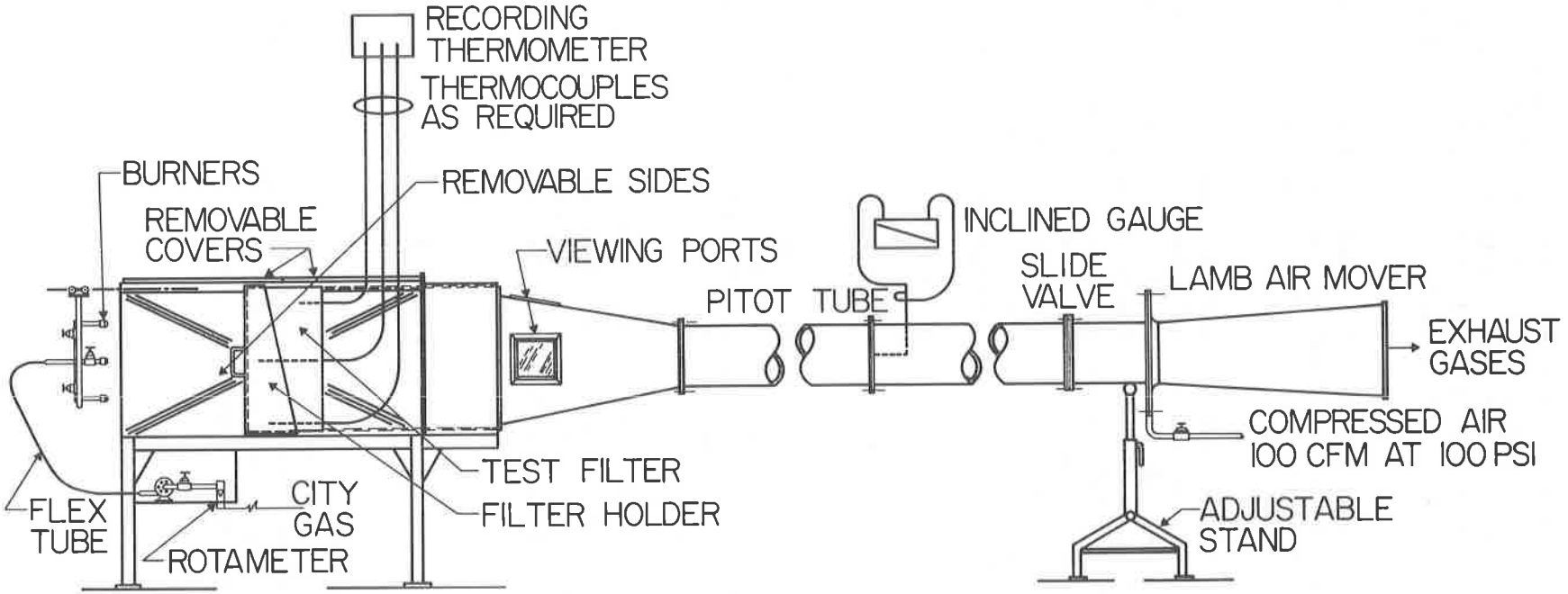


Fig. 1, Test equipment, schematic

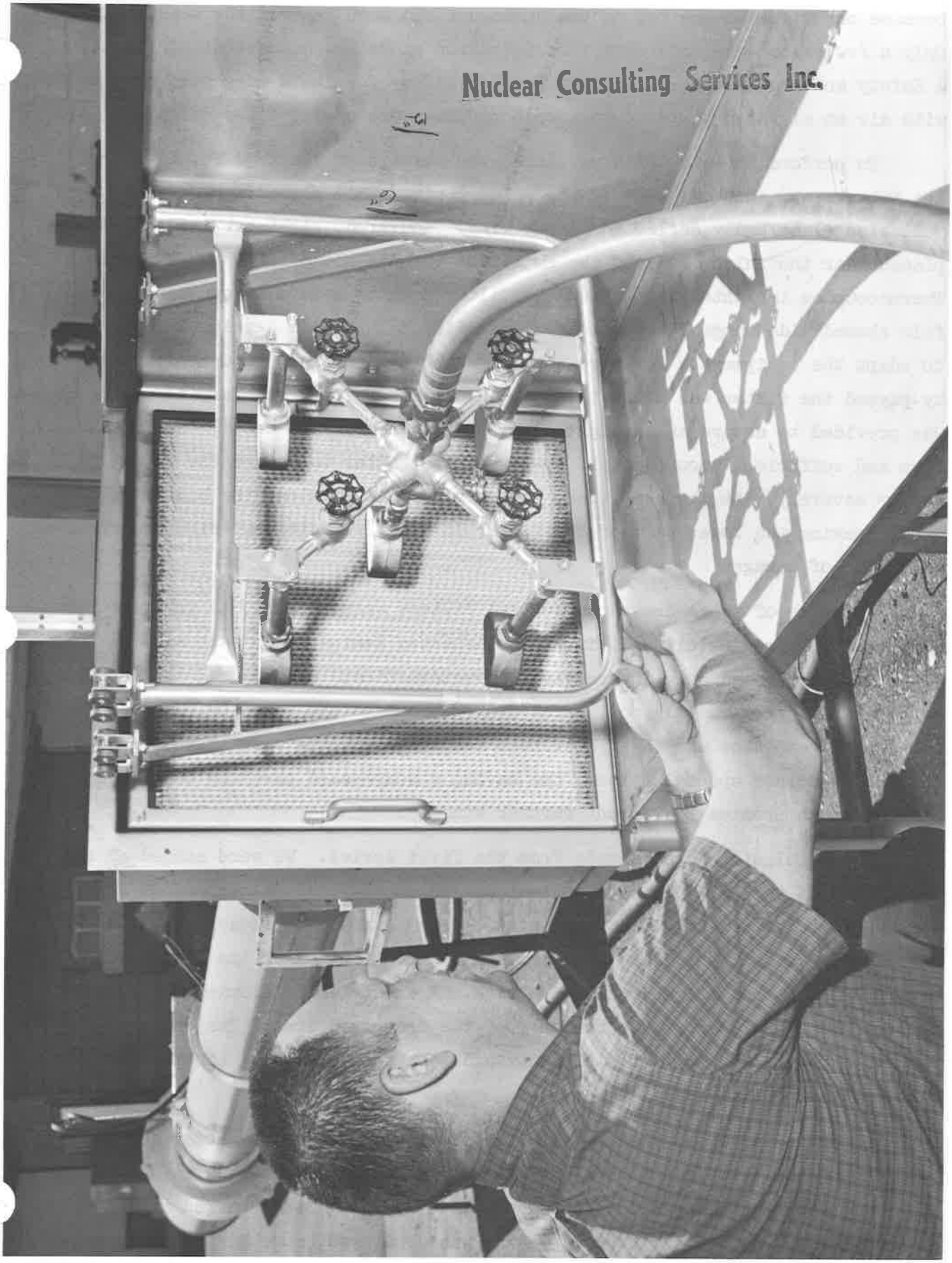


Figure 2. Test Set Up with Top and Side Removed

because one side and the top of the enclosure had been removed for observation. Only a few tests were made with fire intrusion since Mr. Gilbert of AEC Health & Safety and Mr. Keigher of the AEC Reactor Safety Committee suggested that tests with air at elevated temperatures would provide more useful information.

To perform hot-air tests we placed the burners at least 36 in. away from the filters and shut off most of the primary air. This formed a wavering, yellowish flame badly deflected by the wind. Louvered, sight-barrier screens, placed near the inlet, reduced the amplitude but did not eliminate the problem. Thermocouples implanted throughout the filter pack to obtain a temperature profile showed wide range fluctuations. An additional problem developed in trying to adapt the equipment. For fire-intrusion tests, the small amount of air that by-passed the filter was of little consequence, therefore, no clamping mechanism was provided to assure an airtight seal. During heated air tests, the hot air rose and sufficient amounts of it by-passed the filter to damage the frame exterior severely. At the same time, unheated air flowed along the bottom of the duct, leaving the lower part of the filter in "mint" condition. Figure 3 shows this type of damage.

In spite of these drawbacks several filters were tested. An experimental filter with approximately 1/16 in. thick asbestos laminated on each side of the plywood frame showed some interesting characteristics; Heat caused the asbestos to delaminate from the plywood, which charred beneath the asbestos. The joint between the asbestos and the filter pack reacted about the same as in standard filters. Another special filter, one having a compressed particle board frame, showed enough promise to warrant further studies.

Few conclusions can be made from the first series. We were amazed at the resistance of the HEPA filter (fabricated with glass fiber filter medium and aluminum separators) to direct and intense fire intrusion. Because heat was rapidly dissipated, only localized melting and destruction of the medium and separators occurred at the point of attack. A thin film of aluminum appeared to flow over the glass at the boundary of the destroyed area. The depth of destruction depended on flame intensity and length of exposure. Most of the filters reacted similarly.

As discussed above, the hot-air tests were ranging in character due to by-passing and air stratification. The filters were severely damaged at the top. The frame was charred outside because of the by-passing, and charred more deeply on the inside. As the sealant and medium was destroyed, more of the hot gasses passed, causing progressive destruction.

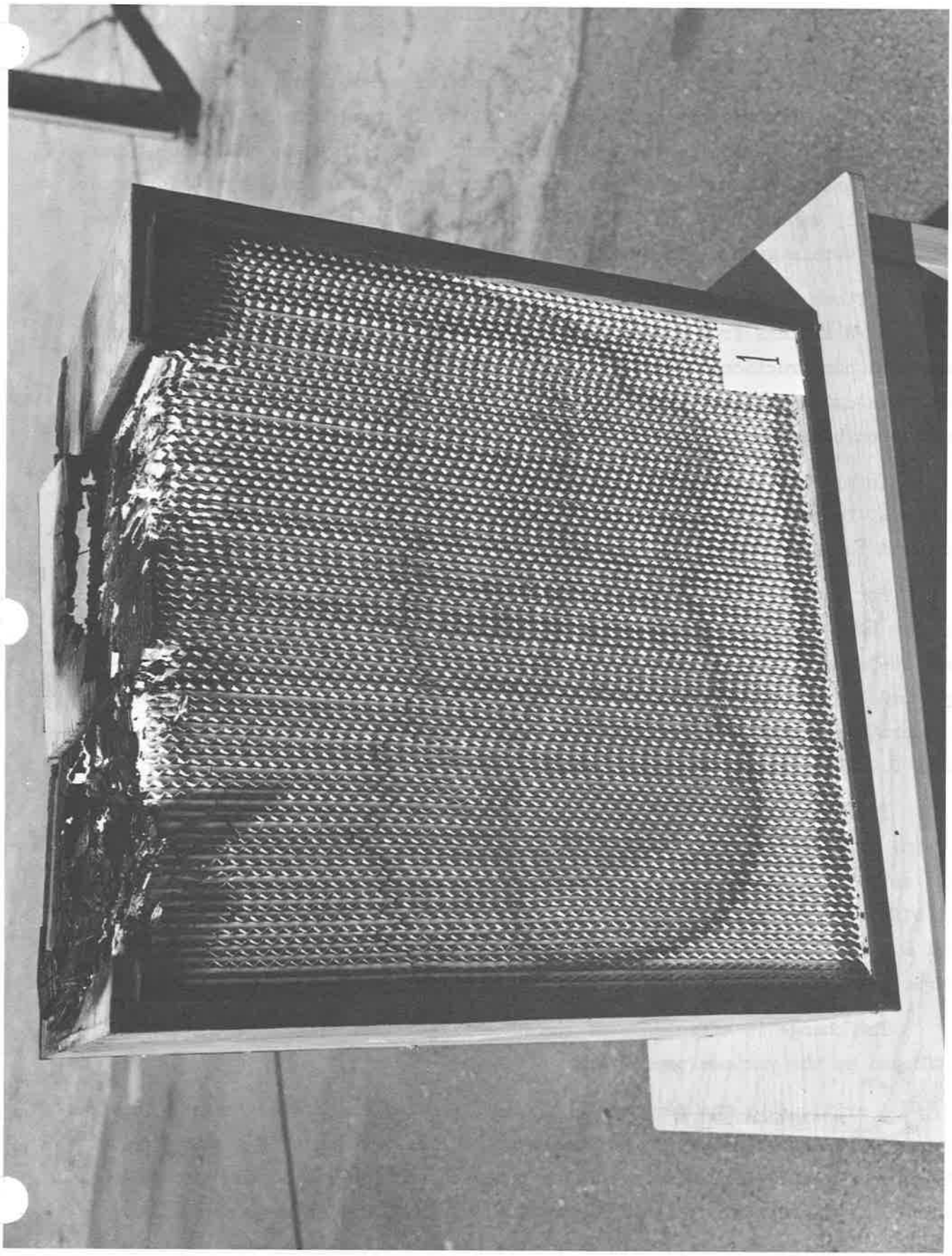


Figure 3. Upstream, Overall

## FIRE-STOP FILTERS

During the summer of 1964, we prepared for a new series of tests to check the relative effectiveness of various metallic filters when used as fire-stop filters ahead of HEPA filters. The equipment used before was modified to permit the insertion of metallic filters either 1- or 2-in. thick by 24-in. square immediately upstream of the HEPA filter. Flanges and clamping equipment were added to obtain good seals on each face of the HEPA filter.

Fifteen metallic filters from six manufacturers were obtained for testing. HEPA filters from a single batch were used for comparison. They were of standard construction, that is, fire-retardant, treated-plywood frames, glass media, aluminum separators, self-extinguishing rubber adhesive and 1/4-in. mesh screen on both faces.

In mid-September 1964, Messers. Humphrey Gilbert, AEC Health & Safety; James A. Young, USNRL, and James Palmer, AEC Consultant, formerly from Hanford, arrived to assist with the tests.

For each test a prefilter, HEPA filter, and appropriate holder were placed in the test unit. The airflow was adjusted to 1000 cfm and the gas burners operated for 5 min. At the end of the test period, the burners were extinguished but the airflow was continued until the equipment cooled to ambient temperatures. The final step was to test the system for efficiency with mechanical D.O.P.

Preliminary tests showed the optimum placing of the burner assembly was 12-in. from the face of the prefilter. A suitable gas-flow rate was determined and set with a control valve, permitting duplication on succeeding tests with an off/on valve. Several prefiring efficiency tests of the system by mechanical D.O.P. showed the same results as that marked by the manufacturer. Therefore, the prefiring test was eliminated.

The change in efficiency of the HEPA filter then indicated the protection afforded by the various prefilters.

A critique by the persons involved in the September 1964 tests emphasized some of the deficiencies in the equipment. Plans were made for future tests. As a result, additional equipment was procured and fabricated to permit better control of the hot-air tests. Figure 4 shows the modified test setup. It consists of a large-capacity, natural gas burner and sections of ducting with baffles ahead of the test filters. The longer, tortuous air path provides an

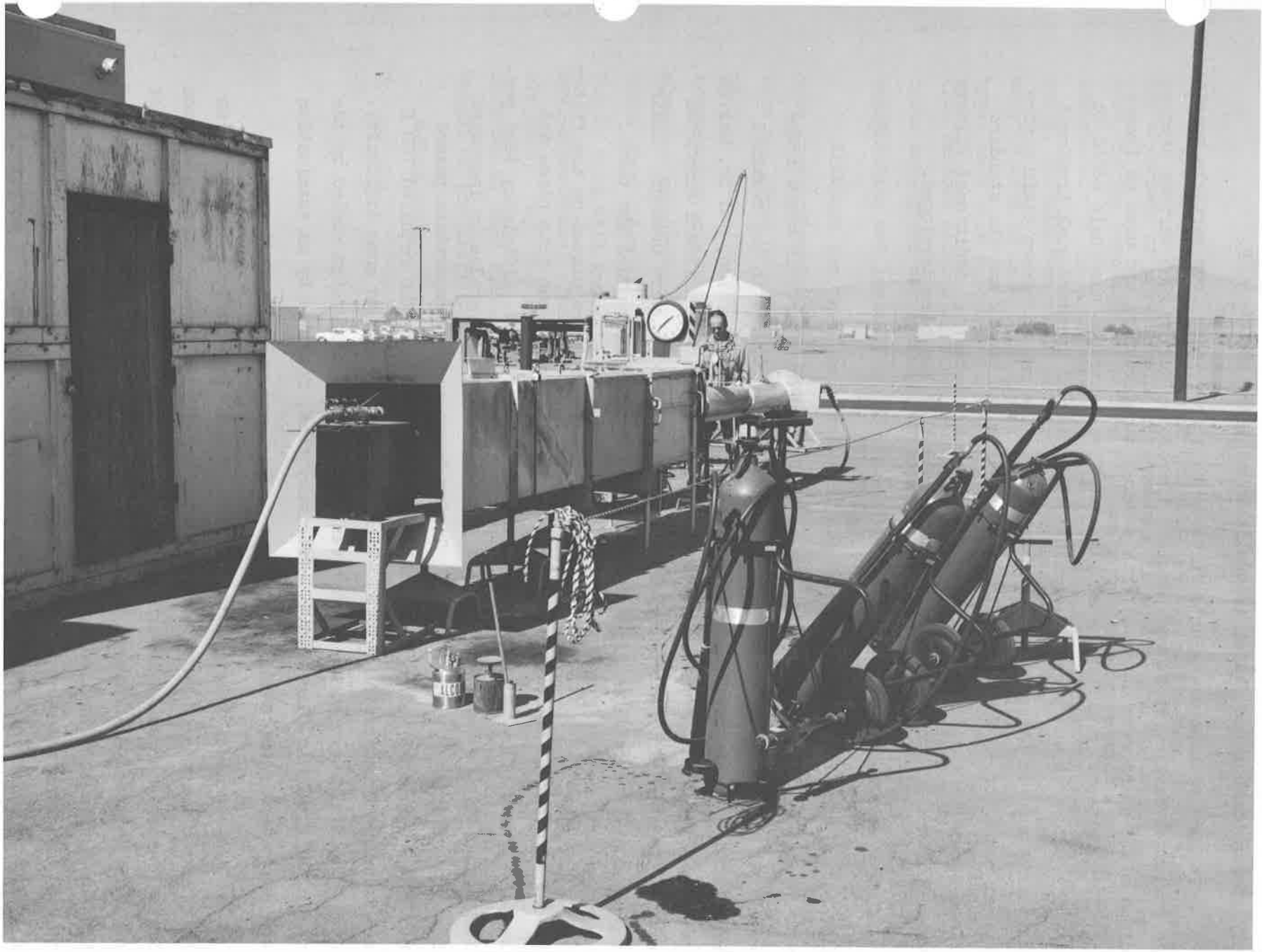

Figure 4. Modified Test Setup

## DISCUSSION

BROWNING: On the first one, Mr. Young, I believe that you tested the efficiency of filters after exposure to shock and, in some cases where you saw no visible damage, you observed deterioration of the efficiency. Do you have any ideas about the mechanism of deterioration of efficiency? When you looked at the medium could you see that there were little cracks in it, that it had been bent, or some other explanation?

YOUNG: We measured the efficiency to find out whether the filter was good or not. You couldn't trust your eye. Cracks or deviations or fractures smaller than what you could detect with your eye would show up by a change in DOP penetration.

Of course, we did not claim that a filter was of no value unless penetration had gone beyond .03 percent. In general, the filters would start out with much lower penetration than .03. It was only when they went beyond the .03 specification that it deemed to be a defective filter.

BROWNING: The question in my mind is, was there ever deterioration that could not be explained by something you could see? Did you always have an explanation as to why it deteriorated? Could you see cracks and things like that?

YOUNG: We could see cracks or find a deviation in the filter in some places.

McFEE: I have a question for Mr. Murrow. Could you tell me whether you made any oxygen availability tests at the filter interface?

MURROW: Not at the filter interface. We made it downstream, before the air mover, which might be considered a sort of average of the conditions under the heat test. Mr. Millham, do you remember the oxygen at that point?

MILLHAM: 16.2 percent in contrast to normal 20.9.

MURROW: 16.2 percent, determined by our calibrated Orsat apparatus.

YOUNG: I might have to amplify the question, which I just answered, and that is that a part of this examination of filter after a shock test was to probe the filter if it exceeded the specification, with a small probe, so you could then locate where the penetration had occurred.

SMITH: In your tests on filters, was the frame exposed, the entire frame exposed, to the high temperatures?

MURROW: On the latter series of tests, those which had the 300 series numbers, the downstream face of the filter was sealed, so that actually, all of the hot air went through the filter and none bypassed, thereby exposing only the inside of the frame. In the earlier tests, before the change in the equipment, some major portion of it went through, but some of it bypassed and went over the top showing deterioration to the outside of the frame.

SMITH: Was the deterioration due mostly to scorching?

MURROW: It depended on a number of things. Usually, the outside was scorching; on the inside, we sometimes saw rather definite damage to the glue line or even to the top of the filter media in addition to scorching or charring of the frame.

One other thing that I didn't mention was that, in general, we feel that the weight of the metallic filter is probably as good a criteria of the protection that will be obtained as any other. In other words, the more mass of metal in front of the high efficiency filter, the better protection for the high efficiency filter.

I would also like to mention that this report will be amplified with more tables and photographs and reproduced as a UCRL Report. Anyone who is definitely interested in receiving a copy may do so by giving me their name and address at some future time during the conference.

BURCHSTED: As a side note to Mr. Murrow's comment about particle board, we have so far found excessive porosity in these materials. We will check that out.

MURROW: My comment was only that as far as fire intrusion, heat, or high temperature resistance was concerned, it was pretty good.

VILES: Did you make any studies to determine whether or not the DOP deposited on the filter had any effect upon these tests?

YOUNG: These were all new filters, of course, all of which had been tested by DOP at the manufacturer's and at Oak Ridge, and by ourselves, after a test. We did not take any filters that had not been evaluated by DOP because we don't know how to evaluate the breakdown mechanism, except by DOP test.

VILES: I just wondered if this was possible. Would you say what effect the DOP might have on the fire resistance of these filters, the ones with DOP deposited on the filter?

MURROW: I don't believe that our equipment as set up is that critical in its evaluation. It's more of a ranging kind of equipment rather than a completely accurate determination. Also, due to the fact that we generally only

tested one of a kind, we realize that the test from another one or 50 more or 100 more would get better statistics and might show something else. We have neither the filters nor the time to do that.

VILES: Did you have any idea how much DOP might have been on the filters?

YOUNG: We have calculated it in the past. The amount of DOP depends mainly on the duration of the test. For a standard 1000 cfm filter, and using 100 micrograms of DOP per liter upstream approximately 3 grams of DOP would be collected for each minute the filter is exposed in this test rig.

MURROW: I don't think that, as far as our tests were concerned, the DOP was on for more than a minute and a half for any one filter. That would add up to much less than five minutes total of all three tests, viz. manufacturer, quality assurance station and our tests.

BILLINGS: I was associated, of course, with the original test at Harvard for the 20-inch shock tube. We, of course, took our direction from Mike Gorman, and the original question that was asked us was the effect of unloading. We weren't really looking for structural damage, although we found it at essentially the same level you did. It is nice to know our results and your results are essentially the same for overpressure, but the original criteria was the filter is loaded and you impose a shock wave in the opposite direction; how much junk cops off back to the building, or does the building become contaminated if the space was never ventilated?

YOUNG: We didn't evaluate that part of it. We realize it is a problem and your question is still a valid one. We were interested only in the effect of shock to the external face of the filter.

BILLINGS: You mentioned wire mesh. One of the filters we tested, one of the original, in which there was a perforated aluminum plate, it was my feeling that essentially what you found would be the case. If you put a lot of mass in front of it you are going to really protect the filter. If you did it with a lot of metal filter screens, something like that, you would normally tend to protect the filter from structural damage.

YOUNG: That is right. It is not the effect on the blast as it is maintaining rigidity of the filter during the shock phase.

GILBERT: The criteria were changed somewhat in this particular set of tests. We only wanted to determine what kind of value we could get to protect the glove box filter, but while we had the opportunity, we stretched it to the other sizes of filter, so this is the change in the application.

# PROGRESS REPORT
# FACTORS INFLUENCING HIGH-EFFICIENCY GASKET LEAKAGE

F. E. Adley

Hanford Occupational Health Foundation

## INTRODUCTION

This report identifies factors which adversely influence the sealing property of High Efficiency, Particulate, Air (HEPA) filter gaskets. Because of the paucity of information on the actual performance of these gaskets with respect to the overall filter operation, this study was conducted so that more detailed study could be made of the significant factors.

The Chemical Warfare Service (CWS) filter developed in the early 40's was designed to produce optimum performance commensurate with the requirements for chemical and biological protection. It was subsequently adopted by the Atomic Energy Commission for the cleanup of radioactive particulates in effluent stack gases. Since its inception the features of this filter, currently called a HEPA filter have been periodically improved by the commercial manufacturers. For example, a guaranteed minimum overall efficiency of 99.97% is now common. A typical HEPA filter is shown in Figure 1.

Efficiency of this order of magnitude for an installed filter demands that the integrity of each structural component must support and not detract from (counteract) such high performance. The filter medium must be free of flaws or imperfections, the frame and its corner joints must be impervious to leakage as must the adhesives which seal the components together. Similarly, the mounting gasket must provide a satisfactory seal of the filter to the mounting surface to prevent leakage of contaminated atmosphere by the filter. Gaskets of various materials and shapes such as closed-cell neoprene, solid rubber, cork-neoprene composition, and glass are employed, the choice being that of the user.

Little or nothing has been reported on the actual performance of these gaskets with respect to the overall filter operation. The purpose of this study was to identify factors such as gasket joints, configuration, and hardness which influence the sealing property of HEPA filter gaskets so that more detailed study could be made of those which are of significance.

Work performed under Contract No. AT(45-1)-1837 between the Atomic Energy Commission and Hanford Occupational Health Foundation, Inc.

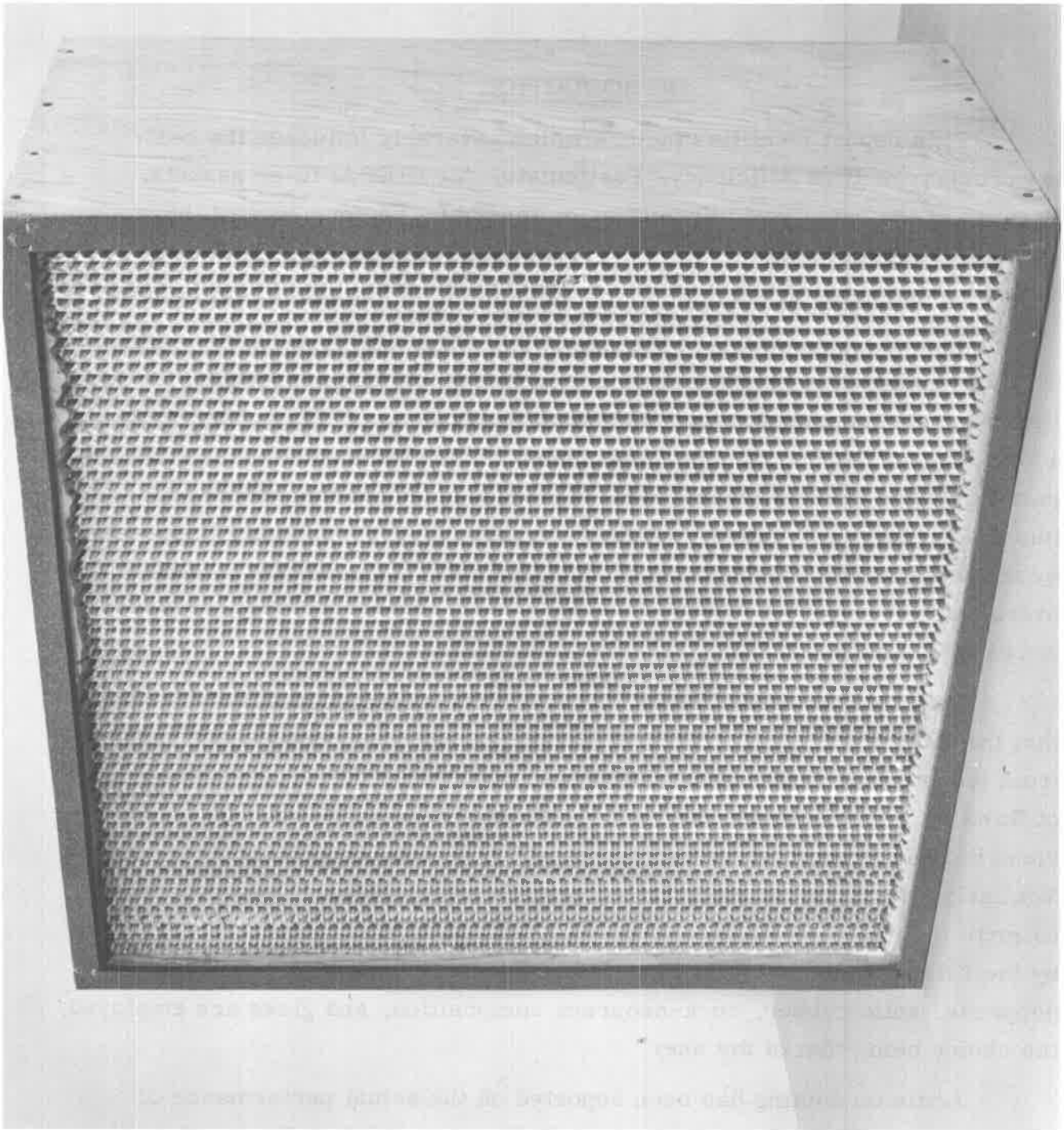

Figure 1. Typical HEPA Filter

## SUMMARY

Tests were performed to develop data which would demonstrate factors related to gasket leakage that warrant more detailed study. A full-scale test facility providing gasket mounting conditions equivalent to a 1000 $ft^3$/min HEPA filter was employed in evaluating various aspects of gasket leakage.

The effect of time on installed gaskets was shown by conducting tests to simulate and measure the effect of various mounting forces on leakage over a period of several weeks. It was found that leakage and compression of the gaskets increased with time whereas pressure diminished.

The change in compression due to dynamic loading was demonstrated for a cellular and a solid gasket over a period of 20 days. In 1 week, the compression of the cellular gasket had increased by a factor of 3 and the cork-neoprene compression had increased by a factor of about 1.5. The compression of each was still increasing at 20 days.

Static force was applied to various gasket specimens for a period of 111 days. The pressure exerted by the cellular and solid gaskets relaxed to an equilibrium of approximately 50 to 60% of the original pressure in about 2 weeks. The solid molded gasket continued to relax over a longer period.

Leakage from inadequately cemented gasket joints was significantly greater than those well-prepared, but moderate clamping pressures reduced joint leakage, particularly with solid elastomers.

High compression of the gaskets studied was found unnecessary to reduce leakage to levels well below the lower limit of sensitivity of the thermal dioctyl phthalate (DOP) filter testing method.

Tests on solid molded gaskets of the same hardness in nine different shapes showed measurable differences in sealing quality although no particular configuration was a definite optimum. The 1/2 in. molded cellular half-round gasket demonstrated relatively poor sealing ability. Gasket hardness failed to show any relationship to sealing quality nor was there any definite advantage between solid and cellular elastomers.

Variations in gasket thickness were found to influence leakage. Findings indicated that gasket thickness tolerance should be ±0.01 in. Mounting surfaces should also be in plane to ±0.01 in.

The results of this study indicate that several facets of gasket leakage warrant more extensive investigation. These facets include the effects of aging during operation, the effects of high compression, and the importance of gasket skin. Leakage of frames under operating stresses should also be evaluated.

## TEST PROCEDURE

### FACILITY

Since the objective of this investigation was to develop data applicable to in-place operation, a full-scale test facility was used which would reflect the effect of dimensional and other influencing variables. Initially, a plywood test frame dimensionally the same as that for a 1000 $ft^3$/min filter was used. Although this frame was constructed carefully with excellent corner joints and internal bracing, it was found that the frame itself embodied uncorrectable leakage which distorted test findings.

Therefore, a test frame, as shown in Figure 2, was constructed of 3/4 in. aluminum plate with welded seams. This frame was suspended and counterbalanced by a weight attached at (A) to provide zero pressure on the test gasket (B). During a test, the gasket was compressed on mounting plate (C) by tightening eight clamping bolts (D). The amount of compression was determined by four corner dial micrometers (E) which could be read to 0.001 in. (equivalent to 0.4% compression for a 1/4 in. gasket).

Force on the gasket was measured by four corner platform scales (F). Approximately 2 in. above the bottom edge of the frame was a welded aluminum panel which formed a chamber below when the gasket seal was made. Gasket leakage was measured by metered makeup air introduced at (G). Airflows as low as $10^{-6}$ $ft^3$/min (about $3 \times 10^{-2}$ $cm^3$/min) were measured. Air pressure on the gasket was measured at (H). To provide

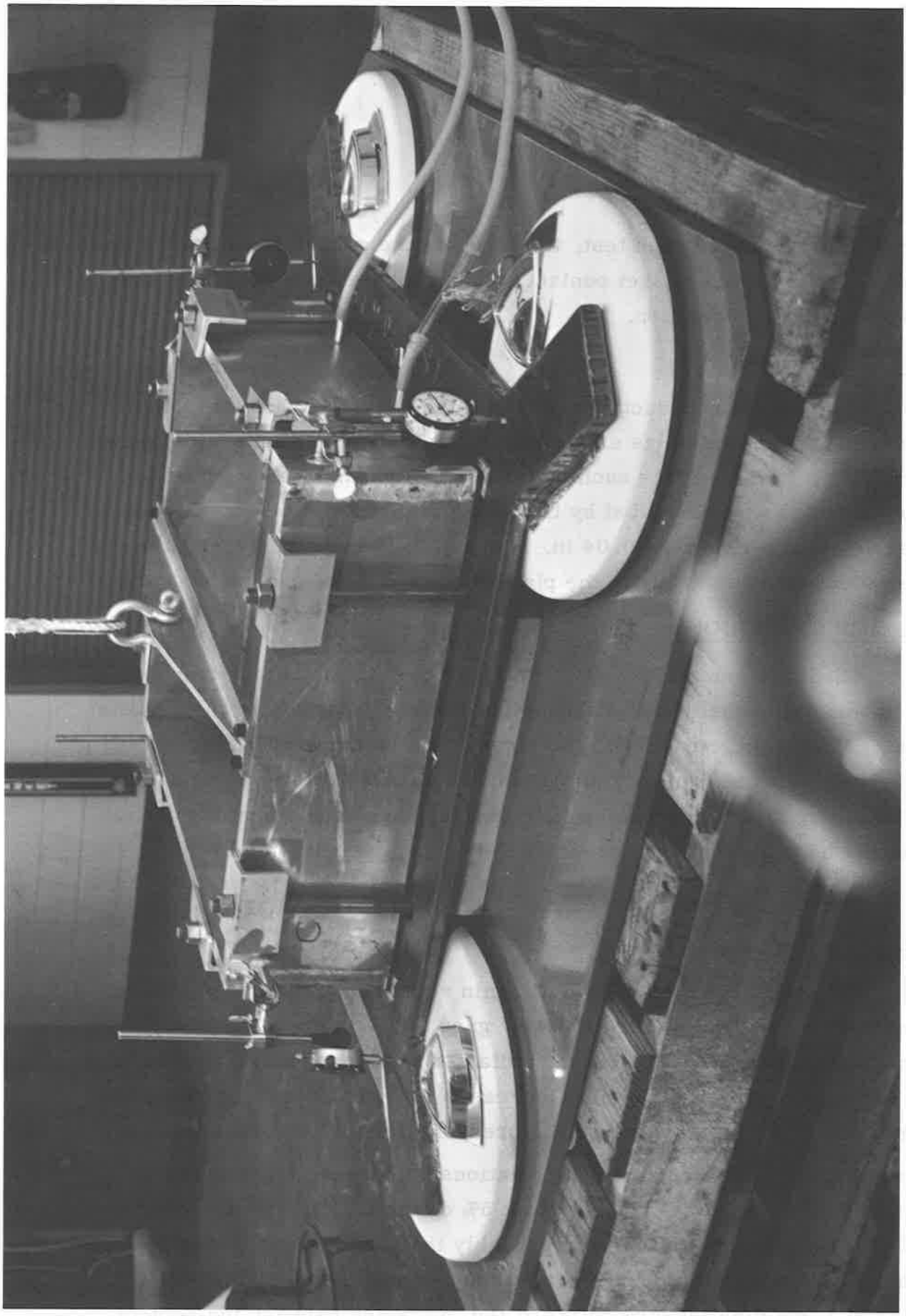

Figure 2. Aluminum Test Frame

a uniform baseline for each test, the force on the gasket was raised 2 lb at each corner to assure gasket contact. This was then assumed to be the zero compression condition.

## SIMULATED DEFECTS

In addition to conducting tests with the gasket seating only on the surface of the steel plate as shown above, the ability to seal against possible mounting frame defects such as improperly ground welding beads or other asperites was simulated by the use of an artificial defect, Figure 3. These defects, which were 0.04 in. high and 0.18 in. wide at the base were added, when desired, to the plate at the center of each side.

## LEAKAGE CRITERION

A leakage rate of $10^{-4}$ $ft^3$/min (2.83 $cm^3$/min), rather than zero was chosen as a baseline for relating the sealing capability of the gaskets tested. This leakage rate could be directly and accurately measured and was below the lower limit of dioctyl phthalate (DOP) filter testing equipment by a factor of $10^{-2}$. In terms of filter performance the effect of this leakage would be equivalent to increasing the percent penetration by $10^{-5}$.

# TESTS

## PRESSURE

Filters of this type of 1000 $ft^3$/min rated capacity have pressure drops in the range 0.8 to 1.1 in. water gage (W. G.) depending primarily on the characteristics of the filter media used. Occasionally, system airflow rates are changed or loading increases over the operating life of the filter, each of which may change the pressure drop by several inches of water. Figure 4 demonstrates the relationship between leakage and pressure up to 5 in. W.G. Up to about 5% compression, the predominating factor influencing leakage was probably the gasket establishing positive contact with the mounting surface. Further compression involved the sealing of remaining leakage points at the joints and between the contact surface of the gasket and the mounting plate.

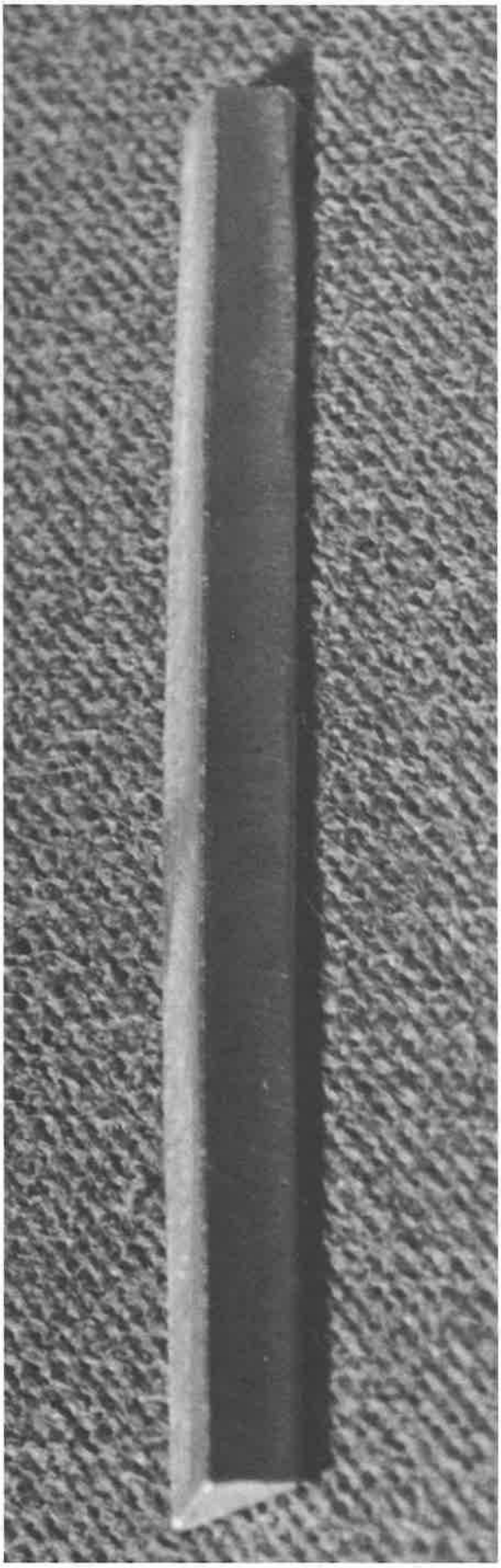

Figure 3. Artificial Defect

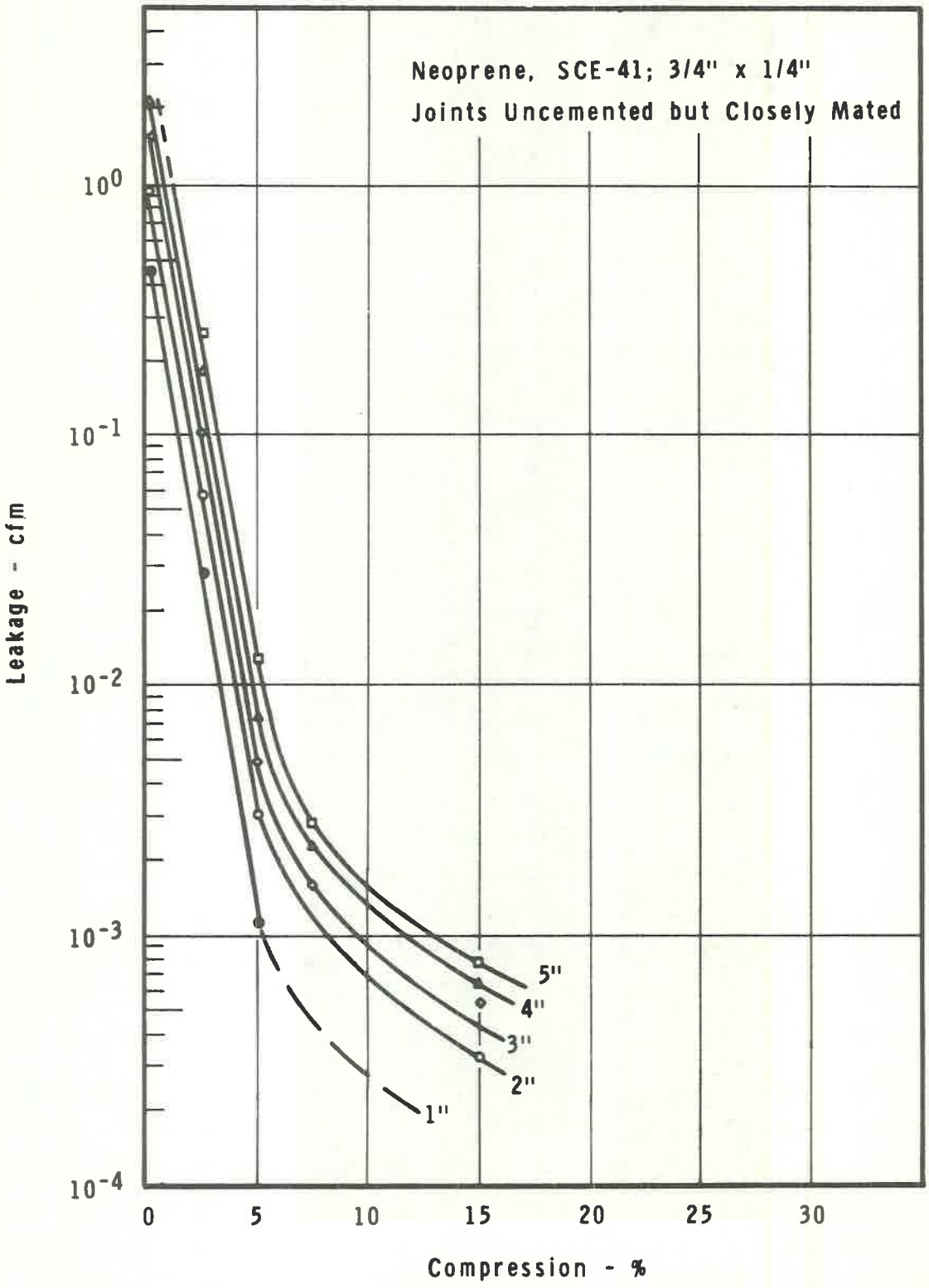


FIGURE 4. Effect of Air Pressure

## JOINT LEAKAGE

Leakage of an impervious gasket can be attributed primarily to inadequate sealing against the mounting surface or to imperfect cementing of the corner joints if such exist. The importance of joint leakage was investigated for solid and cellular gaskets.

A cork-neoprene gasket of durometer 53, Shore A, hardness was selected as a conventional solid gasket. The corner joints were wedge-shaped dovetail as indicated in Figure 5. The same gasket was used in Tests A and B with the joints being securely cemented after Test A. It was found that the gasket with uncemented joints (Test A) had a leakage of about 3 $ft^3$/min at a little less than 5% compression.

This leakage was due to both that of the joints and that caused by the slight variation in thickness of the four gasket strips such that the thinner gasket strips were not well seated when the thicker ones were subjected to minimal pressures. The latter leakage factor was of varying importance in all leakage tests, the effect being most pronounced in the harder gasket materials. To meet the stated leakage criterion of $10^{-4}$ $ft^3$/min, approximately 15% compression of the gasket in Test A was necessary.

Test B, in Figure 5, required an equivalent compression to reduce the leakage to the criterion level.

It was observed that, as the gasket was compressed in each test, the leakage rates gradually approached each other until they became equal at approximately 15% compression. It is believed that the reason for the uncemented joints gradually sealing with increased compression is that the gasket material displaced by compression filled the voids within the joints.

When a solid elastomer is subjected to compression, it behaves as an incompressible fluid and there is a displacement of material to maintain its original volume. This characteristic is shown in Figure 6 which demonstrates specimens, each compressed 40%, of molded solid rubber (A), cork-neoprene (B), and closed-cell neoprene (C). Displacement of each gasket medium is evident particularly with the solid elastomer. Such lateral

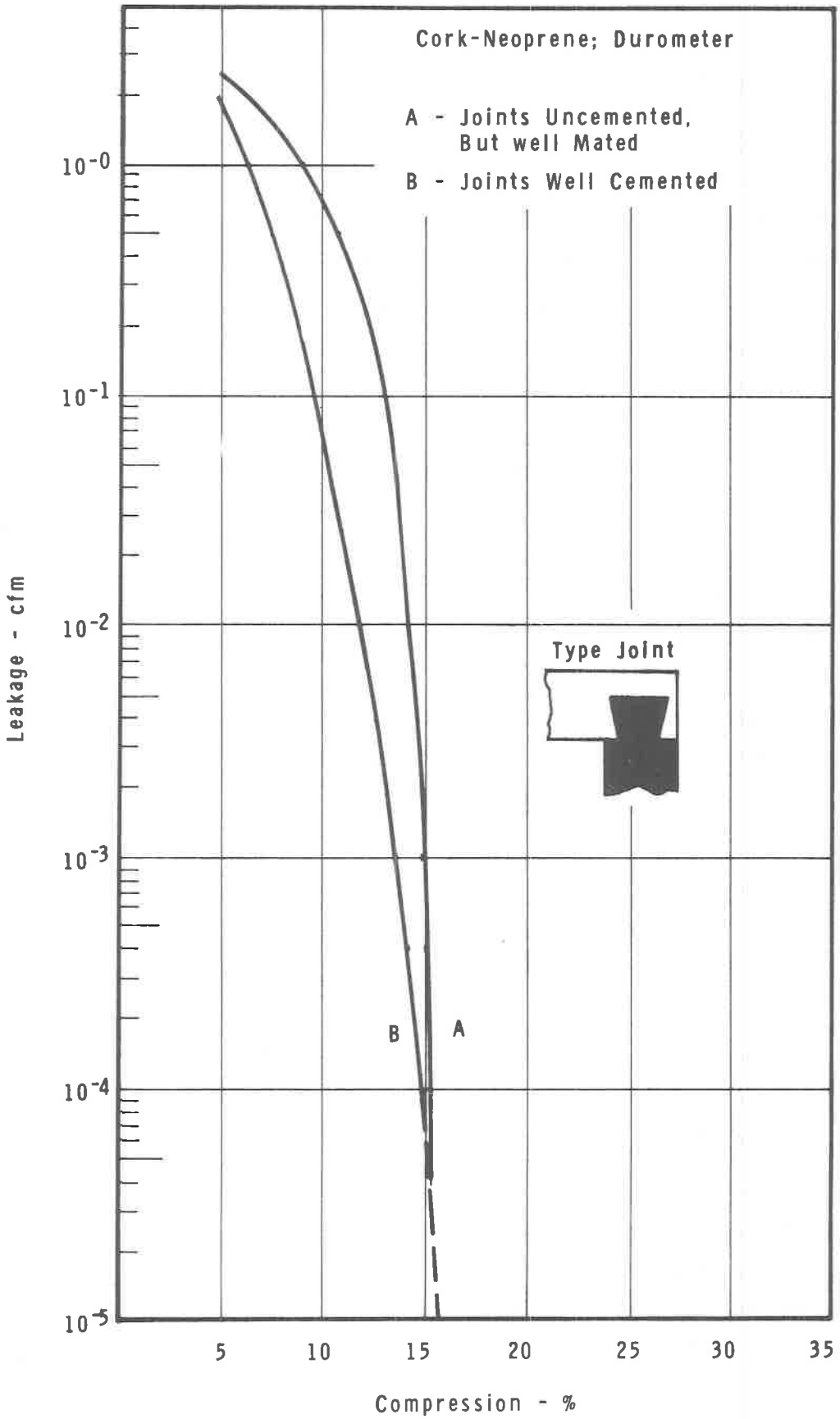


FIGURE 5. Joint Leakage

displacement was also observed during actual leakage tests wherein the gasket medium, particularly the molded solid material, occasionally projected up to 2 mm beyond the edge of the frame. This results in a sheer force where the gasket is in contact with the filter frame and the mounting surface. Expansion in unconfined directions such as within the uncemented joints apparently causes a closing of voids in the joint.

A second test was made using a cellular gasket also containing dovetail joints (See Figure 7). This softer medium permitted the gasket in Test (A) with well cemented joints to achieve the criterion leakage at a compression of only 22%, whereas, about 32% was necessary when the joints were uncemented but closely mated (B). After gasket seating was fairly well established at approximately 10% compression in Test A and 15% in Test B, the leakage for a given compression was higher by a factor of about 5 with uncemented joints. This relationship, which held through 50% compression, was probably due to the absence of any significant change of the voids in the uncemented joints during compression, which was in contrast to the cork-neoprene gasket performance.

Gaskets with partly cemented joints under the conditions discussed would have leakage rates between curves A and B.

## GASKET HARDNESS

One of the physical qualities of gaskets, that of hardness, was investigated to determine its influence on the sealing property. One method for designating the hardness of solid rubber is by the indentation of the material by a hardness measuring instrument, a durometer.[1] The penetration of an indentor point is calibrated to indicate a measure of hardness in durometer units. The hardness of the cellular rubbers employed in this investigation is designated according to ASTM procedure[2] as shown in Table I.

Two types of gaskets were tested; a group of five solid rubber gaskets ranging in hardness from durometer 13 to 53, Shore A, and a second group of conventional gaskets including six closed-cell expanded neoprene with 25% deflection at loads ranging from 1 to 24 psi and a cork-neoprene. Each had well cemented joints.

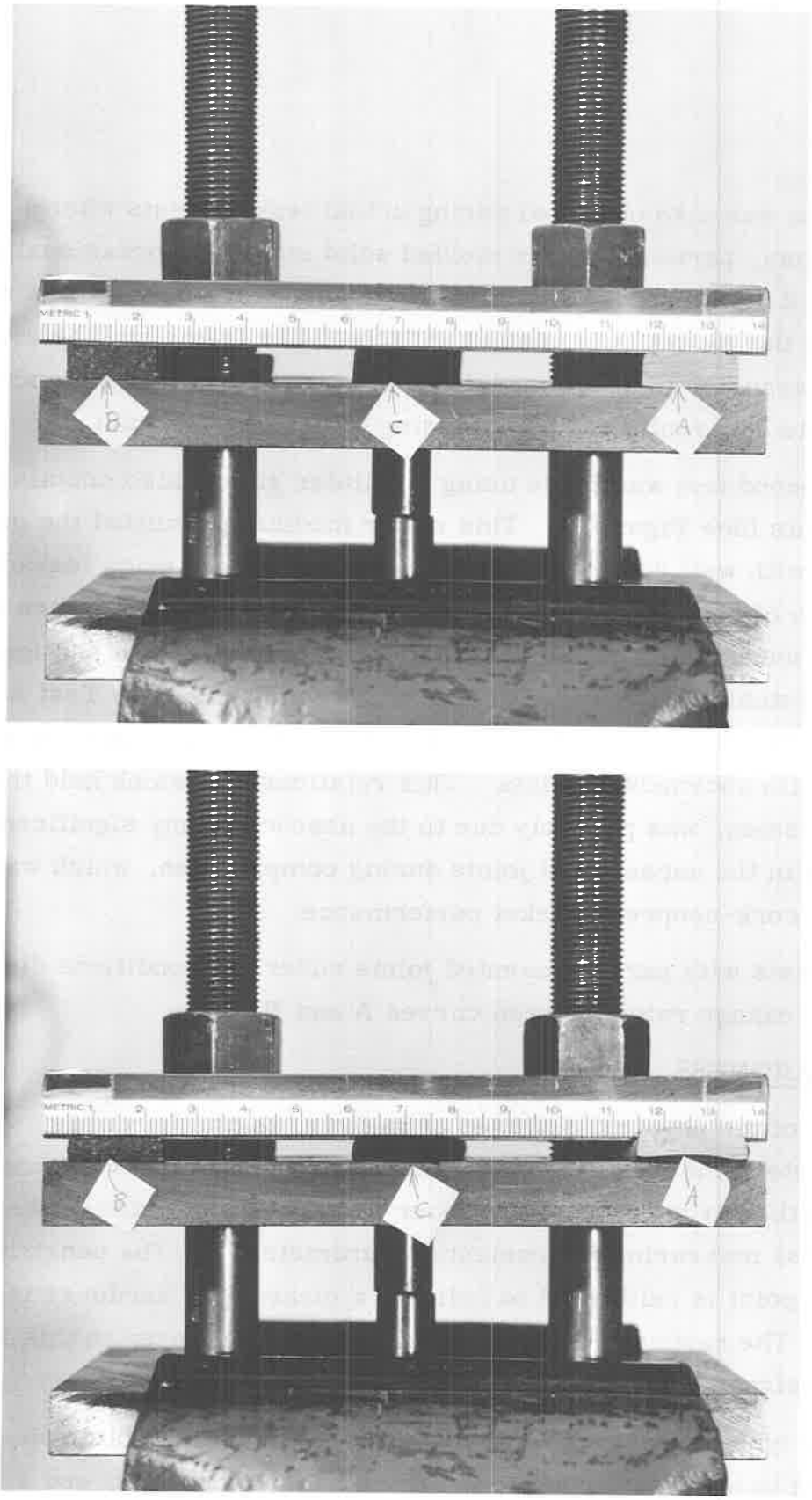


Figure 6. Demonstration of Displacement of Solid Elastomer Under Compression; (A) Molded Solid Rubber, (B) Cork-Neoprene, (C) Closed-Cell Neoprene.

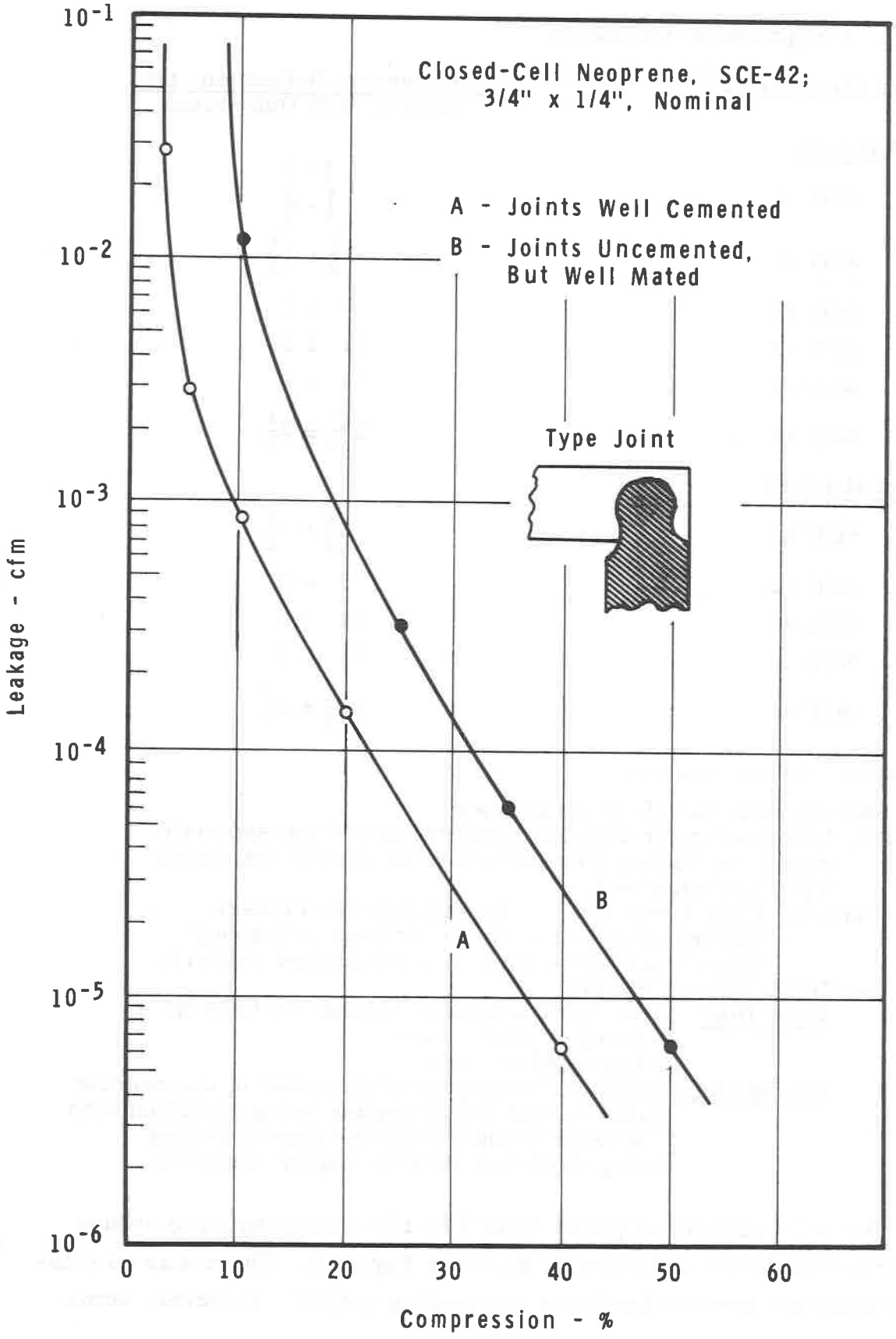


FIGURE 7. Joint Leakage

TABLE I. Compression-Deflection

| Grade Number [a] | Compression Deflection, psi (Limit: 25% Deflection) |
|---|---|
| Sponge Rubbers | |
| SCO 10 | $1 \begin{cases} +1 \\ -\frac{1}{2} \end{cases}$ |
| SCO 11 | $3\frac{1}{2} \pm 1\frac{1}{2}$ |
| SCO 12 | $7 \pm 2$ |
| SCO 13 | $11 \pm 2$ |
| SCO 14 | $15 \pm 2$ |
| SCO 15 | $20\frac{1}{2} \pm 3\frac{1}{2}$ |
| Expanded Rubbers | |
| SCE 41 | $3\frac{1}{2} \pm 1\frac{1}{2}$ |
| SCE 42 | $7 \pm 2$ |
| SCE 43 | $11 \pm 2$ |
| SCE 44 | $15 \pm 2$ |
| SCE 45 | $20\frac{1}{2} \pm 3\frac{1}{2}$ |

[a] Grade Number code is defined as follows:

- SC: Designation for cellular rubbers made from synthetic rubber or rubber-like materials having oil resistance with medium swell.
- O and E: Type S rubbers are divided into two classes designated by the letter O for open cell sponge rubbers and E for closed cell expanded rubbers.
- Two Digit Grade Numbers:
  - First Digit identifies the kind of cellular rubbers as 1-Sponge rubbers, and 4-Expanded rubbers.
  - Second Digit indicates the degree of firmness of the cellular rubbers, the softer grades being identified with the lower numbers and the firmer grades being identified with the higher numbers.

The solid gaskets required from 5 to 15% compression to reduce the leakage rate to the criterion as shown in Figure 8. There was no relationship apparent between hardness and sealing quality. However, some

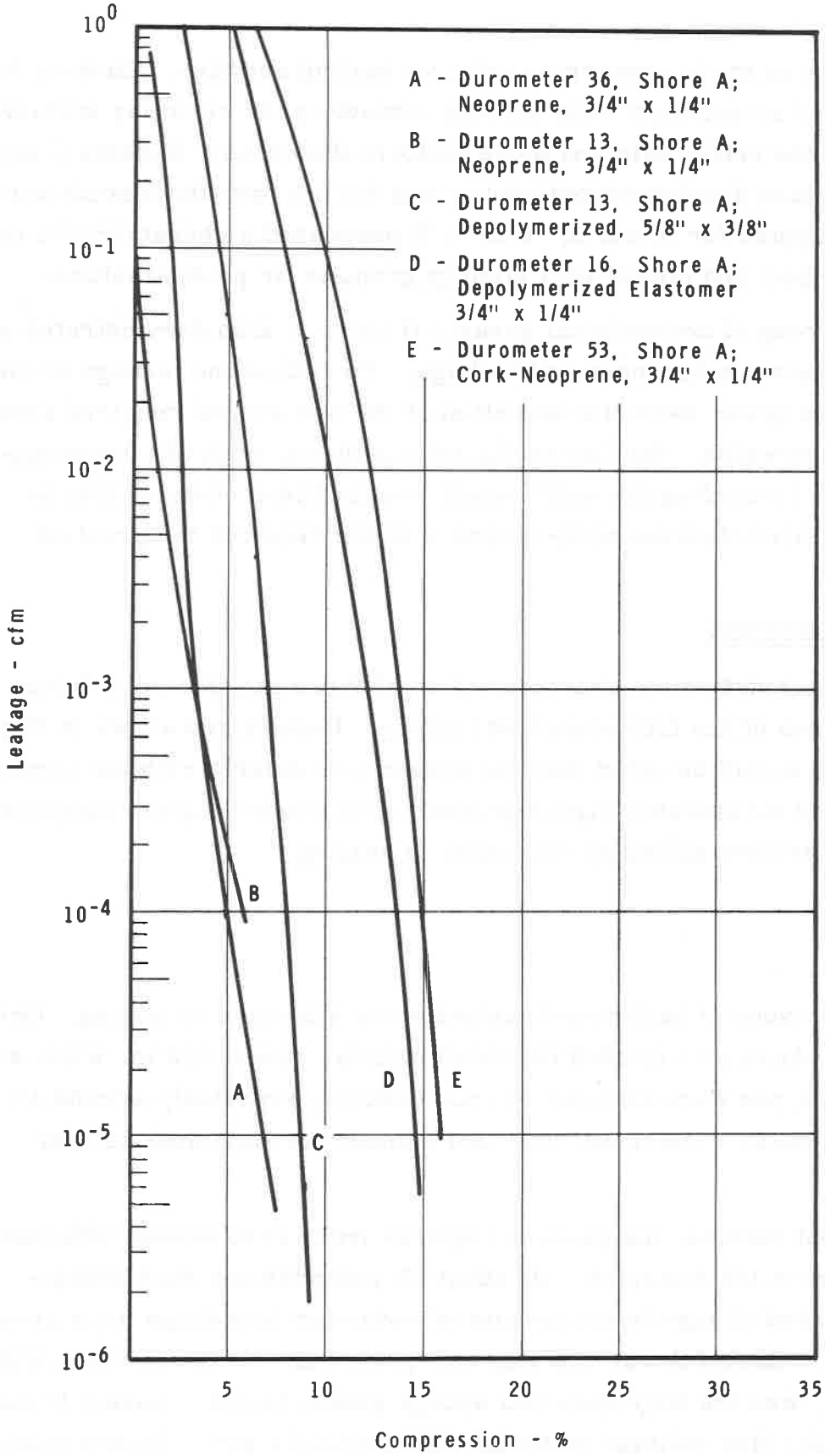


FIGURE 8. Effect of Hardness (Solid Gaskets)

comments can be made concerning relative sealing abilities. Gaskets A and B each had an excellent skin surface contacting the mounting surface; gasket A had the better skin and more uniform thickness. Gaskets C and D were of molded depolymerized rubber and did not have the smooth uniform surface noted for A and B. Gasket E possessed a characteristic cork-neoprene surface and embodied a slightly granular or pebbly testure.

The group of conventional gaskets (Figure 9) also demonstrated no relationship between hardness and leakage. To reduce the leakage to the criterion, this group (with the exception of the half-round) required about 7 to 15% compression. Similar to the solid gaskets, each of the conventional gaskets (excluding the half-round) required less compression to meet the criterion than the cork-neoprene which required the greatest compression.

## LOAD-DEFLECTION

The load-deflection characteristics of these gaskets were determined by means of the full-scale test facility. Results are shown in Figures 10 and 11. It should be noted that the presence of defects with the harder gaskets caused measurably higher pressures to achieve a given compression. Also, greater difficulty was found in sealing.

## SHAPE

### Half-Round

Three types of half-round gaskets were subjected to testing. One was a typical American molded expanded cellular gasket 1/2 in. wide; and the other two types were cellular French gaskets, reportedly around 15 durometer. These were tested with and without the simulated defects (Figure 12).

Without defects, the gaskets required from 17 to almost 30% compression to meet the criterion. At about 5% compression each demonstrated a marked change in the amount of reduction in leakage for a given compression. Gasket A was the only one-piece half-round specimen and, interestingly, was the only open cell sponge gasket tested. Gasket C was an exceptionally fine cellular material and noticeably soft. At 30% compression the leakage ranged from an estimated $10^{-7}$ to about $10^{-4}$ $ft^3$/min.

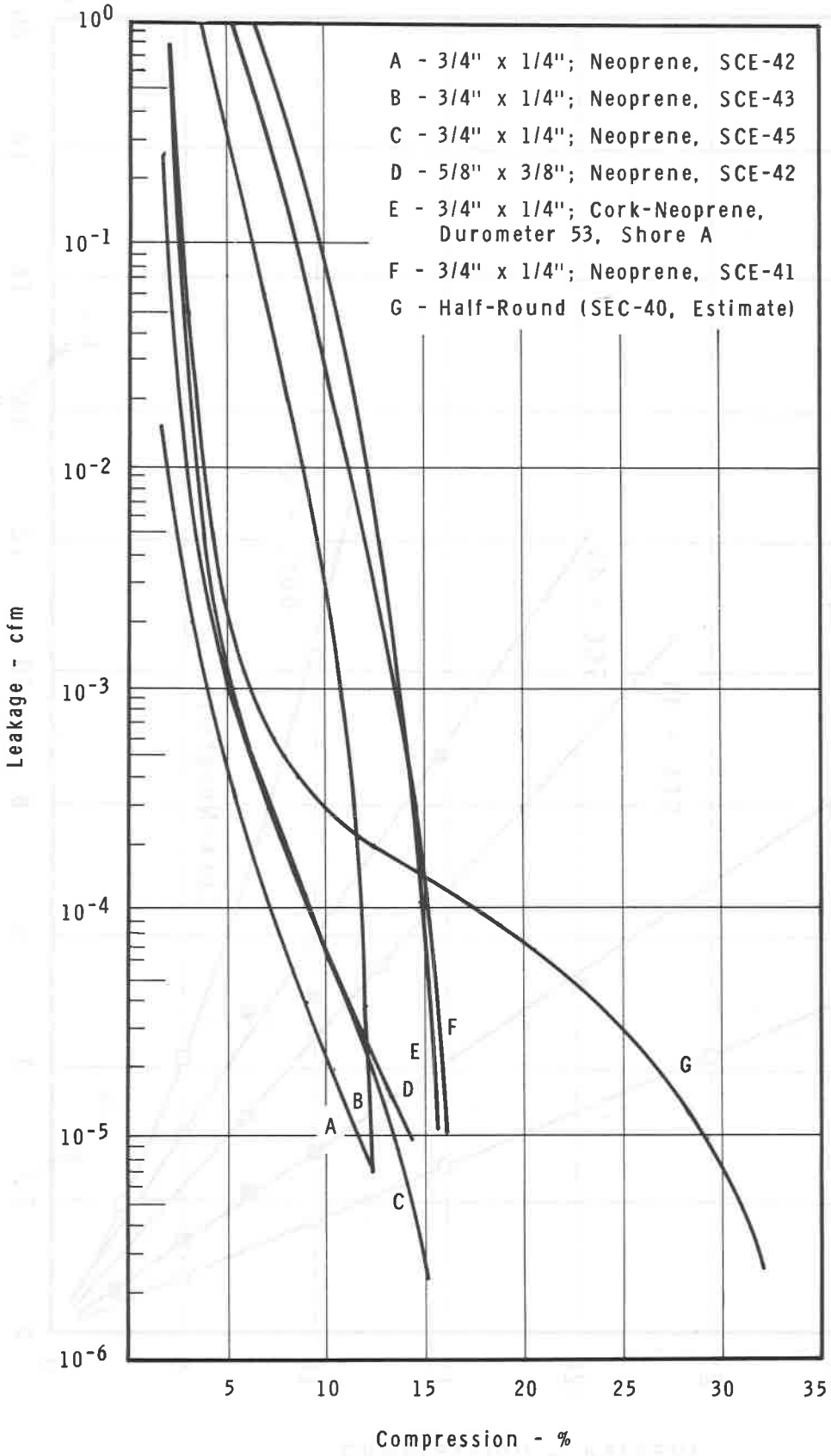


FIGURE 9. Effect of Hardness (Conventional Gaskets)

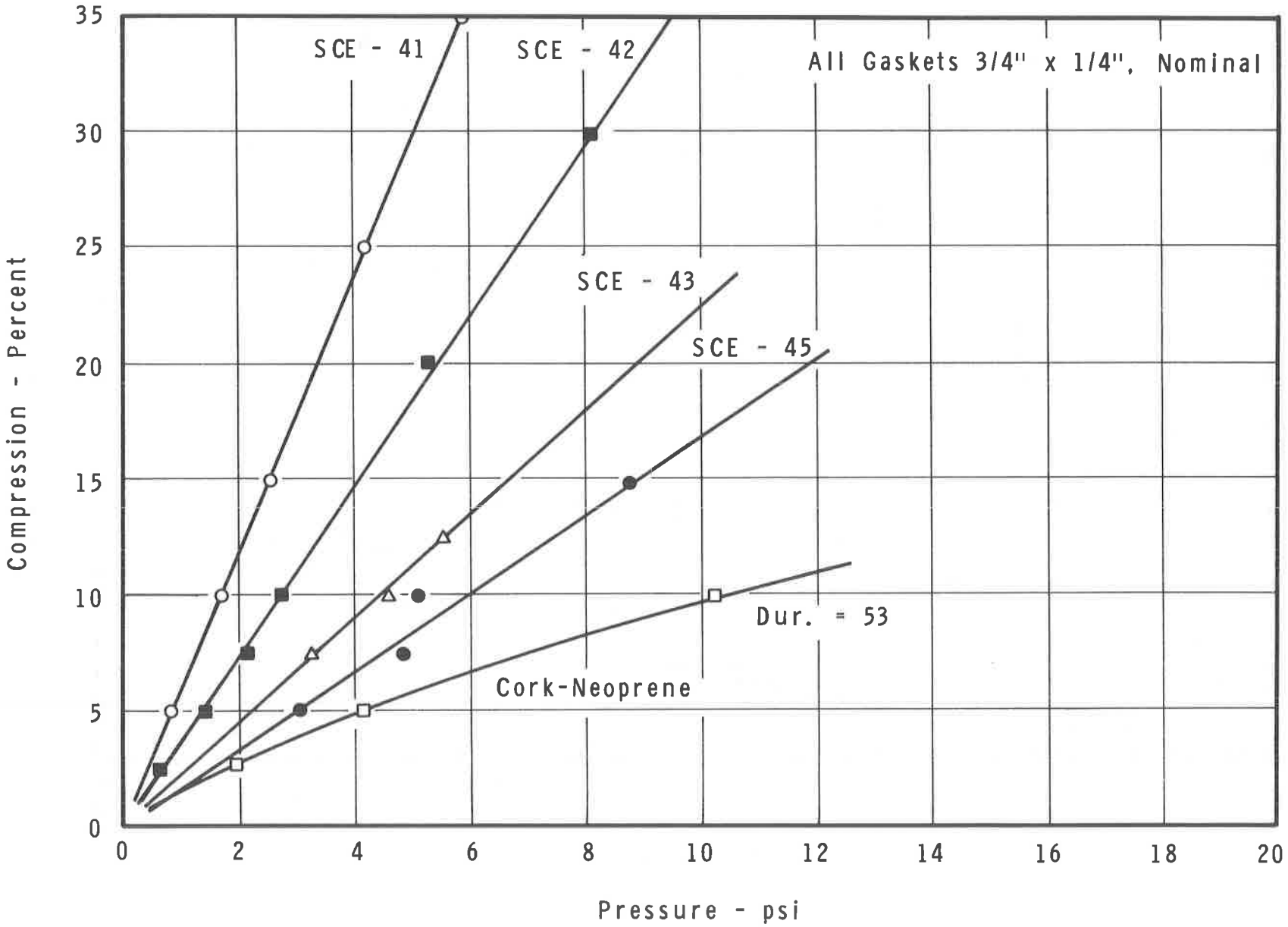


FIGURE 10. Gasket Load-Deflection

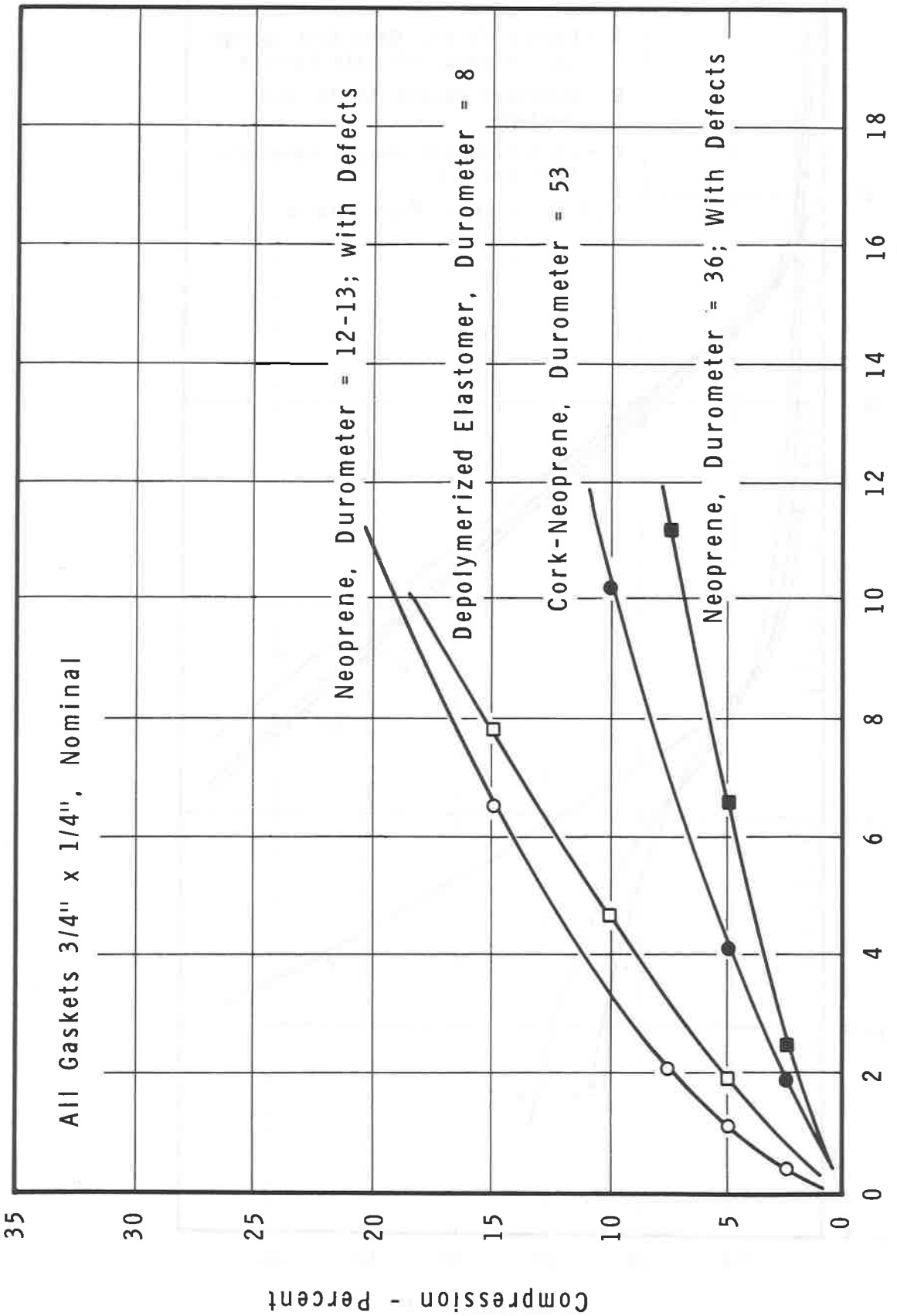


FIGURE 11. Solid Gasket Load-Deflection

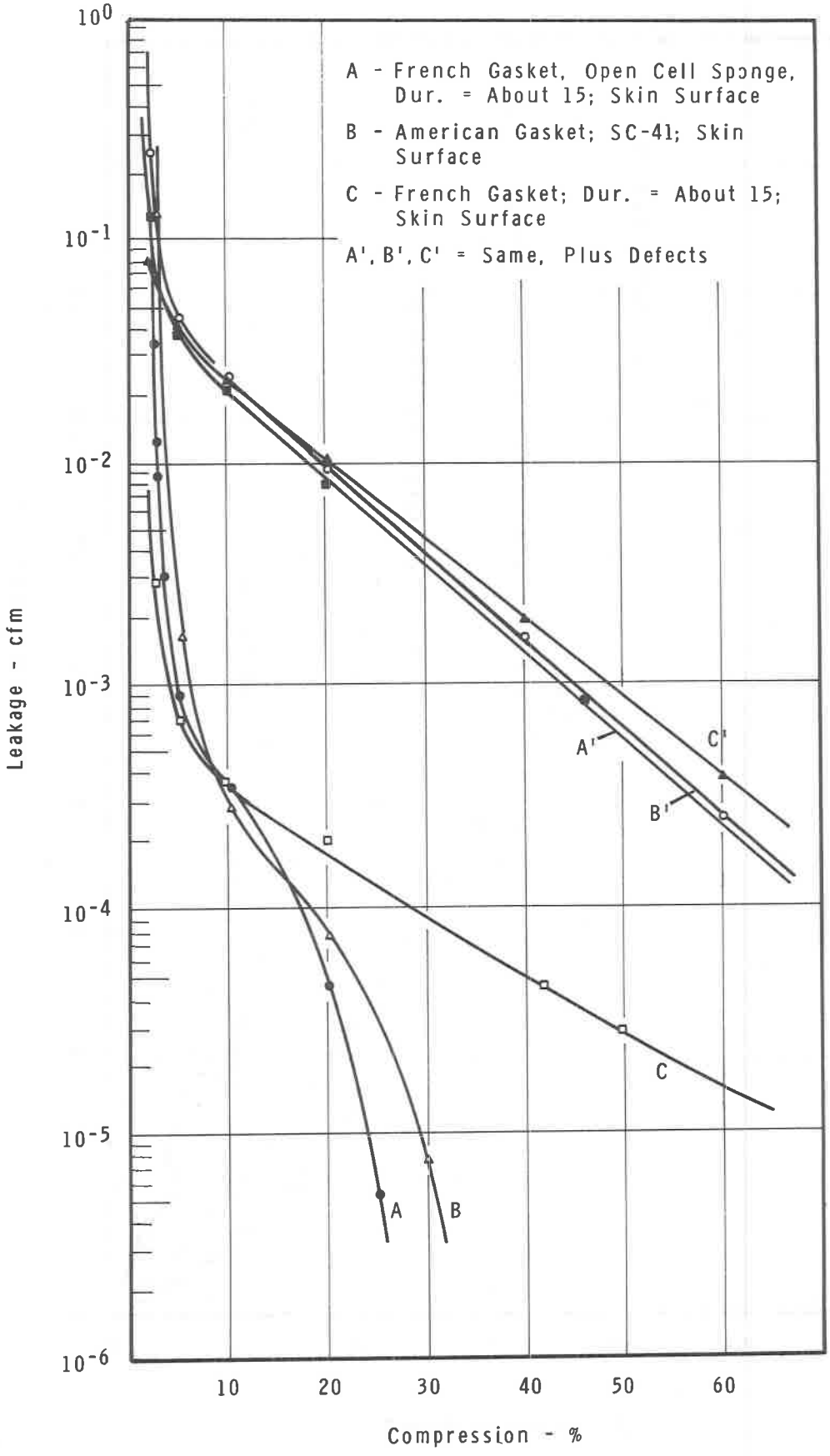


FIGURE 12. Half-Round Gaskets

When defects were added, the compression necessary to attain the leakage criterion was between 70 and 80%. At 30% compression the leakage was approximately $4 \pm 0.5 \times 10^{-3}$ $ft^3$/min.

Molded Shapes

So that a comparison of gasket shape as affecting sealing quality could be attempted, various shapes of specimen gaskets were used. These gaskets were one-piece depolymerized rubber with a durometer 8 to 12, Shore A (See Figure 13). Considering that these gaskets were, by nature, prototypes they were fairly uniform dimensionally although some small surface irregularities did exist. It is felt that these were of minor significance in the leakage tests.

The first series (Figure 14), which was conducted without defects, showed that the gaskets reached the criterion with compressions ranging from about 7 to 17%. Shape J had a noticeably poorer sealing quality than the other shapes.

The same gaskets were also tested with defects added, as shown in Figure 15. The gaskets required a minimum of 25% compression to achieve the leakage criterion, shapes O and P requiring an estimated 50 to 55% compression. At a compression of 30%, the gaskets that provided the least leakage were T, W, L, and R. As found previously, leakage caused by the presence of the defects was reduced rapidly with relatively small compression until the leakage was in the range $10^{-2}$ to $10^{-1}$ $ft^3$/min. Following this, a given compression of all shapes reduced leakage at a slower rate.

## FORCES EXERTED ON GASKETS

Four forces act upon gaskets when in operation. The first, as shown in Figure 16 is a static force exerted by the clamping arrangement. Such clamping, whether it be by bolting or by cam, produces the largest force and may range from a few hundred pounds up to about 2000 lb and is always a positive or sealing force.

The second is a dynamic sealing force created by the air pressure differential across the filter (See Figure 17). At 1 in. W. G. differential

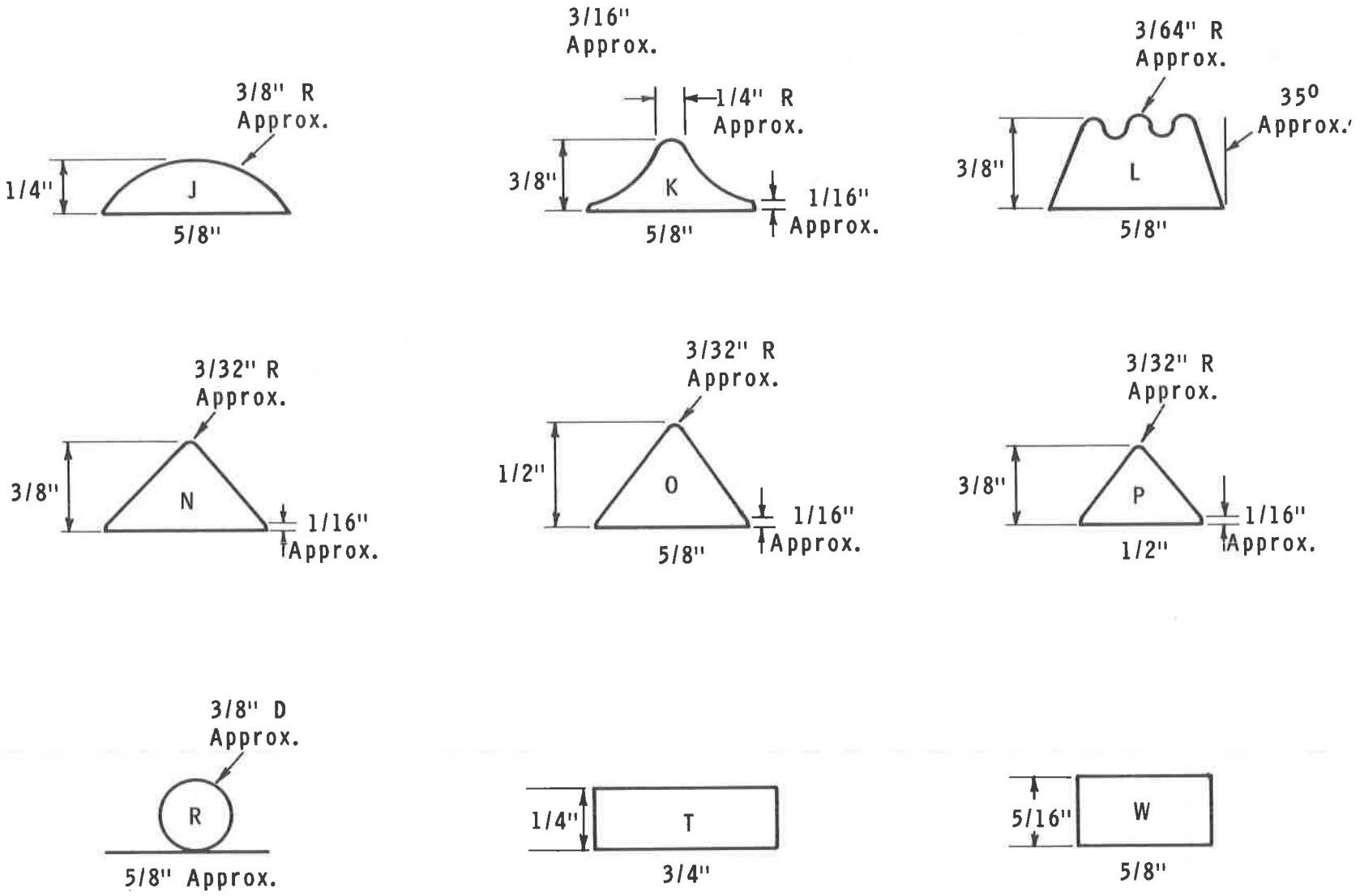


FIGURE 13. Gasket Shapes

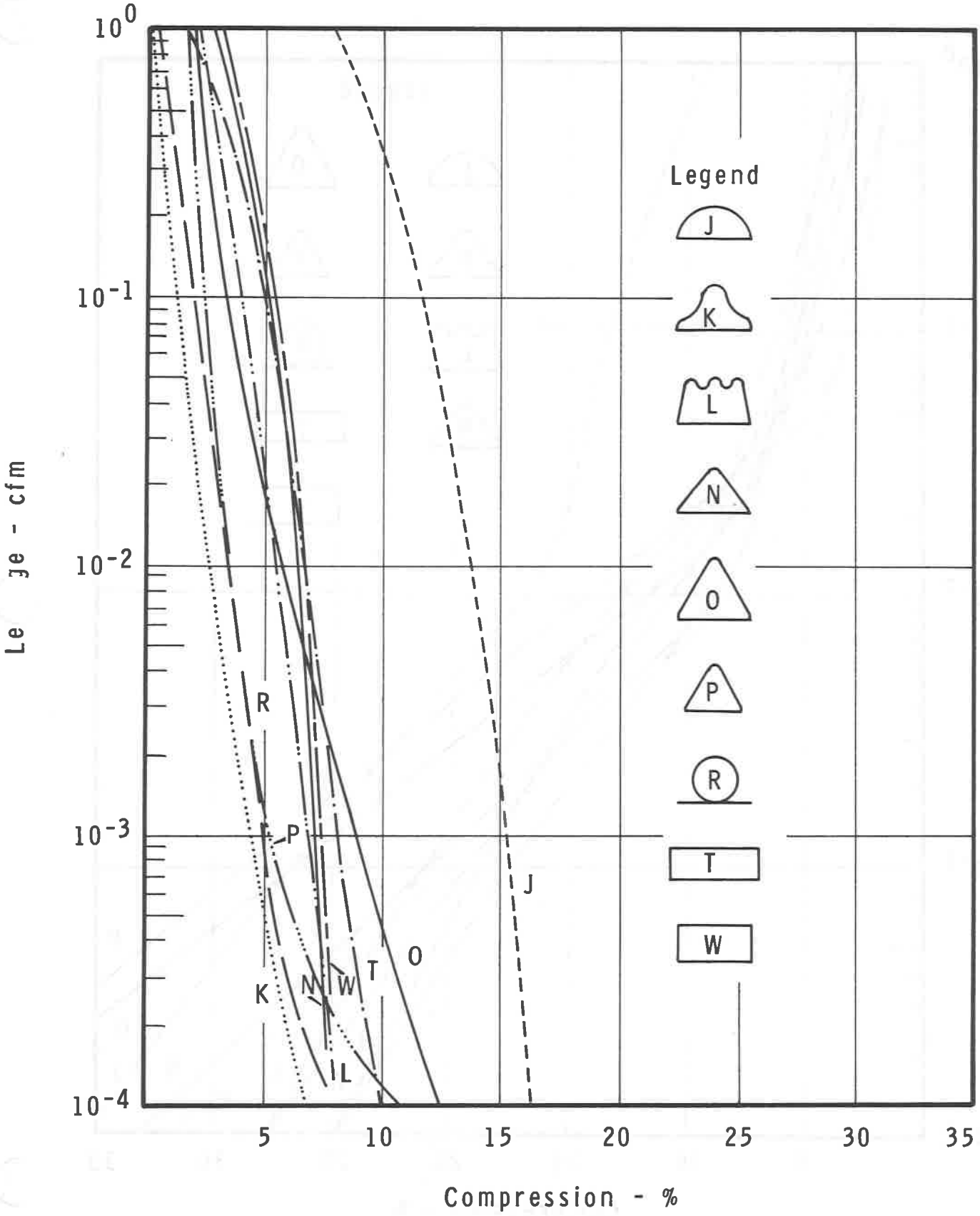


FIGURE 14. Molded Shapes (Without defects)

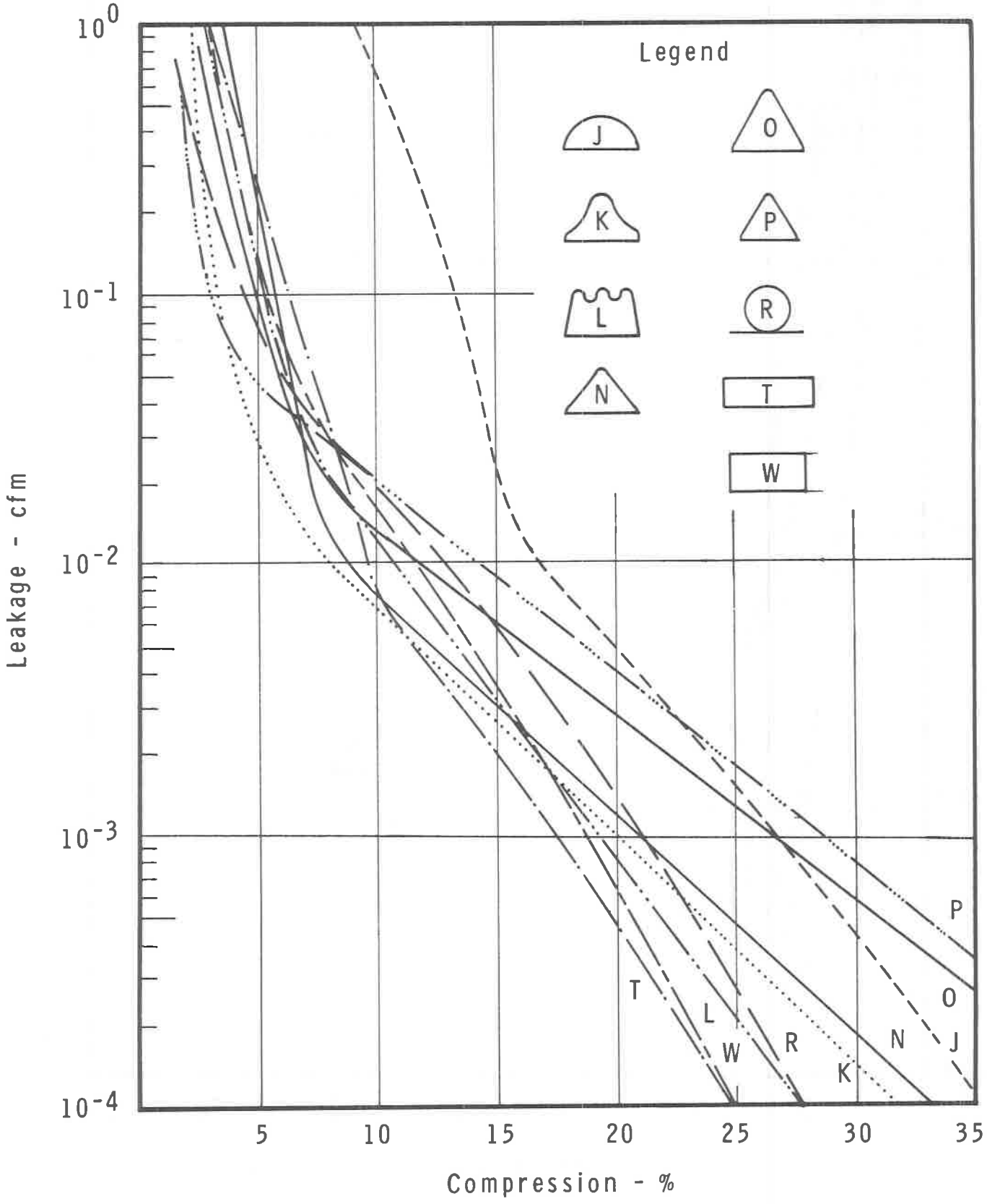


FIGURE 15. Molded Shapes (With defects)

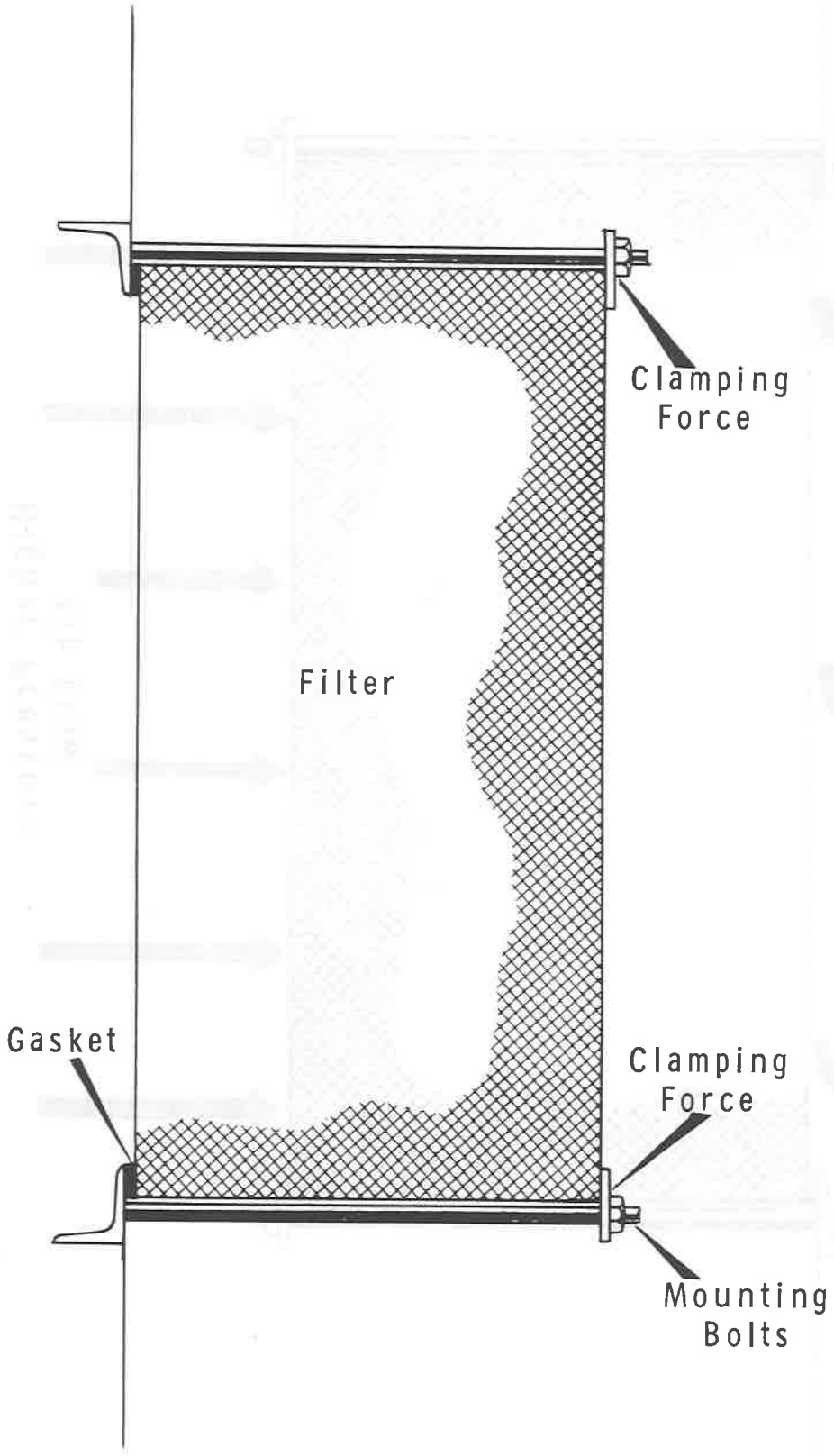


FIGURE 16. Static Force Exerted by Clamping Arrangement

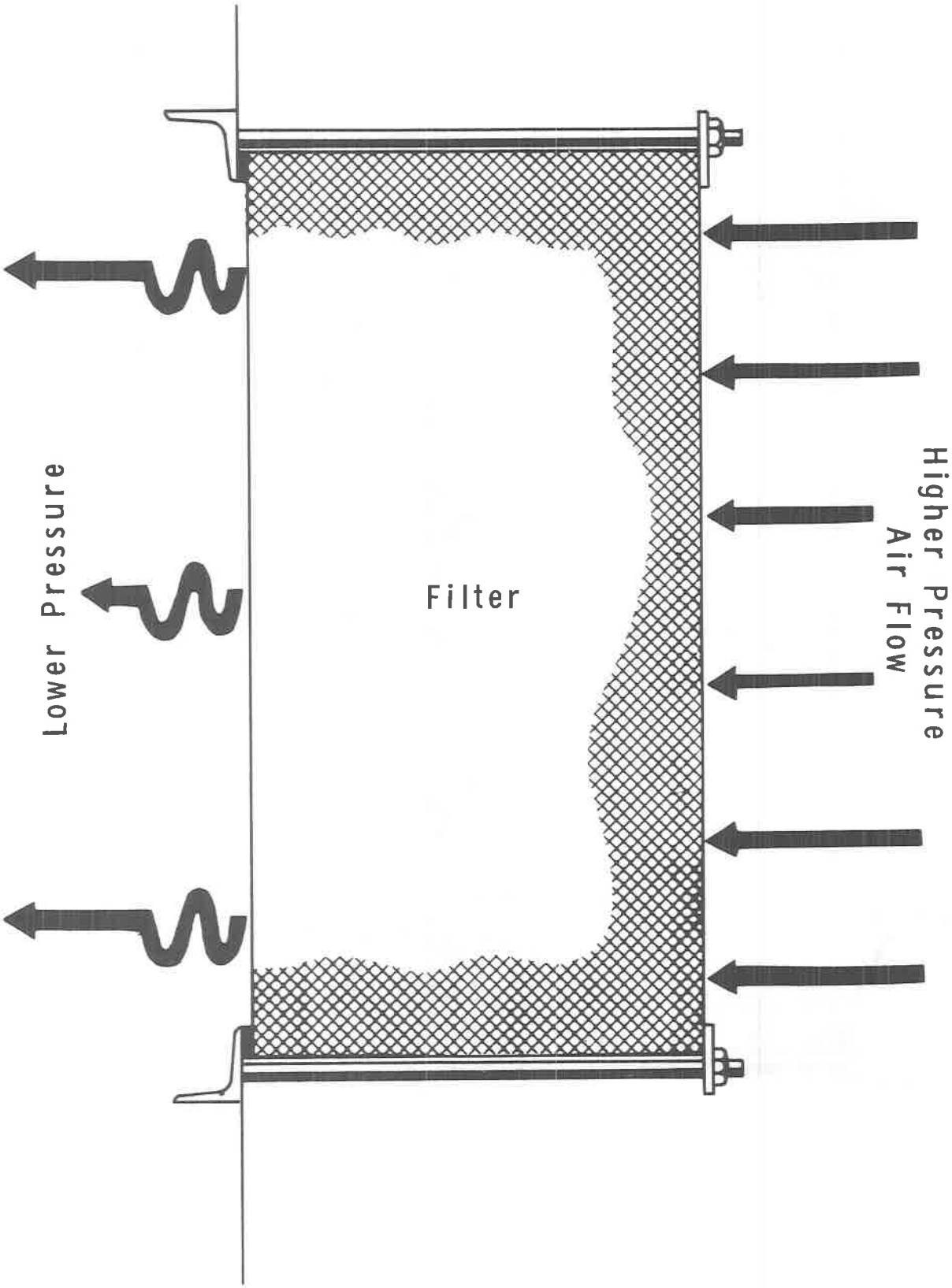


FIGURE 17. Dynamic Sealing Force Created by Air Pressure Differential Across Filter

with a standard 1000 $ft^3$/min filter, this amounts to a constant force of slightly over 20 lb being applied to the gasket at all times. Since filters can be mounted either upstream or downstream of the mounting frame, this force may be positive or negative. When the filter is on the upstream face the force will be positive or compressive. When downstream, it will be negative or tending to decompress the gasket.

The third, as in Figure 18, is another dynamic force created by the mass of the filter which is approximately 35 lb for a 1000 $ft^3$/min unit. This influence may be positive on the gasket if the filter happens, for example, to be mounted horizontally above a ceiling panel or may be zero if it is mounted on a vertical panel.

The fourth force acting on the gasket results from compression springs when used in the clamping device. This is also a dynamic force of a positive nature and continues to apply a decreasing force as the gasket compresses.

DYNAMIC

Dynamic force as experienced during the operation of a filter can be attributed to the parameters of air pressure, spring-type clamping, or the mass of the filter. These may be cumulative or counteractive, depending on the method of installation and operation of the filter facility.

A test device, Figure 19, was used to produce a uniform dynamic load on full-scale specimens. Test gasket (A) was mounted on the bottom edge of the filter frame (B), which was then placed on a mounting base (C), similar in construction to the usual mounting panel. The pressure source (D), a water tank, was then located on top of the frame to provide equal pressure; and water was added to achieve the desired gasket compression. A maximum load of about 1150 lb was possible. The amount of compression was determined by dial micrometers (E), at each corner.

Two common types of gaskets were tested (See Figure 20). A closed cell neoprene, SCE 41, was compressed 27% by 340 lb (4.88 psi) and left undisturbed for 20 days. In less than 1 week, the constant load had increased the compression to more than 80%. The cork-neoprene

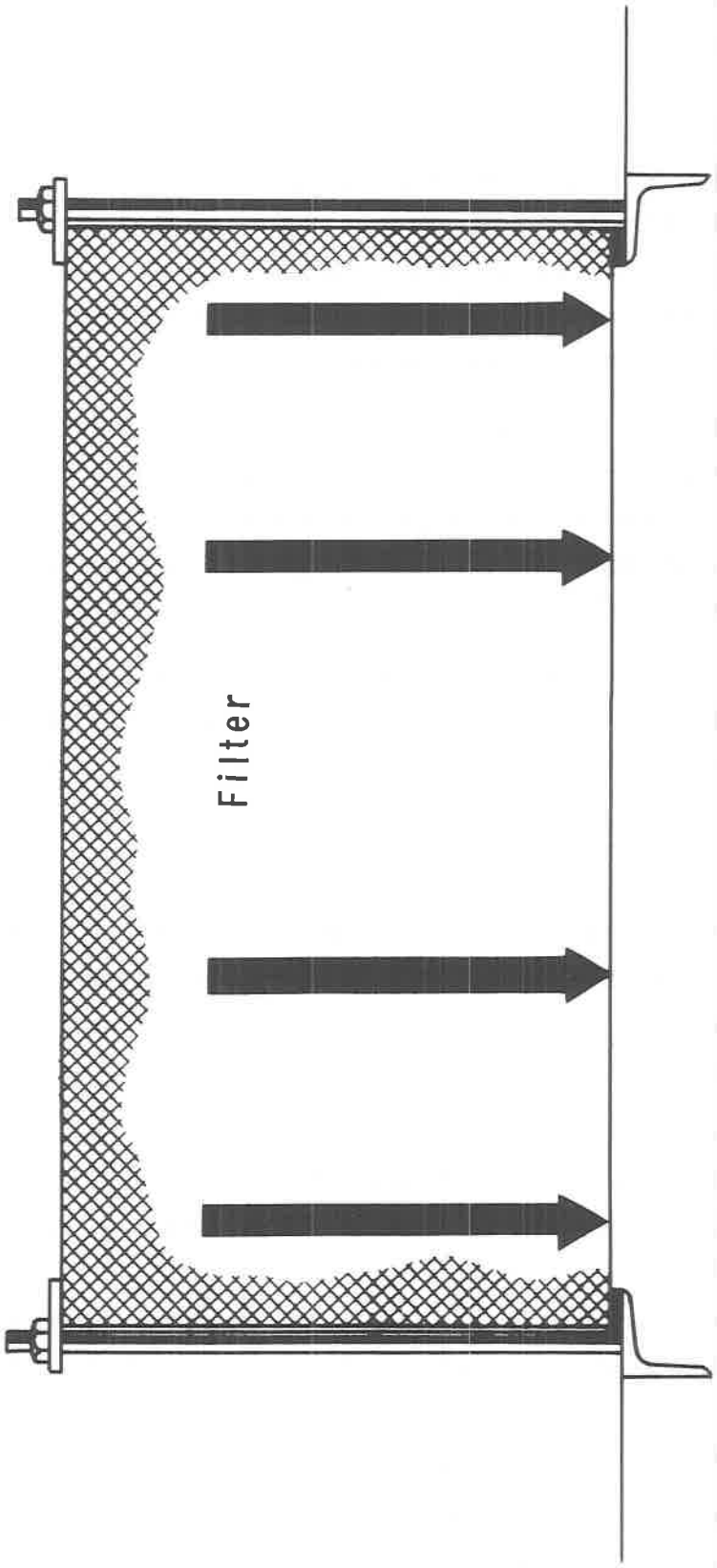


FIGURE 18. Dynamic Force Created by Mass of Filter

Figure 19. Test Device Used to Produce Uniform Dynamic Load on Full-Scale Specimens

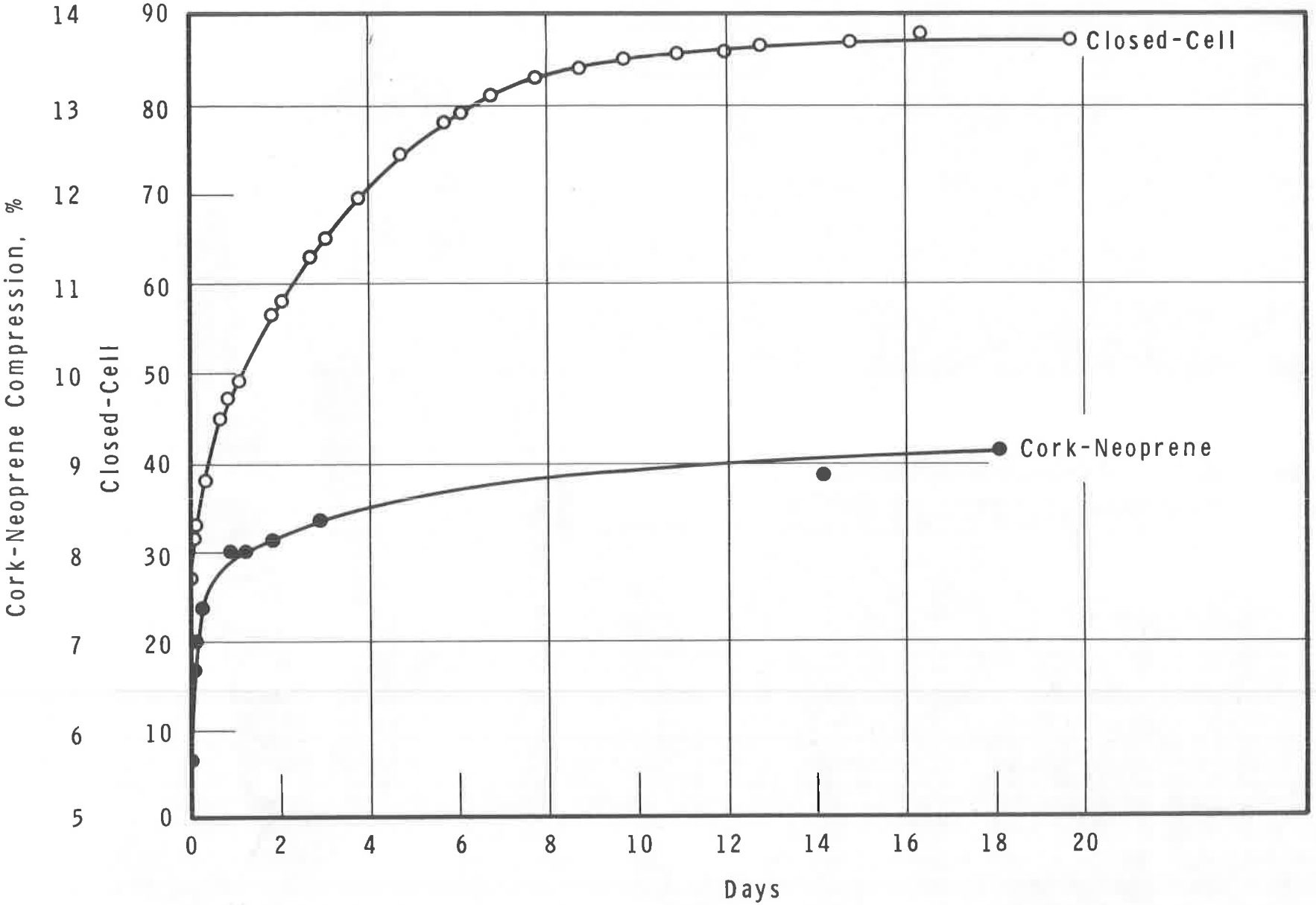


FIGURE 20. Uniform Dynamic Loading

gasket of durometer 41, Shore A, was similarly mounted and compressed to 5.7% by 1077 lb (15.5 psi). In 1 week, compression had increased to 8.5%. The compression of both gaskets after 2 weeks was changing at a relatively slow rate.

STATIC

Clamping of a filter during installation by bolting or by a cam arrangement produces a fixed deflection by the force exerted. Regardless what changes take place in the physical properties of a gasket medium following clamping, the amount of deflection due to clamping remains unchanged. To ascertain what effect this would have, specimens of various gasket materials were placed in an ASTM compression set device[3] with the spring removed (Figure 21). After initial compression, specimens were left in the device for up to 111 days. All specimens, except one, were approximately 3/4 in. x 2.25 in. x 0.25 in. and were compressed approximately 35%.

To determine what change in compression pressure took place, a pseudo torque wrench arrangement was devised (Figure 22) whereby a torque arm (A), was individually attached to each nut (B) on the compression set device and an increasing force applied by the gradual addition of water to container (C) until a slight sustained movement of the torque arm was produced. By having well machined and lubricated threads, a torque of approximately $2.5 \times 10^{-2}$ ft-lb was measurable. This was equivalent to a force of about 1.5 lb. Movement of the torque arm for a reading was sufficiently small such that the complete series of readings change the gasket compression less than 1%.

The closed cell neoprene (SCE 41) and the cork-neoprene (durometer 41, Shore A) gaskets reached equilibrium pressures of 50 to 60% of their original pressures in about 2 weeks (Figure 23). However, the molded rubber did not change as rapidly and continued relaxing for a longer period. The harder specimen was circular, almost 2 in. in diameter. A considerably higher initial pressure was required for this specimen.

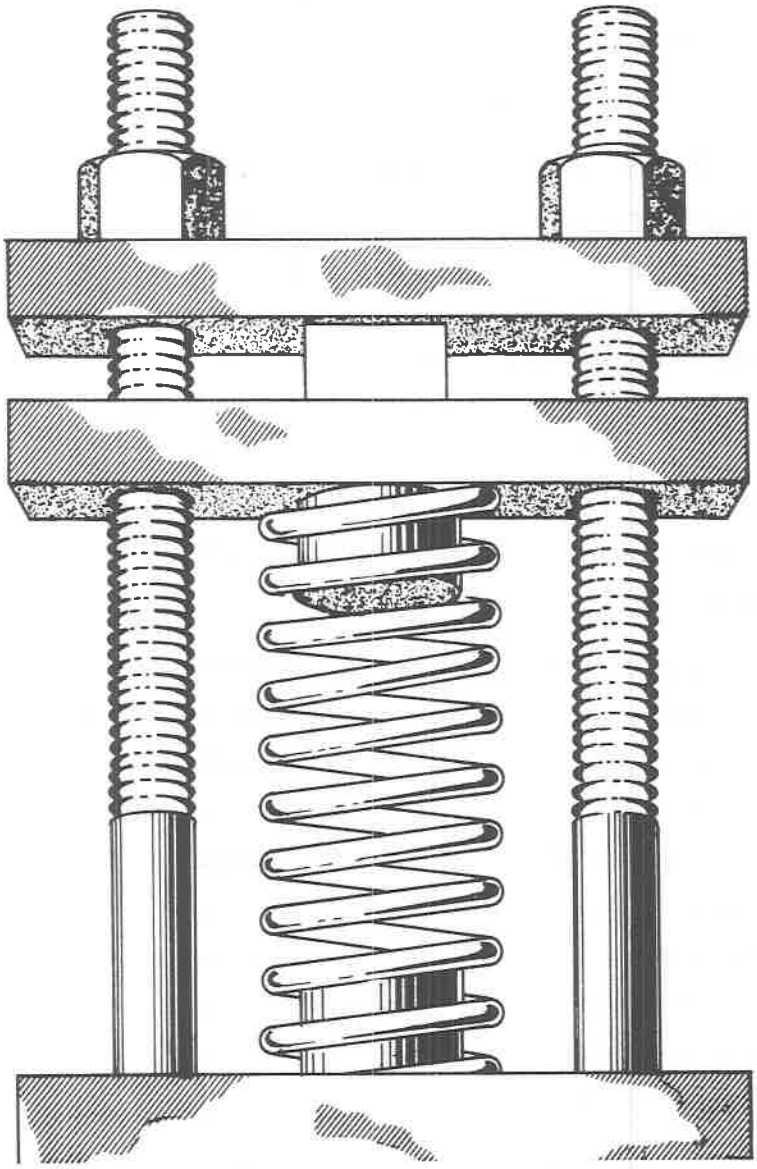

FIGURE 21. Device for Compression Set Test, Using External Loading

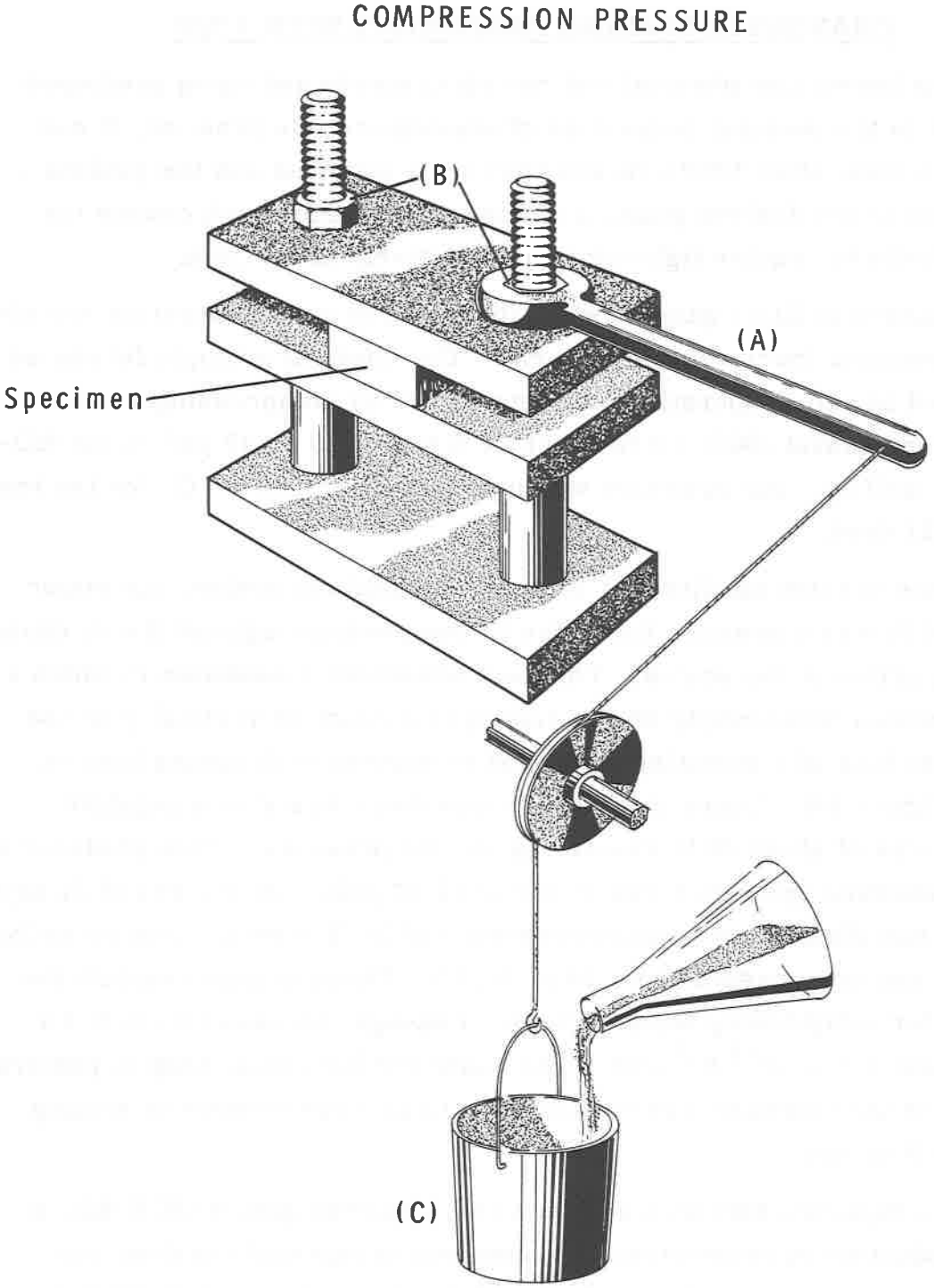


Figure 22. Pseudo Torque Wrench Arrangement

## CHANGES IN SEALING PROPERTIES WITH TIME

It is known that physical and chemical stress and aging predispose to changes in the physical properties of elastomers. In practice, it has been shown that, after HEPA filters have been installed and the gaskets compressed to the desired point, a change takes place which causes the mounting bolts to require tightening in a relatively short time.

Changes in filter gaskets with time when in actual operation are the result of complex forces acting on them. The effect of multiple forces as experienced in actual operation was determined by compressing a closed cell neoprene gasket (SCE 41) to about 24 % by 270 lb (3. 40 psi) in the full-scale test facility. Air pressure was maintained at 1 in. W. G. for the test period of 21 days.

Since the test facility was mounted on platform scales, the major load of 270 lb was a dynamic force due to compression against the mechanical spring action of the scales. This test simulated a condition in which a filter is located horizontally on the ceiling of a room or vertically on the downstream face of a mounting panel and is secured with spring loading clamps (Figure 24). Under these conditions there was also a negative dynamic force of about 20 lb created by the air pressure. This produced a resultant positive dynamic force of 250 lb (4. 31 psi). At the end of 21 days, this force had diminished to approximately 110 lb (1. 9 psi). Concurrently, the gasket had compressed from 24 to 36. 5%. These changes explain the necessity for retightening bolted filters. Leakage increased from $3.4 \times 10^{-4}$ to about $5.5 \times 10^{-4}$ $ft^3$/min. The cause for the initial drop in penetration prior to the increase was possibly due to an improvement in seating during the first day.

In a duplicate test with a closed cell neoprene gasket (SCE 42), a similar reduction in penetration was observed except that the drop and recovery occurred over 4 days. In the 16 day test, the overall dynamic force decreased from 380 lb (5. 52 psi) to about 230 lb (3. 34 psi). Compression increased from 24 to about 35. 5%; and leakage which commenced at $3.2 \times 10^{-4}$ $ft^3$/min dropped to $10^{-4}$ $ft^3$/min then rose to about $2.7 \times 10^{-4}$ $ft^3$/min, and appeared to be still increasing with time.

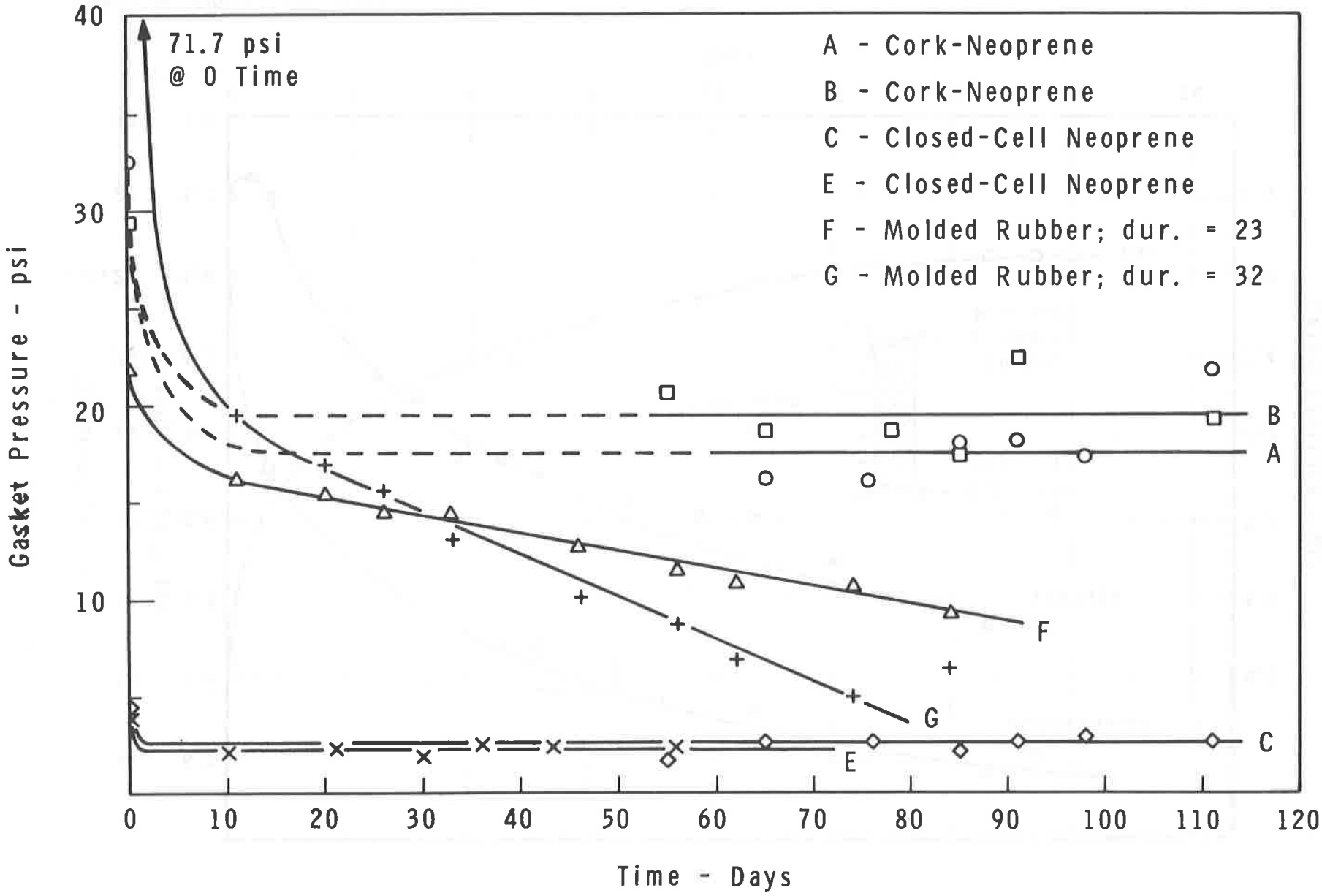


FIGURE 23. Static Loading

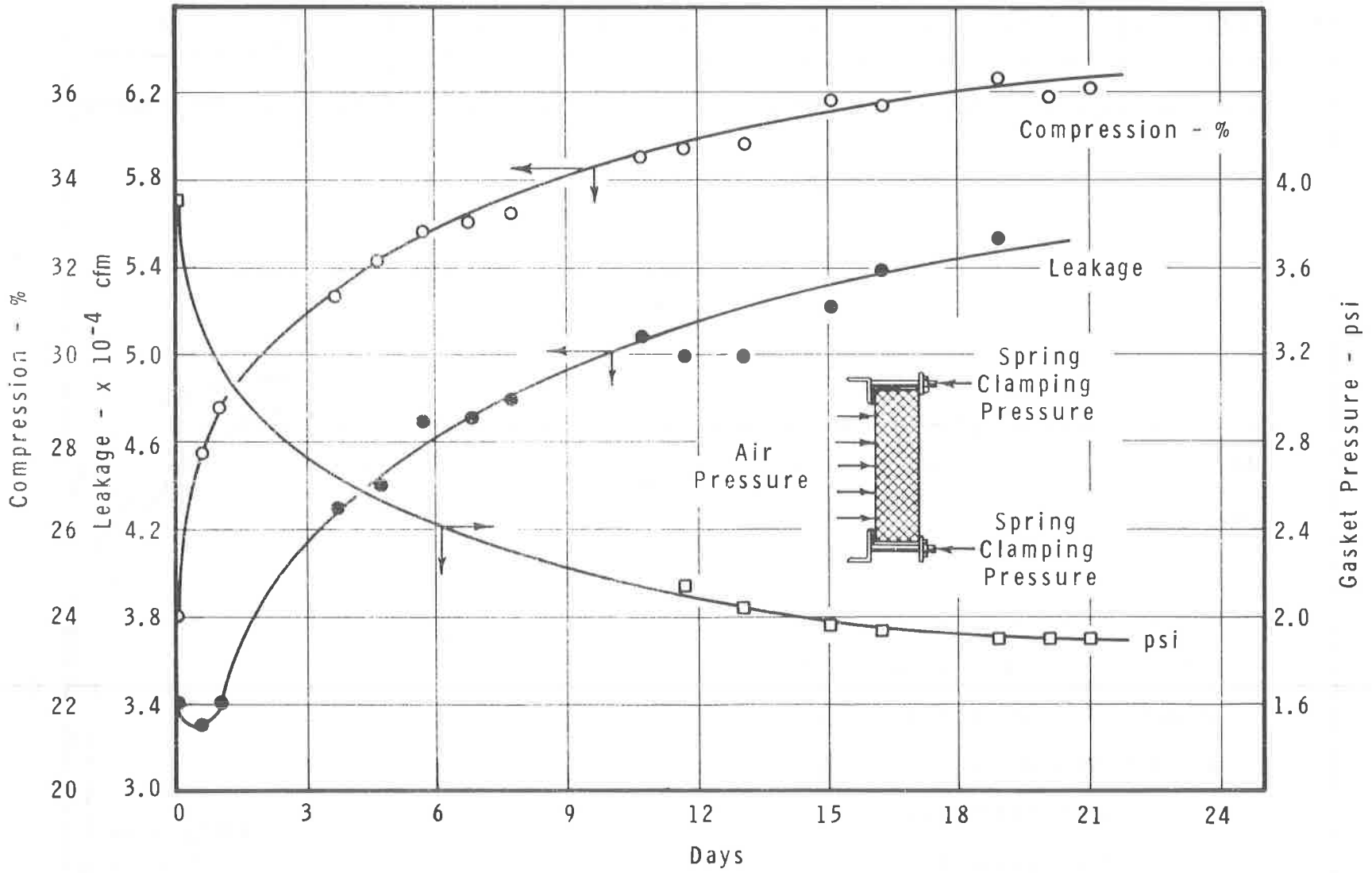


FIGURE 24. Effects of Time (Static-dynamic loading)

To simulate the condition of a filter mounted vertically on the downstream side, the platform scales were disengaged, thus making the clamping a positive static force. A closed-cell neoprene gasket (SCE 41) was used. The 1 in. W. G. static air pressure contributed a negative dynamic force of about 20 lb. The findings are shown in Figure 25. This type of mounting creates considerably less dynamic force, thus, tending to compress the gasket less than in the preceding two tests. As a result, the compression increased with time at a lower rate. Leakage, however, has increased at a higher rate than shown in Figure 24. At the end of 17 days operation, the leakage shown in Figure 25 increased by a factor of 1.7 whereas that in Figure 24 had increased by a factor of 1.6.

## CONCLUSIONS

Investigations, to date, make certain conclusions possible relative to several aspects of gasket leakage.

High compression of HEPA gaskets seems unnecessary. Of the gaskets tested, compression of about 20%, even with defects introduced, reduced the leakage rate to levels below that detectable by DOP filter methods with a 1000 $ft^3$/min filter.

In view of the leakage created by variations in gasket thickness, it is important that thickness be maintained within ±0.01 in. This is particularly important with gaskets of high durometer.

Similarly, it is essential that the mounting surface be in plane to ±0.01 in. to enhance gasket seating and to prevent distortion of the filter frame during clamping. High durometer gaskets would predispose to such leakage if the mounting surface is not in plane.

Although a marked increase in penetration can be attributed to inadequately sealed joints, the leakage rate did not appear to be significant for a 1000 $ft^3$/min filter at gasket compressions over 20%. However, joint leakage is of increasing importance as filter capacity is reduced due to the reduced effect of dilution.

Tests on several different shapes of gaskets showed that all gaskets with the exception of the half-round shape followed the same general

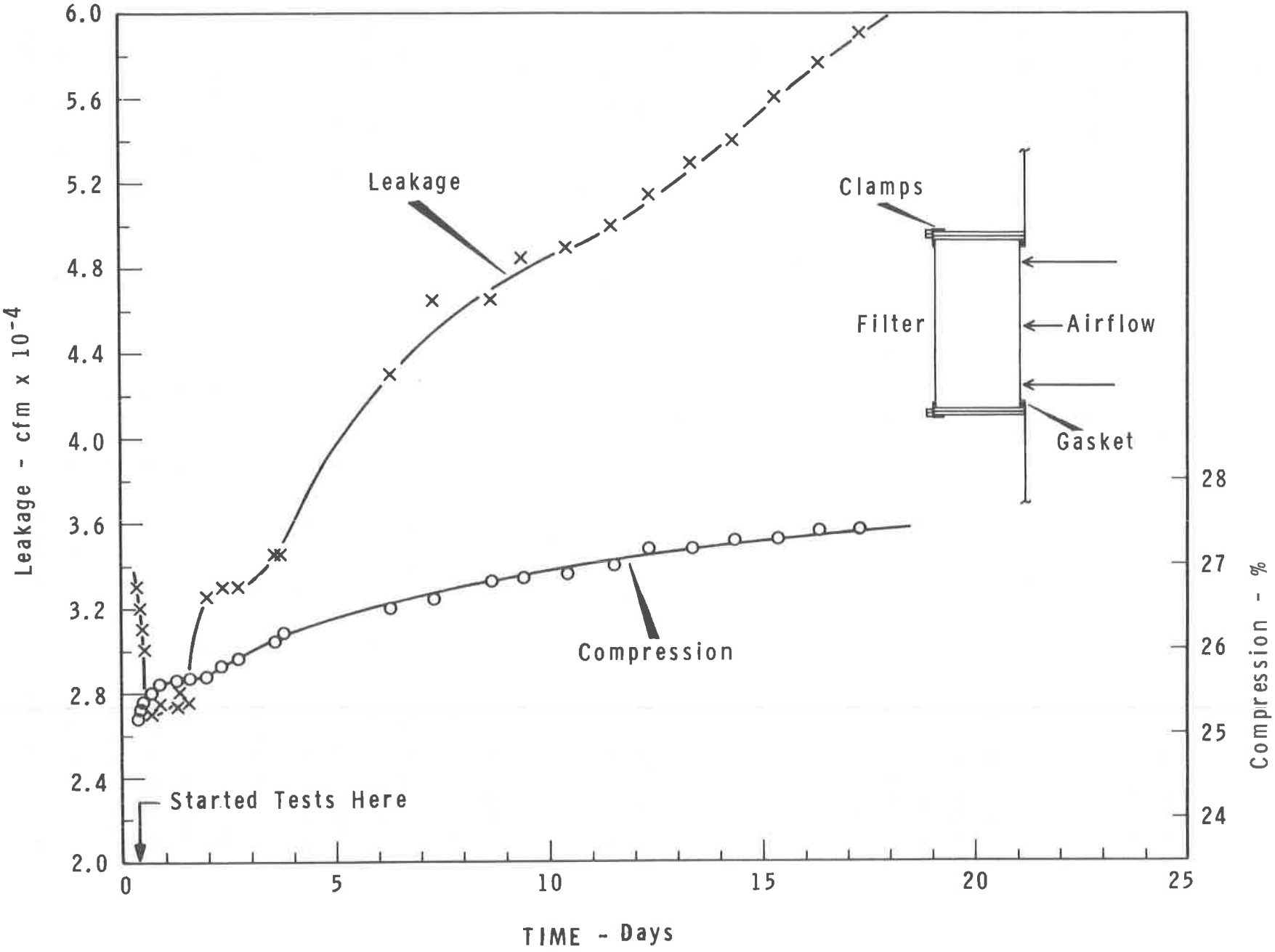


FIG 25. Effects of Time (Static-dynamic loading)

compression-leakage relationships. Shape advantage was not marked so that no particular shape studied could be definitely identified as an optimum. The 1/2 in. molded cellular gasket showed relatively poor sealing ability.

With respect to the effect of time on installed filters, measurable changes in gasket performance were evident. In a period of a few weeks, penetration and compression increased whereas gasket pressure diminished. In view of the change in penetration that occurs with time, in-place filter testing should not be conducted, if possible, until at least 3 weeks following installation.

The findings of this study have identified certain areas of gasket sealing that warrant more extensive evaluation. The more important of these are as follows.

- The effect of aging on gasket leakage of installed filters over extended periods of operation
- The effect of high compression on gasket materials and their sealing qualities
- The importance of gasket skin in various cellular elastomers
- Although related indirectly to gasket sealing, the magnitude and source of frame leakage for various types of filter frames under installation stresses.

## ACKNOWLEDGMENT

The assistance contributed by George A. Golightly, Richland Operations Office, AEC, in conducting certain of the laboratory tests is acknowledged. Recognition is also made of the technical guidance provided by E. H. May, Rubatex Corporation and Philip Hodel, Huntington Rubber Company. The specimens of conventional gaskets were kindly contributed by American Air Filter Company, Mine Safety Appliances Company, Rubatex Corporation, and Flanders Filters, Inc.; the latter also furnished the molded gaskets.

## REFERENCES


1. Tentative Method of Test for for Indentation of Rubber by Means of of a Durometer, ASTM D676-59T.

2. Tentative Specifications and Methods of Test for Sponge and Expanded Cellular Rubber Products, ASTM D1056-62T.

3. Standard Methods of Test for Compression Set of Vulcanized Rubber, ASTM D395-61.

# DEVELOPMENTS IN CONTAMINATED FILTER REMOVAL EQUIPMENT*

C. A. Hahs

Oak Ridge National Laboratory
Oak Ridge, Tennessee

## Abstract

Equipment used to filter gases exhausted from a nuclear facility and the methods by which this equipment will be removed and replaced require careful planning. At Oak Ridge National Laboratory, one filter removal carrier has been designed to remove filters from both the older and the newer filter pit installations and to provide gamma and/or neutron shielding during this operation. Other developments in removal technique are exemplified by the methods used to remotely remove, transport, and deposit in-cell canister filters in disposable casks, and by the methods used to seal glove-box exhaust filters in their own polyethylene tubes before removing them.

## Introduction

When a nuclear facility is being planned, careful consideration must be given to the equipment needed to filter the gases exhausted from the facility and the methods by which this equipment will be removed and replaced. In many cases, filters removed from a facility will not normally require gamma or neutron shielding. However, an accident within the facility could cause the release of particulate matter with a high level of activity, and the filters would then require shielding during their removal. Therefore, the ideal installation would allow the filters to be removed by hand during normal operation and have provisions for their removal within gamma and/or neutron shields if necessary. This consideration must be extended to cover the many types of filtering equipment that may be used in the nuclear facility. The latest developments in contaminated filter removal equipment and technique at Oak Ridge National Laboratory (ORNL) are related to the removal of filters from underground pits, hot cells, and glove boxes, and these developments are discussed in this paper.

---

*Research sponsored by the U. S. Atomic Energy Commission under contract with the Union Carbide Corporation.

## Removal of Filters From Pits

At ORNL, we have designed one filter removal carrier that will serve the most recent filter pit installations still on the drawing boards as well as many of the older installations. This double-jacketed carrier provides for gamma shielding with 3 1/2 in. of steel, and neutron shielding is furnished by filling the 8-in. width between the steel jackets with water. Six tons of water are required for this purpose, and when filled, the carrier will weigh 16 tons. In Fig. 1, the ORNL filter removal carrier is illustrated in place over the cell ventilation filter pit within the Transuranium Processing Plant, one of the newer facilities at ORNL.

## Equipment Arrangement in Newer Pits

The filter pits in the Transuranium Processing Plant are located within the limited access area of the facility. This location permits the carrier to be positioned with the building crane and also allows the building itself to serve as secondary containment for the filters. Three prefilters, MSA Dustfoe filters with an efficiency of from 80 to 90%, and six absolute filters with an efficiency of 99.97% are contained within the filter enclosure in the pit, as shown in Fig. 1. The six absolute filters are arranged in two sets of three filters in series. All filter enclosures are made of steel and are provided with closure plates to seal the end connections before the filter enclosures are removed from the filter pits. The filter enclosures are connected to pipe ducts in the pits by means of clamping devices.

The clamping devices used to connect and seal the filter enclosures with the ducts in the newer filter pit installations are extremely important, and they can cause operational problems if not properly designed. Some trouble was encountered during fabrication of the clamping devices for the Transuranium Processing Plant, and a new concept of the device was developed that has proved satisfactory and warrants mention here.

This new concept of a clamping device involved the use of bellows to connect the pipe ducts and the filter enclosures. This type of device was used in the Thorium-Uranium Recycle Facility, and one such unit is illustrated in Fig. 2. The springs between the flanges preload the bellows in tension and make the unit rigid. They also allow the bellows to pass from tension to compression, which greatly increases the cycle life of the unit. The 6- and 18-in. bellows used to make the clamping devices at ORNL had enough flexibility to allow construction dimensional tolerances of $\pm$1/8 in. to be used on ductwork in the filter pits and on the length of the filter enclosures. The dimensional relationships between the alignment of ducts and the flanges of the connecting equipment are not critical because the bellows may cock approximately 3/8 in. without affecting the sealing capability.

## Removal Procedure For Newer Pits

Before removing the shielding plugs from the top of the filter pit from which filters are to be removed, the clamping devices in the pit are actuated with extension tools through the concrete shielding plugs. After the shielding plugs have been removed, the removal carrier is positioned over the filter enclosure to be removed, as illustrated in Fig. 1, and two 500-watt sealed beam

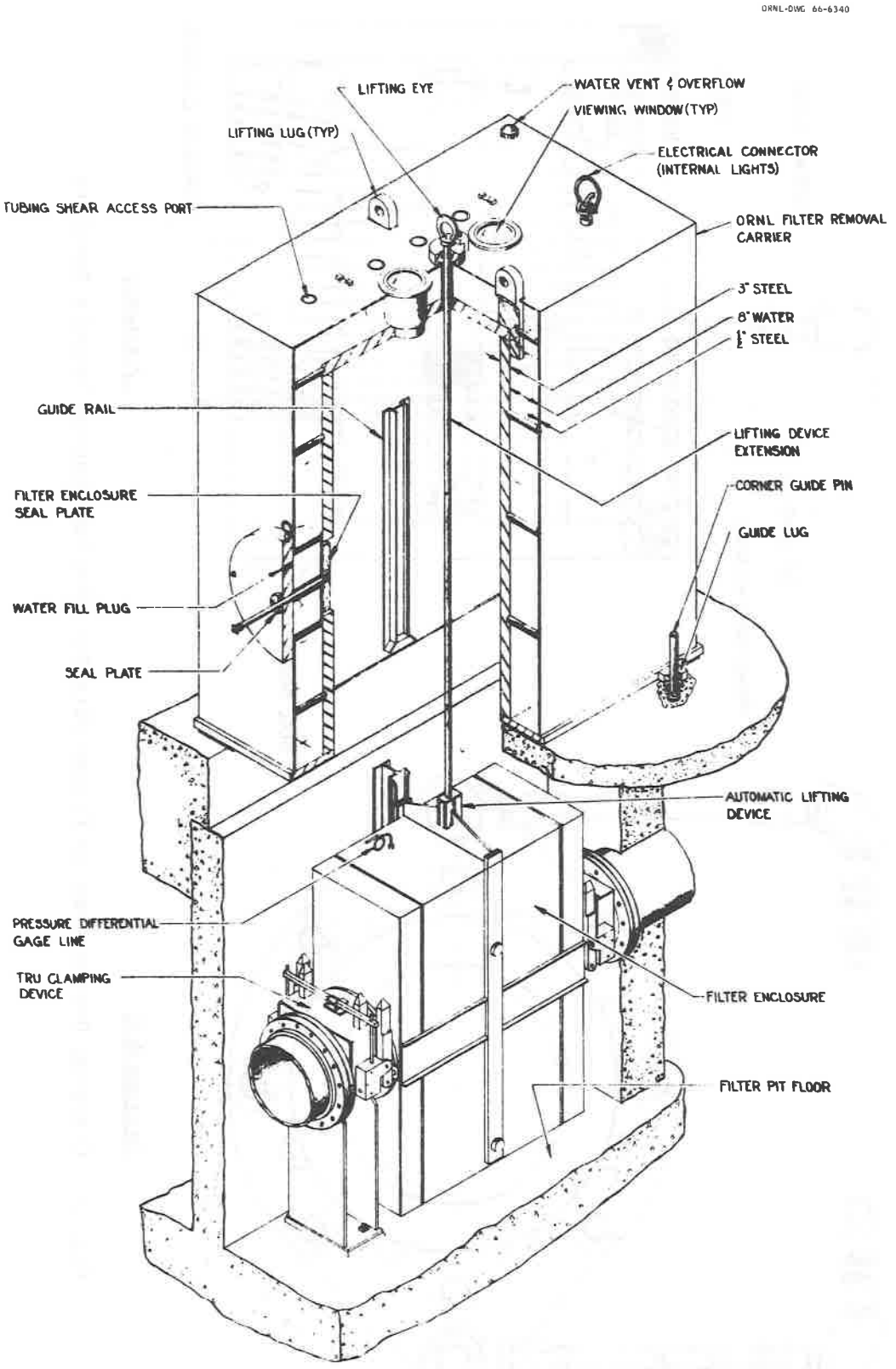


Fig. 1. Filter Removal Carrier Positioned For Removal of a Filter Enclosure From the Transuranium Processing Plant Cell Ventilation Filter Pit.

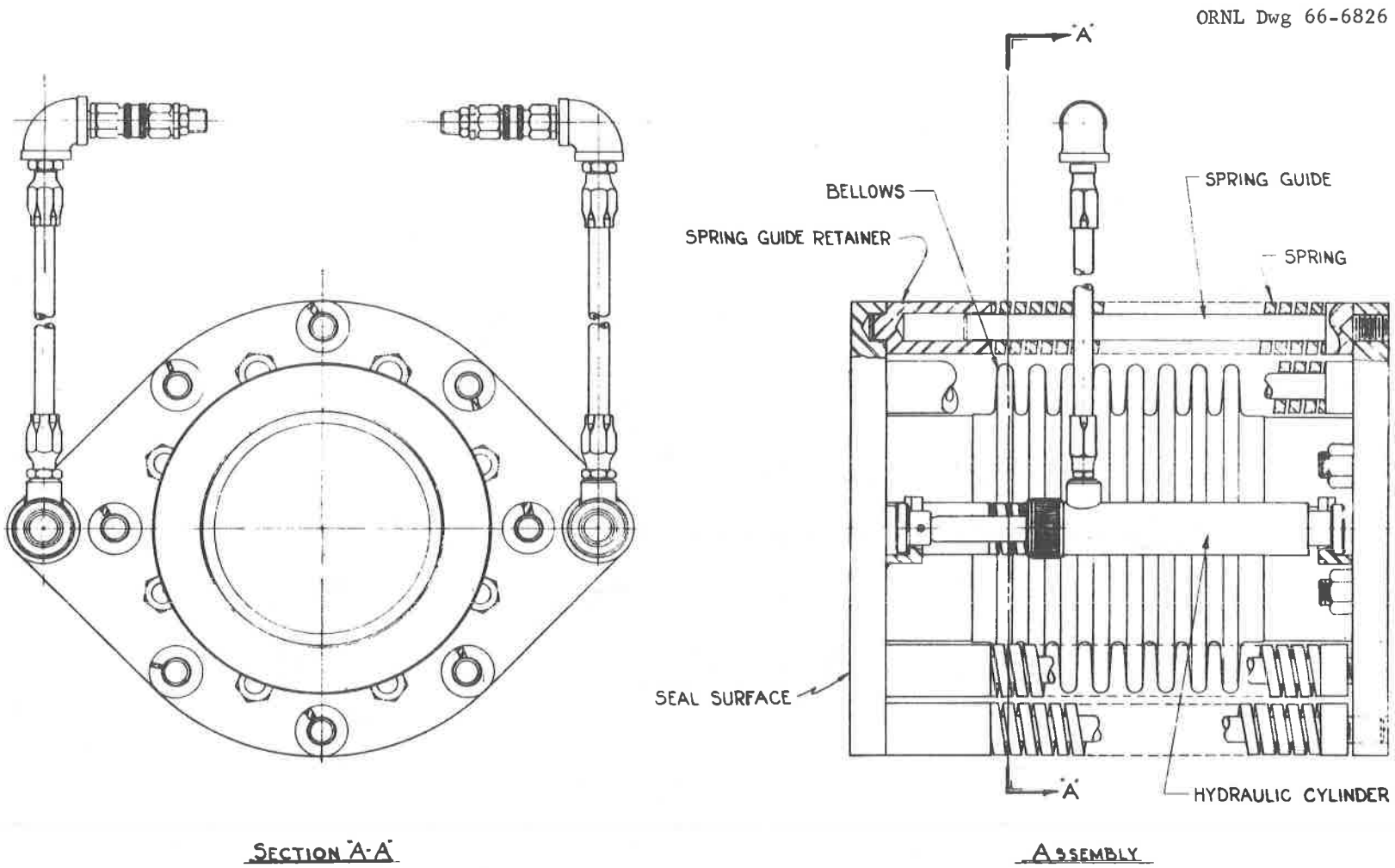


Fig. 2. Clamping Device Used in Filter Pits For Thorium-Uranium Recycle Facility.

lamps in the carrier illuminate the hardware in the pit.

To ensure that the lifting device of the carrier is positioned directly over the lifting support on the filter enclosure, guide pins are inserted through the guide lugs on the side of the carrier. The pressure-differential-gauge line, which is normally connected to the piping in the pit, is sheared remotely with a tubing shear passed through the top of the carrier. Then the automatic lifting device is lowered, and it latches onto the lifting support of the filter enclosure upon contact. Guide rails located in the filter pit and carrier guide the filter enclosure as it is lifted from the pit with the lifting eye. The ends of the filter enclosure are sealed with closure plates while the carrier is over the pit, and the bottom of the carrier is sealed with a steel plate that also provides shielding. The sealed carrier is then transported to the burial ground where its contents are buried.

### Equipment Arrangement in Older Pits

Many of the older filter pits at ORNL have designs similar to that shown in Fig. 3. Three 24- x 24- x 11 1/2-in. filters are banded together and forced against a seal plate with a steel wedge. This system has worked satisfactorily where the sealing surfaces are flat to within 1/16 in. and where joints between the sealing framework and the concrete have been made properly. Filters in these older pits were usually removed without shielding, but the ORNL filter removal carrier was designed to serve these older filter pits as well as the newer ones.

### Removal Procedure For Older Pits

To remove filters from the older pits, a plywood box with a hinged bottom is placed in the carrier. After the shielding plugs have been removed from the top of the filter pit, the carrier is aligned over the filter units to be removed by using guide lugs located on opposite corners of the carrier. A lifting tool is used to elevate the steel wedge about 12 in. to free the filters. Then two units of three filters are lifted into the plywood box with a filter lifting tool. The hinged bottom of the plywood box is then closed and sealed with a mechanism inside the carrier. All penetrations through the top of the plywood box are also sealed before the carrier is removed from the filter pit. The bottom shield is sealed on the carrier, which is then transported to the burial ground where the contaminated filters are buried in the sealed plywood box.

## Removal of In-Cell Canister Filters

There are nine cell cubicles in the Transuranium Processing Plant at ORNL, and a cross section of a typical cubicle is illustrated in Fig. 4. Most of the air within a cubicle is cooled and recirculated, but air removed from each of the nine cubicles passes through a canister-type filter before going through the vessel off-gas filters and on to the stack. Design of the air handling equipment within these cubicles was complicated by the acid atmosphere, high radiation level, and the limited space within the cubicle. All of the equipment, including

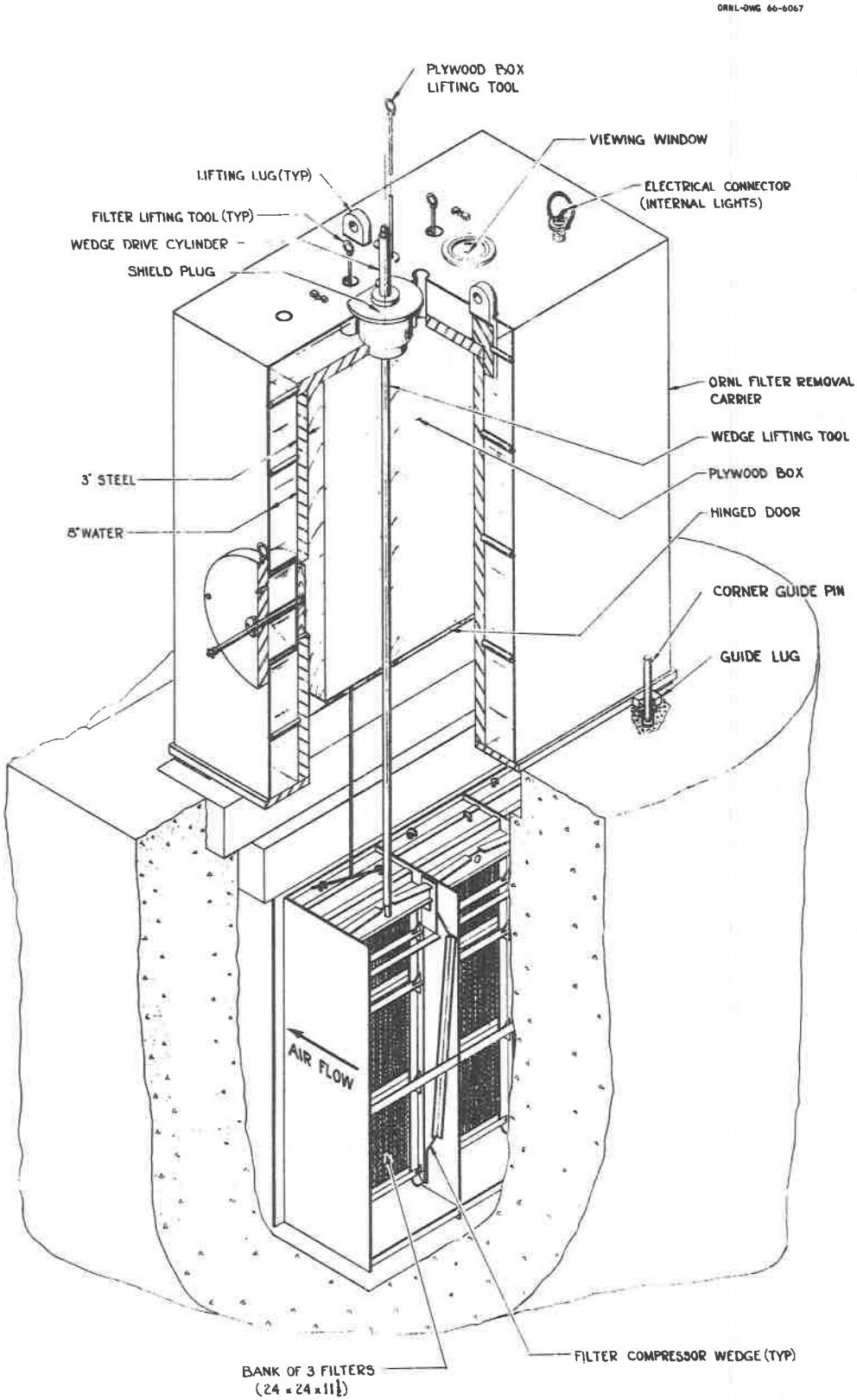


Fig. 3. Filter Removal Carrier Positioned Over Older Type Filter Pit.

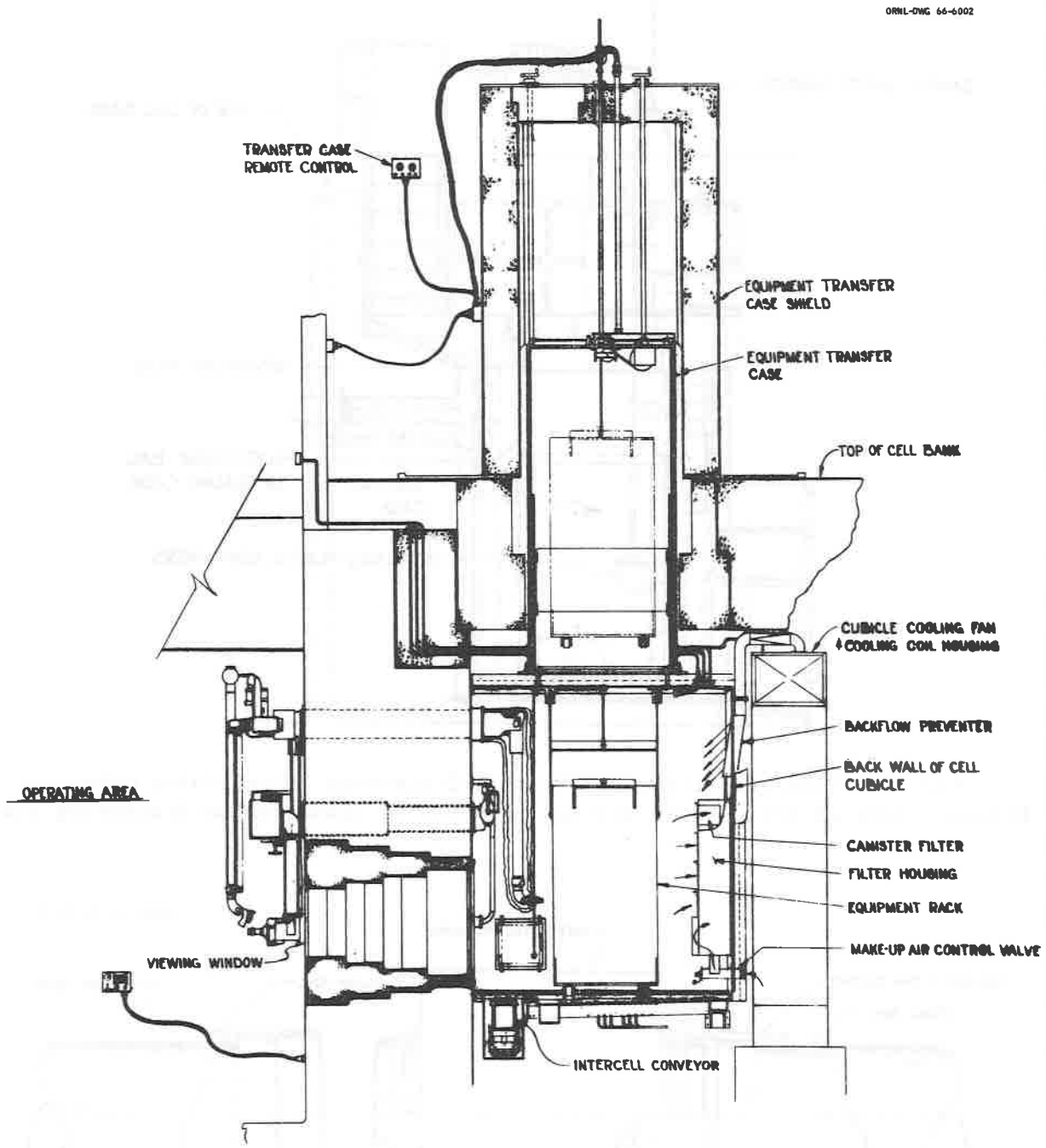


Fig. 4. Cross Section of a Typical Cell Cubicle in the Transuranium Processing Plant.

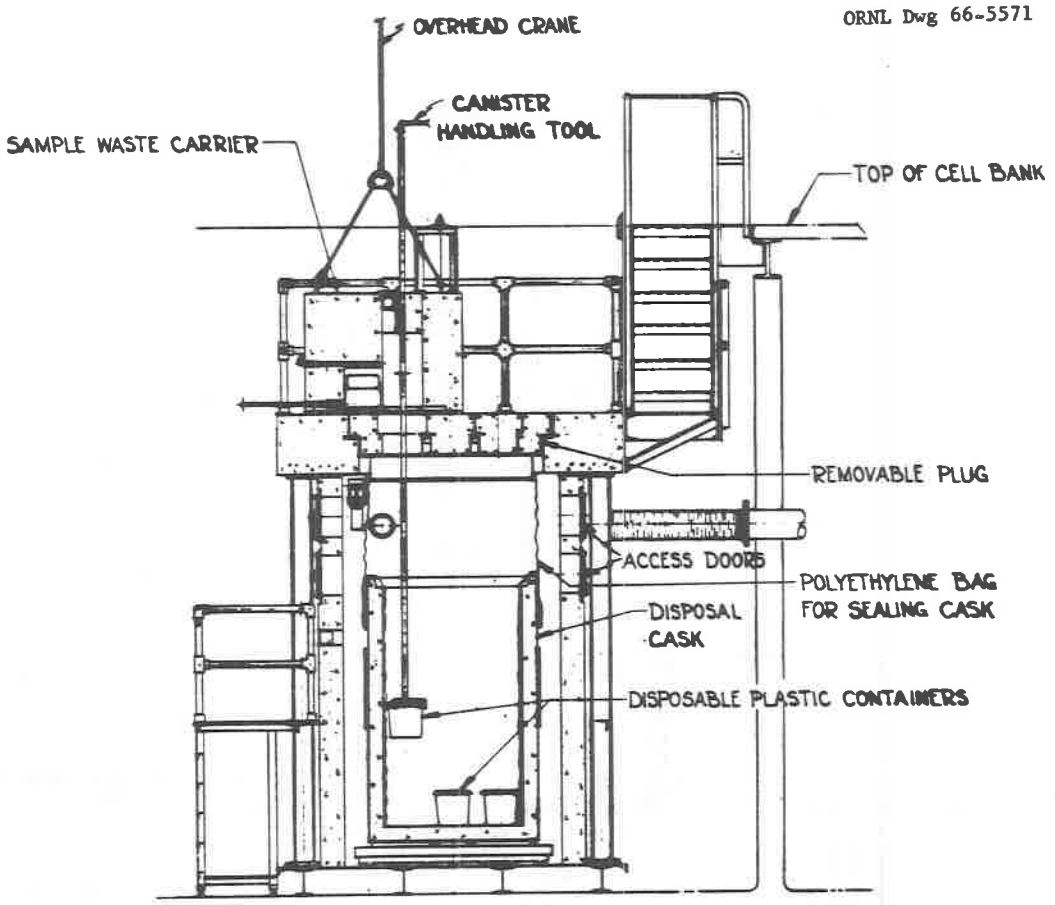


Fig. 5. Canister Filters in Plastic Containers Being Loaded Into Disposal Cask at Solid Waste Disposal Station in Transuranium Processing Plant.

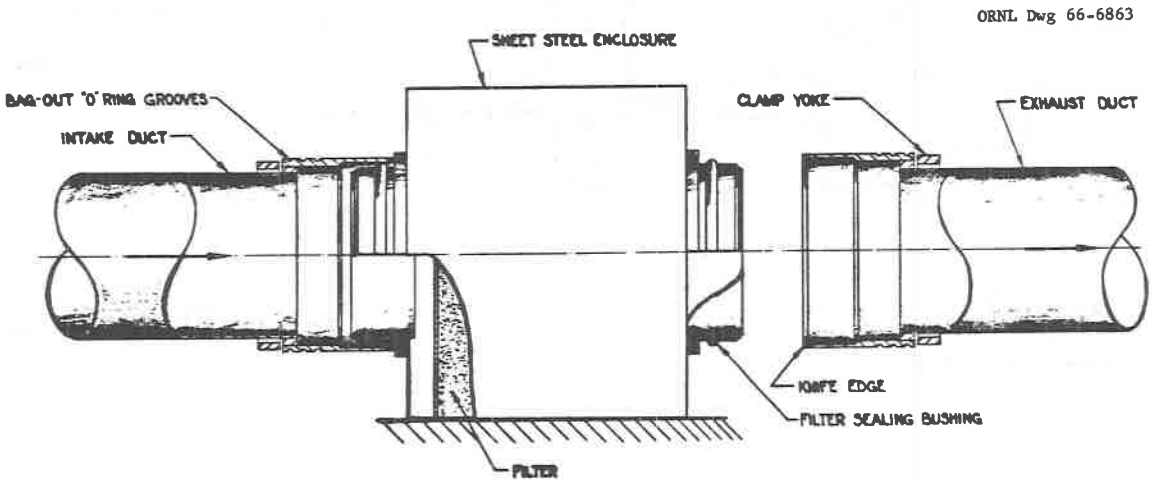


Fig. 6. Exhaust Filter Enclosure For Glove Boxes.

the filter housing and backflow preventer, was designed for remote removal, and the canister-type filter frame was made of stainless steel to ensure a seal with the filter material in this acid environment. These canister filters are 99.97% efficient, and they will contain most of the high level isotopes that leave the cubicle. Therefore, the canisters must be removed in a shielded container.

The canister filters are removed from each cell cubicle and delivered to the transfer area cubicle via the intercell conveyor shown in Fig. 4. These canister filters are deposited in the transfer area cubicle where they are sealed within disposable polyethylene containers and then transferred to the solid waste disposal station in a shielded carrier. The canisters in their plastic containers are shown being loaded into a disposable cask in Fig. 5.

The disposable cask is made from a standard 42-in.-ID concrete pipe, and it will contain 42 canisters. When the cask is full, the turntable upon which it rests is rotated to twist the polyethylene bag lining the cask. The twisted bag is banded with polyethylene, and a hot knife is used to cut and seal the top of the bag. The lid of the cask is sealed with tar before the cask is removed from the solid waste disposal station, and the cask is then taken to the burial ground where it and its contents are buried. All solid waste that will fit in the 8-in.-diameter-by-8-in.-deep canister in the intercell conveyor is disposed of in the same manner.

## Removal of Glove Box Filters

The glove box exhaust filtering equipment recently installed in the Transuranium Research Laboratory at ORNL uses filters enclosed in sheet steel, as illustrated in Fig. 6. Each filter enclosure is contained within its own polyethylene tube at installation. One end of the tube is connected to the inlet duct and the other to the exhaust duct with O-rings. The filter sealing bushings on the filter enclosure inlet and outlet tubes seal these tubes to the connecting ducts. These bushings are made of neoprene and are disposable.

Filters installed in glove boxes in this manner do not require shielding for removal and are simple to change by hand. Before the filter enclosure is moved from its normal position, the ends of its containing polyethylene tube are cut and heat sealed. The ends of the tube remaining on the connecting ducts are contained within the polyethylene tube of the replacement filter. These tube ends may be placed in a pocket formed in the side of the replacement tube and heat sealed to reduce the spread of contamination.

## Summary

The safe removal of filters that are contaminated with radioactive particles has presented a problem at ORNL as well as other AEC installations, and a great effort has been made at ORNL to standardize the equipment used to remove contaminated filters. The filter removal equipment and techniques discussed in this paper have been designed to serve old, new, and future filter installations and to insure safe and dependable handling of contaminated filters.

## DISCUSSION

BURCHSTED: These mounting system filters will frequently be made of structural steel members and the tolerances on these are going to be fairly crude; do you plan to make any tests to simulate the effect of warping of a mounting frame or twisting of the frame itself or twisting of the mounting flange of the filter unit?

ADLEY: I think I visualize what you are concerned about. We don't have any firm plans made on that yet, but that is a real logical one to try and we probably will include it.

REIST: Could you say anything about whether the conclusions that you made for the 1,000 cfm filter could be made also for smaller or larger filter sizes?

ADLEY: I can say this much: I don't know whether I included it in my coverage here or not, but one point with respect to the leakages, of course, where you have a fixed amount of leakage, say, in cc's per minute through a gasket joint, for example, the smaller the filter the more important this gets. The point is that you dilute this leakage with a certain amount of clean air that is available, or essentially clean air, and the smaller amounts of this clean air the more important any leakage becomes.

FULLER: Mr. Adley, would you speculate on whether or not the buildup in pressure drop would tend to compensate for the deterioration of the gasket on a upstream sealing or at least a downstream sealing unit? Do you have any projection?

ADLEY: I don't seem to think so. For example, just from the standpoint of the pressure drop involved, if the pressure drop increases, does it counteract?

FULLER: Yes.

ADLEY: As the pressure drop gets higher, you do get more leakage through any defects that you have in your seal. At the same time, it seems from the tests that we have run so far, that as the installation proceeds with the aging process, that there is a certain amount of changing in the compression and also in the leakage. Now, the tests we have done so far are limited. There are really just two tests, but they are very indicative of what will happen. It does seem that in both of the tests that the leakage does increase with time, so my guess is you would not have any canceling out of leakage.

# THE DEVELOPMENT OF IMPREGNATED CHARCOALS FOR TRAPPING METHYL IODIDE AT HIGH HUMIDITY

by

D. A. COLLINS, L. R. TAYLOR and R. TAYLOR
U.K.A.E.A., Reactor Development Laboratory,
Windscale Works, Sellafield, Cumberland, England

## SUMMARY

Methyl iodide can be present in releases of iodine from irradiated fuel and at high humidity most activated charcoals will not provide efficient permanent retention of methyl iodide.

Impregnation of activated charcoal with certain amines or inorganic halides has been found to improve the retention of methyl iodide at high humidity. The best results are given by triethylenediamine or potassium iodide supported on 207B charcoal. The behaviour of these two impregnated charcoals has been examined in more detail.

Design data are presented in the form of a linear relationship between log DF and stay-time in the charcoal bed, and a predicted allowance for ageing of charcoals exposed to a continuous flow of air. The performance during and after exposure to steam at high temperature has been measured.

The properties of the two recommended impregnants are to some extent complementary. Potassium iodide is not sensitive to carbon dioxide or high temperatures, but will not accept as high a loading of methyl iodide as triethylenediamine and lowers the ignition point of the charcoal. Its mode of action is not so well understood and it may be less consistent in its performance and more readily poisoned. For application in reactor containment systems a mixture of the two types of impregnated charcoal is recommended.

Tests of large scale beds filled with impregnated charcoal have given satisfactory results but re-emphasise the importance of eliminating mechanical defects which can lead to by-passing of the charcoal.

TABLE II

Cumulative penetration of methyl iodide (100ug/g charcoal) through impregnated 207B charcoals with continued passage of saturated air at room temperature

| Impregnant | Stay-time in charcoal bed seconds | Total Penetration after various times % | | | | |
|---|---|---|---|---|---|---|
| | | 1 hour | 4 hours | 24 hours | 100 hours | 168 hours |
| 0.8% pyridine | 3 | 0.45 | 0.49 | - | - | - |
| 1% morpholine | 1.5 | 0.013 | 0.014 | - | - | 0.017 |
| 1% piperidine | 1.5 | 0.005 | - | 0.0065 | - | 0.007 |
| 10% piperazine | 0.5 | 0.0048 | - | - | 0.005 | - |
| 5% TEDA | 0.2 | 0.016 | 0.027 | - | 0.055 | - |
| 0.5% KI | 0.2 | 0.307 | 0.344 | - | 0.363 | - |

## OPTIMUM LEVEL OF IMPREGNATION

23. It is to be expected with the amine impregnants that too low a level of impregnation will be ineffective and too high a level will poison the charcoal. The results of tests to determine the optimum level are shown in Figure 6. In each case the optimum performance is obtained in the neighbourhood of 5 - 10$^{w}/_{o}$ impregnation. In the case of triethylenediamine, which is relatively expensive chemical, cost considerations dictate the choice of 5$^{w}/_{o}$ impregnation for large scale application.

24. Potassium iodide clearly operates by a different mechanism from the amines and performance is not nearly so sensitive to the level of impregnation. The curve is virtually flat over almost two orders of magnitude variation in the level of impregnation but the best performance is obtained within the range of 0.1 to 1$^{w}/_{o}$ on the charcoal. Here cost is not a significant consideration and it is quite reasonable to select the centre of this range for all applications. Impregnation with potassium iodide has been found to lower the ignition point of 207B charcoal to about the same as that of unimpregnated coconut charcoal but measurements have been made only with 0.5$^{w}/_{o}$ KI on 207B.

## EFFECTS OF MASS OF METHYL IODIDE LOADED ON CHARCOAL

25. Earlier work in dry gases has shown that a sharp breakthrough occurs when the mass of methyl iodide per unit weight of charcoal exceeds a certain limit which differs for different charcoals. Similar behaviour is anticipated with impregnated charcoals in wet gases and some measurements have been made with selected charcoals to define their loading limits. The results shown in Fig. 7 illustrate that with triethylenediamine serious overloading does not occur until well over one milligram of methyl iodide per gram of charcoal is presented to the charcoal bed.

Fig. 6

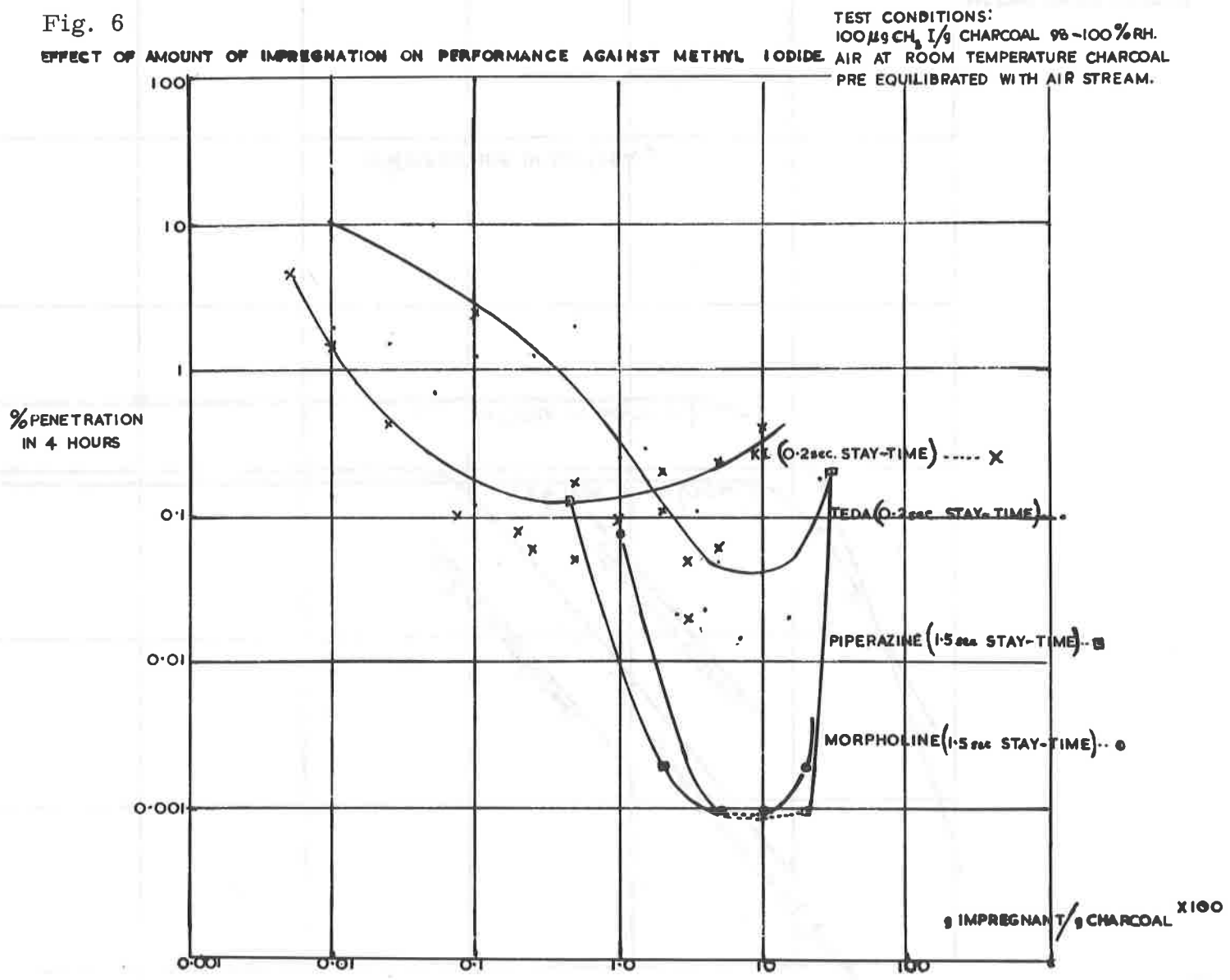
EFFECT OF AMOUNT OF IMPREGNATION ON PERFORMANCE AGAINST METHYL IODIDE.
TEST CONDITIONS:
100 µg CH3 I/g CHARCOAL 98-100% RH.
AIR AT ROOM TEMPERATURE CHARCOAL
PRE EQUILIBRATED WITH AIR STREAM.
% PENETRATION IN 4 HOURS
100
10
1
0·1
0·01
0·001
KI (0·2sec. STAY-TIME) ----- X
TEDA (0·2sec STAY-TIME)
PIPERAZINE (1·5 sec STAY-TIME)
MORPHOLINE (1·5 sec STAY-TIME)
0·001
0·01
0·1
1·0
10
100
g IMPREGNANT/g CHARCOAL X100

Fig. 7

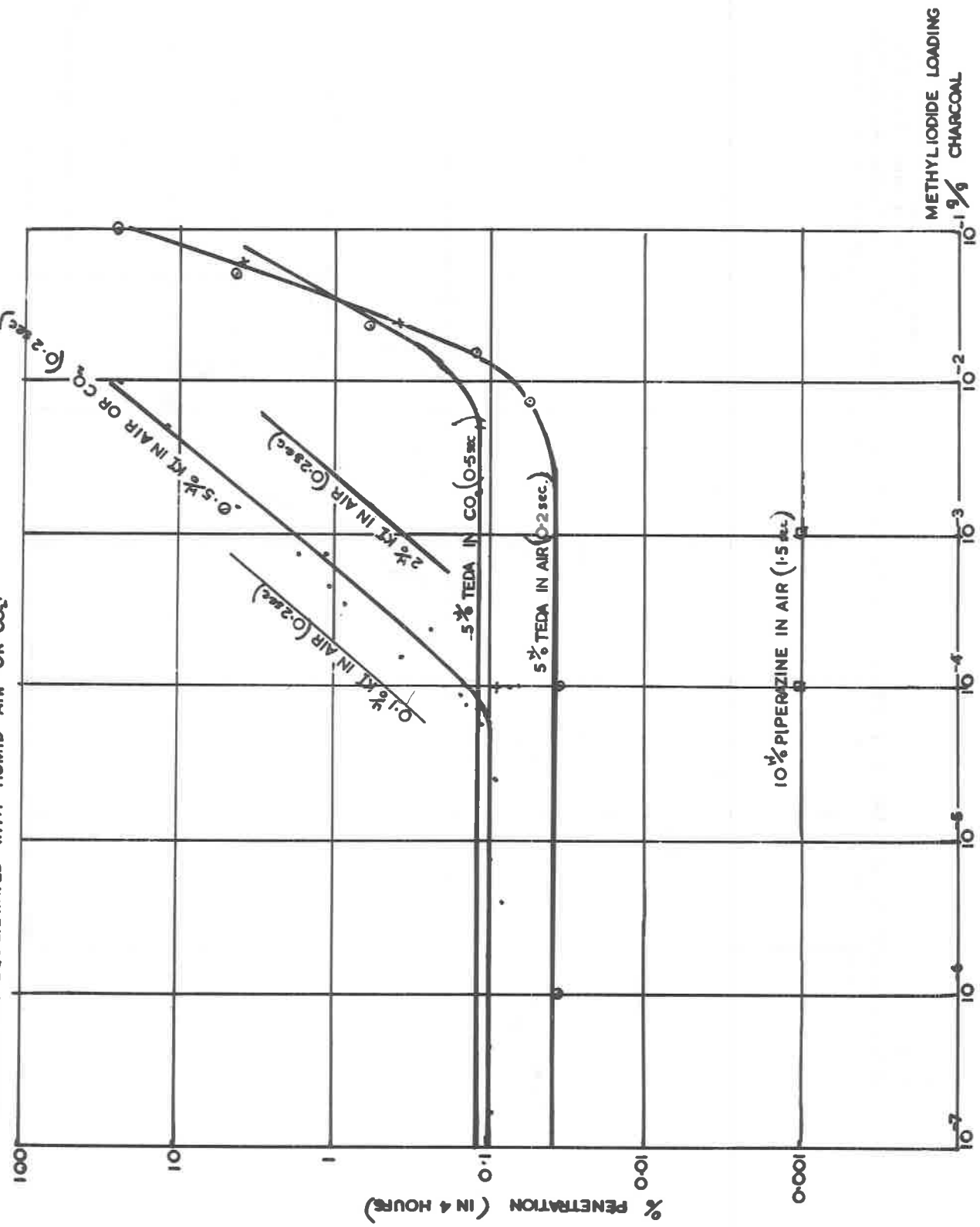
EFFECT OF METHYL IODIDE LOADING ON PENETRATION THROUGH IMPREGNATED 207B CHARCOAL
TEST CONDITIONS: 96-100% R.H. AIR OR CO2 AT ROOM TEMPERATURE.
CHARCOAL PRE EQUILIBRATED WITH HUMID AIR OR CO2.
% PENETRATION (IN 4 HOURS)
METHYL IODIDE LOADING % CHARCOAL
0.5% KI IN AIR OR CO2 (0.2sec.)
2% KI IN AIR (0.2sec.)
0.1% KI IN AIR (0.2sec.)
5% TEDA IN CO2 (0.5 sec.)
5% TEDA IN AIR (0.2 sec.)
10% PIPERAZINE IN AIR (1.5 sec.)

Potassium iodide-impregnated charcoal will not accept such a heavy loading. Breakthrough occurs at just over 100µg methyl iodide per gram of charcoal. Operation in carbon dioxide as opposed to air does not appear to affect the loading at which breakthrough occurs although, in the case of the amine impregnants, it affects the degree of penetration below the breakthrough point.

## THE EFFECT OF AGEING AND EXPOSURE TO IMPURITIES AND SEVERE OPERATIONAL CONDITIONS

26. 207B charcoal impregnated with triethylenediamine or with potassium iodide is capable, when freshly prepared, of providing the performance required by an efficient trapping plant for methyl iodide under conditions of up to 100% relative humidity. For operational purposes however, designers wish to know whether performance is likely to deteriorate over the life of the plant. Some plants are required to operate continuously (as on active cell or some reactor containments extracts) and may be exposed to impurities which could poison the charcoal. In other applications the charcoal may be required to operate for a time under severe conditions of exposure to condensing steam at a high temperature. Attempts have been made to carry out experiments from which the deterioration in performance under various conditions of service can be predicted. It is difficult to simulate all operational conditions in the laboratory and these predictions will need to be backed up by measurements on actual installed plants.

### Ageing

27. The performance of impregnated charcoals deteriorates with time when they are continuously exposed to a flow of air. Ageing is likely to be due to chemical or physical poisoning by impurities in the air or to gradual loss of the impregnant if this is volatile. It was assumed that the effects would be proportional to the number of changes of air to which the charcoal was exposed and could be accelerated in time by increasing the rate of air change. Ageing tests in flowing air were therefore carried out with a very short stay-time in the bed and were performed both in clean air (filtered through un-impregnated charcoal) and in normal un-filtered air. The results (Figures 8 and 9) suggest that ageing is initially more rapid in un-filtered air than in clean air but over a large number of air changes the rate of deterioration seems to be more or less independent of the cleanliness of air. There is a wide scatter in the results but the fall-off in performance can be approximated by an exponential curve whose decay constant results in a halving of the performance (represented by $\log_{10}$DF divided by stay-time) in $10^8$ air changes. The same decay constant applies to both triethylenediamine and potassium iodide-impregnated 207B although their ageing processes are almost certainly different.

28. The results of ageing tests in static air are so far inconclusive. After being exposed to air in a shallow tray for one year the performance of both 5% TEDA/207B and 0.5% KI/207B had measurably deteriorated. A similar increase in penetration was measured after storage of 0.5% KI/207B in a bin for 9 months. All these results (Table III) are, however, within the scatter to be expected with freshyl prepared samples.

29. It is recommended that for the design of charcoal traps to operate in a continuous flow of air it should be assumed that the log DF will

Fig. 8

RESULTS OF ACCELERATED AGEING TESTS WITH 5% TEDA/ 207B

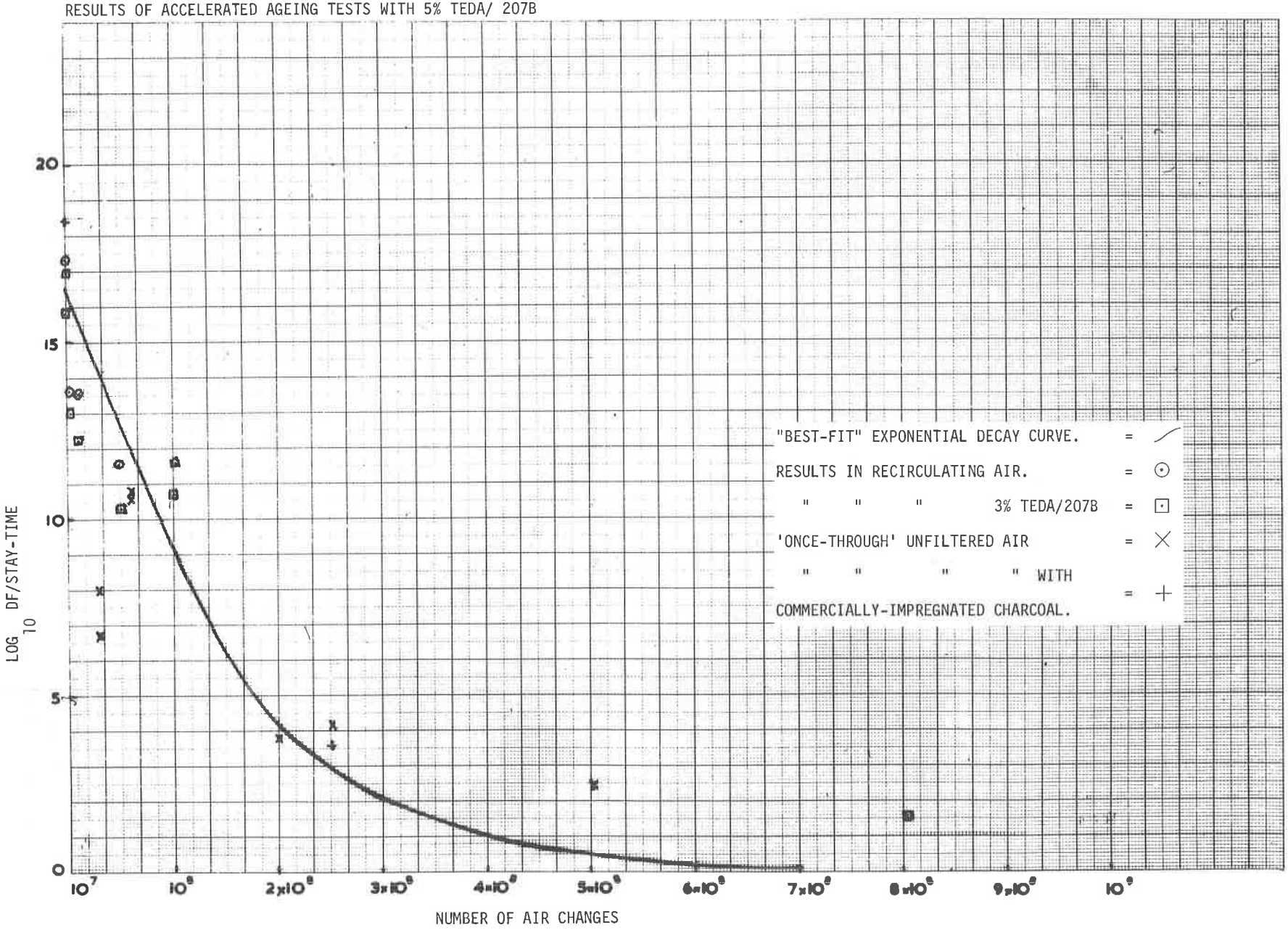

Fig. 9

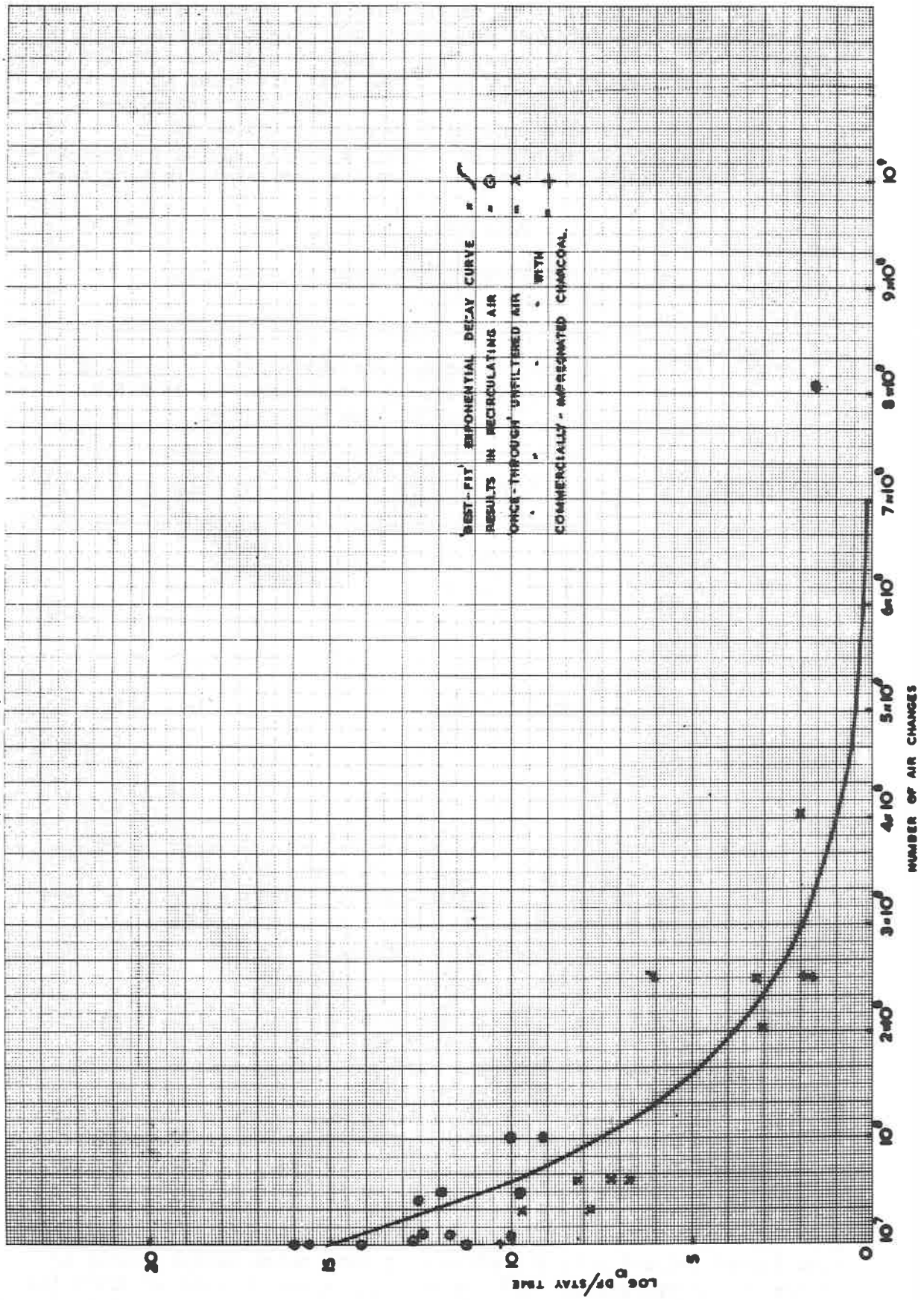
RESULTS OF ACCELERATED AGEING TESTS WITH 5% KI/207B IN AIR
'BEST-FIT' EXPONENTIAL DECAY CURVE
RESULTS IN RECIRCULATING AIR
ONCE-THROUGH UNFILTERED AIR
WITH
COMMERCIALLY-IMPREGNATED CHARCOAL.
LOG10 DF/STAY TIME
NUMBER OF AIR CHANGES

half in $10^8$ air changes. This is equivalent to 18 months operation if the trap is designed for ½ second stay-time. Predicted ageing curves based on this assumption are shown in Figure 10 together with the results of tests on actual samples of charcoal withdrawn at various times from an installed charcoal trap which operates continuously. This trap is filled with a mixture of potassium iodide and triethylenediamine-impregnated 207B and the actual ageing behaviour is in line with the predictions based on the accelerated ageing tests.

TABLE III

Ageing of impregnated charcoals in static air

| | Methyl iodide penetration (%) in standard test 0.2 seconds stay-time 98 - 100% R.H. air at room temperature | |
|---|---|---|
| Aged in shallow tray | 0.5% KI/207B | 5% TEDA/207B |
| 6 months | 0.21 | 0.035 |
| 1 year | 0.43 | 0.066 |
| Aged in bin | | |
| 1 week | 0.48 | - |
| 9 months | 0.63 | - |

Poisoning

30. Some traps will occasionally be exposed to impurities that are not present in normal air. These include common organic solvents which may be used in ventilated fuel-handling cells and, in the case of traps required to treat A.G.R. circuit gas, various organic compounds which are the products of radiolytic reactions occurring in the circuit.

31. Tests in which the charcoal was given a loading of acetone, carbon tetrachloride and trichlorethylene equivalent to 100 mg. sdvent /g. charcoal and then presented with methyl iodide in saturated air at room temperature showed an insignificant increase in penetration in the case of 5% TEDA/207B and an increase by a factor of two in the case of 0.5% KI/207B. This loading of solvents is equivalent to many times the useage in a typical fuel handling cell over a period of years.

32. The organic impurities present in the A.G.R. circuit cause a significant reduction in the efficiency with which methyl iodide is trapped by unimpregnated 207B charcoal in carbon dioxide at 100°C (in the absence of such impurities the efficiency under these conditions is very high). With 0.5% KI/207B (0.25 sec. stay-time) no measurable penetration of methyl iodide occurred under these conditions when the

Fig. 10

ANTICIPATED DETERIORATION IN PERFORMANCE OF IMPREGNATED CHARCOALS IN CONTINUOUS USE.

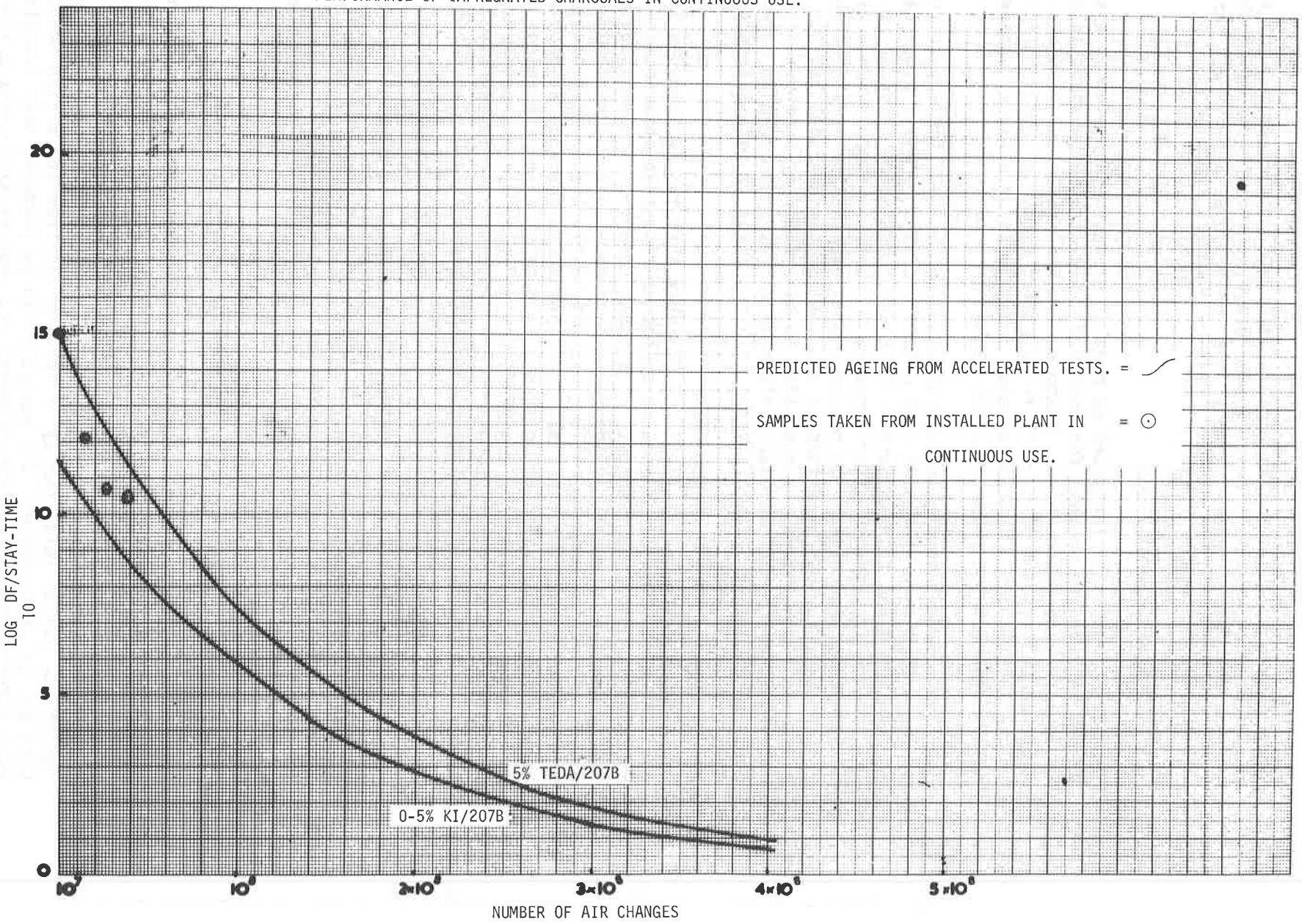

TABLE VII

Effect of high temperature pre-treatment on the performance of impregnated charcoals

| Charcoal | Exposure | Subsequent performance against methyl iodide in saturated air at room temperature | | Performance of unexposed sample for comparison % penetration |
|---|---|---|---|---|
| | | Stay-time, sec. | Penetration % | |
| 5% TEDA/207B | 380°C in air | 0.1 | 56 | 2.5 |
| 1% Morpholine/207B | 360°C in air | 1.5 | 72 | 0.008 |
| 1% Piperidine/207B | 100°C in air 3 h. | 1.5 | 3.2 | 0.008 |
| 0.5% KI/207B | 300°C in $CO_2$ 8 h | 0.25 | 0.1 | 0.02 |

TABLE VIII

Variation in performance of impregnated charcoals

| Description of batch of 207B charcoal | Performance (Methyl iodide penetration at 0.2 sec stay-time in 98 - 100 R.H. air at room temperature) | | | | | |
|---|---|---|---|---|---|---|
| | 0.5% KI impregnation | | | 5% TEDA impregnation | | |
| | Mean | Highest | Lowest | Mean | Highest | Lowest |
| Batch 1 (1 cwt) supplied 24/2/65 for laboratory impregnations | 0.175 (20 results) | 0.72 | 0.05 | 0.05 (10 results) | 0.14 | 0.02 |
| Batch 2 (1 cwt) supplied 26/5/65 for laboratory impregnations | 0.29 (31 results) | 0.78 | 0.11 | 0.06 (8 results) | 0.10 | 0.03 |
| Batch 3 (1 cwt) supplied 7/12/65 for laboratory | 0.48 (18 results) | 0.94 | 0.14 | 0.095 (only 2 results) | 0.11 | 0.08 |
| Batch used for large scale impregnation by manufacturer | 0.65 (38 results) | 1.41 | 0.28 | 0.03 (4 results) | 0.05 | 0.02 |
| Variation within 1 drum of above product | 0.81 (9 results) | 1.0 | 0.53 | - | - | - |
| Charcoal as above, impregnated in laboratory | 0.10 (only 2 results) | 0.11 | 0.09 | - | - | - |
| Batch supplied in 1963 (residue from sack) laboratory impregnation | 0.80 (only 1 result) | - | - | - | - | - |
| Batch supplied 3/9/64 laboratory impregnation | 0.13 (only 1 result) | - | - | - | - | - |

38. There is a much smaller variation in performance with triethylenediamine impregnant than with potassium iodide and this is in keeping with the hypothesis that the latter acts in some way catalytically and may be dependent upon the presence of other trace constituents in the charcoal. Recent work suggests that the variation between batches may be reduced by making small changes to the level of KI impregnation of each batch with potassium iodide. For the design of trapping plants it is recommended that designers should anticipate a performance equivalent to 0.1% penetration at 0.2 sec. stay-time for 5% TEDA/207B and

TABLE XIII

Summary of main results on the basis of index of performance ($\log_{10}$DF/stay-time)

| Test | Index of Performance (for 8 - 12 mesh charcoal granules except where noted) | | | | | | | |
|---|---|---|---|---|---|---|---|---|
| | unimpregnated 207B | 0.5% KI/207B | 5% TEDA/ 207B | 10% Piperazine 207B | British coconut charcoal | | American coconut charcoal | |
| | | | | | 0.5% KI | 5% TEDA | 0.5% KI | 5% TEDA |
| elementary iodine in 100% R.H. air | ~20 | 24 | ~20 | | | | | |
| methyl iodide in dry air (100µg/g loading) | 22 | >40 | >40 | | | | | |
| methyl iodide in 100% R.H. air (100 µg/g loading) | 0.2 | 8-12 mesh 13.8<br>12-16 mesh 22<br>18-30 mesh 32<br>30-50 mesh 50 | 16.5 | 12.3 | 6.5 | 8.6 | 7.8 | 9.35 |
| methyl iodide in 100% R.H. $CO_2$ (100µg/g loading) | 0.2 | 13 | 5.6 | 2.7 | | | | |
| methyl iodide in 100% R.H. air ( 1 mg/g loading) | 0.2 | 8.5 | 16.5 | 12.3 | | | | |
| methyl iodide in 100% R.H. air after $10^8$ air changes (100µg/g loading) | 0.2 | 6.9 | 8.25 | 4 | | | | |
| methyl iodide in dry steam at 110°C (100µg/g loading) | | >20 | >20 | >5 | | | | |
| methyl iodide in 100% R.H. air after heating to 300°C in air or $CO_2$ (100µg/g loading) | 0.2 | 12.0 | 3.0 | | | | | |

54. The results of tests carried out both before and after replacing with impregnated charcoal are shown in Table XII. It is not of course possible to test the beds under accident conditions and the main result of the tests has been to show up mechanical defects which lead to by-passing of the charcoal. Each of the re-filled beds, after modifications where necessary, has shown a good performance in the tests. The condition of the charcoal is monitored at intervals by withdrawing a sample and testing in the laboratory. The continued leak-tightness of the beds is checked by routine in-situ tests with methyl iodide.

## CONCLUSIONS

55. For the retention of methyl iodide in conditions of high relative humidity, greatly improved performance is obtained by impregnating charcoal with amines or with inorganic halides. 5% by weight of triethylenediamine or 0.5% by weight of potassium iodide on 207B charcoal appear to provide the best combination of performance with cheapness and availability. Of the different charcoals examined as bases to support the impregnants none offers a significant improvement upon 207B and most are distinctly inferior.

56. For design purposes the performance of the impregnated charcoals can be represented by a linear relationship between log DF and stay-time in the charcoal bed. In a continuous flow of air performance gradually deteriorates and it suggested that this may be designed for by assuming that $\log_8$ DF will decay exponentially with a halving-time equivalent to $10^8$ air changes.

57. Log DF divided by the stay-time is roughly consistent for a given charcoal and provides a convenient index of performance. The reciprocal of this number is proportional to the amount of charcoal required to do a given job. The main results of this work may be expressed according to this index and are summarised in Table XIII.

58. 0.5% KI/207B performs almost equally well in air and in carbon dioxide and stand up well to exposure to steam at high temperature, but it suffers the disadvantages that its ignition point in air is lowered, the acceptable loading of methyl iodide is limited to about 100 $\mu g/g$ charcoal and, because of its apparently catalytic mode of action, it may be susceptible to poisoning by some impurities.

59. 5% TEDA/207B performs better and rather more consistently in air than does 0.5% KI/207B. It will also accept a much higher loading of methyl iodide. Its disadvantages are that performance is significantly worse in carbon dioxide, the impregnant can be partially lost by exposure to high temperature and subsequent performance is affected, and the impregnant is moderately expensive.

60. For most practical applications in reactor containment it is believed that the best solution is to use a mixture of the two types of impregnated charcoal.

61. These conclusions refer to charcoal in the 8 - 12 mesh size range. Smaller charcoal granules can provide even better performance when impregnated with potassium iodide and their use in certain circumstances may be preferred when more supporting evidence has been accumulated.

62. No matter how good the charcoal, the performance of a charcoal bed will be unsatisfactory unless the mechanical condition of the bed is such that by-passing of the charcoal cannot occur. This is best assured by careful attention to the design and regular in-situ testing after installation. For the in-situ tests the use of labelled methyl iodide is recommended. The condition of the charcoal should also be monitored at intervals by withdrawal of a sample and application of a standard test for methyl iodide penetration in the laboratory.

## APPENDIX 1

## SUMMARY OF COMPLETE RANGE OF IMPREGNANTS EXAMINED

63. In addition to the useful impregnants with which the body of this report is concerned, a large number of other compounds were examined. Some of these had little or no effect on the ability of 207B charcoal to trap methyl iodide, others caused a significant improvement but for one reason or another did not appear so promising as those chosen for more detailed study. After preparation, each impregnated charcoal was subjected to the standard test for methyl iodide penetration, which involved pre-equilibrating with saturated air (98 - 100% relative humidity) at room temperature, then loading 100μg $CH_3I$/g charcoal and integrating the penetration over four hours as saturated air continued to flow through the charcoal. The data are divided into organic impregnants and inorganic impregnants.

Organic impregnants

| Impregnant supported on 207B charcoal | Stay-time, sec. | Methyl iodide % penetration in standard test |
|---|---|---|
| 3 w/o isoquinoline | 3 | 2.7 |
| 1 w/o pyridine + $K_2Cr_2O_7$ | " | 4 |
| 1-amino-4-diethylaniline | " | 10 |
| 1.4 w/o pyrrole | " | 14.1 |
| 19 w/o N, N dimethyl p-phenylenediamine | " | 31.7 |
| 1.4 w/o quinoline | " | 38.0 |
| chloramine-T | " | 96.8 |
| 5 w/o morpholine + 5 w/o N-silver succinimide | 1.5 | 0.028 |
| 5 w/o 4-aminopyridine - 1% glycerol | " | 0.21 |
| 5 w/o hexamine | " | 0.37 |
| 5 w/o diethanolamine | " | 0.54 |
| 5 w/o 3-diethyl-aminopropanol | " | 1.2 |
| 5 w/o 2-diethylaminoethanol | " | 1.86 |
| 3.6 w/o dicyclo hexylamine | " | 2.86 |
| 5 w/o tri-n-butylamine | " | 3.36 |
| 2 w/o iminazole - 2% glycerol | " | 3.4 |
| 5 w/o n-propanolamine | " | 7.1 |
| 5 w/o succinimide | " | 7.9 |
| 5 w/o N-(2-aminoethyl) ethanolamine | " | 10 |
| 5 w/o ethanolamine | " | 10.9 |
| 5 w/o triethanolamine | " | 13.7 |
| 5 w/o iminazole | " | 14.5 |
| 1 w/o pyridine - 5 w/o guanidine carbonate | " | 16.9 |
| 2 w/o isopropanolamine | " | 16.7 |
| 2 w/o succinimide - 0.2% glycerol | " | 17.7 |
| 6 w/o 5-amino acridine | " | 25.7 |
| 1.2 w/o sym-diphenylguanidine | " | 27.8 |

Organic impregnants contd.

| Impregnant supported on 207B charcoal | Stay-time, sec. | Methyl iodide % penetration in standard test |
|---|---|---|
| 2 w/o n-propanolamine | 1.5 | 28.4 |
| 1 w/o benzyl-diphenylamine | " | 29.4 |
| 5 w/o 2-aminopyridine | " | 32.1 |
| 0.2 w/o dicyclo hexylamine | " | 32.6 |
| 1 w/o 4-aminophenazone - 0.2% glycerol | " | 34.9 |
| 2-amino-2-methyl-propan-1:3 diol | " | 35.3 |
| 3 w/o acridine | " | 41.4 |
| 2 w/o p-amino-N, N diethylaniline - 0.2% glycerol | " | 43 |
| 2.4 w/o N, N diphenyl guanidine | " | 45.2 |
| 5 w/o form-dimethyl-amide | " | 48.3 |
| 5 w/o ethyl carbamate | " | 61.1 |
| 2 w/o guanidine carbonate - 0.2% glycerol | " | 63.4 |
| N-benzyldiphenylamine | " | 63.4 |
| 1 w/o N-benzyl-N-methyl-aniline | " | 66.3 |
| 4 w/o toluene-p-sulphonamide | " | 73.6 |
| 5 w/o 4-aminophenazone | " | 78.4 |
| 3 w/o diaminoethane tetra-acetic acid | 0.2 | 77.8 |
| 3 w/o triethylenediamine/HCl | 0.1 | 1.0 |
| 3 w/o triethylenediamine/HBr | " | 0.9 |
| 3 w/o triethylenediamine/HI | " | 0.74 |
| 3 w/o triethylenediamine/$H_2SO_4$ | " | 1.2 |

Inorganic impregnants

| Impregnant supported on 207B charcoal | Stay-time sec. | Methyl iodide % penetration in standard test |
|---|---|---|
| 5 w/o bromine | 1.5 | 0.001 |
| 5 w/o iodine | " | 0.001 |
| 3 w/o hydrogen iodide | " | 0.001 |
| 10 w/o potassium salts (KBr, KI, $KIO_3$, $K_2Cr_2O_7$ | " | 0.001 |
| 5 w/o potassium bromate | " | 0.003 |
| 5 w/o potassium bromide | " | 0.005 |
| 5 w/o potassium chloride | " | 2.1 |
| 5 w/o potassium dichromate | " | 7.5 |
| 5 w/o sodium acetate | " | 9.0 |
| 5 w/o potassium permanganate | " | 12.6 |
| 5 w/o potassium sulphamate | " | 17.9 |
| 5 w/o potassium hydroxide | " | 57.0 |
| 5 w/o sulphamic acid | " | 68.5 |
| 3 w/o hydrogen iodide | 0.5 | 0.007 |
| 2 w/o sodium chloride | " | 8.5 |
| 1 w/o silver nitrate | " | 24.4 |
| Ammonium hydroxide | " | 41.5 |
| 5 w/o bromine | 0.25 | 0.001 |
| 0.5 w/o caesium iodide | " | 0.001 |
| 2 w/o sodium iodide | " | 0.002 |
| 5 w/o iodine | " | 0.24 |
| 3 w/o hydrogen iodide | " | 0.53 |
| 2 w/o $ICl_3$/0.5 w/o potassium iodide | 0.2 | 0.24 |
| 1 w/o $(Co(NH_3)_6)Cl_3$ | " | 60.2 |
| 2 w/o $ICl_3$ | " | 69.7 |
| 3 w/o Aluminium sulphate | " | 78.6 |
| $NH_3$ + methanol | " | 85.2 |
| 3 w/o Aluminium nitrate | " | 95.8 |
| 50 w/o bromine (10 min. before $CH_3I$) | 0.1 | 0.001 |
| 10 w/o bromine (4 hrs before $CH_3I$) | " | 0.076 |
| 2 w/o nickel iodide | " | 0.34 |
| 2 w/o magnesium iodide | " | 0.37 |
| 2 w/o calcium iodide | " | 0.83 |
| 0.25 w/o potassium iodide + 0.25 w/o cesium iodide | " | 0.88 |
| 1 w/o magnesium iodide | " | 1.0 |
| 1 w/o rubidium chloride | " | 1.0 |
| 2 w/o ammonium iodide | " | 1.22 |
| 2 w/o potassium hydroxide + 5 w/o iodine | " | 1.65 |

Inorganic impregnants contd.

| Impregnant supported on 207B charcoal | Stay-time sec. | Methyl iodide % penetration in standard test |
|---|---|---|
| 0.5 W/o potassium iodide + 10 W/o iodine | 0.1 | 3.3 |
| 10 W/o iodine (loaded 30 mins before $CH_3I$) | " | 9.0 |
| 2 W/o lithium bromide | " | 10.0 |
| 2 W/o ferrous iodide | " | 10.3 |
| 2 W/o ferrous bromide | " | 12.2 |
| ammonium hydroxide | " | 85 |

## APPENDIX II

## THE MECHANISM OF METHYL IODIDE RETENTION BY IMPREGNATED CHARCOALS

64. No serious attempt has been made to elucidate the mechanism of the reactions by which methyl iodide is retained. The retention of elementary iodine itself on charcoal is not clearly understood although it obviously involves chemisorption rather than physical adsorption. With methyl iodide it is assumed that some initial reaction must occur to make the iodide more readily available for chemisorption. In wet atmospheres the problem is at least partly one of access to the charcoal surface.

### Amine-impregnants

65. Impregnation of charcoal with amines was an attempt to cover part of the surface of the charcoal with a material that would be more receptive to methyl iodide molecules than to water molecules. The initial reaction of the amine group with methyl iodide coverts the iodine to an ionic form, after which it is presumably more readily capable of reacting with the base charcoal and is unlikely to be deterred from doing so by the presence of water.

with secondary amines $R_2NH + CH_3I \longrightarrow R_2CH_3N + HI$

with tertiary amines $R_3N + CH_3I \longrightarrow R_3N^+CH_3I^-$

The quartenary iodide produced by reaction with tertiary amines is frequently a stable non-volatile compound (that formed from triethylenediamine has a melting point of 390°C) but the significant differences in retention provided by different base charcoals make it likely that a further stage of reaction with the base charcoal is involved.

66. The superiority of heterocyclic amines containing a second amine grouping or other reactive grouping at the opposite end of the molecule, may be associated with the need to attach the amine firmly to the charcoal and yet retain a sufficiently reactive basic nitrogen atom to react with methyl iodide.

### Potassium iodide

67. The lowered ignition temperature of potassium iodide impregnated charcoal is evidence of its greater chemical reactivity and it may be postulated that it is therefore more reactive towards methyl iodide. It is also possible, however, that isotopic exchange between the natural iodine of the impregnant and the radioactive iodine in the methyl iodide contribute towards the retention of radioactive iodine.

68. Experiments in which $CH_3{}^{132}I$ was presented to charcoal impregnated with $K^{131}I$ have shown that isotopic exchange does occur, but it cannot be the sole mechanism because the total mass of methyl iodide which penetrates the charcoal in these experiments is much smaller than that loaded, indicating that there must have been some adsorption. Also it has been shown in a number of experiments that when the amount of iodine loaded as methyl iodide exceeded the amount of iodine present as potassium iodide on the charcoal, the measured penetration was much smaller than would have been the case if complete isotopic exchange had occurred. Finally, if isotopic exchange were sufficiently rapid to account for very low penetrations at the normal loading ratio of 0.1 mg. $CH_3I$ to 5 mg of potassium iodide impregnant, then it would be difficult to explain the observed dependence of penetration upon stay-time.

| KI on charcoal mg/g | $CH_3I$ loaded mg/g charcoal | measured penetration % of $^{131}I$ activity | % Penetration on isotopic exchange mechanism |
|---|---|---|---|
| 5 | 10 | 19 | 50 |
| 1 | 5 | 49.3 | 80 |
| 0.13 | 1 | 6.8 | 87 |
| 0.1 | 0.5 | 6.4 | 80 |
| 0.05 | 0.1 | 2.2 | 50 |
| 0.01 | 0.05 | 13.6 | 80 |

69. The chemisorption of methyl iodide may involve its decomposition and is almost certainly catalytic. The wide variations in performance when potassium iodide is supported on different base materials suggests that interaction with the base charcoal is critical.

REFERENCES .

1. COLLINS, D.A., TAYLOR, R., TAYLOR, L.R. The removal of methyl iodide from reactor effluent gases. TRG Report 789(W) 1964.

2. TAYLOR, L.R., TAYLOR, R. Internal Document. 1966

# RETENTION OF METHYL IODIDE BY IMPREGNATED CARBONS UNDER AMBIENT CONDITIONS

G. W. Parker, G. E. Creek, and A. Ferreli

Reactor Chemistry Division
Oak Ridge National Laboratory
Oak Ridge, Tennessee

## ABSTRACT

The extent of the production of methyl iodide and the containment of this form of radioiodine have become two of the most important factors that must be considered in the preparation of reactor safeguards analyses. Various estimators of the amount and mode of formation of methyl iodide have generally concluded that less than 5 percent of the iodine should be present in this form; however, even this amount leads to serious implications because conventional carbon-filter systems are relatively ineffective in trapping this compound. In April of 1965, this problem was brought to the attention of the nuclear safety authorities by papers presented at the International Symposium on Fission Product Release and Transport Under Accident Conditions at Oak Ridge.

Since that time, significant advances in methods of trapping methyl iodide have been discovered independently in the U. S. and in England. Very promising results from the testing of various chemical additives to coconut charcoals were obtained. An isotopic exchange reaction apparently occurs when the additive is molecular iodine ($^{127}I_2$) and a compound is formed when the additive is an organic amine. The mechanism responsible for improved retention when the additive is an iodide salt is not clear at present.

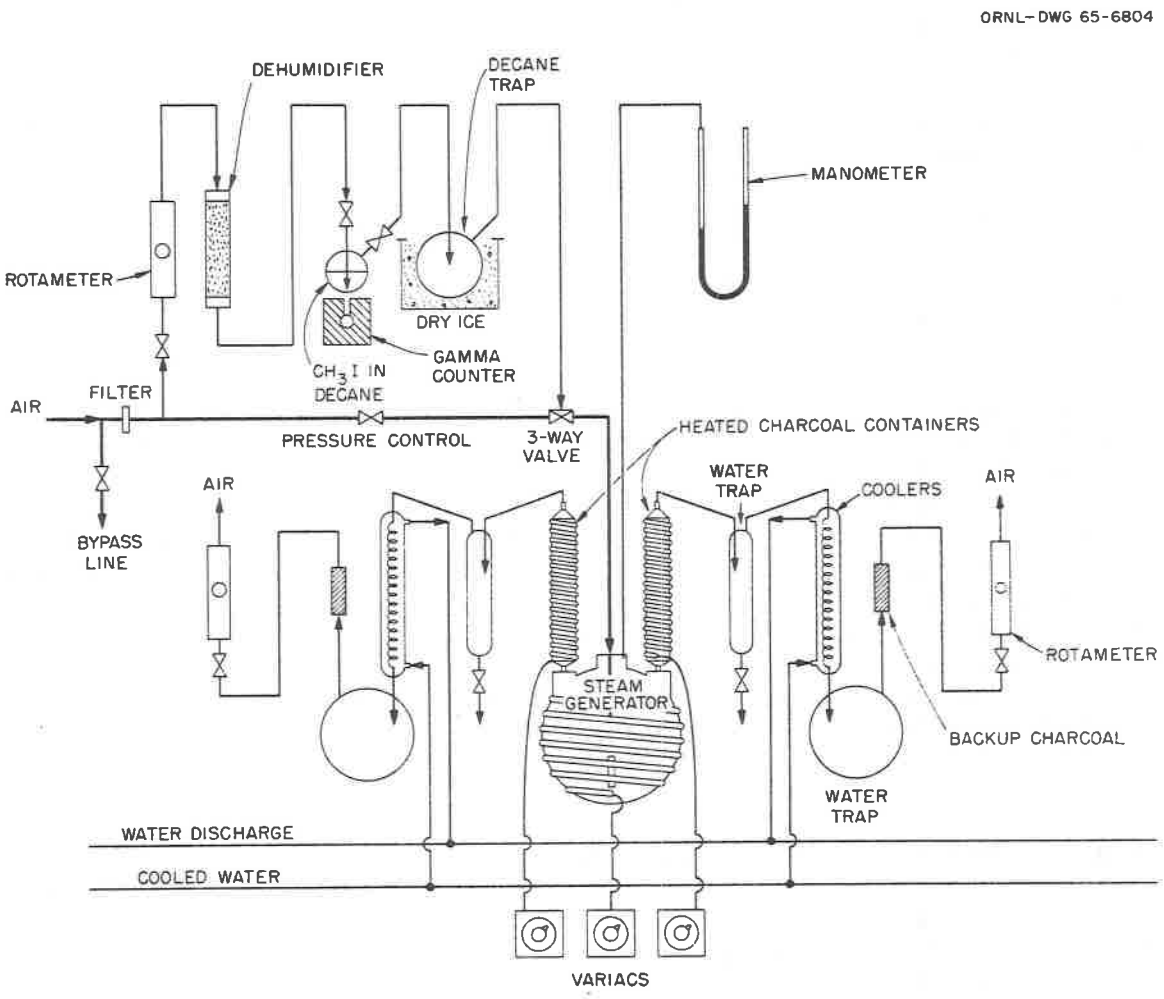


**Fig. 1. Schematic Diagram of Experimental Apparatus.**

Data on the retention of methyl iodide by various impregnated activated carbons and some untreated materials are given in Table 1. All tests were conducted at the temperature (25°C) and the relative humidity (70%) specified as HFIR accident conditions. Part were run at the flow velocity (38 fpm) to be used in the HFIR filter system, but some were run at half the HFIR velocity, which was near the velocity used in the LOFT system. Part of these data are displayed in Fig. 2. Data obtained under similar conditions are shown in Fig. 3.

Air at 100°F and 100% relative humidity was the carrier gas used in determining the methyl iodide retention efficiency of charcoal samples under LOFT conditions. A flow rate of 1070 cc/min was used which gave a face velocity of 17.5 fpm and a residence time of 0.225 sec per cartridge. The charcoal cartridges used were 2-$cm^2$ in cross section and 2-cm long, and they were maintained at 115°F during the tests in conformance with LOFT test conditions. The total bed depth presently specified for the LOFT system is 3-3/8 in. (8.6 cm).

In most of the tests, in order to obtain a 20-hr loading period, the $CH_3{}^{131}I$ mixed with $CH_3{}^{127}I$ carrier was adsorbed on charcoal with inferior retention capacity. A portion, usually about one-third of the $CH_3{}^{131}I$, was then eluted from this charcoal by passing air through it at a rate of 30 cc/min over a period of 20 hr. The eluted $CH_3{}^{131}I$ was mixed with the main air stream going to the charcoal cartridges under test.

After the loading operation was completed, the cartridges were subjected to a 4-hr sweep by air at 100°F and 100% relative humidity containing no tracer $CH_3I$. The results are summarized in Table 2, and part of the data are shown graphically in Fig. 4. In all the tests except Run 10-14, the amount of iodine activity penetrating the first three cartridges (6-cm total bed depth) was negligible.

## PERFORMANCE TESTS AT 75°C AND 100% RELATIVE HUMIDITY

The performance of one commercially available iodine-impregnated carbon (MSA 85851) was tested under conditions approximating those specified in the LOFT sequence prior to initiation of containment sprays. At that time the temperature of the contained air is expected to be 75°C and the relative humidity is postulated to be 100%.

The apparatus used in these studies was that shown schematically in Fig. 1. It was mounted in a hood that is connected to a hot off-gas system and was arranged so that parallel gas streams from the same source could be used to determine the effect of variations in conditions or materials. Methyl iodide containing $CH_3{}^{131}I$ tracer was prepared by

TABLE 1

Retention of Iodine From Methyl Iodide by Various Samples of Activated and Impregnated Charcoals

| Impregnant | Amount of Impregnant (mg/g of charcoal) | Manufacturer[a] | Charcoal Identification | Air Velocity (fpm) | Loading Time (hr) | Iodine from $CH_3I$ Loaded on 8-g Bed (mg) | Residence Time in 5-cm-Deep Bed (sec) | Penetration of 5-cm-Deep Bed (%) |
|---|---|---|---|---|---|---|---|---|
| None | | SS | 207 | 19 | 2.5 | 0.5 | 0.52 | 30 |
| None | | BC | 513 | 19 | 3.0 | 0.5 | 0.52 | 26 |
| None | | MSA | 25725 | 19 | 2.0 | 0.5 | 0.52 | 12 |
| Piperidine | 50 | SS | 207 | 19 | 3.0 | 0.75 | 0.52 | 2.76 |
| NaI | 50 | BC | 416 | 19 | 3.5 | 0.2 | 0.52 | 0.54 |
| $I_2$ | 76 | MSA | 85851 (lot 15) | 38 | 2.0 | 1.0 | 0.26 | 0.06 |
| $I_2$ | 10 | MSA | 25725 | 19 | 3.0 | 0.5 | 0.52 | 0.033 |
| $I_2$ | 70 | MSA | 25725 | 19 | 3.0 | 0.5 | 0.52 | 0.027 |
| $I_2$ | 70 | BC | 416 | 19 | 3.0 | 1.0 | 0.52 | 1.0 |
| $I_2$ | 70 | PCC | PCB | 19 | 3.0 | 0.75 | 0.52 | $1.6 \times 10^{-4}$ |
| $I_2$ | 70 | PCC | PCB | 19 | 3.5 | | 0.52 | $4 \times 10^{-4}$ |
| $I_2$ | 70 | PCC | PCB | 38 | 4.0 | 2.0 | 0.26 | $9 \times 10^{-3}$ |
| $I_2$ | 70 | PCC | PCB | 19 | 5.0 | 1.5 | 0.52 | $1 \times 10^{-4}$ |
| $I_2$ | 70 | PCC | SGL | 19 | 3.0 | 0.5 | 0.52 | 0.35 |
| KI | 10 | PCC | PCB | 19 | 3.0 | 1.0 | 0.52 | $7 \times 10^{-8}$ |
| KI | 10 | PCC | PCB | 19 | 4.5 | 35.0 | 0.52 | $1.3 \times 10^{-3}$ |
| KI | 10 | PCC | PCB | 38 | 4.5 | 2.0 | 0.26 | $4 \times 10^{-5}$ |
| KI + $I_2$ | 10 each | PCC | PCB | 38 | 3.5 | 2.0 | 0.26 | $4 \times 10^{-6}$ |
| TED[b] + KI | 50 and 100 | MSA | 25725 | 38 | 4.0 | 2.0 | 0.52 | $7 \times 10^{-4}$ |
| TED | 50 | MSA | 25725 | 19 | 4.5 | 3.5 | 0.52 | $1.8 \times 10^{-4}$ |
| TED | 50 | MSA | 25725 | 19 | 5.0 | 1.5 | 0.52 | $1.5 \times 10^{-5}$ |

[a]SS — Sutcliffe-Speakman, BC — Barnebey-Cheney, MSA — Mine Safety Appliance, PCC — Pittsburgh Coke and Chemical Company; all samples were 8-14 mesh size except PCB, which was 12-30.

[b]Triethylenediamine.

TABLE 2

Penetration of Treated and Untreated Coconut Charcoal by Methyl Iodide Under LOFT Conditions

Air velocity: 17.5 fpm
Air temperature: 100°F
Relative humidity: 100%
Charcoal bed temperature: 115°F
Loading period: 20 hr

| Run No. | Loading Time (hr) | Charcoal Type | Mesh Size | Carrier $CH_3{}^{127}I$ Used (mg) | Penetration of 2-cm Cartridges (%) | | | | | |
|---|---|---|---|---|---|---|---|---|---|---|
| | | | | | Cartridge 1 | Cartridge 2 | Cartridge 3 | Cartridge 4 | Cartridge 5 | Cartridge 6 |
| 9-13 | <18 | MSA 85851 | 8-14 | 1 | 7.4 | 0.51 | 0.003 | | Negligible | |
| 9-22[a] | 20 | MSA 85851 | 8-14 | 1 | 0.06 | 0.005 | 0.002 | | Negligible | |
| 9-27 | 20 | MSA 85851 | 8-14 | 27 | 2.5 | 0.1 | 0.03 | | Negligible | |
| 10-4 | 20 | MSA 85851 | 8-14 | 57 | 4.0 | 0.33 | 0.07 | | Negligible | |
| 10-6[a] | 20 | PCB + 6% $I_2$ | 12-30 | 27 | 0.16 | 0.04 | 0.002 | | Negligible | |
| 10-7 | 20 | PCB + 6% $I_2$ | 12-30 | 27 | 6.1 | 0.091 | 0.01 | | Negligible | |
| 10-14 | 17 | PCB (untreated) | 12-30 | 1 | 81 | 61.5 | 40 | 22 | 9 | 2.3 |
| 10-10 | 20 | PCB + 5% $I_2$ | 12-30 | 1 | 1.2 | 0.028 | 0.0011 | | Negligible | |
| 10-16 | 20 | PCB + 5% $I_2$ | 12-16 | 1 | 5.3 | 0.39 | 0.019 | 0.0012 | | |

[a]First portion of methyl iodide eluted from charcoal in trap.

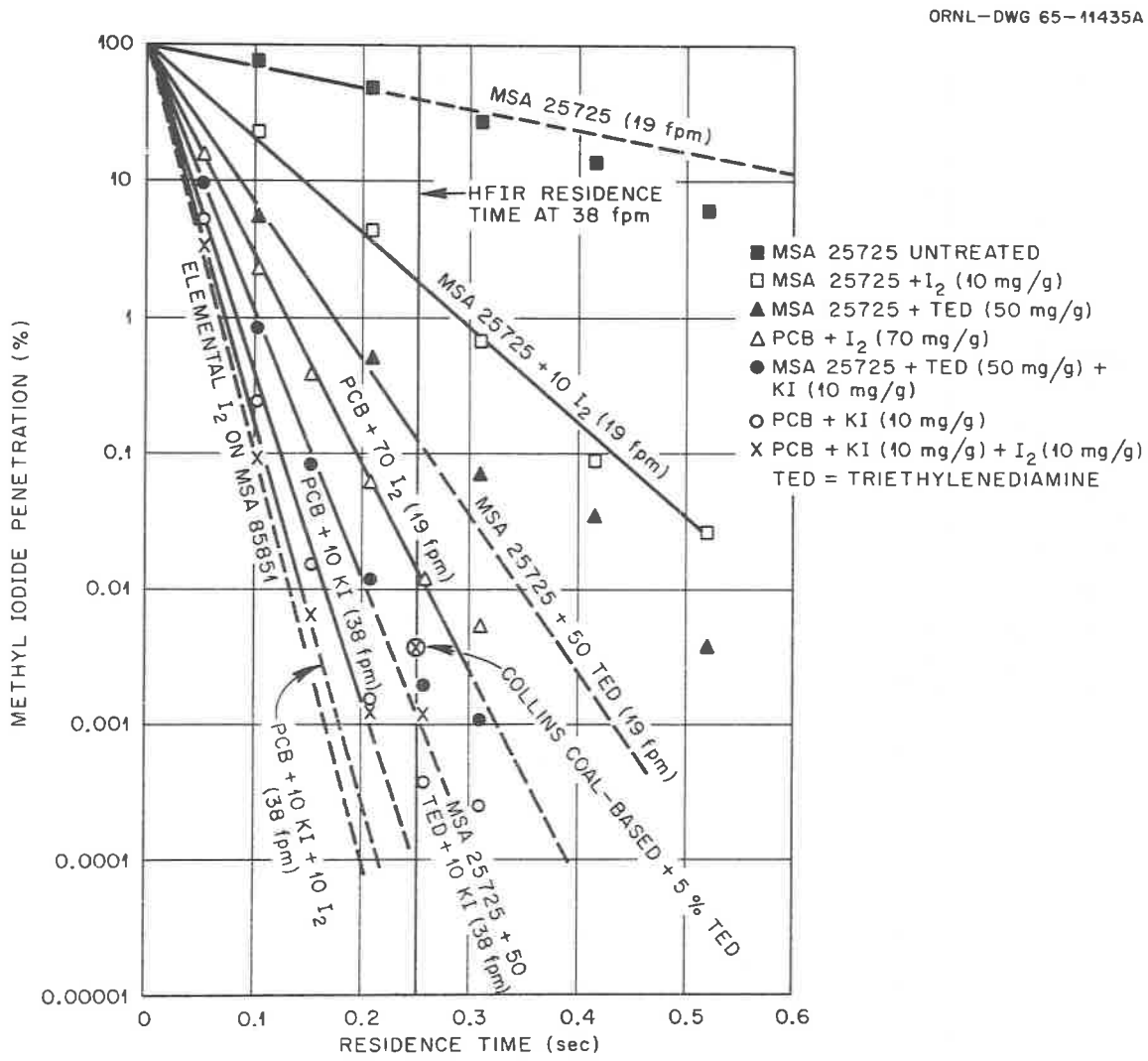


Fig. 2. Effect of Residence Time on Methyl Iodide Penetration of Treated and Untreated Coconut Charcoal at 25°C and 70% Relative Humidity.

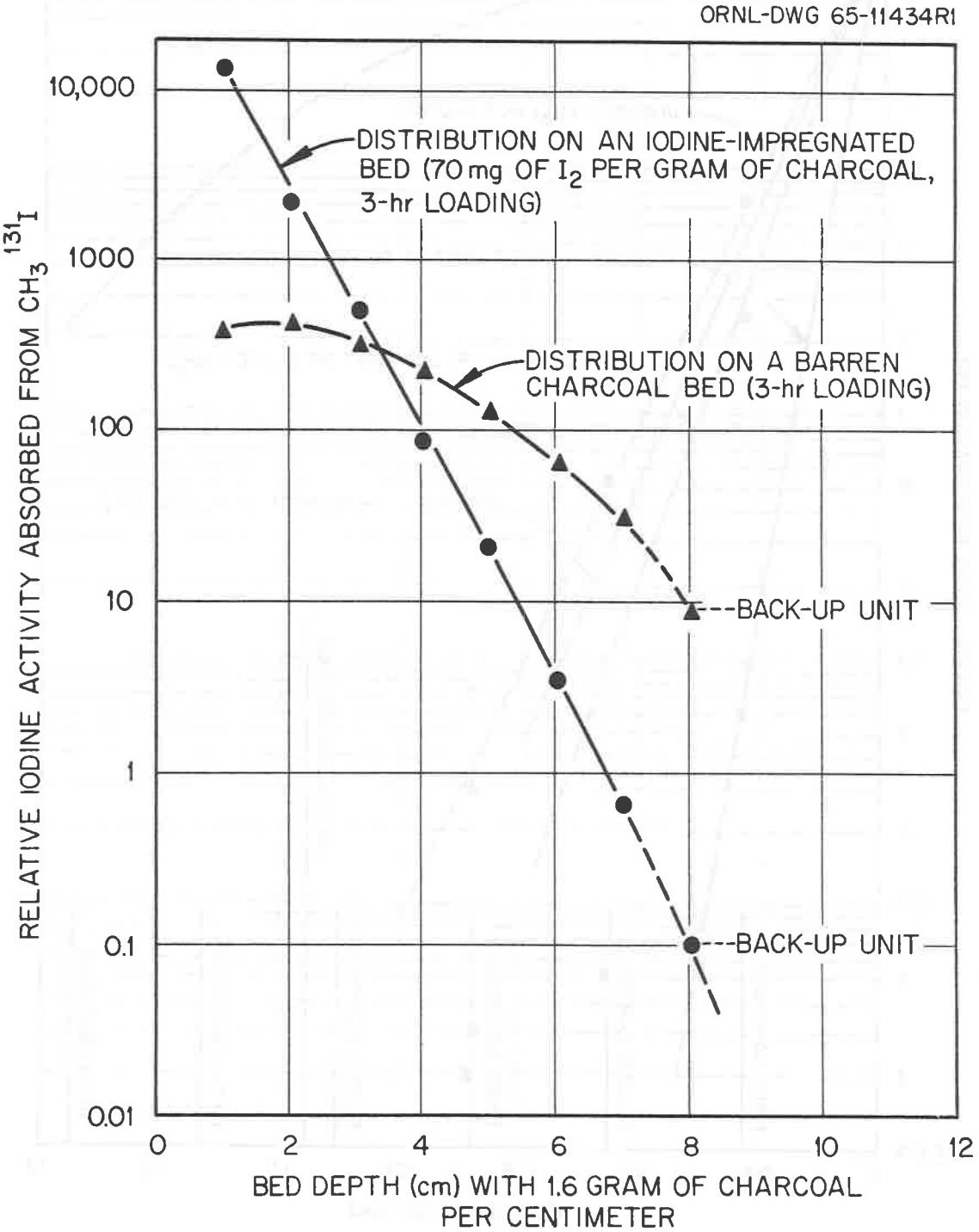


Fig. 3. Retention of Methyl Iodide by Treated and Untreated Coconut Charcoal Under HFIR Conditions.

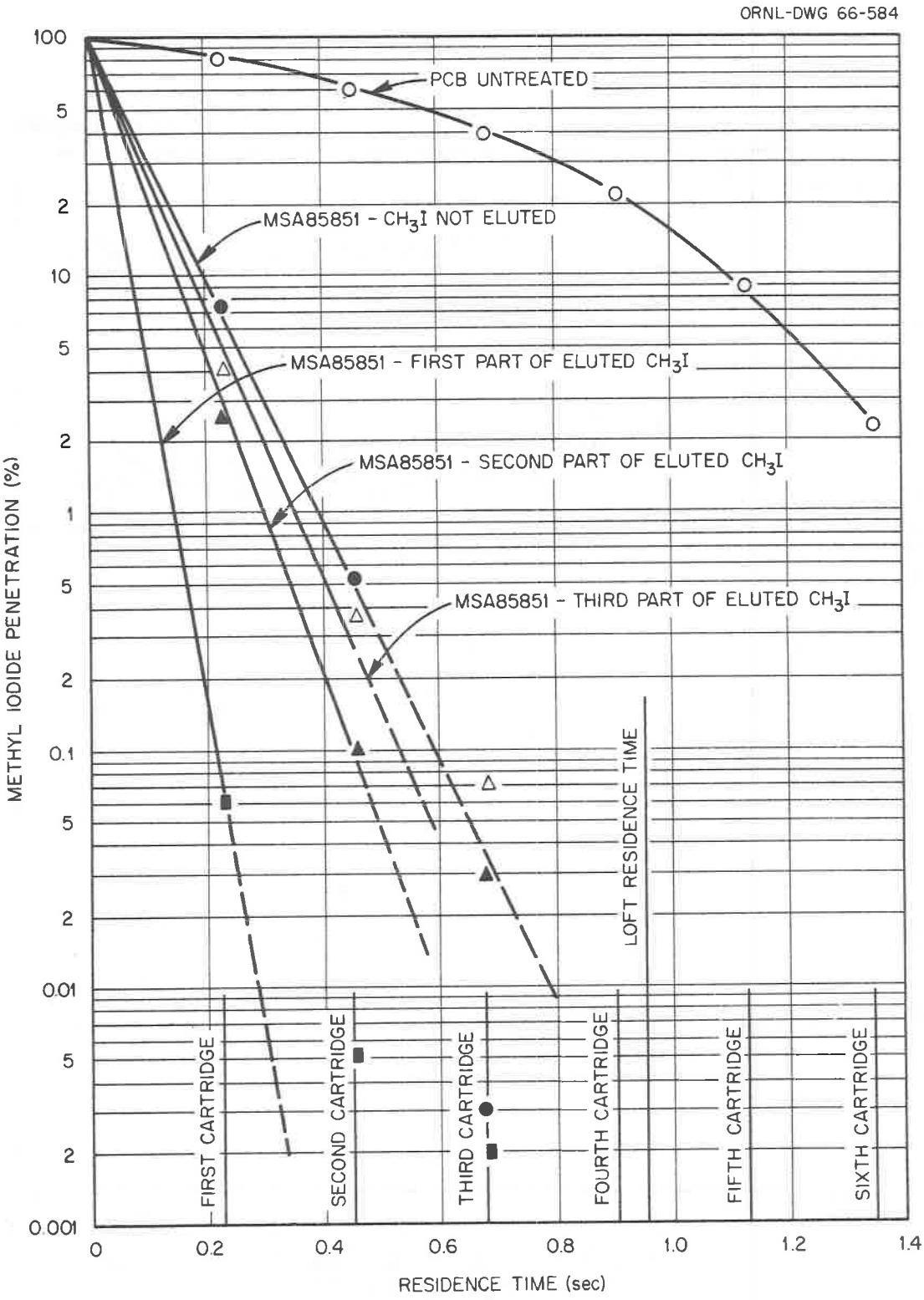


Fig. 4. Penetration of Treated and Untreated Coconut Charcoal by Methyl Iodide Under LOFT Conditions (Air at 17.5 fpm, 100°F, and 100% Relative Humidity; Bed at 115°F).

isotopic exchange between $CH_3{}^{127}I$ and $Na^{131}I$ in 95% ethyl alcohol. The tracer-tagged methyl iodide was dissolved in decane and the mixture was carried by a metered flow of air through a dry-ice-cooled trap, to remove the decane, and it was then bubbled through water at a controlled temperature to saturate the gas stream. The effluent gas was passed through a series of charcoal beds in a heated holder which had the bottom half of the holder empty to permit temperature equilibrium and then through traps and condensers for removal and measurement of the water content of the gas stream. Finally, the low-humidity gas passed through a backup charcoal trap held at room temperature to trap any residual methyl iodide penetrating the first (wet) charcoal beds and then through a rotameter before discharging into the hood off-gas line.

After the heated charcoal traps had been exposed to the saturated gas stream for the predetermined length of time, the traps were disassembled, the iodine activity of the individual charcoal cartridges was measured, and the water content of the individual cartridges was determined by weighing. Iodine activities were converted to weights of methyl iodide by use of previously determined specific activity values.

The penetration of coconut charcoal beds by methyl iodide at a concentration of 0.7 $\mu$g per liter of air saturated with water vapor at 75°C was studied as a function of bed depth at different residence times. Two different sizes of charcoal cartridges were used, 1 cm and 2 cm deep, but the volume was the same, 4 $cm^3$ (1.6 g of charcoal), for both bed depths. Cartridges of both sizes were arranged in series of six and tested simultaneously as described above.

Four runs were made at a slight positive pressure ranging from 1 to 10 cm Hg. The pertinent data relative to the performance of the charcoal beds in the extraction of methyl iodide from saturated air are given in Table 3.

The duration of each run was 1 hr. Air at 75°C and 100% relative humidity was passed through the cartridges for 1/2 hr prior to the addition of methyl iodide in order to approach the conditions expected to prevail in a loss-of-coolant accident. (In a water-cooled reactor accident, fission products may be released to the containment system approximately 30 min after rupture of the primary system releases a large volume of steam.) The relatively severe atmospheric conditions of 75°C and 100% relative humidity were selected because these conditions are predicted for LOFT 5 days after blowdown, at which time use of the trapping system will begin.

The penetration of the cartridges by $CH_3I$ is shown in Fig. 5 as a function of bed depth (cartridge number) at

TABLE 3

Performance of Charcoal* Beds in Extracting Methyl Iodide From Air Saturated With Water at 75°C

Initial concentration of methyl iodide: 0.7 μg per liter of saturated air
Weight of charcoal per cartridge: 1.6 g
Volume of charcoal per cartridge: 4 $cm^3$
Temperature of charcoal: 75°C
Duration of each experiment: 1 hr

| Experiment No. | Air Flow Rate (liters/min) | Charcoal Cartridge Length (cm) | Air Residence Time (sec/cartridge) | Total $CH_3I$ Trapped (μg) | Percentage of $CH_3I$ Trapped per Cartridge | | | | | | |
|---|---|---|---|---|---|---|---|---|---|---|---|
| | | | | | 1 | 2 | 3 | 4 | 5 | 6 | Backup Trap |
| 1 | 1.75 | 1 | 0.140 | 71.8 | 66.8 | 27.8 | 4.4 | 1.0 | Not Used | | 0 |
| | | 2 | 0.140 | 71.8 | 72.4 | 23.7 | 3.6 | 0.3 | | | 0 |
| 2 | 3.5 | 1 | 0.070 | 145.2 | 42.8 | 33.3 | 17.5 | 4.6 | 1.0 | 0.5 | 0.3 |
| | | 2 | 0.070 | 141.9 | 45.8 | 32.5 | 15.6 | 4.7 | 0.9 | 0.3 | 0.2 |
| 3 | 7.0 | 1 | 0.035 | 284.9 | 28.5 | 25.9 | 19.7 | 13.3 | 7.5 | 3.3 | 2.1 |
| | | 2 | 0.035 | 284.1 | 37.5 | 28.7 | 19.4 | 9.5 | 3.1 | 1.1 | 0.7 |
| 4 | 14.0 | 1 | 0.0175 | 569.4 | 20.6 | 21.4 | 18.2 | 13.2 | 9.4 | 6.7 | 10.5 |
| | | 2 | 0.0175 | 591.4 | 29.6 | 22.5 | 16.8 | 11.9 | 7.8 | 5.7 | 5.7 |

*Impregnated charcoal (MSA #85851).

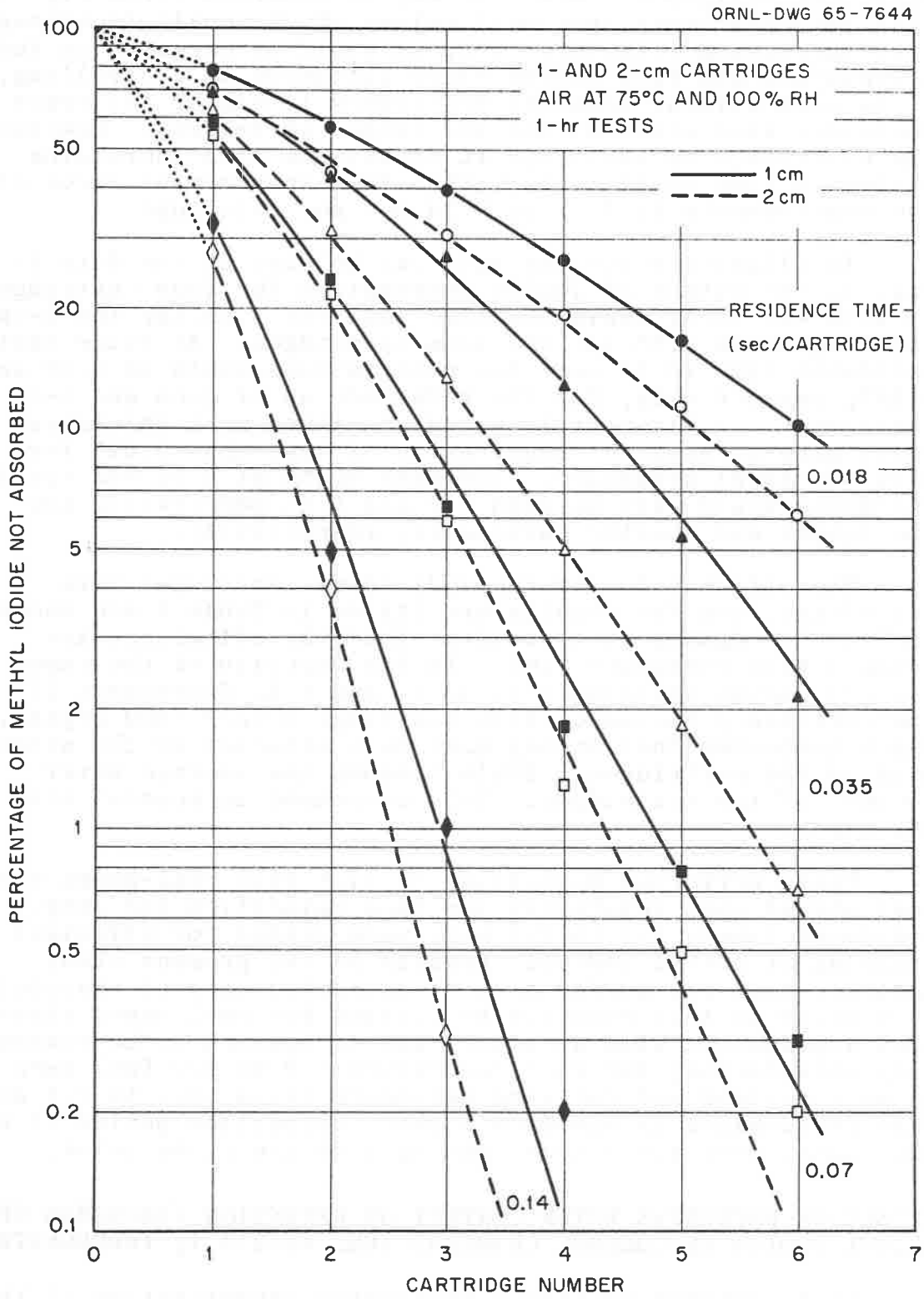


Fig. 5. Effect of Residence Time on Performance of Charcoal Beds (Air at 75°C and 100% Relative Humidity).

different residence times. It may be observed (from Fig. 5) that the efficiency (per unit volume of charcoal) increases with increasing residence time, as would be expected in the streamlined gas flow regime where diffusion is controlling. It is also evident that the efficiency is higher (at every residence time studied) for the longer cartridges. However, the difference is small and it diminishes with increasing residence time until it is within the experimental error of the measurements at 0.07 or 0.14 sec per cartridge.

To illustrate the use that can be made of the data in Fig. 5, the extent of iodine penetration for four cartridges at 0.28 sec total residence time would be 1.8% for the 2-cm cartridges and 2.5% for the 1-cm cartridges. At twice that residence time (0.56 sec) the penetrations would be 0.07 and 0.18%, respectively, for the beds made up of 2-cm and 1-cm cartridges. A six-cartridge bed of either unit thickness would give an apparent penetration of less than 0.01% for 0.84 sec total residence. The same depth at 0.42 sec total residence would give between 0.2 and 0.3% penetration for the longer and shorter cartridges, respectively.

The efficiencies of the individual cartridges were calculated, and the results are listed in Table 4 and shown in Fig. 6. Again, it is evident that the efficiency increased with residence time. In the majority of the cases (in all except cartridges 3, 4, 5, and 6 in Experiment 2) the efficiency increased with cartridge number (bed depth), which indicates that it may have been affected by the water held by the cartridges. Table 5 shows the average water content of the cartridges. This decreased in general with bed depth.

Tests performed by Collins et al.[4] with coal-based charcoal showed that relatively low face velocities and long residence times, 0.5 to 1.5 sec, were needed for efficient trapping of methyl iodide. Results of the present study indicate that the performance of untreated coconut charcoal is similar to that reported by Collins for coal-based charcoal impregnated with an amine, and it appears to be reasonably satisfactory for face velocities (30 to 120 fpm) used in most designs and for long residence times (0.4 to 0.8 sec). This performance is based on a short deposition period (1 hr). Additional data for a 4-hr loading time are given below.

## EFFECT OF EXCESSIVE WATER CONTENT ON RETENTION (EXCHANGE OF METHYL IODIDE BY COCONUT CHARCOAL (MSA #85851 $I_2$ IMPREGNATED)

In an attempt to make a systematic investigation of the effect of water uptake by charcoal at 75°C and 100% relative humidity, a series of tests was made in which charcoal beds were first exposed to various volumes of water-saturated air

TABLE 4

Efficiency of Charcoal* Beds in Extracting Methyl Iodide From Air Saturated With Water at 75°C

Initial concentration of methyl iodide: 0.69 μg per liter of saturated air
Weight of charcoal for cartridge: 1.6 g
Volume of charcoal per cartridge: 4 $cm^3$
Temperature of charcoal: 75°C
Duration of each experiment: 1 hr

| Residence Time (sec) | Charcoal Cartridge Length (cm) | Efficiency of Cartridge (%)[a] | | | | | |
|---|---|---|---|---|---|---|---|
| | | 1 | 2 | 3 | 4 | 5 | 6 |
| 0.140 | 1 | 67 | 84 | 82 | 100 | | |
| | 2 | 73 | 86 | 92 | 100 | | |
| 0.070 | 1 | 43 | 58 | 73 | 72 | 56 | 63 |
| | 2 | 46 | 60 | 72 | 77 | 64 | 66 |
| 0.035 | 1 | 29 | 36 | 43 | 50 | 58 | 61 |
| | 2 | 38 | 46 | 57 | 66 | 63 | 61 |
| 0.0175 | 1 | 21 | 27 | 31 | 33 | 35 | 39 |
| | 2 | 30 | 32 | 35 | 38 | 41 | 50 |

[a]Efficiency of cartridge (%) = $\frac{CH_3I \text{ sorbed} \times 100}{CH_3I \text{ reaching cartridge}}$.

*MSA #85851.

TABLE 5

Average Water Content of Charcoal Cartridges

Weight of charcoal per cartridge: 1.6 g
Volume of charcoal per cartridge: 4 $cm^3$
Partial pressure of water in air: 289 mm Hg
Temperature of charcoal cartridges: 75°C

| Cartridge Length (cm) | Average Water Content of Cartridge (% of dry weight) | | | | | |
|---|---|---|---|---|---|---|
| | 1 | 2 | 3 | 4 | 5 | 6 |
| 1 | 67 ± 18 | 45 ± 6 | 39 ± 12 | 39 ± 9 | 37 ± 10 | 31 ± 12 |
| 2 | 52 ± 5 | 45 ± 6 | 45 ± 6 | 41 ± 8 | 40 ± 7 | 39 ± 7 |

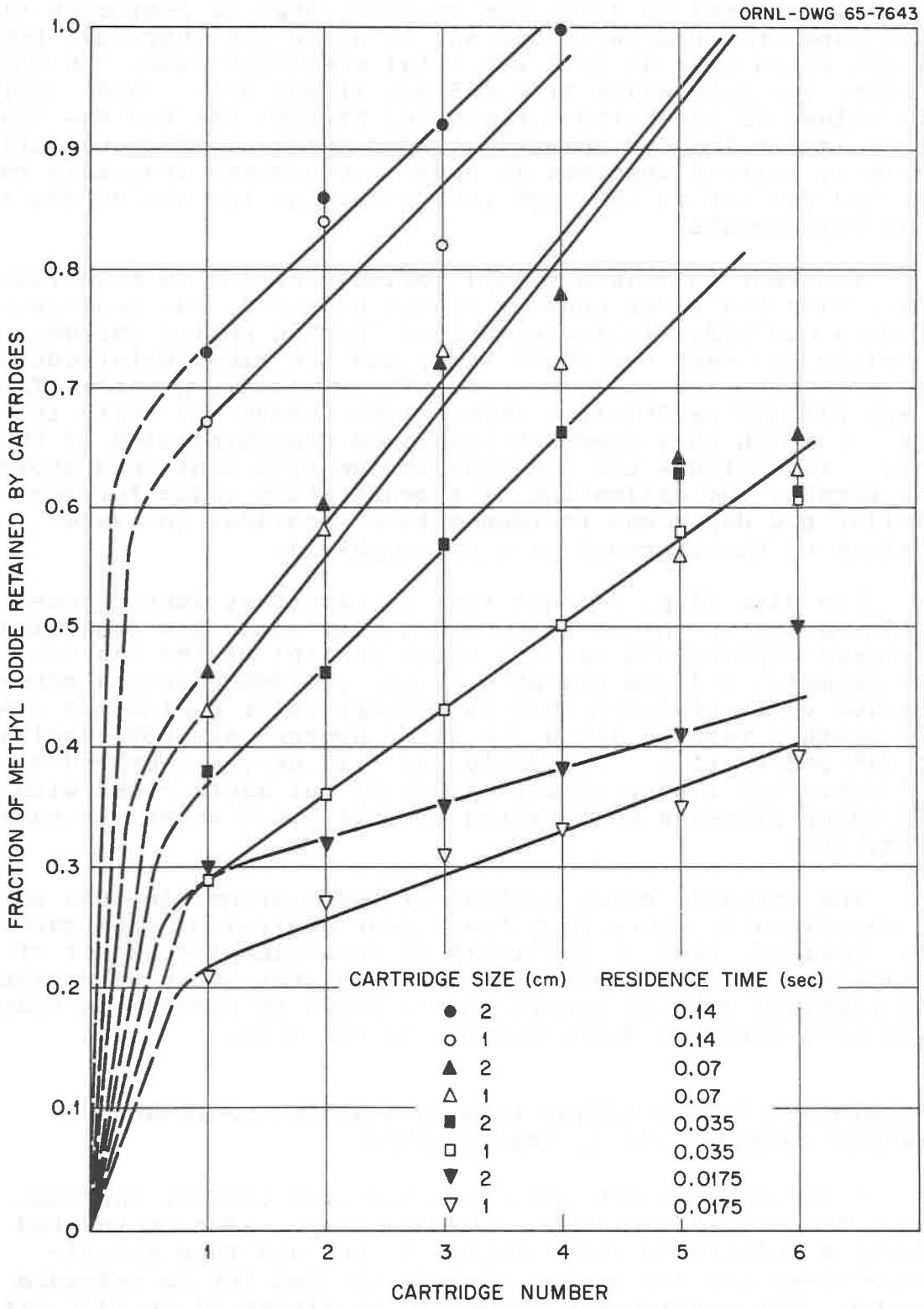


Fig. 6. Efficiency of Cartridges at Various Bed Depths (Air at 75°C and 100% Relative Humidity.

during a 30-min period. The flow rates were varied from 1.75 to 14 liters/min to cover the desired range of residence times. This exposure apparently did not saturate the charcoal, because it was found that at 0.42 sec total residence time, the water content was 35%, while at 0.105 sec it was 47%. (Note that the volume of saturated air passing through the bed was four times larger for the shorter residence time.) Wide variations in water content observed in these experiments indicated that the bed was not at the same temperature as the gas stream in some experiments.

In order to relate methyl iodide behavior to both residence time and water content of the charcoal, the penetration of each cartridge following a 1-hr loading period was determined for each residence time, and the final water content of each cartridge was measured. These values, given in Table 6 are plotted as fraction penetrating versus bed depth in Fig. 7, which is a somewhat idealized representation of the data. It excludes the non-equilibrium data mentioned above and permits the estimation of a penetration value for any similar bed depth and residence time, provided the water content of the charcoal is also comparable.

The data (Fig. 7) show that an important factor controlling the retention of methyl iodide under the conditions of these experiments was the water content of the charcoal. For example, a 12-cm bed at 0.21 sec residence gave a penetration value of 0.07% with an average water content of 41%, but another test in which the water content was 63% resulted in 24% penetration. Similarly, at 0.42 sec, a 3-cm bed with 35% water had a penetration of 0.84%, but another bed with 30% water showed a penetration of only 0.01% under the same conditions.

The variable water content of the charcoal in this series of experiments, where relatively poor control of this parameter was obtained, made it difficult to determine the effect of residence time. However, it was found that the penetration of the charcoal beds by methyl iodide could be correlated reasonably well with the water content of the beds.

## ATTEMPTS TO DESORB IODINE FROM METHYL-IODIDE-LOADED COCONUT CHARCOAL (5% $I_2$ IMPREGNATED)

A series of tests was conducted with coconut charcoal in which the methyl iodide was continuously loaded on the bed during a relatively short period (1 hr) and then methyl-iodide-free gas was passed through the bed for an extended period. The loading was conducted at either 25 or 75°C with saturated air. The flow velocities used were 60 and 120 linear fpm. Tests were made with both deep beds (six 2-cm cartridges) and shallow beds (six 1-cm cartridges).

TABLE 6

Penetration of Coconut Charcoal* Beds by Methyl Iodide at Various Bed Depths, Residence Times, and Water Contents

| Residence Time per Cartridge[a] (sec) | Residence Time for Six Cartridges (sec) | Water Content of Cartridges (% of dry weight)[b] | Fraction of Methyl Iodide Penetrating Bed | | | | | | | | |
|---|---|---|---|---|---|---|---|---|---|---|---|
| | | | Bed Depth (cm) | | | | | | | | |
| | | | 1 | 2 | 3 | 4 | 5 | 6 | 8 | 10 | 12 |
| 0.003 | 0.018 | 65 | 0.80 | 0.73 | | | | | | | |
| 0.006 | 0.036 | 53 | 0.73 | 0.64, 0.58 | | 0.50 | | | | | |
| 0.009 | 0.054 | 51 | | | 0.40 | | | 0.34 | | | |
| 0.012 | 0.072 | 48 | 0.57 | 0.54, 0.46 | | 0.35, 0.27 | | | 0.20 | | |
| 0.015 | 0.090 | 48 | | | | | 0.12 | | | 0.12 | |
| 0.018 | 0.108 | 46 | | | 0.26, (0.54/53%)[c] | | | 0.15, 0.11 | | | 0.06 |
| 0.023 | 0.138 | 44 | 0.33 | 0.27, 0.24 | | 0.22, 0.13 | | | 0.05, (0.41/70%)[c] | | |
| 0.030 | 0.18 | 42 | | | | | 0.054, (0.22/47%)[c] | | | 0.019, (0.24/66%)[c] | |
| 0.035 | 0.21 | 41 | | | 0.06 | | | 0.06, 0.021 | | | 0.0073 (0.24/63%)[c] |
| 0.047 | 0.28 | 40 | 0.052 | (0.055/38%),[c] (.003/26%)[c] | | 0.38, 0.014 | | | (0.015/44%),[c] (0.15/53%)[c] | | |
| 0.060 | 0.36 | 39 | | | | | 0.005 | | | 0.0028 | |
| 0.07 | 0.42 | 35 | | | 0.008, (0.001/30%)[c] | | | 0.003 | | | |

[a] Each charcoal cartridge contained 4 cm³ of granular charcoal.

[b] Average water content of the charcoal cartridges after 90 min exposure to air at 75°C and 100% relative humidity at the flow rate (3.5 to 14 liters/min) giving the residence time shown in the first column.

[c] Values in parentheses are penetrations and water contents observed when the charcoal beds were either above or below the temperature of the flowing gas stream.

* Impregnated charcoal (MSA #85851).

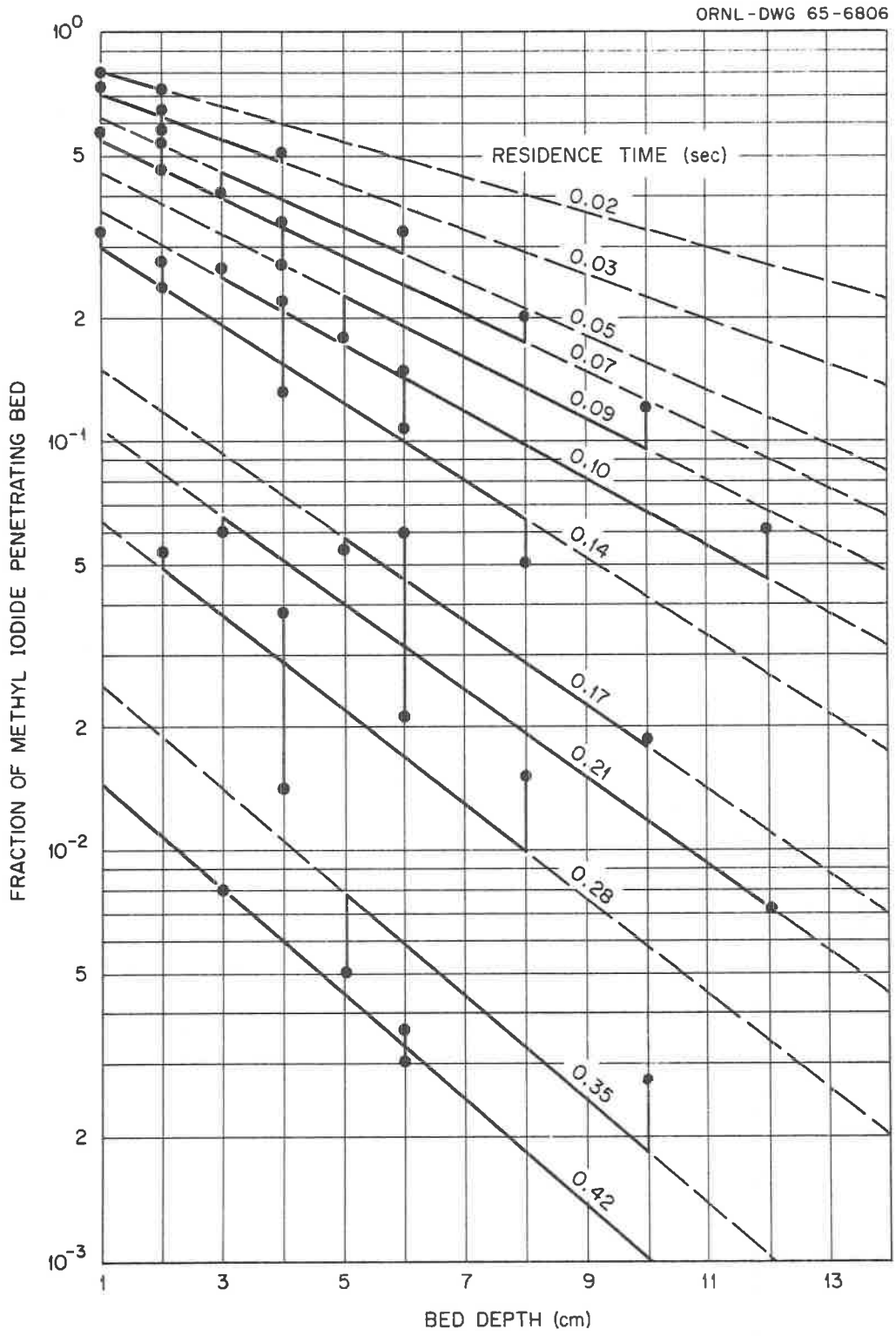


Fig. 7. Fraction of Methyl Iodide Penetrating Charcoal Beds as a Function of Bed Depth and Residence Time.

Two points stand out from these tests. First, penetration of a bed of coconut charcoal by methyl iodide is strongly dependent upon the amount of water held in the charcoal. Second, once adsorbed, exchanged iodine resists desorption from coconut charcoal through many hours of airflow even at a high relative humidity. These two points are illustrated by the data in Figs. 8 and 9. In these tests, $CH_3{}^{131}I$-labeled methyl iodide was loaded on parallel beds at a rate that would give an average loading (assuming homogeneous distribution) of 28 $\mu$g per gram of dry charcoal.

In Figs. 8 and 9 the values of Curve A represent amounts of $CH_3I$ adsorbed from an air stream at 25°C and 100% relative humidity, with no visible condensation of water occurring in the cartridges. The values of Curve B represent $CH_3I$ content of charcoal cartridges after being subjected to a stream of air (without $CH_3I$) at 25°C and 100% relative humidity for 8 hr. The flow rate was 7 liters/min or 60 linear fpm in the 1-cm cartridges (Fig. 9) and 120 linear fpm in the 2-cm cartridges (Fig. 8). The corresponding residence time in the beds was 0.2 sec. The data show that negligible changes in methyl iodide distribution occurred under these experimental conditions.

Since no detectable loss (less than $10^{-4}$ percent) was apparent during the passage of saturated air through the beds for 8 hr at 25°C (Curve B), more severe conditions were selected for the next desorption test: 4 hr at a temperature of 75°C and 100% relative humidity (Curve C) and 2 hr at 90°C (Curve D). After the 4-hr exposure at 75°C, the peak of the curve had shifted downstream a distance equivalent to one cartridge length, or through about one-sixth of the bed. The subsequent exposure for 2 hr at 90°C produced no further change, so the distribution profiles shown by Curves C and D in Figs. 8 and 9 are superimposed.

In seeking to explain the difference between the results of the 90°C test and those obtained in the previous test at 75°C, the water content of the charcoal was compared for the two runs. It was found that the 75°C run was made under temperature control conditions that left the charcoal with an amount of water approximately equal to 100% of its dry weight; whereas the 90°C run was made under better controlled conditions (bed at same temperature as the gas stream) and water was adsorbed to the extent of only about 60% of the dry weight of the charcoal.

A final desorption test was made with saturated air between 95 and 100°C and the bed at 95°C so that condensation in the bed would occur. Exposure of the beds for 2 hr under these conditions produced a measurable displacement of the iodine activity in both beds; however, the shallow (1-cm bed)

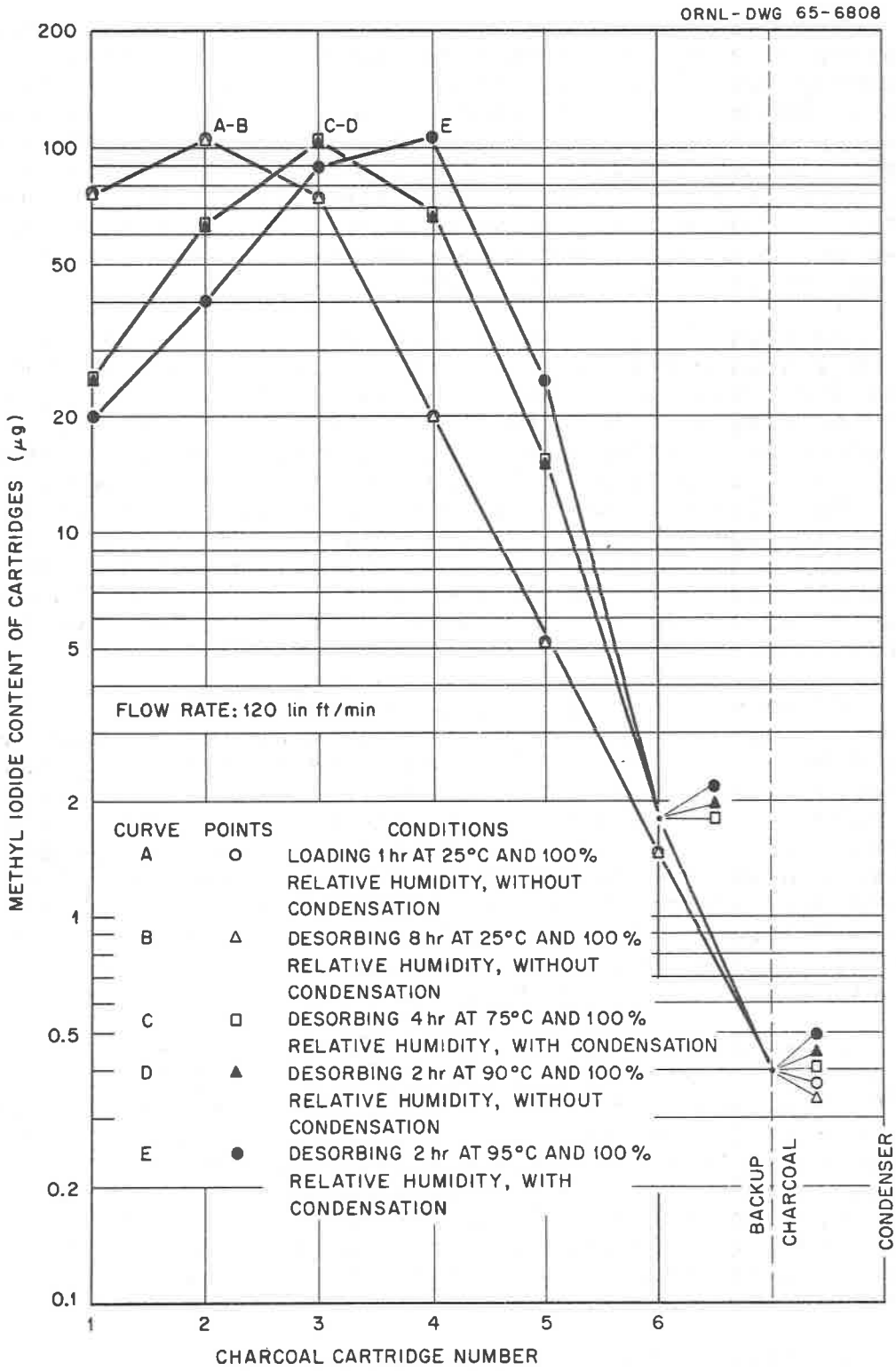


Fig. 8. Distribution of Methyl Iodide After Sorption at 25°C in Water-Loaded 1-cm Coconut Charcoal Cartridges and After Exposure to Flowing Saturated Air at Temperatures up to 95°C.

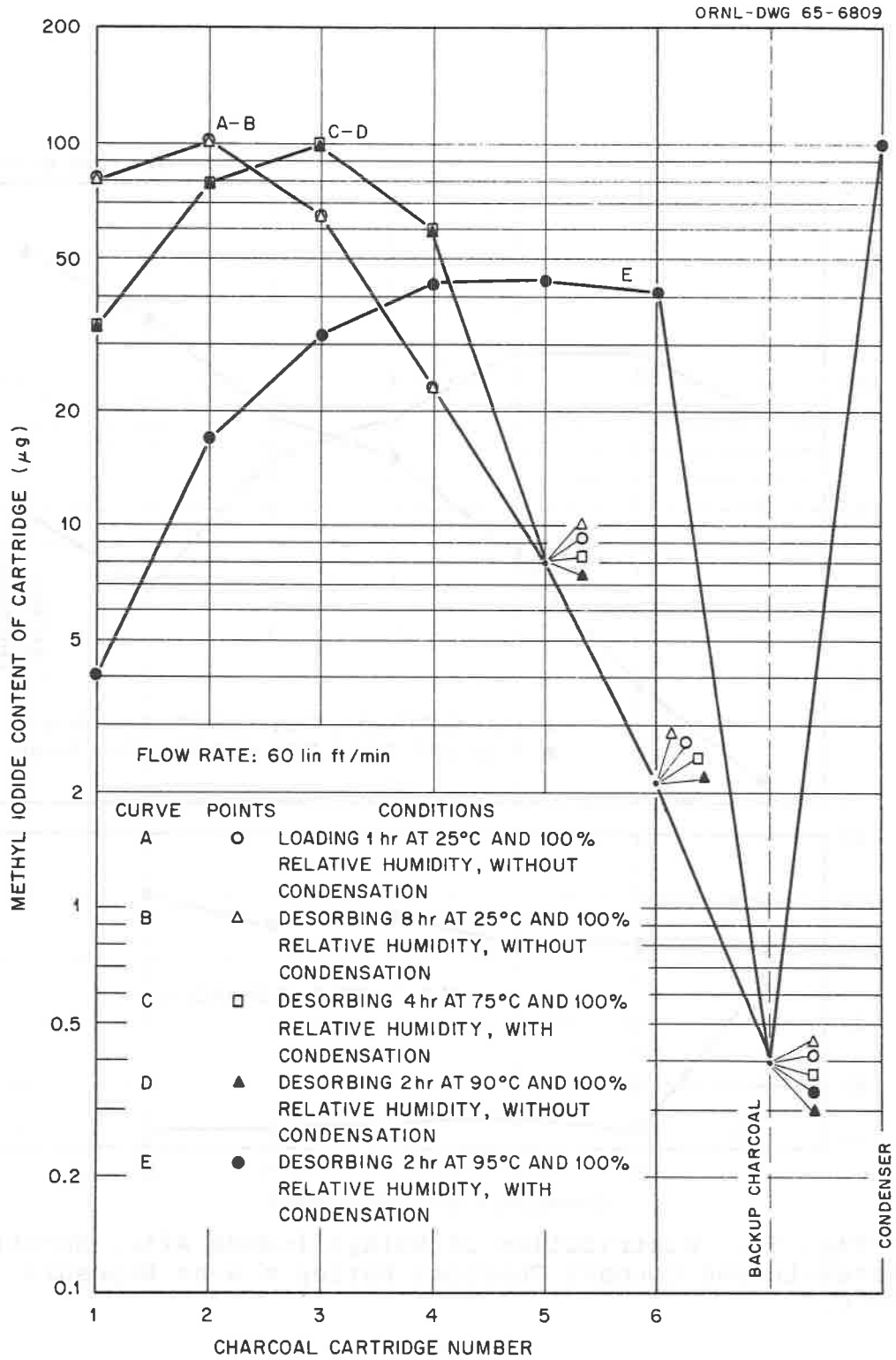


Fig. 9. Distribution of Methyl Iodide After Sorption at 25°C in Water-Loaded 1-cm Coconut Charcoal Cartridges and After Exposure to Flowing Saturated Air at Temperatures up to 95°C.

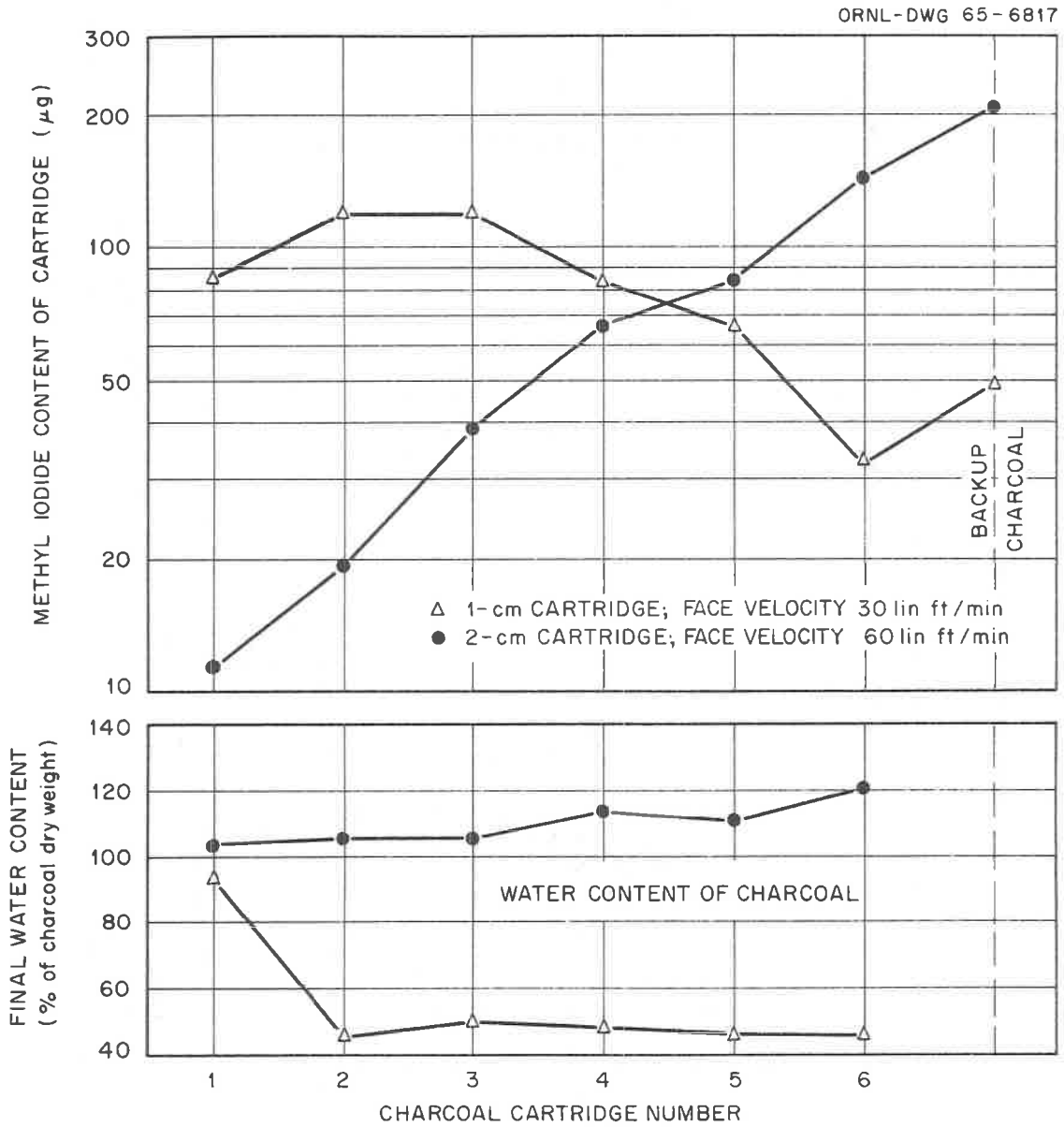


Fig. 10. Distribution of Methyl Iodide After Sorption on Water-Loaded Coconut Charcoal During a 4-hr Exposure at 75°C.

showed significant loss of $CH_3I$ (~ 35%), and the activity removed from the bed was not found in the backup charcoal (Curve E, Figs. 8 and 9). It was accounted for by examining the condensate in the air-cooled condenser (Fig. 1). However, the iodine appeared to be entirely in an ionic form, since it was completely inextractable by $CHCl_3$. Further tests showed the form to be iodide, which would be its form if the impregnant were being leached as HI. It is interesting to note that the amount of iodine activity leaving the beds exposed to flowing saturated air for 8 hr at 25°C and 4 hr at 75°C was below the limit of detection, while only 5 parts in $10^4$ was lost during the 1-hr loading period.

Examples of the sensitivity of the retention process to the duration of the loading period and the accumulation of excess water in the charcoal are shown in Fig. 10. In these experiments, the loading time was increased to 4 hr at 75°C with an air flow of 3.5 liters/min. Excessive water accumulation in the beds occurred, particularly in the 2-cm cartridges. Penetration under these rather severe conditions (75°C and 100% relative humidity, with condensation) was about 8% in the shallow bed, which showed a 50% water gain, and 40% in the deep bed with a water gain of 100% of the charcoal dry weight.

## CONCLUSIONS

The results of these tests indicate that the retention of methyl iodide by impregnated coconut charcoal adsorbed from humid air may be adequate for reactor safety containment systems. This conclusion is limited to conditions under which the water content of the beds is held to less than approximately 50% of the dry charcoal weight and the bed dimensions permit a residence time of several tenths of a second at the maximum gas velocity that can be experienced under accident conditions.

REFERENCES


1. C. J. Barton, Compiler, Proceedings of the International Symposium on Fission Product Release and Transport Under Accident Conditions, Held at Oak Ridge, Tennessee, April 5-7, 1965, USAEC Report CONF-650407, September 1965.

2. Karl B. Brown, Jr. Re-examining the Significance of Fission Products in Accident Situations, Nucleonics 23(6), 55 (1965).

3. R. D. Collins, Trapping Radioiodine, Nucleonics 23(9), 7 (1965).

4. D. A. Collins, R. Taylor, and L. R. Taylor, The Removal of Methyl Iodide from Reactor Effluent Gases, USAEC Report CONF-650407, p. 853, September 1965.

TABLE 1

Retention of Iodine From Methyl Iodide by Various Samples of Activated and Impregnated Charcoals

| Impregnant | Amount of Impregnant (mg/g of charcoal) | Manufacturer[a] | Charcoal Identification | Air Velocity (fpm) | Loading Time (hr) | Iodine from $CH_3I$ Loaded on 8-g Bed (mg) | Residence Time in 5-cm-Deep Bed (sec) | Penetration of 5-cm-Deep Bed (%) |
|---|---|---|---|---|---|---|---|---|
| None | | SS | 207 | 19 | 2.5 | 0.5 | 0.52 | 30 |
| None | | BC | 513 | 19 | 3.0 | 0.5 | 0.52 | 26 |
| None | | MSA | 25725 | 19 | 2.0 | 0.5 | 0.52 | 12 |
| Piperidine | 50 | SS | 207 | 19 | 3.0 | 0.75 | 0.52 | 2.76 |
| NaI | 50 | BC | 416 | 19 | 3.5 | 0.2 | 0.52 | 0.54 |
| $I_2$ | 76 | MSA | 85851 (lot 15) | 38 | 2.0 | 1.0 | 0.26 | 0.06 |
| $I_2$ | 10 | MSA | 25725 | 19 | 3.0 | 0.5 | 0.52 | 0.033 |
| $I_2$ | 70 | MSA | 25725 | 19 | 3.0 | 0.5 | 0.52 | 0.027 |
| $I_2$ | 70 | BC | 416 | 19 | 3.0 | 1.0 | 0.52 | 1.0 |
| $I_2$ | 70 | PCC | PCB | 19 | 3.0 | 0.75 | 0.52 | $1.6 \times 10^{-4}$ |
| $I_2$ | 70 | PCC | PCB | 19 | 3.5 | | 0.52 | $4 \times 10^{-4}$ |
| $I_2$ | 70 | PCC | PCB | 38 | 4.0 | 2.0 | 0.26 | $9 \times 10^{-3}$ |
| $I_2$ | 70 | PCC | PCB | 19 | 5.0 | 1.5 | 0.52 | $1 \times 10^{-4}$ |
| $I_2$ | 70 | PCC | SGL | 19 | 3.0 | 0.5 | 0.52 | 0.35 |
| KI | 10 | PCC | PCB | 19 | 3.0 | 1.0 | 0.52 | $7 \times 10^{-8}$ |
| KI | 10 | PCC | PCB | 19 | 4.5 | 35.0 | 0.52 | $1.3 \times 10^{-3}$ |
| KI | 10 | PCC | PCB | 38 | 4.5 | 2.0 | 0.26 | $4 \times 10^{-5}$ |
| KI + $I_2$ | 10 each | PCC | PCB | 38 | 3.5 | 2.0 | 0.26 | $4 \times 10^{-6}$ |
| TED[b] + KI | 50 and 100 | MSA | 25725 | 38 | 4.0 | 2.0 | 0.52 | $7 \times 10^{-4}$ |
| TED | 50 | MSA | 25725 | 19 | 4.5 | 3.5 | 0.52 | $1.8 \times 10^{-4}$ |
| TED | 50 | MSA | 25725 | 19 | 5.0 | 1.5 | 0.52 | $1.5 \times 10^{-5}$ |

[a]SS — Sutcliffe-Speakman, BC — Barnebey-Cheney, MSA — Mine Safety Appliance, PCC — Pittsburgh Coke and Chemical Company; all samples were 8-14 mesh size except PCB, which was 12-30.

[b]Triethylenediamine.

TABLE 2

Penetration of Treated and Untreated Coconut Charcoal by Methyl Iodide Under LOFT Conditions

Air velocity: 17.5 fpm
Air temperature: 100°F
Relative humidity: 100%
Charcoal bed temperature: 115°F
Loading period: 20 hr

| Run No. | Loading Time (hr) | Charcoal Type | Mesh Size | Carrier $CH_3{}^{127}I$ Used (mg) | Penetration of 2-cm Cartridges (%) | | | | | |
|---|---|---|---|---|---|---|---|---|---|---|
| | | | | | Cartridge 1 | Cartridge 2 | Cartridge 3 | Cartridge 4 | Cartridge 5 | Cartridge 6 |
| 9-13 | <18 | MSA 85851 | 8-14 | 1 | 7.4 | 0.51 | 0.003 | | Negligible | |
| 9-22[a] | 20 | MSA 85851 | 8-14 | 1 | 0.06 | 0.005 | 0.002 | | Negligible | |
| 9-27 | 20 | MSA 85851 | 8-14 | 27 | 2.5 | 0.1 | 0.03 | | Negligible | |
| 10-4 | 20 | MSA 85851 | 8-14 | 57 | 4.0 | 0.33 | 0.07 | | Negligible | |
| 10-6[a] | 20 | PCB + 6% $I_2$ | 12-30 | 27 | 0.16 | 0.04 | 0.002 | | Negligible | |
| 10-7 | 20 | PCB + 6% $I_2$ | 12-30 | 27 | 6.1 | 0.091 | 0.01 | | Negligible | |
| 10-14 | 17 | PCB (untreated) | 12-30 | 1 | 81 | 61.5 | 40 | 22 | 9 | 2.3 |
| 10-10 | 20 | PCB + 5% $I_2$ | 12-30 | 1 | 1.2 | 0.028 | 0.0011 | | Negligible | |
| 10-16 | 20 | PCB + 5% $I_2$ | 12-16 | 1 | 5.3 | 0.39 | 0.019 | 0.0012 | | |

[a]First portion of methyl iodide eluted from charcoal in trap.

TABLE 3

Performance of Charcoal* Beds in Extracting Methyl Iodide From Air Saturated With Water at 75°C

Initial concentration of methyl iodide: 0.7 μg per liter of saturated air
Weight of charcoal per cartridge: 1.6 g
Volume of charcoal per cartridge: 4 $cm^3$
Temperature of charcoal: 75°C
Duration of each experiment: 1 hr

| Experiment No. | Air Flow Rate (liters/min) | Charcoal Cartridge Length (cm) | Air Residence Time (sec/cartridge) | Total $CH_3I$ Trapped (μg) | Percentage of $CH_3I$ Trapped per Cartridge | | | | | | |
|---|---|---|---|---|---|---|---|---|---|---|---|
| | | | | | 1 | 2 | 3 | 4 | 5 | 6 | Backup Trap |
| 1 | 1.75 | 1 | 0.140 | 71.8 | 66.8 | 27.8 | 4.4 | 1.0 | Not Used | | 0 |
| | | 2 | 0.140 | 71.8 | 72.4 | 23.7 | 3.6 | 0.3 | | | 0 |
| 2 | 3.5 | 1 | 0.070 | 145.2 | 42.8 | 33.3 | 17.5 | 4.6 | 1.0 | 0.5 | 0.3 |
| | | 2 | 0.070 | 141.9 | 45.8 | 32.5 | 15.6 | 4.7 | 0.9 | 0.3 | 0.2 |
| 3 | 7.0 | 1 | 0.035 | 284.9 | 28.5 | 25.9 | 19.7 | 13.3 | 7.5 | 3.3 | 2.1 |
| | | 2 | 0.035 | 284.1 | 37.5 | 28.7 | 19.4 | 9.5 | 3.1 | 1.1 | 0.7 |
| 4 | 14.0 | 1 | 0.0175 | 569.4 | 20.6 | 21.4 | 18.2 | 13.2 | 9.4 | 6.7 | 10.5 |
| | | 2 | 0.0175 | 591.4 | 29.6 | 22.5 | 16.8 | 11.9 | 7.8 | 5.7 | 5.7 |

*Impregnated charcoal (MSA #85851).

**TABLE 5**

**Average Water Content of Charcoal Cartridges**

**Weight of charcoal per cartridge: 1.6 g**
**Volume of charcoal per cartridge: 4 $cm^3$**
**Partial pressure of water in air: 289 mm Hg**
**Temperature of charcoal cartridges: 75°C**

| Cartridge Length (cm) | Average Water Content of Cartridge (% of dry weight) | | | | | |
|---|---|---|---|---|---|---|
| | 1 | 2 | 3 | 4 | 5 | 6 |
| 1 | 67 ± 18 | 45 ± 6 | 39 ± 12 | 39 ± 9 | 37 ± 10 | 31 ± 12 |
| 2 | 52 ± 5 | 45 ± 6 | 45 ± 6 | 41 ± 8 | 40 ± 7 | 39 ± 7 |

TABLE 6

Penetration of Coconut Charcoal* Beds by Methyl Iodide at Various Bed Depths, Residence Times, and Water Contents

| Residence Time per Cartridge[a] (sec) | Residence Time for Six Cartridges (sec) | Water Content of Cartridges (% of dry weight)[b] | Fraction of Methyl Iodide Penetrating Bed | | | | | | | | |
|---|---|---|---|---|---|---|---|---|---|---|---|
| | | | Bed Depth (cm) | | | | | | | | |
| | | | 1 | 2 | 3 | 4 | 5 | 6 | 8 | 10 | 12 |
| 0.003 | 0.018 | 65 | 0.80 | 0.73 | | | | | | | |
| 0.006 | 0.036 | 53 | 0.73 | 0.64, 0.58 | | 0.50 | | | | | |
| 0.009 | 0.054 | 51 | | | 0.40 | | | 0.34 | | | |
| 0.012 | 0.072 | 48 | 0.57 | 0.54, 0.46 | | 0.35, 0.27 | | | 0.20 | | |
| 0.015 | 0.090 | 48 | | | | | 0.12 | | | 0.12 | |
| 0.018 | 0.108 | 46 | | | 0.26, (0.54/53%)[c] | | | 0.15, 0.11 | | | 0.06 |
| 0.023 | 0.138 | 44 | 0.33 | 0.27, 0.24 | | 0.22, 0.13 | | | 0.05, (0.41/70%)[c] | | |
| 0.030 | 0.18 | 42 | | | | | 0.054, (0.22/47%)[c] | | | 0.019, (0.24/66%)[c] | |
| 0.035 | 0.21 | 41 | | | 0.06 | | | 0.06, 0.021 | | | 0.0073 (0.24/63%)[c] |
| 0.047 | 0.28 | 40 | 0.052 | (0.055/38%),[c] (.003/26%)[c] | | 0.38, 0.014 | | | (0.015/44%),[c] (0.15/53%)[c] | | |
| 0.060 | 0.36 | 39 | | | | | 0.005 | | | 0.0028 | |
| 0.07 | 0.42 | 35 | | | 0.008, (0.001/30%)[c] | | | 0.003 | | | |

[a]Each charcoal cartridge contained 4 cm³ of granular charcoal.

[b]Average water content of the charcoal cartridges after 90 min exposure to air at 75°C and 100% relative humidity at the flow rate (3.5 to 14 liters/min) giving the residence time shown in the first column.

[c]Values in parentheses are penetrations and water contents observed when the charcoal beds were either above or below the temperature of the flowing gas stream.

*Impregnated charcoal (MSA #85851).

# MECHANISMS THAT AFFECT THE ADSORPTION OF METHYL IODIDE ON CHARCOAL UNDER HUMID CONDITIONS

Frank J. Ackerman and John Z. Grens

Lawrence Radiation Laboratory,
University of California
Livermore, California

## ABSTRACT

Breakthrough curves of the adsorption of methyl iodide from air on charcoal were experimentally measured over the range of 20-100% humidity. The observed breakthrough curves can be explained by assuming two rate controlling mechanisms for mass transfer; bulk diffusion was found to control the adsorption rate during the early period, while pore diffusion was found to control later in the adsorption process. Water vapor greatly limits the external surface adsorption capacity of the charcoal for methyl iodide. Water vapor also hinders the rate of mass transfer by pore diffusion.

## INTRODUCTION

Fission product iodine released by nuclear reactor fuel elements and nuclear device tests has been found to be only partially trapped on charcoal in some cases.[1,2] Lawrence Radiation Laboratory recently used a gas cleaning plant to bleed the cavity created by the Salmon nuclear test.[3] A significant fraction of the iodine in the processed gas penetrated the charcoal adsorbers of the plant. There is evidence that up to 30% of the iodine from the cavity was in a form other than $I_2$.

Experimental evidence shows that iodine in the form of $I_2$ or hydrogen iodide is effectively adsorbed on charcoal in flow systems.[4,5,6,7] Organic iodides, such as methyl iodide, are only partially retained in continuous adsorbers, especially under humid conditions.[8,9,10] The equilibrium amount of methyl iodide absorbed on charcoal is sufficiently large for complete adsorption even under conditions of high humidity. Therefore, incomplete adsorption of methyl iodide must be due to a low rate of mass transfer.

This study is concerned with the mechanisms that control the rate of methyl iodide adsorption on charcoal, and with the effect of process variables (humidity, flow rate, bed dimension, etc.) on that rate. Our purpose ultimately is to be able to mathematically evaluate charcoal adsorber performance.

The mechanisms that control adsorption rate can be determined by studying the effluent concentration history, or breakthrough curve, of the adsorption process. We measured the breakthrough curves resulting from the adsorption of methyl iodide on charcoal at several humidities.

## THEORY

One would like to predict the performance of a given adsorption process under any set of conditions with a minimum of laboratory experiments. The performance parameter of greatest interest is the concentration history of the effluent stream, the breakthrough curve. The breakthrough curve can be calculated by solving the set of partial differential equations which describe the adsorption process.

The equations for bed and effluent concentrations have been solved for a number of cases.[11,12,13] Of particular significance is the work of Vermuelen.[14,15,16,17,18] To use an existing solution, we must know the stoichiometry, equilibrium relationship, mechanisms and rate of mass transfer in the system, and the effect of water vapor on these factors.

The following analytical treatment is intended only to acquaint the reader with the physical quantities and nomenclature used to describe the behavior of fixed bed processes. It should be mentioned at this point that no single solution now appearing in the literature adequately describes the problem at hand. A detailed mathematical treatment will be the subject of a future paper.

### Stoichiometry

The maximum amount of sorbent a bed can adsorb is designated as its ultimate capacity ($q_\infty$). This capacity is the quantity of material a bed in equilibrium with the feed concentration ($C_o$) would hold. This stoichiometric behavior is usually expressed in terms of a distribution ratio

$$D = q_\infty \rho_b / C_o e \quad , \tag{1}$$

where $\rho_b$ is the bulk density of the bed as packed and, e is the external void fraction of the bed.

### Equilibrium

The equilibrium that takes place on the surface of a particle during adsorption can be written as

$$A + \text{adsorbent} \longleftrightarrow A \bullet \text{adsorbent}.$$

The equilibrium curve which relates the solid phase concentration of A ($q_A$) to the fluid phase concentration ($C_A$) is termed the adsorption isotherm.

It is convenient to express the quilibrium relationship in terms of a separation factor (r),

where $$r = \frac{x(1-y)}{y(1-x)} \quad . \tag{2}$$

Here x and y are dimensionless concentrations; $x = C/C_o$, $y = q/q_\infty$.

The separation factor becomes constant if we assume a Langmuir adsorption isotherm,

$$r = \frac{1}{1 + K_L C_o} \quad . \tag{3}$$

$K_L$ is the Langmuir equilibrium constant.

The Langmuir isotherm is applicable to physical adsorption on homogeneous surfaces where there is negligible interaction between adsorbed molecules.

Four general types of equilibrium behavior are associated with various values of r:

| | |
|---|---|
| 1) Irreversible | $r = 0$ |
| 2) Favorable | $0 < r < 1$ |
| 3) Linear | $r = 1$ |
| 4) Unfavorable | $r > 1$ |

## Mass Transfer Rate

The effective rate of adsorption in packed beds is governed by the mass transfer mechanisms involved. Rate-controlling mechanisms which may operate simultaneously are:

1. Mass transport from the bulk fluid to the external surface of the absorbent particles (bulk diffusion).
2. Longitudinal molecular diffusion or axial dispersion in the bulk fluid (axial dispersion).
3. Diffusion in the fluid phase within the particle pores (pore diffusion).
4. Reaction at the solid surface.
5. Solid-phase diffusion (diffusion of the adsorbed material along the pore surface and within the solid matrix).

Bulk diffusion, pore diffusion, and solid-phase diffusion are generally the most important in gas adsorption. Axial dispersion operates in parallel with bulk diffusion, but it is quite slow and is only important at very low flow rates. Bulk diffusion is followed in series either by pore diffusion and then reaction or by reaction and then solid-phase diffusion. The series with the fastest overall transfer rate will control. But the slowest step in either series controls the effective rate for that series. In physical adsorption the surface reaction is quite fast and is not rate controlling. If bulk diffusion is not appreciably faster than pore diffusion or solid-phase diffusion it behaves mathematically like a resistance in series with them. However, the resistances are not additive in a simple way.[17,19]

In a specific case it may happen that two different mechanisms will control, each during a different part of the adsorption process. It is important to know which mechanism controls, since different design equations apply for different mechanisms.

An estimate of whether mechanism 1, 2, 3, or 5 is controlling can be obtained from the pore and fluid-phase diffusivities, together with the Peclet

number.[18] Details of the method are given in Appendix II. The result of this calculation shows that in the case of $CH_3I$ adsorption, either pore or solid-phase diffusion controls and the external mass transport is relatively fast.

## Mathematical Description of the Process

The adsorption process can be described by the solution of two simultaneous partial differential equations: (1) the material balance equation and (2) the mass transfer rate equation. It is general practice to write these equations in terms of a set of dimensionless variables:

N, number of transfer units $= kv/F$

Z, throughput parameter $= C_o \frac{(V-ve)}{q_\infty \rho_b} \frac{}{v} = \frac{V-ve}{Dve}$

r, equilibrium parameter $= \frac{1}{1 + K_L C_o}$

x, dimensionless fluid phase concentration $= C/C_o$

y, dimensionless particle phase concentration $= q/q_\infty$

When this set of variables is used the material balance equation, which states that material lost by fluid is gained by the solid, becomes

$$\left(\frac{\partial y}{\partial NZ}\right)_N = - \left(\frac{\partial x}{\partial N}\right)_{NZ} . \qquad (4)$$

The rate equation assumes different forms, depending on the mechanism of mass transfer chosen as a model. For example, if a model based on second-order kinetics is chosen to describe the transfer rate,[15] the rate equation is

$$\left(\frac{y}{NZ}\right)_N = x(1-y) - ry(1-x) . \qquad (5)$$

The solution of Eqs. (4) and (5), with appropriate boundary conditions, provides x and y as functions of N, Z and r. This solution was first reported by Thomas,[13] and has been widely discussed in the literature. Solutions using other rate equations and some special cases such as r = 0 or r = 1 also have been reported.

We have found that adsorption of methyl iodide on charcoal involves the parallel operation of two mass-transfer processes, external diffusion or pore diffusion, each controlling at different times. Existing solutions will individually describe either of the two processes. Unfortunately, there is no available solution when these processes take place in parallel. The solutions which do exist are useful in that they provide a framework for examination of the experimental data and a basis for general conclusions.

## EXPERIMENTAL

A diagram of the experimental apparatus used to determine the methyl iodide adsorption rate on charcoal at various humidities is given in Fig. 1a. The humidity is controlled by mixing dry air with saturated air. The dew point of the air stream is continuously monitored and manually controlled within 1° F of the set point.

A mixture of methyl iodide and $I^{131}$ - tagged methyl iodide is added to the air stream at a constant rate of approximately $2.4 \times 10^{-6}$ mole/min. The methyl iodide diffuses through a capillary tube in a constant-temperature bath. Details of the methyl iodide feed system are shown in Fig. 1b. Liquid $CH_3I$ at the bottom of the capillary tube vaporizes and diffuses to the top of the tube where it mixes with the air stream. The rate of methyl iodide diffusion up the tube remains fairly constant over the period of a run (within 4%) since the change in the liquid level is small compared to the length of the tube. The diffusion rate is measured from the drop in liquid level which is measured with a cathetometer during each run.

The air stream passes through the charcoal test bed where $CH_3I$ adsorption takes place. The methyl iodide emerging from the test bed is collected by drying the air stream and passing it through a charcoal trap in a well counter. The total $I^{131}$ —tagged methyl iodide adsorbed in the trap is gamma-counted. The amount of trapped methyl iodide is determined from the count rate of a measured quantity of methyl iodide.

Before each test, charcoal-water vapor adsorption equilibrium is established by passing air at the test humidity through the charcoal bed for at least 4 hours. Immediately before a test run, the air stream is diverted from the test charcoal bed and trap. The stream flows through a bypass line while steady-state $CH_3I$ and water vapor concentrations are established.

Several runs were made without charcoal in the test bed to measure systematic errors and to check the $CH_3I$ feed rate against the $CH_3I$ build-up in the charcoal trap as indicated by gamma counting.

The charcoal used in the tests is steam-activated coconut shell carbon with a maximum ash content of 4% (Barnebey-Cheney type 513). See Appendix I for properties of the charcoal used.

A list of the tests performed is presented in Appendix I. Tests 1 through 8 were run on a 2.7-cm-long charcoal bed of 10-12 mesh particles, and cover a humidity range of 12.5% to 100%. Tests 9 and 10 both were run at 70% humidity but the bed characteristics were changed: in test 9 the bed was 5.4 cm long; in test 10 the bed was 2.7 cm long as before, but 28-32 mesh charcoal particles were used.

## RESULTS

$CH_3I$ breakthrough curves for four tests are presented in Fig. 2. Here the amount of methyl iodide which passed through the adsorption bed is shown as a function of time. The curves were plotted from test data by converting the gamma count measured at the charcoal trap to moles of $CH_3I$. The effect of humidity on adsorption, as shown by these curves, is typical of all tests. The slope of a curve at any point is proportional to the $CH_3I$ concentration leaving the bed at that instant. The desired breakthrough curve is obtained by plotting first derivative (slope) of a curve as a function of time (for example, the breakthrough curve of test 4 is plotted in Fig. 5).

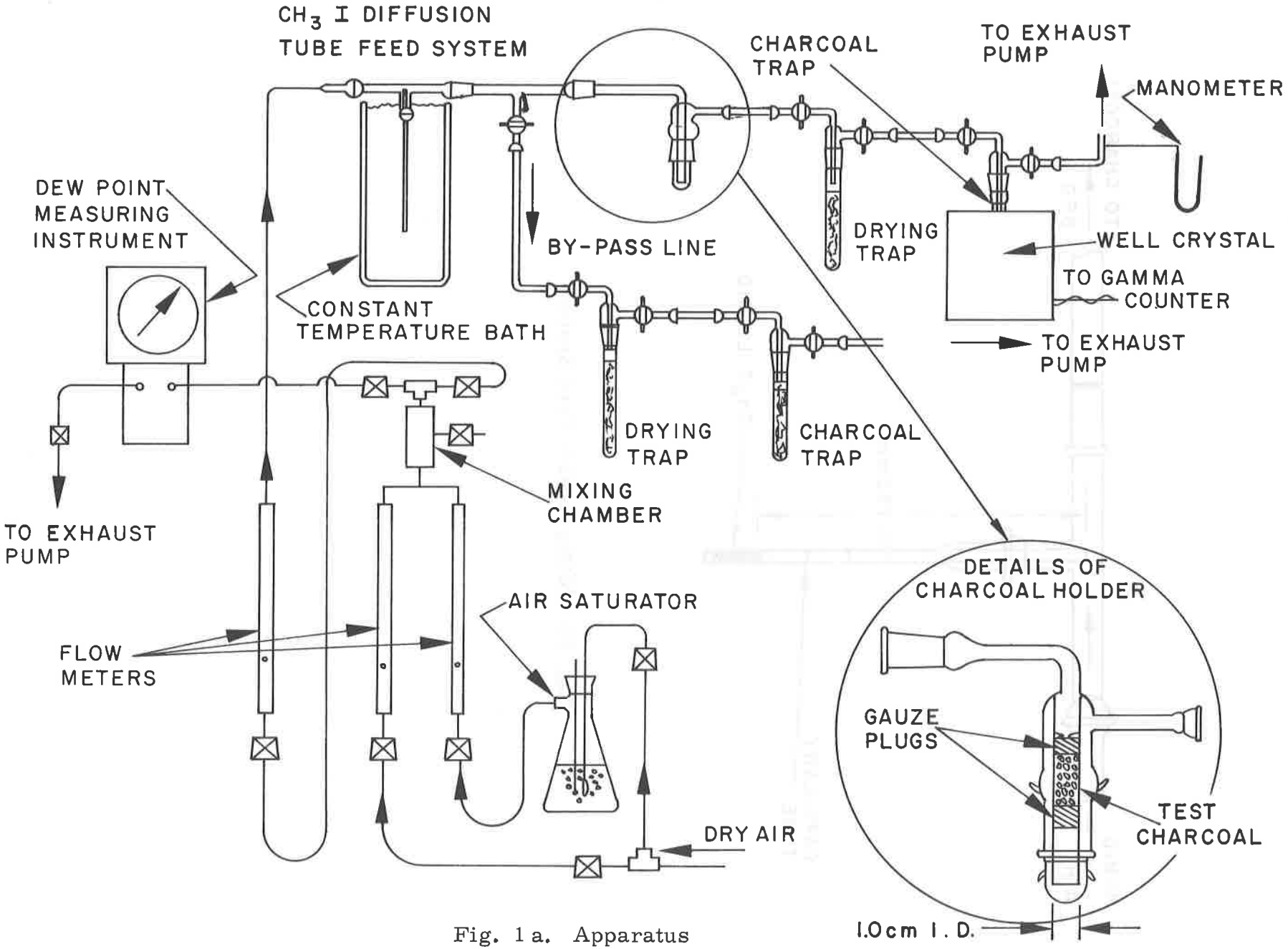


Fig. 1 a. Apparatus

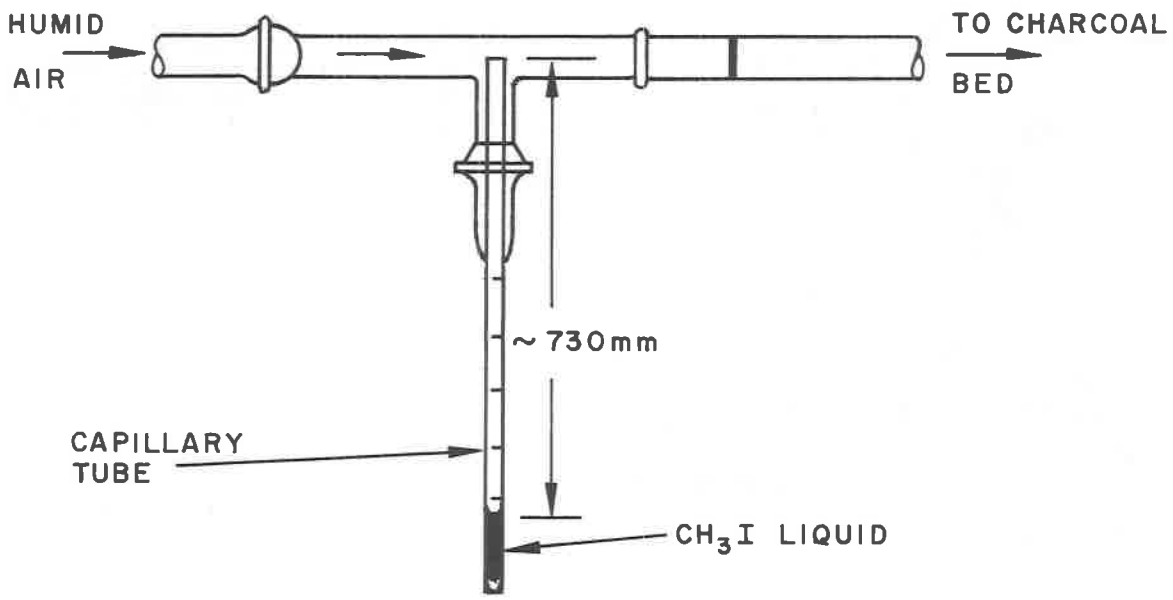


Fig. 1b. Methyl Iodide Feed System

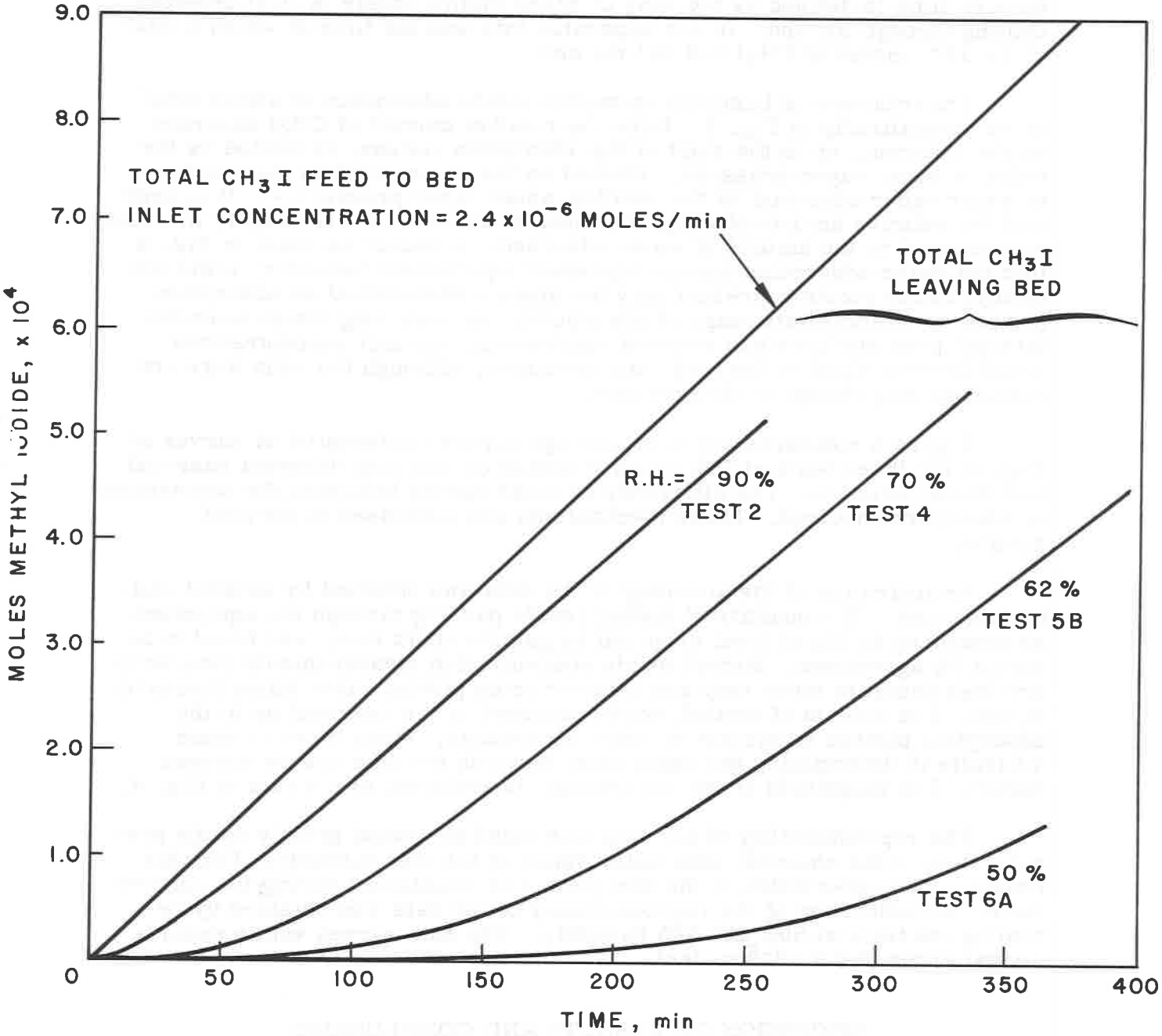


Fig. 2. Typical Data Curves

Note that the slope of each curve becomes constant at late times, indicating an apparently constant methyl iodide concentration leaving the bed. In all tests this "constant" exit concentration was less than the feed concentration ($C_O$). The value of this concentration was found to depend on humidity, decreasing slightly as humidity was decreased. The effect is not great, but it can be perceived in Fig. 2.

In the discussion to follow, the region of apparently constant concentration will be termed the adsorption plateau; the "constant" concentration will be termed the plateau concentration.

Figure 3 shows the effect of humidity on breakthrough time. Breakthrough time is defined as the time at which methyl iodide is first detected coming through the bed. In our apparatus this was the time at which a total of $3 \times 10^{-7}$ moles of $CH_3I$ had left the bed.

The influence of humidity on methyl iodide adsorption is shown even more dramatically in Fig. 4. Here the relative amount of $CH_3I$ adsorbed on the charcoal, up to the start of the adsorption plateau, is plotted vs the relative water vapor pressure. Plotted on the same graph is the fraction of water vapor adsorbed vs the relative water vapor pressure.[20] It is seen that the relative amount of $CH_3I$ adsorbed on the charcoal is roughly inversely proportional to the amount of water adsorbed. It should be noted in Fig. 4 that the water adsorption curves represent equilibrium behavior, while the methyl iodide points represent only the amount adsorbed at an adsorption plateau or intermediate stage of adsorption. At very long times when the internal pore surfaces had reached equilibrium, the exit concentrations would become equal to the feed concentrations, although the runs were not continued long enough to observe this.

Figure 5 compares the breakthrough curves (differential of curves of Fig. 2) for three tests at 70% relative humidity, but with different charcoal bed characteristics. The difference in these curves indicates the mechanism of adsorption involved. These mechanisms are discussed in the next section.

An indication of the accuracy of the data was obtained by several calibration runs. The quantity of methyl iodide passing through the equipment, as measured by liquid level drop and by gamma count rate, was found to be within 5% agreement. Methyl iodide concentration measurements inherently are less accurate since they are obtained from plotted curve slope measurements. The amount of methyl iodide adsorbed in the charcoal up to the adsorption plateau is subject to some uncertainty, since there is some difficulty in determining the exact point at which the data curves become linear. The magnitude of the uncertainty is reflected in the data of Fig. 4.

The reproducibility of the data was found to depend greatly on the presaturation of the charcoal with water vapor at the test humidity. For this reason close supervision of the dew point was maintained during the current tests. An indication of the reproducibility of the data was obtained by repeating the tests at 50% and 62% humidity. The data agrees within experimental error ($\pm 2 \times 10^{-6}$ moles).

## DISCUSSION OF RESULTS AND CONCLUSIONS

We now can evaluate two important aspects of methyl iodide adsorption: 1) the mechanisms which control the mass transfer rate; and 2) the influence of water vapor.

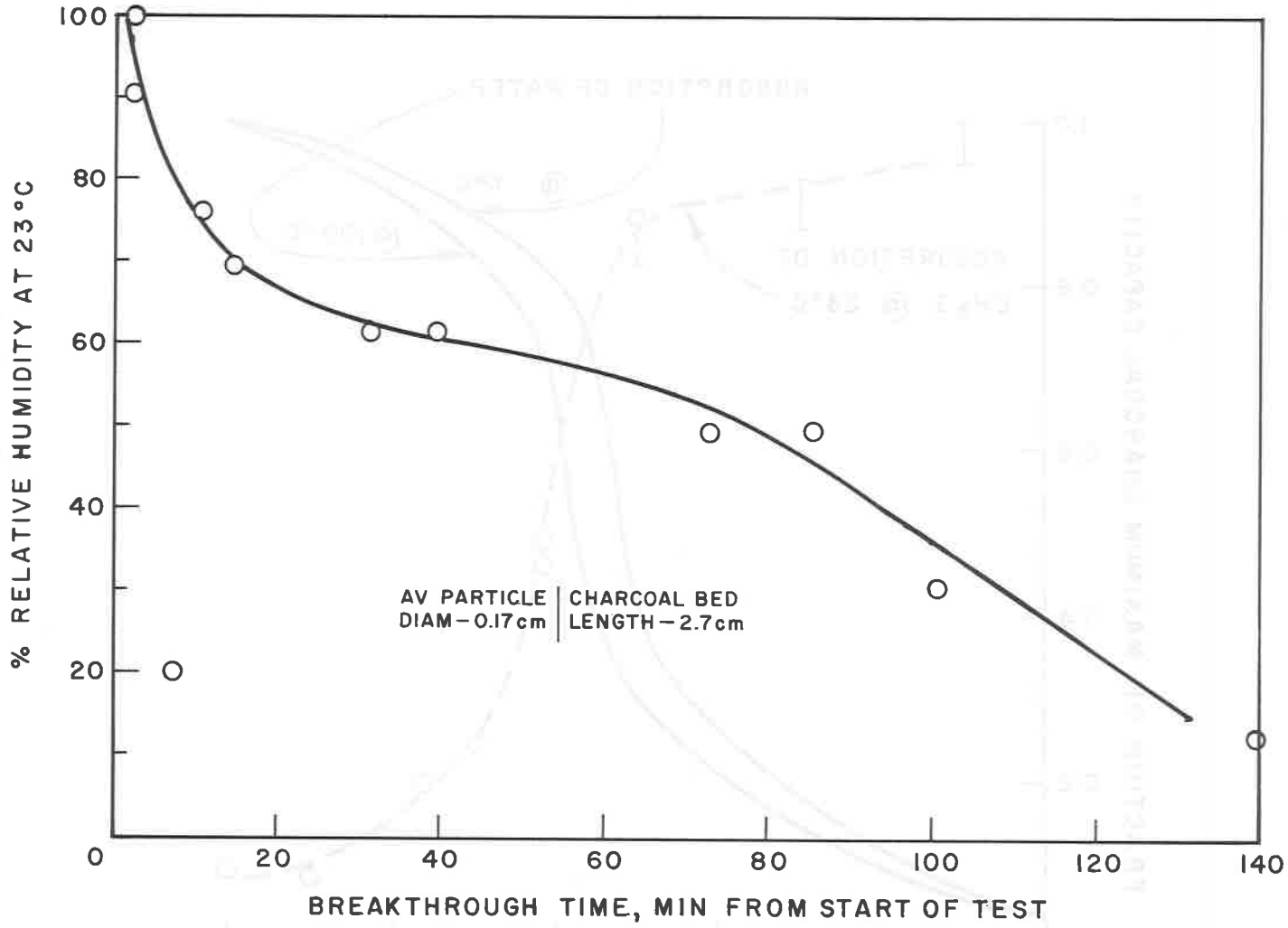


Fig. 3. Effect of Humidity on Breakthrough Time

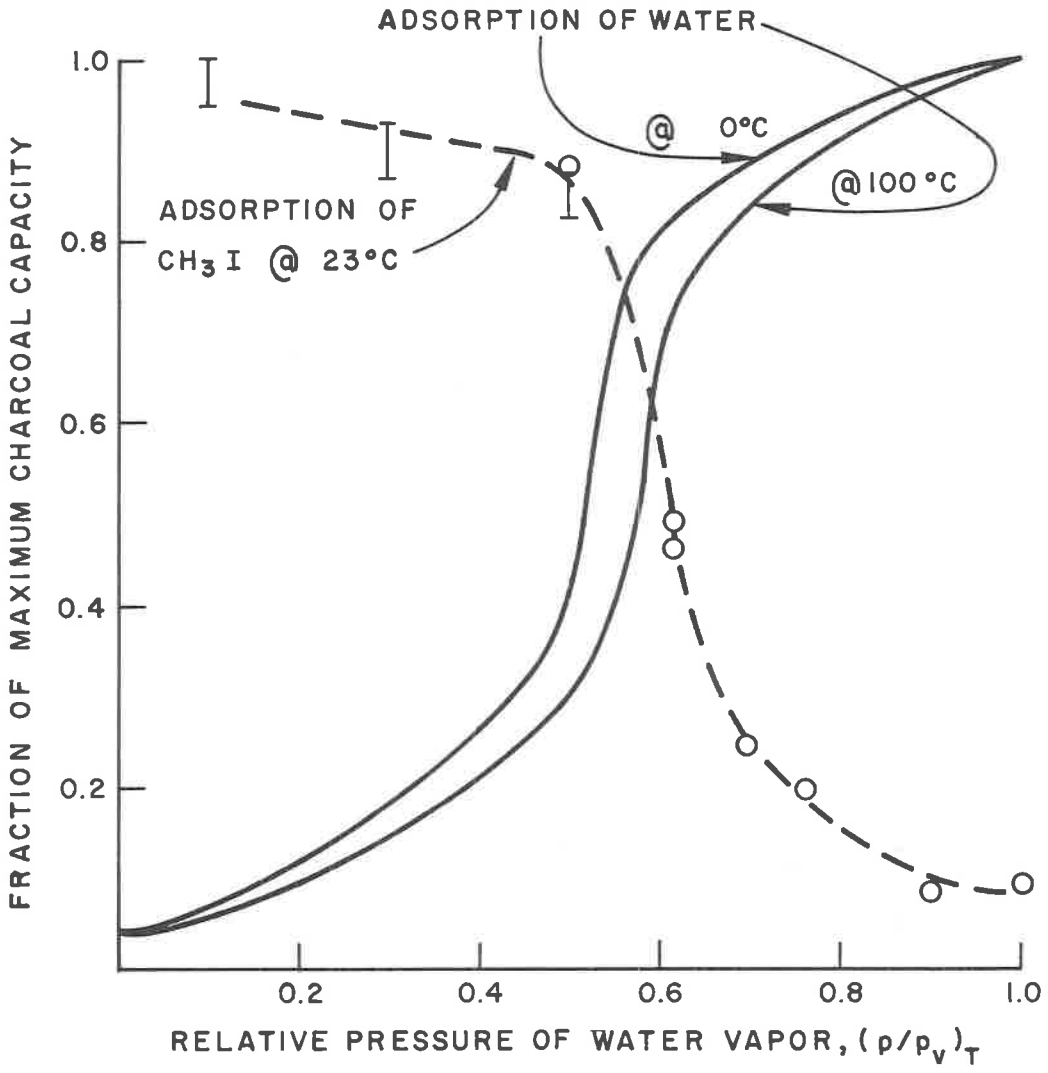


Fig. 4. Adsorption of Methyl Iodide and Water Vapor on Charcoal

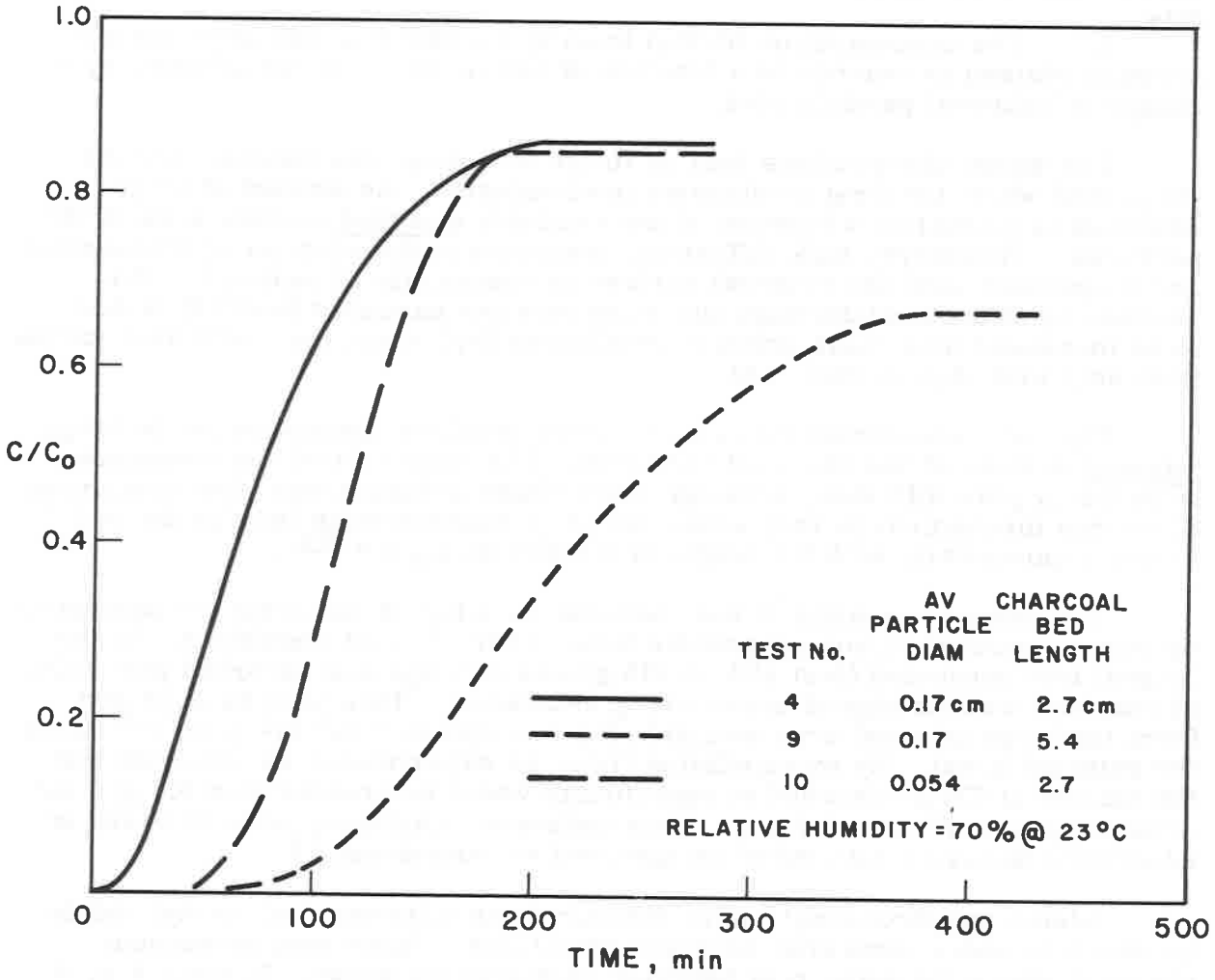


Fig. 5. Breakthrough Curves of Methyl Iodide Adsorption at 70% Relative Humidity

## Rate Mechanisms

The experiments present an interesting and unexpected example of physical adsorption phenomena. The data as seen in Fig. 2 strongly support the conclusion that two adsorption rate mechanisms control, each at different times. One mechanism controls the effective mass transfer rate from early times until shortly after breakthrough. The rate of mass transfer is quite fast when this mechanism is controlling. A second relatively slow mechanism controls at later times (the constant slope portion of the curves of Fig. 2). During this latter period the concentration leaving the charcoal bed apparently is constant but not as high as the entering concentration. Absorption therefore continues, but at a greatly diminished rate.

The curves of Fig. 5, together with Table I, furnish additional evidence that two rate mechanisms are involved and also indicate what the mechanisms are. Two facts are apparent from these three tests:

1. The total quantity of $CH_3I$ adsorbed by the charcoal up to the time the adsorption plateau is reached is a function of both bed length and particle size.
2. The concentration ($C/C_o$) leaving the charcoal bed after the adsorption plateau is reached is a function of bed length; it is not affected by a change in charcoal particle size.

The above observations lead us to the following conclusions: During the period when the first mechanism predominates, the amount of $CH_3I$ adsorbed is primarily a function of the available external surface area of the particles. Therefore, bulk diffusional transport is the controlling mechanism, and it operates until the external surface is essentially at capacity. The sharpening of the breakthrough curve for smaller particles (test 10) is due to an increased bulk mass transfer coefficient ($k_F$) since the coefficient varies inversely with $(d_p)1.6$ (Ref. 15).

The slow adsorption rate at late times involves adsorption on the large internal surface of the charcoal particles. The rate-controlling mechanism is probably pore diffusion, although solid-phase diffusion may also contribute. Since this mechanism is very slow, the $CH_3I$ concentration leaving the bed varies exponentially with the length of the bed ($C/C_o \propto e^{-KL}$).

The internal capacity of the charcoal for $CH_3I$ is too great for saturation by this mechanism in any reasonable time under our test conditions. In the longest test conducted (test 6B), 0.125 grams of $CH_3I$ was adsorbed per gram of charcoal with no sign of approaching saturation. This is to be expected from the large internal area available for adsorption ($\sim 10^3$ $M^2/g$ or $10^5$ times the external area). By extrapolation from the experiments we estimate that the amount of $CH_3I$ adsorbed at equilibrium would be greater than 0.2 g/g but probably not more than 0.7 g/g. This estimated maximum value is based on adsorption behavior with other halogenated hydrocarbons.[18]

Adams and Browning[10] have measured the adsorption of methyl iodide on charcoal under somewhat different conditions. Their data on coconut charcoal shows the same rate behavior as discussed above. In their Fig. 4 (cf. Ref. 10) they plot breakthrough curves at three different bed depths. Their curves are very similar to those of tests 4 and 9 of Fig. 5, and they clearly show an adsorption plateau whose level depends on bed depth.

Table I.

| | Tests | | |
|---|---|---|---|
| | 4 | 9 | 10 |
| Average particle diameter (cm) | 0.17 | 0.17 | 0.054 |
| Bed length (cm) | 2.7 | 5.4 | 2.7 |
| Estimated relative external surface area | 1 | 2 | 1.5-2 |
| $C/C_o$ at plateau | 0.86 | 0.67 | 0.85 |
| Quantity of $Ch_3I$ adsorbed at plateau (moles $\times 10^5$) | 22 | 62 | 33 |

## Effect of Water Vapor

Since the shape of the breakthrough curve is due to two controlling mechanisms instead of the usual case of one, it is difficult to determine the exact influence of water vapor on r, Z, and N.

Stoichiometry. The amount of methyl iodide adsorbed up to the adsorption plateau is just slightly greater than the ultimate capacity ($q_\infty$) of the external charcoal surface since bulk mass transport is controlling. It therefore follows from the results presented in Fig. 4 that $q_\infty$ for the external surface is inversely proportional to the quantity of water adsorbed. In our particular case it is convenient to define ultimate capacity for the surface area acted on by each mechanism $(q_\infty)_{ext}$ and $(q_\infty)_{int}$. It is logical to assume that $(q_\infty)_{int}$ follows the same relationship as $(q_\infty)_{ext}$. This relation appears in the dimensionless throughput parameter Z.

Equilibrium. Comparison of the experimental breakthrough curves with the analytical curves calculated by Vermeulen[15] lead us to believe that the adsorption equilibrium remains favorable regardless of the humidity. Thus the separation factor (r) lies in the range, $0 < r < 1$. Because of the combined influence of both rate mechanisms on the breakthrough curve it is difficult to determine if water vapor causes r to vary significantly within the range of favorable equilibrium.

Mass Transfer Rate. The first mechanism, bulk diffusion, is so fast that water vapor has little observable influence on the rate.

The rate of adsorption by the second mechanism, pore diffusion, is influenced by water vapor to some extent. The effect on the rate is observed in the value of the effluent concentration during the period this mechanism controls. This apparently constant concentration is inversely proportional to the effective adsorption rate. As we previously observed in Fig. 2, the value of the exit concentration decreases slightly as humidity is decreased. Therefore, the effective pore diffusion rate is reduced by the presence of water vapor. The effect is not large; the rate change was not more than 20% between 12% humidity and 100% humidity.

## DESIGN APPLICATIONS

The laboratory data collected thus far, together with some of the more basic theoretical observations on fixed-bed behavior, comprise a basis for rational design of air cleaning adsorbers. Of greatest interest to the designer are:

1. The time of first appearance of $CH_3I$ in the effluent.
2. The long term collection efficiency.

Once inlet $CH_3I$ concentration and humidity have been selected, the items above may be estimated conveniently by the following procedure:

Breakthrough time may be estimated by using the standard design procedure for external-diffusion-controlled mass transfer (see Ref. 15 or Ref. 18). Values of $(q_\infty)_{ext}$ for a particular charcoal may be estimated for any humidity from two experimental breakthrough measurements at separated humidities by assuming $(q_\infty)_{ext}$ inversely proportional to the quantity of water adsorbed. Values of N can be determined by using a calculated bulk mass transfer coefficient. The error involved in this procedure will depend on the relative influence of the second mechanism. For relatively long beds pore diffusion can be significant, and the breakthrough time calculated by the above procedure will be less than the actual.

Outlet concentration for long-term operation can be estimated by assuming pore-diffusion-controlled mass transfer and using the methods detailed in Perry[18] or Ref. 17. Here we can use N = 0, unless the true value is known, or we can use $C/C_o$ values obtained from one experimental measurement.

## ACKNOWLEDGMENTS

This work was performed under the auspices of the U. S. Atomic Energy Commission.

# APPENDIX I

## TEST CONDITIONS

Test Charcoal — (Barnebey Cheney type 513)

| | | |
|---|---|---|
| Coconut shell | | steam activated |
| Maximum ash content | | 4% |
| Total surface area ($M^2/g$) | | $1.2 - 1.3 \times 10^3$ |
| Average pore diameter (Å) | | 17 to 20 |
| Internal porosity | | 0.6 |
| Charcoal density (void free) | | 2.0 ± 0.2 |
| Particle size (mesh) | 10-12 | 28-32 |
| Average diameter (cm) | 0.17 | 0.054 |
| Number of particles (#/g) | 490 | 11,200 |
| External surface area ($cm^2/g$)(a) | 45 | 100 |

Charcoal Bed

| | | | |
|---|---|---|---|
| Temperature (° C) | | 23.0 | |
| Diameter (cm) | | 1.0 | |
| Area ($cm^2$) | | 0.785 | |
| Density of bed ($g/cm^3$) | | 0.51 | |
| Bed void fraction | | 0.40 | |
| Bed length (cm) | 5.4(b) | 2.7 | 2.7(c) |
| Bed volume ($cm^3$) | 4.2 | 2.1 | 2.1 |
| Weight of charcoal (g) | 2.14 | 1.07 ± 0.3 | 1.10 |

Summary of Tests

| | |
|---|---|
| Temperature | 23° C |
| Pressure | 1.013 atm |
| Volumetric flow rate | 500 $cm^3$/min at test temperature & pressure. |
| Mass flow rate | $1.0 \times 10^{-2}$ g/sec |
| | $3.5 \times 10^{-4}$ g-mole/sec |
| Face velocity | 640 cm/min |
| Methyl iodide feed rate | 0.0051 moles/$M^3$ at 0° C 1 atm |

| | | Charcoal Bed | | |
|---|---|---|---|---|
| Test | % relative humidity $100 \times (p/p_2)$ 23° C | Length cm | Particle size mesh | $CH_3I$ adsorbed at start of plateau mg/g charcoal |
| 1 | 100 | | | 12 |
| 2 | 90.5 | | | 9 |
| 3 | 76 | | | 24 |
| 4 | 70 | 2.7 | 10-12 | 29 |
| 5A | 62 | | | 56 |
| 5B | 62 | | | 58 |
| 6A | 50 | | | 99 |
| 6B | 50 | | | 106 |
| 7 | 30 | | | 104 |
| 8 | 12.5 | | | 114 |
| 9 | 70 | 5.4 | | 41.2 |
| 10 | 70 | 2.7 | 28-32 | 42 |

(a) Estimated; based on surface area of sphere with same diameter.

(b) Test No. 9.

(c) Test No. 10.

# APPENDIX II

## CALCULATIONS

The equations used in this section are from Perry,[18] sections 14 and 16. Fluid-phase diffusivity is calculated by Eqs. (14-57).

$$D_f = \frac{B\,T^{3/2}\sqrt{\frac{1}{M_1} + \frac{1}{M_2}}}{P\,r_{12}^2\,I_D}$$

where $$B = \left(10.7 - 2.46\sqrt{\frac{1}{M_1} + \frac{1}{M_2}}\right) \times 10^{-4}$$

(Note: Eq. (14-57a) is in error)

T - abs temp (° K),

M - molecular wt,

P - pressure (atm)

$r_{12} = \frac{(r_o)_1 + (r_o)_2}{2}$, where $r_o = 1.18\,V_o^{1/3}$, subscripts 1 - $CH_3I$ and 2 - air.

$V_o$ - molal volume at boiling point — found in tables.

$I_D$ - collision integral for diffusion — found in table.

$D_f = 0.10\ cm^2/sec$, $CH_3$ - air.

Pore diffusivity is calculated from Eqs. (16-36).

$$D_{pore} = \frac{D_f\,x}{2}\left\{1 - \exp\left[-\frac{4\,\bar{r}}{3\,D_f}\left(\frac{8\,RT}{M}\right)^{1/2}\right]\right\}$$

x - porosity = 0.6

$\bar{r}$ - pore radius = $9 \times 10^{-8}$ cm

$D_{pore} = 0.00135\ cm^2/sec$

$D_{pore}/D_f = 0.0135$

Peclet Number:

$$N_{Pe} = \frac{d_p F}{D_f S}$$

$d_p$ - particle diameter

F - volumetric flow rate

S - cross section area of bed

| $d_p$ | $N_{Pe}$ |
|---|---|
| 0.17 cm | 17. |
| 0.054 | 5.4 |

When we use values calculated above in Fig. 16-9 (Ref. 18), we see that pore or particle diffusion controls in both cases.

## NOTATION

| | |
|---|---|
| C | Concentration of solute in fluid phase |
| $C_o$ | Concentration of solute in feed phase |
| D | Distribution ratio |
| F | Volumetric flow rate |
| e | External void fraction of adsorbent bed |
| $K_L$ | Langmuir constant |
| k | Mass transfer coefficient |
| N | Number of transfer units |
| P | Partial pressure |
| $P_V$ | Vapor pressure |
| q | Concentration in solid phase |
| $q_\infty$ | Ultimate adsorbent of solid phase; the solid phase concentration in equilibrium with $C_o$ |
| r | Separation factor for adsorption |
| V | Solution volume |
| v | Column volume |
| x | Dimensionless fluid phase concentration ($C/C_o$) |
| y | Dimensionless solid phase concentration ($q/q_\infty$) |
| Z | Throughput parameter |
| $\rho_b$ | Bulk density of solid phase |

## REFERENCES


1. D. A. Collings, R. Taylor, W. D. Yuille, Experience in Trapping Iodine-131 and other Fission Products Released from Irradiated AGR-type End Elements, in Eighth AEC Air Cleaning Conference, USAEC Report TID-7677 p. 102, Oct. 1963.
2. G. W. Parker, W. J. Martin, and G. E. Creek, Behavior of Methyl Iodide in the Containment Mockup Facility, Nuclear Safety Program Semiannual Progress Report, ORNL-3843, p. 73, June 1965.
3. Richard A. Heckman, et al, VUF-3016, Vent Gas Treatment Facility, July 1965. See also The Design and Operation of a Vent Gas Treatment Facility, paper 6 session 36, this conference.
4. L. Silverman, R. Dennis, E. Kristal and F. Stein, Iodine Collection Studies, Sixth AEC Air Cleaning Conference, USAEC Report TID-7593, 1960.
5. R. E. Adams and W. E. Browning, Jr., Removal of Radioiodine from Air Streams by Activated Charcoal, ORNL-2872, 1960.
6. J. F. W. Smith and R. H. A. Crawley, Nuclear Engineering 6: 427 (1961).
7. E. M. Morimoto, work on $I_2$ and HI Adsorption on Charcoal, unpublished.
8. D. H. F. Atkins and A. E. J. Eggleton, Iodine Compounds Formed on Release of Carrier-free Iodine-131, British Report AERE M-1211, 1963.
9. D. A. Collins, R. Taylor and L. R. Taylor, The Removal of Methyl Iodide from Reactor Effluent Gases, International Symposium on Fission Product Release and Transport Under Accident Conditions, CONF-650407, p. 853, April 1965.
10. R. E. Adams and W. E. Browning, Jr., Removal of Iodine and Volatile Iodine Compounds from Air Systems by Activated Charcoal, International Symposium on Fission Product Release and Transport Under Accident Conditions, CONF-650-407, p. 869, April 1965.
11. A. S. Michaels, Ind. Eng. Chem. 44: 1922 (1952).
12. E. Glueckauf and J. I. Coates, J. Chem. Soc. 1314 (1947).
13. H. C. Thomas, J. Am. Chem. Soc. 66: 1664 (1944).
14. K. R. Hall, E. C. Lee, A. Acrivos and T. Vermeulen, I & E. C. Fundamentals 5: 212 (1966).
15. N. K. Hiester and T. Vermeulen, Chem. Eng. Progr. 48, 505 (1952).
16. T. Vermeulen, N. K. Hiester, Chem. Eng. Progr. Symp. Ser. 55, 61 (1959).
17. N. K. Hiester, S. B. Radding, R. L. Nelson, T. Vermeulen, A. I. Ch. E. Journal 2: 404 (1956).
18. Perry's Chemical Engineers' Handbook, 4th Ed., McGraw-Hill, New York, 1963.
19. C. J. King, A. I. Ch. E. Journal 10: 671 (1964).
20. A. S. Collidge, J. Am. Chem. Soc. 49: 708, 1927.

# HIGH TEMPERATURE CARBON FOR IODINE ADSORPTION*

by

R. C. Milham

Savannah River Laboratory
E. I. du Pont de Nemours and Co.
Aiken, South Carolina 29801

## ABSTRACT

The Savannah River Laboratory is studying adsorbers that will reduce the probability of igniting existing types of activated coconut-shell carbon in some reactor confinement systems. A new high temperature coconut-shell carbon (ignition temperature ~530°C) has been developed by an American manufacturer, and, in preliminary tests, meets specifications for the Savannah River Plant confinement system.

A standardized procedure has been developed to measure ignition temperature, to evaluate promising new types of carbon, and to evaluate effects of variables (such as air flow, bed depth, impregnants, plant service, and humidity) on ignition temperature. Results of these evaluations are reported.

---

* The information contained in this article was developed during the course of work under Contract AT(07-2)-1 with the U. S. Atomic Energy Commission.

## INTRODUCTION

The objectives of work at the Savannah River Laboratory (SRL) on high temperature carbons for iodine adsorption were to a) find an adsorber that will reduce the probability of fire, b) develop a standard procedure for the measurement of ignition temperature, c) measure the ignition temperature of promising carbons, and d) evaluate the effects of variables (such as air flow, bed depth, impregnants, plant service, and humidity) on ignition temperature.

A survey of the literature showed that activated carbon is the superior adsorber of radioactive, elemental iodine in spite of the risk of ignition. No satisfactory substitute for carbon was found. Carbon has the advantages of:

- high efficiency for adsorption of iodine (>99.9%) under a variety of adverse conditions
- long service life
- essentially maintenance-free operation
- low pressure drop
- relatively inexpensive
- negligible desorption

The temperature of carbon that has adsorbed radioactive iodine increases due to heat generated by the decay of radioiodine. The temperature rise depends primarily on:

- rate of air flow through the carbon; with no air flow, the carbon might be heated to its ignition temperature
- quantity and distribution of the iodine

The ignition temperature can be raised by using carbon:

- with a smaller internal surface area
- with a coarser mesh
- impregnated with materials that inhibit the initiation of ignition such as phosphates, borates, or halogens

- purified to remove impurities such as sodium and potassium that catalyze the oxidation of carbon

A review of commercially available carbons indicated that Barnebey-Cheney Co. had developed a coconut shell carbon with a high ignition temperature. Evaluation of this carbon at SRL showed that its ignition temperature was about 200°C higher than ordinary coconut carbon supplied by Barnebey-Cheney Co. and that it met specifications for the carbon presently used in the Savannah River Plant (SRP) reactors. Measurement of the adsorption properties of carbon are discussed in References 1-3.

## DISCUSSION

### Small-Scale Apparatus

A small-scale apparatus was developed at SRL to measure the ignition temperatures of promising carbons and to evaluate the effects of variables. The design for the apparatus was adapted from equipment used to measure the ignition temperature of coal. The SRL apparatus was made of stainless steel to mock up a full-size bed made from stainless steel. Quartz has been used by other investigators[4] to avoid possible catalytic effects of metals on the oxidation of carbon.

A diagram of this apparatus is shown in Figure 1. Compressed air entering the apparatus is cleaned by a carbon bed and an absolute filter. Air flows up to 6.5 cfm(130 ft/min velocity, based on face area of carbon bed) are measured with a calibrated rotameter. The air temperature is increased 2 to 4°C/min by the preheater; the furnace temperature is kept at the same temperature by a controller connected to thermocouples 1 and 9. Up to 5 thermocouples inserted in the carbon bed record the temperature at various positions. The thermocouples (0.025-inch diameter) are stainless steel clad. Ignition of the carbon is indicated by an abrupt temperature rise of the bed. The downstream air temperature, which also gives prompt indication of ignition, is monitored by thermocouple 3. Carbon beds

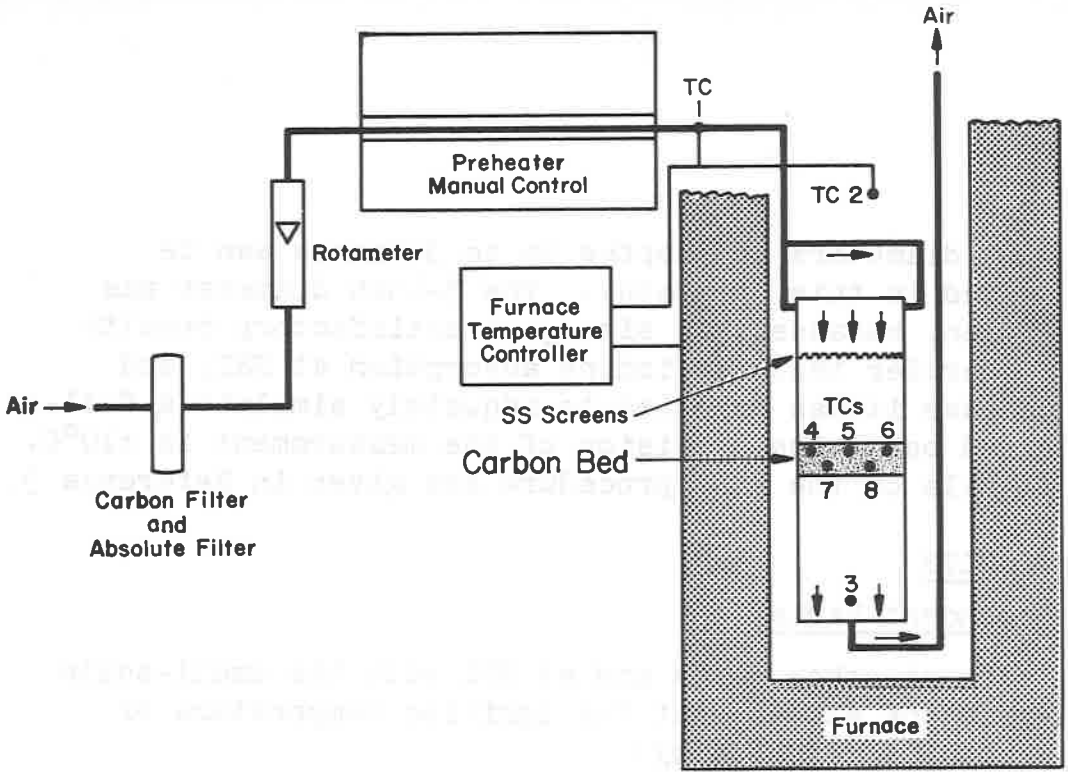


FIG. 1 SMALL-SCALE IGNITION TEST EQUIPMENT

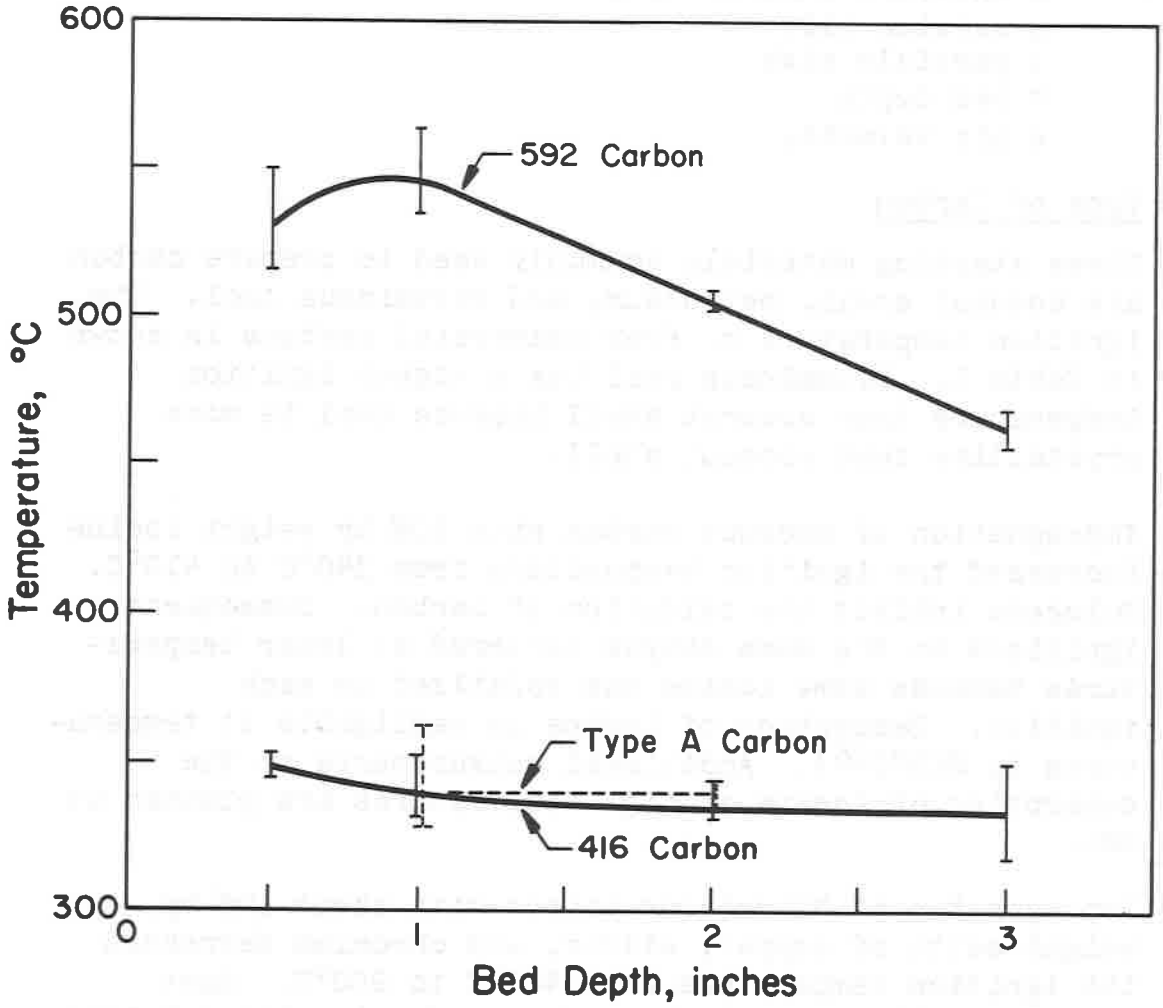


FIG. 2 IGNITION TEMPERATURE OF CARBON VERSUS BED DEPTH
(Air Velocity - 70 ft/min)

with diameters and depths up to 3 inches can be tested in this apparatus. The 3-inch diameter was chosen, because this size gave satisfactory results in earlier tests of iodine adsorption at SRL, and because it was expected to adquately simulate a full-sized bed. The precision of the measurement is ±10°C. Details of the test procedure are given in Reference 5.

## RESULTS

### Dependent Variables

Tests at other sites and at SRL with the small-scale apparatus showed that the ignition temperature of carbon is affected by:

- o type of carbon
- o internal surface area
- o service life
- o particle size
- o bed depth
- o air velocity

### Type of Carbon

Three starting materials commonly used to prepare carbon are coconut shell, petroleum, and bituminous coal. The ignition temperature of four commercial carbons is shown in Table 1. Bituminous coal has a higher ignition temperature than coconut shell because coal is more crystalline than coconut shell.

Impregnation of coconut carbon with 10% by weight iodine increased the ignition temperature from 340°C to 410°C. Halogens inhibit the oxidation of carbon. Subsequent ignitions on the same sample occurred at lower temperatures because some iodine was volatized in each ignition. Desorption of iodine is negligible at temperatures to 250°C(6). Additional measurements on the desorption of iodine at high temperatures are planned at SRL.

Impregnation of bituminous carbon with about 10% by weight salts of copper, silver, and chromium decreased the ignition temperature from 480°C to 250°C. Most metallic salts, especially sodium and potassium, catalyze the oxidation of carbon.

TABLE 1

Ignition Temperature of Various Commercial Carbons

| Carbon | Mesh* | Ignition Temperature** (°C) |
|---|---|---|
| Coconut Shell | | |
| Type 416 (Barnebey-Cheney Co.) | 10 x 14 | 340 |
| Type A*** | 6 x 16 | 340 |
| Petroleum | | |
| Type B*** | 6 x 16 | 420 |
| Bituminous | | |
| Type C*** | 4 x 10 | 480 |

* These variations in mesh should not affect ignition temperature significantly.

** Air velocity, 70 ft/min; 1-inch-thick by 3-inch-diameter bed.

*** Arbitrary designation for carbons available commercially from companies other than Barnebey-Cheney Co.

## Internal Surface Area

The effect of internal surface area was reported by Kovach.[4] He showed a rapid decrease in ignition temperature from 485°C for 750 $m^2/g$ to 370°C for 1500 $m^2/g$. These results agreed with kinetics of the oxidation of carbon as discussed by Kovach.

## Service Life

The ignition temperature of Type 416 (430°C) increased about 80°C after 18-25 months service in the SRP reactors. This increase is attributed to the increased concentration of iodine and chlorine in carbon as shown by mass spectroscopic analysis. These halogens (probably products of the combustion of coal in the vicinity) inhibit the oxidation of carbon, and increase the ignition temperature as shown in Table 2.

## Particle Size

Ignition temperature increases with increasing particle size. However, the effect of particle diameter on ignition temperature was not significant (~25°C) for diameters normally used in confinement applications (1 to 4 mm)[4].

## Effect of Bed Depth

The dependence of ignition temperature on bed depth from $\frac{1}{2}$ to 3 inches was determined with two coconut shell carbons available from the Barnebey-Cheney Co. (Types 416 and 592) and one coconut shell carbon from another company (Type A). Type 592 is a new, commercially available carbon that has been specially treated to increase its ignition temperature.[4] Air velocity was 70 ft/min, the normal face velocity for SRP carbon beds.

The ignition temperature of Type 416 was unaffected as the bed depth increased from $\frac{1}{2}$ to 3 inches as shown in Figure 2. Similar results were also obtained for Type A carbon at 1 and 2-inch depths. However, the ignition temperature of Type 592 carbon decreased from 530 to 460°C as the bed depth increased from 1 to 3 inches. In

TABLE 2

Effect of Service on The Ignition Temperature of Type 416 Carbon

| Service, Months* | Ignition Temperature,** °C |
|---|---|
| 0 | 340 |
| 18 | 400 |
| 18 | 410 |
| 25 | 430 |

* Exposure to flowing air in the exhaust ventilation system of SRP reactors.

** Air velocity, 70 ft/min; 1-inch-thick by 3-inch-diameter bed.

TABLE 3

Ignition Temperature of Full-Sized SRP Carbon Bed

| Carbon | Ignition Temperature, °C | Air Velocity, ft/min |
|---|---|---|
| Type 416 | 340 | 70 |
| Type 592 | 530 | 105 |

the deeper Type 592 beds, ignition usually occurred inside the bed instead of near the face of the bed.

## Effect of Air Velocity

The dependence of the ignition temperature of Type 416 and of Type 592 carbon on air velocity is shown in Figure 3.

The ignition temperature of Type 416 carbon did not vary as the velocity increased from 10 to 120 ft/min. The ignition temperature of Batch A, Type 592 carbon increased from 470 to 550°C as the velocity increased from 10 to 70 ft/min. For Batch B, Type 592 (from full-size bed discussed later) the ignition temperature increased from 430 to 520°C as the velocity increased from 20 to 105 ft/min. This increase is attributed generally to more uniform heat transfer which minimizes local heating.

## Independent Variables

Tests also showed that the ignition temperature of carbon in the small-scale apparatus was unaffected by several other variables:

- o variation of bed diameters from 1 to 3 inches
- o installation of baffles in the bed
- o corrosion products of stainless steel
- o re-ignition of a bed that was not impregnated
- o relative humidity of supply air to the bed
- o reduction of the oxygen content of the air to the bed from the normal 20.9% to 15.9%
- o increasing the heating rate up to 4.8°C/min

## Bed Diameter

Variation of the bed diameter from 1 to 3 inches had no effect as expected, because the ignition temperature was measured under nearly isothermal conditions. The air is preheated to about the same temperature of the carbon bed.

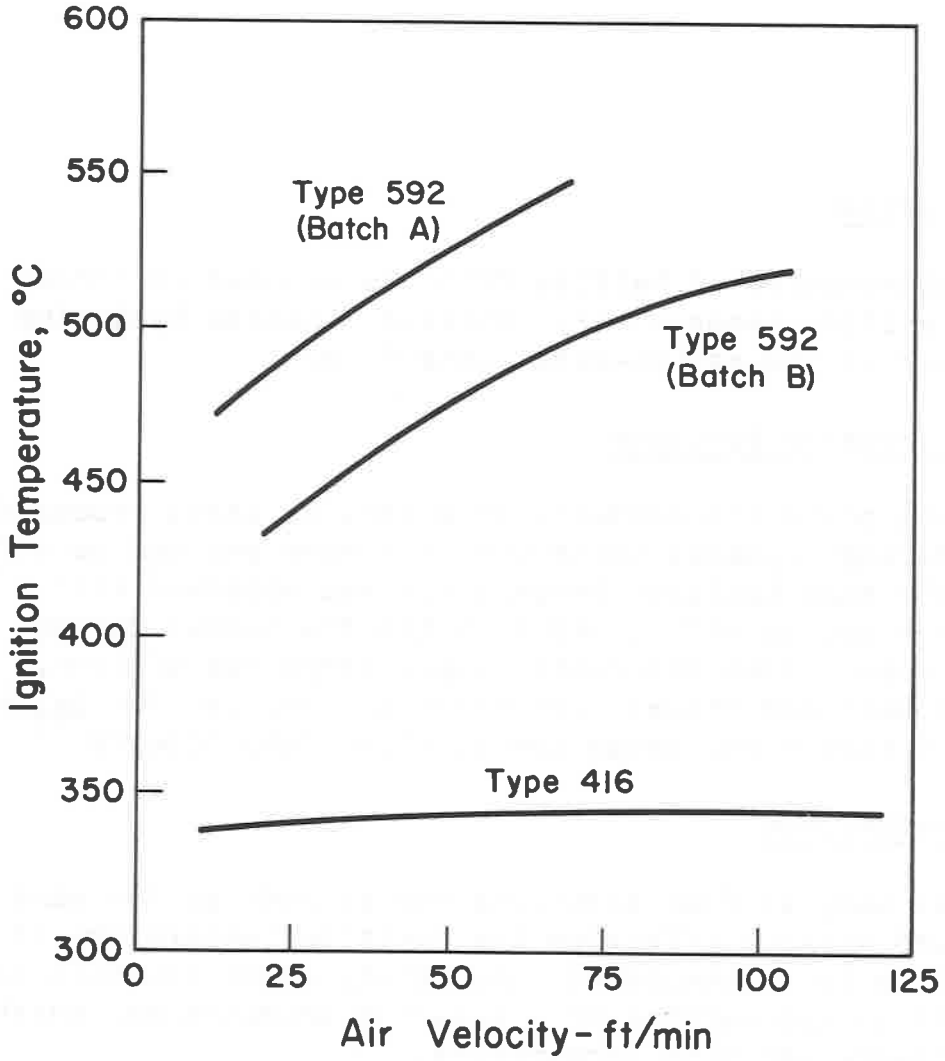


FIG. 3 IGNITION TEMPERATURE OF CARBON AS A FUNCTION OF AIR VELOCITY

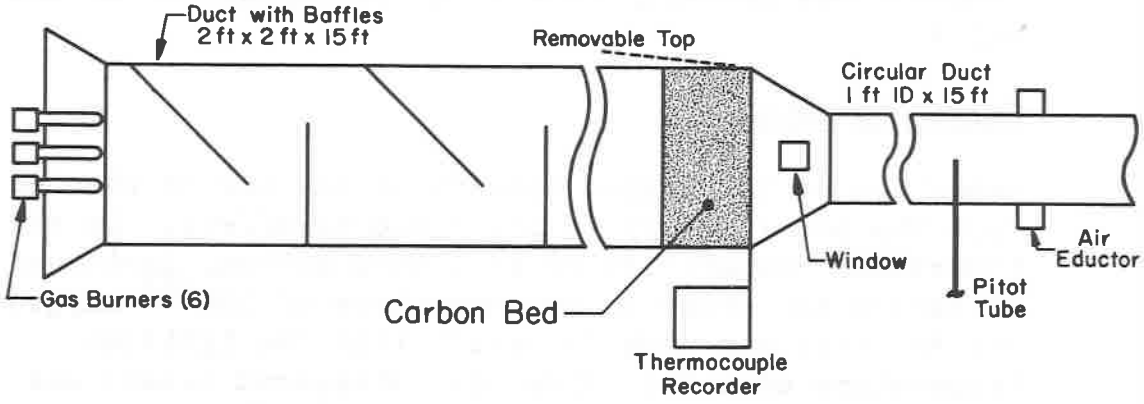


FIG. 4 FULL-SIZED IGNITION TEST EQUIPMENT

## Baffles

Elimination of baffles from the bed had no effect on ignition temperature. Baffles minimize bypassing of air at the carbon-metal interface.

## Corrosion Products

The corrosion products of stainless steel produced during repeated tests with the same bed had no effect. The same ignition temperature was observed with a new bed as with a bed that had discolored during reuse. Some materials (e.g., compounds of iron, cobalt and nickel) are known to catalyze the oxidation of carbon and cause low ignition temperatures[7].

## Reignition

As many as four ignitions can be made on the same bed without affecting its ignition temperature if the fire is extinguished immediately after ignition occurs. Prolonged burning of the carbon produces ash which lowers ignition temperature.[4]

Re-ignition of carbon impregnated with halogens (inhibitors of ignition) produces lower ignition temperatures because of the loss of some of the halogens. Re-ignition of whetlerite (carbon impregnated with salts of copper, silver, and chromium) produces increased ignition temperatures probably because of decomposition of the salts.

## Oxygen Content

Reduction of the oxygen content of the air to the bed from the normal 20.9% to 15.9% had no effect. In the industrial preparation of activated carbon, ignition of carbon can occur in an atmosphere of 10%[6] oxygen. The SRL test was made to verify that the ignition temperature of a full-size bed (discussed later) was not affected by air that contained 16.2% oxygen.

## Heating Rate

Increasing the heating rate of the bed up to 4.8°C/min (maximum obtainable in test apparatus) had no effect. As discussed later, a heating rate of 10°C/min had no effect on the ignition temperature of full-sized carbon beds.

## Humidity of Air

In preliminary measurements, no effect of the humidity of the supply air to the bed was found. Air, saturated with moisture at 43°C, produced a normal ignition temperature.

## Full-Sized SRP Carbon Beds

The ignition temperature of Type 416 and Type 592 carbon in a bed framed with stainless steel[3] was measured at the Lawrence Radiation Laboratory. Unfiltered air and the combustion products from six gas burners entered a horizontal, uninsulated metal duct 2 feet square and 15 feet long as shown in Figure 4. This duct contained four baffles to mix the air to uniform temperature before it entered the carbon bed attached to the end of the duct. Effluent air from the carbon bed passed through a 1-foot-diameter duct, 15 feet long.

The downstream face of the bed was observed through three glass windows in the duct. An air eductor, operated by compressed air, was used to adjust air flow through the bed.

The temperature of the bed was measured with 20 calibrated iron-constantan thermocouples (0.025-inch-diameter, stainless steel sheath) that were inserted where ignition was likely. Temperature at each thermocouple was recorded every 26 seconds.

Air flow was measured with a pitot tube connected to an inclined manometer. Air temperature was

increased by adjusting the burners in ~50°C increments, and the bed temperature was allowed to come to equilibrium after each increase in temperature. At about 50°C below the ignition temperature, the air temperature was increased continously at ~10°C/min.

The oxygen content of air flowing through the apparatus at the ignition temperature decreased from the normal 20.9% to 16.2% because of the combustion products from the burners. As expected, the decrease in oxygen had little effect on the ignition temperature as shown by tests in the small-scale SRL apparatus.

At the ignition temperature, the thermocouples in the center of the bed suddenly indicated a rapid temperature rise. As shown in Table 3, Type 416 carbon ignited at 340°C and Type 592 carbon at 530°C. Both measurements agreed with results from the small-scale laboratory apparatus.

When the 416 carbon ignited, glowing particles of carbon blew out of the center of the bed. The gas burners and air flow were stopped immediately and the top of the upstream duct was removed. The upstream face was sprayed with 160 pounds of carbon dioxide, but the fire was not extinguished. The carbon dioxide solidified on the stainless steel mesh and plugged the perforation. This treatment cooled the upstream face, but the thermocouples in the middle of the bed indicated that the bed was still burning. Because it appeared that carbon dioxide would not extinguish the fire quickly, water was used.

Water reacts with hot carbon to produce a mixture of hydrogen and carbon oxides that might form an explosive atmosphere. Therefore, air flow was restored and the bed was flooded with water from a 1-inch-diameter hose. The water melted the solidified carbon dioxide and steam flowed out of the apparatus.

After 10 minutes of flooding, two areas of the bed continued to burn, so two of the glass windows on the downstream face were opened and water was sprayed

on the downstream face. After 5 minutes, the fire appeared to be extinguished and all thermocouples indicated normal temperature.

The bed was removed from the apparatus and inspected. A noticeable amount of carbon was consumed by the fire. The only apparent damage to the framing was a 4 by 4-inch area of corrosion on the upstream face and a 6 by 6-inch area of discoloration on the downstream face.

The fire in the Type 592 carbon was extinguished easily with a water spray that blanketed the face of the bed. The gas burners were stopped immediately after the carbon ignited and the air flow was maintained at a velocity of 10 ft/min to avoid an explosion of the effluent gases. The water spray, at a rate of 8 gpm, cooled the bed from a maximum of 850°C to ambient temperature in 5 minutes.

There was no significant damage to the bed or to the neoprene gaskets from the brief exposure to high temperature. The upstream face of the bed showed no corrosion and there were only a few square inches of a white deposit on the downstream face. There was no visible loss of carbon due to ignition.

In an endurance test, the bed of Type 592 carbon was not significantly damaged from exposure at 280°C for 35 minutes. The neoprene gaskets maintained a seal against leaks around the bed and the stainless steel frame was not buckled nor warped. A test at SRL of the bed of Type 592 carbon, showed that leakage through the bed was less than 0.01%. A method developed at SRL[8,9] was used.

## CONCLUSIONS

A high temperature carbon with excellent iodine adsorption properties (~99.9% for iodine) is commercially available. The use of this carbon in confinement facilities reduces the risk of ignition

# A Nondestructive Method for Determining The Residual Gas Life of Charcoal Beds

H. F. BOGARDUS,* V. R. DEITZ,* AND A. STAMULIS*

A nondestructive method has been developed for determining the residual gas life of charcoal beds used to remove gases from air streams. It makes use of the fact that a direct relationship exists between the manner in which $CO_2$ penetrates a charcoal bed and the capacity of that bed for strongly adsorbed gases. A pulse of $CO_2$ is introduced upstream of the charcoal bed, and a very sensitive indicator-recorder system is used to sample the downstream air and to trace the shape of the $CO_2$ pulse as the gas emerges from the charcoal bed. The pulse shape is directly relatable to the residual gas life of the bed.

Activated charcoal is used extensively as a means of removing gases from air streams. Each charcoal bed has a certain adsorption capacity, and when this capacity has been reached the bed must be renewed. If the gas being adsorbed is toxic, the charcoal bed often must be renewed before its capacity has been reached, that is, while it still has a certain amount of residual gas life. Currently, the residual gas life of a charcoal bed is determined by introducing a strongly adsorbent test gas into the air stream and then sampling the air as it emerges from the charcoal bed to determine when the test gas has penetrated the charcoal. This method, however, destroys any further usefulness of the charcoal bed.

In the absence of a nondestructive method for determining the residual gas life of charcoal, the bed must be renewed according to a schedule established on the basis of past experience. Such a schedule cannot take into account circumstances that may have changed the air pollution level. Hence the need for a truly nondestructive method.

In order to be truly nondestructive, the method must be so designed that determination may be made at intervals during the time the charcoal bed is in use without destruction of a significant portion of its gas life. In order to be practical, the method must be independent of the moisture content of the charcoal and of the relative humidity of the air stream; it must be applicable to both laboratory and field use; it must not employ toxic materials; it should not employ obnoxious materials; and it should be rapid. In the past, various Freons have been tried as test gases and, under very limited conditions, are being used to indicate the residual gas life of charcoal beds (1,2); but the interaction between the Freons and the charcoal surface is not independent of the moisture content of the charcoal. As a result, while the Freons can be made to work very well under dry conditions in the laboratory or in a charcoal bed assembly plant, their use in the field is limited to newly installed beds and to beds which can be dried in place.

This article describes a new method in which carbon dioxide ($CO_2$) is employed as the test gas for determining the residual gas life of a charcoal bed. It makes use of the fact that a direct relationship exists between the manner in which $CO_2$ penetrates a charcoal bed and the capacity of that bed for strongly adsorbed gases. In order to conduct a determination, a pulse of $CO_2$ is introduced upstream of the charcoal bed. A very sensitive indicator-recorder system samples the downstream air and traces the shape of the $CO_2$ pulse as the gas emerges from the charcoal bed. The height of the $CO_2$ pulse increases and the width decreases as the charcoal surface becomes contaminated with strongly adsorbed materials. The pulse shape is thus relatable to the residual gas life of the charcoal bed. The method is nondestructive; it is independent of the moisture content of the charcoal and the relative humidity of the air stream over a range of relative humidities normally encountered in the field; it is applicable to both laboratory and field use; it employs nontoxic quantities of $CO_2$; and it is rapid, the elapsed time from introduction of the $CO_2$ until completion of the pulse traces being about 20 seconds.

A block diagram of the $CO_2$-pulse method is shown in Figure 1. The $CO_2$ must be introduced rapidly into the air stream and, for a given series

*Protective Chemistry Branch, Chemistry Division.



*Preprint from Report of NRL Progress, September 1966.*

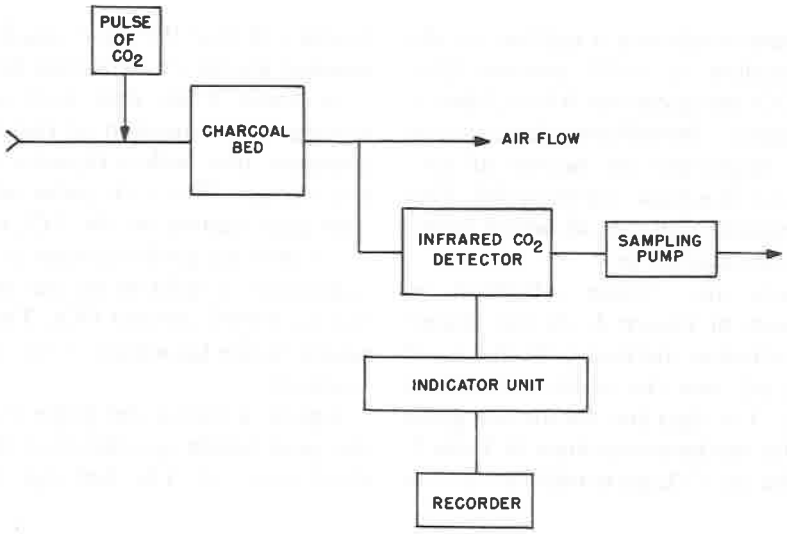


Figure 1 – Block diagram of the $CO_2$-pulse method for nondestructive determination of residual gas life of charcoal beds

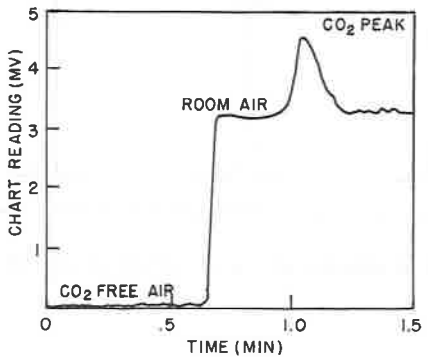


Figure 2 – Typical $CO_2$ pulse as it appears on recorder chart. This trace was obtained with a clean charcoal bed.

of experiments, always at the same rate. Various procedures may be used, such as puncturing a small balloon, activating a quick-release valve in a pressure bottle, or injecting with a hypodermic syringe. The $CO_2$ detector is an infrared meter with a response time of 0.1 second for 90 percent of full-scale deflection. The low impedance output of the $CO_2$ indicator unit is connected to a 10-millivolt recorder by means of a 25-ohm, multiturn potentiometer. A typical $CO_2$ pulse as it appears on the recorder chart is shown in Figure 2.

In order to show that $CO_2$-pulse data can be used to predict residual gas life, a charcoal bed was systematically exposed to various adsorbates, and the $CO_2$ pulse for various degrees of contamination was recorded. The initial studies were carried out by exposing the charcoal to decane and methylacetoacetate. The charcoal used in these studies was a 12-30 mesh, low-density, PCC-ASC impregnated type used in military gas-mask canisters. The charcoal bed was 1.6 centimeters in diameter by 1.9 centimeters deep. The air flow rate through the bed was 8.3 centimeters per second. The concentration of adsorbate in the influent air stream was 6 milligrams per liter, and the relative humidity of the air stream was 20 percent. Gain control on the $CO_2$ indicator unit was set at 700, and the potentiometer between the indicator unit and the recorder was set

at 135. Under these conditions, 1 millivolt on the recorder is equivalent to 0.077 percent $CO_2$. The volume of $CO_2$ per pulse was 0.5 milliliter at atmospheric pressure. Periodically the charcoal was weighed to determine the degree of contamination, and the $CO_2$ pulse was recorded. This process was continued until the adsorbate began to emerge from the charcoal bed.

$CO_2$-pulse traces for decane adsorbed on charcoal are shown in Figure 3. As the degree of surface contamination increased, the height of the pulse increased, and the width at half the height decreased. The data for decane are given in Table 1, that for methylacetoacetate in Table 2. The data show that the $CO_2$ pulse width at half the height will give the most reliable estimate of the residual gas life of a charcoal bed.

In Table 3 are data from another study involving the adsorption of decane by a collective protector unit with a capacity of 100 cubic feet per minute. The $CO_2$ pulse was 100 milliliters. The gain control on the $CO_2$ indicator unit was set at 900, the potentiometer at 810. Under these conditions, 1 millivolt on the recorder is equivalent to 0.0095 percent $CO_2$. These data were obtained in the laboratory in normal (low-humidity) room air.

Figure 4 shows the pulse trace width at half the peak height as a function of bed depth for a clean charcoal. The bed was 1.6 centimeters in

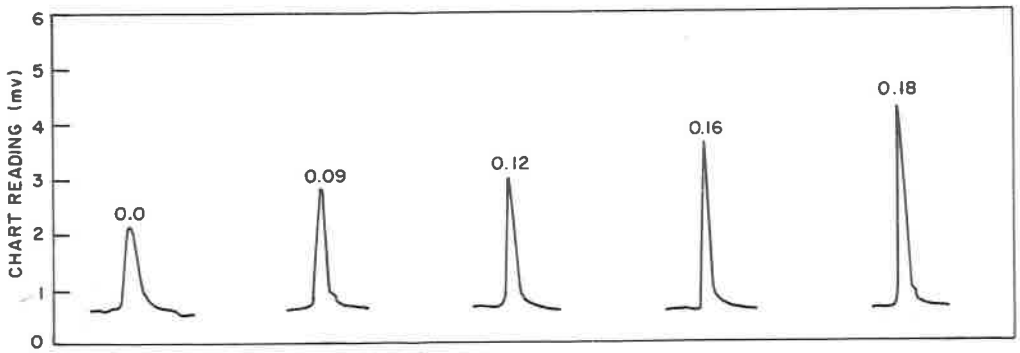


Figure 3 — Variation of $CO_2$ pulse with grams of adsorbed decane per grams of charcoal

TABLE 1
Residual Gas Life of Charcoal Contaminated with Decane

| Gram of Decane per Gram of Charcoal | Residual Gas Life (%) | $CO_2$ Pulse | | Residual Gas Life (Calculated from $CO_2$ Pulse) | |
|---|---|---|---|---|---|
| | | Height (mm) | Width (mm) at Half Height | Height* | Width† |
| 0 | 100 | 15 | 3.2 | 100 | 100 |
| 0.09 | 50 | 23 | 2.2 | 62 | 47 |
| 0.12 | 33 | 25 | 1.8 | 52 | 26 |
| 0.16 | 11 | 32 | 1.6 | 19 | 16 |
| 0.18 | 0 | 36 | 1.3 | 0 | 0 |

*Percent Residual gas life = $(L - U/L - C) \times 100$
†Percent Residual gas life = $(U - L/C - L) \times 100$
$C$ = Pulse height, or width, clean charcoal
$L$ = Pulse height, or width, charcoal contaminated to penetration point
$U$ = Pulse height, or width, contaminated charcoal

TABLE 2
Residual Gas Life of Charcoal Contaminated with Methylacetoacetate (MAA)

| Gram of MAA per Gram of Charcoal | Residual Gas Life (%) | $CO_2$ Pulse | | Residual Gas Life (Calculated from $CO_2$ Pulse) | |
|---|---|---|---|---|---|
| | | Height (mm) | Width (mm) at Half Height | Height* | Width† |
| 0 | 100 | 17 | 3.0 | 100 | 100 |
| 0.04 | 78 | 21 | 2.6 | 78 | 75 |
| 0.06 | 67 | 22 | 2.4 | 72 | 62 |
| 0.08 | 55 | 24 | 2.2 | 61 | 50 |
| 0.10 | 44 | 26 | 2.0 | 50 | 37 |
| 0.15 | 17 | 29 | 1.8 | 33 | 25 |
| 0.16 | 11 | 31 | 1.6 | 22 | 12 |
| 0.18 | 0 | 35 | 1.4 | 0 | 0 |

*Percent Residual gas life = $(L - U/L - C) \times 100$
†Percent Residual gas life = $(U - L/C - L) \times 100$
$C$ = Pulse height, or width, clean charcoal
$L$ = Pulse height, or width, charcoal contaminated to penetration point
$U$ = Pulse height, or width, contaminated charcoal

TABLE 3
Residual Gas Life of a 100-cfm Collective Protector Unit Exposed to Decane

| Total Decane Absorbed (gm) | Residual Gas Life (%) | $CO_2$ Pulse | | Residual Gas Life (Calculated from $CO_2$ Pulse) | |
|---|---|---|---|---|---|
| | | Height (mm) | Width (mm) at Half Height | Height* | Width† |
| 0 | 100 | 9.2 | 14.0 | 100 | 100 |
| 150 | 90 | 8.5 | 13.2 | >100 | 90 |
| 300 | 75 | 12.0 | 12.2 | 60 | 75 |
| 600 | 50 | 12.0 | 11.2 | 60 | 50 |
| 900 | 25 | 15.0 | 9.2 | 15 | 25 |
| 1200 | 0 | 16.0 | 8.4 | 0 | 0 |

*Percent Residual gas life = $(L - U/L - C) \times 100$
†Percent Residual gas life = $(U - L/C - L) \times 100$
$C$ = Pulse height, or width, clean charcoal
$L$ = Pulse height, or width, charcoal contaminated to penetration point
$U$ = Pulse height, or width, contaminated charcoal

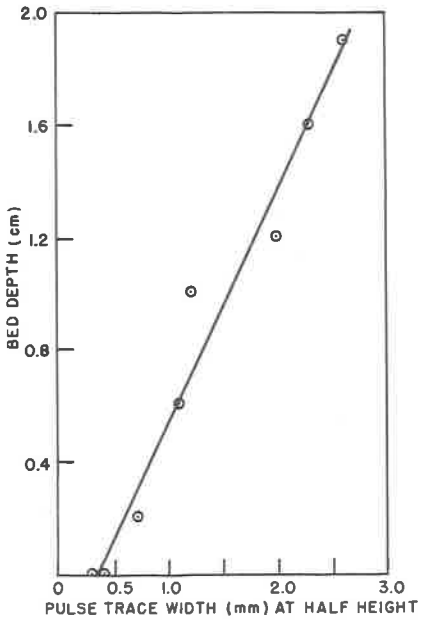


Figure 4 — Pulse trace width (at half height) *vs* bed depth for a clean charcoal surface

diameter and contained the same type of charcoal mentioned above. The moisture content of the charcoal was as received, and the relative humidity of the air stream was approximately 20 percent. The flow rate of air through the bed was 8.3 centimeters per second, the volume of $CO_2$ used per pulse was 0.5 milliliter. The straight line relationship shown in the figure is a convenient feature of the $CO_2$-pulse method as a means of determining the residual gas life of a charcoal bed.

Our data show that the shape and size of the $CO_2$-pulse trace is affected by a number of factors: the quantity of $CO_2$ used per pulse; the rate at which the $CO_2$ is introduced into the air stream; the shape of the charcoal bed; the dimensions of the ductwork from the point at which the $CO_2$ is introduced to the point where a sample is drawn off for analysis; the ratio of the sampling rate to the total flow rate; the gain setting of the $CO_2$ indicator unit and of the potentiometer; the chart speed of the recorder; and *the degree of contamination of the charcoal surface by strongly adsorbed materials.*

The $CO_2$-pulse method has been used successfully with larger charcoal beds and with air flows of 1500 and 4100 cubic feet per minute. Precautions must be used, however, to obtain reliable data. Our studies show that the new method will give a reliable estimate of the degree of contamination of the charcoal surface, but only if all variables that would affect the $CO_2$-pulse trace are kept constant.

## REFERENCES

1. C. B. Yoder and H. E. Gaffney, "Improved Expectancy Testing and Surveillance Testing of Charcoal End Items," Final Report—U.S. Army Chemical Center, Contract No. DA 18-108-CML-6519, with U.S. Testing Company, Inc., Hoboken, N.J., February 1962
2. A. H. Peters and D. Muhlbaier, "Non-destructive Test of Carbon Beds for Reactor Containment Applications; Progress Report: June 1962—December 1963," AEC Report DP-870, E. I. duPont de Nemours and Co., Savannah River Laboratory, Aiken, S.C., February 1964

## DISCUSSION

BOYD: One, Mr. Hillary, please redefine your index of performance; and, second, on Table XIII, the chart for the performance of the TEDA charcoal would indicate that it gave better performance with larger loadings of methyl iodide than with smaller loadings of methyl iodide. Could you explain?

HILLARY: The index of performance is defined as $\log_{10}$ of the contamination factor, divided by the stay-time.

I think one could just make a general comment on the second part of your question; the amine-impregnated one is able to accept a higher loading than the potassium iodide impregnated one. This may well be due to the different mechanism which apply. We haven't done very much work on the mechanism, as Dr. Parker was indicating; therefore, it is that the mechanism for removal of methyl iodide by charcoal which is impregnated by iodine or an iodine compound is probably isotopic exchange.

The little work we have done on potassium iodide-impregnated charcoals suggests that this may be true at high mass loadings, somewhat in the region of one to five milligrams per gram of charcoal, but that at the low mass loadings, which we have used, 100 micrograms point of charcoal that may be a catalytic mechanism is more practical.

In case of amine-impregnation, this is a direct chemical reaction held by the additional physical adsorption which you would have applying for methyl iodide on the charcoal; because of the large surface area, you have got a relatively long time for the chemical reaction to take place.

RIVERS: This is directed to Mr. Hillary. I think you suggested that on the large-scale beds the degradation of performance with time was due to mechanical failures primarily. Do you have an explanation for the degradation observed in laboratory scale tests?

HILLARY: I don't know that we have anything more than speculation here because we haven't a very clear idea of the mechanisms involved. The aging with time which we have found, certainly, in the case of amine-impregnation, it is quite possible this is due to loss of the volatile amine, although the TEDA Triethylenediamine has a boiling point of something like 170° Centigrade, I think, obviously, it would be much reduced when it is at charcoal or distributed over a large surface area.

In the case of potassium iodide-impregnated charcoal, it may be simple oxidation of the active sites, which would otherwise be effective for methyl iodide.

ETTINGER: Since methyl iodide is one of the many nonelemental forms of iodine you run into, have either of you looked into your impregnated charcoals as to how well they do against nonelemental and nonmetallic forms of iodine which are present?

PARKER: Let me venture an answer first. We are not, of course, concerned about forms of iodine which we cannot find. We are mainly interested in accident control and, therefore, as long as no new varieties are cropping up, why, they are not pertinent.

Hydrogen iodide has been tested at Oak Ridge. We do guarantee that there are no wisps of iodine getting through our detection system, and we feel certainly that methyl iodide represents the most illusive form that nature can devise. We wish it had not come along, in fact, but there it is and the answer to it didn't turn out to be too difficult.

HILLARY: I think I would endorse what Dr. Parker has said and add that we have done experiments in which we have released iodine in all its forms, from irradiated fuel which include methyl iodide; that at different temperatures, mainly high temperatures in terms of melting off the fuel, and iodine which is released and which is usually at something like 2000°C, a major part of the iodine content of the fuel, we passed this through charcoals. We have found, and I think this was published at a conference last year by Mr. R. D. Collins, that certainly on long elution with an untreated charcoal you can get fairly high penetrations (by methyl iodide); however, when one replaces the untreated charcoal by an impregnated charcoal, the performance then becomes satisfactory.

The charcoal, of course, is supported by a high efficiency filter, so this is a small scale model of the treatment plant, if you like, so this, we feel, we have done some tests under conditions where we think realistic iodine is being generated and find that the performance of the treatment plant as a whole is satisfactory.

GUSSMAN: Mr. Bogardus, can you tell the difference by the pulse between the bed which is worn out or saturated and a bed which is leaking?

BOGARDUS: The only work which we have done in this respect was in the laboratory where we ran tests in which we removed the charcoal from the bed; or, in some cases, we replaced the charcoal with glass beads.

There is a sharp rise in peak height. I hesitate to make a firm statement, but a peak height was approximately twice what you saw here.

STEINBERG: Mr. Bogardus, have you, or are you going to try to relate this to toxic gas life?

BOGARDUS: Yes, we most certainly are going to. We haven't yet, but we are going to.

# REMOVAL OF IODINE AND METHYL IODIDE BY AEROSOL FORMATION WITH HYDRAZINES

by

F. J. Viles, Jr., and L. Silverman*

Harvard Air Cleaning Laboratory
School of Public Health, Harvard University
665 Huntington Avenue
Boston, Massachusetts

---

## ABSTRACT

As an approach to handling radioiodine releases from nuclear installations, studies were made of the gas phase reactions of iodine with hydrazine and with its unsymmetrical dimethyl derivative. These reactions lead to the formation of aerosols which could be effectively removed by filtration or by settling, diffusion and solubility processes. Hydrazine air concentrations of 765 to 890 ppm proved adequate for efficient aerosol formation and removal of both iodine and methyl iodide. For dynamic conditions involving aerosol filtration, reaction times of several minutes were required. Reaction and natural aerosol removal processes under static conditions required several hours. Hydrazine concentrations of approximately 37 ppm were effective in removing methyl iodide only when alkali was present to remove the interference created by normal air concentrations of carbon dioxide (350 ppm est.). Although tests were not made to determine carbon dioxide interference with the methyl iodide--unsymmetrical dimethyl hydrazine reaction at low concentrations, methyl iodide removal was complete with 90 to 180 ppm of this reactant in the absence of carbon dioxide. Efficient aerosol formation and removal of iodine by reaction with low hydrazine concentrations (20 ppm) occurred in the presence of normal levels of carbon dioxide.

* Deceased

## INTRODUCTION

Many compounds and physical states of radioiodine can be released from nuclear reactors and associated operations.[1] These include (a) elemental iodine, either free or adsorbed on inert (carrier) particles, (b) gaseous hydrogen iodide, (c) iodide, iodate and periodate particles, and (d) methyl iodide and higher alkyl iodide vapors.

A method proposed for the control of the gaseous forms of radioiodine in contained atmospheres is based on their conversion to aerosols. Removal is effected by high efficiency filtration normally available or, in the case of loss-of-coolant accidents involving pressurized or boiling water reactors, by solubility in water.

Initially, effort was centered on aerosolization of elemental iodine, with the concept that if reduction of iodine to iodide could be effected at the early stages of iodine release, methyl iodide formation and iodine plate-out might be prevented or at least minimized. Hydrazine was selected for this task since it is one of the strongest reducing agents known (in neutral or alkaline solution) and possesses adequate vapor pressure for gas phase reactions at ambient temperatures. In addition, its alkalinity qualified it as a reactant to form a stable iodide aerosol salt with hydrogen iodide, one of the forms of iodine released and also the end product of iodine reductions.

In the course of the initial studies, the interaction and aerosol formation of methyl iodide with hydrazine was noted. More recent studies also demonstrated the reduction of iodates and periodates to iodides by reactions with hydrazine.

Thus it appeared that hydrazine and potentially its derivatives (i.e. alkyl and dialkyl hydrazines) were capable of forming iodide aerosols by reacting with all forms of radioiodine thus far identified with fission products released (or formed after release) from nuclear reactor accidents. The exception to this statement would be iodide particles (metal iodides) already formed prior to the application of hydrazine.

This report presents data and conclusions obtained from studies on the aerosolization and removal of iodine and methyl iodide by reaction with hydrazine and unsymmetrical dimethyl hydrazine. This work is still in progress.

## REQUIREMENTS FOR REMOVAL BY AEROSOLIZATION

The current MPC (maximum permissible concentration) for soluble iodine-131 in air in the general environment in the vicinity of a nuclear installation (assuming an exposure time of 168 hours/week) is $10^{-10}$ μCi/cc.[2]

This corresponds to a concentration of $7.5 \times 10^{-14}$ parts of $^{131}I$ per million parts of air, or a vapor pressure of $5.7 \times 10^{-17}$ mm of Hg. This extremely low permissible concentration, although not directly applicable to problems of accidental release, is not only indicative of the need for high filtration efficiency of iodide aerosols but also the necessity of forming stable aerosols of negligible vapor pressures.

Production of water soluble, or preferably hygroscopic iodide aerosols, would provide an additional removal factor in the case of reactor loss-of-water coolant accidents. In contained reactors, these aerosols would be removed efficiently by absorption during the cooling (water spray) and steam condensation periods following the loss of coolant accident. The large amounts of water present (thousands of gallons) would produce highly diluted solutions of these substances, thus effecting further reduction in vapor pressure by many orders of magnitude in accordance with the relationships of Raoult's Law (i.e., V. P. is proportional to the mole fraction of solute in solution).

Ideally, for all conditions including gas as well as water cooled reactors, efficient removal of iodine and its compounds by aerosolization requires the formation of aerosols of very low vapor pressure and high water solubility.

Formation of iodide aerosols of high stability and negligible volatility involves first, reduction of iodine and its compounds in elevated states of oxidation (iodates and periodates, etc.) to the iodide state, using a reducing agent, and secondly, formation of a non-volatile form of the iodide.

Aerosolization of iodine contaminants in a contained atmosphere may be accomplished by one of three methods, namely: (a) atomization of absorbing or reactive liquid aerosols with which the iodine contaminants react to become part of the original aerosol, (b) dispersion of reactive solid aerosols which effect removal in a manner sililar to (a), and (c) addition of one or more gaseous reactants to the gas to react with the iodine contaminants to produce a stable iodide aerosol. The latter method was investigated in this research.

## REACTION OF IODINE AND ITS COMPOUNDS WITH HYDRAZINE

Hydrazine will reduce elemental iodine to iodide according to the following equation:[3]

$$H_2N\text{-}NH_2 + 2I_2 = N_2 + 4HI$$

These chemicals react violently when anhydrous or highly concentrated hydrazine is used.

Since hydrazine is a base, it will react with hydrogen iodide to form solid mono and di-iodides (hydrazinium iodides).

$$N_2H_4 + HI = N_2H_5I$$

$$N_2H_5I + HI = N_2H_6I_2$$

The hydrazinium iodides are salts of a weak base and will release hydrazine when present with stronger bases such as the alkali hydroxides.

$$N_2H_6I_2 + 2NaOH = N_2H_4 + 2H_2O + 2NaI$$

Iodine in its highest states of oxidation as iodates and periodates react with hydrazine to form iodides.

$$2IO_3^- + 3\ N_2H_4 = 2\ I^- + 3\ N_2 + 6\ H_2O$$
$$IO_4^- + 2\ N_2H_4 = I^- + 2\ N_2 + 4\ H_2O$$

Methyl iodide and hydrazine react to form mono and dimethyl (asymmetrical) hydrazines[3].

$$CH_3I + N_2H_4 = CH_3N_2H_3 + HI$$
$$CH_3I + CH_3N_2H_3 = (CH_3)_2N\text{-}NH^2 + HI$$

Since methyl hydrazine contains a more basic nitrogen than free hydrazine, methylation tends to continue to the dimethyl compound.[3]

Unsymmetrical dimethyl hydrazine reacts mole for mole[4] with methyl iodide to give the tri-alkyl hydrazinium salt.

$$(CH_3)_2N\text{-}NH_2 + CH_3I = \left[H_2N \cdot N\ (CH_3)_3\right] I$$

As with hydrazine, the methyl hydrazines will react with hydrogen iodide to form methyl hydrazinium iodides.

$$CH_3N_2H_3 + HI = CH_3N_2H_4I$$

$$(CH_3)_2\ NNH_2 + HI = (CH_3)_2\ NNH_3I$$

Initial studies between gaseous iodine and hydrazine demonstrated rapid and apparently complete aerosolization of the element. Similar reactions between methyl iodide and hydrazine were not so apparent although a high degree of aerosolization occurred. Since this is an organic reaction involving the methylation of the hydrazine molecule, its quantitation was questioned, particularly at low concentrations in air.

## HIGH CONCENTRATION STUDIES

The first studies of the reactions of hydrazines with iodine and its compounds involved high concentrations of each reactant. This permitted adoption of existing analytical techniques for non-radioactive iodine compounds and favored interaction of the compounds if they were to occur at all.

### Methyl Iodide-Hydrazine, Dynamic Conditions

Investigation of the methyl iodide-hydrazine reactions first involved gas phase studies under dynamic conditions in which air containing methyl iodide at a concentration of 13,900 ppm was passed over solutions of 64% hydrazine in water (hydrazine hydrate - $N_2H_4 \cdot H_2O$) (Fig. 1). The concentration of methyl iodide was prepared by saturating 60 ml/min of air at 0°C (concentration equal to $1.85 \times 10^5$ ppm - see Fig. 2) followed by its dilution with 740 ml/min of clean air. Following filtration, the air stream was analyzed for methyl iodide by catalytic thermal decomposition at 850°C to hydrogen iodide and iodine, absorption of the hydrogen iodide and iodine in sodium carbonate-arsenite solution and titration for iodide with silver nitrate using the Volhard procedure.[5] The data obtained are presented in Table 1.

The first four tests did not involve complete flushing of the system at the conclusion of the 5 minute runs which resulted in an incomplete accounting of the unreacted methyl iodide. Maximum corrections for this error are noted as minimum efficiencies in parenthesis. Tests 5 - 7 involved a 25 minute period of flushing of the system with the clean dilution air at a flow of 740 ml/min.

Possible errors in the analyses due to interference of hydrazine vapor would have caused these determinations to produce low removal efficiency values. The residual hydrazine in the sampled air would have resulted in formation of nitrogen oxides during catalytic combustion of methyl iodide with the possible removal of silver ions by their reduction to elemental silver during titration. This removal would be credited to silver iodide to produce increased downstream iodide values. In later work where hydrazine might interfere with analyses, its efficient removal was accomplished by absorption on beds of sodium acid phosphate ($NaH_2PO_4$).

Reduced methyl iodide removal efficiencies were also caused by hydrazine vapor pressures lower than anticipated due to hydrate formation which resulted in hydrazine-air concentrations lower than that of methyl iodide. Saturated air concentrations of hydrazine over different hydrazine-water mixtures were determined by analysis using the p-dimethylaminobenzaldehyde colorimetric procedure.[6] For contrast, theoretical saturated air concentrations calculated from Raoult's Law and actual concentrations of hydrazine are presented in Figure 3.

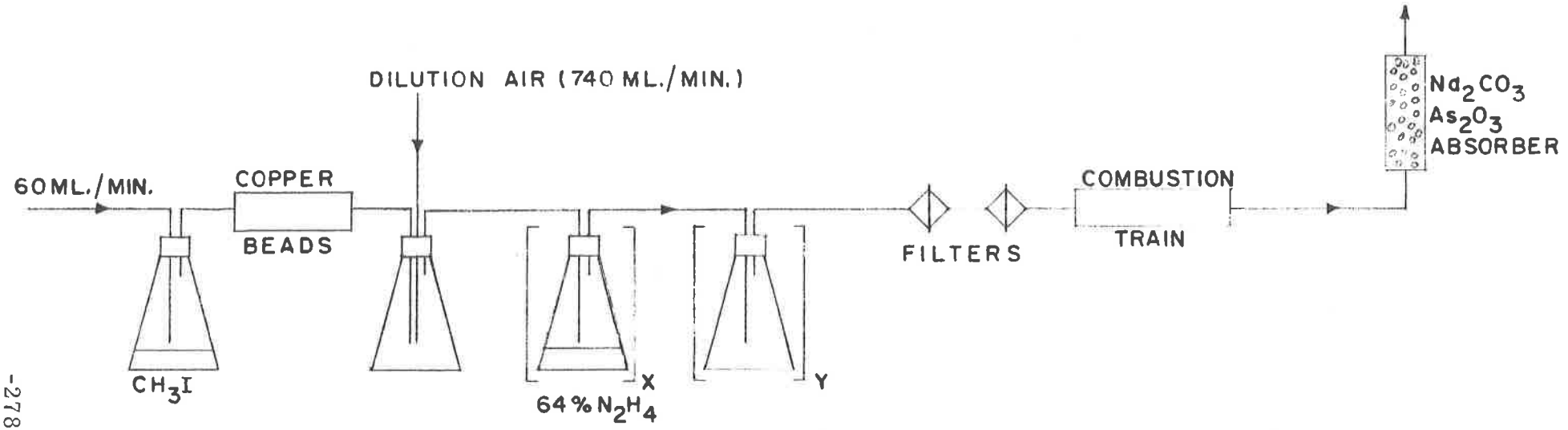




FIGURE 1. SCHEMATIC DIAGRAM OF SYSTEM FOR AEROSOLIZATION AND REMOVAL OF METHYL IODIDE VAPOR BY 64% HYDRAZINE.

TABLE 1

REMOVAL OF METHYL IODIDE BY AEROSOLIZATION WITH HIGH CONCENTRATIONS OF HYDRAZINE, DYNAMIC CONDITIONS

| Test No. | Number of Flasks $N_2H_4$ | Empty | $H_2O$ | Removal Efficiency% | Approximate Reaction Time (Min.) |
|---|---|---|---|---|---|
| 1 | 1 | 0 | 1 | 79.5(59.3)* | 2.5 |
| 2 | 1 | 0 | 1 | 79.2(58.5)* | 2.5 |
| 3 | 1 | 0 | 2 | 92.2(68.6)* | 3.75 |
| 4 | 1 | 0 | 2 | 92.6(70.5)* | 3.75 |
| 5 | 3 | 3 | 0 | 81.6 | 7.5 |
| 6 | 3 | 0 | 3 | 84.3** | 7.5 |
| 7 | 3 | 0 | 4 | 95.0*** | 8.75 |

* Low value = minimum calculated efficiency due to incomplete flushing of system.

** Membrane filter used instead of glass.

*** Feeds to $H_2O$ flasks submerged below $H_2O$ surface and membrane filter used instead of glass.

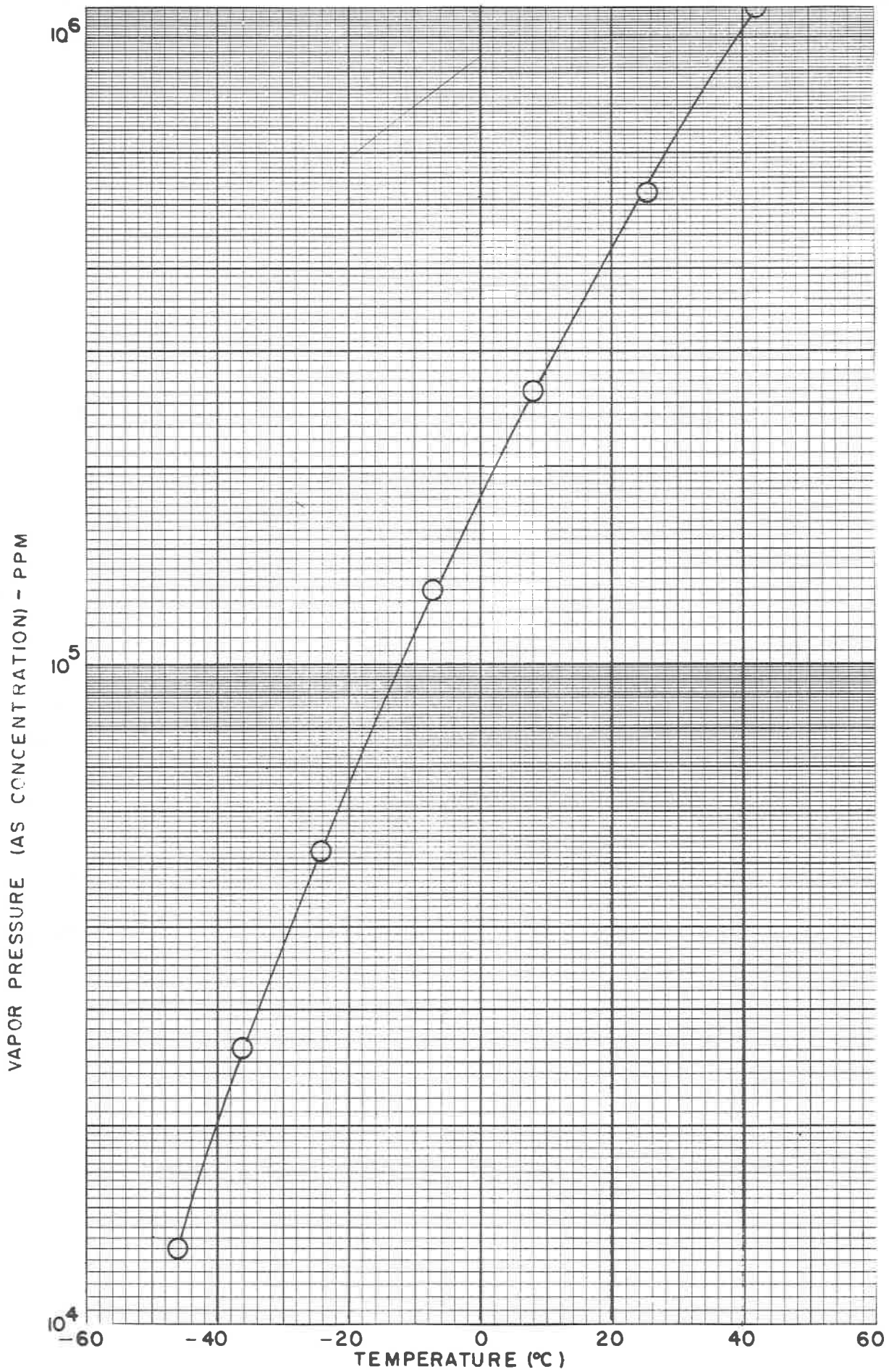


FIGURE 2. VAPOR PRESSURE OF METHYL IODIDE.

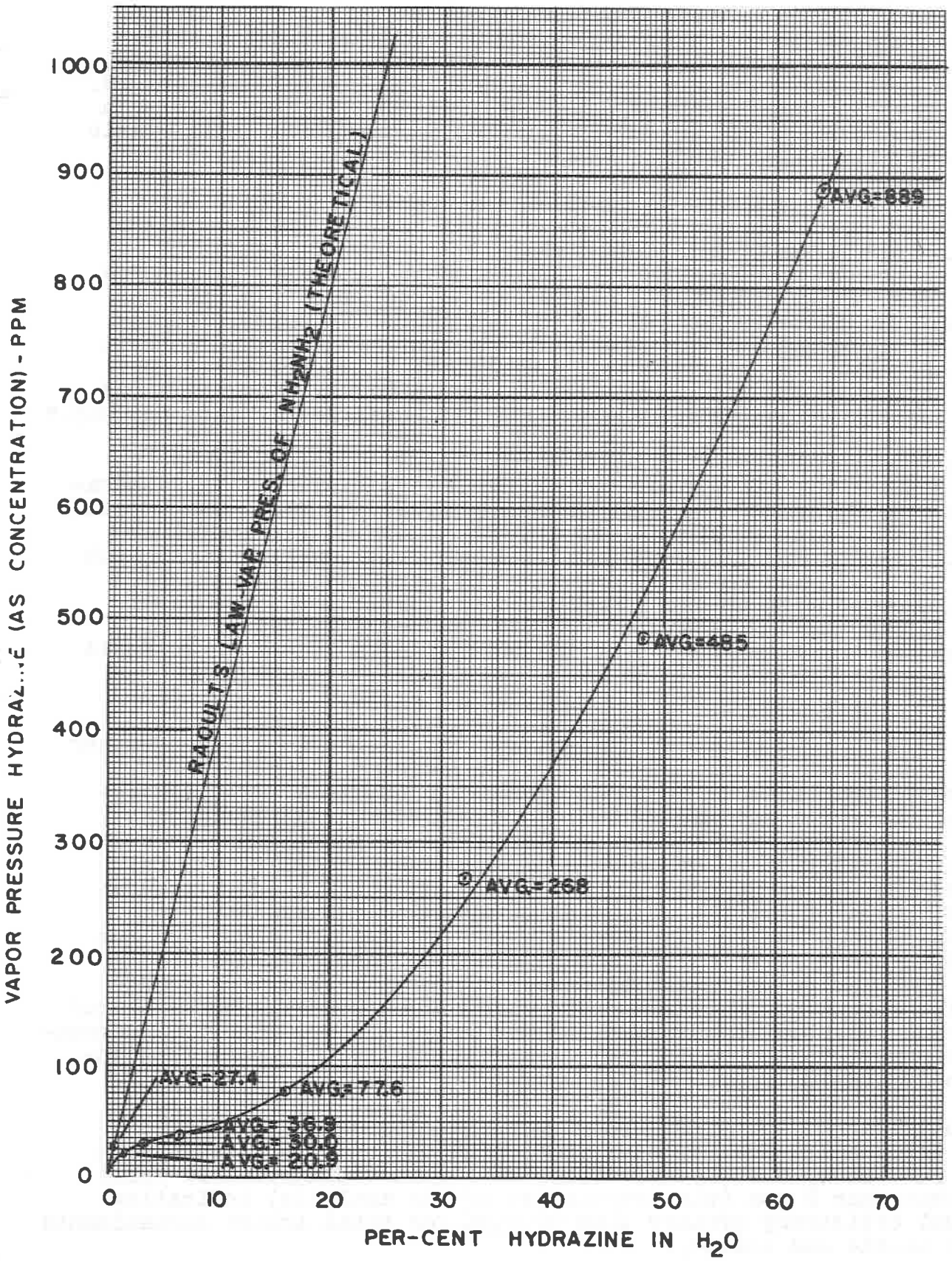


FIGURE 3 VAPOR PRESSURE HYDRAZINE – $H_2O$ MIXTURES AT ROOM TEMP.

Although high removal efficiencies were not obtained in these studies, significant gas phase reactions between methyl iodide and hydrazine with the formation of an iodide aerosol were demonstrated. Since these gas phase reactions require reaction times greater than desired for dynamic conditions, studies were continued under static conditions where long reaction times would be possible.

Methyl Iodide and Iodine-Hydrazine, Static Conditions

Air in a 500 ml flask was saturated with methyl iodide at 25.5°C (concentration equal to $5.27 \times 10^5$ ppm - see Fig. 2). A few milliliters of 64% hydrazine-water solution were injected into the flask and the contents left to react overnight (18 hours). Rapid formation of an aerosol was observed. The following day no aerosol was noted. The gas phase was analyzed (without filtration) for methyl iodide by the gas chromatograph. No methyl iodide was found in the gas phase indicating a removal efficiency greater than 99.998%.*

In a second static test, 5.0 grams of iodine were added to a clean 20.3 liter Pyrex glass bottle. For saturation at room temperature (420 ppm), only 0.044 gms. of iodine were required. The excess was allowed to evaporate or react with the walls of the container until the iodine had all evaporated and the flask was saturated with iodine. A 22.7 gram solution of methyl iodide was added and the flask stoppered with an aluminum covered rubber stopper. When the methyl iodide had completely evaporated, the excess pressure was released and 100 ml of 64% hydrazine were added to the flask. Rapid formation of an aerosol, which increased in density with time, was noted.

The 22.7 grams of methyl iodide on evaporating would add another 3.9 liters of gas to the 20.3 liter flask corresponding to a total gaseous content of 24.2 liters at standard conditions. The concentrations of iodine and methyl iodide in the flask then became 352 and $1.62 \times 10^5$ ppm, respectively. Assuming uniform mixing, these were the concentrations of these substances when the pressure was released and the flask contained 20.3 liters (actually 20.2 liters after addition of the 100 ml hydrazine solution) at standard conditions. The hydrazine vapor addition to the gas phase was 890 ppm (0.089%) (Figure 3) which was essentially unchanged throughout the static test due to the unlimited amount present in the 100 ml 64% hydrazine solution. Mole per mole reactions between the contaminants would have resulted in a removal of 5.2 grams of hydrazine or a concentration change in the 100 ml solution from 64% to 58.8% (air concentration 890 to 765 ppm).

Following 48 hours reaction time, the gaseous contents of the bottle were analyzed without filtration by the catalytic combustion method previously described.[5] Total iodide contaminants were found to be less than 2 ppm (the sensitivity of the analysis) indicating a removal efficiency greater than 99.999% for total iodide contaminants (methyl iodide and iodine).

* At the time of these tests, chromatographic analysis was not fully developed and provided a 10 ppm $CH_3I$ limit of sensitivity.

These tests demonstrated that relatively high concentrations of hydrazine (0.089 to 0.0765%) are essentially 100% efficient in the removal of iodine and methyl iodide by aerosolization after sufficient reaction time (18 - 48 hrs.). It is believed that the time for essentially complete aerosol formation (from interaction of the methyl iodide and iodine with hydrazine) is only a matter of an hour or two. The longer times are required for the removal of the aerosols by settling and diffusion.

## LOW CONCENTRATION STUDIES

Production of sustained high air concentrations of hydrazine (890 ppm - 64% hydrazine in water) in loss of coolant accidents involving pressurized or boiling water reactors would not be practical because of the large amounts of water present (~10,000 gallons) and the high solubility of hydrazine in water. Hydrazine in air concentrations of 10 to 30 ppm (~0.5 to 4.0% hydrazine in water) could be obtained with realistic amounts of hydrazine. These concentrations are in the same range as the total airborne iodine contaminants anticipated from accidental fission product release in a conventional containment.

To determine aerosolization removal efficiencies at these low concentrations of reactants, an ultra sensitive method of iodide analysis, based on the catalytic reduction of ceric sulfate by iodide in the presence of arsenite ions[7] was utilized. Iodine samples for this analysis were collected in clean copper bead beds. Analysis for methyl iodide first involved its catalytic thermal decomposition as described previously[5] followed by the ceric sulfate method for iodide analysis. A sensitivity of 0.01 microgram of iodide by this method permitted determinations as low as 0.007 ppm of methyl iodide and 0.0035 ppm of iodine ($I_2$) in a 300 ml sample of air.

Use of this method required iodide-free chemicals and glassware. In addition, the air used for the dynamic studies and for flushing the 300 ml flask samples through the combustion unit ($CH_3I$ samples) had to be free of this element. The building supplied compressed air, analyzed and found to contain >0.054 µg total I/liter, was cleaned to negligible levels of iodides by its passage through all glass and membrane filters in series followed by a three quarter inch diameter, 3 foot long copper tube packed with Barneby-Cheney MI-1 activated charcoal.

Low concentrations of methyl iodide were later analyzed by the gas chromatograph with an electron capture detector (Wilkens Aerograph Model 600-C) which had been successfully adapted to suitable analytical sensitivity and accuracy for these studies.

### Methyl Iodide-Hydrazine, Dynamic Conditions

A single dynamic study of the removal of methy iodide by aerosol formation with hydrazine was made at low concentrations of each reactant (Fig. 4). A concentration of 15 ppm of methyl iodide was

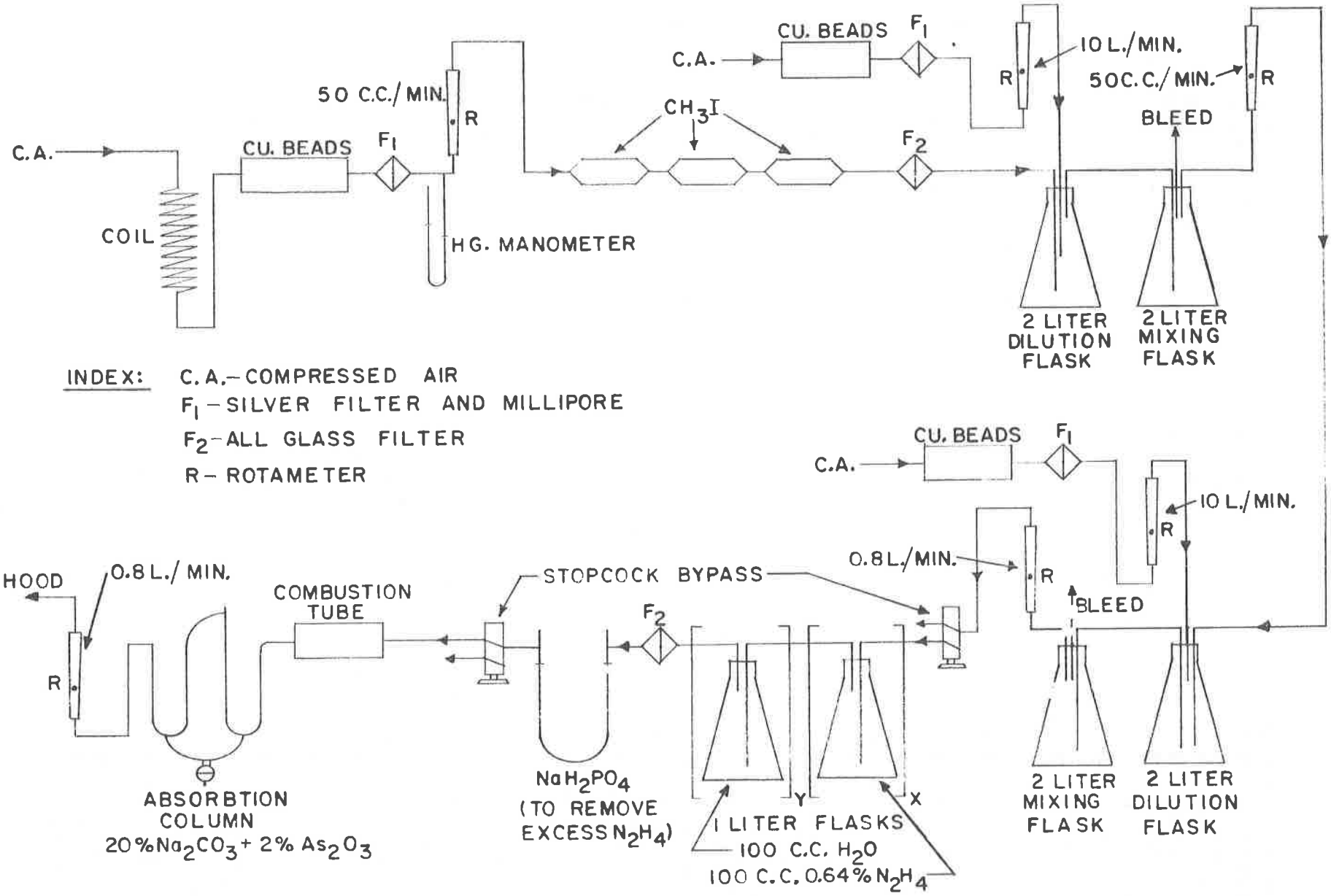


FIGURE 4. SCHEMATIC DIAGRAM OF SYSTEM FOR AEROSOLIZATION AND REMOVAL OF METHYL IODIDE VAPOR BY HYDRAZINE (LOW CONCENTRATION).

synthesized by measured dilutions of known amounts of air originally saturated with methyl iodide at a known temperature. A metered amount of the first dilution was again diluted with metered air to produce the desired concentration. An 800 ml/min sample of this air was passed through single 1 liter flasks containing 100 ml of 2% hydrazine (air concentration equal to 25 - 30 ppm hydrazine, Fig. 3) and 100 ml $H_2O$. Following filtration and removal of hydrazine vapor (with $NaH_2PO_4$), the methyl iodide in the airstream was combusted and collected as iodides as described previously. Analysis was made by the ceric sulfate iodide method.[7] The time required for the gas phase interaction of methyl iodide with hydrazine was approximately 2.5 minutes.

Under the conditions of this test, a removal efficiency of only 2.7% was obtained. The long time required for low concentrations of reactants to form removable aerosols heavily favored future studies under static conditions.

Methyl Iodide-Hydrazine, Static Conditions

Two tests were made involving the aerosolization and removal of methyl iodide by reaction with hydrazine at low concentrations under static conditions. Methyl iodide concentrations were obtained by flushing two 20.3 liter bottles for 20 minutes at a flow of 10 liters per minute with air containing known concentrations of methyl iodide prepared with the apparatus shown in Figure 4.

In Test #1, 10 ml of $H_2O$ were injected into the static reaction flask. Air samples were taken from the flask using evacuated sampling flasks ($\sim$ 300 ml) to determine the initial methyl iodide concentration. (The air sampled was replaced with clean air.)

Following a period of 61 minutes, 1.1 ml of 6.4% hydrazine-water solution were added to provide approximately 11 ml of 0.64% hydrazine solution in the flask (air concentration equal to 15 - 20 ppm hydrazine, Fig. 3). Methyl iodide analyses were then performed over a total period of 48 hours. Methyl iodide was analyzed by its decomposition to iodides using the combustion technique previously described, followed by iodide analysis using the ceric sulfate procedure. Results of these analyses are presented in Table 2.

This test demonstrated that low concentrations of hydrazine (15 - 20 ppm) do not react with low concentrations of methyl iodide in water-saturated normal air. This conclusion is supported by the dynamic test involving low concentrations of these reactants presented previously.

Hydrazine reactions, particularly as a reducing agent (although this is not involved in the methyl iodide reactions), occur mostly in neutral or alkaline media. It was suspected that the 350 - 400 ppm of carbon dioxide normally present in air created an acid environment and prevented the hydrazine-methyl iodide reaction by neutralizing

TABLE 2

METHYL IODIDE REMOVAL BY REACTION WITH HYDRAZINE (0.64%) AT LOW CONCENTRATIONS UNDER STATIC CONDITIONS.

| Time | Flask Contents | Corrected* ppm Methyl Iodide |
|---|---|---|
| 0 | Original $CH_3I$ Concentration | 11.25 |
| 13.5 min. | $CH_3I$ + 10 ml $H_2O$ | 9.83 |
| 60 min. | $CH_3I$ + 10 ml $H_2O$ | 9.40 |
| 61 min. | $N_2H_4$ added | |
| 3 hours | $CH_3I + H_2O + N_2H_4$ | 11.5 |
| 24 hours | $CH_3I + H_2O + N_2H_4$ | 10.0 |
| 48 hours | $CH_3I + H_2O + N_2H_4$ | 10.8 |

* Values were corrected for the loss of methyl iodide due to its removal by previous air samples ( $\sim$ 300 ml each).

the hydrazine. This theory is supported by the success of initial methyl iodide-hydrazine reactions where the suspected interference of carbon dioxide was prevented by significantly greater concentrations of hydrazine (890 - 765 ppm).

In Test #2 of this series, a concentration of 5.75 ppm of methyl iodide in a 20.3 liter flask was exposed to 7.0 ml of 0.1N NaOH for a period of three hours during which three air samples were taken to determine the methyl iodide decay for the system. At the end of 3.25 hours, 0.75 ml of 64% hydrazine in water was added to result in a 7.75 ml solution of 6.2% hydrazine in 0.0903N NaOH. The latter would neutralize 420 ppm of carbon dioxide in this size flask (as $Na_2CO_3$) while the hydrazine air concentration would be approximately 37 ppm (Fig. 3) assuming no interference due to the presence of sodium hydroxide or carbonate.

Results, shown in Fig. 5, indicated a sharp reduction in methyl iodide concentration on addition of the hydrazine, with removals of 94.3% and 95.3% after 3 and 6 days, respectively. It is noted, however, that the concentration of methyl iodide decreased during the 3.25 hour period prior to the addition of hydrazine. This reduction may have been caused by (1) solubility of methyl iodide in the 7 ml solution of 0.1N NaOH initially added to the flask, or (2) adsorption on the glass surfaces of the flask. However, the latter effect was not noted in Test #1.

These tests indicate that hydrazine will react with methyl iodide to form a removable aerosol if an alkali is present to remove carbon dioxide. The complete removal of methyl iodide by this process is still in doubt, however, since 5% of the total iodide remained after 6 days. The actual concentration (0.25 ppm) is in the range of total iodides (0.1 to 0.3 ppm) we have found in our laboratory air. This air may be a source of contamination in the analysis of these samples where air is used to flush the samples through the combustion unit for decomposition of the methyl iodide prior to iodide analysis.

Methyl Iodide-Unsymmetrical Dimethyl Hydrazine

The ease with which unsymmetrical di-alkyl hydrazines is reported[4] to add on one molecule of an alkyl halide to form trialkyl hydrazinium salts prompted gas phase reaction studies betwen methyl iodide and unsymmetrical dimethy hydrazine (UDMH). In these studies, analyses for methyl iodide were made by gas chromatography (Wilkens Aerograph Model 600 C) utilizing an electron capture detector. Calibration of the chromatograph was made with known concentrations of methyl iodide prepared by the apparatus shown in Fig. 6. Metered air saturated with methyl iodide at a known temperature (Fig. 2) was diluted with a metered (orifice meter corrected for pressure) large excess of clean air in a Ventura type mixer. A metered aliquot of this air was diluted further with a large amount of clean metered air to produce the known concentration. Syringe samples (5 - 50 microliters) of this air were then injected

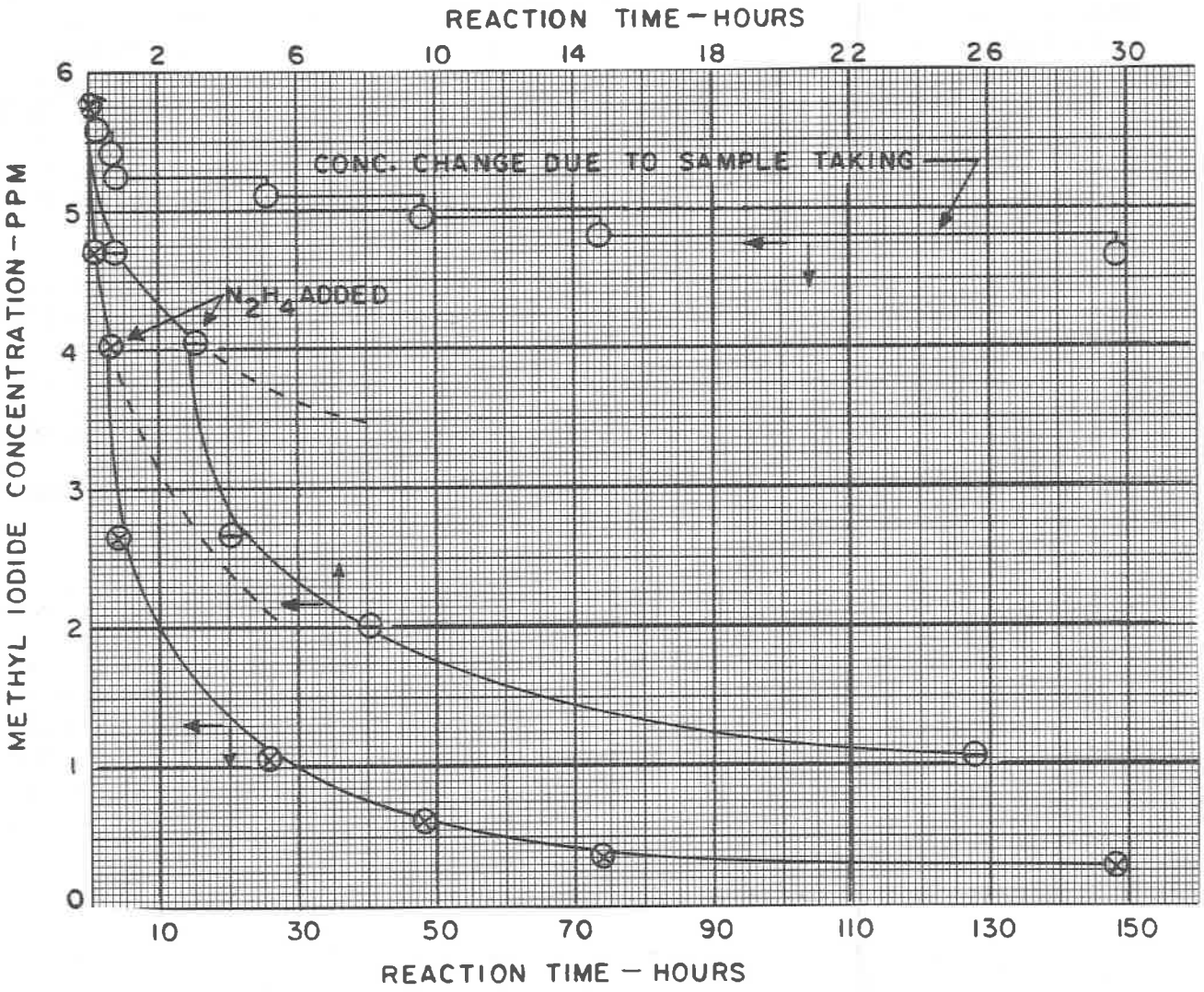


FIGURE 5. STATIC TEST METHYL IODIDE HYDRAZINE – 7.75 ML. OF 0.0903 N. NaOH, 6.2 % HYDRAZINE SOL. (CONC. $N_2H_4$ = 37 PPM)

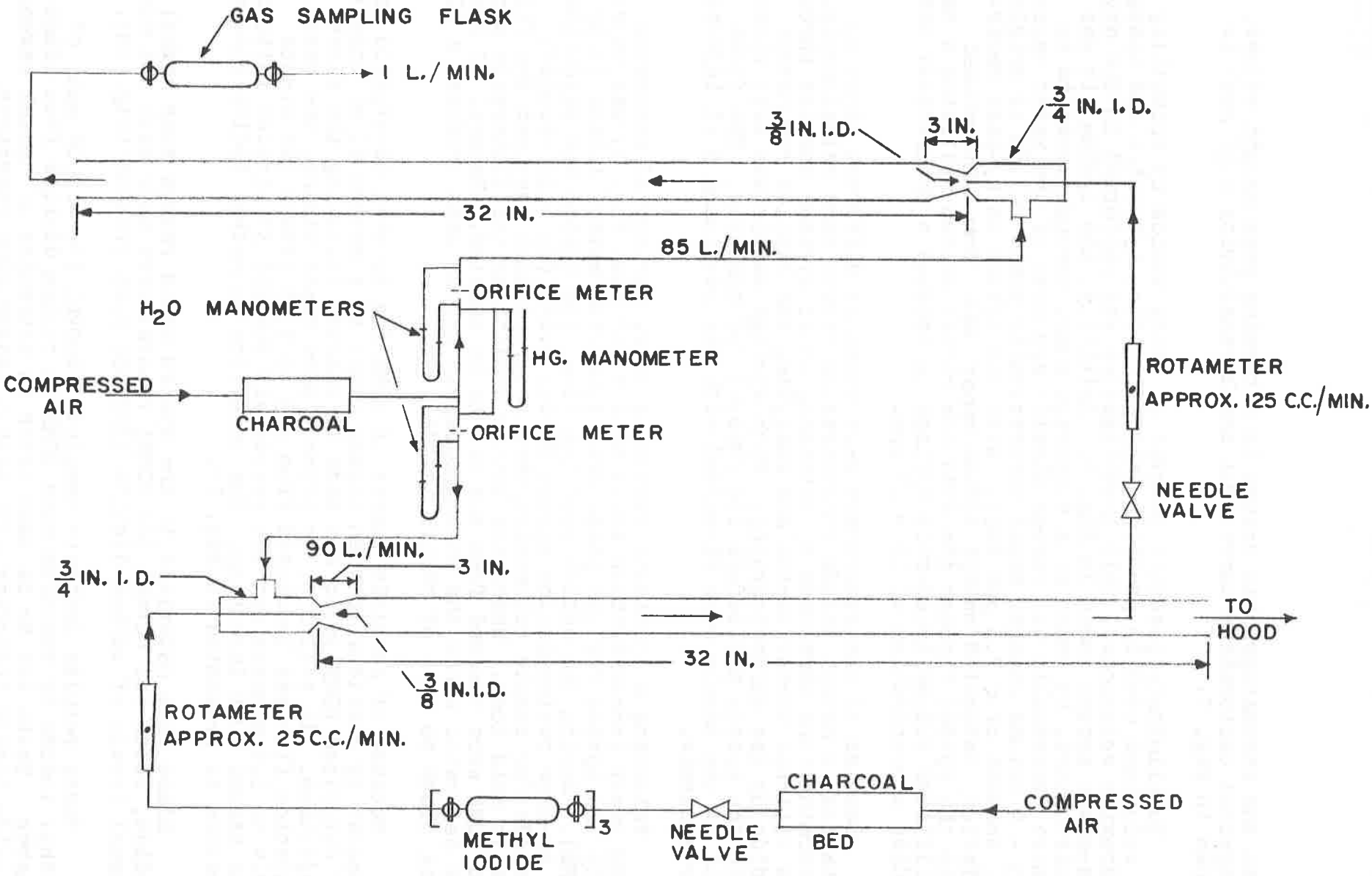


FIGURE 6. APPARATUS FOR LOW METHYL IODIDE CONCENTRATION SYNTHESIS (0.003 TO 20 P.P.M.).

into the chromatographic column to determine peak height values. A typical calibration curve (5µl sample sensitivity 0.02 ppm) is shown in Fig. 7.

To eliminate possible removal of methy iodide by solubility in solutions used in previous studies (water, hydrazine and sodium hydroxide solutions), this investigation was performed in the dry-gas-phase system shown in Fig. 8. Initially, the system air was recirculated, by means of a diaphragm pump, through ascarite to remove essentially all carbon dioxide and most of the water vapor ( 3 - 4 volume changes would theoretically yield <1.8% of original $CO_2$ content or < 7.5 ppm CO2). With the system on by-pass recirculation, saturated methyl iodide vapor was then introduced into the system through the silicone rubber septum utilizing a half milliliter volume hypodermic syringe to produce a theoretical methyl iodide concentration of 10 - 12 ppm.

Samples of the atmosphere were taken at different times to establish a methyl iodide concentration versus time relationship. Determinations were made by obtaining 10 µl syringe samples through the silicone rubber septum and analyzing the samples for methyl iodide by gas chromatography. Each syringe sample was well flushed with the system air before its removal for analysis. The first 5 µl of the sample were discarded with the remaining 5 µl injected for analysis.

Following a 15 minute period, a 10 ml syringe of saturated UDMH vapor (concentration equal to $2 \times 10^5$ ppm, Fig. 9) was injected into the system for gas phase reactions with methyl iodide (~90 ppm UDMH). During the entire reaction time, the system was maintained on by-pass recirculation except during brief (20 - 30 seconds) periods for sample collection when recirculation involved the filter-oxalic acid loop. Under the latter conditions the filterable aerosols and UDMH were removed from the air to be sampled. Removal of UDMH was desirable since the chromatographic column used produced a UDMH peak close to that of methyl iodide.

Because of possible losses of UDMH due to wall adsorption and removal by oxalic acid when taking samples, a second 10 ml injection of saturated UDMH vapor was made 16 minutes following the first injection. In addition, to promote more rapid mixing, the recirculation flow was increased from 2.3 to 5.75 liters per minute (9.4 to 3.8 minutes for one system air change) 37 minutes following the second UDMH injection. The reduction in methyl iodide concentration is presented in Fig. 10.

Since some materials in the system would remove some methyl iodide, tests for normal (no UDMH) removal were made with and without normal levels of carbon dioxide (350-400 ppm) present (Fig. 10).

These results indicate complete removal (to < 0.02 ppm) of methyl iodide by reaction with UDMH in carbon dioxide free atmospheres. Tests are to be made later to determine if normal carbon dioxide levels interfere with methyl iodide-UDMH reactions.

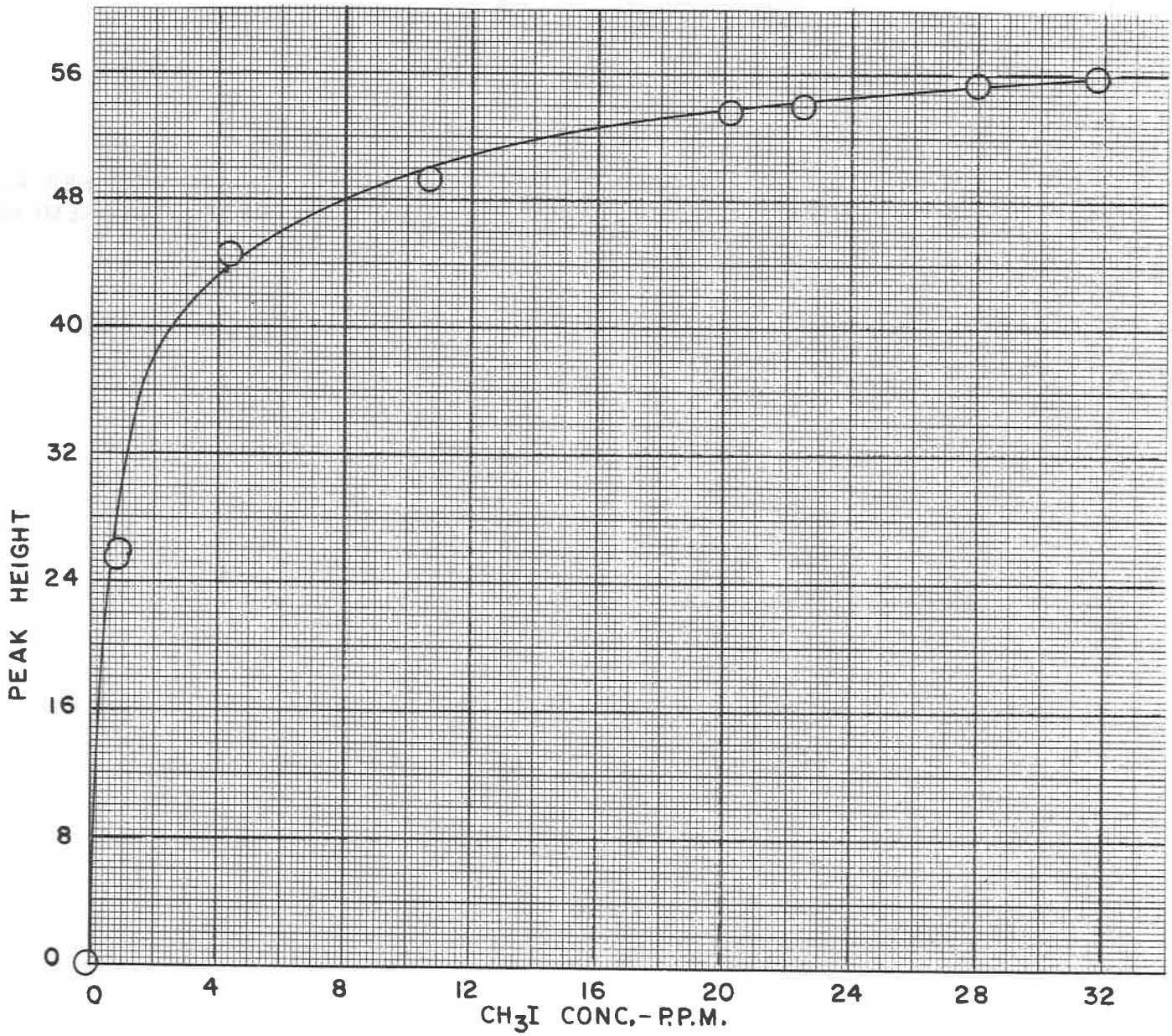


FIGURE 7. METHYL IODIDE CALIBRATION OF GAS CHROMATOGRAPH (ELECTRON CAPTURE). SAMPLE - 5 µL. OF 10µL. SYRINGE. SILICONE COLUMN = 5% SE 30 60/80 MESH CHROMOSORB.

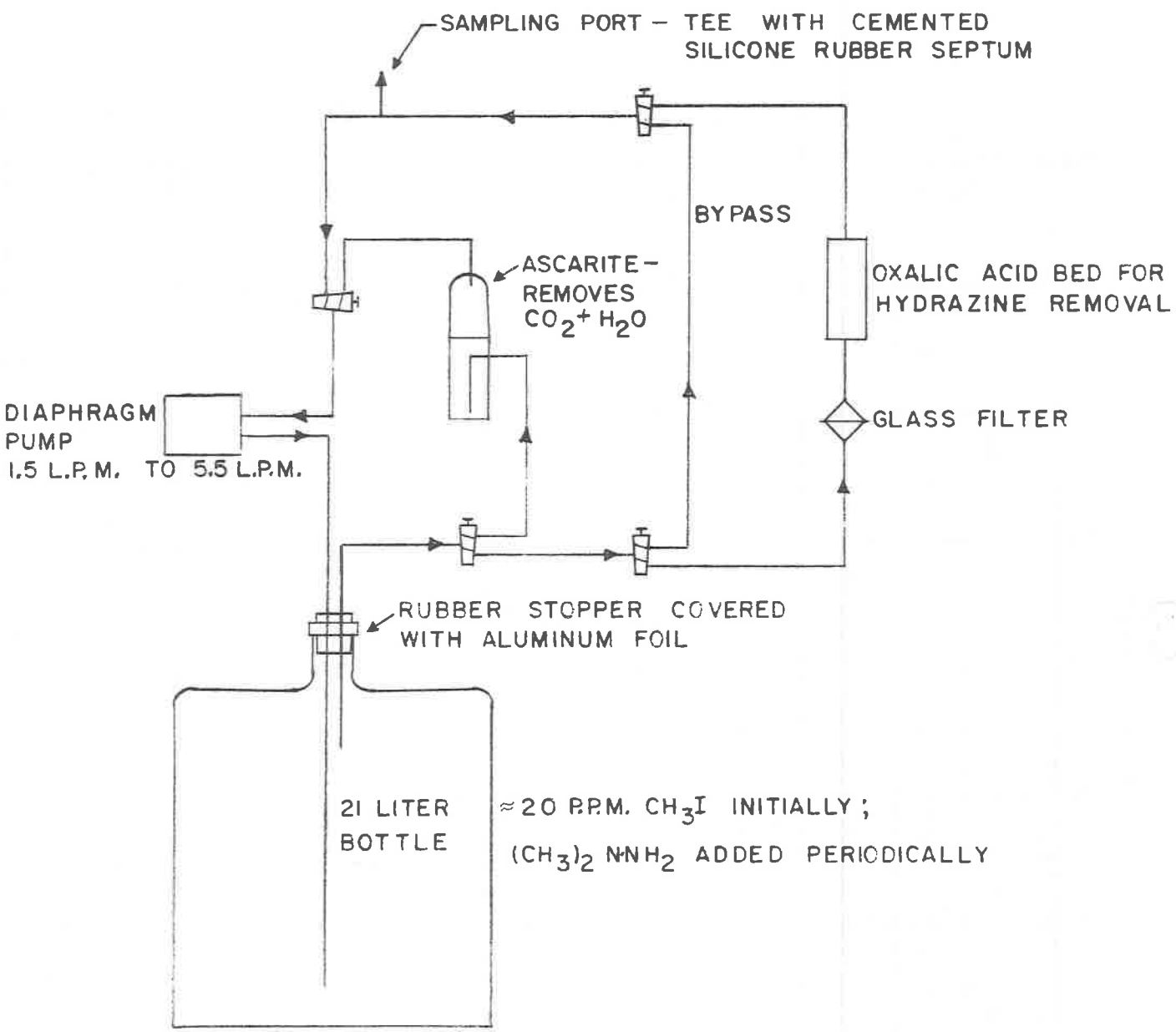


FIGURE 8. APPARATUS FOR STUDY OF DRY GAS PHASE REACTIONS BETWEEN METHYL IODIDE AND HYDRAZINES [PRINCIPALLY $(CH_3)_2 N{\cdot}NH_2$]

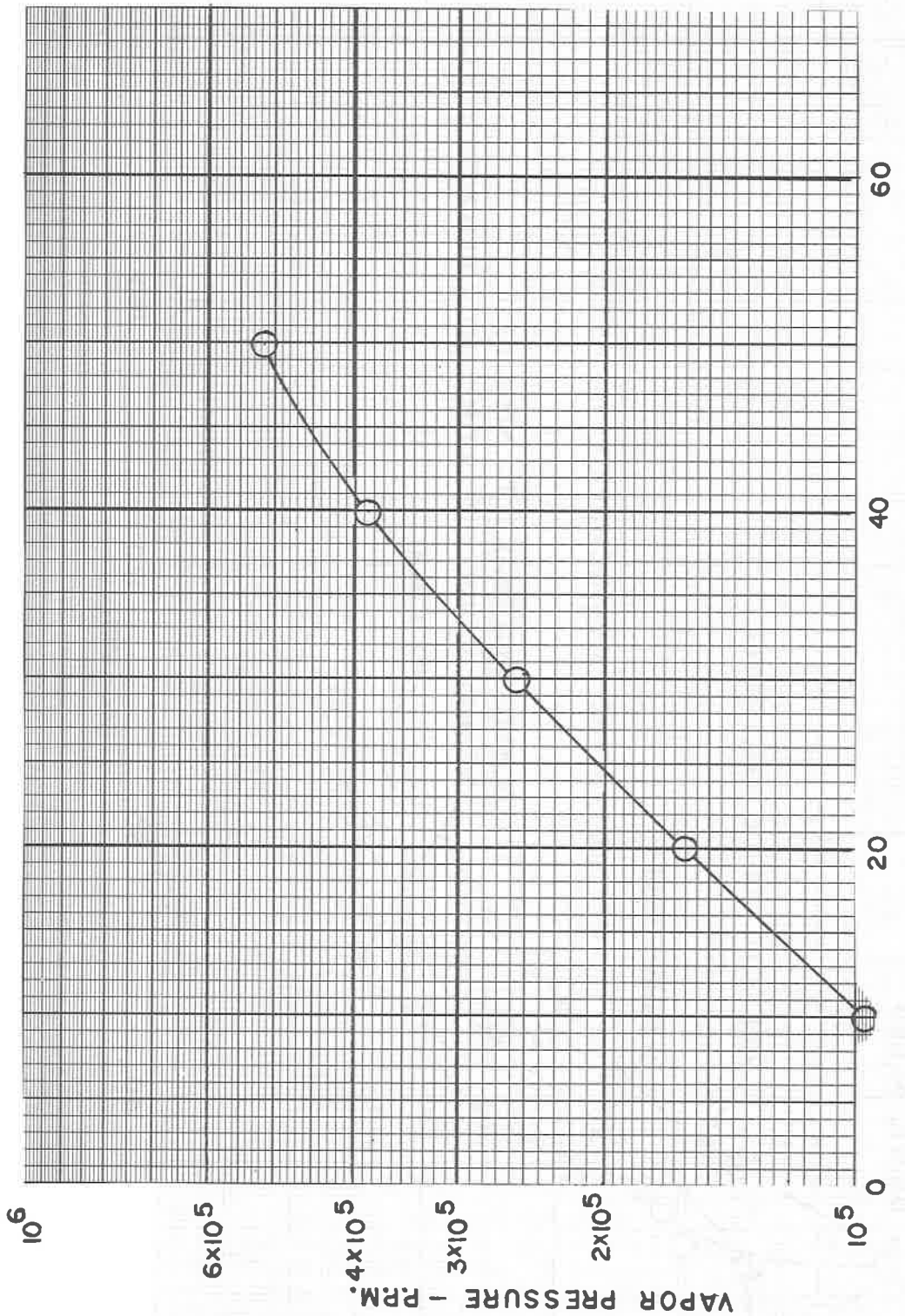


FIGURE 9. VAPOR PRESSURE OF UNSYMMETRICAL DIMETHYL HYDRAZINE.

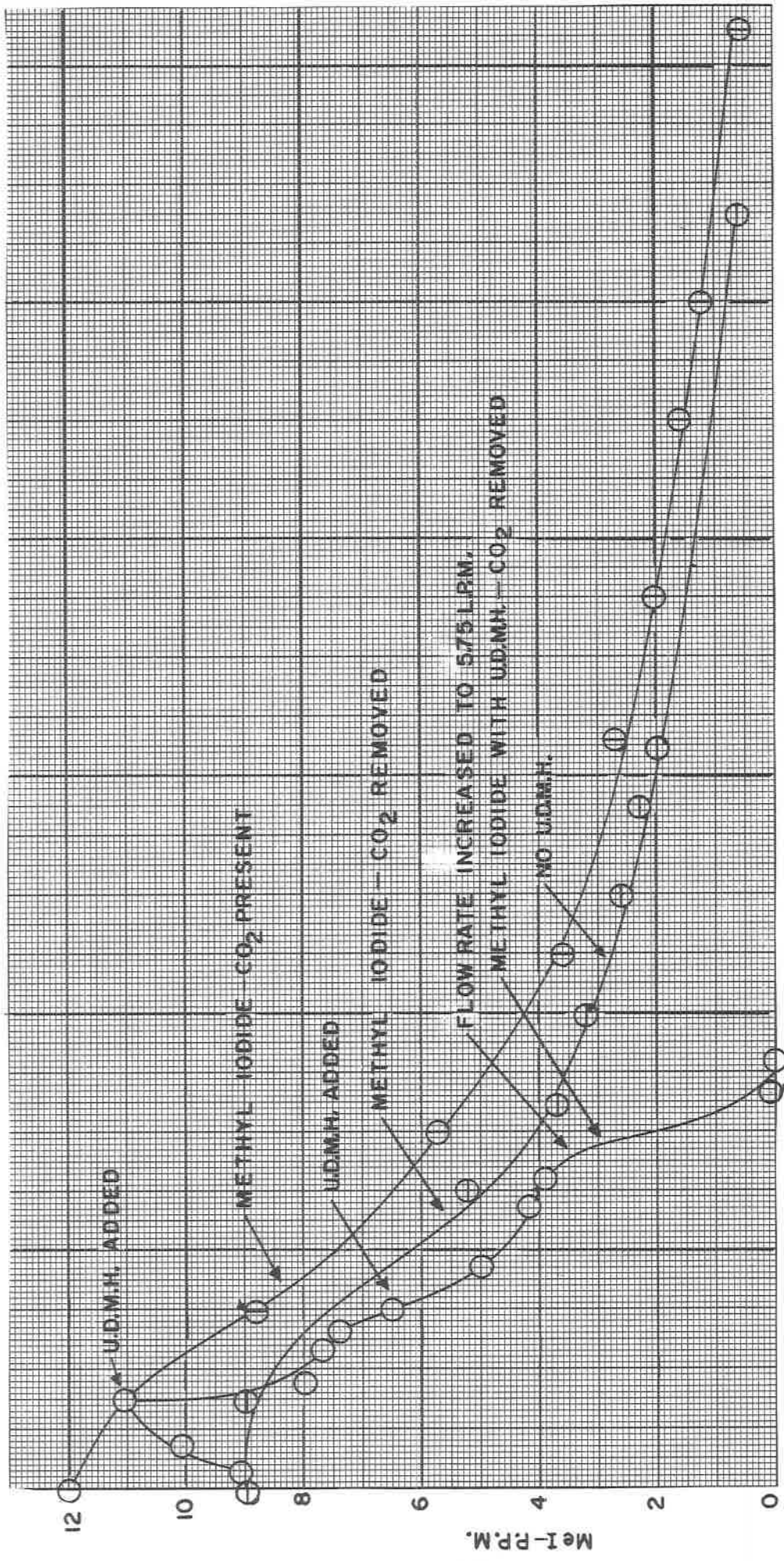


FIGURE 10. METHYL IODIDE DECAY CURVES.

Iodine-Hydrazine Static Conditions

The interference created by carbon dioxide in the methyl iodide-hydrazine reactions at low concentrations necessitated studies on the effect of this gas on the iodine-hydrazine reaction.

Static studies of low iodine concentrations in 20 liter flasks were attempted but difficulty was encounted in maintaining significant iodine concentrations for the time required to determine concentration changes due to hydrazine-iodine reactions. Success in this endeavor was achieved by maintaining a saturated iodine concentration for a prolonged period (> 24 hours), following which the excess solid iodine was removed from the flask and the contained gas diluted with clean air to a desirable concentration range. Although the final concentration decreased with time, its decay rate was low enough to demonstrate marked concentration reductions on the addition of 100 ml of 1% hydrazine solution ( air concentration equal to 20 ppm) to the flask (Fig. 11). The persistent residual 0.2 ppm of iodine indicated incomplete reaction.

A second test identical with the one described but including 0.06N NaOH in the 100 ml 1% hydrazine demonstrated the same marked reduction in concentration and residual 0.2 ppm iodine content in the flask. It was suspected that the residual iodine was caused by contamination in the samples. In these studies, iodine concentrations were determined by sampling 100 ml of the gas through a bed of clean iodide-free copper beads ($\sim$ 1 mm diameter) and analyzing the collected iodine by the ceric sulfate method.[7] To assure sampling exactly 100 ml of gas through the copper beds, 100 ml of room air were used to flush the sampling train following collection of the sample.

An additional sample was taken, with the 100 ml of room air used for flushing the train being cleaned by its passage through a bed of activated charcoal. This test demonstrated less than 0.01 ppm iodine in the flask, indicating that the 0.2 ppm in the previous samples was due to room air contamination. This was confirmed by several 100 ml room air samples taken at 15 minute intervals which revealed room air concentrations ranging from 0.1 to 0.3 ppm iodine (iodine, hydrogen iodide and other iodides).

Since the 0.2 ppm iodine observed in the flask samples was due to contaminated air used in the sampling procedure, it can be stated that the removal of iodine by its reaction with hydrazine at low concentrations is complete and without significant interference from normal levels of carbon dioxide.

## CONCLUSIONS

1) Airborne methyl iodide reacts with relatively high concentrations of hydrazine (800 - 900 ppm) under dynamic conditions to form an aerosol which is removable by filtration. Among other factors, the efficiency of aerosol formation and removal is dependent on reaction time between the two vapors. For removal efficiencies greater than 80%, reaction times of several minutes are required.

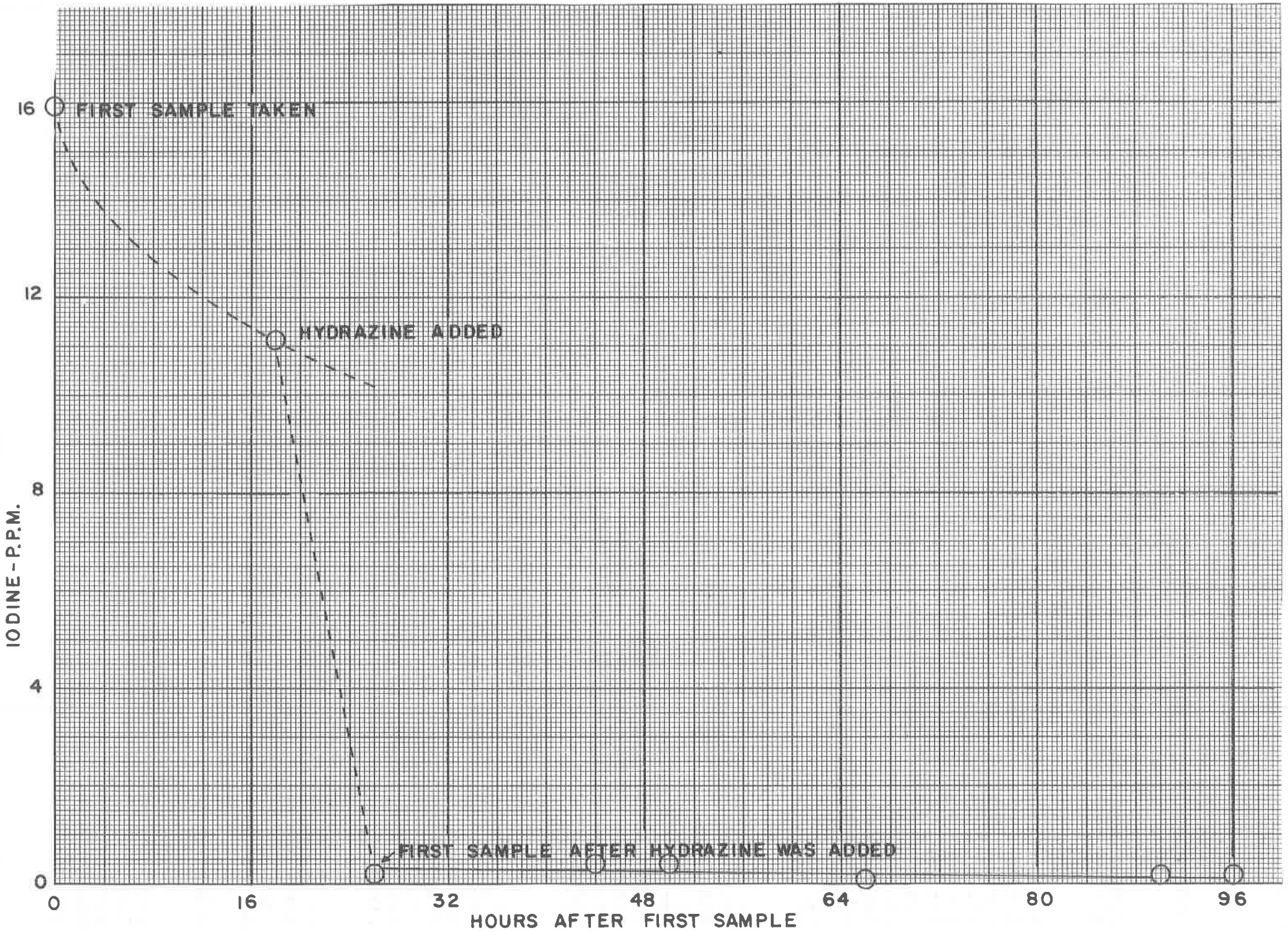


FIGURE 11. STATIC TEST $I_2 + N_2H_4$. 100 ML. OF HYDRAZINE SOL. (NORMAL $CO_2$ PRESENT).

2) High concentrations of hydrazine (765-890 ppm) react with iodine and methyl iodide vapors under static conditions to form aerosols which are efficiently removed ( >99.99%) by settling, diffusion and solubility processes.

3) Iodine in the gas phase reacts with low concentrations of hydrazine (20-30 ppm) under static conditions and in the presence of normal levels of carbon dioxide (300-400 ppm) to result in 100% removal.

4) Efficient removal of methyl iodide vapors by low air concentrations of hydrazine ($\sim$35 ppm) under static conditions requires the presence of free alkali to remove carbon dioxide and prevent its interference.

5) Removal of gaseous methyl iodide by low air concentrations of unsymmetrical dimethyl hydrazine (90-180 ppm) in a dry carbon dioxide free atmosphere is highly efficient under dynamic conditions.

6) The time required for removal of iodine and methyl iodide in static studies is dependent on the rate of aerosolization, the properties of the aerosols formed, and the shape and size of the containment vessel.

REFERENCES


1. Cowser, K. W. Current Practices in the Release and Monitoring of I-131 at NRTS. Hanford, Savannah River and ORNL, Nuclear Information Center, Oak Ridge National Laboratory (ORNL-NSIC-3) Aug. 1964.

2. Title 10, Part 20, Code of Federal Regulations Supt. of Documents, U. S. Government Printing Office, Washington, D. C.

3. Clark, Charles C., Hydrazine, Mathieson Chemical Corporation, Baltimore, Maryland, Aug. 1953.

4. Karrer, Paul, Organic Chemistry, Nordemann Publishing Co., Inc., New York, p. 120, 1938.

5. Tebbens, B. D., Portable Combustion Apparatus for Field Determination of Chlorinated Hydrocarbons, Journal of Industrial Hygiene and Toxicology, 19: 204, 1937.

6. Watt, R. W., and Chrisp, J. D., Spectrophotometric Method for the Determination of Hydrazine. Analytical Chemistry 24: 2006, 1952.

7. Viles, F. J., Jr., and L.Silverman, In-Place Removal Efficiency Test, Proceedings 9th Air Cleaning Conference, Boston, Mass., Sept. 1966.

# REMOVAL OF METHYL IODIDE FROM SIMULATED REACTOR CONTAINMENT ATMOSPHERES WITH HYDRAZINE

J. Mishima
L.C. Schwendiman
L.L. Burger
R.A. Hasty

Battelle Memorial Institute*
Pacific Northwest Laboratory
Richland, Washington

## ABSTRACT

The reaction of hydrazine and methyl iodide is under study to determine the feasibility of using hydrazine in reactor spray systems to remove organic and molecular forms of radioactive iodine. Rate studies showed that the static removal of methyl iodide from the vapor phase over a 50% hydrazine solution proceeds with a half-life of about six minutes at 50°C.

Reaction rate and/or rate of transfer to the solution varies with airborne methyl iodide concentration, liquid hydrazine concentration and the available liquid surface area. Spraying 35% hydrazine solutions through air containing methyl iodide at room temperature and at 75°C effectively scavenges methyl iodide even in the presence of 50 mg/m$^3$ of molecular iodine.

## INTRODUCTION

The control of radioiodine released to the environment in the event of a reactor fuel meltdown is of great importance to nuclear safety and a considerable amount of research has been performed in this area.[1] Airborne iodine concentrations ranging from ∿ 9 to 300 mg/m$^3$ are postulated for several power reactors.[2] The relatively recent identification of organic iodides as a constituent of systems containing airborne radioiodine[3] has already resulted in extensive study to understand the formation and behavior of methyl iodide (iodomethane), and to devise trapping systems.[4] The organic iodides have been found to comprise up to 30% of airborne active iodine.[1] One potential approach to the removal of airborne organic radioiodine is the vapor phase reaction with hydrazine. Parameters governing this reaction are under study at the Pacific Northwest Laboratory with the aim of ascertaining the mechanism and demonstrating feasibility of effective removal of airborne organic iodide.

The research at Pacific Northwest Laboratory was undertaken in late 1965, following preliminary work performed at Harvard University[5] which indicated that a filterable aerosol could be formed under certain conditions when hydrazine and methyl iodide were allowed to react in the gas phase. Some scouting ex-

*Work performed under Contract No. AT(45-1)-1830 between the Atomic Energy Commission and Battelle Memorial Institute.

periments subsequently carried out in our laboratories and described in this report gave promise that methyl iodide could be removed from an atmosphere by sprays containing hydrazine.

Based on these data, a study was initiated to investigate in greater detail the reaction between methyl iodide and hydrazine under conditions approaching those anticipated in a reactor accident. The work has proceeded along two fronts during the ensuing interval.

1. A physical chemistry study to establish the theoretical aspects of the reaction, products formed, etc.

2. Demonstration studies of the removal of methyl iodide from contained atmospheres approximating those anticipated from a reactor accident.

This report presents the data and conclusions from these studies which are still in progress.

## SUMMARY

The feasibility of using aqueous hydrazine solutions for the removal of airborne radioactive methyl iodide is under study at the Pacific Northwest Laboratory. Two areas are currently being investigated.

1. A chemical study of the hydrazine-methyl iodide reaction.

2. Demonstration of the removal efficiencies of various aqueous hydrazine solutions on contained airborne methyl iodide under simulated post-accident reactor containment atmospheres.

The rate of disappearance of methyl iodide vapors injected into hydrazine vapors in equilibrium over 17.5 to 50% aqueous hydrazine solutions, 0.05 and 0.2 N in sodium hydroxide, has been determined at 29° and 50°C. The half-life of the reactions found ranged from 6.3 to 42 minutes. The data fit the equation:

$$\frac{dc}{dt} = K\ S\ C_{H_L}\ C_{M_G}$$

where $K$ is a constant,
$S$ is the liquid surface area,
$C_{H_L}$ is the concentration of aqueous hydrazine,
$C_{M_G}$ is the concentration of the airborne methyl iodide.

In the absence of hydrazine, methyl iodide losses to the surfaces of the reaction vessel are negligible for the time period involved. The decrease in gas chromatograph peak height (methyl iodide concentration) was linear over several orders of magnitude.

Bubbling methyl iodide, airborne in hot air or steam, through hydrazine solutions was not efficient under the conditions studied. The small contact time between the liquid and gas phases and the large size of the bubbles are the probable reasons for the low removal. Only 11 - 14% of the airborne methyl iodide was removed by a 35% aqueous hydrazine solution. Water under the same conditions extracted 0.2%.

Airborne methyl iodide was quantitatively removed by spraying a 35% aqueous hydrazine solution through the contained gases at room temperature and at 75°C. Solutions were pumped through a spray nozzle at the top of a 45" tall ×14"

diameter aluminum chamber holding the gases. Methyl iodide concentrations of 0.5 and 1000 mg/m$^3$ were used in the room temperature runs and 1 mg/m$^3$ used at 75°C. The presence of 50 mg/m$^3$ of molecular iodine in some of the experiments did not interfere.

Installation of a 10' tall × 4' diameter, stainless steel spray chamber is nearing completion. Demonstrations of the efficiencies of hydrazine sprays upon methyl iodide under simulated post-accident, reactor containment atmospheres are scheduled. Additional small-scale, scouting studies in the small chamber to optimize hydrazine concentrations and study the effects of ammonium hydroxide additions and other temperatures will be continued in the interim. Additional experiments to characterize the mechanisms, and parameters controlling the gas phase reactions as well as some of the products are in progress.

## CHEMICAL STUDIES OF THE METHYL IODIDE-HYDRAZINE SYSTEM

The study of the physical chemistry of the methyl iodide-hydrazine system was undertaken to determine the properties of the products of the reaction, the rate of reaction and to define those parameters which control the reaction. These data are expected to help define the optimum conditions for effective removal of the reaction products by sprays or other engineered aerosol and vapor clean-up systems. The basic studies are also expected to suggest possible related compounds which may be useful in forming easily removed iodine containing products. These areas will be explored as time permits. An essential part of the research program was to develop suitable techniques for following the reaction.

The two principal chemical reactions of interest in the study of the removal of airborne methyl iodide from reactor containment atmospheres by hydrazine sprays appear to be:

$$N_2H_4 + 2CH_3I \rightarrow (CH_3)_2N_2H_2 + 2HI \qquad (1)$$

$$N_2H_4 + 2I_2 \rightarrow N_2 + 4HI \qquad (2)$$

The latter reaction has not been studied in our research undertaken to date, but must eventually be carefully considered because of the large relative abundance of airborne molecular iodine following a reactor-fuel meltdown accident.

The presence of HI, a reactive compound, as a product suggests that the course of the reaction and the removal of radioactive iodine will be contingent not only upon the equilibrium of the initial reaction, but also upon secondary reactions which HI may undergo. Reactions of HI with sundry materials present, particularly basic vapors or liquids will help to immobilize the radioactive iodine.

Various analytical techniques were evaluated to determine which were suitable to follow reaction (1). Four methods were evaluated: gas absorption spectrophotometry, proton nuclear magnetic resonance (NMR), conductometric and gas-liquid chromatography (GLC). For the gas phase only GLC was found adequate for the concentration range desired. Absorption spectrophotometry, although rapid, proved to be less sensitive than desired. The detection limit of ∿ 2.8 g methyl iodide/m$^3$ was far above the expected concentration range. Nuclear magnitude resonance (NMR) and conductometric methods are limited to liquid phase reactions. Each method has limitations which were identified in the study.

Airborne methyl iodide concentrations were determined by separation on a

1/4" OD × 6' or 12' stainless steel column of 20% SE 30 (silicone gum) on Chromosorb P® under isothermal (40°C) conditions. A Research Specialties gas chromatograph[a] was used with a Warner Chilcot[b] electron capture detector. The lower detection limit of the system was determined to be $2 \times 10^{-12}$ g iodine as methyl iodide. Gas samples ranging from 10 to 500 µl were used to follow methyl iodide concentrations during the reaction rate studies. A linear correlation was found between peak height and area for aliquots up to $3 \times 10^{-8}$g iodine. Peak height measurements were found to be reliable for low methyl iodide concentrations.

The half life $(\tau_{1/2})^c$ of removal of gas phase methyl iodide was determined by measuring the decrease in airborne methyl iodide subsequent to injection of methyl iodide into hydrazine vapors at equilibrium with aqueous hydrazine of known concentration, and to which various quantities of NaOH had been added. The reaction was carried out in a jacketed Pyrex reaction vessel 2.7 cm ID × 7.75 cm long.

Half lives for the reaction were found to range from 6.3 to 42 minutes with methyl iodide concentration ranging from 9.3 to 30 mg/m$^3$, aqueous hydrazine concentrations from 17.5 to 50 w/o, and temperatures of 29°C and 50°C. Results are listed in Table 1. The $\tau_{1/2}$ varies with hydrazine and methyl iodide concentration and liquid surface area. The data fit the equation,

$$\frac{dc}{dt} = K\ S\ C_{H_L}\ C_{M_G} \qquad (3)$$

where $K$ = constant

$S$ = liquid surface area

$C_{H_L}$ = concentration of the aqueous hydrazine

$C_{M_G}$ = concentration of methyl iodide in the gas phase.

The temperature coefficient of the rate of methyl iodide removal is small and is dependent on hydrazine concentration. Airborne hydrazine concentrations calculated from available published data for aqueous hydrazine mixtures[6,7] are greatly in excess of the stoichiometric quantity required for reaction of methyl iodide. Losses to the reaction vessel surfaces in the absence of hydrazine are negligible for the time period involved. Figure 1 shows the variation of peak height (methyl iodide concentration) with time. The upper curve shows the data for two separate experiments using different sodium hydroxide concentrations. The lower curve shows the decrease in methyl iodide when a higher concentration (50%) hydrazine is used, and exhibits a much more rapid rate of removal. The curve indicates the linear behavior of peak height over several orders of magnitude. Work is continuing to confirm and better define the apparent increase in removal rate with surface area exposed.

Examination of the data from the various techniques applied to follow concentration changes in the systems of hydrazine and methyl iodide resulted in observations of significance, but not yet fully interpreted. The nuclear

---

® Chromosorb is Johns Manville registered trademark for support material.

a Manufactured by Research Specialties, Richmond, California.

b Manufactured by Warner-Chilcot Laboratory, Instrument Division, Richmond, California.

c The half-life of the reaction ($\tau_{1/2}$) is the time, in minutes, required to reduce the airborne methyl iodide to one half its original concentration.

TABLE 1

GAS PHASE METHYL IODIDE-HYDRAZINE REACTION HALF LIVES

| Temp. (°C) | Wt % $N_2H_4$ | NaOH (N) | Liquid Surface Area ($cm^2$) | Initial Conc. Methyl Iodide ($mg/m^3$) | $\tau_{1/2}$ Half-Life (min) |
|---|---|---|---|---|---|
| 50.1 | 50 | 0.05 | 5.65 | 18.6 | 6.7 |
| 29.7 | 50 | 0.05 | 5.65 | 30 | 7.3 |
| 50.1 | 35 | 0.05 | 4.72 | 18.6 | 11.2 |
| 50.1 | 35 | 0.20 | 4.72 | 9.3* | 11.7 |
| 50.1 | 35 | 0.05 | 4.72 | 18.6 | 11.8 |
| 50.1 | 35 | 0.20 | 4.72 | 18.6 | 12.3 |
| 50.1 | 17.5 | 0.20 | 5.65 | 18.6 | 23.0 |
| 50.1 | 17.5 | 0.05 | 5.65 | 18.6 | 24.5 |
| 50.1 | 27 | 0.04 | 2.87 | 12 | 34.5 |
| 29.7 | 17.5 | 0.05 | 5.65 | 30 | 42 |
| 50.1 | 0 | 0.05 | 5.65 | 11.6 | 1270† |

* Peak height observed for aliquot size not consistent with this value; indicates concentrations of ∿ 30 to 40 $mg/m^3$.

† Reaction followed for 17.5 hours. Half life calculated by extrapolation.

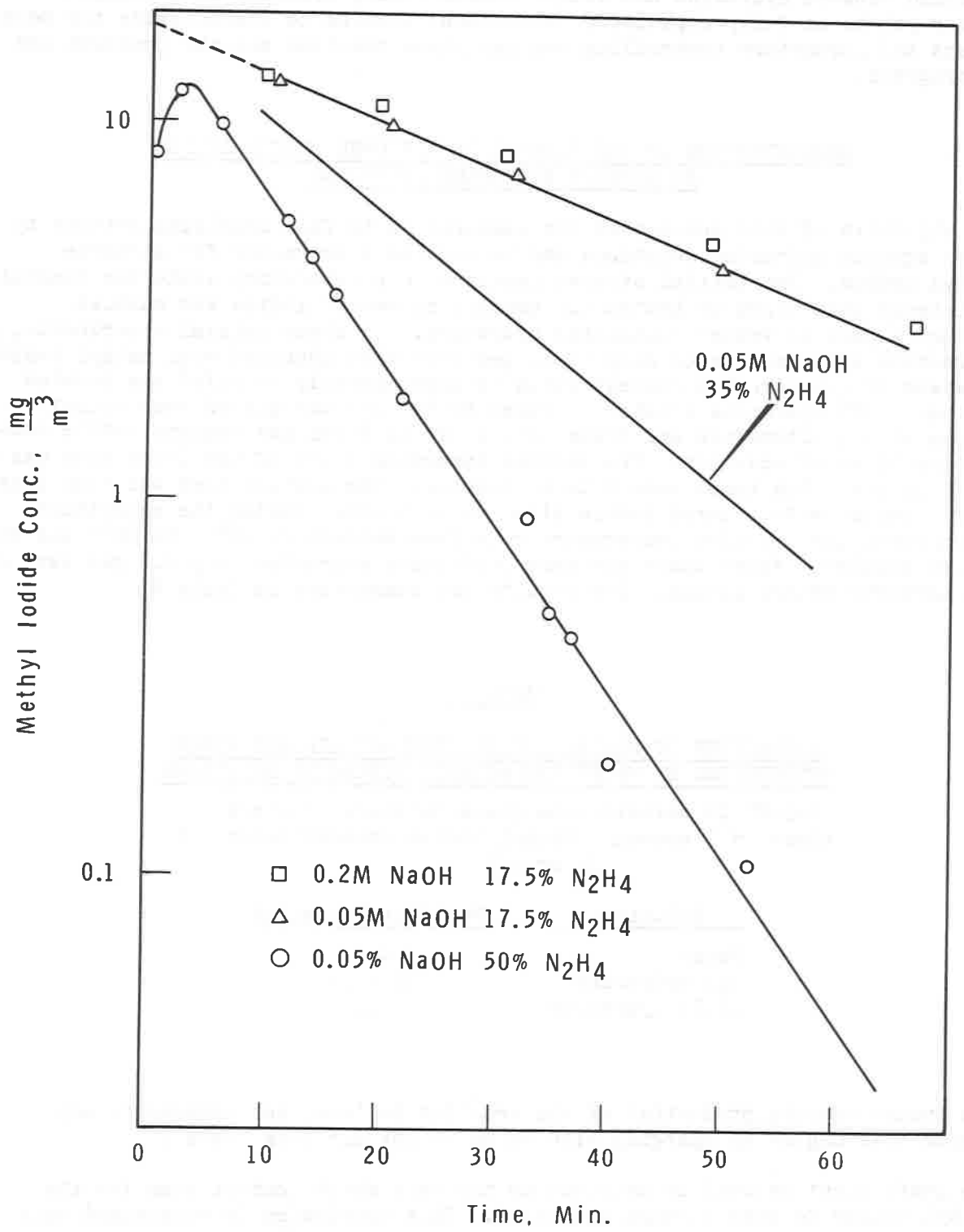


Figure 1. Reaction Rate Determinations at 50°C

magnetic resonance experiments in liquid systems confirmed that one product appearing was 1,1-dimethyl hydrazine. Spectrophometry of the gaseous system showed a rapid initial change in composition after methyl iodide was added to hydrazine. Slower changes in composition followed. The data indicate that the reaction between hydrazine and methyl iodide likely proceeds in a complex manner yet to be fully explained. Additional studies to characterize the mechanisms and parameters controlling the gas phase reaction and the products are in progress.

## DEMONSTRATION OF THE REMOVAL OF AIRBORNE METHYL IODIDE BY AQUEOUS HYDRAZINE SOLUTIONS

The objective of this portion of the research is to find promising methods by which aqueous hydrazine solutions can be used as a scavenger for airborne methyl iodide. The initial studies examined on a laboratory scale the removal efficiency when steam or heated air containing methyl iodide was bubbled through a pool or vessel containing hydrazine. In these initial experiments, extraction efficiencies of only 11-14 per cent were obtained when methyl iodide in steam or hot air, at a concentration of approximately 25 $mg/m^3$ was bubbled through a 35% hydrazine solution. Steam or hot air was passed over methyl iodide at ∿ 3 liters/min and drawn into a 125 ml Pyrex gas washing bottle containing 50 ml of solution. The initial immersion depth of the inlet tube was ∿ 2-1/2 inches. Run times were 8 to 10 minutes. The contact time was much less than 1 second with a large bubble size (up to 5 mm). During the experiments using steam the solution temperature rose from ambient (∿ 23°C) to 80°C and the volume doubled. Water under the same conditions extracted only 0.2 per cent of the airborne methyl iodide. The results are summarized in Table 2.

TABLE 2

EXTRACTION OF METHYL IODIDE FROM HOT AIR AND STEAM ATMOSPHERES BY WATER AND AQUEOUS HYDRAZINE SOLUTIONS

(1-5/8" ID borosilicate glass bubbler. Contact time: < 1 second. Methyl iodide concentration: ∿ 25 $mg/m^3$)

| Solution | Per Cent Extracted |
|---|---|
| Water | 0.2 |
| 35% Hydrazine | 11 - 14 |
| 17.5% Hydrazine | 11 |

The iodine bearing product(s) of the reaction is (are) not removed to any appreciable degree by sparging with steam or hot air (see Table 3).

The inefficient removal is ascribed to the very short contact time for the methyl iodide to pass through hydrazine. This conclusion is consistent with the reaction rates indicated in the chemical studies. Diffusion of methyl iodide to the bubble-liquid interface probably limits the reaction.

Spraying with water containing reactive compounds such as hydrazine may be a feasible method to immobilize airborne organic iodides. Included in the engineered safeguards of most reactors is a depressurization water spray system which may serve with little modification as the means for adding the reactive compound to the atmosphere. Reactions which result in aerosols which can

TABLE 3

RETENTION OF IODINE BEARING METHYL IODIDE-HYDRAZINE PRODUCTS BY AQUEOUS PHASE

(4.7 to 13.4 mg/cc methyl iodide in 35% hydrazine solution sparged with steam or heated air.)

| Time After Initial Contact (hour) | Indicated Retention (Per Cent) |
|---|---|
| 0 | 100 |
| 0.1 | 110 |
| 1 | 113 |
| 4 | 111 |
| 16 | 92 |
| 17 | 90 |
| 40 | 114 |

be removed in existing gas clean-up facilities or which yield soluble iodides which will be held in the water should prove useful.

A 114 liter chamber, 45" tall and 14" in diameter, was constructed to determine the feasibility of this approach.

Efficient methyl iodide removal was obtained by spraying a 35% aqueous hydrazine solution through airborne methyl iodide in air at ambient condition. Tagged methyl iodide and molecular iodine were released into the aluminum tank by heating alcohol and carbon tetrachloride solutions of iodine and methyl iodide in a Pyrex generator. The vapors were mixed by means of a bellows made from a 1 liter polyethylene bottle attached to one of the eight 1" NPT couplings welded to the chamber wall. Spray solutions were pumped from a 1 liter polyethylene reservoir with a stainless steel gear pump capable of flows up to 400 cc/min at ∿ 100 psi. The solution was carried to the stainless steel spray nozzle projecting into the chamber via 1/4" OD aluminum tubing. The sprayed liquid was collected in the conical bottom of the chamber and could be returned to the pump via 1/4" OD aluminum tubing. The system is shown schematically in Figure 2. After the solution had been sprayed through the chamber atmosphere (12 minutes for the single-pass and 60 minutes for recycle), the system was allowed to equilibrate for 1 hour before removal of the liquid and the transfer of the chamber atmosphere. The latter was pulled through 2 charcoal cold-traps in series. Aliquots of both the sprayed solution and charcoal were counted in a 9" well crystal-gamma spectrometry system. Removal efficiency was calculated by

$$\text{Removal efficiency} = \frac{^{131}\text{I in liquid}}{^{131}\text{I on charcoal} + ^{131}\text{I in liquid}} \times 100 \qquad (4)$$

The removal efficiencies found are listed in Table 4. The 35% hydrazine solution appears to quantitatively remove the airborne methyl iodide even in the presence of an appreciable quantity of elemental iodine (50.5 mg/m$^3$). Decreasing the hydrazine concentration decreased the removal efficiency somewhat. Use of ammonium hydroxide improves the removal. Reaction rate was such that the 12 minute single pass followed by the one hour waiting time removed 93% as compared with 100% removal for a recycle of the hydrazine for sixty minutes. These observations suggest that the reaction under these conditions may be fairly rapid, although the importance of the settling or equilibration period in methyl iodide removal is yet to be determined.

The foregoing experiments were performed at essentially ambient temperatures. The 114 liter chamber was later outfitted with surface heating units controlled by transformers and the walls were insulated with glass fiber pads. The chamber temperature could be raised to 100°C and maintained reasonably constant. A mixing propeller was installed and other improvements incorporated to assure consistent operation. Figure 3 is a diagram of the modified chamber.

Four runs were completed with the modified chamber with the principal objective of determining whether higher temperatures and steam would favor the scavenging reactions.

During each run the chamber temperature was raised to the desired level using the heating cable. Steam was passed into the chamber from an all-glass steam generator. After stabilization of conditions, methyl iodide and elemental iodine were passed into the chamber from an all-glass generator. The gases were mixed and the liquid sprayed through the atmosphere for 60 minutes. During this period, the temperature of the spray liquid rose from ambient to ∿ 50°C while the chamber temperature decreased from 75°C to 50°C. After a 60 minute settling period, the liquid was pumped from the chamber and the air

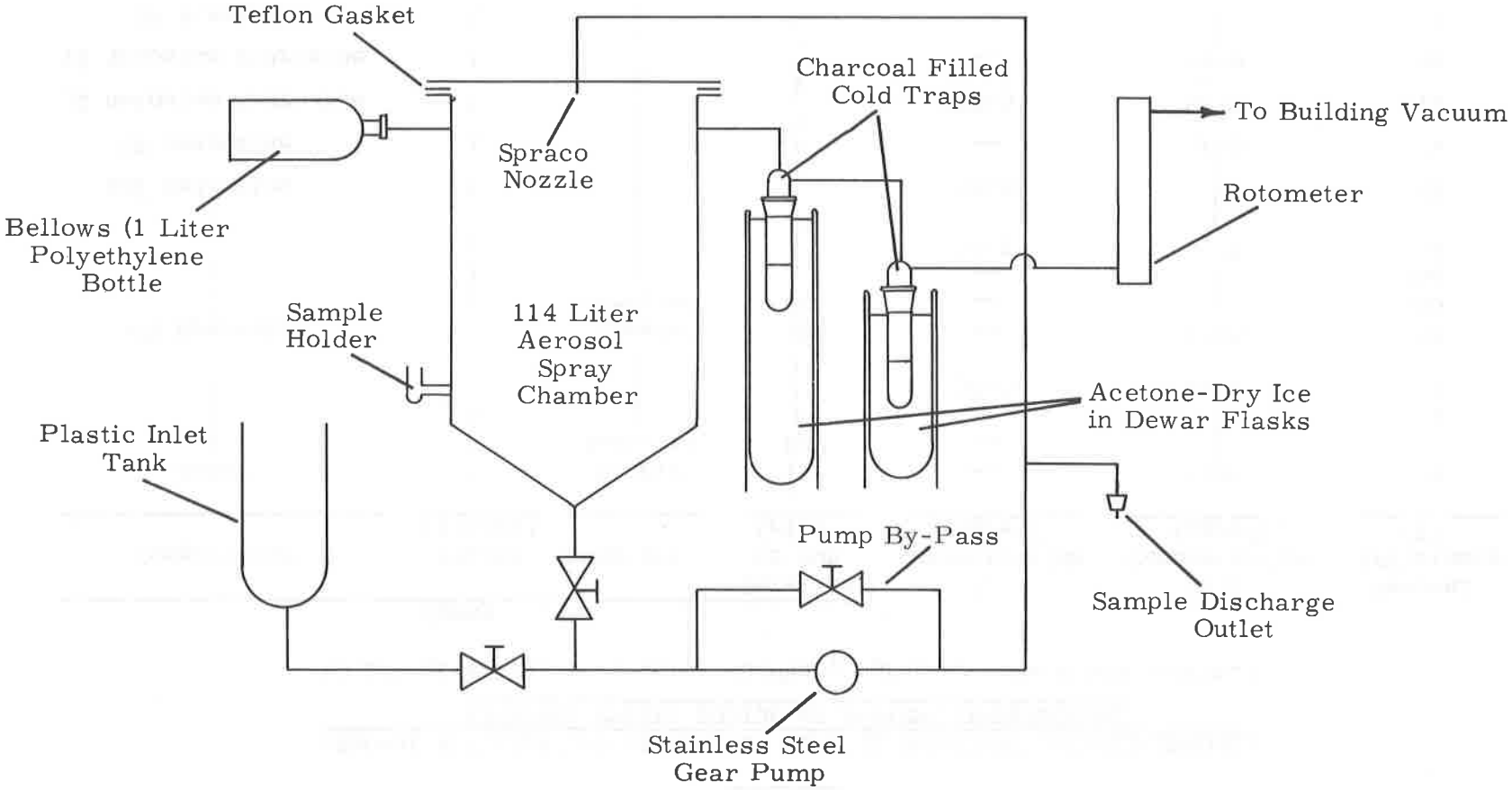


Figure 2. Schematic Diagram of 114 Liter Aluminum Spray Chamber

TABLE 4

REMOVAL EFFICIENCIES OF VARIOUS AQUEOUS SOLUTIONS SPRAYED THROUGH AIRBORNE METHYL IODIDE AT AMBIENT TEMPERATURES

(0.114 liter aluminum spray chamber, spraying rate = 400 cc/min.)

| Composition | Spray Volume (liters) | Spray Contact | Duration Of Run (min) | $I_2$ Concentration ($mg/m^3$) | $CH_3I$ Concentration ($mg/m^3$) | Removal Efficiency (%) |
|---|---|---|---|---|---|---|
| Water | 4 | Single | 12 | -- | 1000 | 5 |
| | 1 | Recycled | 60 | -- | | |
| | 1 | | | -- | | 5 |
| | 1 | | | 50.5 | 0.57 | 4 |
| 35% Hydrazine | 4 | Single | 12 | -- | 1000 | 93 |
| | 1 | Recycled | 60 | -- | | 100 |
| | 1 | | | -- | | 100 |
| | 1 | | | 50.5 | 0.57 | 99 |
| 10% Hydrazine | 1 | | | 50.5 | | 88 |
| 5% Hydrazine | 1 | | | -- | 1000 | 74 |
| 5% Ammonium Hydroxide | 1 | | | 50.5 | 0.57 | 19 |
| 1% Ammonium Hydroxide | 1 | | | -- | 1000 | 30 |
| 5% Ethanol | 1 | | | -- | | 5 |

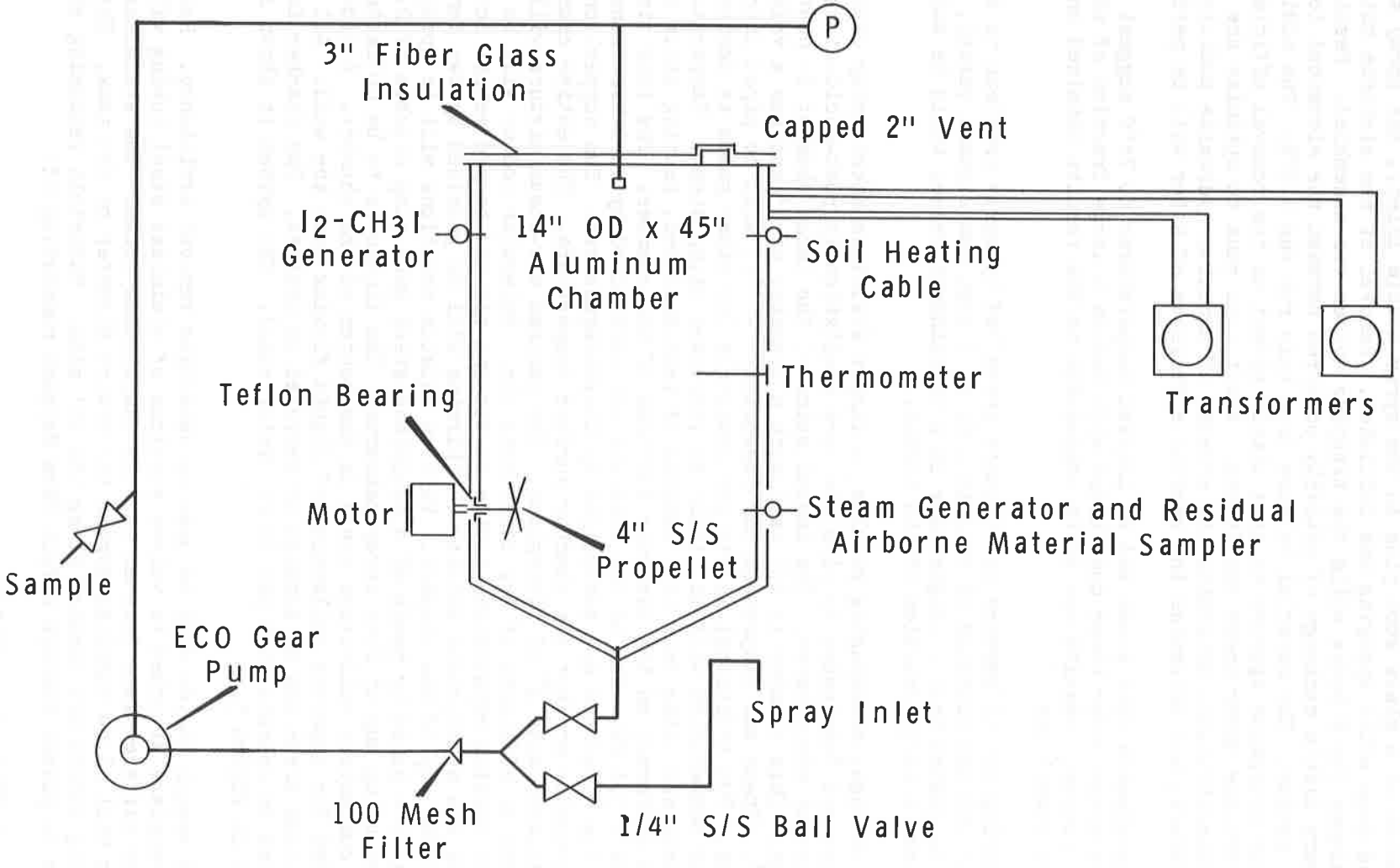


Figure 3. Schematic Diagram Modified 0.114 $M^3$ Aluminum Spray Chamber

pulled through a trapping system consisting of a fiberglass filter, 1 N sodium hydroxide in a gas washing bottle, a glass "U" tube condenser at -78°C, and a charcoal trap at -78°C. Two to three tank volumes were passed through the system. The system is shown schematically in Figure 4.

Results from the four runs are listed in Table 5. In run 1 (prior to the installation of a glass wool plug in the spray nozzle inlet), the spray system plugged soon after spraying was initiated. Removal of the airborne material was delayed for 2 hours while the trapping system was assembled. Results indicate very little exchange of activity occurred between the elemental iodine and methyl iodide. The material balance from this run was ∿ 97%. The addition of ammonium hydroxide appears to have little effect on the removal efficiency of 35% hydrazine under these conditions. Additional runs to optimize the hydrazine concentration, determine the effects of ammonium hydroxide addition and temperature, and determine the removal efficiency of water will be performed.

The experiments with steam and at initial temperatures to 75°C suggest that 35-37% hydrazine under these conditions will remove a large fraction of airborne methyl iodide. Results are quite comparable to the results obtained under ambient conditions.

Considering the difference in distance travelled by spray droplets in the 45" chamber and the distance of fall in a 65 - 70 foot containment vessel, the results suggested that a single pass in a containment vessel would be sufficient to remove a large fraction of the iodine.

Based on these encouraging results, a larger stainless steel spray chamber was designed and fabricated to simulate more realistically, post-accident reactor containment atmospheres. The installation of the large chamber is nearing completion. This chamber is 10' tall with a diameter of 4' and has a volume of ∿ 4 $m^3$. Steam and compressed air (dewpoint ∿ -50°F) will be piped into the chamber. Two additional inlets are available for other gases as desired. The chamber temperature will initially be increased using steam. Temperature will be maintained using four 110' lengths of lead-sheathed, heating cable positioned uniformly on the exterior surfaces of the chamber. The four circuits provide ∿ 3.1 KW. Two of the circuits are controlled by variable transformers while the other two are controlled by thermoregulators. Two copper-constantan thermocouples monitor the chamber surface temperature. The entire chamber will be insulated with 3" of fiberglass. The desired air-steam mixture will be obtained by additions of dry compressed air. Molecular iodine will be generated by heating crystalline iodine in flowing air and tagged methyl iodide by heating the appropriate solution. Stirring will be provided by two fans located at the top of the chamber. Various aqueous solutions will be sprayed through the gases by means of a stainless steel gear pump capable of 2.5 gpm at 100 psi using any of four spray patterns. The liquid is to be collected in three concentric collection areas in the bottom of the chamber. A trough is provided for separate collection of liquid flowing down the wall. All four collection areas can be sampled or recycled as desired. The chamber is constructed to operate at 1 psi (a 24" water seal). The system is shown schematically in Figure 5.

Tagged methyl iodide will be used to determine removal efficiency. Heated Maypack samplers attached to valved sections of stainless steel tubing will be used to differentiate between various radioiodine forms. The stainless steel tubing will allow sampling across the entire diameter of the tank. Three sampling points are located along the 10' side. Materials remaining airborne are to be passed through a full flow Maypack consisting of:

a. A fiberglass filter.
b. A water cooled condenser.

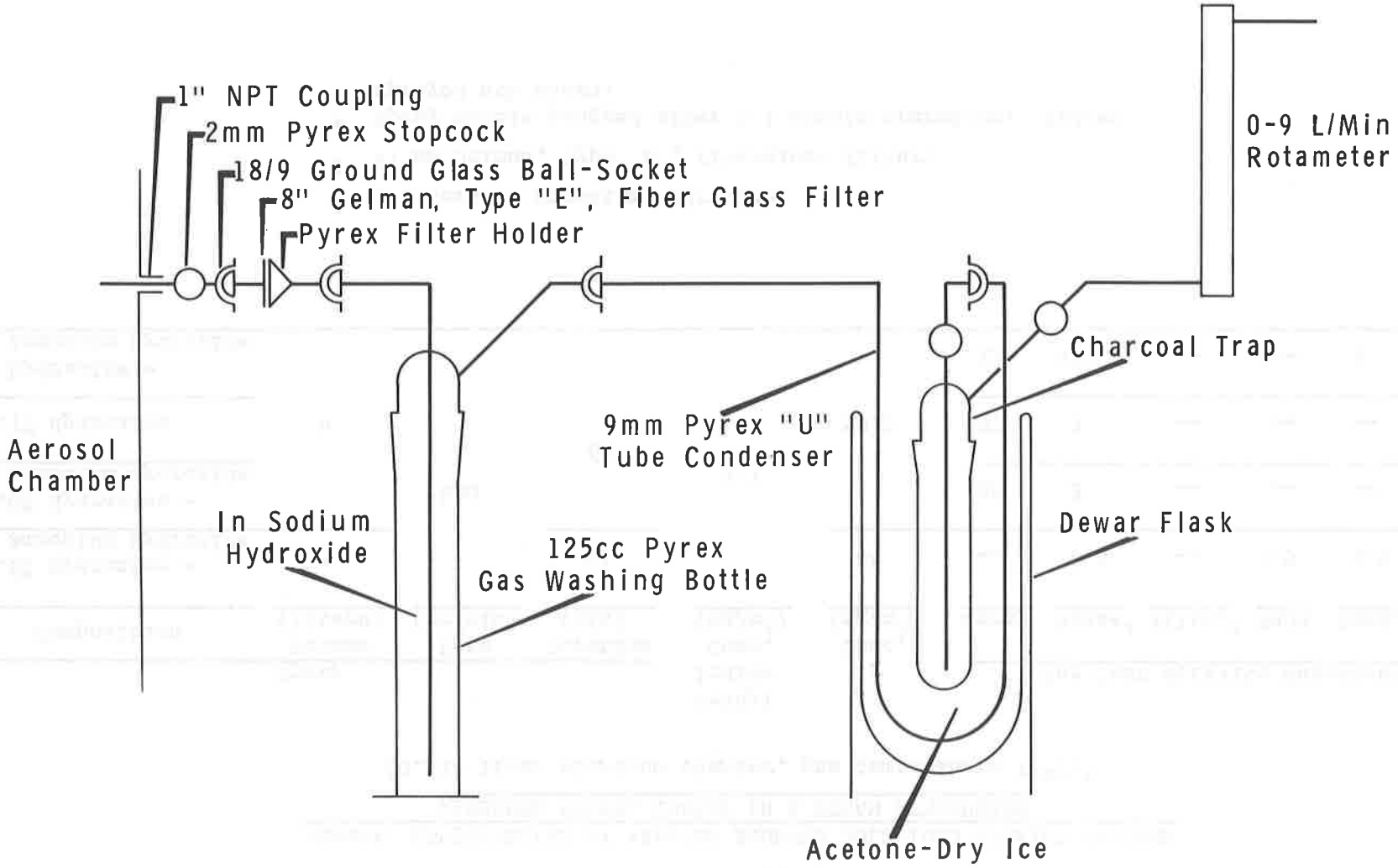


Figure 4. Schematic Diagram Iodine Trapping System

TABLE 5

REMOVAL EFFICIENCIES OF VARIOUS AQUEOUS SOLUTIONS SPRAYED THROUGH AIRBORNE METHYL IODIDE IN A STEAM ATMOSPHERE

(0.114 liter aluminum chamber, gas temperature 75°C.)

| Composition | Spray Volume (liters) | Spray Rate (cc/min) | Spray Duration (min) | Methyl Iodide Conc. ($mg/m^3$) | $I_2$ Conc. ($mg/m^3$) | Per Cent Activity Recovered In: Spray | Rinse[1] | Filter[2] | NaOH | Cond. | Charcoal |
|---|---|---|---|---|---|---|---|---|---|---|---|
| 35.6% Hydrazine - 5% Ammonium Hydroxide | * | 400 | ∿1 | 1.1 | 44 | -- | 6.5 | -- | 0.5 | 9.5 | 83.5 |
| 35.6% Hydrazine - 5% Ammonium Hydroxide | 4 | | 60 | | | 98 | 2 | -- | -- | -- | -- |
| 37.7% Hydrazine | | | | | 50.5 | 97 | 3 | -- | -- | -- | -- |
| 5% Hydrazine - 5% Ammonium Hydroxide | | | | | | 75 | 12 | -- | -- | 1 | 12 |

[1] 2 liters 5% ammonium hydroxide.

[2] 47 mm Gelman, type "E", fiberglass filter.

* Spray nozzle plugged after ∿ 1 minute operation. Volume sprayed not known.

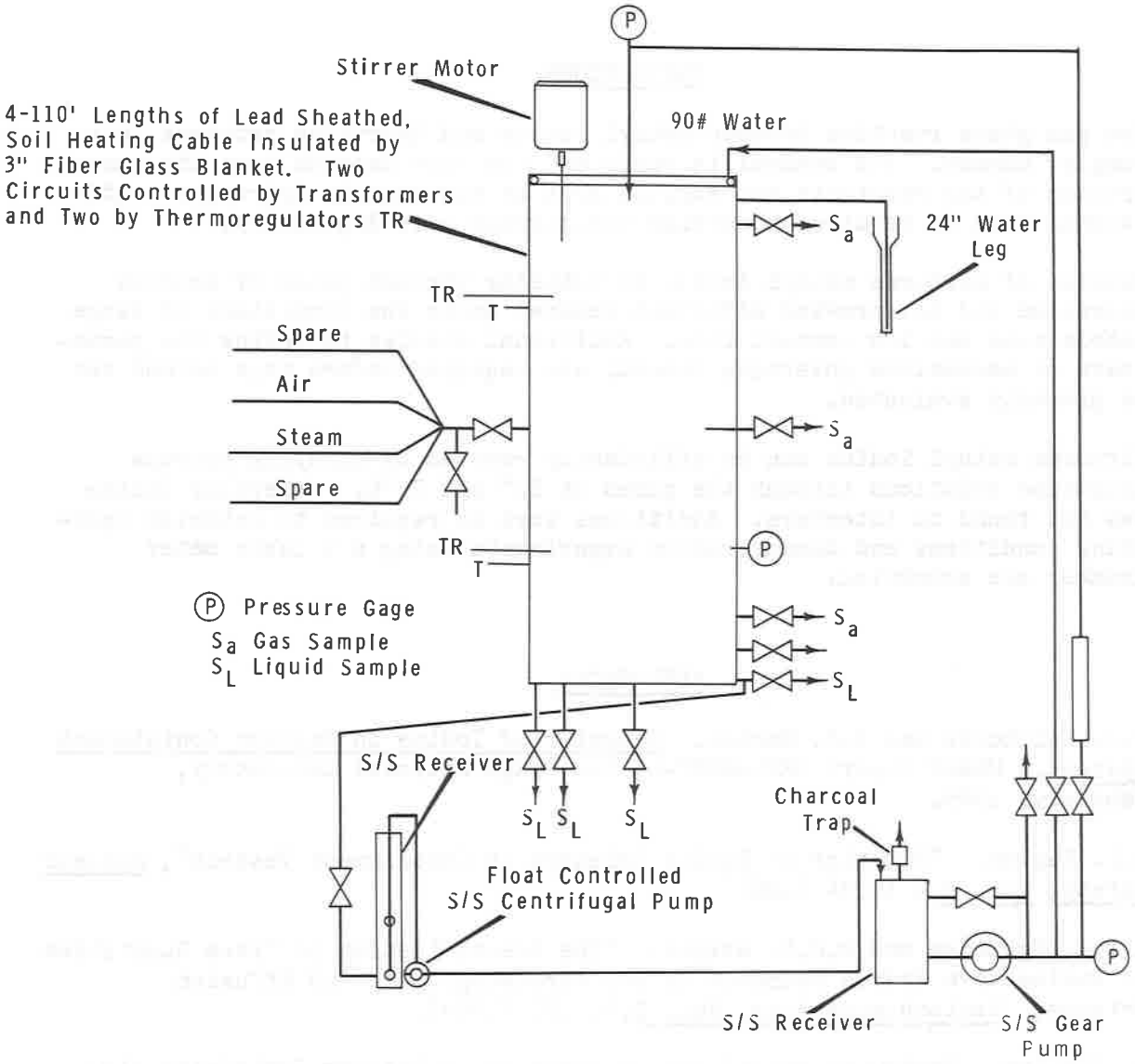


Figure 5. Schematic Diagram 4 $M^3$ Stainless Steel Spray Chamber

c. A series of silver screens.
d. A "U" tube condenser at acetone-dry ice temperature.
e. A deep bed charcoal trap.

The system is shown schematically in Figure 6. Methyl iodide diffusion to the wall and wash-out from a condensing system will be determined using the wall-washing ring located at the top of the chamber and the wall condensate trough.

## CONCLUSIONS

1. The gas phase reaction between methyl iodide and hydrazine proceeds in a complex manner. The removal is rapid and the rate depends upon the concentration of the reactants and surface area of the aqueous hydrazine. Additional work is required to define the surface area dependency.

2. Removal of airborne methyl iodide by bubbling through pools of aqueous hydrazine did not provide efficient removal under the conditions of large bubble size and low contact time. Additional studies to define the parameters or mechanisms governing removal are required before this method can be properly evaluated.

3. Airborne methyl iodide can be efficiently removed by spraying aqueous hydrazine solutions through the gases at 23° and 75°C. Molecular iodine was not found to interfere. Additional work is required to optimize operating conditions and demonstration experiments using a 4 cubic meter chamber are scheduled.

## REFERENCES


1 G.W. Keilholtz and G.J. Barton. Behavior of Iodine in Reactor Containment Systems. USAEC Report ORNL-NSIC-4, Oak Ridge National Laboratory, February, 1965.

2 S.I. Kaplan. "Behavior of Iodine Released in Containment Vessels", Nuclear Safety, Vol. 5,4 : 254 (1964)

3 A.E.J. Eggleton and D.H.F. Atkins. "The Identification of Trace Quantities of Radioactive Iodine Compound by Gas Chromatographic and Effusion Methods," Radiochimica Acta, Vol. 3,3: 151 (1964).

4 J. Mishima. Review of Methyl Iodide Behavior in Systems Containing Airborne Radioiodine, USAEC Report to be published, Pacific Northwest Laboratory.

5 F.J. Viles, Jr., Harvard Air Cleaning Laboratory, personal communication, 1966.

6 J.G. Burtle. "Vapor Pressure Composition Measurements on Aqueous Hydrazine Solutions," Industrial and Engineering Chemistry, Vol. 44,2: 1675 (1952).

7 C.C. Clark, Hydrazine, 1st Ed., pp 19-22, Mathieson Chemical Co., Baltimore, Maryland, 1953.

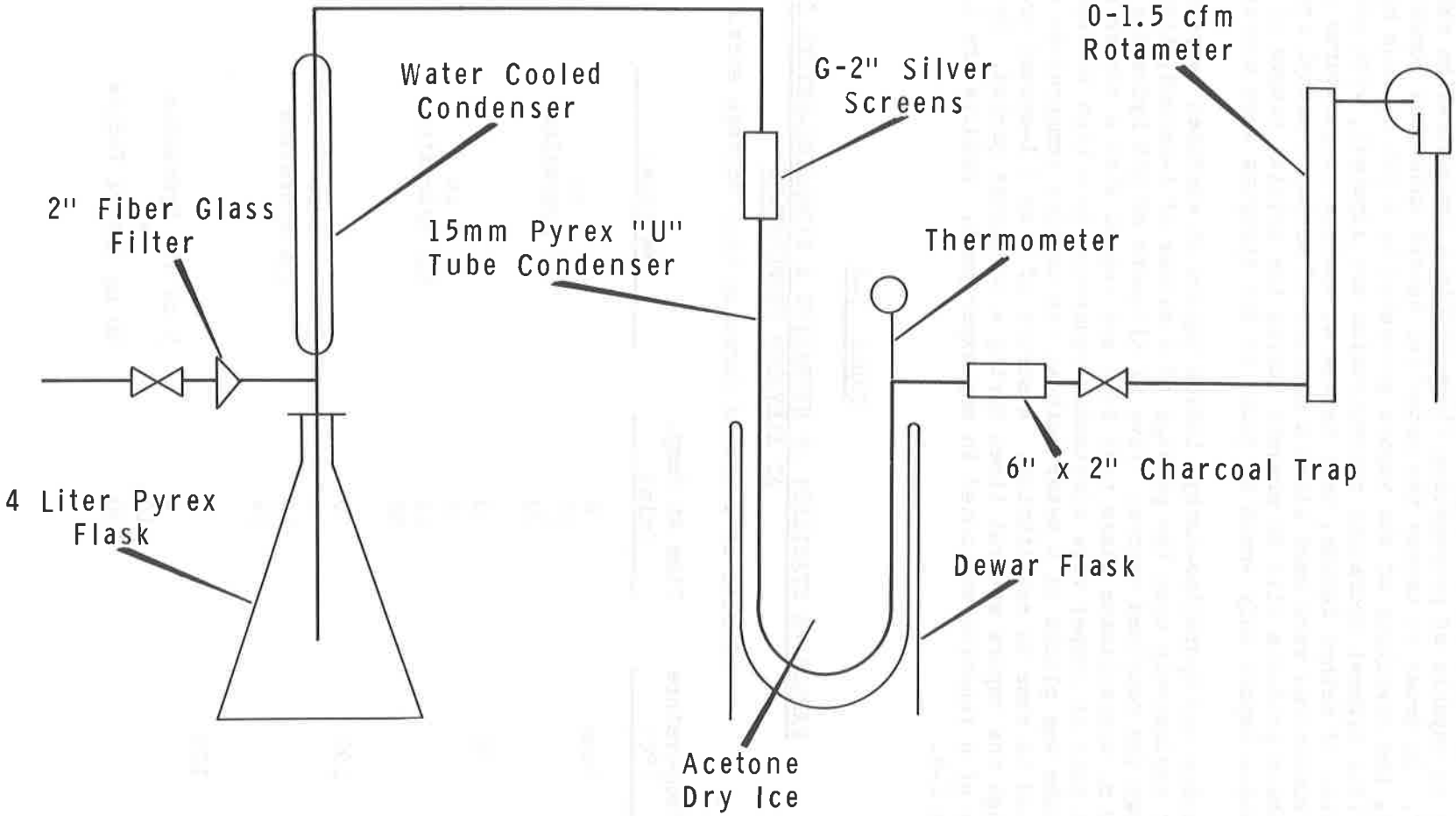


Figure 6. Schematic Diagram Proposed Full Flow Maypack

## APPENDIX

### The Chemical Stability of Aqueous Hydrazine Solutions

At 104° to 135°C and roughly atmospheric pressure, hydrazine vapor mixed with water is capable of propagating flame within a concentration range of 30.9 to 100%*. In order to assess the potential hazard under the conditions of our study, the stability of the vapors generated by a 35% aqueous hydrazine solution (the highest hydrazine concentration anticipated), with and without the addition of methyl iodide, were tested at various temperatures up to 100°C. Both conditions were used since a mixture of airborne methyl iodide, hydrazine and their products will be present during the initial stages of a run while hydrazine vapors only would be found if the spraying were successful.

Hydrazine and hydrazine-methyl iodide vapors at elevated temperatures did not react explosively upon the passage of a series of 1-second, high voltage arcs through the confined vapors. Five ml aliquots of 35% hydrazine were placed in a 100 ml borosilicate glass test tube and capped with a rubber stopper containing a pair of copper wire electrodes connected to a high voltage transformer. The tube was placed in a water bath at the testing temperature and the vapor allowed to come to equilibrium. A series of 3 to 5 1-second arcs were passed through the vapors several times during a 30 minute period. No visible evidence of a reaction was noted in any experiment. Results are listed in Table I-A.

TABLE I-A

EXPLOSIVE STABILITY OF HYDRAZINE & HYDRAZINE-METHYL IODIDE AT ELEVATED TEMPERATURE

(Series of 1-second duration high voltage arcs.)

| Temperature (°C) | Time At Temp. (min) | Material | Observation |
|---|---|---|---|
| Room | 0<br>10<br>30 | 5 cc<br>35% Hydrazine | No reaction |
| 75 | 0<br>6<br>11<br>30 | 5 cc<br>35% Hydrazine | No reaction |
| 100 | 0<br>6<br>12<br>24 | 5 cc<br>35% Hydrazine | No reaction |
| 100 | 0<br>6<br>10<br>30 | 5 cc 35% Hydrazine<br>+<br>50 µg Methyl Iodide | No reaction |

* H.F. Coward and G.W. Jones. Limits of Flammability of Gases and Vapors, Bulletin 503, Bureau of Mines, U.S.Government Printing Office, (1952).

## DISCUSSION

NOBLE: I would like to direct my question to the author of the last paper, Mr. Mishima. I notice in the paper that your studies are carried out at a temperature of approximately 50° C. Now, on large power reactor containment systems, we would be operating at pressures from 40 to 60 PSI for design and temperatures from 125° to 140° C. Are you planning to run any tests under these conditions?

MISHIMA: Well, the runs shown at elevated temperatures were at 75. I have run one at 100° C. We find the increase in temperature aids the removal of methyl iodide.

BERNARD: This is directed to both Messrs. Viles and Mishima. With the action time shown, of about 18 hours, 60 hours, you get 95% to 99% removal; what application does this have to the reactor accident? Can we afford to wait this long to obtain the noted removal; can we afford to utilize this much time to have the reaction go to completion?

MISHIMA: Our experiments are run for 60 minutes. The values that I gave on the elevated temperature were for a 60-minute run using five weight percent hydrazine. At an initial temperature of 75° C, we get between 95% and 98% removal within four hours; and this is using a 45" tank. If you extrapolate, consider it takes 15 minutes to spray four liters of solution in my pump, then it's equivalent to, as best as I can make it, one fall through the 70-foot reactor containment sphere, and so I would feel that the time for removal of the spray is very short, really.

VILES: The experiments I described were long-time experiments under the static condition. The point to be noted here is that the reaction probably is fairly rapid, relatively speaking, but there is a time factor that is required to have the aerosol diffuse, settle, and remove itself from the gas phase, and I think most of this time is devoted to that second phase and not to the initial reaction.

The first time an analysis was conducted, was overnight. We were trying to see that there was, in fact, a complete removal.

On the dynamic systems, we have much better, much shorter times for the removal because we have mixing going on. The unsymmetrical hydrazine experiments, methyl iodide was a dynamic system. The time for this test I have forgotten; it is a matter of hours. In the report you will note it isn't an 18-24 hour period.

The point, I think, that should be made here is that the work has not been completed by any means. Certainly, we want to see how rapidly we can remove the aerosol by having the reaction occur and then filter

the air stream. Most of the static studies did not involve any filtration, and this is why it took so long to get the removal efficiency result by settling. But, actually, in the containment that we had, we would have reaction occur within a reasonable period of time, I would say a matter of an hour, till we start cleanup, if we had the filtration system to remove the aerosol which should have formed in that period.

PARKER: In summary, I would like to comment that you haven't heard the worst yet. I think Mr. Ackley will give you a little something to worry about this afternoon. Everybody has a solution to the methyl iodide and, of course, methyl iodide is the major form that is hard to control. I think it is a credit to the chemists working on the program that solutions have come up as quickly as they have.

THEOS THOMPSON
Professor of Nuclear Engineering
Director of MIT Reactor

The education, ability, and the contributions of our speaker today are very well known. Really, he needs no introduction in my opinion.

He is a member of the American Academy of Arts and Sciences and the National Academy of Sciences, the General Advisory Committee to the Atomic Energy Commission and its Past Chairman, Past President of the American Nuclear Society; he is this year's winner of the Perkins' Award of the American Chemical Society and many other awards that are far too many to mention here.

I wanted, indeed, just to tell you a story about him. I wanted to say a word about the way he was introduced into the atomic energy field.

As many of you know, he served from 1943 to 1946 as the man in charge of Process Design for the gaseous diffusion plant at Oak Ridge, one of the most fundamental parts in our wartime atomic energy effort. I understand from others that his introduction to atomic energy went something like this: The laboratory at Oak Ridge was sent a man from Los Alamos, whose name was Edward Teller, not so well known then as now, and this man's job was to review and to stamp approval of every drawing which came through the office. These drawings began to pile up. Edward Teller received them in his office but he didn't send any out, and very soon the project began to grind to a halt because there were no drawings with which to work. Finally, Edward Teller came out of his office one day and he said, "I must go on a trip." He went away and came back and immediately called in several people, including Manson Benedict, to his office.

He said, "Now, I have received permission to tell you what the problem is. The difficulty is that I really am not familiar enough with blueprints to know how to read them, and I, at the same time, could not tell you what we were really hunting for because of secrecy problems and, therefore, I was stuck.

But, now," he said, "I have received permission to tell you what fission is and what we are hunting for," and he described then the process of fission and the chain reaction. He described why they were hunting for enlargements in pipes and collection regions of that sort where a critical mass could occur. He described what to hunt for and, of course, everyone else in the room except Edward Teller could read blueprints. Right away the pile vanished from his desk and things got started. This was Manson Benedict's introduction, so far as I know, to the real secrets of atomic energy.

In my own personal opinion and those of many of my friends, the development of the gaseous diffusion plant was as much a part of one effort that has led us into this era as anything that has been happened. To my best knowledge, Manson Benedict was one of, if not the principal leader of, that entire project.

I want to make one brief comment in another area. He came to MIT in 1951 and there started and developed the Nuclear Engineering Department as it stands today at MIT. In my own opinion, the Nuclear Engineering Department is primarily his creation. He taught most of the courses first, he set the standards, and he has developed a high espre that we have in nuclear engineering. To my way of thinking that is one of his great contributions.

Along the way, he somehow managed to find a chance to be a member of ACRS (Advisory Committee on Reactor Safeguards to the AEC). He is now a member and Past Chairman, as I said, of the General Advisory Committee. Therefore, he is extremely knowledgable up to date in the field of nuclear reactors. He has just come back from Europe a few days ago, after a very infirmative review of fast reactor developments there.

He is not only a scientist and an engineer. He is a lover of nature; he likes his summer and he also likes the winter, which is unusual. The first snowfall is something that he used to really enjoy, but I think in the last few years, he has had some doubts about this. He is one of the world's greatest golf bugs, and he misses hardly any opportunity to play golf. In fact, I too enjoy the fact he is a golf bug, because this means I can play a little golf, too, you know since I am in his department.

He is a real friend, a man of great understanding and a man of great knowledge, and one handful of real pioneers who has given life to the nuclear age. Manson Benedict.

MANSON BENEDICT
Professor and Head of Department of Nuclear
Engineering -- MIT

Thank you, Tommy, for your most kind and appreciated introduction. I should say in return that if the planners for this meeting had really known where to find a well-informed and authoritative speaker on nuclear reactors, they would have asked Tommy, the man who introduced me, rather than myself, to speak about nuclear power projects because of the vantage point of his membership on the Advisory Committee on Reactor Safeguards. He is in the position to see every reactor project that comes through, and he understands and contributes to the development of this very important field. But, I will do the best I can as sort of a second-hand observer on what is going on in nuclear power. Tommy's reference to my trip abroad gives me an opportunity to tell you a little bit more about planning for it.

This trip was the idea of Mr. William Webster, President of the New England Electric Company and a fellow member with me of the General Advisory Committee. He had an invitation to give several lectures in Europe and thought it would be interesting to visit power reactors and power reactor development centers in Europe before his special engagements came along. It was my good fortune to be invited to go along with him, and we mapped out a program which took us to seven different reactor development centers or power reactor installations.

As it turned out, the first one of these installations was at Dounreay at the extreme northern tip of Scotland. I probably don't have to tell you that this was all I needed to know in order to suggest to me where and how I should spend the two weeks' vacation this summer that I was able to take. You guessed it! My wife and I toured the golf courses of Northern Scotland before visiting Dounreay and other reactor centers.

I am very glad to have the opportunity to speak to this group today for a number of reasons. Perhaps the most important one is that the invitation to speak today was extended to me by Leslie Silverman, for whom I have a great admiration and whose loss I regret just as keenly as I am sure you do. I hope that I may be in a sense paying my respect to Leslie by speaking before you today.

The other reason why I am glad to be with you today is I feel that this group, the air cleaning fraternity, has made many important contributions which has brought nuclear power to where it is today and has many more additional contributions which it will have to make in order that this development may come to its full fruition. I will try to bring this out later in my talk.

In the brief time that I have to speak to you today, I am going, first of all, to outline very hurriedly some of the dramatic advances that have been taking place in nuclear power, both in this country and abroad. Then I would like to mention a few of the problems which have to be solved as nuclear power continues to expand, some of which are right down the alley of the air cleaning fraternity.

Actually, most of the dramatic advances in nuclear power have taken place since the previous conference of this series, which, I understand, was held in 1963. At that time, it was generally thought that nuclear power was feasible, and a few plants were being built, but the costs were high. Costs of the order of 5 1/2 or 6 mills per kilowatt hour were quoted, and this still priced nuclear power out of the competitive market, except in a few locations in the country very remote from fuel sources. New England was perhaps one of them; California was perhaps another. But it was pretty clear that nuclear power wouldn't penetrate very much into the utility market unless costs could be brought down by 25 percent or so.

What happened then was that the experience gained with a few of the pioneering plants, notably, Shippingport, Dresden and Yankee, gave equipment manufacturers sufficient knowledge so that they could tell where the plants were over-designed, where the belt-and-suspenders type of safety engineering was no longer required, and where costs could perhaps be reduced in the next generation of reactors.

In addition it took a very forward-looking attitude to realize that if prices were reduced markets would develop, production would go up and, because of the increased volume of sales, lower costs would become attainable.

Whatever the reason was, the Jersey Central Power & Light Company asked for bids on a new power station to be built on the Atlantic Seaboard about 100 miles South of New York. The equipment suppliers came in with such low prices for nuclear power plants in direct economic competition with coal-fired plants that the Jersey Central Power & Light Company was able to convince itself and its stockholders that it would have a cheaper source of electricity generation by buying a nuclear plant than by buying a coal-fired plant at a location only some 300 miles from the Pennsylvania coal fields.

The Jersey Central Power & Light Company put out a report which has become almost a bible in the economics of nuclear power, which showed that a coal-fired plant would cost $110 per installed kilowatt and would generate electricity for about 4.2 mills per kilowatt hour averaged over the life of the plant, whereas a nuclear plant, whose capacity at that time, and still is, somewhat uncertain but would lie between 515 and 620 megawatts, would cost somewheres between $132 or $110 per kilowatt, depending upon whether or not its increased capacity or design capacity was reached. This makes its initial cost somewhat higher than coal, but the cost of electricity from it would be in the range of 4.1 mills down to 3.7, depending on whether its capacity was at the lower or upper end of the range I mentioned.

This gave the nuclear plant a clear enough margin over a coal-fired plant so that in a part of the country where no one had thought nuclear power could be competitive, it clearly was.

These cost figures were based on a 30-year plant life and a 6.4 percent return on investment, and they don't include a charge for local taxes which comes to about 10 percent. Even so, comparatively, nuclear power evidently made the grade here.

There are some who thought that this was just a flash in the pan; that G. E., the winner of the competition for this plant, had priced the plant below cost and that it couldn't happen again. Well, the interesting and important thing is that it has happened again; it has happened again a good many times since the Oyster Creek Plant was announced. There have been 29 large nuclear, power units placed on order with more than 20,000 megawatts of electric capacity. This is about 10 percent of the entire generating capacity in the United States at the present time; and this has all taken place in just about two years.

The total volume of sales involved here is over two billion dollars. Even more dramatically, during the last few months in 1966, from 40 to 50 percent of all new power generating capacity in the United States has been nuclear, in contrast with the very small amount that was being ordered prior to this time.

This boom in nuclear power sales reached a climax with a recent announcement by TVA, which had conducted an even more thorough exercise than Jersey Central Power & Light, on the relative costs of electricity from coal and from nuclear plants.

TVA had invited competitive bids on 2,000 megawatt units of either coal-fired or nuclear-fired capacity, and investigated the possibility of making long-term contracts either for coal on the one hand or for nuclear fuels on the other hand. They issued a very impressive report, very completely documented, with quite firm guarantees on what nuclear power costs and nuclear fuel costs would be, which showed a very marked advantage for nuclear power in their part of the world.

The thing which is remarkable about this is that TVA's plants are next door to some of the lowest cost strip-mined coal in the United States.

To summarize the TVA figures, the unit cost of these two types of plants were just about the same; they showed a unit cost of $117 per kilowatt for a coal-fired plant and $116 for nuclear. These were just about a standoff. But nuclear fuel costs were so much lower than coal costs, even in this part of the country, that when figured in terms of mills per kilowatt hour, the costs come out 2.9 mills for coal and 2.4 mills for nuclear power, almost a 25 percent advantage for nuclear power compared with coal.

The conclusion should not be drawn from these figures that suddenly nuclear power costs have gone down from 4.1 mills for Oyster Creek down to 2.4 mills for Tennessee Valley, because TVA, not being an investor-owned utility, is a government agency and is able to obtain its money at a 4 1/2% return on capital. Also TVA has based its costs on a 35-year rather than 30-year plant life.

If TVA's analysis had been made on the same basis as Jersey Central's, these costs would have been above three mills. Nevertheless, this is a clear demonstration of two things: That almost everywhere in the country, nuclear power is cheaper than power from coal, and that nuclear power costs are still going down.

Now, because of this spectacular reduction in the cost of nuclear power, there is great optimism about the extent to which nuclear power will be introduced as the electric generating capacity of this country is increased still further. You hear utility executives in parts of the country like New England and California predicting that there will be very few, if any, coal-fired plants built in those parts of the country. There will be some hydro expansion, but much of the new capacity will be nuclear.

Various estimates have been made as to how rapidly nuclear power generating capacity in the country will increase. One which the AEC made in 1965 and which is probably on the low side already because of these favorable cost figures shows that nuclear capacity will increase from something like 1780 megawatts operating today to over 12,000 megawatts which is already on order for operation in 1970, and is thus a firm figure, to estimates of 37,000 megawatts for 1975, 92,000 megawatts for 1980, 295,000 for 1990, which is all more than all the generating capacity in the United States today, to 700,000 by the year 2000.

These latter figures are no more than really wild guesses; nobody knows how rapidly the economy of the country is going to expand and how great the demand for nuclear power, or power of any sort, will be that far in the future. But, one thing you can be pretty sure of -- most, if not all, of the large generating stations in these distant future dates will be nuclear. Through 1980, it is clear that the types of stations which will be built will be improved versions of the ones which we see coming on the line today; that almost all will be boiling water or pressurized water reactors.

Other reactor types are under development at the present time and have certain technical advantages over water reactors, and there is hope that the costs of these other types can be reduced. But it takes a long, long time and a great deal of development effort to bring a new type of reactor to dependable, reliable, low-cost operation; and it is pretty clear, I think, that it will be at least the late 1970s before we have any substantial amount of other types of reactors.

I should say why work is being done extensively on other types of reactors. There are two rather serious drawbacks to the light-water reactors which are in use today, even though they produce electricity at low cost. They do it at low thermal efficiency, only about 30 percent as compared with 40 percent for modern coal-fired stations. Even more seriously, a light-water reactor can utilize only one percent of the atoms in natural uranium before the uranium is too depleted for further use. You have to disregard the rest of the fuel. This makes rather poor use of a natural resource which is still in somewhat limited supply.

So, other types of reactors which may make better use of natural uranium and may have higher thermal efficiency are being developed in this country and abroad.

There are the so-called advanced converter types, which can utilize from two to three percent of the atoms in natural uranium and, thus, would stretch resources of uranium two or three times as far as the light-water reactors do. There is an even more satisfactory conserver of resources, the breeder type of reactor, which, in theory, could utilize close to 100 percent of the atoms in natural uranium by converting it all successively to plutonium and burning the plutonium. The AEC has mounted a substantial development effort on both these types of reactors. I think it is too early today to predict the extent to which either of them will be used after 1980, but we are all very hopeful that one or the other will succeed, because there is apt to be a shortage of uranium if we do not have better means of burning it in reactors than today's type.

I will have more to say about the uranium reserve picture, later.

Now, I would like to turn for a moment to developments abroad which Mr. Webster and I had an opportunity to observe in some of the countries which are carrying out parallel development efforts and parallel expansions of power capacity to ours.

At present, England is the country which has the largest amount of nuclear generating capacity in the world; it has 4100 megawatts in operation now. This is all of the same type as the first type of reactor which was developed by the United Kingdom Atomic Energy Agency, the so-called Magnox Reactor, which is a gas-cooled, natural uranium-fueled, magnesium alloy-clad reactor. This reactor has many of the disadvantages that our light-water reactors do -- it doesn't make very efficient use of uranium and it has a low thermal efficiency; and, as we will see in a moment, it has rather high costs. So, the U.K.A.E.A. has developed a better type of reactor called the Advanced Gas-Cooled Reactor; or, for short, the AGR. One AGR unit is being built. This is a twin-reactor, 1200 megawatt station called the Dungeness B Station. There are plans to introduce 8,000 megawatts of additional capacity by 1975. In the AGR Reactor, slightly enriched uranium fuel clad with stainless steel is used, gas temperatures are higher, thermal efficiency is higher, and costs are definitely lower than with Magnox Reactors.

The U.K.A.E.A. and its captive customer, the Central Electric Generating Board in England, which produces all of the electricity South of the Scottish border, issued a report comparing the costs of electricity from different types of plants in England, which is also something of a landmark in nuclear power development. This showed natural uranium Magnox Reactors producing electricity at 7.3 mills per kilowatt hour; a modern coal-fired plant in England producing electricity for 6.1 mills per kilowatt hour; a boiling water reactor of the type which TVA and Jersey Central have ordered in this country, but supplied by British manufacturers working under license with G.E., producing electricity for 5.6 mills per kilowatt hour, well below coal; but, the advanced gas-cooled reactor coming in at a slightly lower figure of 5.4 mills per kilowatt hour.

This comparison indicates that the first Magnox reactors are not economic. It has convinced the Central Electric Generating Board that the A.G.R. type reactor is the type which will produce electricity at the lowest cost on their system, and they plan and hope to build additional units of this type.

Now, you may wonder why a higher figure was given for the boiling-water reactor in England than the lower figure quoted, for instance, by Jersey Central down in the 4 mill range. This is partly due to an apparent markup in prices which occurs when United States technology has to be relearned and offered by British firms, but it is partly due, also, to a cost penalty which the CEGB assessed to the light-water reactors because of the fact they have to be shut down for two weeks or more for refueling, at which time they have to buy power from some of their more costly coal-burning stations, and this constitutes an economic penalty for the nuclear power stationswhich have to be interrupted.

The gas-cooled reactors have the advantage of being refueled continuously while in operation and never having to be shut down for this cause. The Central Electric Generating Board has quite extensive plans for increasing nuclear capacity. By 1980, they estimate that they will have some 30,000 megawatts of nuclear capacity in operation.

There is one other difference in the British program, and it is an important one. The development of breeder reactors in England is proceeding on a more rapid time schedule than in the United States, and I would say at a more advanced stage. It has been made a matter of national policy to go into this development with the expectation of having at least one commercial plant in operation by 1978. The CEGB is keeping open the possibility that some of the units to be installed in the latter part of the 1970s will be of the fast-breeder type. There is very little possibility that this will occur in the United States because our own program is not that far advanced.

In the U.K.A.E.A., construction has already started on a prototype fast breeder reactor, a 300 megawatt, sodium cooled, plutonium fueled, fast-breeder reactor to be built at the remote site in Northern Scotland, which was the excuse for my golfing vacation.

The hope is that this plant will operate so dependably and so reliably that it will confirm the feasibility of this concept and the favorable low-cost estimates which have been made for it. If this turns out to be as successful as its developers in England hope, we can expect that sodium-cooled reactors will start to operate in England by the late 1970s.

After England and the United States, Germany is the country of the Free World expected to make the next heaviest use of nuclear power.

At the present time, very little nuclear power capacity is in operation in Germany. They have a small, U. S.-designed boiling-water reactor and a small German designed heavy-water reactor, and these are all that are producing electricity. This is due to the fact that for a number of years after the war, German science technology wasn't allowed to work in the fission field at all. The Germans are making up very rapidly for the delay which was put in their way; they have turned some of their best scientists over to development of nuclear power and the big German industrial companies are very heavily committed to nuclear reactor development. They have an excellent national laboratory at the Karlsruhe Center for Nuclear Research, and they are rapidly closing the gap between German technology in this field and the United States.

The predictions for Germany are that nuclear power capacity will increase to 1200 megawatts in 1970, 9,000 in 1975, and 23,000 in 1980. This is about a quarter the amount that we predict for the United States at the same time.

Germany, like England and like Russia, is very active in fast reactor development. We were impressed to see the good program, both of experimental development work and engineering design, which was being undertaken at Karlsruhe in support of fast reactors in Germany.

The Germans have made a decision already and have started down the road towards building not one but two fast reactor prototypes, one of them a sodium-cooled reactor quite similar in general concept to the British design and to the one which is being worked on in the United States, and another which is cooled

by steam. The steam-cooled reactor has a good deal of appeal for the German industrial firms which have been working on water-cooled reactors because they feel that it will be easier to translate their knowledge to a steam-cooled fast reactor than to one which is cooled with sodium. Another German group headed by Siemens-Schuchert interests is working on the sodium-cooled reactor and has equal optimism about success in this development. A thermal efficiency over 40 percent, doubling time under 10 years and low costs are predicted. It is likely that these optimistic estimates will be somewhat disappointed when the first reactors come on the line. That was the experience with light-water reactors, but it is certainly possible, and I think even likely, that with the amount of intensive effort which is going into them now fast reactors will ultimately prove to be the wave of the future in the reactor field.

Now, just a word or two about where the rest of the Free World stands. It would take far too long to attempt to describe every national program, but you do find a considerable variety from country to country.

In France, where nuclear power development and electricity production are both state monopolies, nearly all of the power reactors are of the gas-cooled, natural uranium type, not too different from the type found uneconomic in Britain. The French think they can improve the efficiency and lower the cost of these reactors by going to a new type of fuel element, in which the uranium is formed as a tube rather than a solid rod, and they are continuing down this line of development.

In Canada, India, and Sweden, most reactors are of the heavy-water type, cooled and moderated by heavy water and fueled with natural uranium.

In Italy and Spain, several types of reactors are used; some are of the natural uranium type, and others use enriched uranium.

Just to conclude this kind of statistical account, by 1980 it is estimated that the total nuclear generating capacity in the Free World will be some 237,000 megawatts, which is a little more than the total generating capacity in the United States at the present time. This will be divided, roughly, the United States, 38 percent; United Kingdom, 14 percent; Germany, 10 percent; and the balance of the Free World, the remaining 38 percent.

One has to ask himself the question, is there enough low-cost uranium to support this rapid expansion of nuclear power? I will try to answer the question for the United States; but, in answering it for the United States, you can draw about the same conclusions for the Free World because the estimated United States reserves of uranium are about 35 percent of the reserves of the world, which is also about the ratio of the estimated generating, nuclear generating capacity in this country compared to the rest of the world.

The AEC has estimated that some 800,000 tons of uranium can be mined in the United States for less than $10 a pound, and that another 900,000 tons can be mined for less than $30. The present price is $8 a pound.

If we estimate the uranium requirements for the projected increase in generating capacity in the United States, all of the $10-a-pound uranium would be used up by 1995. If we had only light-water reactors, all of the $30-a-pound uranium would be used up shortly after the year 2000.

Increase in uranium price to $10 would add about a tenth of a mill per kilowatt hour to power cost. This, we could stand. In short, I am saying we have enough uranium to carry us through till 1995, even if we don't get better types of reactors. But the increase in price of uranium to $30 a pound would add over one mill per kilowatt hour to the cost of power and would probably put nuclear power out of competition with coal again; thus, something needs to be done to develop either more supplies of uranium at low cost or better reactors, if, beyond 1995, we are to have enough uranium to go around.

The advanced converter reactors would carry us sometime into the future, to after the year 2000, without running out of uranium. The cost of power from advanced converters is not as sensitive to the price of uranium because they don't use so much to make electricity. Advanced converters would help, but they wouldn't be the last word either. To obtain assurance of uranium for an unlimited time and unlimited expansion of capacity, we need the fast breeder reactor, and that is the reason why I attach so much importance and significance to the work which is being done in England and Germany.

While I am glad that a substantial effort is being made in the United States, I can't help feeling regret that our own program hasn't reached the program where construction of some sort of a demonstration fast reactor has been authorized. It is only by going into a full construction project that you learn to make a real reactor that can be built and run successfully, that you can be sure you have identified all the problems. I'm afraid that if we don't take this step soon, we'll be in the position of having the British and German equipment manufacturers able to offer fast reactors to American power stations before our own manufacturers can.

I have already mentioned that the British expect to have their prototype fast reactor operating in 1971; Germany expects to have its on the line in 1973; and the Russians, who have gone out ahead of everybody here, are building a 350 megawatt fast reactor on the shores of the Caspian Sea, which they predict will be in operation as early as 1969. This is a measure of how far ahead of us these other countries are.

I have discussed reactors in this way so you can see that what types of reactors we are going to have to be most concerned with in the future. Water reactors will be most generally used for the next 15 years and probably sodium-cooled reactors after that time.

Let's see what are the most serious air-cleaning problems in connection with these two types of reactors. Water reactors, of course, can give off various forms of contamination. Most of these are minor nuisances; but,

in a serious reactor accident or in a serious fuel element failure, fission products would possibly escape from the reactor and would have to be prevented from getting into the environment.

Of the fission products, radio-iodine is the one which gives the most trouble and is the one which has to be removed from reactors effluents and ventilation air, to the most stringent levels. I was interested to note that there were a number of papers dealing with radio-iodine removal at this conference.

Gas-cooled reactors, such as are being developed in Britain, are liable to some of the same possible modes of failure as water reactors. The escape of fission products, notably radio-iodine, is the major problem that has to be guarded against.

In the case of sodium-cooled reactors, iodine doesn't appear to be as much of a problem, because even if it should escape from the fuel, it reacts with sodium and tends to be held back. The most serious air contamination problem in the event of an accident with a sodium-cooled reactor would be a large-scale sodium fire, especially of radioactive sodium. This would produce a radio-sodium aerosol, which would have to be removed to very low levels. I note that there were papers dealing with this subject at this conference.

Finally, when these large amounts of nuclear power are being generated, the reprocessing plants handling fuel from these reactors will handle much more krypton 85 than at present. It is probable that measures will have to be taken to hold back the krypton 85 and keep it until it decays before it can be released. As far as I know, this is not being done by reprocessing plants at the present time. This is another problem that air-cleaning authorities will be asked to deal with.

The last thing I would like to say about nuclear power development is that these optimistic predictions that I have made are going to depend upon favorable experience with the first reactors, upon the prevention of accidents, which would give rise to public antagonism toward nuclear reactors, and upon a solution of what is proving to be a very serious problem, that of finding suitable sites for nuclear reactors.

One sees this in Britain as well as in the United States, because suitable sites for reactors at the present time have to be remote from population centers and have to have adequate cooling water. They have to be acceptable to local residents from the standpoint of the amenities of the local situation. People don't like industrial plants in some places.

In the United States, up till now, except in California, sites have been found. Having found a site, however, there's a tendency to put additional nuclear stations on it. This is because you don't have to go through the problem of gaining public acceptance all over again for opening up a new area to this kind of development.

As an example, at the Dresden site near Chicago, three large reactors are being built; in Britain, four reactors are being built at the Dungeness site. This multiplication of reactors on a given site places stricter limits on the routine release if airborne contaminants from any one plant in order to keep the total release from the site down to acceptable levels. This, also, makes the work of the air-cleaning experts more difficult.

Another problem in siting reactors has been getting permission to run transmission lines from reactors in remote sites into the cities where the principal load centers are. Suburban people don't like overhead transmission lines, and I don't know that you can blame them. This is particularly acute in Great Britain where the population density is high and where a large portion of the land has been declared to be of national value for historic or scenic reasons. Around some of the cities in England have been set aside what are known as "Green Belt Areas," in which no industry is allowed and through which transmission lines are not allowed to penetrate except under very special circumstances.

The result is that there's strong pressure in England, and to a lesser extent in this country, for siting nuclear power plants in cities. People feel this is an inevitable development and that means will have to be found to make nuclear power stations safe enough so that they can be put in large cities withou any serious harm to the population. Among other things, this will mean that airborne contaminants released from these plants will have to be so low in concentration that even if there are a million people around the plant, over-exposure to them on a population basis will not take place.

This, I think, provides the strongest challenge to air-cleaning experts. Engineering designs are being made of new containment schemes which are thought to be sound enough, impervious enough, to provide protection for reactors in cities. But people have to live and breathe inside these structures from time to time; air will have to be discharged from them, and measures will have to be found to make this air clean enough so it won't hurt the population of a large city.

I would like to leave you with the thought that nuclear power is going to expand rapidly and that there are very severe and important problems in the air-cleaning field which will have to be solved if this expansion is to take place safely.

# REMOVAL OF RADIOACTIVE METHYL IODIDE FROM STEAM-AIR SYSTEMS*

R. D. Ackley, R. E. Adams, and W. E. Browning, Jr.

Reactor Chemistry Division, Oak Ridge National Laboratory, Oak Ridge, Tennessee

ABSTRACT

Certain specially-impregnated charcoals have been observed to have the capability of effectively trapping radioactive methyl iodide, by an isotopic exchange mechanism, from air streams of fairly high relative humidity at temperatures as high as 115°F. In the event of a nuclear reactor accident, however, the methyl iodide trapping problem may be complicated by the production of steam with attendant elevation of the air temperature. The objective of this work was to obtain applicable data under these more severe conditions. Removal of radioactive methyl iodide from flowing steam-air by impregnated charcoals has been investigated in two series of tests. Temperatures and pressures for one series were around 212°F and 14.4 psia, and, for the other series, generally around 280°F and 60 psia. According to the results obtained, $CH_3{}^{131}I$ can still be trapped effectively at these higher temperatures and, also, at the higher pressures by an appropriately selected impregnated charcoal provided the charcoal has not been damaged and provided the prevailing relative humidity in the charcoal does not exceed 90%.

## INTRODUCTION

When fission-product iodine is accidentally released into the air of a containment vessel, the iodine may assume a variety of forms. The most important of these include elemental iodine vapor, iodine adsorbed on or occluded in particles, and a generally small but often significant proportion as methyl iodide. Authorization for nuclear reactor operation may require the installation of engineered safeguards with the capability of removing practically all of the radioiodine from air thus contaminated. The problem may be further complicated by the production of steam and elevation of the air temperature as a result of the nuclear accident. Elemental iodine is readily trapped from air streams by activated charcoal, even at relative humidities approaching saturation, and iodine-laden particles may be removed by high efficiency filters. However, methyl iodide is not removed effectively from air streams by the more usual types of charcoal, unless the relative humidity is low, and it is not stopped by the filters. Consequently, considerable research has been performed in an effort to obtain a solution to this rather urgent problem. As a result, at least two successful methods for removal of radioactive methyl iodide from air streams corresponding to fairly high

*Research sponsored by the U. S. Atomic Energy Commission under contract with the Union Carbide Corporation.

relative humidities have been developed. The two methods are very similar in that they both involve the use of specially-impregnated activated charcoal for trapping the radioactive methyl iodide but differ in that they involve two very different reaction mechanisms.

One of the methyl iodide[1,2] removal methods was developed as the result of work at Oak Ridge National Laboratory. This method is based upon isotopic exchange and utilizes charcoal that, as commercially available, is impregnated with one or more iodine-containing substances. The mechanism is indicated to be as follows:

$$CH_3{}^{131}I + {}^{127}I \text{ (on charcoal)} \rightarrow CH_3{}^{127}I + {}^{131}I \text{ (on charcoal)}.$$

That is, when molecules of $CH_3{}^{131}I$ enter the charcoal bed, they encounter non-radioactive $^{127}I$ atoms of the impregnant. Some of the encounters result in exchange of the two types of iodine atoms. Thus, the methyl iodide that is radioactive when it enters the charcoal tends to be transformed into non-radioactive methyl iodide which ultimately emerges downstream of the charcoal while a corresponding amount of the radioactivity remains behind.

The other method, which utilizes the alkyl halide-organic amine reaction, was developed by researchers of the United Kingdom Atomic Energy Authority. They reported that charcoal impregnated with morpholine, piperidine, piperazine, or 4-aminopyridine was effective for removing methyl iodide[3] from air streams at high relative humidity. More recently, triethylenediamine was reported to be an especially good impregnant, as judged by its high efficiency for methyl iodide[4] removal. It also has the advantage of being relatively non-volatile, having a boiling point of 174°C.

Both of the radioactive methyl iodide trapping methods have been investigated rather thoroughly for conditions of fairly high relative humidity, a pressure of one atmosphere, and ambient or only moderately higher temperatures. However, conditions of temperature and pressure considerably higher than these have been postulated for the atmosphere in a reactor containment vessel following a certain type of nuclear accident. As a consequence, investigation of radioactive methyl iodide removal by impregnated activated charcoals has been extended so as to include tests made under more severe conditions, and the essentials of the results obtained are reported herein.

These tests may be divided into two series. Some of the more pertinent conditions that were employed in the first series of tests were: approximately 212°F and 14.4 psia, and relative humidities, with one exception, within the range 60 to 90%. Analogous conditions for most of the tests of the second series were: approximately 280°F and 60 psia, and relative humidities ranging up to 100%.

In addition to methyl iodide, lesser quantities of ethyl and propyl iodides have, on occasion, also been observed in conjunction with elemental radioiodine, but these compounds have not received very much

attention. This is because of the small amounts involved and because removal methods for radioactive methyl iodide would generally also tend to be applicable to the removal of radioactive ethyl and propyl iodides.

## DESCRIPTION AND IDENTIFICATION OF THE ACTIVATED CHARCOALS

The following will more fully identify and describe the various activated charcoals that are concisely designated in subsequent sections of this report.

| Activated Charcoal(s) | Description |
|---|---|
| MSA 85851 | This is an impregnated charcoal from Mine Safety Appliances Company and is the material that was used in the early tests where radioactive methyl iodide removal due to isotopic exchange was observed. Several different lots, all 8-14 mesh, have been tested. Except to say that the charcoal is impregnated with one or more iodine-containing substances, the nature of the impregnation is not precisely specified here due to proprietary considerations. A similar remark is also applicable to the other commercially impregnated charcoal. |
| BC-727 | This charcoal, 8-14 mesh, is from Barnebey-Cheney and is impregnated with iodine-containing substance or substances. |
| PCB | This charcoal, unimpregnated and, as used in this work, either 6 x 16 or 12 x 30 mesh, is from Pittsburgh Activated Carbon Company. |
| Laboratory-impregnated Charcoals | A few of these have been prepared and tested. The method of impregnation consisted of immersing the base charcoal, which was PCB, in a solution of the impregnant, stirring, and allowing the solvent to evaporate. An example of the manner of designation for a laboratory-prepared impregnated charcoal follows: 5% $I_2$, PCB, 6 x 16, corresponding to percent by weight and nature of impregnant, base charcoal, and mesh size, respectively. |

## RADIOACTIVE METHYL IODIDE REMOVAL TESTS AT TEMPERATURES AROUND 212°F

The way in which each of these tests was conducted is illustrated in Fig. 1. The charcoal in the test beds was pre-equilibrated with respect to moisture content by passing air at the relative humidity for the test through the charcoal for a sufficient period of time prior to methyl iodide injection. The three test beds, all with a diameter of 1 in., were,

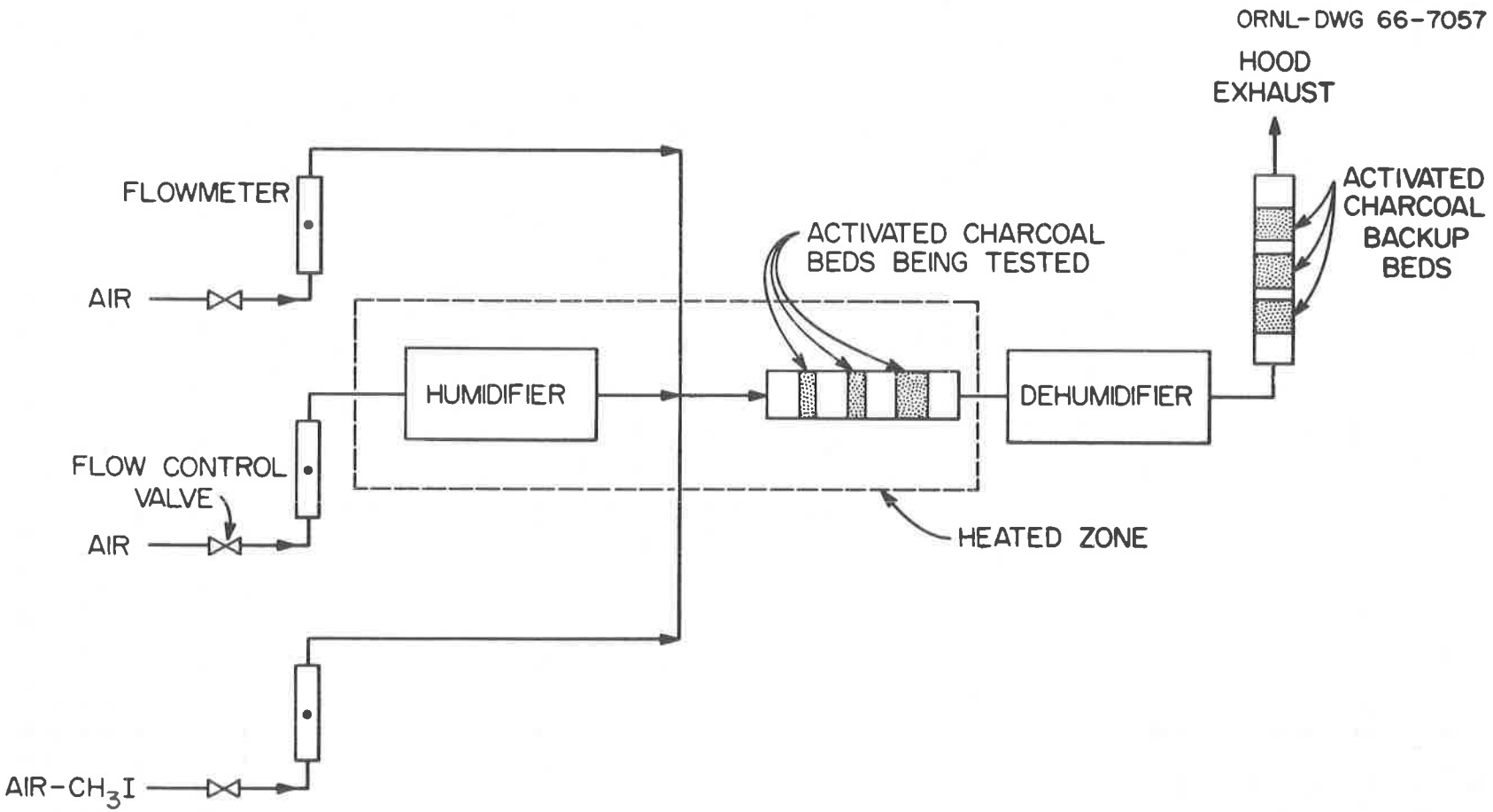


Fig. 1. Simplified Drawing of Setup for Investigation of Removal of Radioactive Methyl Iodide from Flowing Steam-Air by Impregnated Charcoals at Temperatures Around 212°F.

successively, 1/2, 1/2, and 1 in. in depth. Methyl iodide, labelled with $CH_3{}^{131}I$, was introduced over a period which was usually 2 hr; its rate of introduction was measured by gas chromatography with electron-capture detection which is particularly useful for methyl iodide. After the methyl iodide introduction period, the flow of air (with no deliberate change in relative humidity) was continued for an additional period, usually 4 hr. The downstream or backup charcoal beds, replaced for each test, contained both MSA 85851 and PCB charcoal to an extent sufficient to trap quantitatively the radioactive methyl iodide penetrating the test beds. Finally, the setup was disassembled, and the amounts of $^{131}I$ radioactivity in the test beds and the downstream sections were determined by means of a gamma spectrometer equipped with a scintillation crystal.

The more pertinent of the results obtained are presented in Tables 1 and 2. The data in Table 1 show that MSA 85851 impregnated charcoal effectively traps radioactive methyl iodide under the conditions employed in the tests. Under dry conditions (test LTPS-1), very high efficiencies are obtained. Because of the mechanism involved, isotopic exchange, the efficiencies quoted are for $CH_3{}^{131}I$; but, of course, that is the substance for which retention in the charcoal is desired. To a first approximation, at least, the percentage removal efficiency for $CH_3{}^{131}I$ should be independent of the specific activity of the inlet methyl iodide.

The data in Table 2 show that the laboratory-impregnated charcoals also exhibited good efficiencies. Again, the iodine-containing charcoals are effective only for $CH_3{}^{131}I$ (not $CH_3{}^{127}I$). In the case of the triethylenediamine impregnated charcoal, however, the efficiencies would correspond to overall methyl iodide removal (i.e., of both $CH_3{}^{127}I$ and $CH_3{}^{131}I$).

## RADIOACTIVE METHYL IODIDE REMOVAL TESTS AT TEMPERATURES AROUND 280°F

### Testing Procedure and Results

The manner of conducting each of these tests is illustrated in Fig. 2. While the charcoal in the test beds was not always pre-equilibrated with respect to moisture content prior to methyl iodide injection, the rate of steam flow was such that the charcoal would have been equilibrated in a period of time that was short relative to the time corresponding to methyl iodide injection. The rate of methyl iodide introduction was obtained from its known concentration in a supply tank and the flow rate of the air-$CH_3I$ mixture. The "dehumidifier" in Fig. 2 consisted of a water-cooled condenser supplemented by a drying column. (A similar arrangement regarding dehumidification was used in the 212°F tests.) Temperatures at various points in the setup were monitored by means of thermocouples. As in the 212°F tests, the methyl iodide was labelled with $CH_3{}^{131}I$ and the charcoal test beds, with a diameter of approximately 1 in., were, successively, 1/2, 1/2, and 1 in. in depth. With one unimportant exception, the backup charcoal beds were prepared with unused MSA 85851 impregnated charcoal. Times for methyl iodide injection and for subsequent additional steam-air flow differed slightly from those used in the 212°F tests. After stopping the flows, the $^{131}I$ distribution in the setup, including the condenser and drying column, was determined as

Table 1. Efficiency of MSA 85851 Impregnated Charcoal for Removing Radioactive Methyl Iodide from Flowing Steam-Air at Temperatures Around 212°F

| Test Designation | LTPS-1 | LTPS-2 | LTPS-3 | LTPS-4 | LTPS-5 | LTPS-6 |
|---|---|---|---|---|---|---|
| Charcoal Lot No. | 23 | 13 | 23 | 33 | 53 | 63 |
| Temperature, °F | 212 | 221 | 221 | 221 | 208 | 217 |
| Proportion as Steam, % | < 0.1 | 75 | 74 | 79 | 82 | 82 |
| Relative Humidity, % | < 0.1 | 62 | 61 | 65 | 87 | 72 |
| Steam-Air Velocity (superficial), fpm | 50 | 33 | 41 | 39 | 45 | 44 |
| Methyl Iodide: | | | | | | |
| Injection time, hr | 2 | 1 | 2 | 2 | 2 | 2 |
| Inlet concentration in steam-air, $mg/m^3$ | 11 | 10 | 9 | 8 | 9 | 10 |
| Amount injected per g of charcoal (a), mg | 0.8 | 0.2 | 0.5 | 0.5 | 0.6 | 0.6 |
| Time of Flow After Stopping Methyl Iodide Injection (b), hr | 4 | 5 | 4 | 4 | 4 | 4 |
| $CH_3{}^{131}I$ Removal Efficiency, % | | | | | | |
| For bed depth of 1/2 in. | 91.67 | 63.6 | 76.8 | 38.7 | 50.8 | 63.9 |
| For bed depth of 1 in. | 99.38 | 88.7 | 96.7 | 80.7 | 82.7 | 86.8 |
| For bed depth of 2 in. | 99.99 | 99.3 | 99.8 | 99.0 | 99.1 | 98.6 |

a. Based on 13 g for 2 in. depth of charcoal, 1 in. in diameter.

b. For each of these tests, the overall time of steam-air flow after initiation of methyl iodide injection totaled 6 hr.

Pressure for each test was approximately 14.4 psia.

Table 2. Efficiency of Laboratory-Impregnated Charcoals for Removing Radioactive Methyl Iodide from Flowing Steam-Air at Temperatures Around 212°F

| Test Designation | LTPS-7 | LTPS-8 | LTPS-9 |
|---|---|---|---|
| Impregnant, charcoal, mesh size | 5% $I_2$, PCB, 6 x 16 | 1% KI, PCB, 12 x 30 | 5% TED[c], PCB, 6 x 16 |
| Temperature, °F | 210 | 221 | 212 |
| Proportion as Steam, % | 83 | 80 | 86 |
| Relative Humidity, % | 84 | 66 | 84 |
| Steam-Air Velocity (superficial), fpm | 47 | 42 | 58 |
| Methyl Iodide: | | | |
| Injection time, hr | 2 | 2 | 2 |
| Inlet concentration in steam-air, $mg/m^3$ | 7 | 8 | 7 |
| Amount injected per g of charcoal (a), mg | 0.5 | 0.5 | 0.6 |
| Time of Flow after Stopping Methyl Iodide Injection (b), hr | 4 | 4 | 4 |
| $CH_3{}^{131}I$ Removal Efficiency, % | | | |
| For bed depth of 1/2 in. | 65.0 | 65.7 | 72.43 |
| For bed depth of 1 in. | 89.8 | 93.6 | 95.35 |
| For bed depth of 2 in. | 99.0 | 98.9 | 99.89 |

a. Based on 13 g for 2 in. depth of charcoal, 1 in. in diameter.
b. For each of these tests, the overall time of steam-air flow after initiation of methyl iodide injection totaled 6 hr.
c. Triethylenediamine.

Pressure for each test was approximately 14.4 psia.

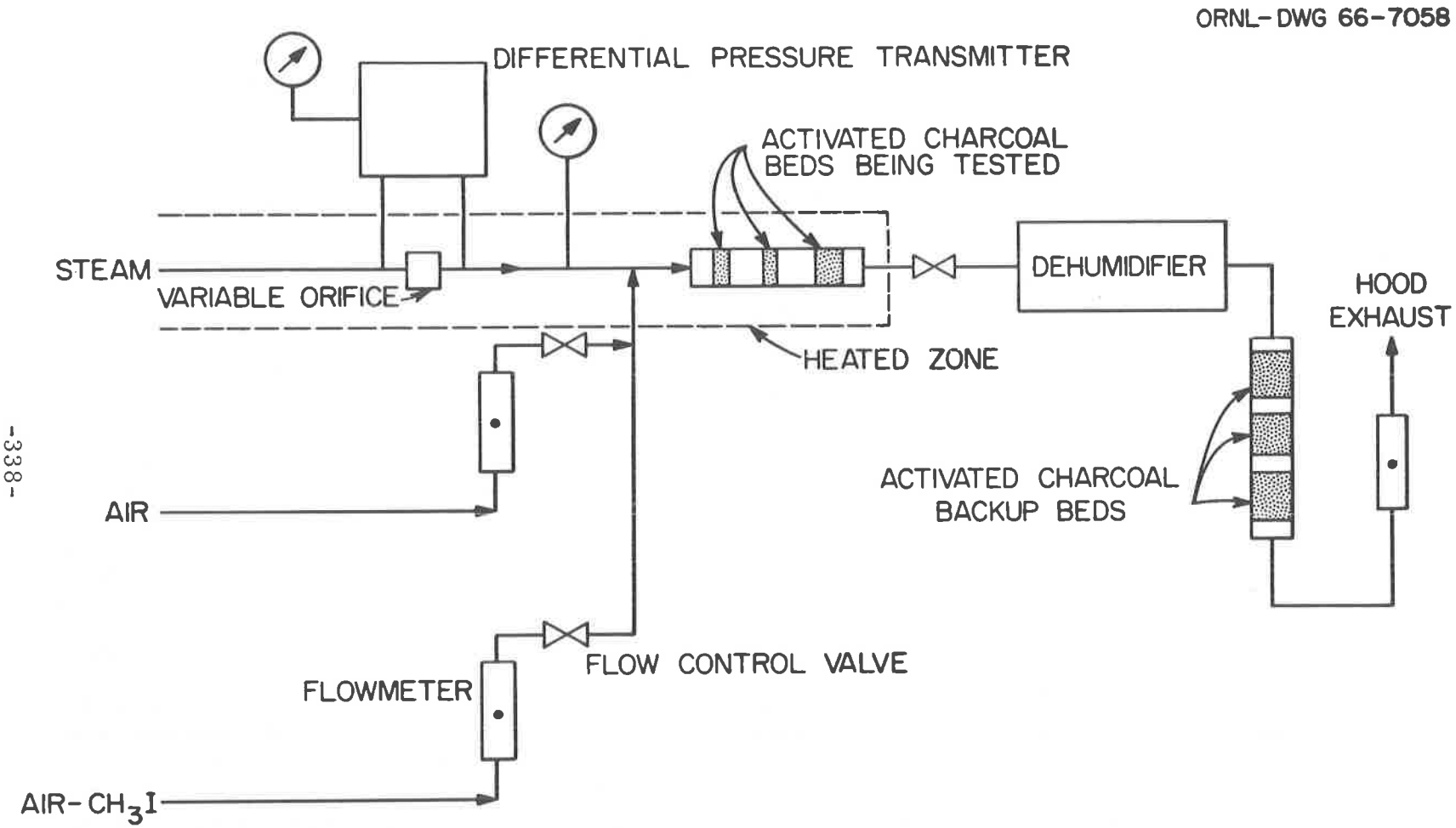


Fig. 2. Simplified Drawing of Setup for Investigation of Removal of Radioactive Methyl Iodide from Flowing Steam-Air by Impregnated Charcoals at Temperatures Around 280°F.

mentioned previously. A selection of the results obtained is given in Tables 3, 4, and 5.

## Discussion of Results

A brief comment on the effect of relative humidity may be in order. Relative humidity is a very important factor in methyl iodide trapping by activated charcoal since the trapping efficiency decreases with increasing relative humidity, the effect becoming most pronounced in the higher relative humidity region. This decrease is associated with the increase in the amount of water adsorption (with increasing relative humidity), and adsorbed water interferes with the interaction of methyl iodide and the charcoal to an extent depending upon the amount of adsorbed water.

Considering the results in Tables 3, 4, and 5, each of the three charcoal types tested exhibited useful $CH_3{}^{131}I$ trapping capability except in those instances where the relative humidity was excessive. In test HTPS-4 (only), Table 3, the test bed holder was not externally heated. Also, the situation was far from adiabatic. The individual $CH_3{}^{131}I$ removal efficiencies obtained in this test suggest that channeling, resulting from condensation, may have occurred in the two downstream test beds. The methyl iodide loadings employed in these tests might be characterized as being relatively high, especially in the case of HTPS-5 of Table 4. The steam-air velocity for this test was also high. However, operating under these two rather extreme conditions, of methyl iodide loading and of velocity, did not result in greatly impaired removal efficiencies.

As judged from the results herein, from earlier results, and from unpublished results, the $CH_3{}^{131}I$ trapping capabilities of MSA 85851 and BC-727 appear to be essentially independent of temperature over the range 75 to 290°F. (More data than those presently available are probably needed in order to comment on this aspect with regard to triethylenediamine-impregnated charcoal.) The higher pressures employed in the HTPS series of tests did not produce any readily apparent effect. Remarks made earlier, in conjunction with the 212°F tests, regarding the methyl iodide species trapped by different charcoals, are also applicable to the tests at higher temperatures.

The results of Tables 3, 4, and 5, exclusive of those for test HTPS-5 due to its particular conditions making it less comparable, are summarized in Fig. 3. The composite curve in the figure depicts the severe loss in $CH_3{}^{131}I$ removal efficiency encountered when the relative humidity approaches 100%. In considering this graph, particularly in the relative humidity region around 90% and upward, it should be recognized that small errors in relative humidity could importantly affect the locations of data points and, also, the location of the curve shown. Obviously, in the design of a $CH_3{}^{131}I$ removal system using impregnated charcoal, the inclusion of some provision that would maintain the prevailing relative humidity below 90% would be a highly desirable objective.

Table 3. Efficiency of MSA 85851 Impregnated Charcoal for Removing Radioactive Methyl Iodide from Flowing Steam-Air at Temperatures Around 280°F

| Test Designation | HTPS-1 | HTPS-2 | HTPS-3 | HTPS-4 |
|---|---|---|---|---|
| Charcoal Lot No. | 23 | 23 | 23 | 33 |
| Temperature, °F | 284 | 280 | 275 | 262 |
| Pressure of Steam-Air, psia | 61 | 61 | 61 | 62 |
| Proportion as Steam, % | 70 | 73 | 71 | 59 |
| Relative Humidity, % | 82 | 91 | 95 | 100 |
| Steam-Air Velocity (superficial), fpm | 41 | 44 | 41 | 27 |
| Methyl Iodide: | | | | |
| Injection time, hr | 1.5 | 1.3 | 1.5 | 2.0 |
| Inlet concentration in steam-air, mg/m³ | 72 | 81 | 73 | 93 |
| Amount injected per g of charcoal (a), mg | 3.2 | 3.2 | 3.2 | 3.5 |
| Time of Flow After Stopping Methyl Iodide Injection (b), hr | 3.5 | 3.7 | 3.5 | 3.0 |
| $CH_3{}^{131}I$ Removal Efficiency, % | | | | |
| For bed depth of 1/2 in. | 72.3 | 64.3 | 62.9 | 49 |
| For bed depth of 1 in. | 92.1 | 86.5 | 85.0 | 52 |
| For bed depth of 2 in. | 98.9 | 97.1 | 88.6 | 54 |

a. Based on 13 g for 2-in. depth of charcoal, 1 in. in diameter.
b. For each of these tests, the overall time of steam-air flow after initiation of methyl iodide injection totaled 5 hr.

Table 4. Efficiency of BC-727 Impregnated Charcoal for Removing Radioactive Methyl Iodide from Flowing Steam-Air at Temperatures Around 280°F

| Test Designation | HTPS-5 | HTPS-6 | HTPS-7 | HTPS-8 | HTPS-9 |
|---|---|---|---|---|---|
| Temperature, °F | 246 | 285 | 284 | 279 | 278 |
| Pressure of Steam-Air, psia | 27 | 61 | 61 | 60 | 62 |
| Proportion as Steam, % | 62 | 72 | 73 | 73 | 73 |
| Relative Humidity, % | 61 | 83 | 86 | 91 | 95 |
| Steam-Air Velocity (superficial), fpm | 92 | 42 | 43 | 45 | 42 |
| Methyl Iodide: | | | | | |
| Injection time, hr | 1.5 | 1.5 | 1.5 | 1.4 | 1.5 |
| Inlet concentration in steam-air, $mg/m^3$ | 163 | 70 | 69 | 66 | 72 |
| Amount injected per g of charcoal (a), mg | 16 | 3.2 | 3.2 | 3.0 | 3.2 |
| Time of Flow After Stopping Methyl Iodide Injection (b), hr | 2.5 | 3.5 | 3.5 | 3.6 | 3.5 |
| $CH_3{}^{131}I$ Removal Efficiency, % | | | | | |
| For bed depth of 1/2 in. | 40.7 | 74.2 | 71.2 | 79.2 | 55.1 |
| For bed depth of 1 in. | 70.7 | 93.3 | 91.6 | 89.9 | 71.9 |
| For bed depth of 2 in. | 95.1 | 97.9 | 98.7 | 93.0 | 75.0 |

a. Based on 13 g for 2-in. depth of charcoal, 1 in. in diameter.
b. For each of these tests except HTPS-5, the overall time of steam-air flow after initiation of methyl iodide injection totaled 5 hr and for HTPS-5, it totaled 4 hr.

Table 5. Efficiency of Triethylenediamine-Impregnated Charcoal (5% by wt. on PCB, 6 x 16 mesh) for Removing Radioactive Methyl Iodide from Flowing Steam-Air at Temperatures Around 280°F

| Test Designation | HTPS-10 | HTPS-11 | HTPS-12 |
|---|---|---|---|
| Temperature, °F | 286 | 285 | 274 |
| Pressure of Steam-Air, psia | 61 | 61 | 61 |
| Proportion as Steam, % | 70 | 71 | 72 |
| Relative Humidity, % | 80 | 82 | 100 |
| Steam-Air Velocity (superficial), fpm | 40 | 42 | 42 |
| Methyl Iodide: | | | |
| Injection time, hr | 1.8 | 1.8 | 1.6 |
| Inlet concentration in steam-air, $mg/m^3$ | 75 | 70 | 73 |
| Amount injected per g of charcoal (a), mg | 3.8 | 3.9 | 3.5 |
| Time of Flow after Stopping Methyl Iodide Injection (b), hr | 3.2 | 3.2 | 3.4 |
| $CH_3{}^{131}I$ Removal Efficiency, % | | | |
| For bed depth of 1/2 in. | 58.2 | 40.0 | 10 |
| For bed depth of 1 in. | 85.3 | 71.5 | 14 |
| For bed depth of 2 in. | 98.2 | 94.7 | 20 |

a. Based on 13 g for 2-in. depth of charcoal, 1 in. in diameter.
b. For each of these tests, the overall time of steam-air flow after initiation of methyl iodide injection totaled 5 hr.

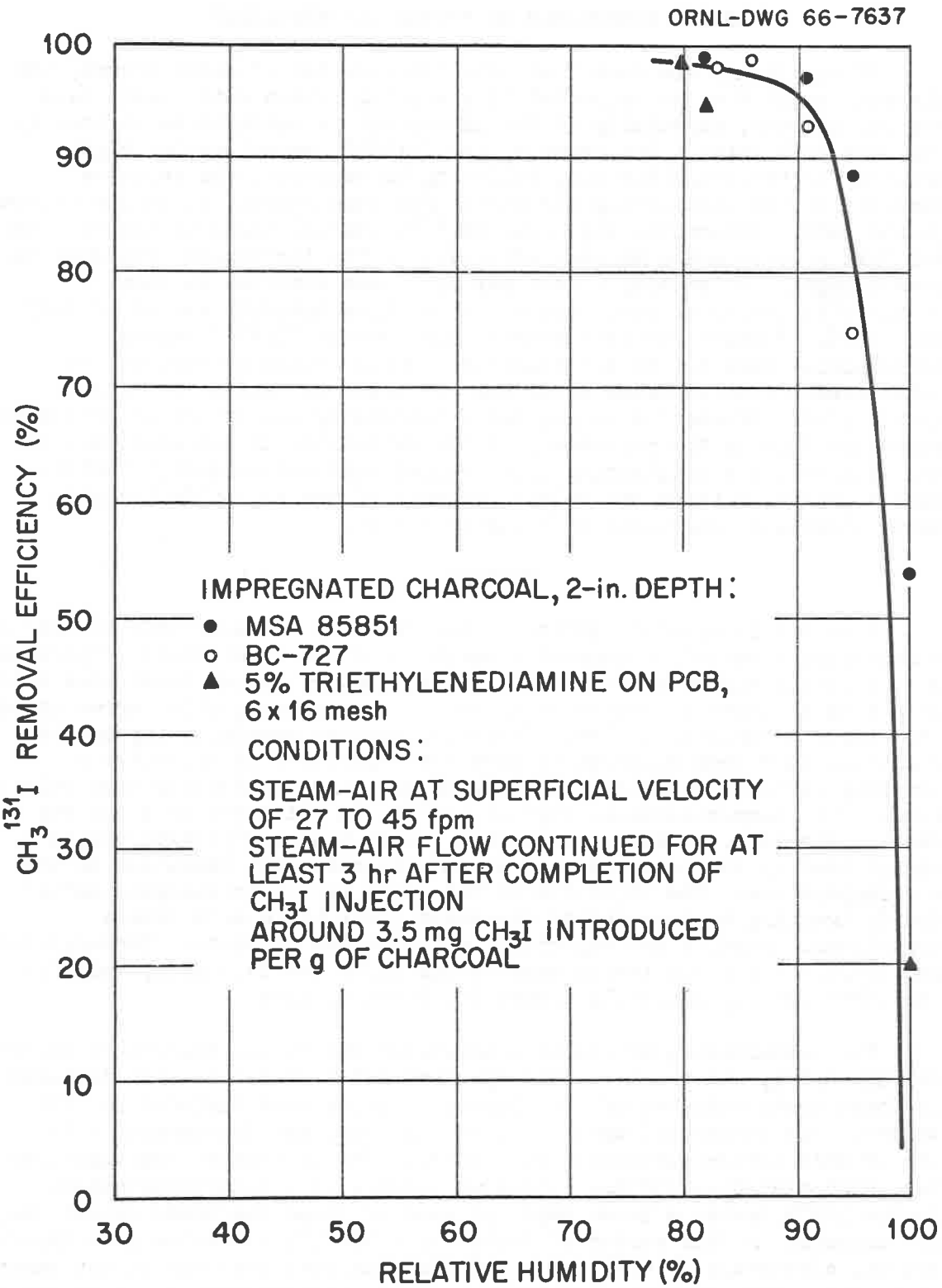


Fig. 3. Effect of Relative Humidity on the Removal of Radioactive Methyl Iodide by Impregnated Charcoals at Temperatures and Pressures Around 280°F and 60 psia.

## BRIEF DISCUSSION OF FUTURE INVESTIGATION

If conditions are such that bulk condensation of water occurs, the charcoal might then be subjected to a washing action which could have serious effects, especially if the impregnant is susceptible to loss by leaching with water. For example, the $CH_3{}^{131}I$ removal system might provide for recirculation and, following an accident, the relative humidity of the circulating air might, for some reason, fluctuate between 90 and 100%. Intermittently, some $CH_3{}^{131}I$ removal might be accomplished, but this process would be less effective if the impregnated charcoal has been damaged. A leaching effect may have been involved in those of the HTPS series of tests where the relative humidity was at or very near 100%. However, to what extents the lowered $CH_3{}^{131}I$ removal efficiencies were due to the possible washing action or were due to interference from adsorbed water are difficult to delineate. Also, insufficient information is available concerning the effect of prolonged steam-air flow on the permanency of the retention, in the charcoal, of the radioactivity originating from trapped radioactive methyl iodide. Investigation of these and related aspects of methyl iodide trapping under steam-air conditions is being initiated.

## SUMMARY

When fission-product iodine is accidentally released into the air of a containment vessel, a generally small but often significant proportion of the iodine may occur as methyl iodide. Methyl iodide penetrates beds of the usual types of activated charcoal to an unacceptable degree unless the relative humidity is low. Recently, certain specially-impregnated charcoals have been observed to have the capability of effectively trapping radioactive methyl iodide from air streams of fairly high relative humidity at temperatures as high as 115°F. In the event of a nuclear reactor accident, however, the methyl iodide trapping problem may be complicated by the production of steam with attendant elevation of the air temperature. The objective of this work was to investigate methyl iodide trapping by impregnated charcoals under these more severe conditions. Results are reported for two series of tests. Temperatures and pressures for one series were around 212°F and 14.4 psia, and, for the other series, generally around 280°F and 60 psia.

Two commercially available impregnated charcoals, designated BC-727 and MSA 85851, and three laboratory-impregnated charcoals were included in these tests with two of the charcoals having been included in both series. The commercial materials, as received, are impregnated with one or more iodine-containing substances. The laboratory impregnations were with elemental iodine, potassium iodide, or triethylenediamine. In the 212°F tests, a 2-in. depth of each of these charcoals except one not included in this series of tests, viz. BC-727, exhibited good $CH_3{}^{131}I$ removal efficiency (> 98%) for a relative humidity that was in the range 60 to 90%. The corresponding methyl iodide loadings were ~ 0.5 mg per g of charcoal and the steam-air velocities were ~ 40 fpm. In this series (212°F), MSA 85851 was tested more extensively than the other varieties of impregnated charcoal. The 280°F, 60 psia series included tests of

BC-727, MSA 85851, and triethylenediamine-impregnated charcoal. The BC-727 and MSA 85851 both exhibited $CH_3{}^{131}I$ removal efficiencies in excess of 90% for 2-in. depths at relative humidities of 90% or lower. The triethylenediamine-impregnated charcoal at this depth exhibited > 90% efficiency at relative humidities around 80% but was not tested at relative humidities around 90%. Methyl iodide loadings of ~ 3.5 mg/g and velocities of ~ 40 fpm were generally employed in this series. One test, made with BC-727, indicated that the $CH_3{}^{131}I$ trapping process was still effective at conditions of loading and velocity considerably more severe than those just given.

The results obtained confirmed that the deleterious effect of high relative humidity on radioactive methyl iodide trapping becomes more pronounced as relative humidity increases.

Further investigation of methyl iodide trapping is to include the following areas: effect of leaching by condensed steam on subsequent $CH_3{}^{131}I$ removal performance of impregnated charcoals and effect of prolonged steam-air flow on retention by impregnated charcoals of trapped $^{131}I$, that originates from $CH_3{}^{131}I$.

## REFERENCES


1. R. E. Adams, W. E. Browning, Jr., Wm. B. Cottrell, and G. W. Parker, The Release and Adsorption of Methyl Iodide in the HFIR Maximum Credible Accident, USAEC Report ORNL-TM-1291, pp. 24-26, 40, Oak Ridge National Laboratory, October 1, 1965.

2. R. D. Ackley, R. E. Adams, W. E. Browning, Jr., G. E. Creek, and G. W. Parker, Retention of Methyl Iodide by Charcoal Under Accident Conditions, in Nuclear Safety Program Semiannual Progress Report for Period Ending December 31, 1965, USAEC Report ORNL-3915, pp. 61-80, Oak Ridge National Laboratory, March 1966.

3. D. A. Collins, R. Taylor, and L. R. Taylor, United Kingdom Atomic Energy Authority; The Removal of Methyl Iodide from Reactor Effluent Gases, in International Symposium on Fission Product Release and Transport Under Accident Conditions, Oak Ridge, April 5-7, 1965, USAEC Report CONF-650407 (Vol. 2), pp. 853-868.

4. R. D. Collins, Trapping Radioiodine (letter), Nucleonics, Vol. 23, No. 9, 7 (1965).

## DISCUSSION

PETERS: Because of the interest and time limit this morning, we changed the schedule to hear the paper "Removal of Radioactive Methyl Iodide from Steam-Air Systems" by R. D. Ackley, R. E. Adams and W. E. Browning, Jr., Oak Ridge National Laboratory, Oak Ridge, Tennessee. Because of the interest and the results presented by Mr. Ackley, as compared to others, both in this country and abroad, we will entertain two or three questions at this time, before proceeding with the rest of the session.

PARKER (ORNL): I again wish to emphasize the significance of this region, 90 to 100 per cent relative humidity. I wonder, however, rather than commenting again, would Mr. Noble or someone else from the contractor line, please tell us at what relative humidity they expect to operate.

NOBLE: I would like to comment on this relative humidity and the practicality of obtaining a 90 per cent relative humidity in a contained atmosphere.

We are talking, here, about containment, and the remarks are particularly appropriate for dry containment, pressurized water type of reactors. We have containment volumes of from 900,000 cubic feet up to well over a million cubic feet. We are talking about temperatures from 125 to 140° C, with pressures, for design purposes, of about 40 to 60 P.S.I. Now, the purpose of the iodine removal filters is to remove the iodine, so we get a lower average concentration over our leakage period. With this large containment volume, it requires rather large flows.

In the case of the Connecticut Yankee containment, we are talking about a flow per filter of assembly of approximately 50,000 C.F.M., with three fans or filter assemblies, in operation for design purposes. If we try to cool this down to about 90 per cent relative humidity, this requires first, cooling the flow down, letting it back up, and then once again cooling it down, so that we have a net heat removal from the flow.

The point I am questioning is, really, whether it is practical, in a containment system, to get a 90 per cent relative humidity, which appears to be necessary, on the basis of some of the information presented here today.

I, personally, feel that unless we can get this charcoal to operate at relative humidity, or relative humidities, either at 100 per cent or close to it, then it may not be practical to use charcoal for this application.

That is the end of my comment, and if anybody would like to take issue with me or make further comment, I shall appreciate it.

HILLARY: When one compares the work that Mr. Ackley has been describing with the work that I presented this morning, then I think it would be better to compare detailed notes outside of the meeting, in the sense that we do not find this effective relative humidity in our work.

One recent experiment is perhaps worth noting, though. We did have commercially prepared impregnated materials for our test, which gave a penetration of something in the order of 10 per cent. This test, in fact, was a little different, in the sense that it was found that the water content of it was about 45 per cent, whereas the normal water content was more nearly 20 per cent. I just want to offer this as a suggestion, or rather as one suggestion for discussion.

LOUROS: In view of the fact that your data showed increased removal efficiency was greater, could you go to much deeper bed depths, four to six inches, and get your removal efficiency up one hundred per cent.

ACKLEY: Well, I believe it might be true that there would be a bed depth which would take care of the situation. Perhaps its pressure drop might be a disadvantage. A bed depth of four, five or six inches would, of course, give considerably improved removal efficiency.

LOUROS: One more point; do you know the particle sizes of the various samples of carbons tested, if they were within the same order of magnitude, i.e., that which would give you the mean diameter, in a short, failure result.

ACKLEY: The commercial materials were 8-14 mesh; that is about all of the information which I have on that point.

# PERFORMANCE OF AIRBORNE ACTIVITY CONFINEMENT SYSTEMS IN SAVANNAH RIVER PLANT REACTOR BUILDINGS*

by

W. S. Durant

Savannah River Laboratory
E. I. du Pont de Nemours and Co.
Aiken, South Carolina 29801

## ABSTRACT

A filtration-adsorption system is installed in the ventilation exhaust of each reactor building at the Savannah River Plant for confinement of airborne particulate and iodine vapor activity that might be released in the highly unlikely event of a reactor accident. Air from the process areas of each building is passed continuously through moisture separators, then through particulate filters, and finally through iodine adsorber beds of activated carbon. The system has the demonstrated ability to confine over 99% of airborne particulate activity and over 99.9% of all forms of airborne halogen activity that could form under emergency conditions that might exist following an accident in the SRP reactors. A continuing program of development, testing, and maintenance ensures that these high efficiencies will be maintained during operation. Experience has been satisfactory for over 3 years of operation.

* The information contained in this article was developed during the course of work under Contract AT(07-2)-1 with the U. S. Atomic Energy Commission.

## INTRODUCTION

The activity confinement system for reactors at the Savannah River Plant (SRP) is designed to collect airborne particulate and halogen activity, that might be released from the reactor in the highly unlikely event of an accident.[1] It represents one of many lines of defense that include preventing accidents, limiting the consequences of accidents, and confining activity that may be released from the fuel and reactor.

The confinement system for airborne activity consists of moisture separators, particulate filters, and halogen adsorbers in the exhaust air portion of the ventilation system. Air is exhausted from the reactor process areas through the filters and adsorbers, and discharged to a stack. Noble gases are not contained. The system has been in full operation in all reactor areas since 1964.

Development work on the confinement system started in 1960 and has been a continuing major effort of both the Savannah River Laboratory (SRL) and Plant (SRP) organizations.[2-6] Considerable laboratory work was required to develop a satisfactory system that would function properly under the possible accident conditions. SRL and SRP personnel participated closely in the design, installation, and operation of the system. A comprehensive evaluation of the performance of the operating system has led to several improvements in reliability and efficiency. A substantial technical effort is continuing.

This paper presents the results of an evaluation of the operating systems after about three years of continuous service.

## DISCUSSION

### Filter Compartments

The filtration-adsorption units are contained in compartments (Figure 1) located on the roof of the reactor buildings. Each parallel compartment contains three banks of filters or adsorbers in series: moisture separators,

NEG. 9173-3

Filter Compartment Prior to Installation

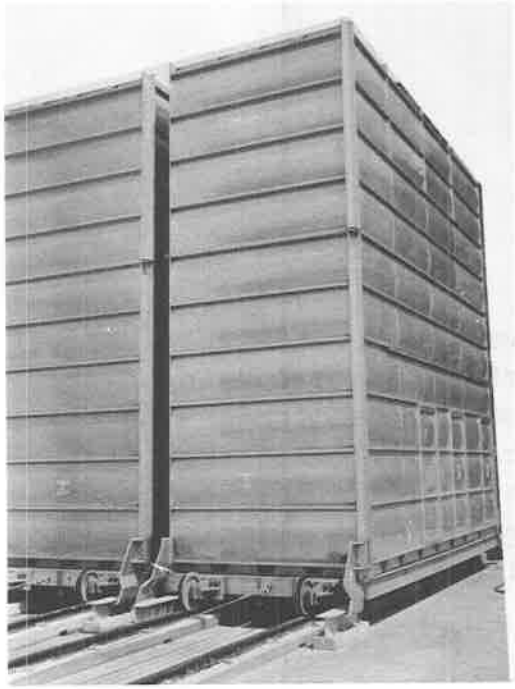

NEG. 9173-2

Filter Compartments in Operating Position on Reactor Building Roof

FIG. 1 SRP FILTER COMPARTMENTS

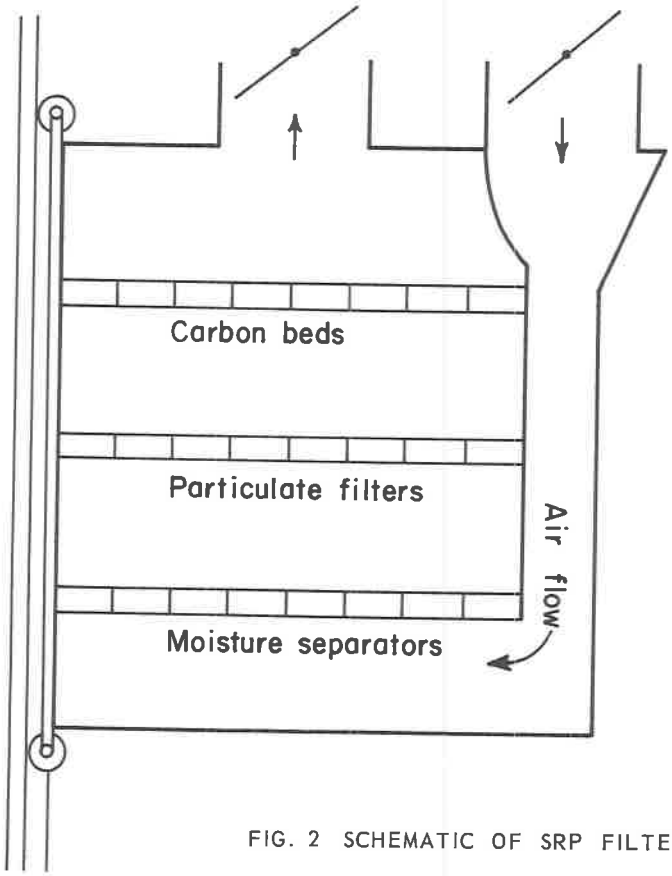


FIG. 2 SCHEMATIC OF SRP FILTER COMPARTMENT

particulate filters, and activated carbon beds (Figure 2). These compartments are located in the process area ventilation system between the exhaust air duct and the exhaust fans; hence, the compartments operate with a negative pressure.

Should any of these compartments become highly contaminated, they would be remotely delatched from the ventilation system, rolled on tracks to the edge of the building, removed from the roof by a crane, and shipped as a unit to the burial ground. The compartments can be pulled away from the air plenum for service. If an accident occurred with a release of steam, the resultant contaminated water would be drained to the process areas.

Because of the possibility of a momentary positive pressure surge during a reactor accident, the walls were fabricated with convex panels of 1/8-inch-thick Type 3003 aluminum as shown in Figure 1. Each compartment was tested at a sustained pressure of 2 psig and a momentary pressure of 3 psig.

Operating experience with the compartments has been excellent for more than three years. Only minor corrosion of the aluminum walls in one reactor area has been observed. The maximum depth of pitting, caused by attack from trace amounts of nitrogen compounds, was about 0.005 inch and is of no consequence to the structural integrity of the compartments.

The filtration-adsorption system depends upon continuous operation of the exhaust air fans. Two fans are normally operating and a third is available. Power for the fans is fed in a loop circuit from two or three power plants that are widely separated. In the very unlikely event that all power plants should fail, power to maintain full system air flow would be supplied by a diesel generator in each reactor area. The exhaust fan system has never experienced an unscheduled stoppage in over 10 years of operation.

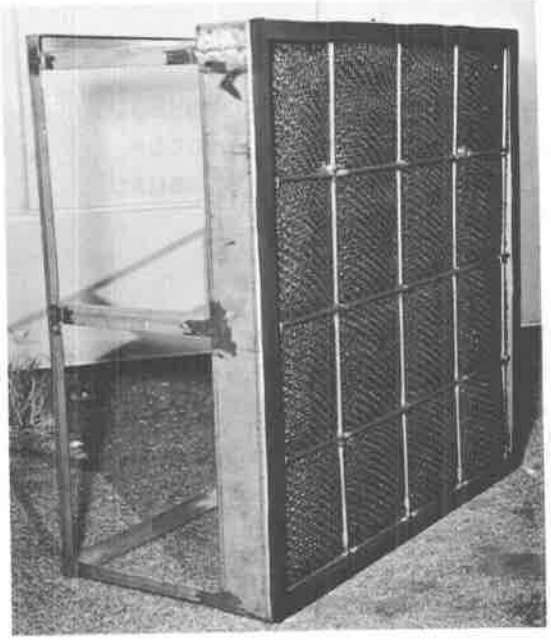

DPSPF-8699-8

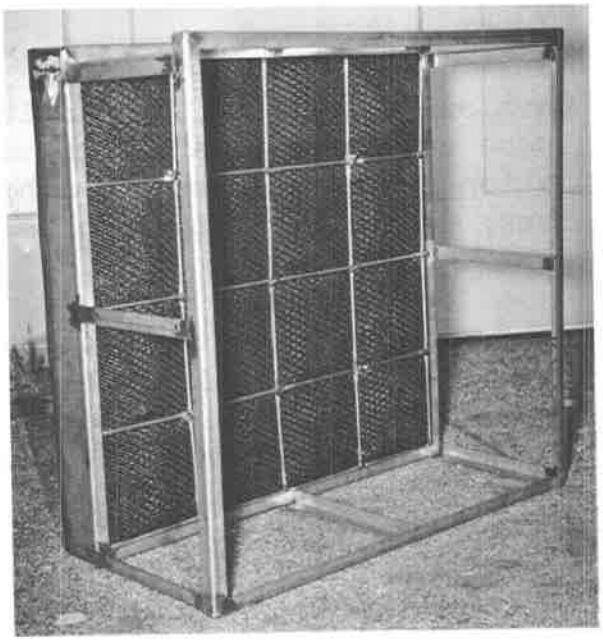

DPSPF-8699-7

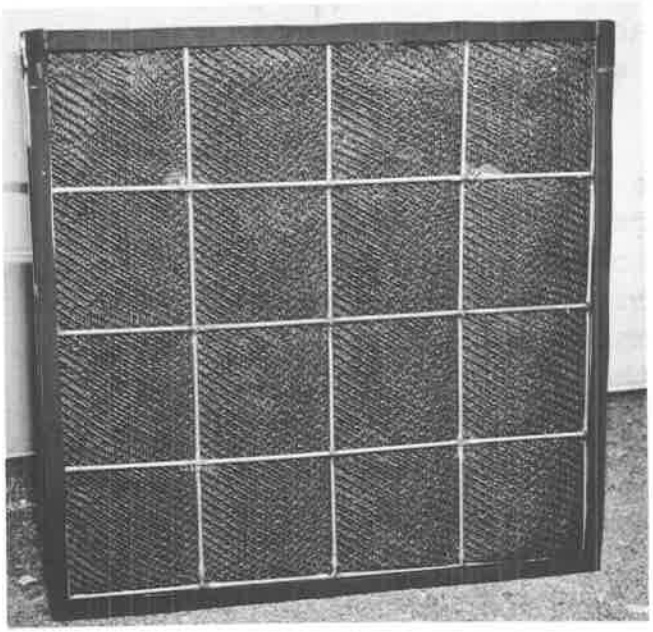

DPSPF-8699-2

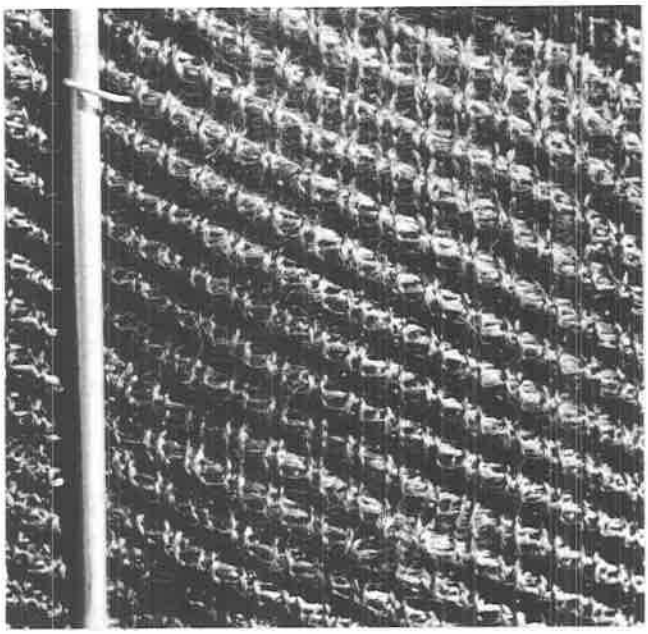

DPSPF-8699-1

FIG. 3 MOISTURE SEPARATOR USED IN SRP ACTIVITY CONFINEMENT SYSTEM

Moisture Separators

The moisture separators ("Demisters"*) are designed to remove about 99% of 1- to 5-μ entrained water particles to protect against significant rupture of the water-repellent particulate filters.[4] The separator, Figure 3, consists of about 24 mats woven from "Teflon"** yarn (individual fibers about 0.001-inch diameter) and stainless steel wire forming a pad 24 x 24 inches x 2 inches thick. The number of mats in each pad is dictated by the desired removal efficiency, which was correlated in terms of a flow resistance requirement of 0.95 ±0.05 inch $H_2O$ at the rated air flow of 1600 cfm. The case, mat, and support mechanism are designed and tested to withstand flows equivalent to about 10 times the rated air flow through the separator.

Because no information was available in the literature on the performance of commerical separators for removal of water particles in steam-air mixtures (fog), extensive tests were conducted at SRL on canddidate units. These tests showed that the specified "Demisters" were the only commercially available units that were satisfactory at the time of installation in the SRP facilities. The "Demisters" successfully withstood the test conditions (wet steam flow to about 10 times the normal air flow and exposure to fog for 10 days), and prevented damage of the particulate filters. On the basis of calculated efficiencies and the observed test results, most of the water particles in the fog were removed by the "Demister" made of "Teflon". The calculated maximum water load on each "Demister" is about one pound of liquid water per minute, and the manufacturer's rating is 8 pounds per minute before flooding occurs.

Tests of standard type prefilters and conventional wire-mesh separators showed that they were practically useless in removing the entrained water particles. One type of prefilter was blown from its containing frame after 10 seconds exposure to wet steam at a maximum rate of 7 times the rated air flow.

---

* Registered trademark of Otto H. York Co.

** Registered trademark of E. I. du Pont de Nemours and Co.

The minimum temperature at which thermal degradation of the "Demisters" might begin is about 150°C. At this temperature the neoprene gasket would begin to deteriorate. The gasket is self extinguishing, however. At about 260°C, the "Teflon" would begin to deteriorate, but the strength of the unit essentially would be unaffected because of the stainless steel wires on which the "Teflon" is woven. Radiation effects on "Teflon" have been measured. Calculations showed that at radiation levels associated with the accumulation of fission products in the filter compartments, the reduced fiber tensile strength is far in excess of the actual stress on the fibers for several hours after an accident.

Because the moisture separators are fabricated of stainless steel and "Teflon", no corrosion from trace acidic compounds has been observed. Also, no degradation of the "Teflon" has been detected.

The only problem with the separators has been an accumulation of an oily substance and particulate matter on the upstream face. Units are removed and cleaned with steam at a nozzle pressure of 15-20 psi to restore flow-pressure drop characteristics to values equal to those of new units without damaging the mat. The front face is steam-cleaned for three minutes in a vertical position, and then the back face is steam-cleaned by blowing steam downward onto the back for three minutes with the separator in a horizontal position.

No units have been replaced because of mechanical damage. The stainless steel and "Teflon" mat is quite tough and flexible; it is not easily damaged from handling during installation or maintenance.

With steam-cleaning about once per year, an indefinite service life is expected.

Particulate Filters

The particulate filters, Figure 4, are designed to remove 99+% of all particulate matter.[4] The filter medium is made of 18-mil-thick glass-asbestos felt sheet

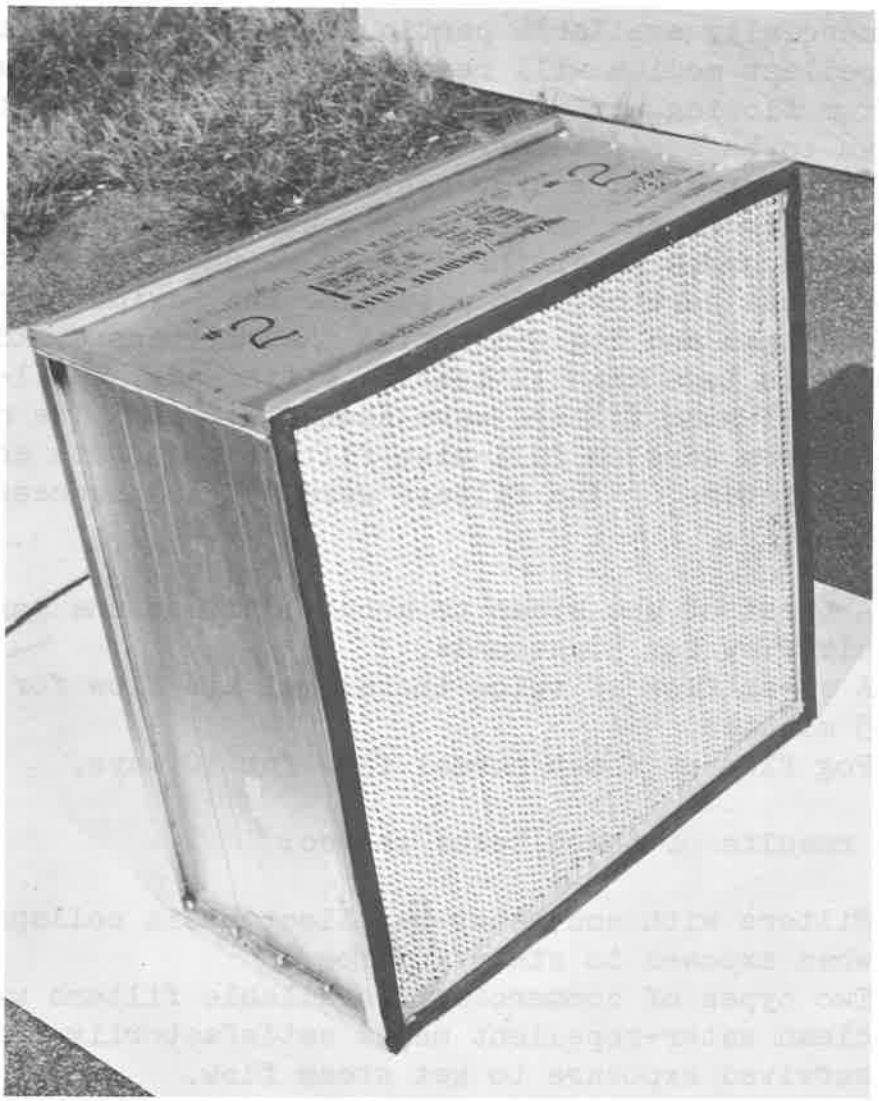

FIG. 4 PARTICULATE FILTER USED IN SRP ACTIVITY CONFINEMENT SYSTEM

which is fire resistant and water repellent for high wet strength characteristics. Under accident conditions, the filters could be exposed to hot air, wet steam at 100°C, or fog.

Commercially available particulate filters with a water repellent medium will remove 99.9+% of particulate matter from flowing air or other dry gases. Such filters were known to be satisfactory for humid air, but were not designed for wet steam and/or fog. The wet-strength characteristics of the various media were not known if the water load occurred after the filters accumulated dust from continuous service. To determine the maximum conditions of steam and fog filtration that filters could withstand with less than 1% loss in efficiency, small-scale and full-size filters were tested by SRL. The most important tests were on full-size filters both with and without "Demisters". The filters were exposed successively to:

- o A burst of wet steam to about 10 times the normal air flow for 30 seconds.
- o A steam flow of twice the normal air flow for 5 minutes.
- o Fog flow at about normal flow for 10 days.

The results of these tests showed:

- o Filters with non-water-repellent media collapsed when exposed to steam and fog.
- o Two types of commercially available filters with clean water-repellent media satisfactorily survived exposure to wet steam flow.
- o Only one commercially available filter with clean water-repellent medium survived the entire sequence of tests.
- o None of the filters survived the 10-day fog test when loaded with atmospheric dust and without a "Demister".

Based on these results, a water-repellent filter made by Cambridge Filter Corp. was selected and extensively tested with clean and dusty media with a "Demister"

upstream. These tests demonstrated that the combination of "Demister" and particulate filter selected would withstand the exposure conditions for any accident that would not significantly damage the reactor building.

Significant design features and specifications for the water-repellent particulate filters include:

- The filter is constructed by folding the felt sheet over corrugated aluminum inserts into closely spaced pleats in a steel frame forming a unit 24 x 24-inches x 11-1/2-inches thick. The unit is designed for 1000 cfm air at a pressure drop not exceeding 1.00-inch $H_2O$ when clean.
- Each roll of medium is qualified by the manufacturer by testing samples for tensile strength and elongation, both dry and wet, and with and without a flat fold in the medium.
- One full-size filter assembled from each roll of filter medium and selected randomly by a Du Pont inspector is required to pass the following sequence of tests:

  a) $\Delta P$ across the filter must not exceed 4 times the normal when exposed to wet steam flow at two times normal flow and with water spray injected upstream of filter for 15 minutes.
  b) Flow resistance after drying must not exceed normal $\Delta P$ at rated air flow.
  c) $\Delta P$ must not exceed 2 times normal when filter is loaded with 4 pounds of dust at normal air flow.
  d) Filter must not fail when exposed for 10 minutes at 6 times normal $\Delta P$.
  e) Maximum penetration of test filter must not exceed 0.1% of 0.3-$\mu$ dioctyl phthalate (DOP) at rated air flow after completion of all sequence tests.

- Each production unit is tested for pressure drop and DOP penetration by the manufacturer. DOP penetration must not exceed 0.03% for 0.3-μ diameter homogeneous particles at 20% and 100% of rated flow.
- After installation in the filter compartments, the units are tested with 0.6-μ DOP[7,8] prior to operation of the compartment. Any filter with a detectable leak (greater than 0.05%) is replaced because small holes may enlarge if the unit remains in service. The in-place DOP test is repeated at about one-year intervals to determine if leaks develop during service.

The gasket, adhesive, and binder in the particulate filter might begin to deteriorate at about 150°C. However, the efficiency of the filters would not be affected because:

- Significant deterioration would not occur until after the fission products were confined.
- All components of the filter are self-extinguishing.
- The strength of the filter is more than adequate to resist damage even without binder.
- Underwriters Laboratory tests showed that damage to the filter is negligible up to 370°C.

Particulate filters have a relatively short life (1 to 2 years is typical) compared to "Demisters" because there is no practical method for cleaning the medium. Wet fly ash from the powerhouse stack is the primary material that accumulates on the filters. More efficient prefilters in the supply air system currently are being installed to reduce the fly ash on the particulate filters as well as on the separators. Although removal of the fly ash from the high efficiency particulate filters is not practical, drying with electrical heaters at reduced flow and use of more efficient prefilters are expected to prolong the filter life. Experimental heaters proved the feasibility of drying the filters, and permanent installation of 80 kw heaters in each filter compartment has been authorized.

Early models of the particulate filters had no protection against puncture of the medium during

installation, and the rejection rate was 1% based on DOP tests of each unit after installation. To protect against puncture, galvanized hardware-cloth face guards are now specified.[9]

The ability of the particulate filters to withstand the severe conditions which might exist under emergency conditions was demonstrated in typical tests on two filters that were removed for tests after 13 months exposure to flowing, normally dust-laden exhaust air in a reactor building ventilation system. The filters, with clean "Demisters" upstream, were subjected to flowing fog under specification conditions. Although very minor damage of one of the filters was observed, the efficiency of each filter for removing 0.6-micron particles of DOP was 99.9+% after 12 days of exposure to the flowing fog.

A fog test was performed also with a dusty "Demister" installed upstream of two dusty particulate filters. The units were removed for testing after 34 weeks exposure to flowing air that contained normal atmospheric dust. After 10 days of exposure to a fog mixture, both filters had an efficiency of 99.9+% for 0.6-micron DOP.

The required efficiency of the filters for removal of 0.3-micron* particles is 99%, although measured efficiences are greater than 99.9%. A high efficiency can be maintained even though the filters may contain a considerable number of holes. For example, four banks of 128 clean particulate filters (about 30,000 square feet total surface area) can contain about 1100 1/4-inch-diameter holes, yet allow only 1% of the rated air stream to pass through the holes.[10]

Activated Carbon Beds

Activated carbon beds, Figure 5, were designed to remove more than 99.9% of elemental iodine vapor that might be released from a reactor if an accident should occur.[9] Numerous tests of small-scale carbon beds showed that more than 99.99% of elemental iodine vapor can be removed

* Tests by the vendor are with 0.3-micron aerosol; the tests at SRP are with 0.6-micron aerosol.

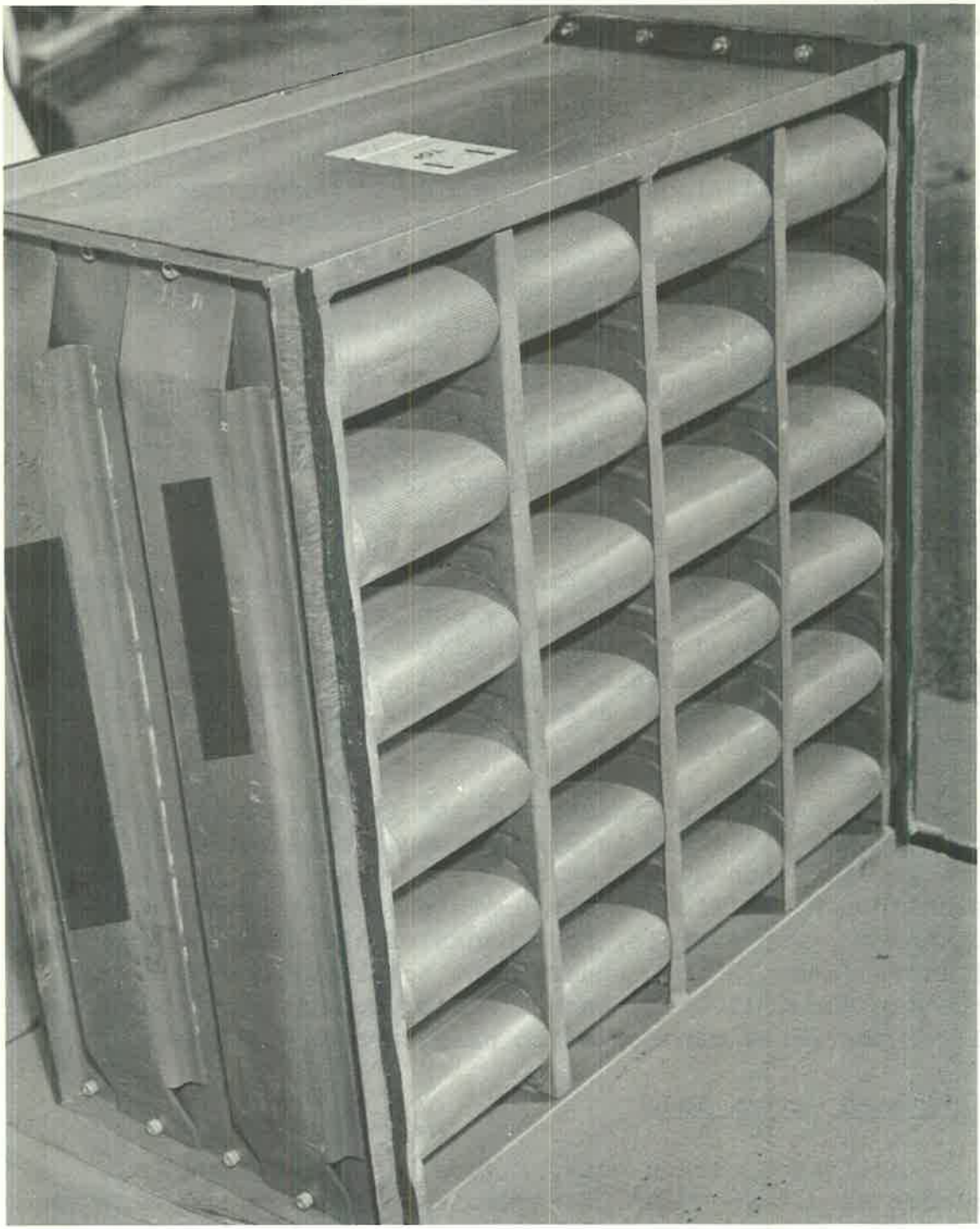

FIG. 5 ACTIVATED CARBON BED USED IN SRP ACTIVITY CONFINEMENT SYSTEM

consistently with a 1-inch-thick bed of new activated carbon of the type specified for SRP. These beds were tested under a wide range of conditions that included:

- Prefiltered fog mixtures at 65°C and at face velocities to 80 feet per minute (normal face velocity is 65-70 feet per minute).
- Unfiltered fog mixtures with liquid water entrainment rates up to 5 times that expected downstream of the particulate filters, and with the carbon beds dry or saturated with liquid water.
- Steam at 70 feet per minute and from a wet condition at 100°C to superheated conditions at 130°C.
- Air at 5 times the normal flow and at temperatures to 110°C.
- Iodine loadings to 6 milligrams $I_2$ per gram of carbon.

In addition, the tests demonstrated that mass transfer was the controlling mechanism for elemental iodine adsorption under SRP conditions. The results were correlated with the semiempirical equation for critical bed depth developed by Dole and Klotz[11] and discussed in detail in Reference 3. A bed depth of only 0.4 inch is required for an iodine removal efficiency of 99.99% at rated air flow. The design efficiency for the 1-inch-thick SRP bed was maintained at flows about 10 times the rated air flow.[3] A 1-inch-thick bed was specified as an added measure of conservatism to increase capacity and to extend service life.

No known commercial adsorber beds could satisfy the test requirements; hence, it was necessary for SRL to design and develop improved beds. The carbon beds developed by SRL and in use at SRP pass all of the above tests. The full-size unit consists of a one-inch-thick bed of activated carbon enclosed between perforated metal sheets. The carbon and frame are subjected to stringent tests by the manufacturer (Barnebey-Cheney Co.) and SRL. Significant design features, shown in Figure 6, and specifications of the unit currently specified include:

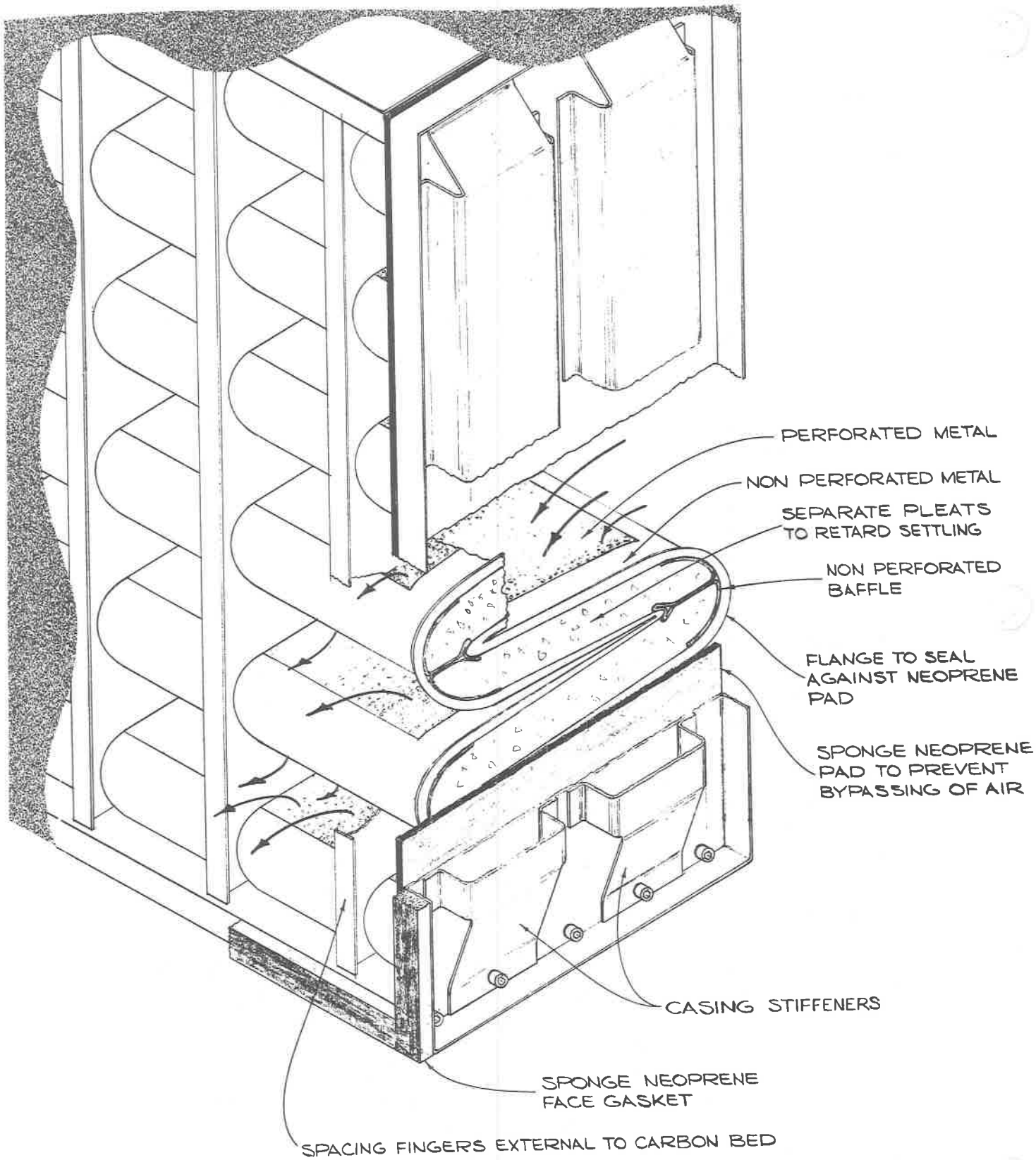


FIG. 6 SECTIONAL SCHEMATIC OF SRP ACTIVATED CARBON BED

- Type 304L stainless steel construction to retard corrosion. (Beds currently in service are made with frames of cadmium-plated or painted mild steel. These have the same adsorption characteristics as those made of stainless steel but shorter life. Beds made with stainless steel frames are being installed now in all filter compartments.)
- Rigid framing to prevent warping or buckling from mishandling and to withstand steam blasts to at least 10 times the normal air flow.
- Spacing fingers external to the carbon bed to maintain the bed thickness at 1 inch. Internal spacers are not used because flow channeling at the carbon-metal interface could occur, and they may interfere with packing uniformity.
- 12 separate pleats to retard settling of the carbon during shipment or during continuous exposure to flowing air for several years. The pleats are formed by 11 shielded baffles between two continuous sheets of perforated metal. Leaks are possible in units where each pleat is individually removable, but not where the unit is continuous. Shields direct the flow through a tortuous path in the curved portions of the units where minor settling may occur.
- Beds installed with pleats horizontal, to further minimize settling of carbon during service.
- A 1-inch baffle at all sides of the bed formed by omitting perforations at the edge of metal sheet to prevent channeling at the carbon-gasket interface.
- Each carbon bed unit packed with 53 pounds (minimum) of activated coconut shell carbon that is relatively dust free (97% hardness, minimum).[12]
- The carbon packed with a gravity system in which the carbon falls a minimum distance of three feet before entering the bed. Two mechanical vibration periods of 30 seconds each are permitted during the loading operation. This method provides a high packing density and a more uniform distribution of the carbon particles.

- After packing, carbon fines and dust blown from each unit with compressed air at a minimum nozzle velocity of 5000 ft/min.
- A mesh distribution of 10 x 14 (Tyler), selected because tests showed that coarse particles could segregate with carbon containing a wider range of carbon particles, i.e., mesh distribution of 6 x 14.
- A perforated face area of about 15 square feet that can pass 1000 scfm of air at a $\Delta P$ of about 0.8-inch $H_2O$. The unit measures 24 x 24 x 11-1/2 inches.
- Physical and chemical tests of representive samples from each batch of carbon made and certified by the vendor.
- Carbon with an ignition temperature greater than 330°C.
- Representative samples of the carbon submitted by the vendor to SRL for analysis. The carbon must remove 99.99% of elemental iodine when exposed to fog at 65°C and flowing at a face velocity of 70 ft/min and with an iodine loading of 1 milligram per gram of carbon.
- All units inspected by a Du Pont representative for quality construction and freedom from obvious and obscure flaws, before, during, and after charging with carbon. Particular attention is directed to construction details affecting quality of airtight seals and the carbon loading operation.
- Each unit tested for leaks with "Freon"* by SRL prior to installation in the confinement system. Beds containing leaks greater than 0.1% of the total flow are unacceptable. Details of the preinstallation "Freon" test are given in Reference 13.
- Carbon beds leak tested in place. The technique was recently developed and demonstrated by SRL. "Freon-112"* is used as a tracer to determine if leaks exist in the carbon beds or at gasket surfaces. The test will be conducted on a routine basis. The technique is described in References 14-18.

* "Freon" and combinations of "Freon-" or "F"- with numerals are Du Pont's trademarks for its fluorinated hydrocarbons.

Activated carbon beds as well as "Demisters" and particulate filters, have neoprene gaskets which begin to deteriorate at about 150°C. In the ignition test[19,20] a full-size prototype of the new SRP carbon bed, the neoprene gasket was not significantly damaged. The carbon bed ignited at 340°C and burned for about 18 minutes before the fire was extinguished.

The efficiency of activated carbon after about 2 years of continuous exposure to exhaust ventilation air from Savannah River Plant reactor buildings remains greater than the design objective of 99.9% for the removal of elemental iodine.[21] Table 1 shows the results of elemental iodine tests on carbon exposed to reactor building exhaust ventilation air for about 2-1/2 years.

Although the beds continue to provide adequate protection from halogen activity, two problems have arisen. The first is that the mild steel frames which contain the carbon are corroding from nitrogen and sulfur compounds that are in the building exhaust air in trace quantities. The corrosion is intergranular which results in severe embrittlement of the metal. Both the original cadmium-plated units and the later painted frames have been attacked. Failure of the perforated metal screen of only two units has been detected, but these failures resulted in a negligible loss of carbon. New units fabricated of Type 304L stainless steel are now being installed in all reactor areas.

The second problem is that of slow degradation of the carbon from adsorption of impurities, primarily $NO_2$. $NO_2$ is formed by radiolytic decomposition of atmospheric nitrogen and subsequent reaction with oxygen in the space between the reactor tank and the biological shield. The separations plant and nearby industrial plants also contribute $NO_2$ to the atmosphere. Analysis of used carbon shows only the presence of NO, so it is assumed that because free NO would not normally exist in air, $NO_2$ oxidizes the carbon and the residual NO sorbs on available sites. NO can be removed from the carbon by drying the bed in-place at about 60°C. The drying operation partially restores the iodine adsorption efficiency to about 99.98%, and increases the service life of the carbon.

TABLE 1

Iodine Tests of Used Carbon Samples from SRP Reactor Areas

| Test No. | Area | Bed Serial No. | Months of Service | Type Test | Efficiency % | Bed Loading $mgI_2/g$ Carbon | Notes |
|---|---|---|---|---|---|---|---|
| 113 | R | 24 | 14 | Steam-air | 99.95 | 1.3 | (1,2) |
| 114 | R | 24 | 14 | Steam-air | 99.92 | 0.9 | (1,2) |
| 115 | R | 24 | 14 | Air | 99.99 | 0.8 | (1,2) |
| 117 | R | 24 | 14 | Steam-air | 99.89 | 0.6 | (1,2) |
| 119 | R | 24 | 14 | Steam-air | 99.99+ | 0.5 | (1,3) |
| 122 | R | 23 | 14 | Steam-air | 99.98 | 0.5 | (1,2) |
| 123 | R | 23 | 14 | Steam-air | 99.98 | 0.4 | (1,4) |
| 124 | R | 23 | 14 | Steam-air | 99.98 | 0.4 | (1,5) |
| 111 | P | 114 | 15 | Air | 99.99+ | 1.6 | (1,2) |
| 112 | P | 114 | 15 | Steam-air | 99.99+ | 1.2 | (1,2) |
| 118 | P | 114 | 15 | Steam-air | 99.99+ | 1.2 | (1,2) |
| 164 | P | 613 | 15 | Steam-air | 99.99+ | 0.6 | (2,15) |
| 187 | P | 91 | 28 | Steam-air | 99.97 | 0.4 | (1,2) |
| 189 | P | 91 | 28 | Steam-air | 99.96 | 0.3 | (2,15) |
| 202 | P | 91 | 28 | Steam-air | 99.98 | 0.6 | (2,15) |
| 203 | P | 91 | 28 | Steam-air | 99.92 | 0.4 | (2,15) |
| 204 | P | 91 | 28 | Steam-air | 99.98 | 0.5 | (2,15) |
| 205 | P | 91 | 28 | Steam-air | 99.98 | 0.5 | (2,15) |
| 206 | P | 91 | 28 | Air | 99.98 | 0.7 | (2,15) |
| 133 | L | 132 | 20 | Steam-air | 99.97 | 0.4 | (1,2) |
| 134 | L | 132 | 20 | Steam-air | 99.99+ | 0.5 | (1,6) |
| 135 | L | 132 | 20 | Steam-air | 99.99+ | 0.5 | (7,2) |
| 136 | L | 132 | 20 | Steam-air | 99.99+ | 0.6 | (8,2) |
| 137 | L | 132 | 20 | Steam-air | 99.99 | 0.6 | (9,2) |
| 138 | L | 132 | 20 | Steam-air | 99.94 | 0.6 | (10,2) |
| 139 | L | 132 | 20 | Steam-air | 99.99 | 0.6 | (11,2) |
| 185 | L | 40 | 28 | Steam-air | 99.96 | 0.5 | |
| 140 | K | 76 | 20 | Steam-air | 99.99+ | 0.6 | (1,2) |
| 141 | K | 76 | 20 | Steam-air | 99.89 | 0.7 | (8,2) |
| 143 | K | 76 | 20 | Steam-air | 99.60 | 0.4 | (8,2,12) |
| 144 | K | 76 | 20 | Steam-air | 99.93 | 0.6 | (8,2,13,14) |
| 145 | K | 76 | 20 | Steam-air | 99.96 | 0.6 | (1,2) |
| 146 | K | 76 | 20 | Steam-air | 99.92 | 0.6 | (10,2) |
| 180 | K | 185 | 28 | Air | 99.99+ | 0.7 | (2,15) |
| 184 | K | 185 | 28 | Steam-air | 99.98 | 0.5 | (2,15) |
| 120 | C | 668 | 7 | Steam-air | 99.99 | 0.6 | (1,2) |
| 121 | C | 668 | 7 | Steam-air | 99.99+ | 0.7 | (1,2) |
| 158 | C | 650 | 17 | Steam-air | 99.98 | 0.5 | (1,2) |
| 201 | C | 650 | 17 | Air | 99.99+ | 0.9 | (2,15) |

Notes:

(1) Test bed was packed with 3 layers of carbon taken from the front, middle, and back of the 1-in.-thick layer in the full-size bed.
(2) Carbon was not dried.
(3) Carbon was dried for 20 hr at 95°C and 70 fpm air flow.
(4) Carbon was dried for 24 hr at 95°C and 70 fpm air flow.
(5) Carbon was dried for 24 hr at 65°C and 70 fpm air flow.
(6) Carbon was dried for 16 hr at 65°C and 70 fpm air flow.
(7) Test bed was packed with carbon from the front 1/2" of full-size carbon bed.
(8) Test bed was packed with carbon from the front 1/8" of full-size carbon bed.
(9) Test bed was packed with carbon from the back 1/2" of full-size carbon bed.
(10) Test bed was packed with carbon from the center 1/3" of full-size carbon bed.
(11) Test bed was packed with carbon from the back 1/8" of full-size carbon bed.
(12) Carbon removed from full-size bed 1 wk after carbon removed for test No. 141.
(13) Carbon for tests No. 143 and 144 identical.
(14) Carbon was dried for 16 hr at 95°C and 70 fpm air flow.
(15) Test bed was packed with a thoroughly mixed carbon sample removed from full-size bed.

Conditions for air test:

Duration of test: 2-1/2 - 3 hr
Face velocity: 70 ft/min
Temperature at test bed: 35°C (95°F)
Isotopic dilution: 1.5 mCi $^{131}I$ per 100 mg $^{127}I$

Conditions for steam-air test:

Duration of test: 2-1/2 - 3 hr
Face velocity: 70 ft/min
Steam flow: 1 $ft^3$/min
Temperature of test bed: 68°C (155°F)
Isotopic dilution: 1.5 mCi $^{131}I$ per 100 mg $^{127}I$

Contaminants in the carbon that reduce efficiency migrate through the bed even at room temperature. Initially, the material is sorbed in greatest concentrations on the front face of the bed. Although the efficiency at the front face may be low, the overall efficiency of the bed still remains high. This was demonstrated by tests on carbon beds from K Reactor Area, as shown in Table 1.

As would be expected, the efficiency of used carbon in air was higher than in steam-air mixtures.

As mentioned above, all carbon beds are scheduled for replacement which started in the summer of 1966. Carbon will be tested periodically to ensure that beds will be replaced when efficiencies decrease below a satisfactory level.

REFERENCES


1. W. S. Durant, et al, Activity Confinement System of the Savannah River Plant Reactors, USAEC Report to be issued, E. I. du Pont de Nemours & Co., Savannah River Laboratory, Aiken, S. C.

2. J. A. List, The SRP Production Reactor Containment Program, Eighth AEC Air Cleaning Conference, TID-7677, pp. 273-279, October 1963.

3. G. H. Prigge, Application of Activated Carbon in Reactor Containment, USAEC Report DP-778, E. I. du Pont de Nemours & Co., Savannah River Laboratory, Aiken, S. C., September 1962.

4. A. H. Peters, Application of Demisters and Particulate Filters in Reactor Containment, USAEC Report DP-812, E. I. du Pont de Nemours & Co., Savannah River Laboratory, Aiken, S. C., December 1962.

5. J. W. Walker and A. H. Peters, Use of Filters in Reactor Containment, Mech. Eng., 85 (9): 46 (1963).


DP 1071

6. J. B. Hays, Performance of High Efficiency Particulate Filters Subject to Steam-Air Mixtures, Summary of the Seventh AEC Air Cleaning Conference, Oct 10-12, 1961 (August 1963).

7. H. W. Knudson and W. Locke, Development of Smoke Penetration Meters, Report P-264, U. S. Naval Research Laboratory, September 1945.

8. Filter Units, Protective Clothing, Gas Mask Components and Related Products, Performance Test Methods, Method 102.9.1 pp. 33-38, MIL Std. 282, May 28, 1956.

9. Military Specification: Filter Particulate, High Efficiency, Fire Resistant, MIL-F-51068A, 23 April 1964.

10. J. W. Thomas and G. D. Crane, Aerosol Penetration Through 9 Mil HV-70 Filter Paper With and Without Pinholes, Eighth AEC Air Cleaning Conference, TID-7677, October 1963.

11. M. Dole and I. M. Klotz, Sorption of Chloropicrin and Phosgene on Charcoal from a Flowing Gas Stream, Ind. Eng. Chem., 38: 1289 (1946).

12. Military Specification, MIL-C-13724A, May 4, 1960.

13. A. H. Peters and D. R. Muhlbaier, Nondestructive Test of Carbon Beds for Reactor Containment Applications - Progress Report-June 1962 to December 1963, USAEC Report DP-870 E. I. du Pont de Nemours & Co., Savannah River Laboratory, Aiken, S. C., February 1964.

14. D. R. Muhlbaier, Nondestructive Test of Carbon Beds for Reactor Containment Applications - Progress Report-January-March 1964, USAEC Report DP-910 E. I. du Pont de Nemours & Co., Savannah River Laboratory, Aiken, S. C., September 1964.

15. D. R. Muhlbaier, Nondestructive Test of Carbon Beds for Reactor Containment Applications - Progress Report: April-June 1964, USAEC Report DP-920, E. I. du Pont de Nemours & Co., Savannah River Laboratory, Aiken, S. C., November 1964.

16. D. R. Muhlbaier, Nondestructive Test of Carbon Beds for Reactor Containment Applications - Progress Report: July-September 1964, USAEC Report DP-950, E. I. du Pont de Nemours & Co., Savannah River Laboratory, Aiken, S. C., April 1965.

17. D. R. Muhlbaier, Nondestructive Test of Carbon Beds for Reactor Confinement Application - Progress Report: October 1964-January 1966, USAEC Report DP-1053, E. I. du Pont de Nemours & Co., Savannah River Laboratory, Aiken, S. C., June 1966.

18. D. R. Muhlbaier, In-Place Nondestructive Leak Test for Iodine Adsorbers, 9th AEC Air Cleaning Conference, Boston, Mass., September 1966.

19. R. C. Milham, High Temperature Carbon for Iodine Adsorption, USAEC Report to be issued. E. I. du Pont de Nemours & Co., Savannah River Laboratory, Aiken, S. C.

20. R. C. Milham, High Temperature Carbon for Iodine Adsorption, 9th AEC Air Cleaning Conference, Boston Mass., September 1966.

21. W. S. Durant, Performance of Activated Carbon Beds in SRP Reactor Confinement Facilities, Progress Report September 1962-September 1965, USAEC Report DP-1028, E. I. du Pont de Nemours & Co., Savannah River Laboratory, Aiken, S. C., January 1966.

## DISCUSSION

PETERS: We will take one or two questions from the floor at this time.

PARKER (ORNL): I am going to be very unpopular. I don't believe the indicated efficiency, 99.99% for removal of radioiodine. I know the report, of course. However, I think that the audience should realize that what you are saying is that your safety analysis says that you will not produce methyl iodide, and on that basis, your filter system will operate at that efficiency, which leaves the margin on methyl iodide, certainly, really still a little controversial.

PETERS: We recognize that. I think I might make one point with reference to the report that Mr. Durant mentioned. The methyl iodide question is quite a controversial one. What we report in that document does not allow one to necessarily draw the same conclusion that we have drawn for different applications. The application is quite important, we feel. But, in the report, we do spend a great deal of effort on the chemistry, the kinetic effect of radiation on decomposing methyl iodine, etc.

HEYSE: You concluded that only one filter media actually satisfied the steam bath requirement. I believe you concluded this in December of 1962, and I don't believe this represents the current state of the art.

DURANT: We agree with that. But no one has come forth with a filter challenging the one that we use. We will welcome all comers.

# FLOATING ROOF CONTAINMENT VESSELS

by

Melvin W. First, Leslie Silverman*, Daniel Pender, and Stanley Dawson

Harvard Air Cleaning Laboratory
School of Public Health, Harvard University
Boston, Mass. 02115

## A B S T R A C T

Theoretical and experimental evaluations show that complete containment of the products of a nuclear reactor accident can be accomplished using a modified commercial gas holder. A holder capable of storing in excess of 20 x $10^6$ cubic feet could retain such releases at a pressure substantially the same as ambient. As a first step in the evaluation of this concept, a small pre-pilot model was constructed to obtain information on seal mechanisms, lubricants, and functional parameters. Based on the resulting data, a 500 cubic foot floating type pilot-scale gas holder has been designed and is currently under construction. Advantages of the proposed system include its relative low cost and the fact that the radioactive materials retained in the holder can later be removed by one or a combination of several decontamination methods.

This work was performed under terms of a contract between Harvard University and the U.S. Atomic Energy Commission

*Deceased

## I. INTRODUCTION

The purpose of this investigation is to develop mechanisms for, and to study the performance characteristics of, a floating roof reactor and off-gas containment vessel. The pressure surge following a major coolant line rupture would be absorbed and suppressed by movement of a leak-tight movable roof. Activation of cooling water sprays following the accident would condense steam and permit the roof to fall slowly to its normal position. The advantages of this containment vessel concept are: (1) In the event of a Maximum Credible Accident, the roof would rise in response to the applied pressure, preventing the shell from being subjected to stresses in excess of a fraction of a pound per square inch. As recovery measures took effect, the floating roof would settle and return to its original position when the pressure inside the containment vessel returned to normal. (2) As the pressure of the stationary parts of the containment shell would not exceed 0.25 psi, it might be possible to lighten and simplify the structure and thereby effect substantial savings while maintaining an equal degree of safety.

An additional use for this containment vessel concept is in connection with chemical plant operations on nuclear fuel dissolvers. Flexible gas storage capability will make it possible to hold radioactive rare gases and $NO_X$ for prolonged periods for slow treatment steps.

Theoretical and experimental investigations are being conducted to develop new methods for constructing gas tight seals in rapidly moving floating pistons, and to determine dimensions and dynamic similarity parameters so that the results of pilot model tests may be extended to full-scale units. The next step in the experimental program will be performed with the aid of a 500 cu. ft. floating piston gas holder. This gas holder has been designed to maintain gases at temperatures in excess of 215°F with the use of a tempering water jacket. In addition, provision has been made for introducing water and chemical sprays of various types to investigate the decontamination factors obtainable by this simple gas purification method. Finally the pilot unit has been designed to test the gas tightness and drag resistance of various piston edge sealing systems.

## II. CHARACTERISTICS OF GAS STORAGE CYLINDERS

Two types of large, low-pressure, cylindrical storage containers are in common use. One employs a floating piston inside a cylindrical metal shell (Figure 1A). The gas is stored below the piston and a gas tight edge seal is made for the piston with mechanical gaskets and a liquid reservoir over the gasket of sufficient hydrostatic head to overcome the pressure of the gas below. The sealing liquid seeps through the edges of the gasket but is collected automatically

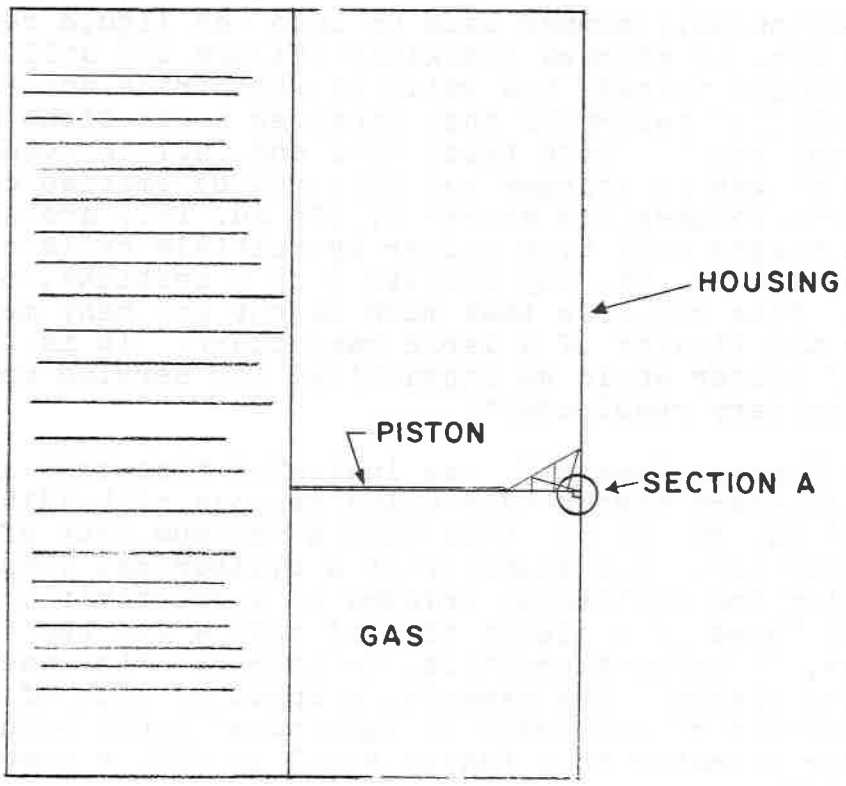


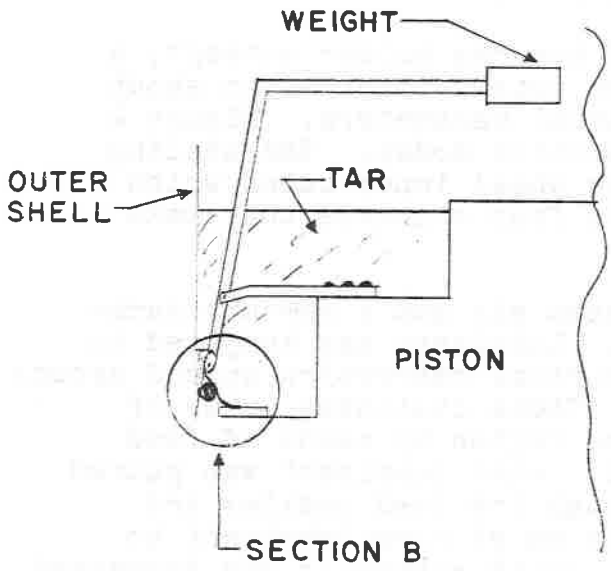


SECTION A ENLARGED

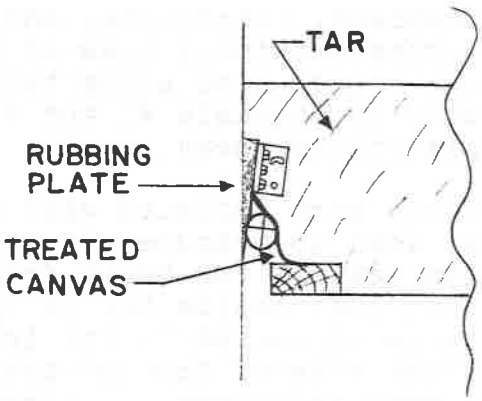


SECTION B ENLARGED

WATERLESS PISTON-TYPE GAS HOLDER

FIGURE 1A

and continuously pumped back up into the liquid reservoir. The second type of storage container (Figure 1B) utilizes a movable bell storage vessel, the walls of which rise and fall in an annular, liquid-filled reservoir that provides a gas tight seal and buoys the metal shell. Both types rise and fall in response to the volume of gas in storage and both may be emptied completely. Large gas volumes (in excess of $10^6$ cu. ft.) are accommodated in the rising bell type holder by multiple bells so that a single unit of $10^7$ cu. ft. may involve 4 or 5 sections, one on top of the other. This requires that much weight and many mechanisms be moved during the filling of a large gas holder. It is believed that this type of holder would be impractical for service where rapid filling was a primary requirement.

The Koppers Company* has indicated that they are prepared to build standard piston-type units capable of holding in excess of $2 \times 10^7$ cu. ft. of gas that have a maximum rate of piston rise of 4 ft. per min. The diameter of a cylindrical vessel capable of absorbing the accidental release of a reactor's coolant would be far too large if a piston rise of only 4 ft. per min. was utilized. However, it appears practical to increase the speed of rise of the floating piston. For example, a speed of rise of 40 ft. per min., (an increase of one order of magnitude) would reduce the required cylinder diameter by a factor equal to $\sqrt{10}$, a more manageable dimension.

## III. LABORATORY INVESTIGATIONS OF RAPIDLY MOVING FLOATING PISTONS

As a first step in the evaluation of the gas holder concept, a small pre-pilot model was constructed to obtain information about seal mechanisms, lubricants, and functional parameters. Figure 2 shows a cross sectional view of the pre-pilot model. The sealing tubes were constructed using two bicycle wheel inner tubes which were seated in channels #1 and #3 of the four channels that make up the piston periphery.

The tubes were inflated with compressed air and a mercury manometer was used to measure air pressure. Lubricant was supplied to the region between the seals from cylindrical reservoirs spaced around the piston, just inside the periphery. These cylinders, made of Lucite, were connected to the inter-tube region by means of feed nozzles that entered through channel #2. When lubricant was poured into the open cylinders, it flowed through the feed nozzles and filled the inter-tube region. The addition of more lubricant to the cylinders raised the height of the liquid reservoir and increased the hydrostatic pressure in the region of the seals. The center piston guide post prevented canting of the piston as it moved up and down the cylinder. A close tolerance fit between the lubricated guide post and the piston sleeve prevented air flow (or leakage) through the center sleeve when the piston moved.

---

* The Koppers Company, Gas Apparatus Section, Baltimore, Md.

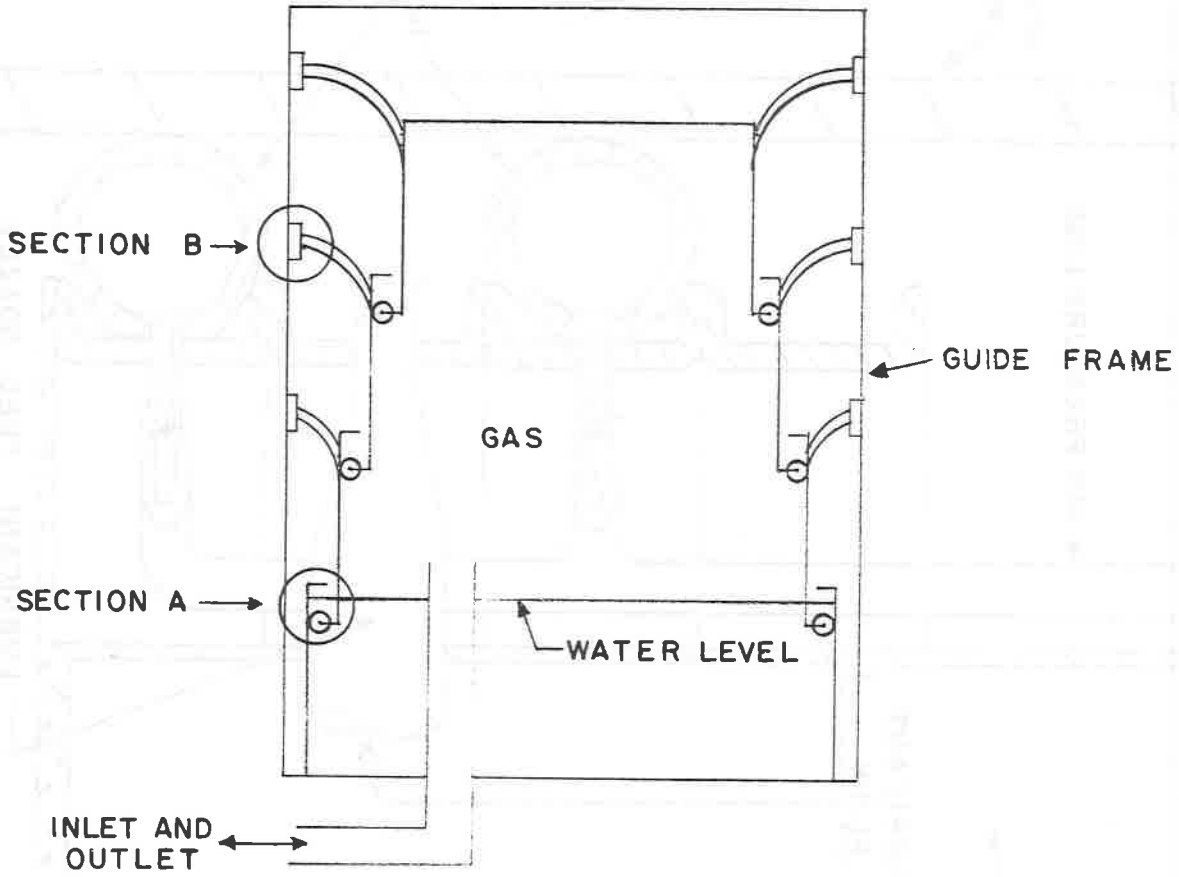


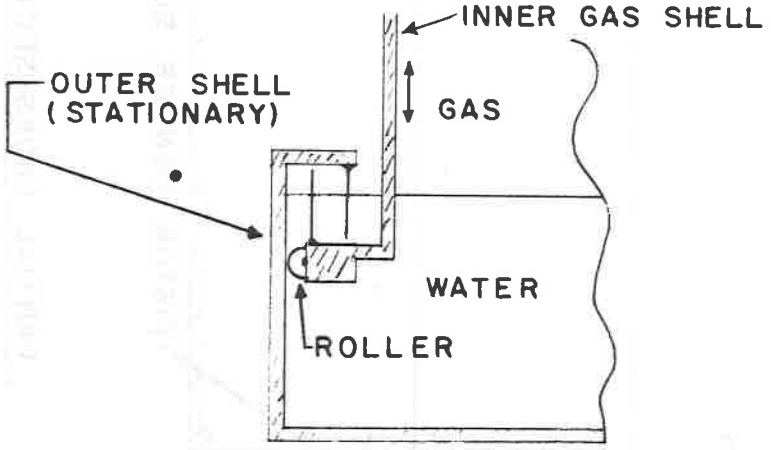


SECTION A – SEAL CUP

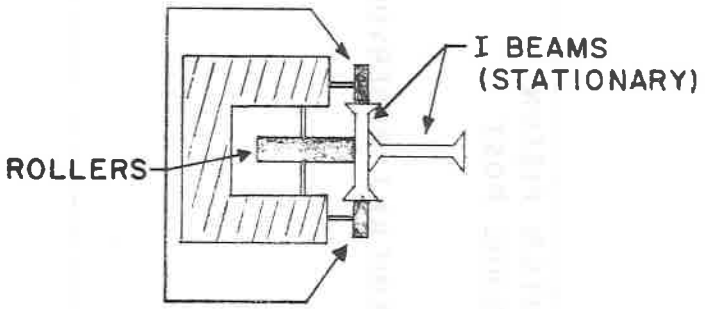


SECTION B – ROLLER MECHANISM

THREE LIFT, WATER SEALED, GAS HOLDER.

FIGURE 1B

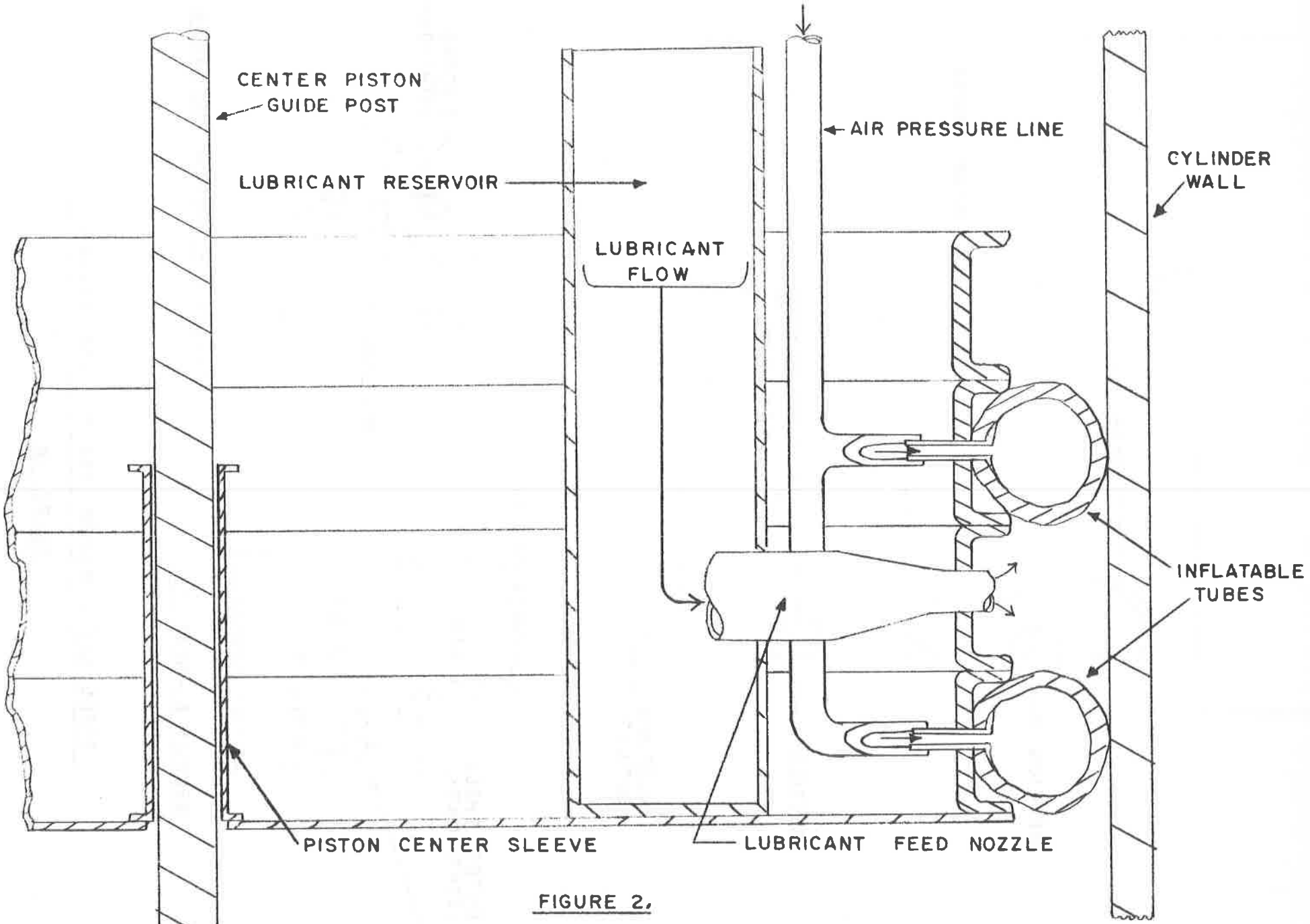


FIGURE 2.

PARTIAL CROSS SECTION OF ACTUAL PISTON SEAL DESIGN

A water manometer, tapped into the lower chamber of the tank, measured steady state pressure in the tank. A mercury manometer connected to the valve stems of the seal tubes, measured tube pressure. Lubricant pressure was measured by noting the height of the liquid in one of the transparent storage cylinders. Air to drive the piston upward was supplied from a laboratory compressed air supply or a mechanical pressure blower. Speed of ascent of the piston was measured by clocking the time to move a measured distance of 2.5 feet. Systematic variation of seal tube air pressure, seal lubricant pressure, and rate of rise permitted evaluation of operating characteristics. The initial impulse needed to bring the piston to its steady state speed was measured, also, to determine peak transient force. This value was of interest as a back pressure limit might be imposed on a full scale unit.

A. Results

1. Lubricants

The first lubricant tested was water. It was found unsatisfactory because, rather than lubricating, it increased the tube's tendency to stick to the surface it contacted. As a result, the tubes were pulled out of the seats when the piston was moved. Therefore, it was concluded that a more viscous liquid with lower surface tension was needed. Glycerine was chosen in preference to an oil as its viscosity may be varied by mixing with water. However, undiluted glycerine was found to provide satisfactory lubrication and all results obtained were with glycerine alone.

2. Seal Lubrication

The theory of lubrication is well known for ideal models and may be quantitated in the formula for viscous drag between lubricated surfaces:

$$\tau = \mu \frac{1}{h} \frac{dx}{dt}$$

where:

$\tau$ = shear drag force

$\mu$ = viscosity of the fluid

$h$ = gap width

$\frac{dx}{dt}$ = relative velocity between the lubricated surfaces.

For constant viscosity, it may be seen from this equation that drag will increase with velocity (dx/dt) and decrease for greater gap widths (h). Applications to real systems often yield results that can be used only in a qualitative way to gain insight into what is happening. This occurs when all the variables employed in the theory can not be measured directly. For example, during a run,

neither the effective contact area between cylinder wall and seal nor the thickness of the dynamic layer of lubricant can be measured directly. These two parameters varied during different tests and were affected by changes in tube pressure, lubricant pressure, quantity of lubricant available, and piston speed as well as lubricant viscosity and surface tension.

Therefore, it was decided to start with the simplest form of lubrication, i.e., swabbing liquid on the inside of the cylinder and the contact surfaces of the seal tubes prior to each test. During this series of runs, the inter-tube region was not filled with lubricant and the lubricant coating the surfaces was not under hydrostatic pressure. The results of these runs are shown in Figure 3. These data show the variation of forcing (cylinder) pressure with seal tube pressure for two different piston speeds. The seal threshold indicated on the curve is the pressure required to inflate the tubes to the point where they made contact with the cylinder wall. As may be seen, cylinder pressure (which is convertible to seal resistance) is approximately linear with seal tube pressure in the range of 7 - 10 inches of Hg.

Considering Curve A, Figure 3, it may be seen that when piston speed was constant at 5.8 ft./min., drag increased for greater seal tube pressures. At the same time, gap width decreased because of greater tube pressure and drag increased in the manner predicted by the formula.

Shifting attention to Curve B (piston speed 8.9 ft./min.) an initial increase in drag (over that for piston speed of 5.8 ft./min.) was observed at 7" Hg seal tube pressure but drag did not increase as rapidly with increases in tube pressure because greater fluid influx was induced at the higher speed and better lubrication resulted.

The next step was to fill the inter-tube region as well as the uppermost channel with lubricant. With this arrangement, a slight hydrostatic pressure was imposed by the volume of fluid supported and retained by the seal. This pressure was less than 2 inches of water. Results of these runs can be seen in Figure 4. Here seal resistance is plotted against piston speed, with lubricant pressure approximately constant at 2 inches of water.

Two factors appear to affect the seal resistance. One, the increased shear effect, would tend to increase seal resistance with increasing velocity. The other, the greater transport of fluid into the seal area with a resulting widening of the gap, would tend to cause the seal resistance to decrease with increasing velocity. The combined effect of these two factors determined whether seal resistance increased or decreased with velocity. If the gap were fixed and not elastically variable, as in this case, only the velocity shear factor would be present and seal resistance would increase proportionally with velocity

FIGURE 3.

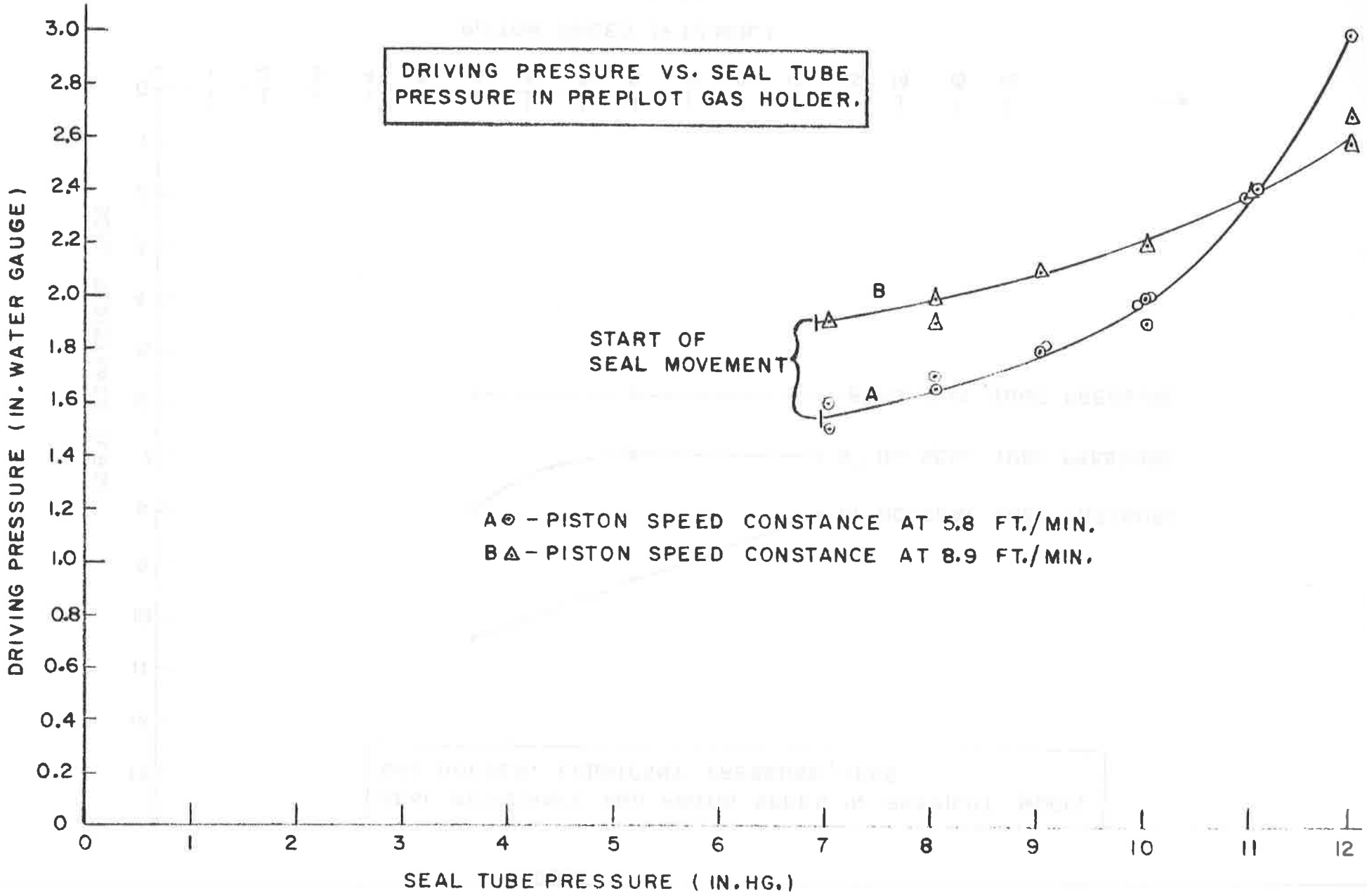
DRIVING PRESSURE VS. SEAL TUBE PRESSURE IN PREPILOT GAS HOLDER.
DRIVING PRESSURE (IN. WATER GAUGE)
3.0
2.8
2.6
2.4
2.2
2.0
1.8
1.6
1.4
1.2
1.0
0.8
0.6
0.4
0.2
0
0
1
2
3
4
5
6
7
8
9
10
11
12
SEAL TUBE PRESSURE (IN. HG.)
B
START OF SEAL MOVEMENT
A
A ⊙ - PISTON SPEED CONSTANCE AT 5.8 FT./MIN.
B △ - PISTON SPEED CONSTANCE AT 8.9 FT./MIN.

FIGURE 4.

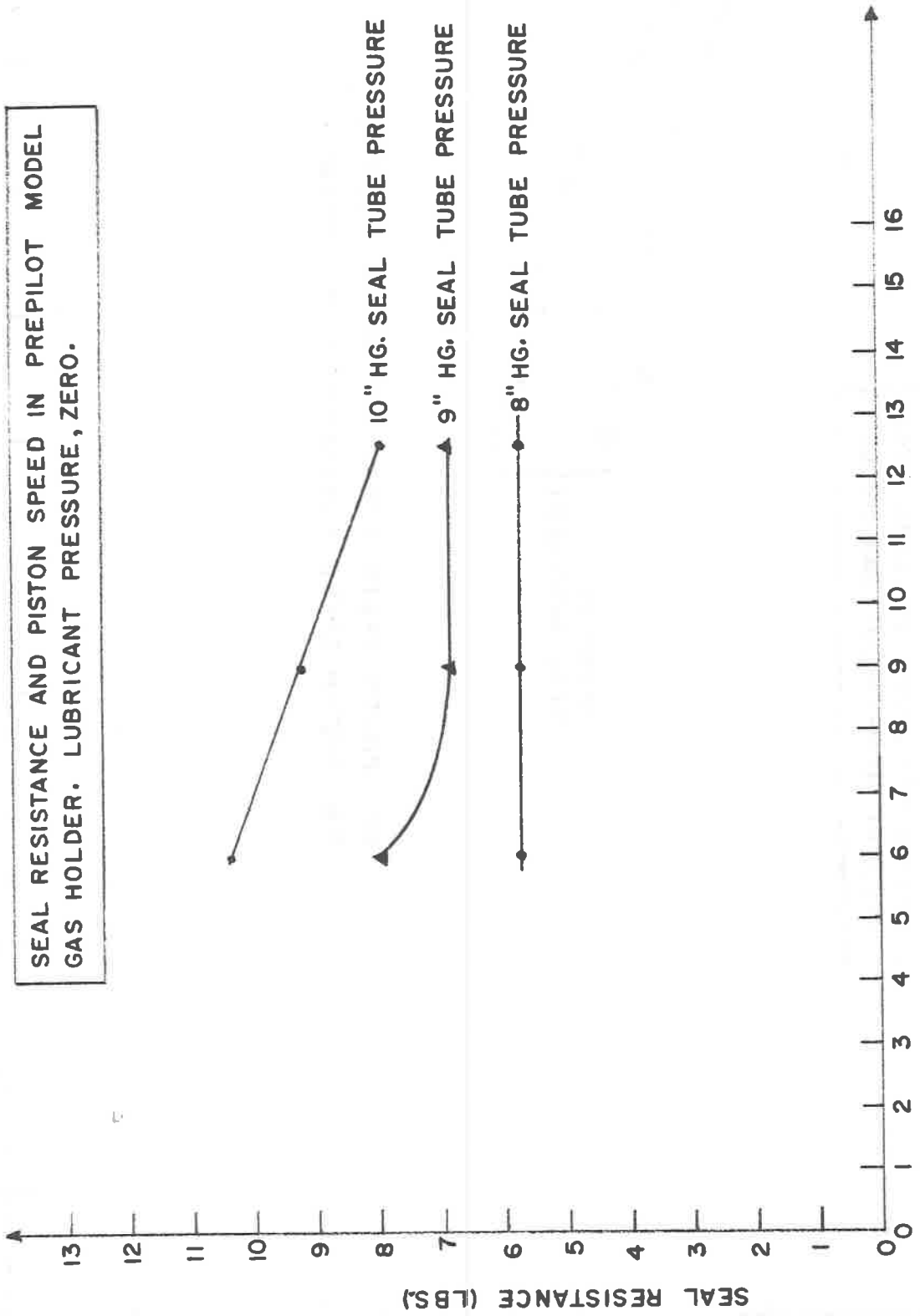
SEAL RESISTANCE AND PISTON SPEED IN PREPILOT MODEL GAS HOLDER. LUBRICANT PRESSURE, ZERO.
10" HG. SEAL TUBE PRESSURE
9" HG. SEAL TUBE PRESSURE
8" HG. SEAL TUBE PRESSURE
SEAL RESISTANCE (LBS.)
PISTON SPEED (FT./MIN.)
0
1
2
3
4
5
6
7
8
9
10
11
12
13
14
15
16

Considering Figure 4, it may be seen that for a seal tube pressure of 8" Hg, resistance was constant as piston speed increased, indicating that the two factors were equal and canceled each other. At 9" Hg seal tube pressure, the transport effect predominates initially (as resistance fell for increased speed), but at higher speeds the velocity effect increased in magnitude and exceeded the transport effect. At 10" Hg seal tube pressure, the transport effect was dominant and seal resistance decreased continuously at greater speeds. It is possible that this curve approaches a constant value at higher speeds in the same manner as the curve for nine inches of mercury seal pressure. The results shown in Figure 4 indicate that resistance to movement by a lubricated piston is a complex function and investigation may indicate practical methods for minimizing resistance at high speeds.

With pressurized lubricant (6-10" of glycerine), there was no observable gas leakage through the seal. This was anticipated, as the pressure of the lubricant (>5" w.g.) was greater than the forcing gas pressure; therefore any fluid flow that took place across the seal would be by the lubricant rather than the gas. It was found, however, that no significant amount of glycerine, as measured by changes in the height of the lubricant reservoir columns, was lost through the seal in this way. It was also observed that pressurizing the lubricant did not result in a significant increase in lubricant consumption. There appears to be no general effect attributable to lubricant pressure. This leads to the conclusion that slight pressurization of the lubricant produces no significant effect on seal performance characteristics other than assuring a positive gas seal. Higher lubricant pressures have not been investigated to date.

It was observed that allowing the piston to remain stationary in the cylinder for some period of time permitted the pressurized seal tubes to force lubricant out of the space between tube and cylinder wall. It was then necessary to exert considerably more force to start the piston than was required to maintain it in motion. This effect was observable after only a few minutes. For brief periods (of the order of 10 seconds) little lubricant flow occurred and the retardation effect was not pronounced but it became more marked the longer the piston was held stationary. To measure this effect, the piston was allowed to remain static for a measured length of time and then pulled upward at constant velocity by means of an electrically operated overhead hoist. A tensile strain element mounted with strain gages was inserted, series-wise, in the hoisting cable. These strain gages and the associated recorder permitted initial-peak and steady state measurement of cable tension as the piston moved.

In all cases, tension quickly reached a peak and then dropped to a steady state value. Seal resistance increased rapidly during the first few moments of standing time and then approached an asymptotic value for periods much longer than ten minutes, indicating that most of the fluid had been lost from the seal by this time. Increased seal tube pressure resulted in a higher

value after five or more minutes of standing but there was no significant difference for shorter periods.

The maximum peak starting transient overpressure ratio was 8.6 for 8" Hg seal pressure and 7.25 for 10" Hg. Thus for an operating tank pressure of 2.5 inches of water, the peak pressure at the start of filling might be as high as 21.5 inches. However, it should be noted that this transient is completed within 1 second and this tends to decrease the importance and significance of a high peak pressure.

Although some small amount of starting overpressure appears to be unavoidable, there are ways to overcome initial piston resistance, no matter how long the period between piston rises. These involve increasing lubricant pressure just before the start of cylinder filling to produce a copious flow of lubricant through the gap between seal and cylinder wall. The effect of this induced fluid layer would be to decrease initial seal resistance and counter the starting transient peak overpressure that has been observed. Alternatively, the piston may be kept in constant short amplitude vibratory movement by a "dither" mechanism that would assure continuous seal lubrication over long periods of time (i.e., years).

B. Projection of Results to Large Scale Units

It was found that steady state piston movement was reached in approximately one second, indicating that it moved under equilibrium conditions during most of its rise. The steady state motion of the piston may be described by the following equation if we assume that the pressure exerted by the incoming gas is essentially constant.

$$\underbrace{W\pi R^2}_{\text{piston weight}} + \underbrace{(2\pi Rb)\ \frac{u}{h}\ \frac{dx}{dt}}_{\text{seal resistance}} = \underbrace{P\pi R^2}_{\text{gas pressure force}}$$

where

W = piston weight/unit area

R = radius of piston

$\mu$ = lubricant viscosity

h = gap width of the seal

$\frac{dx}{dt}$ = piston velocity

P = gas pressure

b = width of the seal contact area

$2\pi Rb$ = total seal contact area

(all in compatible units)

Reducing and rearranging, we obtain the following equation for velocity.

$$\frac{dx}{dt} = \frac{(P-W)\ Rh}{2\mu b}$$

To extrapolate the pilot plant data to a full scale system, we impose the following conditions: (a) gas pressure will remain the same; (b) viscosity of the lubricant will be the same. In addition, we will make the following assumptions: (a) gap width will be approximately the same; (b) piston weight per unit area will be approximately the same.

The scale-up equation that results is as follows:

$$\frac{dx}{dt} = K\ \frac{R}{b}$$

Where

$$K = \frac{(P-W)h}{2\mu} = \text{constant}$$

This predicts that piston speed will increase in proportion to size. Speed is also dependent on "b", the width of the seal contact area, which will increase in larger gas holders because larger tubes will be used to provide seals in larger tanks. If the seal area width were to increase directly proportionally to scale:

$$b = cR$$

Where c is a constant of proportionality

and then $$\frac{dx}{dt} = K\ \frac{R}{b} = K\ \frac{R}{cR} = \frac{K}{c}$$

indicating that piston speed would not vary with scale. Calculations for pre-pilot unit and pilot unit designs indicate the following relations:

| Scale (R) | Seal width (b) | Ratio $(\frac{R}{b})$ |
|---|---|---|
| .84' | 2 1/4" | 4.45 |
| 4' | 6" | 8 |
| 200' | 100" (max) | 24 |

These figures indicate that the value $(\frac{R}{b})$ increases as the system is scaled up to larger units and that the overall effect will be to increase permissible piston velocities. On the basis of these conclusions, the results from the pre-pilot tank may be used to predict performance of a proposed pilot unit in the following manner.

For a particular run with the pre-pilot unit, the following values were observed.

speed = 12.5 ft. per min.
tube pressure = 9 inches of mercury
lubricant pressure = 2 inches of water
seal resistance = 6.8 pounds
piston diameter = 20"
piston wt. = 13 pounds
cylinder pressure = 2.3 inches of water
seal width = 1 1/8"

For the pre-pilot unit,

$$W = \frac{13}{\pi (\frac{10}{12})^2} = 5.8 \text{ pounds per square foot}$$

For a 500 cu. ft. pilot unit, piston weight is estimated at,

$P_w$ = 300 pounds

and

$$W = \frac{300}{(4)^2} = 5.9 \text{ pounds per square foot}$$

Thus, W is approximately the same for both units, verifying the previous assumptions.

Equations for the two units are:

$$\frac{dx}{dt}_{pp} = \frac{(P-W)h}{2\mu} \quad \frac{R_{pp}}{b_{pp}}$$

$$\frac{dx}{dt}_{p} = \frac{(P-W)h}{2\mu} \quad \frac{R_p}{b_p}$$

where

pp = pre-pilot

p = pilot

As $\frac{(P-W)h}{2\mu}$ is constant

it is the same value for both, and

$$\frac{dx}{dt}_p = \frac{(R/b)_p}{(R/b)_{pp}} \quad \frac{dx}{dt}_{pp}$$

so

$$\frac{dx}{dt}_p = \frac{8.0}{4.45} * 12.5 = 22.5 \text{ feet per minute}$$

(Note that this projected speed is based on the validity of the assumptions made; especially that of seal gap width being the same for both units).

Extending this projection to a full scale unit, one would predict even higher speeds because of the increased R/b ratio. Proceeding as before, and based on the assumed values for R and b,

$$\frac{dx}{dt}_{\text{full scale}} = 67.5 \text{ feet per minute}$$

The pistons of the full scale units manufactured by the Koppers Company operate at speeds of only four feet per minute. For this reason, the predicted speed of 67.5 feet per minute at 2.3 inches of gas holder pressure requires close examination (in spite of the fact that the Koppers Company may never have had a requirement for speeds in excess of 4 feet per minute or that their speeds are limited by the tar sealant employed). First, the unit area weight (w) of the full scale unit may be greater than the assumed value (5.9 pounds per square foot). Second, the increased seal width (b) may cause a decrease of the gap width (h). Both factors would tend to decrease speed for a given gas pressure.

An estimate can be made of the weight of a full scale piston. This is based on photographs of a full scale unit designed by the Koppers Company. The basic piston design is that of a circular plate reinforced on the upper surface with 28 radial I-beams. These beams are approximately 24-inch I-beams weighing 28 pounds per linear foot when fabricated from aluminum. The circular plate is estimated to be 0.25 inch thick. For a 100 foot radius tank, total weight of aluminum I-beams = (28) x (100) x 28 = 78,400 pounds. This weight, distributed over the piston, yields a specific weight of $\frac{78,400}{\pi 100^2}$ = 2.46 pounds per square foot. One square foot of 1/4" aluminum plate (density = 0.1 pound per cubic inch) has a weight of 12 x 12 x 1/4 x 0.1 = 3.6 pounds per square foot.

Thus the specific weight of a 200 foot diameter piston constructed of aluminum would be 6 pounds per square foot. Increasing this value by an amount of one pound per square foot to account for reinforcing and seal structures, results in a value of 7 pounds per square foot.

This calculation shows that the piston of a full scale gas holder would have a specific weight that is somewhat greater than

that of the pilot models if made of aluminum, indicating that full scale models may have piston speeds lower than those predicted. Nevertheless, it seems likely that gas holders with filling rate capacities much greater than those commercially available can be constructed, using seals and lubricants of the types discussed, in conjunction with pistons designed for minimal weight.

### C. Mathematical Analysis of Piston Movement

A theoretical analysis was made to study the movement of large air-driven pistons. The results indicate that a persistance oscillation must modify the steady progress of a piston during a rapid rise and must continue as an overshoot at the end of the rise. The analysis is in terms of dimensionless parameters, which facilitate the use of model data in the design of a full scale system. Details of the assumptions and equations are contained in NYO-841-3R.[1] Analysis of results indicates for a 275 foot diameter gas holder and a piston movement of 40 ft/min that the amplitude of oscillation of displacement of the pistons will be 0.2 ft. initially and 0.54 ft. at the end of its rise. Amplitude of oscillation of velocity will be 2.5 ft/sec. initially and 0.9 ft/sec. at the top. The period of oscillation at the start is 0.6 sec., and at the end the period of the over-shoot oscillation is 4.5 sec.

## IV. DESIGN OF A 500 CUBIC FOOT PILOT-SCALE GAS HOLDER FOR ADVANCED STUDIES

An important objective of the theoretical and laboratory studies that were conducted was to provide guidance for the design of an advanced type of pilot unit that would provide close analogies with the performance characteristics of large, full-scale units. A 500 cubic foot floating piston type pilot-scale gas holder is currently under construction.

The pilot unit design includes provision for almost complete emptying by allowing the movable piston to descend to within one inch of the tank floor. To evaluate the pilot unit under simulated conditions, a heating jacket has been provided on the sides and bottom of the tank through which steam can be circulated. Operating the pilot unit at this temperature will make it possible to investigate how lubricants perform under anticipated operated conditions. To make certain that the test unit will be gas tight for the anticipated operating pressure range, all seams and welds are to be gas tight under at least 2 psig.

Provision is to be made to collect the lubricant that flows through the seals in a circular retaining ring inserted in the bottom of the tank to form a collecting channel for the fluid flowing down the cylinder walls. Drain plugs will permit this channel to be emptied periodically.

In commercially available gas holders, pistons are of such aspect ratio (height/diameter) that canting is practically impossible. For the laboratory unit, however, it was concluded that a piston of the same aspect ratio would be too bulky for the space available. Therefore, a relatively low aspect ratio piston was designed. To prevent canting, a center guide post was added.

## V. DISCUSSION AND COMMENTARY

These evaluations show that complete containment of the products of a nuclear reactor accident can be accomplished using a modified commercial gas holder. A holder capable of storing in excess of $20 \times 10^6$ cubic feet could retain such releases at a pressure substantially the same as ambient. Decontamination of these gases prior to their release, and emptying of the gas holder could be conducted at the rate of 1,000 cfm over a period of 7 to 15 days. It may be noted, also, that decay of short-lived radionuclides would be appreciable over a storage period of one week (e.g., $^{131}I$ with a half-life of slightly over eight days would decay to almost one half its initial activity during this period) so that storage for seven days combined with a somewhat higher rate of gas cleaning over the next seven days would give obvious benefits.

Possible gas decontamination steps following storage and in situ cleaning are the following: (a) dry the gases by refrigeration or use of a solid adsorbent, (b) filter through fibrous prefilters plus absolute particulate filters, and finally, (c) adsorb residual contaminant gases, such as $^{131}I$, on activated carbon beds. This represents an intensive treatment cycle but because, (a) the volumetric cleaning rate will be low (~1,000 cu. ft. per min.), and (b) the amount of contaminant to be removed and stored in the gas cleaner will be substantially decreased by prior treatment, both capital and operating costs of this size of a gas decontamination system will be insignificant in relation to the total cost of a test. At a rate of 1,000 cu. ft. per min., approximately $1.5 \times 10^6$ cu. ft. can be treated per day.

The cost of a $10^7$ cu. ft. commercial gas holder, erected on site, has been estimated by one experienced fabricator in this field to be $2,000,000. This cost figure may be used in evaluating the savings that may be expected by substituting a floating roof containment vessel for a conventional pressure resistance containment structure.

An added advantage of a floating roof containment vessel is the possibility of further raising the floating roof, after an accident so as to put the entire container vessel under slight negative pressure. Leakage, if any would then be inward and atmospheric contamination prevented.

References

1. First, M.W., Silverman, L., Pender, D., and Dawson, S., Proposed Gas and Air Cleaning Systems for Rover Engine Test Stands. Harvard School of Public Health, Boston, Mass. Issued as USAEC Report NYO-841-3R, 1964.

## DISCUSSION

HAKE: This isn't a question, but it is a comment. At our Pickering station situated very close to metropolitan Toronto, which has 1500 megathermal units, we are fitting a vacuum type building, which is similar in function to a piston device. I think the capacity of this is in the order of 2 million cubic feet. I am not too sure, but our price seems to be about the same as you quoted for a piston device of similar size.

We have one advantage in a separate building for the four units which will eventually be on this site, so that one building will handle about 6,000 thermal mega-watts. I believe this has been described in the literature.

PETERS: What was the size of this building?

HAKE: I think it is about 2 million cubic feet. It is at very low pressure, about 1/2 PSI absolute with valves in systems to switch to the several power units.

FIRST: Thank you for that comment. It is obviously another application of this general plan, as opposed to putting the reactor inside the vessel. It is entirely possible to build the vessel and allow it to increase or decrease in pressure through a connecting tunnel.

LAWROWSKI: Is there anyone here from D. L. R. who might want to comment on the mechanization of the bedding?

No comment.

# CONFINEMENT SYSTEMS TESTS PERFORMED DURING DEACTIVATION OF THE 100 F REACTOR

M. L. Smith, Engineer
Radiological Engineering
DOUGLAS UNITED NUCLEAR, INC.
Richland, Washington 99352

## ABSTRACT

Permanent shutdown of 100-F plutonium production Reactor at Hanford made the system for confining the particulate and halogen, in the exhaust air, available for testing. The following tests were performed and the results are shown throughout the text: Iodine deposition from the airstream, Iodine removed from airstream by fog spray, Encapsulation of the reactor exhaust air in foam, Effectiveness of fog spray for removing noble gases from the air, Effectiveness of the filter system for removing iodine from the exhaust air.

## INTRODUCTION

The permanent shutdown of the 100-F plutonium production Reactor at Hanford, shown in Figure 1, provided the opportunity to perform full scale tests on the confinement system used to collect the radioactive materials from the exhaust airstream. This confinement filter system has been in service nearly five years. This testing program was intended to measure the efficiency of the current system and test some possible methods of improving the system.

## SUMMARY

### Filter Efficiency Test

The efficiency of the F Reactor absolute filter system was measured by three methods. The efficiency of filter systems of other reactors was measured with the condensation nuclei counter where the condition or efficiency of the filters was known.

The test results indicate that the nuclei counter would be satisfactory for monitoring the integrity of the absolute filters on a continuous basis. More testing is required to obtain the optimum aerosol for use with nuclei counter. The uranine dye method promises to be a satisfactory means of measuring the efficiency of the absolute filters. However, results of the laboratory measurement of the concentration of particles on the filter samples will not be available for a few days.

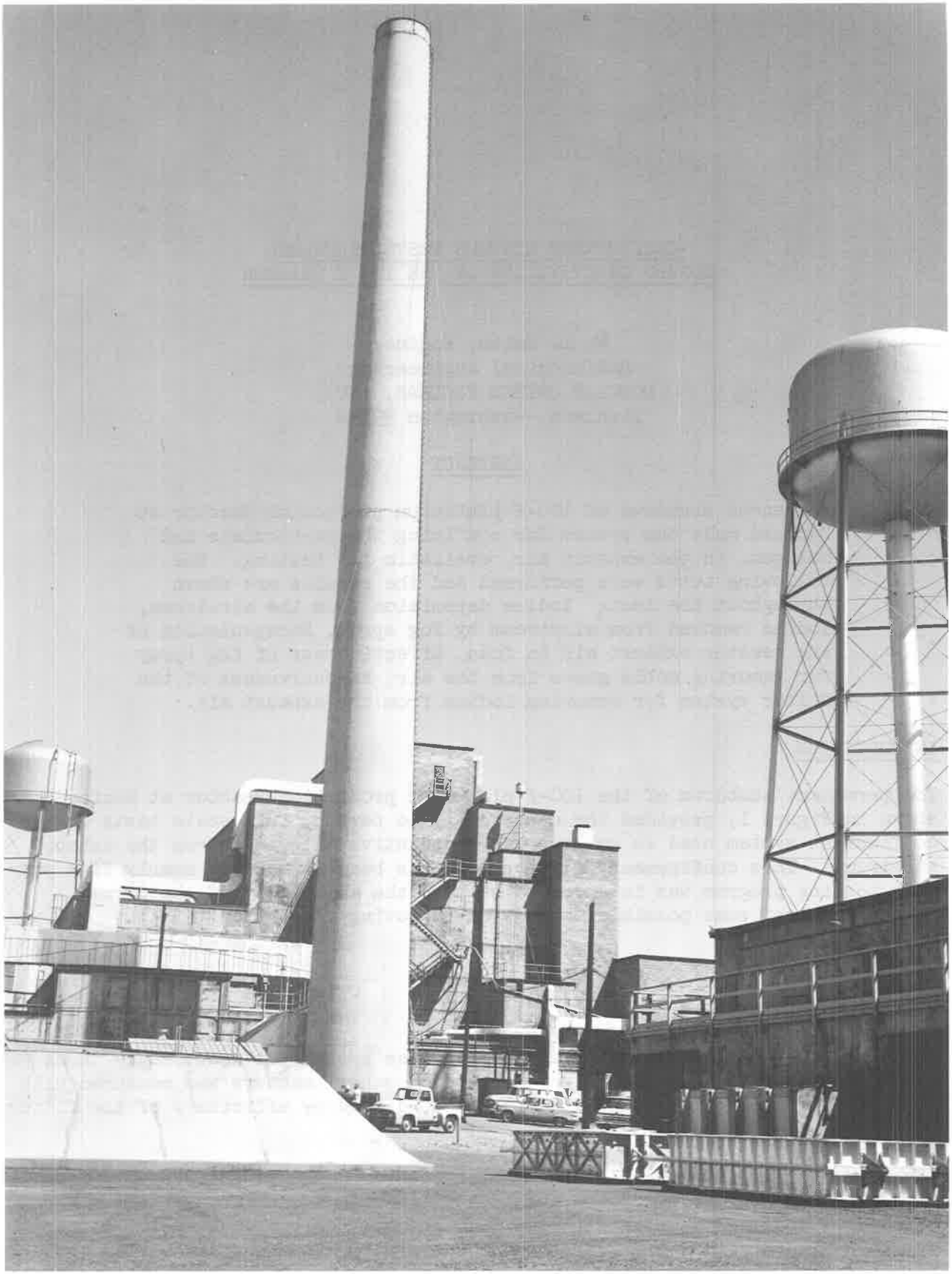

FIGURE 1

F Reactor

## Iodine Deposition Test

Radioactive I-128 was released into the discharge area supply air, and the clean-up of the airstream due to deposition on the reactor surfaces and in the duct was measured. The results varied with concentration of iodine released. The lowest plateout factor was obtained when the concentration of iodine in the air was low. In this case, the methyl iodide form immediately after release was only 0.2 percent. After eight minutes of exposure in the building air and to the surfaces, 52.0 percent of the iodine was of this hard-to-remove organic form. The test when the iodine concentration was high gave a plateout factor of 86 percent on the same surfaces and duct. The significance of the presence of the organic iodide forms is that the coconut shell charcoal filters have been shown to be 97.3 percent efficient in air with a relative humidity of 77 percent at room temperature(1). Efficiency greater than 95 percent should not be expected if the relative humidity is near 100 percent with coconut shell charcoal. Efficiencies of greater than 99.95 percent for the removal of methyl iodide have been obtained using coal based charcoal treated with 1 percent by weight of piperidine, with 99 percent to 100 percent relative humidity in the air(2). A test should be performed to verify these results under field conditions prior to the application of treated-coal-base charcoal to the confinement systems.

## Removal of Iodine by Fog Spray

Approximately 100 curies of I-128 was released into the discharge area supply air with the fog spray operating. The fog spray reduced the concentration in the air exhausted from the discharge area by a factor of 500. The application of a well designed fog spray system in series with the confinement system filter greatly increases the efficiency of the system. It will also provide cooling to reduce the heat load generated by the fission products that may deposit on the filters. A fog spray located near the source of release minimizes exposure to organic compounds available and removes the elemental iodine before the organic compounds of iodine can be formed. The effectiveness of fog spray on the removal of organic forms of iodine should be established in additional tests.

## Iodine Removal Efficiency of the Confinement System Filter and Supplemental Fog Spray

The iodine was released at a location selected to minimize plateout, permitting the maximum amount of the iodine to reach the filter system. Approximately 100 curies of I-128 was released into the exhaust air stream. The efficiency of the absolute filter for removal of iodine was 88.2 percent. The absolute filter plus charcoal filter removed 99.45 percent of the iodine. When a supplemental fog spray, absolute and charcoal filters were used, the efficiency was 99.94 percent for the removal of the iodine. The relative humidity during this test was less than 30 percent. This test with a larger quantity of iodine present in the air confirms the filter system efficiency inherent in the original design of the system(3).

## Encapsulation of the Reactor Exhaust Air in Fire Fighting Foam

Sixteen curies of A-41 and thirty-five curies of I-128 were released into the reactor building air. The air was exhausted from the reactor without filtration and converted into foam at base of the 200 foot exhaust stack and released to the atmosphere from the top of the stack. Most of 500,000 cubic feet of foam then settled back to the ground and released the radioactive argon and iodine to the environment slowly over a two hour period. The purpose of the slower release is to allow the variability of the wind to increase the dispersion of the noble gases. The application of foam as a containment aid is evident. If an overhead foam generator were installed in reactor work space, the air in that space could be converted into foam and dissipated by water near a drain on the floor while

keeping the building volume filled with foam. The foam method of fission product entrainment has been demonstrated by Silverman and Yoder[4]. While the techniques for foam generation for firefighting purposes are well established and the foaming agent well designed for that purpose, this is not the case for use of foam as a containment aid. Development work is needed on a foaming agent with longer life and with chemical additives to improve its capability to hold iodine compounds. A test program to establish the best method of using foaming agents as containment aid within a reactor building would be necessary prior to the adoption of the method.

Removal of Noble Gases from the Exhaust Air by Fog Spray

Approximately ten curies of Kr-85 were released into the exhaust air. The dose was measured up and down stream of a fog spray installed in the duct. Ninety-five percent of the Kr-85 was still in the exhaust air after it passed through the fog spray. The exposure of the air to the fog was less than three seconds.

## DESCRIPTION OF THE SYSTEM

The confinement system for the production reactors utilizes negative pressure and filtration as a means of controlling the release of radioactive particulates and halogen to the atmosphere. The filter system currently consists of a bank of absolute filters followed by a bank of coconut shell charcoal filters. The air is pushed through the filter system by electric exhaust fans and with steam exhaust fans for emergency backup. The layout of the filter, the reactor, and sampling points is shown in Figure 2. The sampling points are identified by the letter S-3, S-6, S-9, S-10, and S-11. In addition to the filter system, there is a fog spray system in the reactor discharge work space (shown in Figure 3) that is automatically activated when the concentration of I-131 exceeds one microcurie/$ft^3$ in the exhaust air.

A special fog spray was installed in the exhaust air duct downstream of the filters, and a 45,000 cfm foam generator was installed in the base of the exhaust air stack as shown in Figure 2.

## TEST A - FILTER EFFICIENCY

Objective: The object was to test the efficiency of the absolute particulate filters while in service at F plutonium production Reactor by the following methods:

1. The condition of the absolute filters was determined by dioctylphthalate method (with filters out of service).

2. The efficiency of the absolute filter was measured with the uranine dye technique while the filter system was in normal operation.

3. NaCl nuclei were generated and mixed into the exhaust air stream and the efficiency of the absolute filters measured with a condensation nuclei counter, shown in Figure 4.

Description: The methods for generating the aerosol and measurement techniques are described in References 5, 7, and 8.

Test Results: A-cell absolute particulate filters were tested with a portable dioctylphthalate equipment. A total of 22 of the 56 filters had single or multiple small penetrations. The penetrations were approximately one-sixteenth

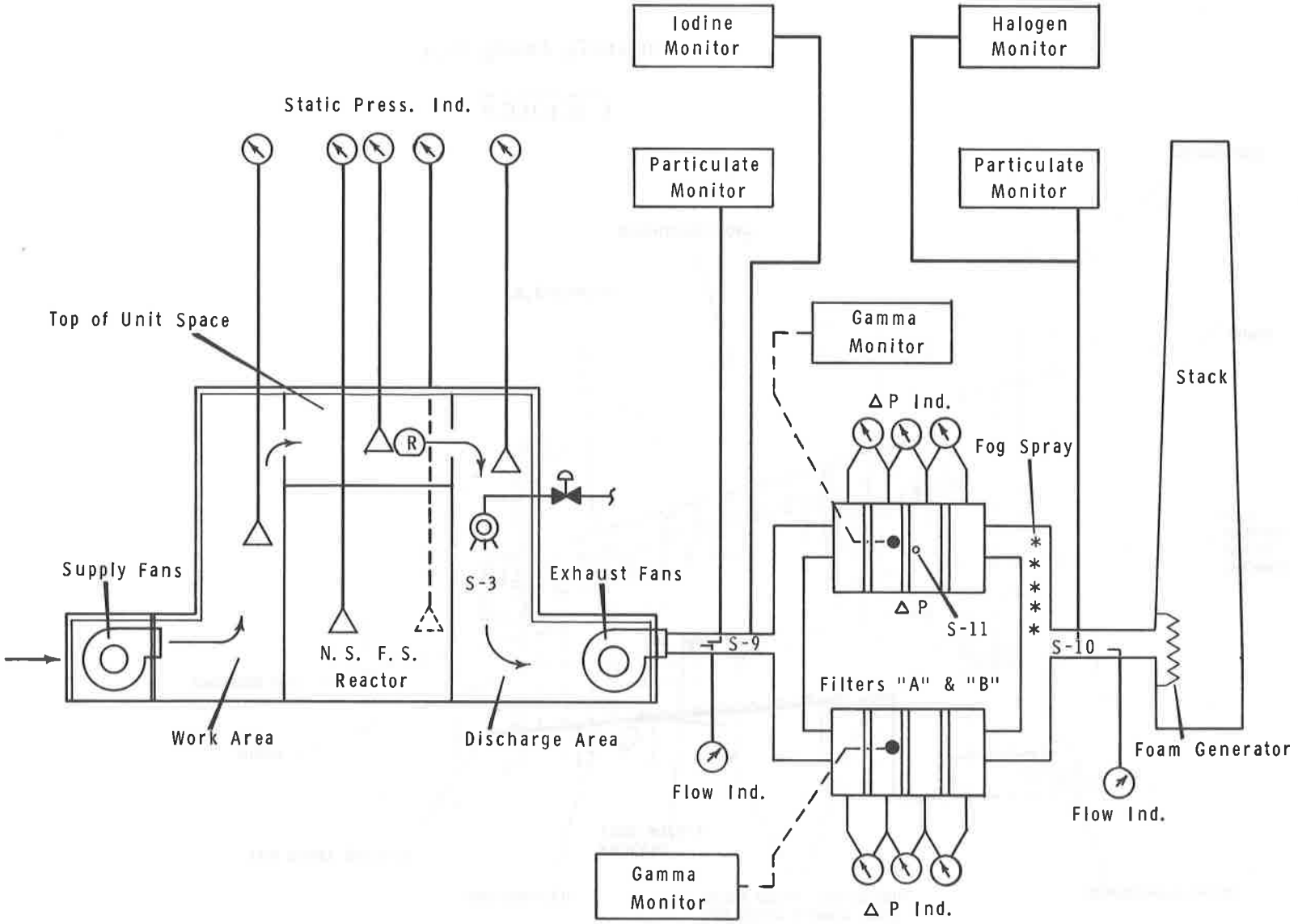


FIGURE 2

Confinement System

# REAR FACE ENCLOSURE FOG SPRAY SYSTEM

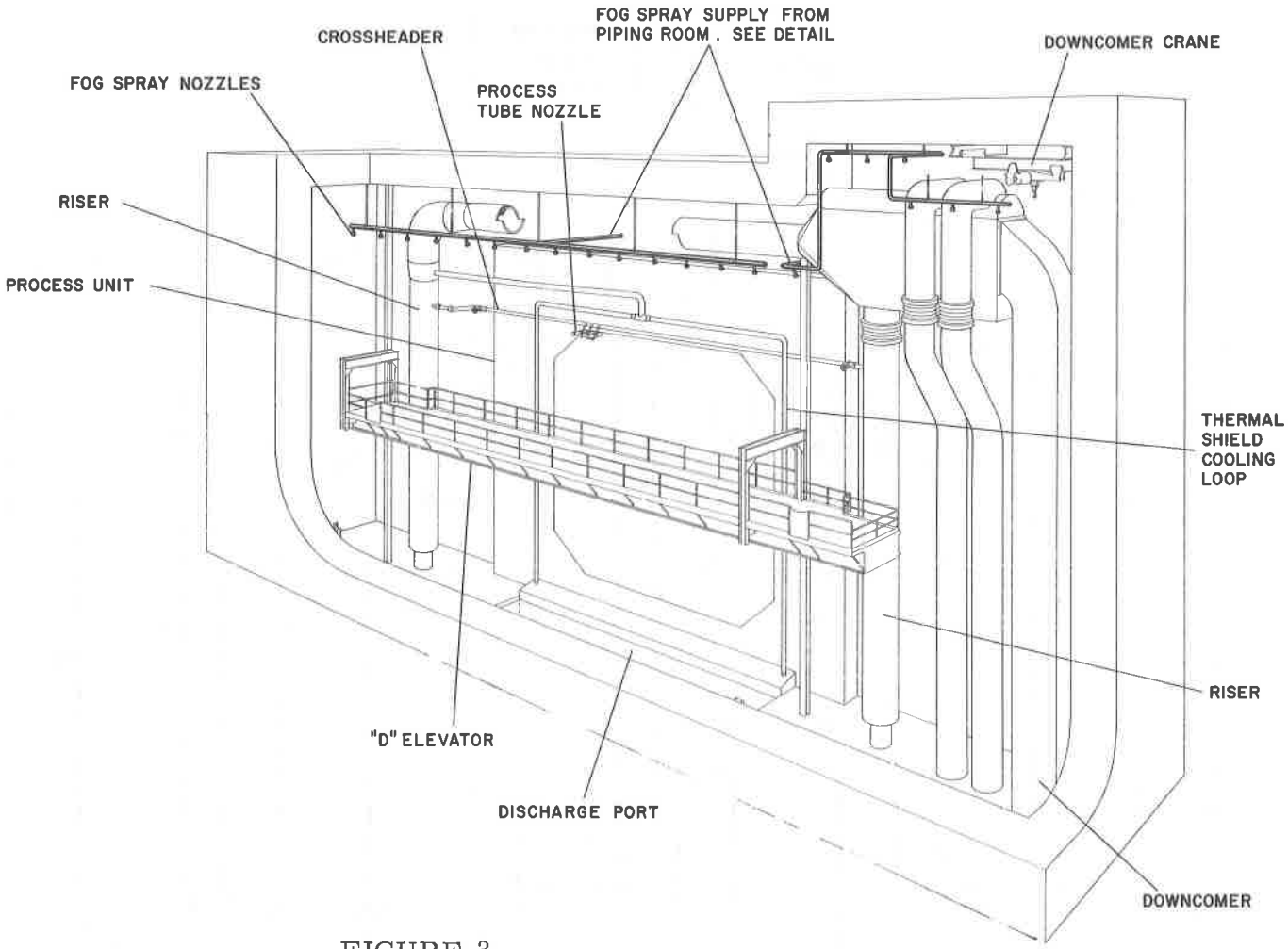


FIGURE 3

Fog Spray System

FIGURE 4

Condensation Nuclei Counter

of an inch in diameter, and most of them were in upstream folds in the filter media. The efficiency determined by the dioctylphthalate method is shown in Table I. This efficiency is based on an estimate of a 6 $mm^2$ penetration per filter(6). The efficiency of the absolute filters measured by the uranine method shown in Table I was measured by the method described in Appendix IA. The efficiency of absolute filters using condensation nuclei shown in Table I was measured by the method shown in Appendix IC.

TABLE I

F REACTOR

ABSOLUTE FILTER EFFICIENCY MEASUREMENTS (by various methods)

| Aerosol | Percent Penetration | Percent Efficiency |
|---|---|---|
| Dioctylphthalate | 1.0 | 99.+ |
| Uranine Condensation | .1 | 99.9 |
| Nuclei | .4 | 99.6 |

The test data indicated the uranine(5) and the condensation nuclei methods are about equivalent. Data taken with the nuclei generator and counter on filter systems with new filters containing no penetrations have also been made. In addition, measurements have been made where known defects were present in the filter system, and examples are shown in Table II.

TABLE II

MEASUREMENT OF FILTER EFFICIENCY WITH CONDENSATION NUCLEI COUNTER

| Reactor | Date | Percent Efficiency | Comments |
|---|---|---|---|
| 105 K | 10/8/64 | 99.96 | All known defective filters had been previously replaced. |
| 105 KE | 8/13/65 | 98.86 | DOP test indicate numerous small penetrations. |
| 105 B Cell | 9/25/64 | 97.0 | Four filters loose in frames due to failure of adhesive. |
| 105 B Cell | 9/28/64 | 99.94 | New filters had been installed in B Cell with flow of 100,000 cfm through the cell. |

The two measurements on the KE filters are an example of the change in filter efficiency occurring in less than one year. The DOP test is required annually. The small penetrations occurring over a period of time cause a slow decrease in pressure differential and are offset by the normal dust loading of the filter, so little or no change is noted in the pressure differential across the absolute filters. The two tests at B Reactor are examples of fairly rapid failure of good filters that were caused by excessive heat and water. These failures were accompanied by a noticeable change in the pressure differential across the filters.

Test Conclusions: The condensation nuclei counter(9) can be used to monitor the efficiency of the confinement system particulate filter and assure that any changes in the condition of the filter system will be detected. If direct correlation of efficiencies is needed, a large salt spray or uranine generator could provide a source of larger particles that will more nearly correlate with DOP test methods.

TEST B - IODINE PLATEOUT

Objective: The object was to measure the removal of iodine from the exhaust air stream by deposition on the building surfaces, in the ducts, fans and filters.

Description: The test involves the release of iodine-128 into the building supply air at the locations designated by (R) in Figure 5. The air was sampled at the locations indicated by the letter (S) in Figure 2. The air sampled is pulled through a May Pack iodine sample cartridge having the configuration shown in Figure 6.

The May Pack iodine sample cartridge is designed to distinguish between the forms of iodine present in the air sampled(10). The first filter element is a silver screen to remove the elemental iodine vapors. The screen is next followed by a fiber glass filter to remove the particulates; following next is a charcoal load filter paper used to remove the readily absorbed organic iodine compounds. The last absorber is a one inch granular charcoal bed which absorbs the remaining organic iodine compounds. The principal iodine compound of interest is methyl iodide and the radioactive iodine absorbed in the charcoal granules is considered to be of this form.

These iodine samplers were installed with snap connectors to allow quick removal. The air was drawn through the samplers with positive displacement air pumps. The cartridges were installed on sample lines of minimum length, and, where possible, in the air stream being sampled. The sample cartridges were removed, capped at the completion of a release, and taken to the counting laboratory where each component of the May Pack was counted. The cartridges were then cleaned and re-assembled with new components for the next test.

Fifty grams of natural iodine-127 were irradiated to form about 800 curies of iodine-128 at time of discharge. This was transported to F Reactor and the ampule perforated and heated with hot air to release the iodine into the air stream. The release mechanism is described and shown in Appendix III. The curie content of the iodine in the ampule at the time of release was established by the decay time allowed. In Test B, the release was made with 16 curies in the ampule, and approximately 10 curies were released to the exhaust air. The May Pack sample was run during the release period and for fifteen minutes after the termination of the release by cooling the ampule. The data shown in Table III are the counts occurring in the channels resulting from five channels below to four channels above the center of the .45 MeV gamma peak emitted by I-128, in each component of the May Pack samplers. The spectrum indicates very nearly 100 percent of the gamma activity present is from the I-128. The data listed are normalized for dilution, decay, and flow.

The count recorded in the different sections of the May Pack sampling the air immediately downstream of the release point (sample point #3) show only 0.20 percent in the methyl iodide form, while after dilution in the building air (sample point #6) 52.6 percent of the iodine is of methyl iodide form. The cleanup resulting from deposition left 50.36 percent of the iodine in the air

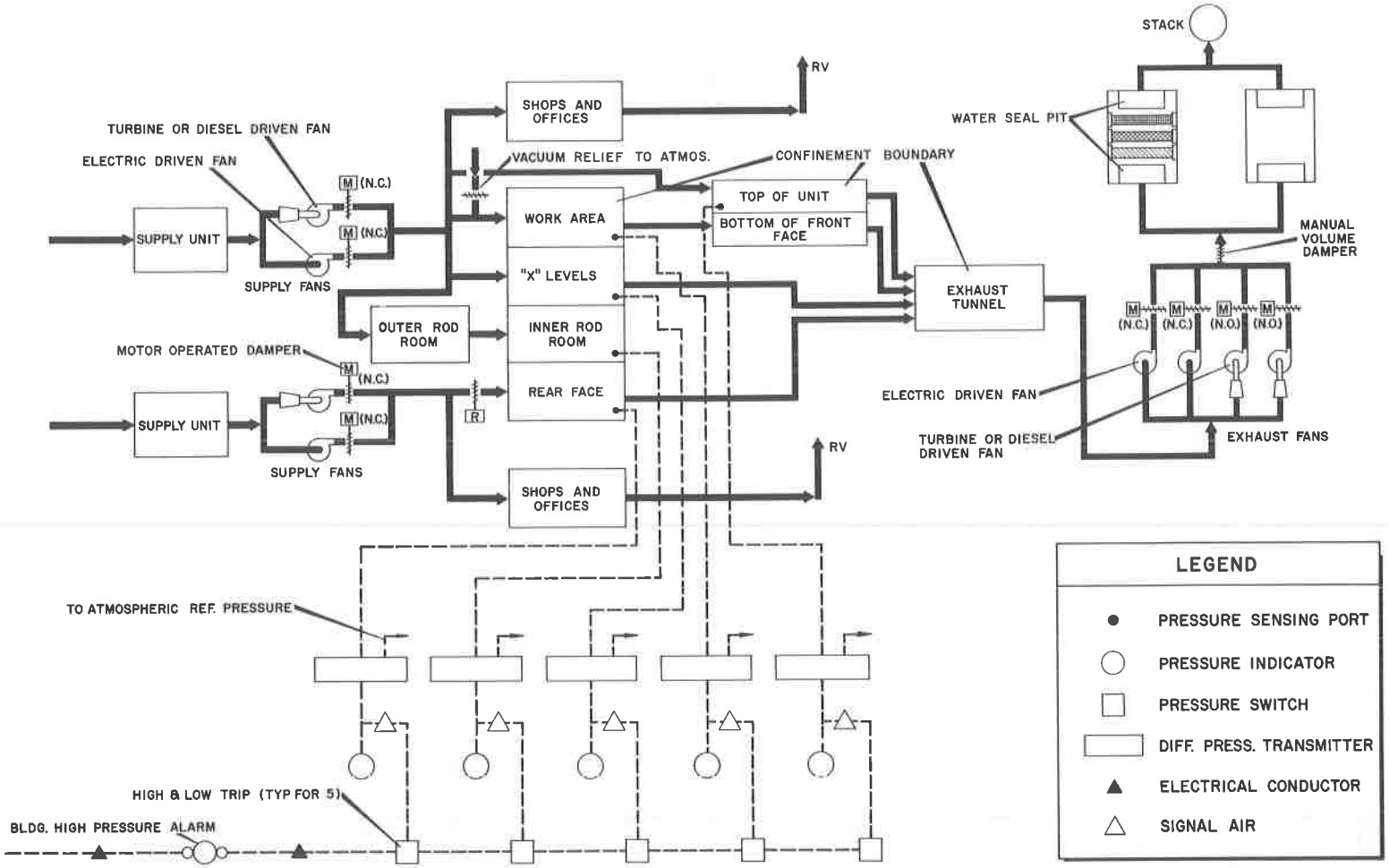


FIGURE 5

Typical Flow Diagram

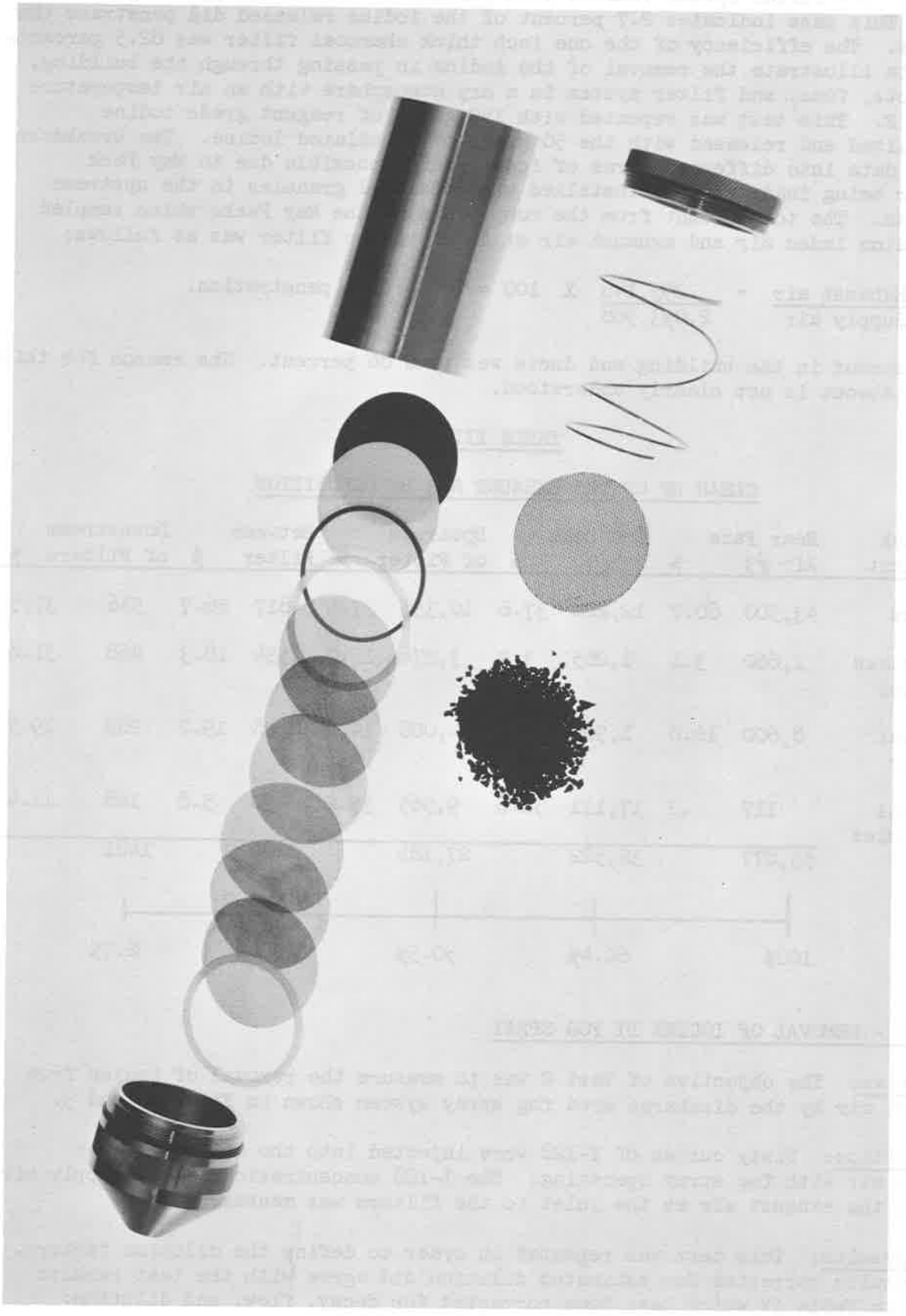

FIGURE 6

Maypack for Airborne Iodine Sampling

stream. The filter system removed 94.6 percent of the iodine reaching the filters. This case indicates 2.7 percent of the iodine released did penetrate the filters. The efficiency of the one inch thick charcoal filter was 82.5 percent. The data illustrate the removal of the iodine in passing through the building, the ducts, fans, and filter system in a dry atmosphere with an air temperature of 74° F. This test was repeated with 150 grams of reagent grade iodine volatilized and released with the 50 grams of irradiated iodine. The breakdown of the data into different forms of iodine isn't possible due to May Pack sampler being inadvertently installed with charcoal granules in the upstream position. The total count from the components of the May Packs which sampled the iodine laden air and exhaust air at inlet to the filter was as follows:

$$\frac{\text{Exhaust air}}{\text{Supply air}} = \frac{293,146}{2,093,968} \times 100 = 14 \text{ percent penetration.}$$

The plateout in the building and ducts was then 86 percent. The reason for this high plateout is not clearly understood.

TABLE III

CLEAN UP OF THE EXHAUST AIR BY DEPOSITION

| May Pack Component | Rear Face Air #3 | % | Fan Cell #6 | % | Upstream of Filter | % | Between Filter | % | Downstream of Filters | % |
|---|---|---|---|---|---|---|---|---|---|---|
| Screens | 43,500 | 80.7 | 12,226 | 37.6 | 10,338 | 37.9 | 4817 | 56.7 | 556 | 37.5 |
| Fiberglass Filter | 1,660 | 3.1 | 1,265 | 3.9 | 3,274 | 12.0 | 1554 | 18.3 | 468 | 31.6 |
| Charcoal Paper | 8,600 | 16.0 | 1,920 | 5.9 | 4,008 | 14.7 | 1628 | 19.2 | 289 | 19.5 |
| Charcoal Granules | 117 | .2 | 17,111 | 52.6 | 9,565 | 35.2 | 490 | 5.8 | 168 | 11.4 |
| | 53,877 | | 32,522 | | 27,185 | | 8489 | | 1481 | |
| | 100% | | 60.4% | | 50.5% | | 15.8% | | 2.7% | |

TEST C - REMOVAL OF IODINE BY FOG SPRAY

Objective: The objective of Test C was to measure the removal of iodine from exhaust air by the discharge area fog spray system shown in Figure 2 and 3.

Description: Sixty curies of I-128 were injected into the discharge area supply air with fog spray operating. The I-128 concentration in the supply air and in the exhaust air at the inlet to the filters was measured.

Test Results: This test was repeated in order to define the dilution factors. The results corrected for estimated dilution did agree with the test results shown in Table IV which have been corrected for decay, flow, and dilution.

TABLE IV

REMOVAL OF IODINE WITH FOG SPRAY

| May Pack Component | Rear Face Air Supply | Inlet to the Confinement Filters |
|---|---|---|
| Silver Screens | 628234 | 425 |
| Fiber Glass Filter | 53070 | 486 |
| Charcoal Load Paper | 295679 | 1008 |
| Charcoal Granules | 22582 | 330 |
| | 999565 | 2249 |

The fraction of the iodine released that reached the inlet to the filter was:

$$\frac{2249}{999565} \times 100 = .22\%$$

The fog spray in the discharge area exposed the air to a diluge of water for an average time of seven minutes. This effected a reduction of five hundred in concentration of iodine in the air before it reached the filter system inlet sampling point.

TEST D - IODINE REMOVAL EFFICIENCY OF THE CONFINEMENT FILTERS AND SUPPLEMENTAL FOG SPRAY

Objective: The objective was to measure the efficiency of confinement system filters and supplemental fog spray in removing iodine from the reactor exhaust air stream.

Description: The release point in this test was selected to minimize the plate-out on the surface and in the ducts and still retain adequate mixing of the sample with air stream prior to reaching the filters. The iodine was released in the plennum 150 feet upstream of the filter system. The air had to make two turns through turning vanes prior to reaching the sampling point in the duct ahead of the filters. The linear velocity in the duct was 1000 ft/min., and the face velocity through the filter cell was 250 ft/min. The velocity allowed only 25 seconds flow time to elapse from the time iodine entered the air stream until the final sampling point was reached. The release was made by the method discussed in Appendix II. The sampling points are shown in Figure 2. The ampule contained 136 curies of I-128 at the time of the release. Approximately 100 curies of the I-128 were released into the exhaust plennum.

Test Results: The May Pack cartridges were counted starting with sample farthest downstream and working upstream. Only one sample at a time was opened to prevent any possible mixing of the samples. The flow through each May Pack was checked before the release and again after the release to insure accurate estimates of the total flow. Dilution was not a factor in this test so that corrections were made for flow and decay only. The sampling lines were monitored to evaluate the buildup of iodine in the lines due to plateout. The

maximum measured on any line was on the stainless steel line which is 15 feet in length connecting to sample point S-9. There was a maximum of about 600 c/m in on this line. Preferential deposition in sample lines was not significant in this test. The results obtained from the measurements described are shown in Table V.

The time required for the exhaust air to traverse the distance between sample point S-9 and S-11 on Figure 2 is approximately 15 seconds. The percentage change of particulate matter resulting from the air traversing the charcoal filter is interesting. The penetration of the absolute filter was 11.8 percent. The penetration of the absolute filter and the charcoal filter was 5.5 percent. The penetration of the absolute and charcoal filters plus the fog spray installed in the duct was 0.065 percent. The organic iodide form constituted 75 percent of the iodine penetrating the entire system. Only 6 percent of the total material penetrating the system was in the particulate form.

## TEST E - REMOVAL OF NOBLE GASES BY FOG SPRAY

Objective: The purpose was to measure the ability of a fog spray system to remove noble fission gases from the reactor exhaust air stream.

Description: Dosimeters were set up in the tunnel upstream and downstream of the fog spray system. The configuration of the dosimeter is shown in Figure 7. The xx's indicate pocket ion chambers; the X's indicate stray radiation chambers.

FIGURE 7

Dosimeter Configuration in the Exhaust Tunnel

The curies of Kr-85 were released into the air stream and the dose upstream and downstream of the fog spray was measured.

Results: The total dose up and down stream of the fog spray was 89.5 versus 83.5 on a total of 22 dosimeters in each location with background response subtracted. The fog spray was installed in the exhaust duct shown in Figure 8. The error possible in the measurement is less than $\pm$ 5 percent. These results simply indicate a slight cleanup of the noble gases by the fog spray, probably less than 7 percent. The air would have been exposed to the fog spray for about three seconds. If the exposure time were increased, the noble gas cleanup would not be sufficient to eliminate the problem created by the noble fission gases; however, the effect on iodine and the particulates would be beneficial and the small cleanup of the noble gases would be an added benefit.

MEASUREMENT OF THE FILTER SYSTEM EFFICIENCY

| May Pack Sampler Sections | Sample Point S-9 | Percent of Total | Absolute F Filter | Sample Point S-11 | Percent of Total | Charcoal Filter | Sample Point S-8 | Percent of Total | Fog Spray | Sample Point S-10 | Percent of Total |
|---|---|---|---|---|---|---|---|---|---|---|---|
| Silver Screens | 770,431 | 43.8 | | 95,552 | 45.8 | | 4,855 | 49.7 | | 209 | 18.3 |
| Fiber Glass Filter | 177,558 | 10.9 | | 9,842 | 4.7 | | 2,197 | 22.5 | | 70 | 6.1 |
| Charcoal Loaded Paper | 807,780 | 45.9 | | 92,640 | 44.5 | | 2,513 | 25.7 | | 684 | 59.8 |
| Charcoal Granule | 4,387 | 0.2 | | 10,303 | 5.0 | | 196 | 2.1 | | 180 | 15.8 |
| | 1,760,158 | 100.0 | | 208,337 | 100.0 | | 9,761 | 100.0 | | 1143 | 100.0 |

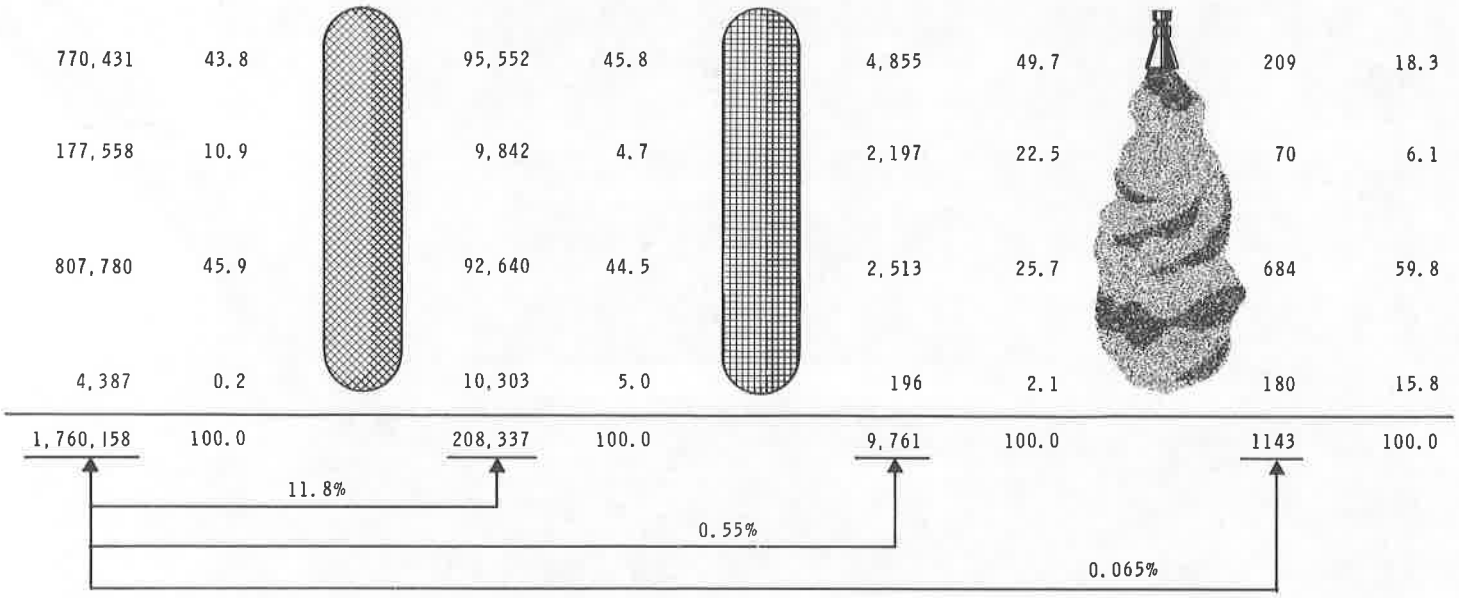


TABLE V

Measurement of the Filter System Efficiency

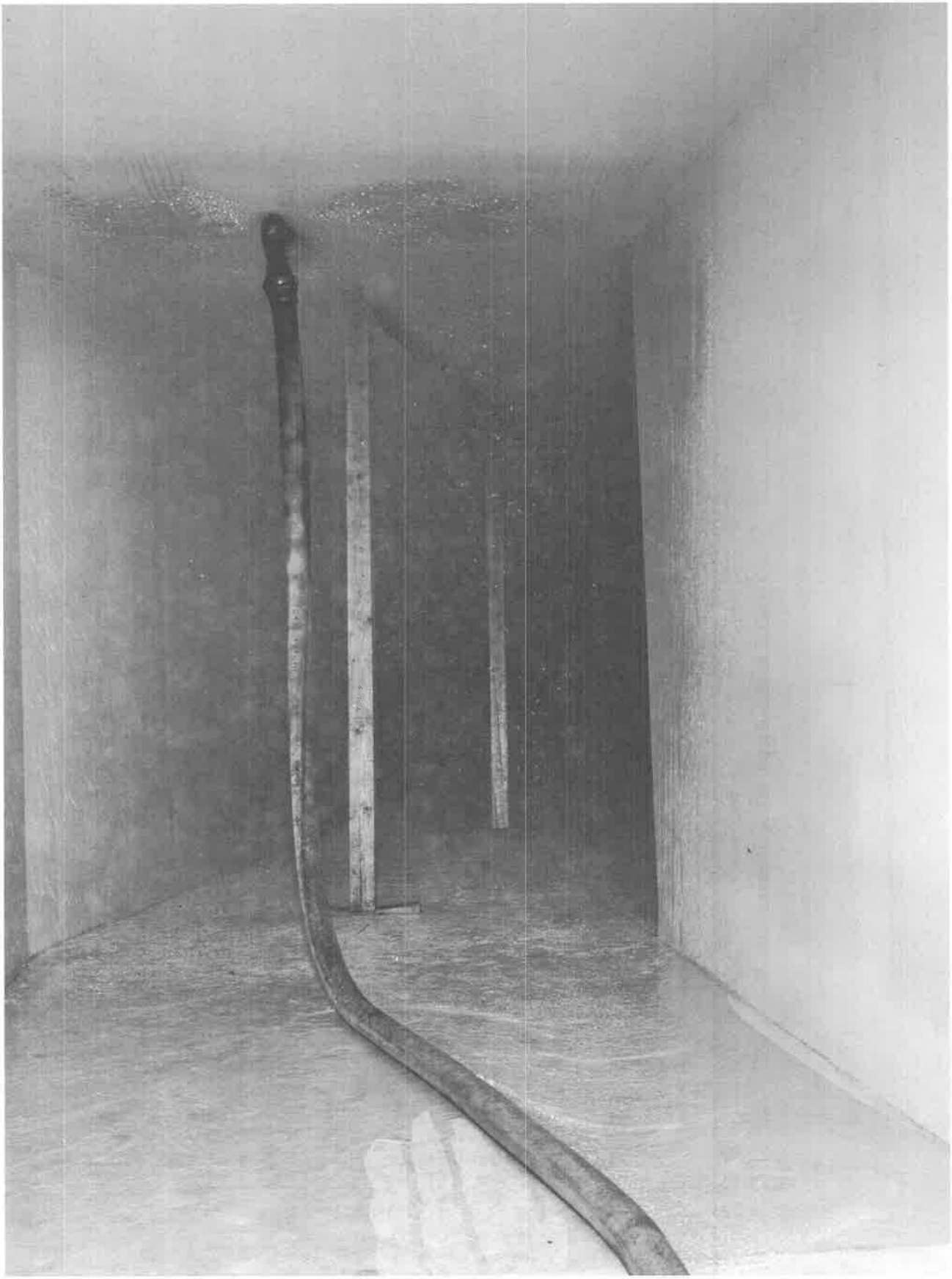

FIGURE 8

Fog Spray System Installed in Exhaust Air Tunnel

## TEST F - REMOVAL OF NOBLE GASES FROM THE EXHAUST AIR BY FOAM

Objective: Measure the capability of firefighting foam to serve as a containment aid for the noble fission gases and gaseous iodine, when these fission products are released into the exhaust air of the reactor.

Description: A reactor accident was simulated by the use of 16 curies of A-41 and 100 curies of I-128. The radioactive gas was released into the reactor charging area, and the iodine was released into the reactor discharge area. The radioactivity in each location was monitored by the fixed radiation monitoring system, and the radiation levels recorded during the test. The recorder chart shows the decrease in the radiation level with time. This decrease is the result of removal and decay of the radioactive material in the building air. The radioactive material removed from the building air is discharged into the reactor confinement system by the exhaust fans. The reactor exhaust air in this test was allowed to pass through the system without filtration into the exhaust tunnel and up the 200 foot stack. The exhaust air flow was set at 45,000 cfm. A foam generator was installed in the base of the exhaust air stack as shown in Figure 1 and 9. A sampling system was installed to sample the gas plume after discharge from the top of the 200 foot stack and is shown in Figure 12. The gas sampled was pulled through a flow-through gas ionization chamber, and the radioactivity of the sample was measured and recorded on the system shown in Figure 10.

In addition to the above measuring system, Environmental Survey Operation of Battelle-Northwest Laboratory established field monitoring station downwind of the point of release as well as sampling the plume by flying the surveillance air craft through the plume at a distance of one-half mile downwind. The reactor plant monitoring forces monitored the radioactivity in the foam according to established procedure after the release was complete. The details of the operation of the foam generator are given in Appendix III.

Test Results: The effect of releasing the A-41 and I-128 into the reactor work spaces is shown in Figure 11 by the recorder chart, recording the gamma radiation in those locations. The release of the radioactive materials and the effect on the radioactivity in the exhaust plume is shown on the traces in Figure 11. The chart recording shows only a slight increase in the radioactivity in the plume until the foam generation was terminated. The marked increase in radioactivity in the air sampled from the plume corresponds to the termination of the encapsulation of the exhaust air in the foam. Figure 12 shows the foam being released from the stack, and Figure 13 shows it being deposited on the ground in a typical release. The radiation levels around the perimeter of foam at four feet high was 17 m RAD/hr. The radioactivity in the foam, when measured by immersing a GM tube in the foam, was generally around 100,000 cpm. Two releases of I-128 and A-41 were made and equivalent dose rate information was obtained from separate tests. On the second release the A-41 and I-128 were released separately, and samples were taken of the foam by drawing samples into the stack May Pack sampler. The spectrum of foam with A-41 encapsulated is shown in Figure 14. The spectrum of foam with I-128 entrained is shown in Figure 15. The exhaust air bearing I-128 and A-41 was passed through the filter system. The iodine trapped in the charcoal of the May Pack was from the fractional percent penetrating the filters. The A-41 was also trapped along with the water in the charcoal of a second May Pack. These spectra were the result of one minute counts and there were 14,300 counts per major division of the paper used. The spectra verify qualitatively that the foam did contain both radioisotopes.

FIGURE 9

Foam Generator Installed in the Stack

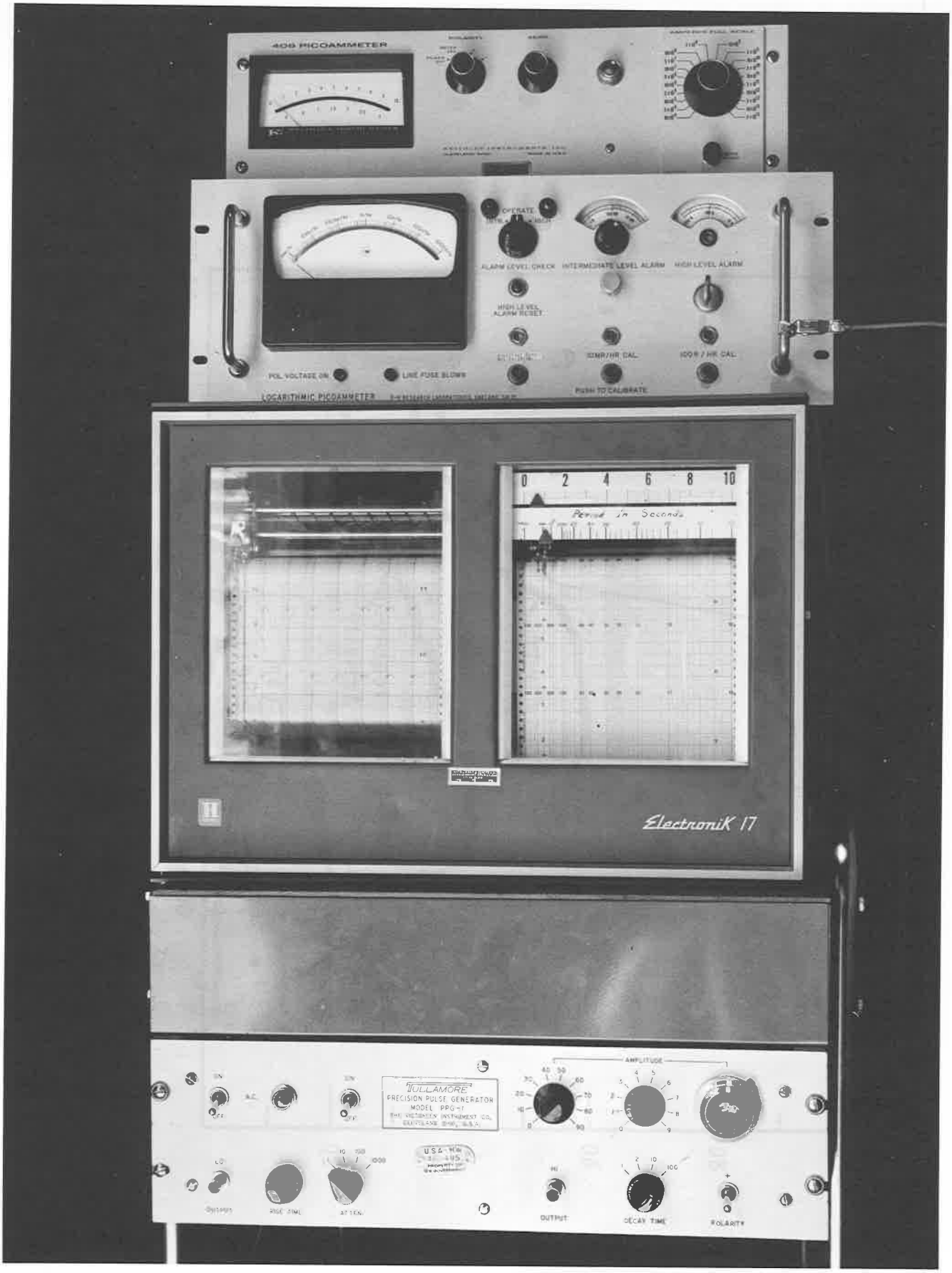


FIGURE 10

Plume Monitor

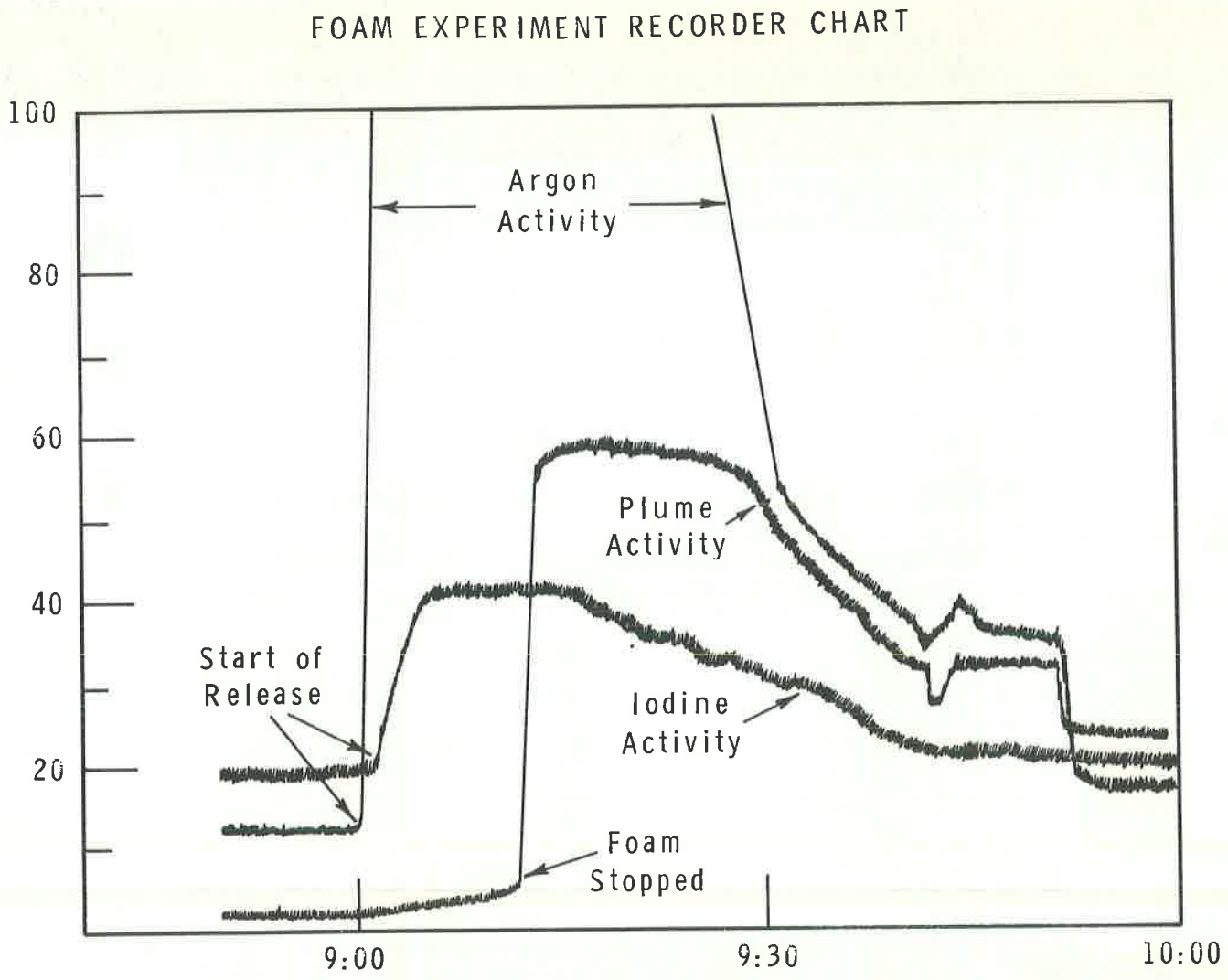


FIGURE 11

Foam Experiment Recorder Chart

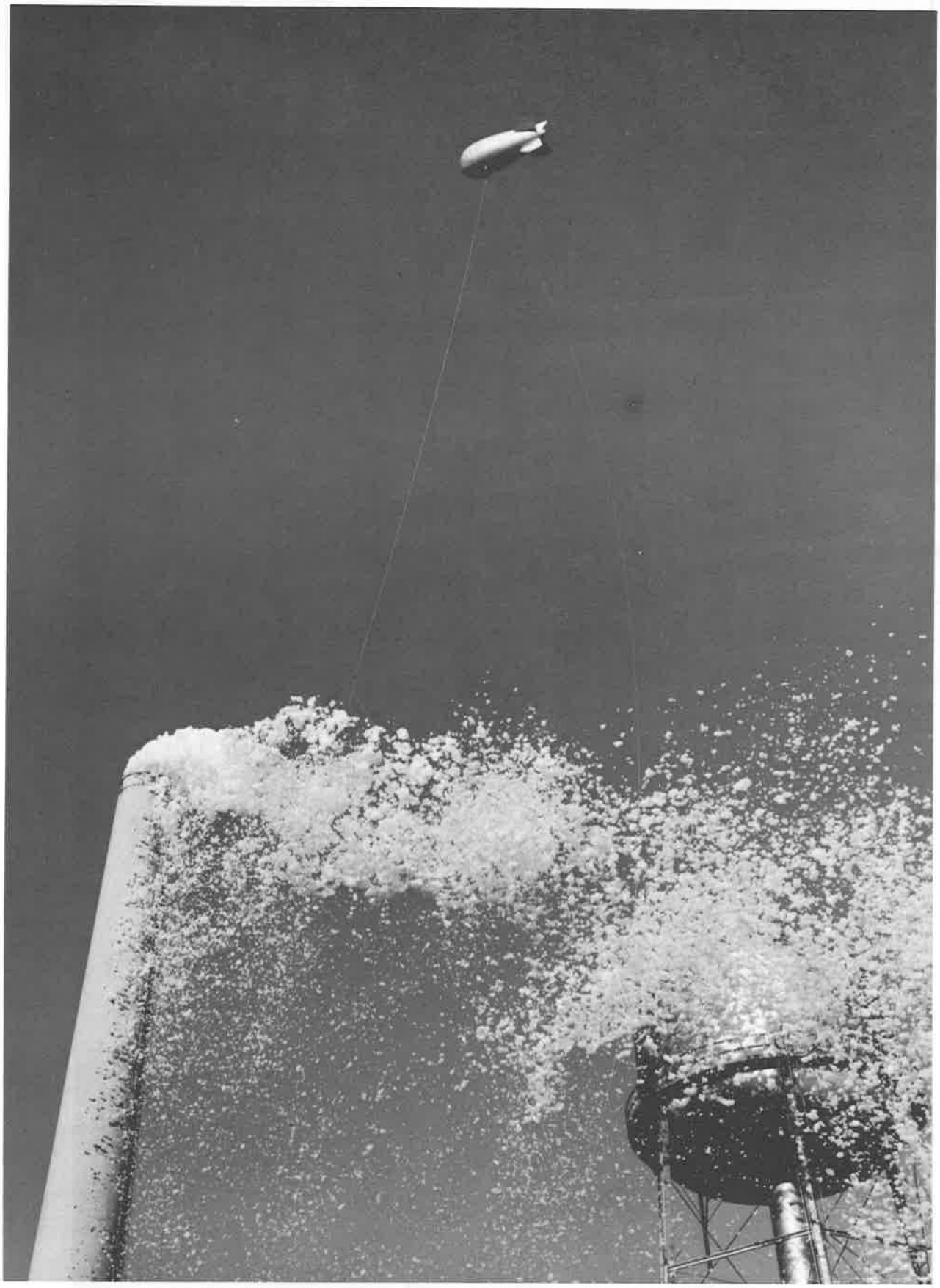

FIGURE 12

Foam Encapsulated Reactor
Exhaust Air Release at 200 Feet

FIGURE 13

Foam Depsoition on Ground

Gamma Spectrums of Foam

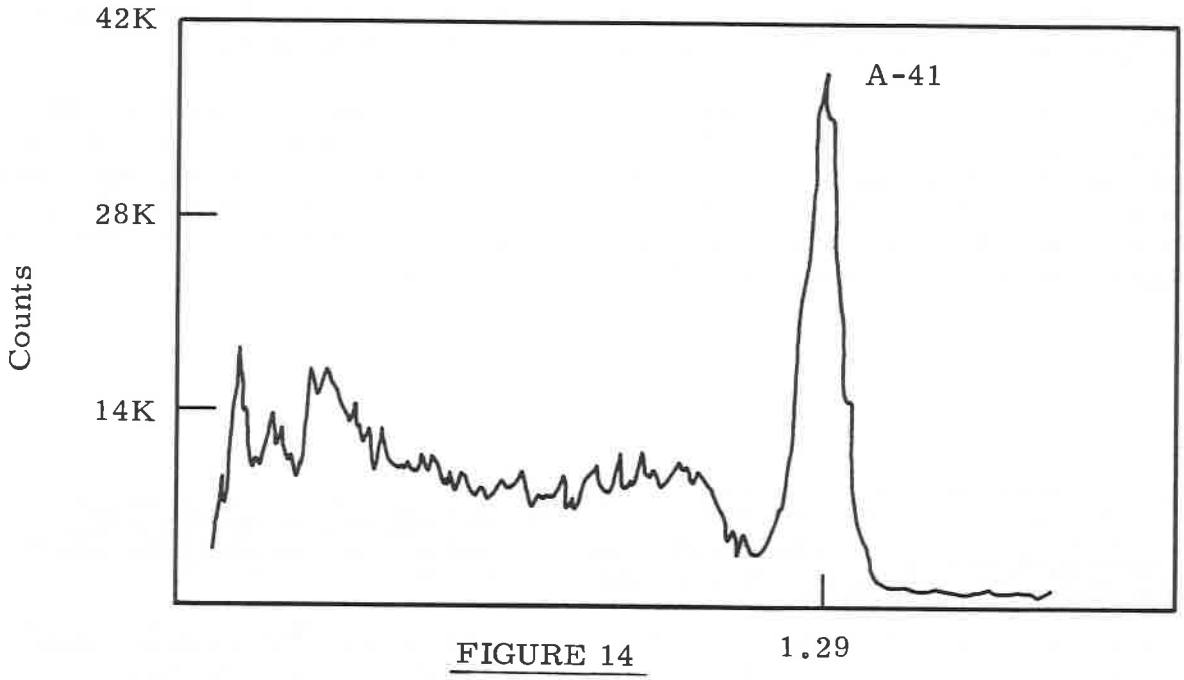


FIGURE 14

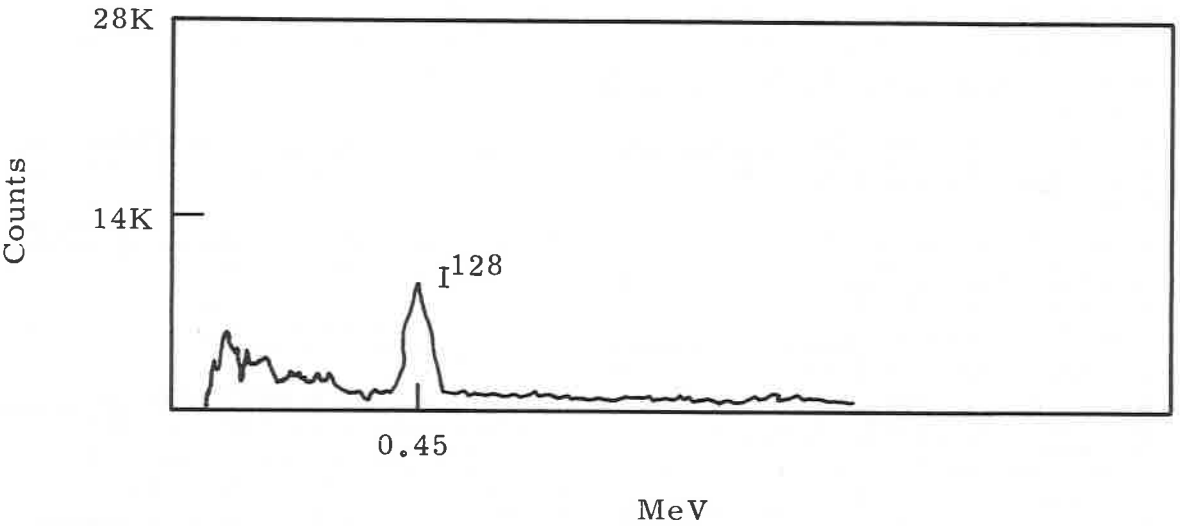


FIGURE 15

The encapsulation of the exhaust air in foam was estimated to be 85 percent efficient. This estimate is the result of comparing the calculated time for the foam generator to fill the volume of the 200 foot stack and the actual time required. The breakdown of the foam after release and prior to reaching the ground was estimated to be less than 10 percent.

The foam used was a commercial firefighting foam which is deliberately designed to rapidly break down. Even with this short lived foam, 75 percent of the exhaust air containing the A-41 and I-128 was brought to the ground and gradually released as the foam dissipated. The foam when exposed to an eight mile per hour wind dissipated to half the original volume in one hour. Increased life of the foam can be obtained by proper design of the foaming agent.

The limitation on the volume of foam that can be generated is limited by the amount of storage and cost of the foaming agent. The conversion of 45,000 cubic feet per minute of air into foam required five gallons of the foaming agent and 300 gallons of water per minute. By the use of an installed foam generator, it may be possible to convert a short duration elevated release to the environment into a ground level release of many hours duration.


(1) Browning, Jr., W. E. and R. E. Adams, Removal of Iodine and Volatile Iodine Compounds from Air System by Activated Charcoal - Nuclear Safety Program Semi Annual Progress Report. ORNL-2691. June 30, 1964 Oak Ridge National Laboratory

(2) Collins, D. A., R. Taylor & L. R. Taylor, Removal of Methyl Iodide from Reactor Effluent Gases - Reactor Development Laboratory Windscale. TRC 982(W). August, 1965

(3) Arthur D. Little, Inc., Halogen Collector Test Program. HW 65587 March, 1960. Hanford Atomic Products Operation

(4) Silverman and Yoder, "Foam Suppression of Radioactive Iodine & Particulates." Eighth Annual Air Cleaning Conference, Page 297, TID-7677 October, 1963,

(5) Wisehart, Donovan, Field Method Using Uranine to Measure Penetration of High Efficiency Filters. HW 79303, October, 1963. Hanford Atomic Products Operations

(6) Adley, F. E. and D. E. Anderson, The effect of Holes on the Performance Characteristics of High-Efficiency Filters. HW 77912. October 25, 1963 Hanford Atomic Products Operation

(7) Etheridge, Edward, Field Test for Confinement System Filters. HW 67471 January, 1960, Hanford Atomic Products Operation

(8) Smith, M. L., Measurement of Filter Efficiency with a Condensation Nuclei Counter. RL-SA-47. October, 1965. Hanford Atomic Products Operation

(9) Skala, George F, "New Instrument for the Continuous Measurement of Condensation Nuclei," Analytical Chemistry, 35: 702. May, 1963.

(10) Megaw, S. J. & F. G. May. "The Behaviour of Iodine Released in Reactor Containers," J. Nuclear Energy pt A&B, 16: 427-436 (1962)

## APPENDIX I

## FILTER TEST METHODS

### A. Dioctylphthalate (DOP)

The filters are masked off so that the rated flow is through the filter that has not been blanked off. The DOP smoke is released upstream of the filter, and the penetration of the filter is measured with a linear photometer.

The smoke is generated by aspirating the heated dioctylphthalate into the air stream with a standard smoke generator of the naval laboratory design. This gives a homogeneous smoke with a particle size of .3 microns.

### B. Uranine

The filter system test with uranine is performed by releasing the uranine and water vapor into the exhaust air stream well ahead of the exhaust fans and mixing vanes. This insures a uniform distribution of the uranine in the air stream. The concentration of uranine in the air is determined by sampling the air upstream and downstream of the filter through the installed isokinetic sampling system. The concentration of the uranine collected on the millipore filter was measured using a spectrophotometer.

The uranine dye particles are generated by aspirating a 15 percent solution of uranine and water into the exhaust air stream. The water is evaporated in the dry air giving a particle with a mass mean diameter of .5 microns.

For complete detail of this test method, refer to Reference 1 in this document.

### C. Condensation Nuclei

The mist was generated by forcing air through a $\frac{1}{4}$" stainless steel tube with a .040 hole drilled about one inch up from the capped end of the tube. Twenty pounds of air pressure was used to inject the air into a 30 percent by weight solution of salt water. The mist is aspirated from the bottle by the acetylene flow into the fan as shown in Figure 16. The salt mist is mixed with the acetylene and burned. When the acetylene is burned, the water is vaporized leaving the salt nuclei to be dispersed by the blower into the building air.

# CONDENSATION NUCLEI GENERATOR

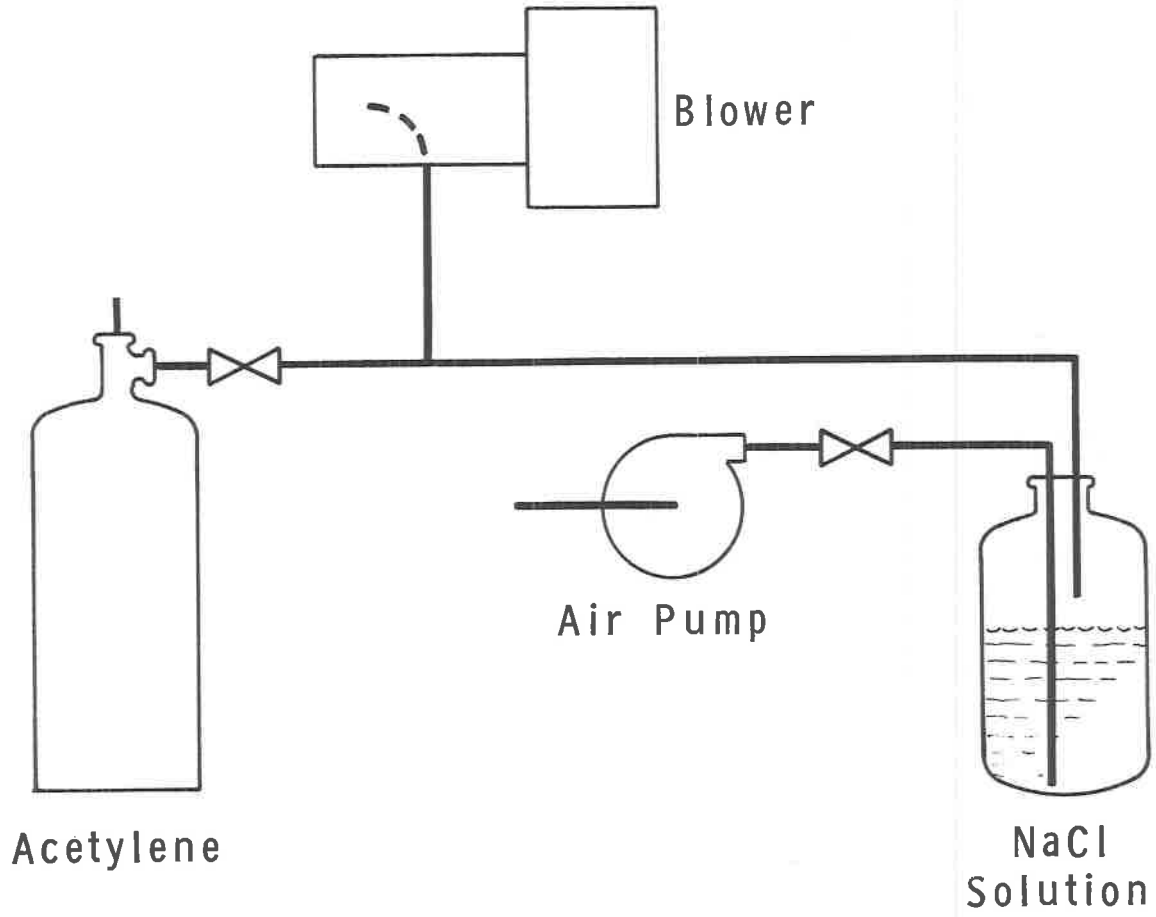


FIGURE 16

Condensation Nuclei Generator

## APPENDIX II

## METHODS GENERATING AND RELEASING THE RADIONUCLIDES

### A. Iodine-128

Iodine-128 was obtained by irradiating 50 gram samples of 99.9 percent pure I-127. The irradiation was accomplished in a poison column control tube at D Reactor at Hanford. The iodine was sealed in a quartz ampule and canned in an aluminum can sized to fit the irradiation facility hardware.

The samples were irradiated for various times depending on the number of curies desired at the planned release time. After irradiation, the outer can was immediately removed under water. Then after thirty minutes decay, the sample was transferred in air to the shipping cask using ten foot tongs. The shipping cask shown in Figure 17 is also the release mechanism for the iodine. A 1 kw electric heating element was installed in the cask plug assembly. In addition, a hot air supply was connected to the cask using a commercial air heater. The air was blown in around the outside of the plug assembly and exhausted up through the center around the ampule. The ampule was perforated prior to heating by piercing it with a steel pin shown in Figure 18. During the piercing operation, a vacuum was placed on the cask with the pump discharging through a charcoal bed.

When the release was essentially complete, the system was cooled by blowing cold air through the system.

### B. Argon-41

The argon-41 was obtained by irradiating argon gas. The gas was in a tank made for the snout facility at KW Reactor. The tank was charged into the reactor and irradiated and then discharged into the biological shield for three hours prior to transfer into the shipping cask. The argon was transported in a five ton shipping cask to F Reactor for release. The argon was released from the shipping cask by cutting the sealed fill tube with an air operated guillotine attached to the shipping cask. The argon very rapidly diffused into the reactor front work space which has a 300,000 $foot^3$ volume. The diluted argon provided the source of A-41 in the exhaust air.

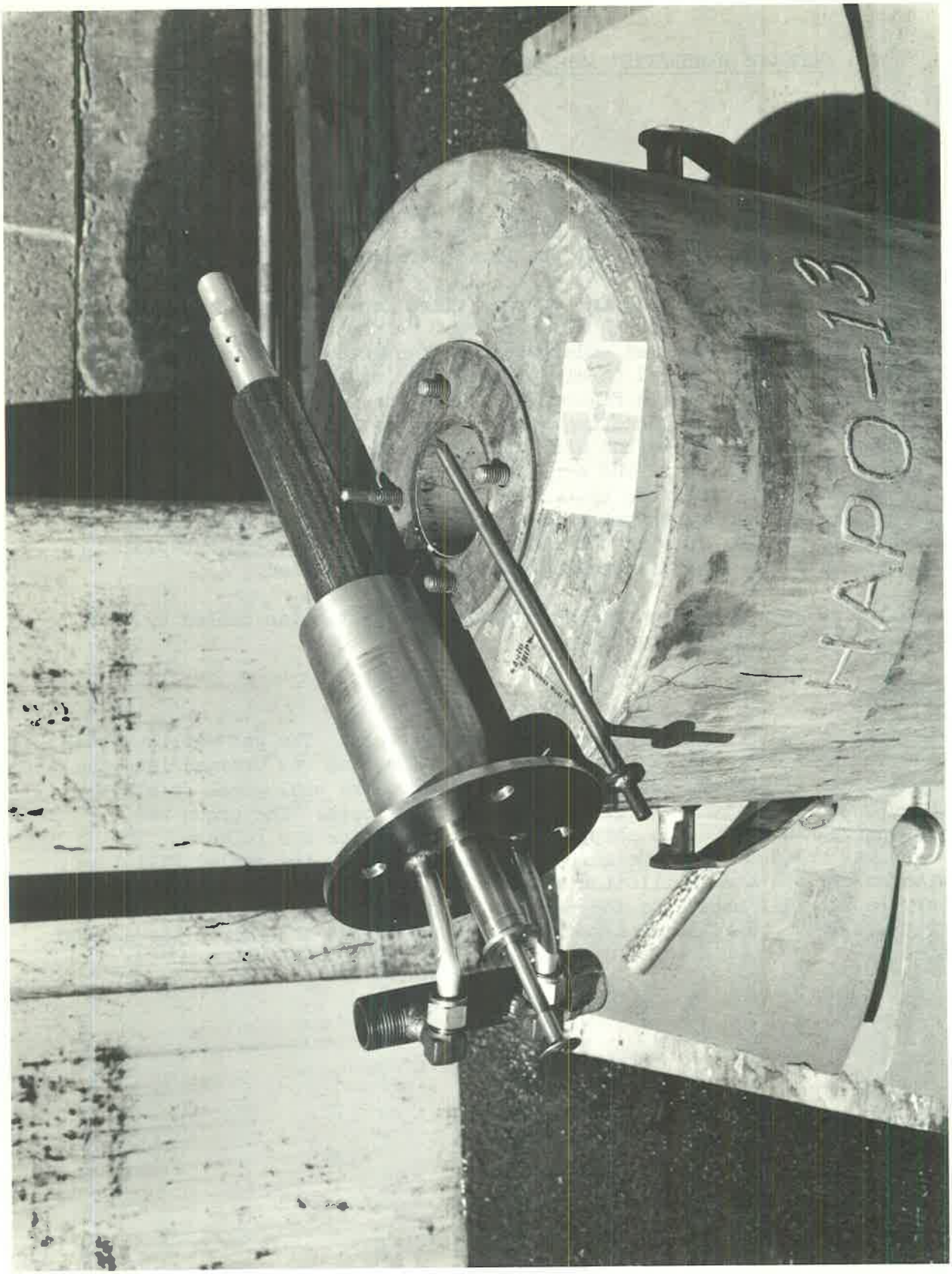


FIGURE 17

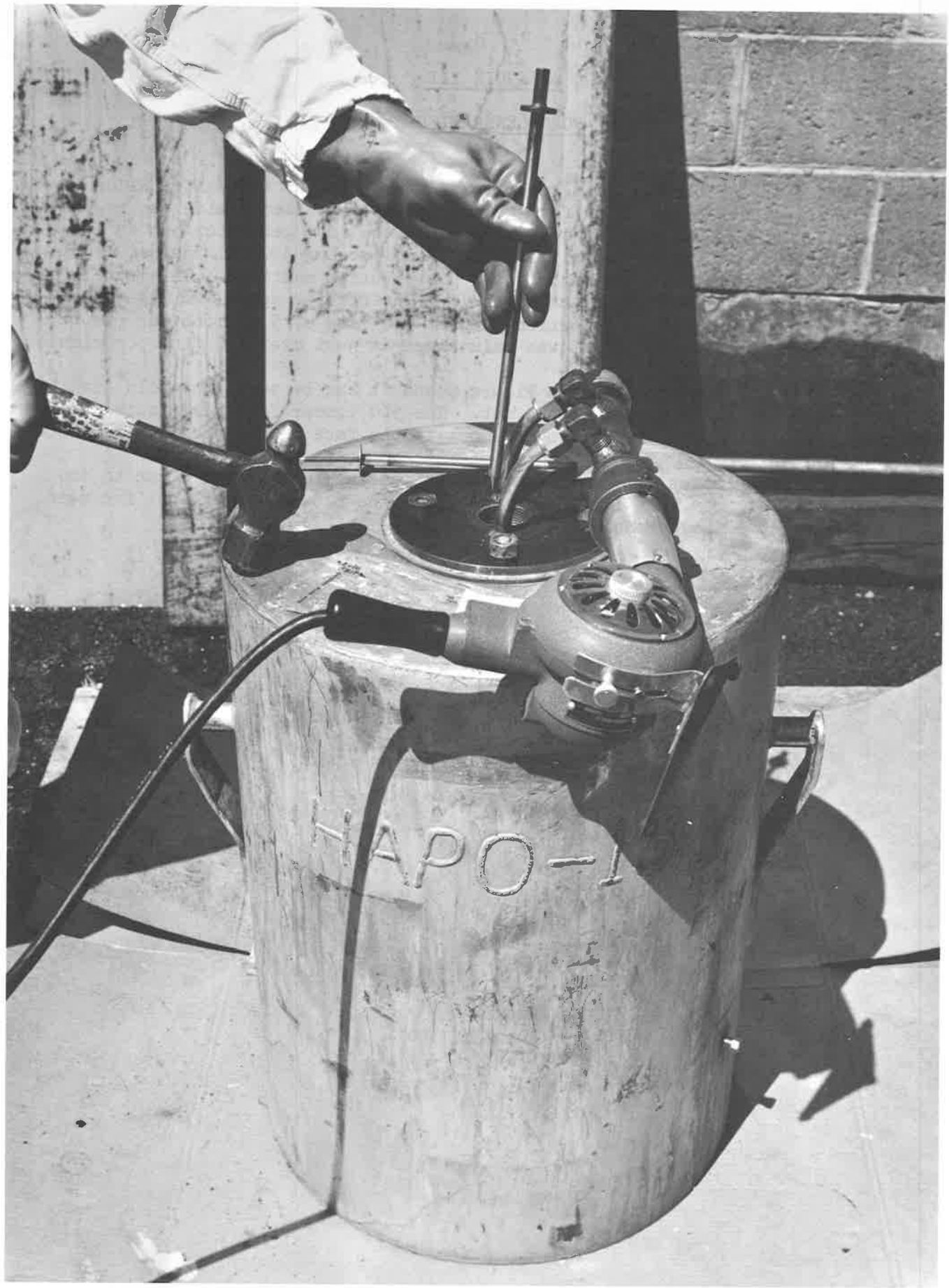


FIGURE 18

## APPENDIX III

## FOAM GENERATION

The foam and the 45,000 cfm foam generator was supplied by the Walter Kidde Co. of Belleville, New Jersey. The foam generator was installed inside the base of the stack. The exhaust air had to pass through the foam generator net as it entered the stack. A water supply capable of delivering 320 gallons per minute was connected to the foam generator water distribution manifold. This supplied 12 psi water to the nozzles on the manifold. The foaming agent was injected into the water supply by an injection pump at the rate of 5 gallons per minute. The air velocity through the net was maintained at just over 500 feet per minute.

The foam generator net is shown in Figure 9 and it can be seen that folds in the net increase the surface area of the net. The 500 linear feet per minute applies to the velocity through the netting and not to the face velocity of the generator.

The fan characteristics were such that the increasing back pressure due to the 200 foot head of foam made little difference in the flow. The exhaust fan used is American Blower Co., Model 10 Vane Axial Fan.

# AIR CLEANING FOR REACTORS WITH VENTED CONTAINMENT

by

R. D. COLLINS, J. J. HILLARY AND J. C. TAYLOR
U.K.A.E.A., Reactor Development Laboratory,
Windscale Works, Sellafield, Cumberland, England

## SUMMARY

A programme of experimental work has been carried out under conditions appropriate to possible depressurisation-type accidents to the Steam Generating Heavy Water Reactor (SGHW) at Winfrith Heath which has vented containment. The work has included small-scale experiments in glass or silica apparatus in which measurements have been made of the extent and form of the iodine release from zircaloy-clad $UO_2$ into steam under melting conditions and at about 1000°C. A number of tests have been conducted with simulated forms of iodine on two large-scale steel models of the reactor water lute steam suppression system. Tests have also been carried out on 1000 cfm filter units to develop droplet disentrainment devices. Work on the development of charcoals to deal with penetrating iodine (methyl iodide) under wet conditions is reported separately.

The results of this work show that:

(a) An effective trapping plant can be specified to deal with fission product iodine in wet atmospheres.

(b) At least up to 1000 MWD/te U fuel burn-up, a can retention factor of 10 applies for iodine expected to be free within the can; also that passage through a water lute is likely to reduce the iodine release by a further factor of 10.

## INTRODUCTION

1. The containment of the Steam Generating Heavy Water Reactor is designed to deal effectively with a wide range of postulated accidents to the reactor and during the design of the prototype further information was sought on the behaviour of fission products under some of these conditions. A principle feature of the containment is the large concrete structure which houses the primary coolant circuit and forms a primary containment. This structure is completely enclosed in a much larger building which acts both as the turbine hall and a secondary containment. Extraction of air through a fission product trapping plant enables the secondary containment to be maintained at a pressure less than atmospheric thus minimising outleakage without requiring an exceptional degree of tightness.

2. In the event of a rupture of the primary coolant circuit the pressure generated in the primary containment is relieved through a water lute which is connected by flumes to the secondary containment. The flumes are situated at one end of the secondary containment which acts as a large buffer volume for uncondensed gases and vapour. Subsequent to blowdown of the circuit, the negative pressure differential in the secondary containment allows it to act as a collecting facility for any fission products escaping from the primary containment, thereby providing double containment. During the short period that the lute is open it is possible to show that the release of fission products is acceptably small and this arrangement avoids the difficulties associated with holding a containment at high pressure for a long period during which a substantial release of activity from the fuel may occur.

3. The experiments were directed to the following points:

(a) The effectiveness of the trapping plant in dealing with all known forms of gas-borne fission products

The main concern was the trapping of organic iodides by charcoal from wet air. A further consideration was the performance of a demister designed to prevent overloading of the high efficiency filter by carry-over of water droplets.

(b) The possibility that novel forms of fission products, capable of penetrating the trapping system, might be produced from zircaloy-clad uranium dioxide fuel heated to a high temperature in steam

(c) The proportion of fission products released by a failed can during period when the water lute is unsealed

The hottest parts of the fuel are cooling due to the drop in reactor power. The can, however, heats up due to partial loss of cooling and if failure occurs some of the volatile fission products previously released from the hottest (central) region of the fuel during normal operation may escape. In the case of the rare gases almost all the release will escape from the can but for the other fission products the proportion will depend on the chemical reactions which take place between different fission products and between individual fission products and the fuel or the can.

(d) The proportion of this release which will be washed out during passage through the primary containment and the water lute

## TRAPPING PLANT

4. It is shown in a companion paper[1] that suitable impregnated charcoals will trap methyl iodide even from wet air and that the life of such a bed is likely to be measured in years.

5. Protection against fission products which are less volatile than iodine depends mainly on the ability of the high efficiency filters to remove aerosols and this can be established by such well known methods as for instance, the sodium chloride flame test. To protect these filters from carry over of water droplets a demister is included in the system.

6. Combinations of filters and demisters were tested to determine whether they would become plugged by the water droplets which might be formed by condensation of steam or be carried over from the lute. It was found that the normal high efficiency filters rapidly blocked unless protected but the situation was much improved by using siliconised filters. The results of some of the tests on full-scale units (1000cfm) are shown in Table I. Steam was injected into the airflow to give 110% relative humidity at 20°C which produced water droplets of which 95% were between 1 and 10 microns in diameter at a concentration of 50 $cm^3$ of water/1000 $ft^3$ of air. The prefilter used incorporates a flame trap but is primarily intended to extend the life of the 'absolute' filter. The importance of arranging pleated paper filters with the paper lying in a vertical plane so that water can drain easily, is shown by comparison of tests 1 and 2. The degree of blockage at the end of the first test in which the air flowed upwards, was so great that the fan used could not pull the full flow. Test 3 shows that the demister (a mat of glass fibres) has considerably reduced the final overall pressure drop even with siliconised filters. Other tests with smaller units showed that a mat of terylene fibres or of PTFE fibres as used by Walker and Peters[2] gave a similar performance and that the system chosen (glass fibre demister, prefilter and absolute filter) was relatively insensitive to large increases in steam: air ratios and hence the droplet concentration. The apparatus used for the 1000 cfm horizontal flow tests is sketched in Fig. 1.

## HIGH TEMPERATURE RELEASE FROM FUEL (SEE APPENDIX I FOR EXPERIMENTAL DETAILS)

7. The temperature of the fuel during irradiation was not considered to be important when specimens were to be heated well above 2000°C. It was convenient to use 0.6 in. dia. x 3 in. long specimens irradiated to 1000 MWD/te in a low flux reactor. They were then heated in steam by radiofrequency induction and the gas stream was carried in silica or glass tubing to a water bubbler, condenser, demister, coarse filter and a May Pack or charcoal bed. The only fission products which were found to be volatile at room temperature were rare gases, and iodine compounds which either behaved as methyl iodide or were more easily retained on charcoal. That is to say, the majority were trapped and retained permanently on the charcoal but unless the humidity was reduced or the charcoal impregnated with an amine, considerable desorption occurred on prolonged elution[3].

8. Table II summarises the results which were reported earlier[3].

TABLE II

High temperature (melting) release of iodine from Zr-2 clad irradiated $UO_2$ (>1800°C)
(up to 100 MWD/te U)

All results expressed as % of fuel iodine inventory

| Test No. | Gas conditions | | Iodine -131 release % | Iodine -131 penetration of condenser-contacting system % | Iodine -131 released as organic-iodides % | Remarks |
|---|---|---|---|---|---|---|
| | Composition | Flow l/min | | | | |
| 1 | Steam | 20 | 28 | 4 | 0.04 | |
| 2 | Steam | 20 | 35 | 0.7 | 0.5 | |
| 3 | Steam | 20 | 34 | 4 | 3 | |
| 4 | Steam | 2 | 31 | 20 | 1.1 | |
| 5 | Steam | 0.3 | 8 | - | 3 | All release passed to hot May Pack |
| 6 | Steam | 2 | 8 | 2.4 | 2.3 | |
| 7 | Steam | 20 | 27 | 12 | 0.1 | Stainless steel can |
| 8 | Air | 10 | 60 | 6 | 0.2 | Steam added to off-gas |

LIQUID: D = DRAINAGE LINES
T = THERMOMETER
ΔP = DIFFERENTIAL PRESSURE MANOMETER

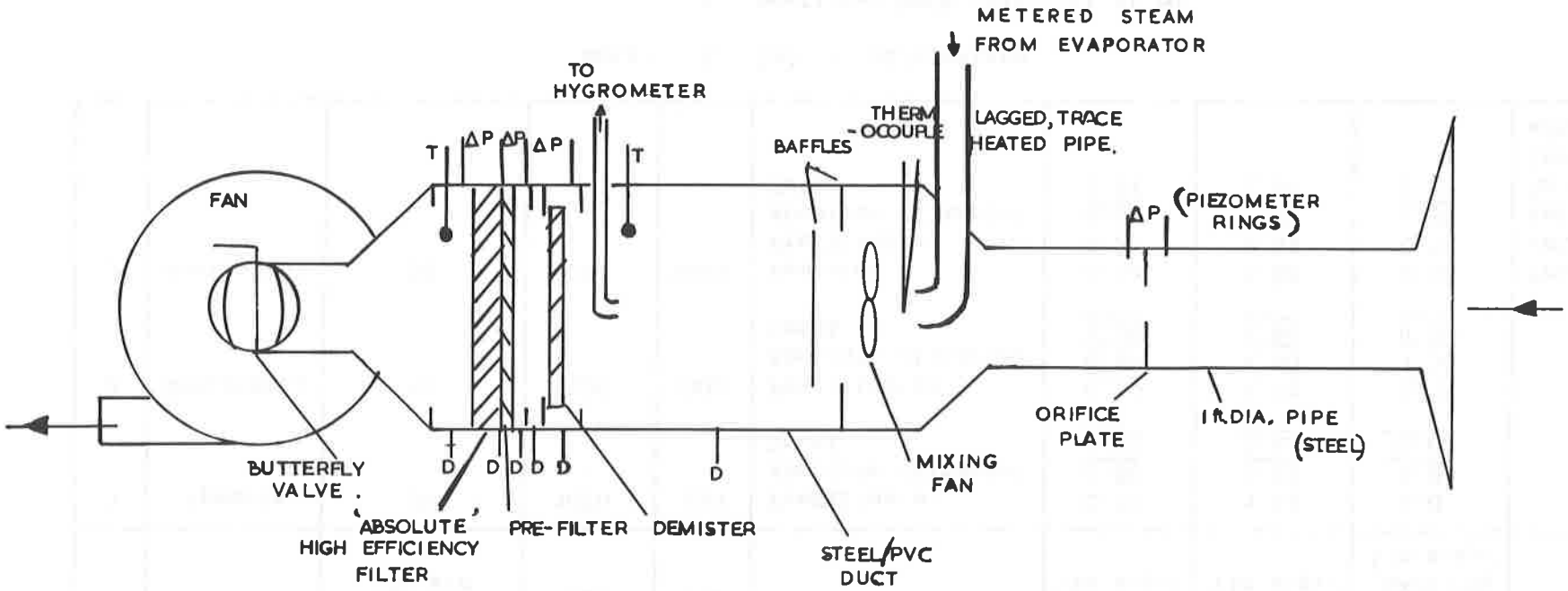


FIG. 1. SECTIONAL SIDE ELEVATION OF 1000 ft³/min. RIG FOR TESTING DROPLET DISENTRAINMENT DEVICES.

TABLE I

1000 cfm droplet disentrainment test

| Test No. | Direction of flow | Entrainment, $cm^3$ water per 1000 cfm air | Initial flow cfm | Final flow cfm | Filter combination | Initial pressure drop (in w.g.) | Final pressure drop (in w.g.) | Final pressure drop scaled to 1000 cfm (in w.g.) | Remarks |
|---|---|---|---|---|---|---|---|---|---|
| 1 | Upwards | 34 | 1070 | 250 | Prefilter(s)<br>Absolute filter(s)<br>Total | 0.10<br>0.89<br>0.99 | 1.63<br>0.79<br>2.42 | 6.0<br>4.0<br>10.0 | |
| 2 | Horizontal | 55 | 1000 | 1000 | Prefilter(s)<br>Absolute filter(s)<br>Total | 0.29<br>0.97<br>1.26 | 3.15<br>1.70<br>4.85 | 3.15<br>1.70<br>4.85 | |
| 3 | Horizontal | 57 | 1000 | 1000 | Demister<br>Prefilter(s)<br>Absolute filter(s)<br>Total | 0.32<br>0.27<br>0.92<br>1.51 | 0.88<br>0.53<br>1.20<br>2.61 | 0.88<br>0.53<br>1.20<br>2.61 | Pressure drops returned to initial values in ambient air (no steam) after 1-2 hours |

Note: 1. (s) = siliconised

2. Prefilter >90% efficient at 5μ

3. Absolute filter >99.95% efficient at 0.5μ

## RELEASE FROM CANS PUNCTURED AT 1000°C (SEE APPENDIX II)

9. Similar fuel specimens were irradiated at up to 43 w/g in order to obtain a high fuel temperature and to free a reasonable proportion of the fission products from the uranium oxide lattice. After irradiation each specimen was held at 300°C in a stream of superheated steam for a period to allow fission products near the can wall to attain chemical equilibrium with their environment at a temperature close to that of normal operation. It was then heated by radio-frequency induction to 1000°C and the can was punctured by focussing a pulse of light from a laser on to the can wall. The pressure of the gas in the interspace between the fuel and the end cap (several atmospheres) carried fission products into the steam flow. The effluent contacted evaporating water droplets sprayed by an air jet and, after passing through a demister to remove the spray, was taken to a condenser, a bubbler, another demister and a May Pack. A separate gas sample measured the helium release (which by comparison with the original filling gave a rough estimate of the extent to which the gas was swept from the fuel interspace). Similarly the rare gas release was measured and correlated with the irradiation conditions. The main purpose was to compare iodine and rare gas release and to determine the proportion of the iodine that remained gas-borne after contact with water and passage through the demister.

10. The first pair of tests used fuel irradiated at a low centre temperature and gave very high retention factors possibly because absorption is favoured by the very low mass (Table III).

11. The rating of the second pair of specimens was higher than is normally used in the reactor but less than 0.4% of the iodine left the can and less than 0.03% penetrated to the May Pack in either case. But the xenon release is also several times less than would be calculated by the accepted methods and it is thus assumed that the release of fission products from the lattice was low. It is possible that the short experimental fuel pencils were more homogeneous than the full length specimens which provided the data on which the methods of calculation are based. Accordingly the results are interpreted in terms of the factors by which the proportional xenon release must be divided to obtain the corresponding iodine or penetrating iodide release. It is to be noted that Test 1 indicates that additional xenon release due to heating the fuel element for a short period at 1000°C in a steam atmosphere is small (0.01% of the fuel inventory).

12. Thus taking the larger of the two releases, the percentage escape of iodine from the can is a tenth of the percentage xenon release and nine tenths of the iodine escaping is in a form which can easily be scrubbed from the air by contact with water. These results are compared with three similar tests in which irradiated fuel was replaced by unirradiated fuel which had been sealed in its can with trace active iodine. The escape figures are in fair agreement on the basis that iodine and xenon are released in similar proportions from irradiated fuel and it appears unnecessary to suppose that special mechanisms operate in the case of irradiated fuel. Increasing the mass of iodine to correspond to the highest burn-up contemplated produced little effect on the fraction which escaped but this point remains to be confirmed with irradiated fuel.

13. A significant amount ($\frac{1}{3}$rd to $\frac{2}{3}$rds) of the released iodine was removed by contacting with evaporating water droplets. This transfer was surprisingly high in view of the small ratio of water:steam + air (1 : 500) and indicates that iodine in whatever form it is released is more easily transferred than data for large concentrations of elemental iodine in pure water suggests[4].

TABLE III

Iodine release from Zr-2 clad $UO_2$ at 1000°C

All results expressed as % of the total fuel inventory (Xe -131 or I -131)

(a) IRRADIATED FUEL

| Test No. | Rating (end of irradiation W/gU | Fuel burn-up MWD/te U | Calc.fuel centre temp. °C | Release temperature °C | Xe-133 escape from can % | Estimated I mass released from $UO_2$ during irradiation ug | I-131 escape from can % | I-131 penetrating condensing/ contacting system % | Can retention factor (Iodine) | Overall retention factor (Iodine) | Remarks |
|---|---|---|---|---|---|---|---|---|---|---|---|
| 1 | 21 | 1150 | 1080 | 925 | not measured | - | $10^{-5}$ | $10^{-6}$ | - | - | |
| 2 | 26 | 360 | 1290 | 700 | 0.01 | 0.01 | $5\times10^{-5}$ | $6 < 10^{-6}$(1) | 200 | 1700 | (1) Mostly organic iodides |
| 3 | 39 | 850 | 2030 | 1050 | 2 | 10 | 0.20 | 0.02(2) | 10 | 100 | (2) Mostly small particles |
| 4 | 43 | 1300 | 2300 | 900 | 5 | 40 | 0.35 | 0.02 | 15 | 250 | |
| (b) SIMULATED FISSION PRODUCT IODINE | | | | | | | | | | | |
| Tracer 1 | - | - | - | 700 | - | 2 | 0.5 | 0.1 | 200 | 1000 | |
| Tracer 2 | - | - | - | 900 | - | 25 | 3.0 | 0.4 | 30 | 250 | |
| Tracer 3 | - | - | - | 900 | - | 1000 | 5.4 | 0.4 | 19 | 250 | Iodine ■ to 12% release from 20,000 MWD/te U burn up fuel |

Notes: (a) Can retention factor = xenon % escape/iodine % escape from can.
(b) Overall retention factor = xenon % escape/iodine % penetrating simple condensing/contacting system.
(c) Retention factors will be greater if the % iodine release from the $UO_2$ lattice is larger than that of xenon.
(d) Col.10 - results from Tests 2 and Tracer 1 and 2 will be a little lower allowing for deposition in the fuel release zone (not measured in these tests).

## LUTE MODELS

14. The largest pressure circuit breaches which are possible, displace the air from the inner containment so rapidly that the pressure there is much greater than the head of water in the lutes, and the water surface is driven well below the level of the bottom of the pipes. To model such a flow it is necessary to satisfy Froudes' criterion (velocity proportional to the square root of the scale factor) so that the dynamic head of the air flow matches the gravity head of the water. But this will lead to an under-estimate of the degree of contact since in a small model the contact time is reduced in proportion to the square root of the scale factor. Furthermore the lower pressure leads to less atomisation whereas similarity requires the size of the droplets to be reduced in proportion to the scale of the model. It is, therefore, necessary to use a large model to minimise scale effects and the results must be expected to be pessimistic.

15. A quarter-scale model of the lute system had been constructed for hydrodynamic studies and decontamination tests were carried out on this. The pressure circuit was simulated by a steam drum, fitted with a nozzle through which a rapid discharge of hot water was initiated by the explosive fracture of a bursting disc. The drum contained demineralised water with, in some cases, 10 p.p.m. of ammonia (typical of reactor operation ) at 100 p.s.i.g. SVP and this was discharged through a primary containment structure and a lute system. The geometry of the top of the flume which leads from the lute to the turbine hall was not modelled and the air was led away by two chimneys. A considerable quantity of water collected at the base of this stack and the major part of the trace material penetrating the lute was in this fall-out. For two tests the trace material used was iodine and in the other two lithium sulphate, the latter having been chosen as a soluble salt which can be easily detected. In two tests the trace material was introduced into the water in the steam drum and in the other two it was released into the jet of water escaping from a pressure vessel by breaking a glass vessel placed below the nozzle. Gas samples were taken from the chimneys and in the first test it was felt that since the air which left the chimney at the start of the blow would contain less tracer than that at the end, a sample of the air in the chimney taken immediately after the blow would provide a pessimistic estimate of the escape of tracer and avoid the problem of sampling a rapidly varying flow. For the remaining tests, however, an approximately isokinetic sample was taken in the stack during the discharge. Appendix III gives experimental details.

16. Table IV shows results of two tests with lithium sulphate, two with iodine and one with methyl iodide.

TABLE V

Intermediate flow rig: iodine penetration VS. Steam flow and proportion of air

| Test No. | Variable | Rig steam flow lb/sec | Rig air flow lb/sec | Proportion of air wt. % | Iodine release mg | Xe-133 recovery % of release | Iodine penetration % (I in chimney x 100 / I in pond + chimney) | Remarks |
|---|---|---|---|---|---|---|---|---|
| 1(a) | ↑ Steam flow W/O Air | 8.8 | 0 | 0 | 3 | - | <3 | High $^{133}$Xe count on charcoal reduced sensitivity |
| (b) | | - | 0.33 | 100 | | | 0.57 | Total penetration <3.6% |
| 2 | | 8.7 | 2.4 | 21.6 | 8 | | 1.06 | |
| 3 | | 7.7 | 7.3 | 48.7 | 7 | 102 | 5.0 | |
| 4(a) | | 6.0 | 0 | 0 | 5 | - | 0.31 | Total penetration 1.0% |
| (b) | | - | 0.33 | 100 | | | 0.70 | |
| 5 | | 6.2 | 1.5 | 19.5 | 5 | 75 | 0.36 | |
| 6 | | 6.0 | 7.3 | 55 | 5 | - | 5.0 | |
| 7 | | 6.0 | 7.3 | 55 | 5 | 107 | 2.9 | |
| 8(a) | | 2.6 | 0 | 0 | 4 | - | 0.72 | Total penetration 1.2% |
| (b) | | - | 0.33 | 100 | | | 0.45 | |
| Elution | | - | 0.7 | 100 | | - | 0.69 | Elution time 10 min. |
| 9 | | 3.1 | 0.7 | 19 | 1 | 85 | 1.43 | |
| Elution | | | 0.7 | 100 | | - | 1.0 | Elution time 10 min. |
| 10 | ↓ | 3.0 | 7.3 | 71 | 11 | - | 5.0 | |
| 11 | Iodine released over a few seconds | 3.6 | 7.3 | 67 | 10 | 95 | 3.5 | |
| 12 | - do - | 7.5 | 1.75 | 19 | 4 | - | 1.52 | |
| 13 | Depth of immersion of lutes 1 ft.only | 3.3 | 0.7 | 18.1 | 12 | 81 | 0.89 | |
| 14 | Higher initial pond temp(60°C instead of normal 0-10°C) | 5.2 | 1.7 | 24.7 | 6 | 89 | 0.80 | |
| Elution | | | 1.0 | 100 | | | 0.42 | |
| 15 | Steam not present (air only) | 0 | 7.3 | 100 | 7 | 88 | 7.1 | |

TABLE IV

| | Mass introduced | Primary Containment | Lute Pond | Chimney fall out | Leaving stack | Gas-borne after experiment | |
|---|---|---|---|---|---|---|---|
| | | | | | | Primary Containment | Chimney and Flume |
| Lithium sulphate below nozzle | 10.8 | 5.2 | 3.0 | 0.077 | $10^{-4}$+ | 0 | 0 |
| Lithium sulphate in drum | 1.6 | 0.6 | 0.24 | 0.020 | 0.0005 | 0 | 0 |
| Iodine below nozzle | 0.9 | 0.12 | 0.21 | 0.029 | 0.0030 | 0 | 0 |
| Iodine in drum | 2.9 | 1.95 | 0.3 | 0.014 | 0.0039 | 0 | 0 |
| Methyl Iodide below nozzle | 8.7 | 0.82 | 0.08 | 0.0045 | 1.65 | 2.25 | 0.64 |

+ based on sample taken after blow

The mass balance varied between 40 and 80%. In the case of the soluble tracers it was difficult to estimate the amounts left on the walls of the rig, while the error in the methyl iodide test may be due to calibration of the electron capture detector or to a mis-match between the flow in the sample pipe and up the chimney. Considering the difficulty of getting representative samples from a rapidly varying flow it is encouraging that the mass balance was as good as 62% in this case. The loss of soluble material from the top of the chimney is seen to be always much less than the fall-out. Penetrations based on the ratio of material introduced, to that in the chimney fall-out are 0.8, 1.25, 3.3, 0.48%, the highest arising from the case in which iodine was introduced into the escaping jet of steam and water. Penetrations based on the gas sample at the top of the chimney show the degree of penetration of forms which do not readily fall out and the corresponding figures are, (not measured) 0.03, 0.3 and 0.14%. Even allowing for some sampling error it is clear that the lute system provides a decontamination factor of at least 10 and that most of the escape is on large drops.

## INTERMEDIATE FLOW MODEL (APPENDIX IV)

17. The largest flows are associated with a very low probability of can failure since even if cooling could be completely removed there would be insufficient time for the can to reach a dangerous temperature before the coolant was discharged. There is therefore more interest in an intermediate range that extends down to flows at which individual pipes may discharge and reseal with a period determined by the resonance period of water flow in the pipe. Since this might have an adverse effect on decontamination the range was explored with a separate model[5].

18. To obtain the best modelling of the conditions around each pipe, the flow velocities and depth of immersion were maintained at full scale but there was a 2.6 : 1 reduction in the horizontal dimensions. In addition only one bank of the parallel tubes was modelled, the width of the pond being reduced accordingly. Since transverse flow is small a 2.6 : 1 distortion in transverse to vertical scale is not thought to be a serious disadvantage. Steam and air were supplied at a steady flow and iodine or fine aerosols could be injected upstream of the lute pipes while xenon was also injected as a check on the sampling system. The flume above the lute pond led to a chimney from which isokinetic samples were drawn and the xenon balance obtained from these samples was generally better than 80%.

19. Table V shows the results of a number of tests in which the iodine penetration varies between 0.3 and 7%. The penetration of iodine depends far less on the flow than on the steam: air ratio as is shown by Fig. 2. The results are not greatly affected by the initial temperature of the water in the lute pond, the depth of immersion of the lute or whether the iodine was released rapidly or over a period of several seconds. The test with air only shows that penetration is small even in absence of any steam condensation mechanism. The results of the work on the two lute system models also imply easier iodine transfer than data at high iodine concentrations suggest[4]. This is in agreement with the dousing tests of Watson et al[6] and work by Diffey et al[7] on removal in a small-scale water lute, and has been discussed theoretically by Eggleton[8] in terms of the various forms of iodine which may exist in water; and also by Griffiths[9]. At low concentrations iodine is probably mostly ionised in aqueous solution.

20. An AERE team carried out some complementary tests in which 0.06 micron aerosols of nichrome were introduced into the flow and the proportion that penetrated the lute was also less than 10% (Table VI). The mechanism by which the particles were removed is not established but condensation onto the aerosol while the steam is mixing with cold air may account for much of it although it should be noted that the highest penetration does not occur at the lowest proportion of air. The air used was drawn from atmosphere and was therefore considerably colder than that in the primary containment of an operating reactor. The results should not necessarily be regarded as quantitatively correct for the reactor system but they do illustrate the large degree of air cleaning even with a fine aerosol which results when rapid condensation occurs, as certainly will be the case in the water lute.

## CONCLUSIONS

21. A trapping plant can be specified which will deal effectively with fission products released from zircaloy-clad uranium dioxide and will operate on air containing a dense mist of water droplets. It consists of a high efficiency filter of siliconized glass fibre paper protected from water droplets by a glass fibre mat and glass fibre prefilter. Behind this is a bed of charcoal impregnated with triethylenediamine or potassium iodide. The impregnation is specified because methyl iodide is a possible consituent of the fission product release.

22. Should the can of a high-rated fuel element rupture in the early stages of a depressurisation accident while the water lute is unsealed and the can temperature is below 1000°C an escape of iodine is to be expected but this should be an order of magnitude less than would be calculated by assuming (1) iodine will be released from fuel in the same proportion as xenon, and (2) all the iodine released from the fuel will escape from the can. Of the iodine escaping from the can 90% will be in a form which is easily removed by contact with water. Following release from the can

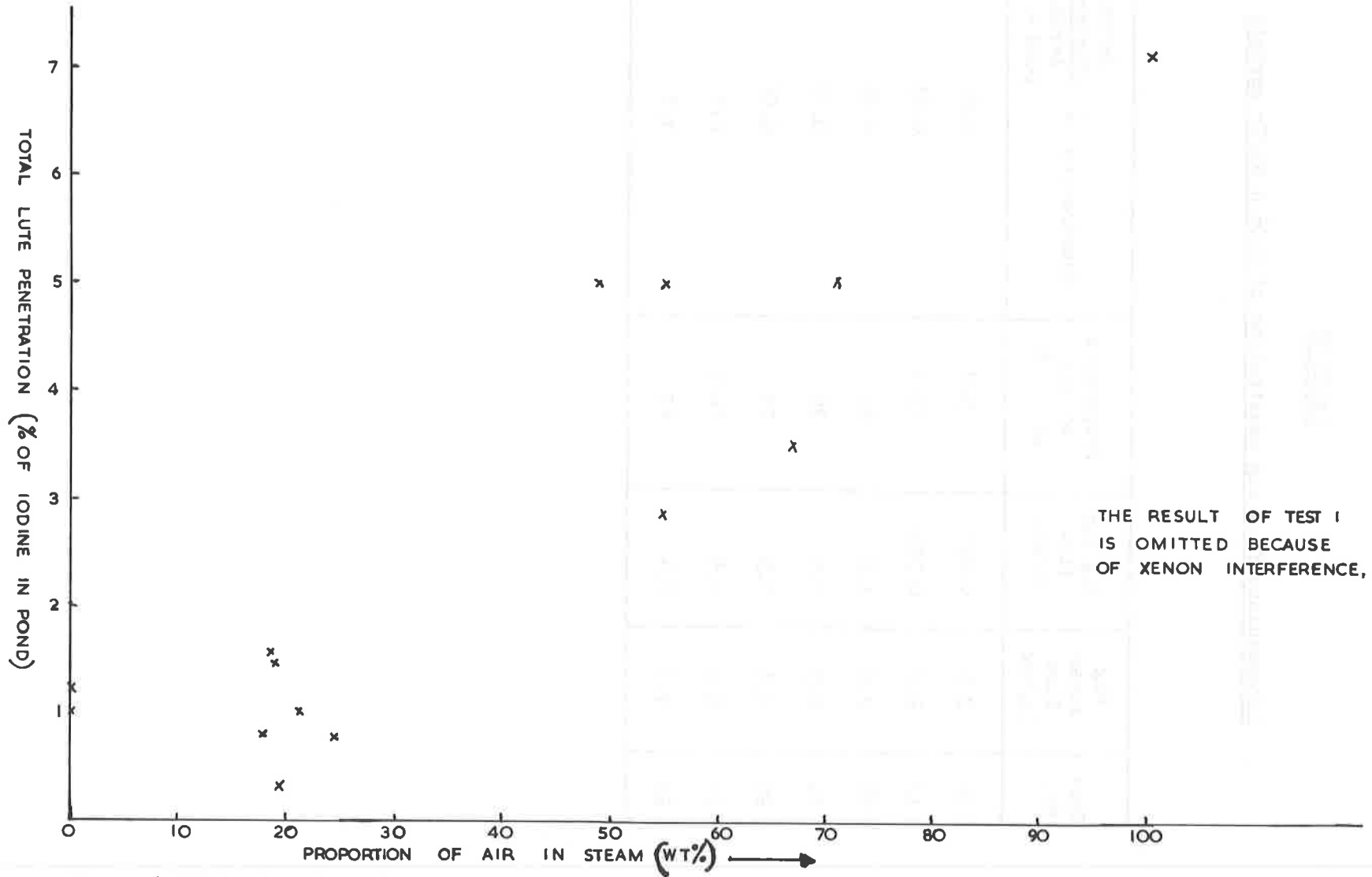


FIG. 2. INTERMEDIATE FLOW RIG TESTS. LUTE PENETRATION Vs PROPORTION OF AIR IN STEAM.

## TABLE VI

### Intermediate flow rig penetration of 0.06 μ Ni/Cr aerosol

| Test No. | Rig steam flow lb/sec | Rig air flow lb/sec | Proportion of air wt % | Penetration = $\frac{\text{Aerosol in chimney} \times 100}{\text{Aerosol in pond + chimney}}$ |
|---|---|---|---|---|
| 16 | 2.5 | 0.097 | 3.7 | 0.81 |
| 17 | 2.5 | 0.375 | 13.1 | 0.83 |
| 18 | 2.5 | 1.8 | 42 | 0.26 |
| 19 | 2.5 | 7.5 | 75 | 0.19 |
| 20 | 2.5 | 7.5 | 75 | 0.06 |
| 21 | 9.0 | 1.8 | 16.7 | 6.7 |
| 22 | 9.0 | 7.4 | 45 | 1.7 |

and passage through the water lute therefore the proportion of iodine escaping is expected to tbe two orders of magnitude less than the proportion of xenon. The latter of course depends on the irradiation history of the charge and particularly on the rating of the leading elements and is estimated by the normal methods.

23. The main value of this work is in assessing the behaviour of a specific reactor design but it does give a general indication of the results to be expected from applying aqueous scrubbing to the effluent from a major depressurisation accident.

## REFERENCES


1. COLLINS, D. A., TAYLOR, L. R. AND TAYLOR, R. The development of impregnated charcoals for trapping methyl iodide at high humidity (1966) TRG Report 1300(W).

2. WALKER, J. W. AND PETERS, A. H., Mech. Eng. Vol. 85, No. 9, p.46 (Sept. 1963).

3. COLLINS, R. D. AND HILLARY, J. J. Some experiments relating to the behaviour of gas-borne iodine, 1965. TRG Report 983(W).

4. TAYLOR, R. F. Absorption of iodine vapour by aqueous solutions. Chem. Eng. Sci. Vol. X, No. 1/2, April, 1959, p. 68.

5. HILLARY, J. J., TAYLOR, J. C., ABBEY, F., DIFFEY, H. R. Iodine removal by a scalemodel of the SGHW reactor vented steam suppression system, 1966. TRG Report 1256(W).

6. WATSON, L. C., BANCROFT, A. R. AND HOELKE, C. W. Iodine containment by dousing in NPD-II. CRCE 979 (AECL 1130) 1960.

7. DIFFEY, H. R., RUMARY, C. H., SMITH, M. J. S. AND STINCHCOMBE, R. A. Iodine clean-up in a steam suppression system. 1965. AERE R.4882.

8. EGGLETON, A. E. J. Private communication.

9. GRIFFITHS, V. The removal of iodine from the atmosphere by sprays. 1963. AHSB(S) R.45.

## APPENDIX I

### High temperature fission product release test: experimental details

24. The apparatus is constructed of silica and glass, and is sketched in Fig. 3; it comprises:-

(a) Fission product release chamber, of silica and provided with a flow of steam (20 l/min) which has been passed through a particulate filter and charcoal bed, and surrounded by a high frequency induction coil which heats the fuel element which is mounted centrally within the coil.

(b) 1.5 litre hold-up vessel, simulating the reactor primary containment, maintained above 100°C so that no condensation occurred. A sample of steam was withdrawn from this vessel through a hot May Pack which comprised copper gauzes, a membrane filter, charcoal papers and granule components and was heated slightly above 100°C to eliminate condensation.

(c) 0.5 litre lute vessel filled with cold, distilled water; the steam inlet pipe was immersed about 6 in. at the start of an experiment. A flow of 10 l/min cold air swept across the top of the lute vessel to displace uncondensed steam and fission products.

(d) The air sweep then passed through a condenser and demister to a full flow sampling or treatment system which was essentially small-scale trapping plant and consisted of pre-coarse and absolute filters, two charcoal beds and post-coarse and absolute filters all in series.

25. In addition, sampling points were provided, leading to May Packs, for other investigations, already reported[3], on the performance of the trapping plant under these conditions.

26. A typical experiment was carried out by trace-heating the apparatus and then setting up correct flows of steam and air. Radiofrequency induction heating was applied to the fuel specimen and its temperature observed by optical pyrometer through a window in the 4 in. lead shielding of the cell. A short warm-up phase was followed by a period of a few minutes at maximum temperature (normally > 2000°C). After switching off the radiofrequency heating, the steam supply was replaced by a flow of argon to displace steam and eliminate condensation during the final cooling down of the apparatus prior to removal of samples.

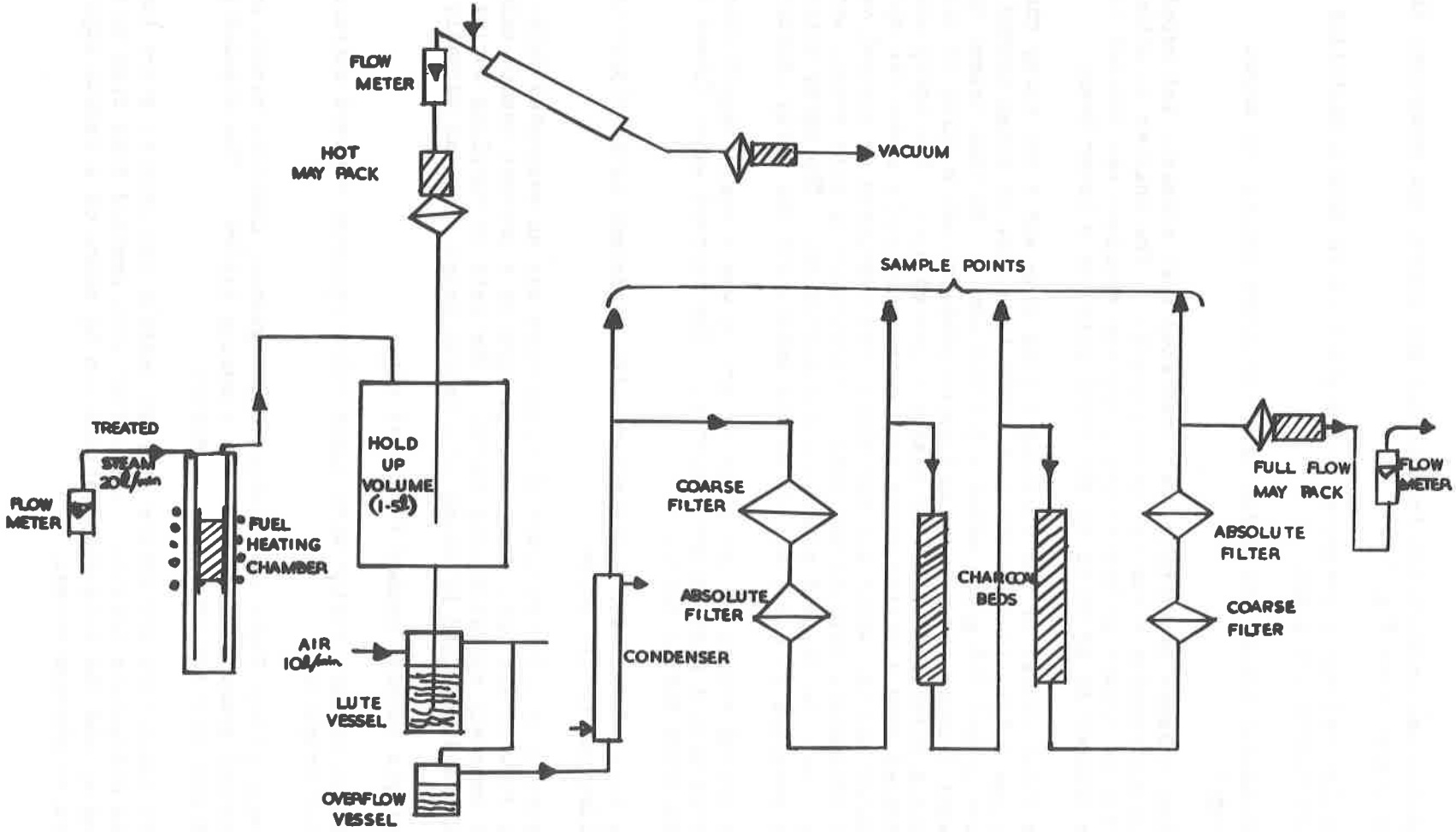


Figure 3. APPARATUS FOR HIGH TEMPERATURE FISSION PRODUCT RELEASE EXPERIMENTS.

## APPENDIX II

### Fission product release at 1000°C: experimental details

27. The apparatus was constructed from silica and glass, and comprised the following main items. (See Fig. 4).

(a) A boiler fed via a rotameter and control valve from a distilled water supply (15 g/min).

(b) A preheater taking the steam from the above boiler, or argon (purge).

(c) A fuel chamber containing the irradiated fuel element, and supplied with superheated steam (or heated argon). The chamber is situated within an induction heater coil, and the specimen was located inside the chamber so as to be at the focal point of a laser beam.

(d) The first vessel of the cleaning system line was a hot spray chamber, (volume 2 litres) maintained at 100°C by a flow of steam around the outer jacket (60 g/min water + 5 l/min air). In this vessel the upward flowing steam carrying fission products met a spray of near-boiling distilled water and heated filtered air. The spray was produced from a heated spray generator immediately above the spray chamber and the water and air flows were regulated by control valves and rotameters outside the cave. Conditions in this vessel were such that the overall process was evaporation. The spray water was retained in a collection bottle underneath the spray chamber.

(e) The second vessel of the cleaning system was a small lagged chamber fitted with a glass fibre demister. The removed water flowed to a collection bottle below.

(f) The third vessel was a condenser; the condensed water flowed to a collection bottle below.

(g) Fitted to a side-arm after the condenser was an evacuated bulb; the flow of air into this was regulated by a pre-set needle valve and remotely operated stop valve. The rate of sampling during a run was determined by means of a vacuum gauge; it was normally 1%.

(h) A simple bubbler washed the moist air.

(i) A small chamber fitted with glass fibre demister removed entrained water droplets.

(j) A bank of May Packs containing copper gauzes, charcoal papers and charcoal granules completed the cleaning system. The cleaned gas was led into the cave extract system.

28. A bank of non-active and active storage vessels was used to store the water from the collection bottles; the latter were emptied from time to time during running-up and the subsequent active run by means of a vacuum applied to the respective storage vessel.

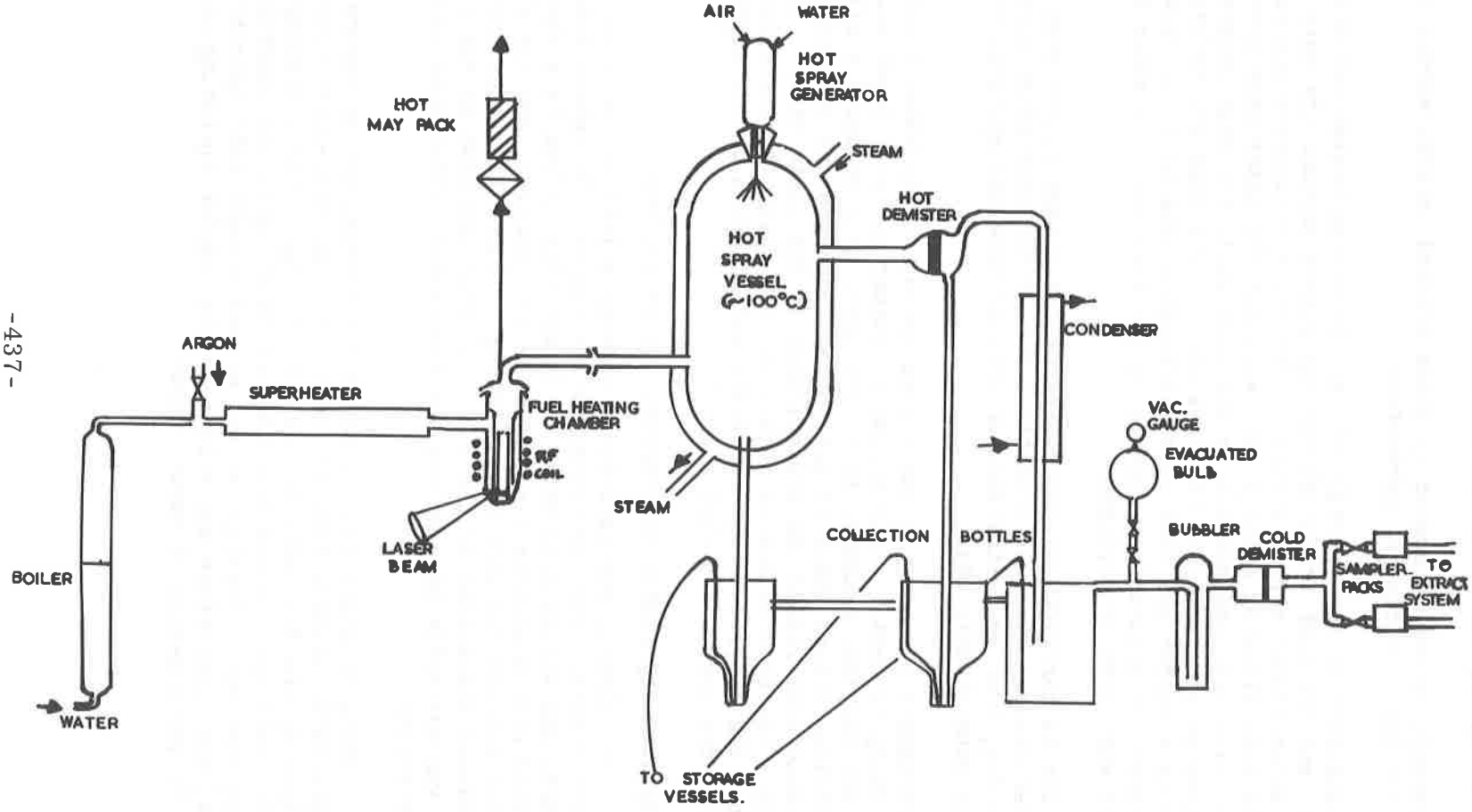


Figure 4. FISSION PRODUCT RELEASE APPARATUS (1000°C)

29. A hot May Pack was connected to the rig by silica and stainless steel tubing along which was withdrawn a small fraction of the steam flow passing out of the fuel heating chamber. The temperature was allowed to fall gradually to about 110°C, the operating condition for the May Pack which consisted typically of copper gauzes, absolute glass fibre filter, charcoal papers and 2 beds of charcoal granules. After passage through a flow meter and control valve, the steam was condensed.

30. Temperatures were measured by glass covered chromel-alumel thermocouples and (of the fuel) by optical pyrometer.

31. In addition to the above a 450 k/c induction heater was situated outside the cave, and the high frequency current passed through the cave walls to the coil by water-cooled copper tubing. The laser condensers and control equipment were also situated outside the cave, and the laser head containing the ruby and flash tube was mounted on the cave wall, the beam passing through a 1 in. diameter pipe inset in the cave wall. The beam was deflected within the cave by a mirror and then passed through a lens of 4 in. focal length to focus within the silica fuel chamber on the fuel can. A pulse of about 30 joules was normally employed.

32. So far in carrying out experiments of this type it has been possible to work under reasonably clean conditions within the cave after cleaning up a previous run, i.e. no restriction on working time has applied, and air counts have been consistently low.

33. Experiments were set up and tested operationally under these conditions, using a dummy element. Only a limited number of trial laser shots was made through any one fuel chamber, since the laser beam produced a slight opacity in the silica through which it passed, and back-scatter of zircaloy on to the silica could also reduce the transmission of the laser beam. The last operation within the cave before an active run was always to check with ordinary light that the laser beam was correctly set to focus on the appropriate section of the irradiated fuel element.

34. A typical experiment was carried out as follows:-

The element was introduced through a port in the cave roof, and after removal from its container was washed with carbon tetrachloride, dried, and washed with water. It was then lifted by a vacuum line fitted with a suction disc into the fuel chamber, and the final ball-joint connections were made remotely. Since radiation from the element produced blackening of the silica chamber and also of the nearby lens, it was advisable to conclude the experiment within some hours of these operations.

Using an argon flow, a check was carried out to ensure that no appreciable leakage resulted from the final ball-joint connections by comparing the flow into and out of the rig. Steam heating and condenser water were applied and then the hot water spray and associated air flow were started. Finally the boiler was brought into operation, and the fuel can temperature was held near its reactor operating conditions of 300°C for a period of about 1 hour.

During this period the collected water was sent to the non-active storage vessels for subsequent examination in the event of a premature can failure.

High frequency current was applied to the coil to bring the can temperature to 1000°C, and the stop valve leading to the evacuated bulb was opened. The laser was then 'fired'. Any water collected during this period of operation was directed to the active storage vessels. The gas sampling rate and can temperature were continuously measured, and the gas flow diverted to fresh May Packs at the end of the cleaning system as required by remote operation of glass taps.

After a period of 10 minutes, induction heating was switched off, and the steam supply to the preheater was replaced by an argon flow. The preheater temperature was then reduced, and when steam had cleared from the system, was switched off. After the fuel chamber temperature had dropped to near 100°C, the argon flow was discontinued, and then the spray water and the rest of the rig heating stopped.

When cold, the ball joints to the fuel chamber were opened, and the element removed, canned, and posted through the roof into a shielded container. Although initially provision was made for remote removal of samples, increase in complexity of the rig and operating experience made the preferred method an entry using protective clothing immediately after removal of the element. All samples were analysed by standard multi-channel $\gamma$-counting techniques except for 90 Sr in which case the samples were treated chemically, dissolved in aqueous solution and the 90 Sr separated for $\beta$-counting.

35. Fig. 5 shows the actual rig as viewed through the cave window.

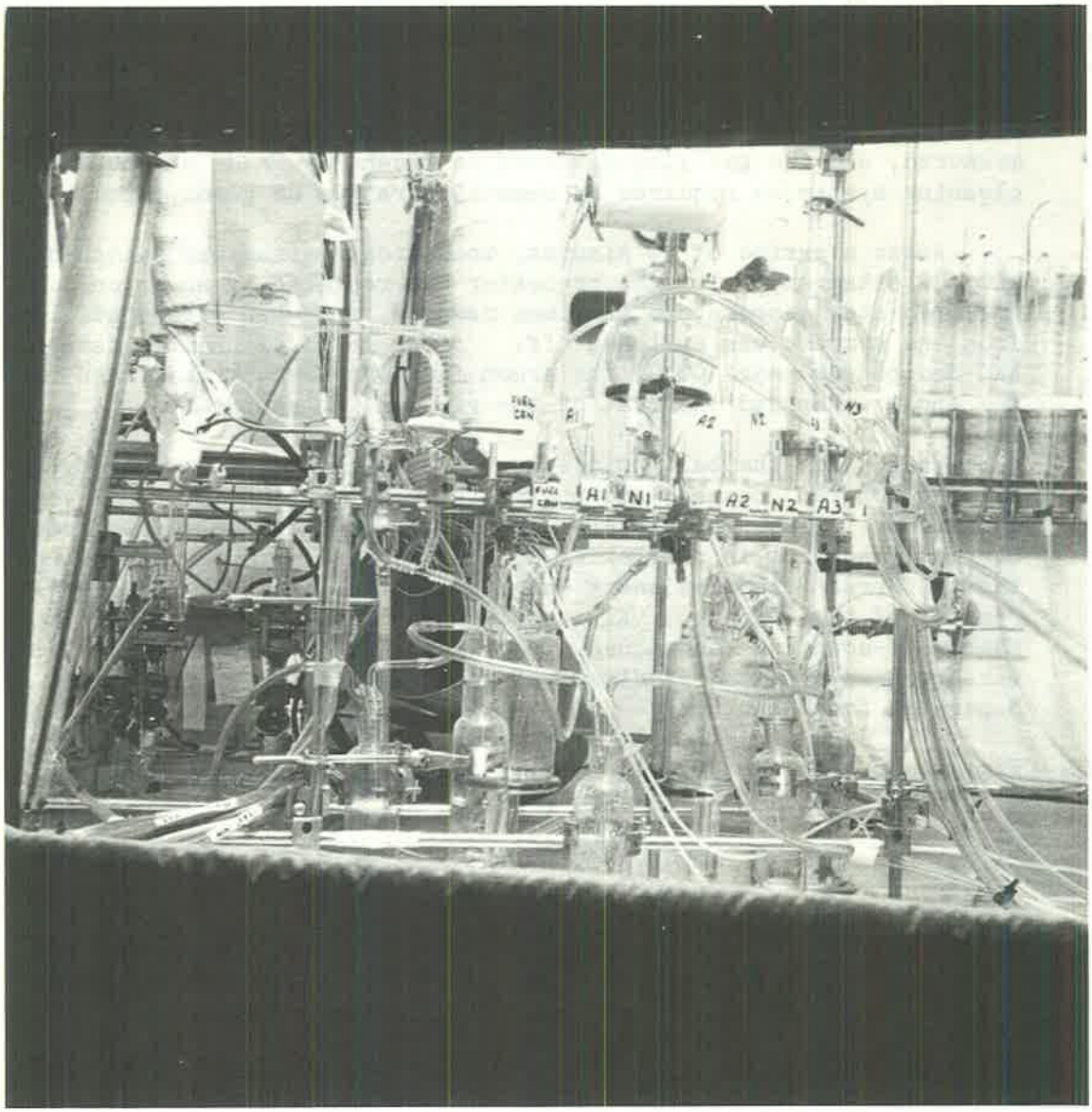


FIG. 5. FISSION PRODUCT RELEASE APPARATUS (1000°C)

## APPENDIX III

### High flow transient rig: experimental details

36. The rig (see Fig. 6) consists of a primary containment, lute system, suppression ponds, and suppression chambers. Inside the primary containment is a steam drum which simulates the reactor primary steam circuit and discharges through an orifice after failure of bursting discs. Pressures, temperatures and water movements are normally measured and release and sampling arrangements were provided for the chemical tests. All the tests were carried out under similar steam release and flow conditions with the largest tested size of steam drum orifice. In two tests a soluble involatile salt chosen for its ease of detection and high solubility ($Li_2SO_4$) was used, iodine in a further two, and finally methyl iodide was released in one test.

37. In a typical experiment, the required quantity of water (841 lb) in the steam drum was heated to reactor primary circuit conditions of temperature and pressure (280°C, 950 p.s.i.a.) and the associated heat exchanger valved off. The steam drum bursting disc was failed, releasing water/steam into the primary containment, air at first and then steam, vented through the water lutes and out through the suppression chambers and the chimneys to atmosphere. Measurement of temperature, pressure and water displaced or collected in various locations was made during and subsequent to the steam discharge. Water mass balance and heat balance was computed for each test.

38. 10 p.p.m. ammonia was added to the suppression ponds in the first iodine test and to the steam drums in the second iodine and the methyl iodide tests.

39. The lithium salt, iodine or methyl iodide was released as indicated below.

40. In the first lithium test, lithium sulphate was dissolved in 0.5 l water in a glass beaker situated in the path of the steam below the steam drum bursting disc. The steam flow dispersed the solution. In the second lithium test the salt was dissolved in the steam drum water and was therefore more evenly distributed during the steam release.

41. The two iodine tests were carried out in a similar sequence, the first involving release from a sealed glass vessel (heated to 80°C to vapourise the crystals) which was in the path of the steam and was fractured a few seconds before the steam release. In the second, iodine was added to the steam drum before failure. Iodine in a small glass bulb was heated (280°C) in a steel pipe and pressure applied from the nitrogen cylinder. This broke the bulb and caused the bursting disc to fail thus injecting iodine rapidly along the pipe into the water in the steam drum; the steam drum already contained an equivalent amount of dissolved ammonium iodide. Within a second or so the steam drum bursting disc was failed and depressurisation began.

42. Finally a fifth test was carried out with methyl iodide released below the steam drum using the same technique as in the first iodine test. The methyl iodide was released without additional heating.

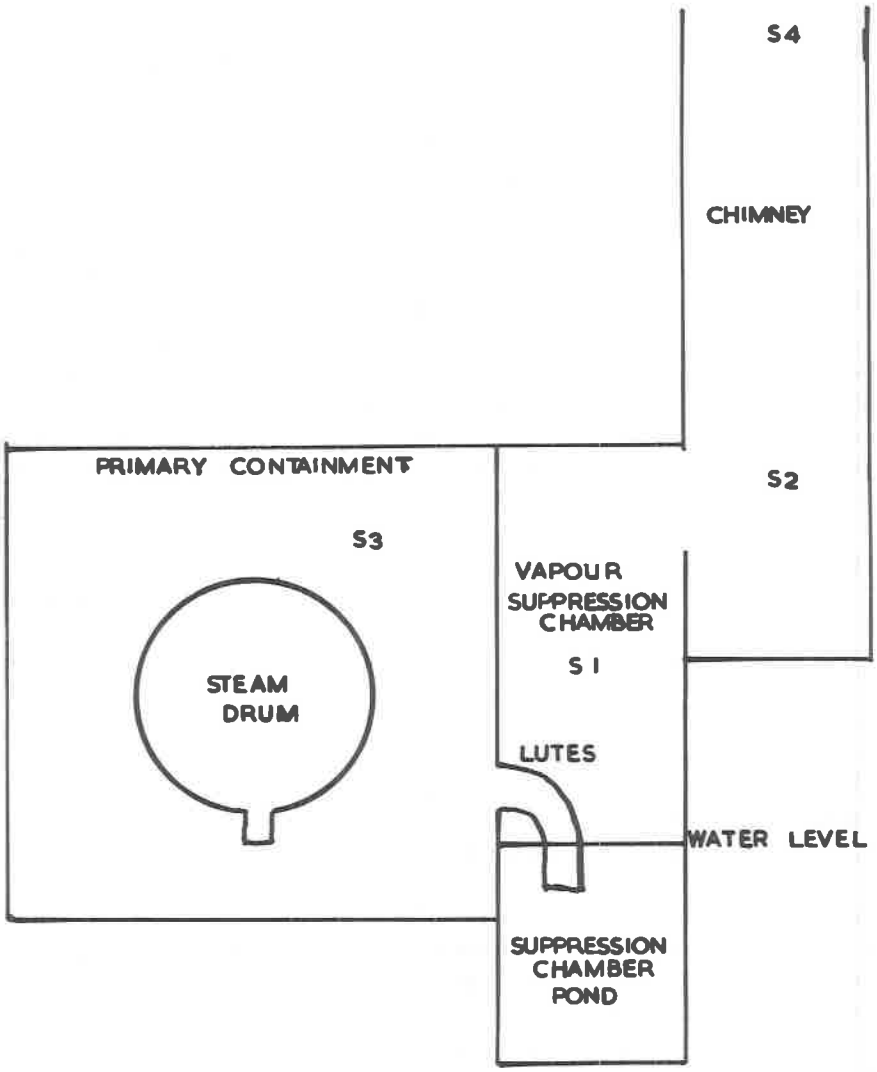


Figure 6. SIMPLIFIED SKETCH OF STEAM SUPPRESSION MODEL.

43. The lithium sampler was constructed in glass and consisted of a Whatman 41 filter paper (of low lithium background) upstream of a short column of silica gel which prevented condensation in the rotameter. Flow rate was 10 l/min. After leaching the filter paper with water, lithium content of the solution was determined by flame photometry. Gas samples were taken from the vapour suppression chambers (S1), chimneys (S2), primary containment (S3) after completion of the steam 'blow', and at the chimney exits (S4) during the 'blow'. The latter consisted of a high flow, iso-kinetic gas sample, some of the gas passing out of the chimney being drawn into an evacuated 10 l glass-bulb. Samples S1, S2, S3 were repeated at intervals following the 'blow' so that initial concentrations could be obtained by extrapolation.

44. Liquid samples were taken following the 'blow' in the primary containment, vapour suppression ponds and bases of chimneys. Background gas and liquid samples were taken before each discharge.

45. The iodine sampler (Fig. 7) was also constructed in glass and consisted of a condenser with condensate collection flask followed by an aqueous potassium carbonate (N/50) bubbler which removed molecular iodine; and a millipore filter paper collected particulate or droplet-borne iodine. Flow rate was 10 l/min. A gas sample, for methyl iodide analysis on a gas chromatographic column, was taken immediately upstream of the millipore component.

46. Samples were taken at the same points and in the same manner as in the lithium tests, including those at the chimney exits during the 'blow'.

47. Between experiments, some washing out was effected and there was at least one chemical-free blow to minimise the effect of carryover of lithium or iodine from one test to the next.

## Ultramicrodetermination of Iodine

### (a) As iodine or iodide (ionised)

48. The method is based on the Kolthoff-Sandell reaction between cerium IV and arsenic III, catalysed by iodine, in sulphuric acid solution.

#### Reagents Used

##### 0.01 M ceric solution

Ceric ammonium sulphate (6.32g) was dissolved in distilled water, concentrated sulphuric acid (44 ml) was added, and diluted to 1 litre. This solution was permanently immersed in the water bath.

##### Composite acid reagent

The reagent consisted of 6N, $H_2SO_4$, 2.1 N,HCl, 0.033N $As_2O_3$. Arsenic trioxide (4.946g) was dissolved in near-boiling water (500 ml), to which concentrated sulphuric acid (5 ml) had been added. A further 500 ml concentrated sulphuric acid was added carefully with cooling, followed by a further 566 ml conc. HCl. The volume was made up to 3 l with distilled water.

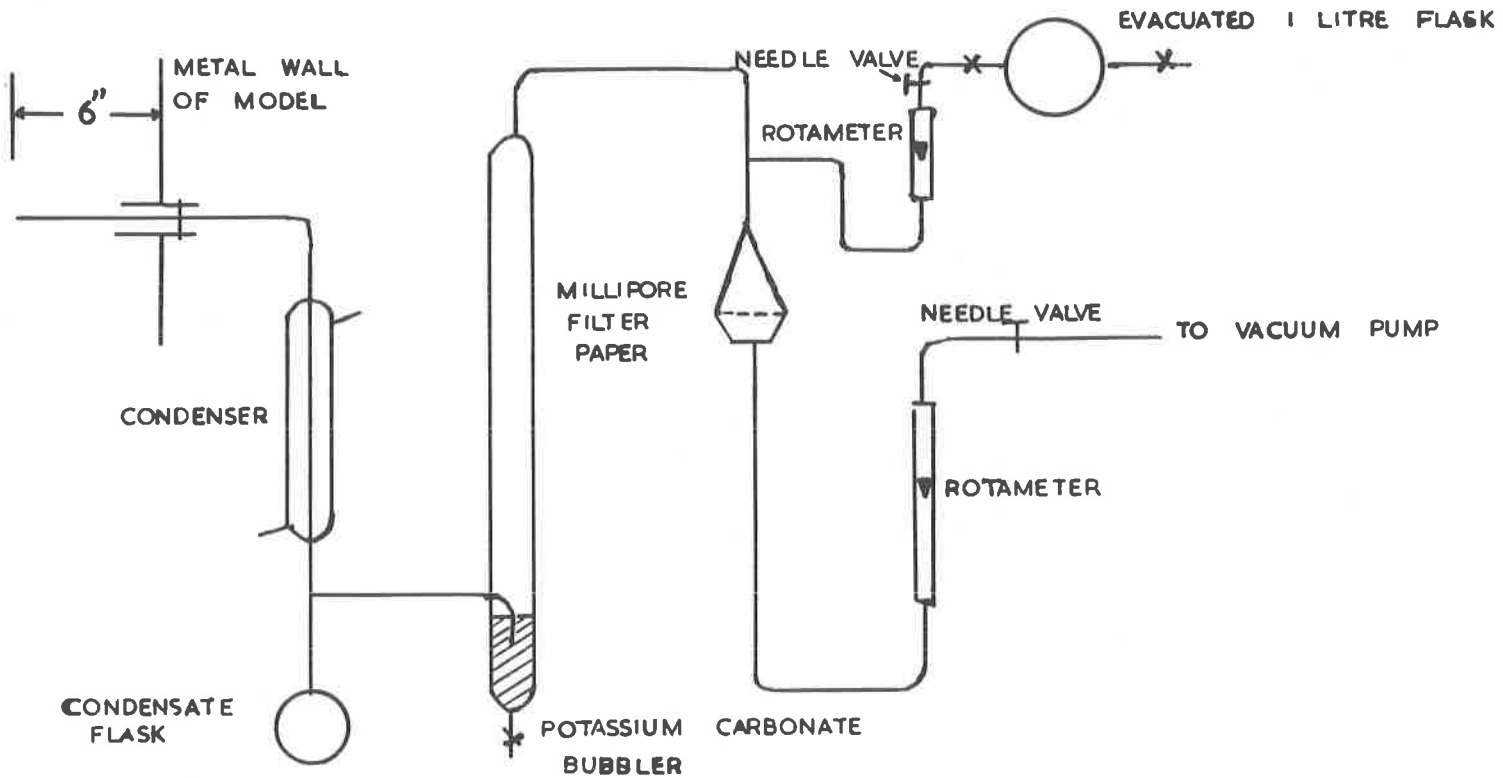


FIG. 7. FLOW DIAGRAM OF IODINE SAMPLING SYSTEM.

Brucine sulphate

Brucine sulphate ($\frac{1}{2}$g) was dissolved in distilled water (100 ml).

Standard potassium iodide solution

Potassium iodide (0.2616g) was dissolved in distilled water (1 litre) to give an iodide concentration of 200 µg/ml. Further dilutions were made as required.

Procedure

Ten ml of each sample were pipetted into 25 ml measuring cylinders, as also were 10 ml of standard iodine samples ranging from 0.001 to 0.010 µg/ml iodine. 5 ml of distilled water were added by pipette to each tube, followed by 3 ml of composite acid reagent. The test tubes and their contents were immersed in the water bath at 30 ± 0.1°C for 15 to 20 minutes to allow temperature equilibration to occur. Ceric ammonium sulphate (2 ml) was added to each tube at 1 minute intervals, and the reaction was allowed to proceed 20 minutes. Brucine sulphate was then added to each tube again at 1 minute intervals. The optical density (O.D.) of the solution was then determined by means of a Unicam S.P. 500 spectrophotometer using 1 cm cells at 440 mµ.

Calculations

A calibration curve was plotted of (1 + $\log_{10}$ O.D. of standards) against iodine concentration, and is a straight line. The iodine concentration of the samples was read off from this calibration curve.

(b) As methyl iodide:

49. A sample of about 5 ml gas was loaded on a dinonyl phthallate (or silicone oil) on celite gas chromatography column and eluted in a stream of dry nitrogen. The methyl iodide was characterised by its retention time. A quantitative mass measurement was made by the use of an electron capture detector (with tritium source) the signal from which had been calibrated against a known amount of methyl iodide prepared by multiple dilution of a benzene solution.

50. In no test (except that in which methyl iodide was released) was methyl iodide detected.

## APPENDIX IV

### Intermediate flow steady state rig: experimental details

51. A sketch of the rig is set out in Fig. 8. Fig. 9 gives a general impression of the scale and arrangement of the rig. Steam at a rate of up to 12 lb/sec was fed to the lute system from a pair of accumulators (supplied direct from a boiler house) through a throttle valve and an orifice plate for flow measurement. The steam then flowed through a control valve to two quick-acting butterfly valves which allowed steam either to be dumped into a large cooling water pond while the required flow conditions were established or to be passed through the lute system. A small buffer volume (simulating the reactor primary containment) was connected to the steam line which then led to a mixing chamber where air at flow rates up to 5,500 $ft^3$/min or 7.3 lb/sec was introduced from a large compressor; air flows up to 600 $ft^3$/min were taken direct from a smaller compressor or from the compressed air main. After passing through the water lute, air was taken up through a flume to a chimney where representative sampling was possible. Air flow was measured by observation of the differential pressure across an orifice in the supply pipe and by anemometer readings in the chimney.

52. A bank of four lutes was provided, immersed for 2 ft into the water of the pond. Pond temperature was measured at intervals of 1 ft depth, and at each depth there were up to 4 thermocouple positions. The rig was constructed mostly of mild steel.

53. Iodine sources, (up to 1 mc $^{132}I$ was used in each test) were received from RCC, Amersham as Sodium Tellurite-132 adsorbed on alumina. Dilute ammonia solution was used to elute the iodide which was then acidified, and 20 mg Potassium Iodide-127 added. The iodide was then oxidised to iodine with potassium dichromate and extracted into carbon disulphide. This was placed in a silica ampoule (20 ml volume) and the solvent evaporated in a stream of argon at -30°C. The ampoule was then sealed with a glass blower's torch.

54. Together with a Xenon-133 source (50 mc) which was sealed in a glass ampoule, the Iodine-132 source was placed in the injection arrangement on the rig. This consisted of a stainless steel pipe with a number of holes drilled at one end to allow release of the iodine and xenon sources into the mixing chamber. The ampoules were broken by driving a stainless steel bar down the pipe. A slotted PTFE cylinder surrounded the iodine capsule to ensure that the release time was at least 20 seconds, i.e. greater than any period associated with flow conditions in the lute due to forms of chugging which are known to occur at low flows. The rate of release was noted by observing the fall of $\gamma$-radiation by a $\gamma$-probe. The injection point was situated in the mixing chamber since this was as near the lute as possible to minimise plate-out upstream of the pond, though in fact little occurred.

55. Iodine sampling points, consisting of glass tubes with stop-cocks, were provided at 1 ft deep intervals in the pond at the same level as the thermocouples; their position was staggered around the perimeter of the pond, but the inlet was normally close to one of the working thermocouples at that level.

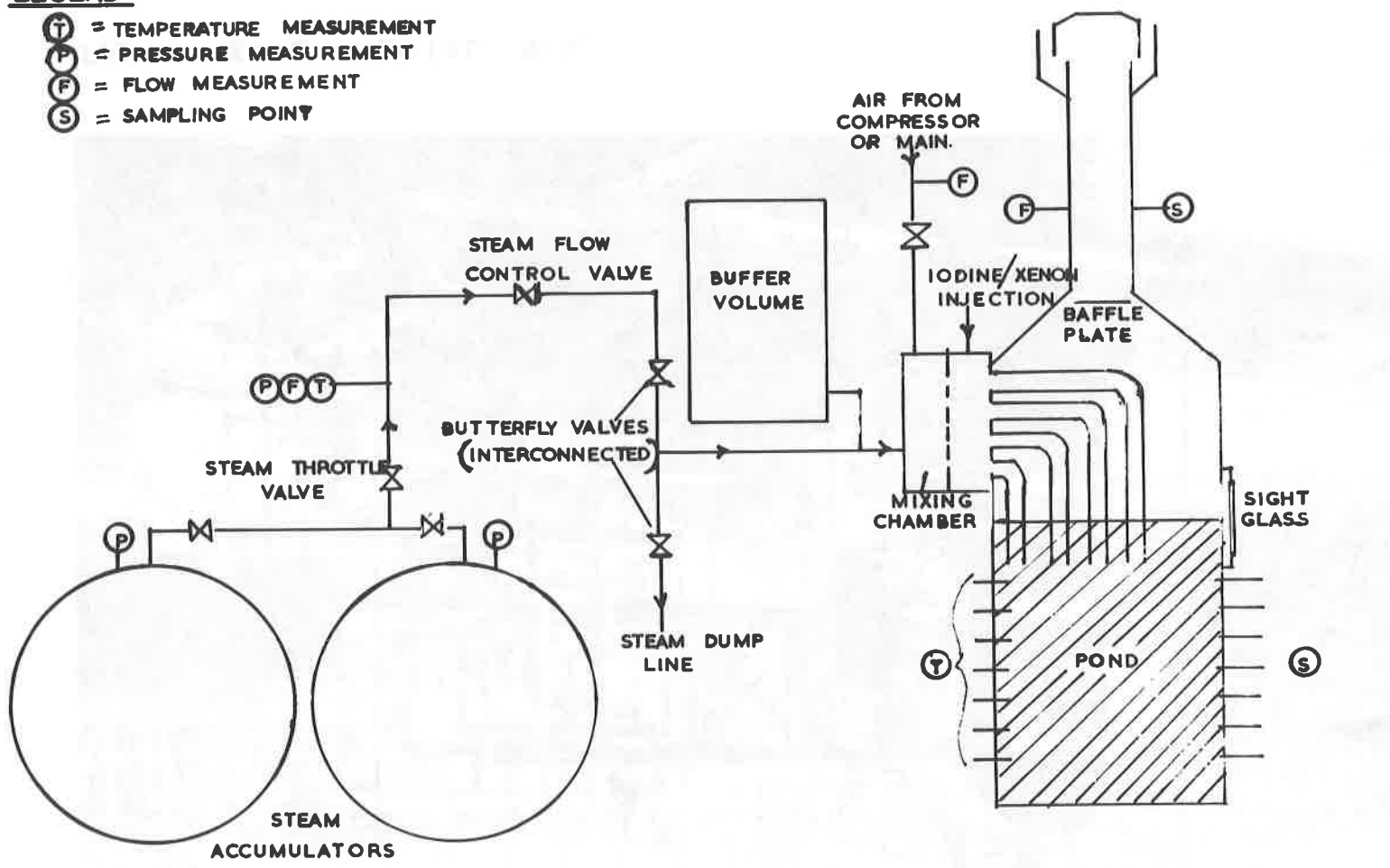


Figure 8. **SKETCH OF EXPERIMENTAL RIG.**

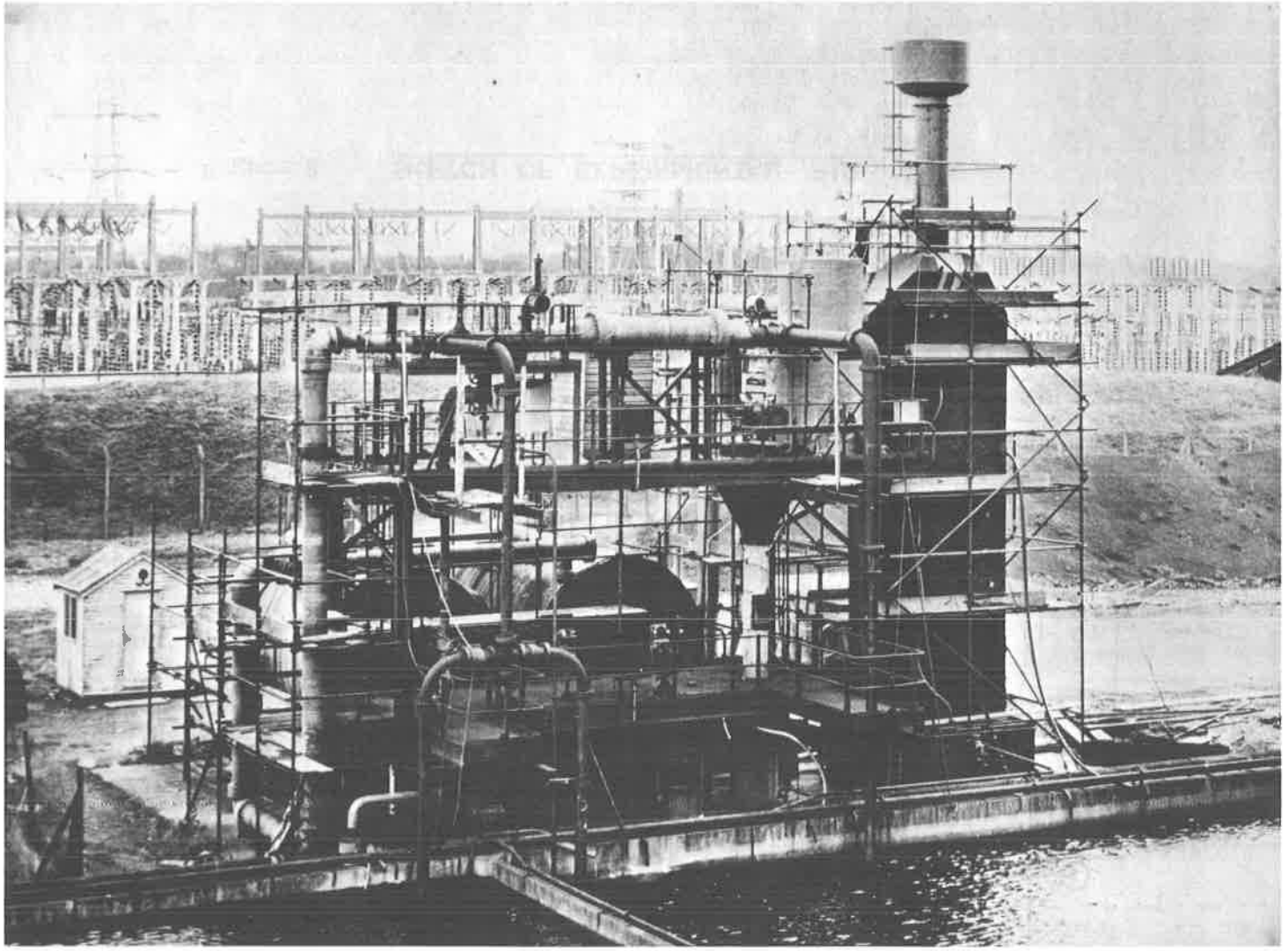

FIG. 9 EXPERIMENTAL RIG.

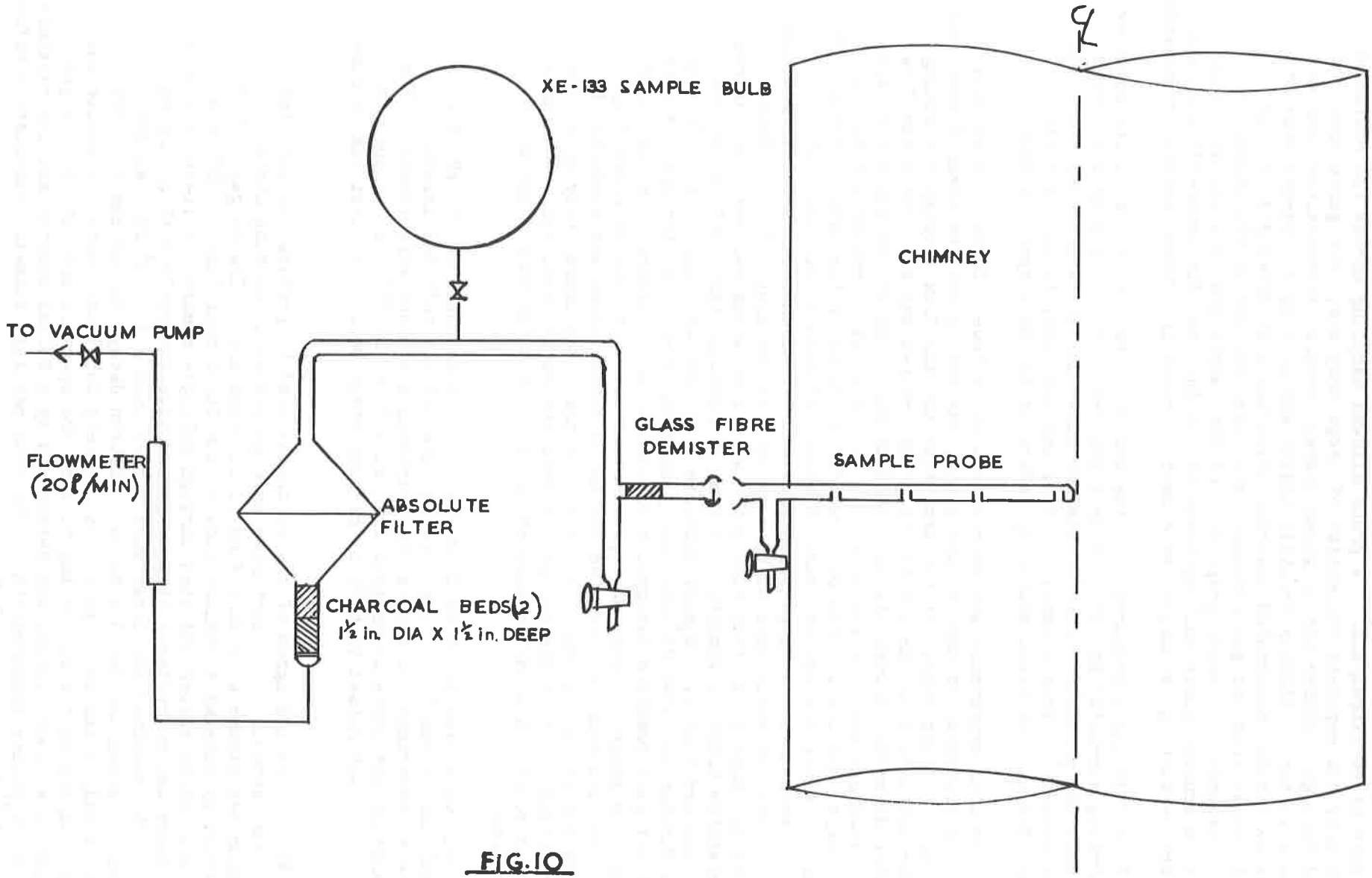


FIG.10

CHIMNEY SAMPLING APPARATUS

56. Samples of the gases flowing up the chimney were withdrawn from a point near the top of the chimney through the glass system shown in Fig. 10 at a flow rate of 20 litres/min. A probe allowed sampling across the radius of the chimney and separate collection of large droplets; the gases then flowed through a coarse mat of glass fibres (droplet disentrainer) and an absolute filter. Finally volatile iodide was held by 2 separate beds of potassium iodide impregnated charcoal which has been developed to trap methyl iodide from wet gas streams; stay time for air in the charcoals was 0.3 seconds. A small proportion of the sample gas flow was withdrawn into an evacuated glass bulb upstream of the charcoal for Xenon-133 analysis. Standard γ-counting techniques were used to count individual sampler components.

57. Xenon-133 was introduced with the iodine to show that the iodine sampling was working correctly and to provide a reference for those runs with steam only when the proportion sampled was not known due to insufficient air flow in the chimney. When chemney air flow was adequate, it was possible to account for all the xenon source by reference to the proportion sampled.

58. A typical experiment was carried out as follows: Correct steam flow, with some superheat at the orifice plate, was set up and the steam dumped into the nearby cooling pond; at the same time the air flow through the mixing chamber and lute pond was set to its predetermined value. The steam flow was then diverted through the lute pond by operation of the butterfly valves, and chimney gas sampling was started. After about 5 seconds the sources were broken, and the γ-probe observed for evidence of the rate of Iodine-132 release. After the correct mass of steam had passed into the pond (i.e. after 25 seconds for a large steam flow and 100 seconds for a small flow) the flows of air and steam were stopped as well as the sample flow. Pond samples of about 50 ml from each point were then withdrawn and a set of pond temperatures noted to compare with similar readings taken before the test. In a standard test two chimney samplers were used as duplicates. In some cases further air (540 $ft^3$/min) was passed for 15-20 min. through the pond to investigate possible desorption of iodine, and a separate sampler used during this purge. Where an experiment involved the use of steam only the normal procedure was carried out but a second stage was conducted by passing air at 250 $ft^3$/min for 2 min into the flume immediately above the water surface to displace the gas between the water level and the chimney sampling point; a separate sampler was also used for this stage of the experiment.

59. Pond water was provided from the local mains supply; the pH of a typical sample was 6.8. The pond was drained and refilled immediately before an experiment to ensure that particules of rust were absent. The temperature was normally ambient initially (i.e. 0-10°C) but in one case, Test 14, it was raised to 60°C by passing steam before the test was carried out.

60. Fig. 11 is a diagram of the equipment used to produce the labelled submicron aerosol. The particles were generated by heating nickel-chromium resistance wire in a flow of filtered air. Thoron gas (220 Rn) was added by passing a smaller flow of air first over Thorium-228 on a stainless steel sinter and then through multiple membrane filters to ensure that there was no contamination by radioactive materials with a long half-life. The combined air flows were passed into a 300 $ft^3$ PVC bag and allowed to stabilise for 1-2 hours. Thoron decays to thorium B ($^{212}Pb$) which rapidly attaches to particles, thereby labelling them. A sample was taken from the centre of the bag to find the specific activity of the gas. The particle concentration was determined by a Pollak counter and the particle size by diffusion measurements. The mean particle diameter immediately before use was found to be about 0.06 microns.

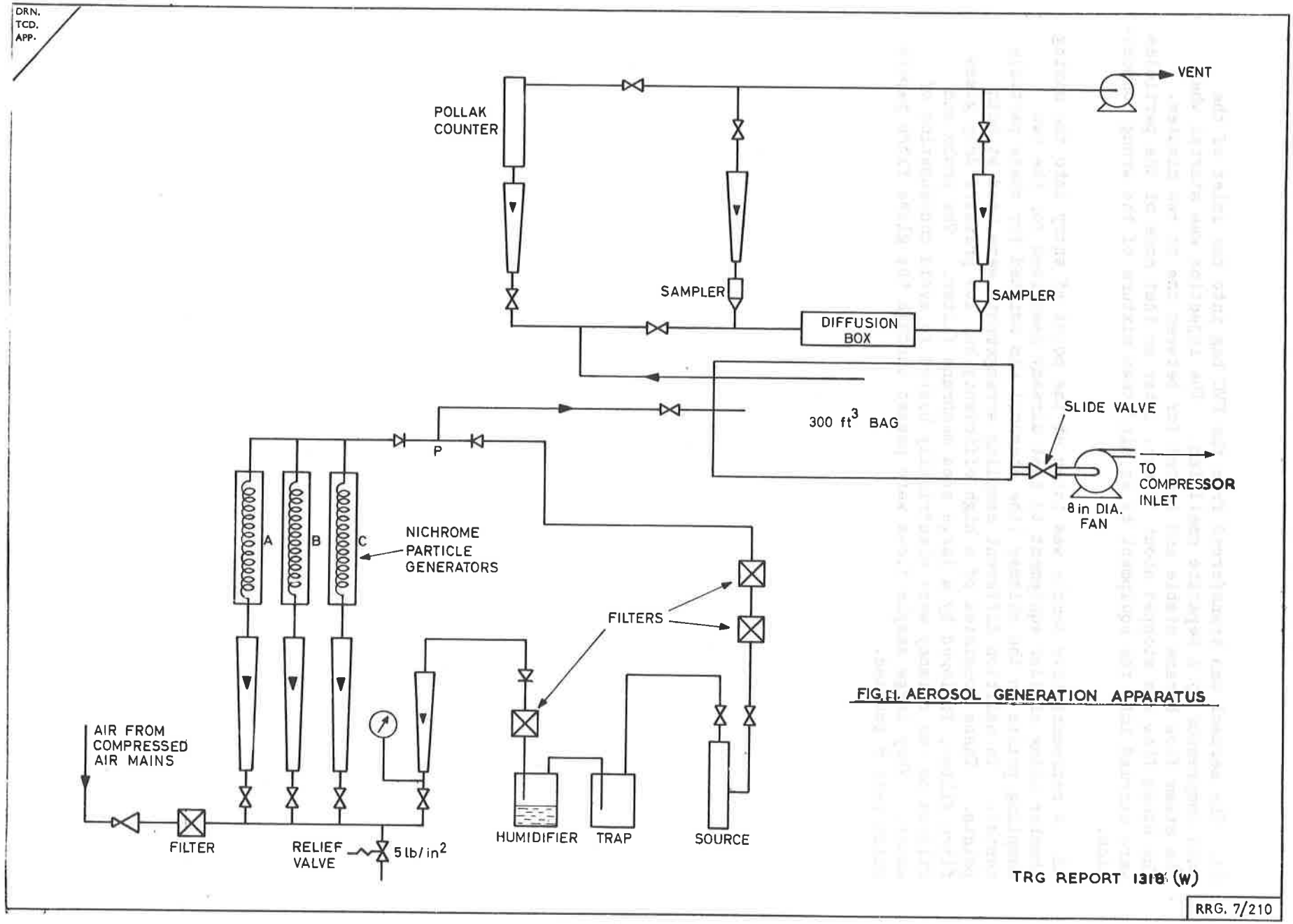


FIG.11. AEROSOL GENERATION APPARATUS

61. The aerosol was transferred from the PVC bag into the inlet of the main compressor by a separate small fan. The injection was started when the steam flow became stable and lasted for between one to two minutes. The steam flow was stopped about 15 sec. later so that none of the particles were carried into the equipment by an air/steam mixture of the wrong composition.

62. A representative sample was taken at the point of entry into the mixing chamber using similar equipment to that already described for the two sampling points in the chimney (the charcoal was omitted for these particle tests). In addition different sampling arrangements were used at both points. These consisted of a high efficiency but low pressure drop glass fibre filter, followed by a large area membrane filter. The probe and filters on the chimney were electrically heated to avoid condensation of water. Very large sample flows were passed through the glass fibre papers which were $\beta$ counted.

## DISCUSSION

PARKER (ORNL): What is the form of iodide in the last experiments in which you had a high burnup in the fuel, and you simply punctured the can? Was the experiment conducted at a time when the radiation level was high enough to have affected the possible decomposition effect that methyl iodide is susceptible to, that is, the radiation decomposition?

HILLARY: I could take the last part first. Perhaps I didn't indicate that these are out of pile experiments, of course. The cooling time of the fuel was about 1 month (1000° C tests).

The first part of the question: On one of the tables, we attempted to list the various forms in which the iodide was released. The two tests, the ones where we knew we had high fuel rating, the iodide in one case appeared to be mostly methyl iodide and in the other case mostly particulate.

# EFFECTS OF CONTAINMENT SYSTEM SIZE ON FISSION PRODUCT BEHAVIOR*

G. M. Watson, R. B. Perez,** M. H. Fontana

Reactor Chemistry Division
Oak Ridge National Laboratory
Oak Ridge, Tennessee

## ABSTRACT

Simple mathematical models to aid in the determination of effect of containment size on plate-out behavior of iodine have been postulated. Two general classes of systems have been considered depending on the absence or on the presence of steam.

In the absence of steam the principal assumptions made were: (1) homogeneous mixing; (2) boundary gas layer enveloping all surfaces; (3) diffusion through boundary layer to be the rate limiting process; (4) molecular iodine present, methyl iodide absent. Mathematical relations in terms of mass transfer coefficients, and surface-to-volume ratios of containers and surface characterization parameters were developed for cases with and without desorption from partially covered surfaces.

In the presence of condensing steam, there is bulk flow of steam toward the walls. In such cases, it has been assumed that the iodine flux which consists of diffusive and bulk flow components may be approximated by the bulk flow component alone, neglecting the diffusive component. Furthermore, it has been assumed that the solubility of iodine in steam-condensate is high enough to permit the iodine and the steam to condense together with the same composition as the gas phase. As a result of these assumptions, mathematical relations have been derived for the concentration of iodine as a function of time in terms of the surface-to-volume ratios, condensing steam fluxes, and steam concentrations.

The case of molecular iodine-methyl iodide-condensing steam has been considered. It was assumed that the deposition of methyl iodide is limited by its smaller solubility in steam condensate. The resulting mathematical expression has two exponential terms differing numerically in the time of relaxation by the magnitude of Henry's law constant for methyl iodide in water.

*Research sponsored by the U. S. Atomic Energy Commission under contract with the Union Carbide Corporation.

**Consultant, University of Florida.

A model for predicting the mass transfer coefficients using film theory and boundary layer analysis was developed for the dry cases based on rough approximations concerning the flow velocity structure within the containment shell; these flows being induced by natural convection. The model shows that observable mass transfer coefficients can be predicted if the temperature differences causing the flow are very small (0.001 °K). Both the velocities and the temperature differences are too small to be observed using current instrumentation. The model also predicts size and pressure scaling effects which appear to be substantiated by limited available data.

Some correlations of the mathematical expressions with experimental data have been performed. Results of iodine-air experiments in the CMF, CRI, and NSPP have been compared with the simple theoretical expressions with moderate success. Experimental results of the condensation of iodine and steam in NSPP, Run No. 8, have been correlated by means of the model. In this case, the agreement with the model is within 20%.

## INTRODUCTION

For many years in the Nuclear Safety Program the need to compare results on plate-out experiments performed in equipment of different size has been appreciated. The great complexity of the experiments, however, has tended to prevent the postulation of useful models for comparison between experiments or for extrapolation to large sizes, or to formulate such complicated models as to be of little use in practical situations. Accordingly, we have attempted to over-simplify our point of view in order to formulate some rather naive mathematical models that may prove useful in producing very rough predictions of the effect of containment size and other experimental variables in the plate-out behavior of iodine.

In each case, we have considered a containment vessel of volume $V_o$ ($cm^3$), and of surface S ($cm^2$). At zero time, we consider the atmosphere in the tank to be homogeneous and to contain a concentration of iodine of $C_o$ moles/$cm^3$. In the various cases treated, the object has been to calculate the concentration of iodine in the atmosphere. Many simplifying assumptions have been introduced and will be enumerated in each case considered. Some general simplifications for all cases are: (1) the assumption that the atmosphere in the tank remains homogeneous throughout the experiment and, (2) radioactive decay can be neglected. Two general classes of systems have been considered depending on the absence or presence of steam.

## I. STEAM ABSENT — AIR PRESENT

### Case 1. No desorption

Assumptions:

(1) Atmosphere consists of air (or inert gas) with a small concentration of iodine.

(2) There is a stagnant film of gas (boundary layer) adjacent to the surfaces. Film thickness = $\delta_c$ cm.[a]

(3) Diffusion across the boundary layer is the rate-limiting process.

---

[a]The evaluation of the film thickness and the mass transfer coefficient will be described in a later section.

(4) No desorption. That is, the wall is considered to be a perfect sink for iodine.

Solution:

Flux of iodine to wall

$$J(t) = - D \frac{dC}{dz} \sim D \left( \frac{C - 0}{\delta_c} \right) = k_c C \qquad (1)$$

where: $J(t)$ = flux of iodine to wall $\left( \frac{\text{moles } I_2}{\text{cm}^2 \text{ sec}} \right)$

$D$ = binary diffusion coefficient of $I_2$ in air (or gas)

$z$ = linear distance - cm

$\delta_c$ = concentration boundary layer thickness, cm

$k_c = \frac{D}{\delta_c}$, mass transfer coefficient, $\frac{\text{cm}}{\text{sec}}$

$C$ = iodine concentration, moles/cm$^3$.

By material balance:

Rate of loss of $I_2$ from atmosphere = rate of plate-out

$$- V_o \frac{dC}{dt} = S \, J(t) \text{ molecules/sec} \qquad (2)$$

$$\frac{dC}{dt} = - \left( \frac{S}{V_o} \right) k_c \, C$$

$$\text{or} \quad \frac{C}{C_o} = e^{-\left( \frac{S}{V_o} \right) k_c \, t} \qquad (3)$$

Since $D = D_o \left( \frac{P_o}{P} \right) \left( \frac{T}{T_o} \right)^{1.5}$[+], and

$$\delta_c = \delta_{c_o} \left( \frac{P_o}{P} \right)^{\frac{1}{2}} \left( \frac{T}{T_o} \right)^{a},$$

$$k_c = k_{c_o} \left( \frac{P_o}{P} \right)^{\frac{1}{2}} \left( \frac{T}{T_o} \right)^{\frac{1}{2}} \qquad (4)$$

---

[a]The evaluation of the pressure and temperature effects on the mass transfer coefficient will be discussed in a later section.

For this simple case, an exponential concentration decay is predicted. The effects of $\left(\frac{S}{V_o}\right)$, pressure, and temperature can be surmised from Eq. (4). That is, Eq. (4) may be useful in the comparison of hydrodynamically similar experiments performed in equipment of different sizes.

Case 2. Desorption with partial wall coverage

Assumptions:

Same as Case I, except for assumption (4). For this case, assumption (4) is changed as follows:

(4) Adsorbed iodine on the wall is in equilibrium with the iodine concentration in the gas phase adjacent to the wall. However only low coverage of the wall is assumed. That is, the coverage is sufficiently low as to be in the linear region of the adsorption isotherm.

So: $C_w = K\,\Theta$, where (5)

$$\Theta = \frac{\text{surface covered by iodine}}{(\text{roughness factor})\ (\text{geometric surface area})} \quad *.$$

Solution:

Net flux to wall:

$$J(t) = k_c\,[C(t) - C_w] \quad . \tag{6}$$

We may express $\Theta$, the fraction covered in terms of concentrations, as:

$$\Theta = \frac{\bar{n}s}{RS} \quad .$$

But $\bar{n} = \bar{N}\ (V_o)\ (C_o - C)$.

Hence $\Theta = \dfrac{\bar{N}\ V_o\ (C_o - C)\ s}{RS}$ ,

and $C_w = K\,\Theta = \dfrac{K\,\bar{N}\ s\ V_o\ (C_o - C)}{RS}$ .

---

*The symbols are defined in the Table of Nomenclature.

Therefore:

$$J(t) = k_c \left[ (1 + \alpha)\, C - \alpha\, C_o \right] , \quad \text{where}$$

$$\alpha = \frac{K \bar{N}\, s\, V_o}{RS} .$$

By material balance:

$$- V_o \frac{dC}{dt} = S\, J(t) = S\, k_c \left[ (1 + \alpha)\, C - \alpha\, C_o \right]$$

$$\text{or} \qquad \frac{C}{C_o} = e^{-\left(\frac{S}{V_o}\right) k_c (1 + \alpha) t} + \alpha \left( 1 - \frac{C}{C_o} \right) \qquad (7)$$

Equation (7) predicts an exponential decay which approaches an asymptote, $\left(\frac{\alpha}{1 + \alpha}\right)$ as $t \rightarrow \infty$ .

Case 3. Unimolecular reversible adsorption

Assumptions:

Same as Case 2, except that coverage of wall is not limited. That is, wall may become saturated with a monomolecular layer.

Further assume that Langmuir's adsorption isotherm is followed. That is:

$$C_w = \frac{\theta}{a\,(1 - \theta)}$$

Solution:

$$J = k_c\, (C - C_w)$$

$$\theta = \left(\frac{\bar{N}\, s\, V_o}{RS}\right) (C_o - C) = \bar{\beta} (C_o - C)$$

$$C_w = \frac{\bar{\beta}\, (C_o - C)}{a[\,1 - \bar{\beta}\, (C_o - C)\,]}$$

$$J(t) = k_c \left[ \frac{a\bar{\beta}C^2 + (a - a\bar{\beta}\, C_o + \bar{\beta})\, C - \bar{\beta}C_o}{a[1 - \bar{\beta}\,(C_o - C)]} \right]$$

$$-V_o \frac{dC}{dt} = S\, J(t) = S\, k_c \left[ \frac{a\bar{\beta}C^2 + (a - a\bar{\beta}C_o + \bar{\beta})\, C - \bar{\beta}C_o}{a[1 - \bar{\beta}\,(C_o - C)]} \right]$$

$$\int_{C_o}^{C} \frac{a[1 - \bar{\beta}\,(C_o - C)]\, dc}{a\bar{\beta}C^2 + (a - a\bar{\beta}C_o + \bar{\beta})\, C - \bar{\beta}C_o} = -\left(\frac{S}{V_o}\right) k_c\, t \quad . \qquad (8)$$

We have integrated this expression and obtained a solution which is implicit in the terms of interest and seems too unwieldy for our purposes here.

## II. STEAM PRESENT — AIR ABSENT

If the atmosphere of the tank consists of steam and a trace of iodine, and steam is condensing on the cooler walls, there will be a net flux of steam toward the walls. In such a situation the flux of iodine will consist of a diffusive component and a bulk flow component. That is:

$$J_1 = -n\, D_{12} \frac{dx}{dz} + J(t)\, x_1 . \qquad (9)$$

We will assume that the contribution of the first group, $n\, D_{12} \frac{dx}{dz}$, is negligible compared to the contribution of the second group. Hence

$$J_1 \approx J(t)\, x_1 \quad . \qquad (10)$$

Equation (10) is believed to be fairly adequate for most cases to be treated and should be a conservative one as the diffusive contribution has been neglected.

Multiplying the right-hand side of (10) by $\left(\frac{n}{n}\right)$

$$J_1 = J(t) \frac{nx_1}{n} = J(t) \frac{C}{n} \quad , \quad \text{since}$$

$nx_1 = C$, the iodine concentration.

The total gas concentration is essentially equal to the steam concentration, and the total flux J is also about equal to the steam flux. Therefore

$$J_1 \approx \frac{J_s(t)\ C(t)}{n_s(t)} \quad .$$

By material balance:

$$-V_o \frac{dc}{dt} = J_1\ S = S \frac{J_s(t)\ C(t)}{n_s(t)} \quad .$$

Integrating, we obtain:

$$\ell n \frac{C}{C_o} = - \left(\frac{S}{V_o}\right) \int_o^t \frac{J_s(t')\ dt'}{n_s(t')} \quad . \tag{11}$$

Equation (11) will be used as a basis for the solution of all the cases solved which involve condensing steam.

Case 4. Constant pressure, constant flux

Assumptions:

Total pressure in tank is kept constant by continuous injection of steam to replace steam condensed and the flux is kept constant by uniform cooling of the walls.

Solution:

$$\ell n \frac{C}{C_o} = - \left(\frac{S}{V_o}\right) \int_o^t \frac{J_s(t')\ dt'}{n_s(t')} \quad . \tag{11}$$

For this case $J_s(t')$, and $n_s(t')$ are constants equal to $J_o$ and $n_o$, respectively.

Equation (11) becomes:

$$\frac{C}{C_o} = e^{-\left(\frac{S}{V_o}\right) \frac{J_o}{n_o} t} = e^{-\left(\frac{S}{V_o}\right)\left(\frac{J_o RT}{P}\right)} \quad . \tag{12}$$

Case 5. Decaying steam pressure

Assumptions:

1. Steam is condensing on the walls at a rate of S $J_s(t)$ $\frac{\text{moles}}{\text{sec}}$ (a variable rate) during the experiment.

2. No steam is admitted into system after t = 0.

Solution:

$$\ell n \frac{C}{C_o} = - \left(\frac{S}{V_o}\right) \int_o^t \frac{J(t')\, dt'}{n(t')}$$

In this case:

$$n(t) = n_o - \left(\frac{S}{V_o}\right) \int_o^t J(t')\, dt' \quad , \tag{13}$$

and

$$\ell n \frac{C}{C_o} = - \left(\frac{S}{V_o}\right) \int_o^t \frac{J(t')\, dt'}{n_o - \left(\frac{S}{V_o}\right) \int_o^{t'} J(t'')\, dt''} \quad . \tag{14}$$

If, in the experiment, the condensate is collected as a function of time, Eq. (14) can be solved numerically.

Case 6. Postulated model for steam flux.

Assumptions:

1. Same as Case 5, except that a model for $J_s(t)$ is postulated as follows:

$$J_s(t) = k_s \left[n_s(t) - n_w\right] \quad . \tag{15}$$

Solution:

$$\ell n \frac{C}{C_o} = - \left(\frac{S}{V_o}\right) \int_o^t \frac{J_s(t')\, dt'}{n_s(t')}$$

Substituting Eq. (15) for J(t′) in Eq. (11) we obtain:

$$\ell n \frac{C}{C_o} = - \left(\frac{S\, k_s}{V_o}\right) \int_o^t \frac{[n_s(t') - n_w]}{n_s(t')}\, dt' \quad . \tag{16}$$

Let $\tau = \dfrac{V_o}{S\, k_s}$ seconds, the relaxation time of the system.

By material balance on the steam we can show that:

$$n(t) = n_w + (n_o - n_w)\, e^{-t/\tau} \quad . \tag{17}$$

Substituting (17) in (16) and integrating we get:

$$\frac{C}{C_o} = \frac{n_w}{n_o} + \left(1 - \frac{n_w}{n_o}\right) e^{-t/\tau} \quad . \tag{18}$$

Equation (18) predicts that the reduced concentration of iodine is identical to the reduced concentration of steam, from Eq. (17).

$$\frac{n_s(t)}{n_o} = \frac{n_w}{n_o} + \left(1 - \frac{n_w}{n_o}\right) e^{-t/\tau} \quad . \tag{19}$$

This is in accordance with our previous postulate that

$$\frac{C(t)}{n(t)} = \frac{C_o}{n_o} \quad .$$

Case 7. Iodine - Methyl Iodide - Condensing Steam

Assumptions:

1. Iodine solubility in water is high enough so that the composition of the condensed mixture is the same as the gas phase.

2. Methyl iodide is considerably less soluble than iodine. It is assumed to follow Henry's law:

$$C_g = \Omega\, x_2 \quad . \tag{20}$$

3. Rate of condensation of MeI = (flux to wall)

$$\text{(ratio condensed)} = \left(J_s \frac{C_g}{n_s}\right)\left(\frac{x}{C_g}\right) = \frac{J_s}{n_s}\ \frac{C_g}{\Omega} \quad . \tag{21}$$

Solution:

$$\ell n \left(\frac{C}{C_o}\right)_{MeI} = \left[\frac{n_w}{n_o} + \left(1 - \frac{n_w}{n_o}\right) e^{-t/\tau}\right]^{\frac{1}{\Omega}} \tag{22}$$

If $\eta$ is fraction of iodine atoms in form of $CH_3I$ and $1-\eta$ is the fraction of atoms as molecular iodine, then

$$\left(\frac{A}{A_o}\right) = \left(1-\eta\right)\left[\left(\frac{n_w}{n_o}\right) + \left(1 - \frac{n_w}{n_o}\right) e^{-t/\tau}\right] + \eta \left[\frac{n_w}{n_o} + \left(1 - \frac{n_w}{n_o}\right) e^{-t/\tau}\right]^{\frac{1}{\Omega}} \tag{23}$$

Equation (23) has two exponentials which correspond to the condensation rates of iodine and of methyl iodide. The time of relaxation of the exponentials differs by the numerical magnitude of Henry's law constant for $CH_3I$.

## III. IODINE – AIR – CONDENSING STEAM

In the case of the iodine-steam systems, with air absent, the transport equation which served as basis for our treatment is Eq. (9):

$$J_1 = - n D_{12} \frac{dx_1}{dz} + J x_1 \ .$$

The significance of each term is clear in this case. For the diffusive component we use binary diffusion coefficients which are, to a good approximation, independent of composition. For the ternary gas mixture of air (considered as one component), steam and iodine the situation becomes considerably more ambiguous. We might be tempted to rewrite Eq. (9) as:

$$J_1 = - n D_T \frac{d\bar{x}_1}{dz} + J \bar{x}_1 \quad ,$$

where $D_T$ is now a ternary diffusion coefficient, which takes into account the retarding effects of the iodine-air and iodine-steam collisions, and $\bar{x}_1$ is the iodine mole fraction in the total mixture. Since in the systems we are considering, air has no bulk flux, J would be the net flux of iodine and steam. Since iodine is in trace amounts we might argue with justification that J can be approximated, as previously, by $J_s$, the steam flux. Since we will neglect the diffusive component of the steam flux, we may not be troubled excessively by the knowledge that ternary diffusion coefficients are cumbersome to calculate and have a strong composition dependence. We may argue that

$$J_1 \simeq J_s \bar{x}_1 = \frac{J_s(t)\ C(t)}{n_a + n(t) + 0} \quad . \tag{24}$$

In the systems we are considering, the air concentration remains constant and if Eq. (24) is correct, the counterpart of Eq. (14), becomes:

$$\ell n \frac{C}{C_o} = - \left(\frac{S}{V_o}\right) \int_o^t \frac{J(t')\ dt'}{n_o + n_a - \left(\frac{S}{V_o}\right) \int_o^{t'} J(t'')\ dt''} \tag{25}$$

The counterpart of Eq. (19) becomes:

$$\frac{C}{C_o} = \left(\frac{n_a + n_w}{n_a + n_o}\right) + \left(1 - \frac{n_w}{n_o}\right) e^{-t/\tau} \quad . \tag{26}$$

At first sight, Eq. (25) and Eq. (26) appear reasonable. However, serious doubts as to their validity arise as we consider that they no longer conform to our basic assumption, that the reduced concentration of iodine and steam should be identical. Furthermore, the asymptote of Eq. (26) is a function of air pressure, which is not very reasonable.

The above considerations have influenced our opinion to the extent that as of today we are inclined to assume, with reservation, that the form of the mathematical equations for air-steam-iodine systems are identical with the corresponding equations of the steam-iodine systems. We feel that air has simply a retarding effect on the processes.

## IV. ESTIMATION OF MASS TRANSFER COEFFICIENTS IN DRY ATMOSPHERES

### 1. Experimental Determination of Mass Transfer Coefficients

Evaluating the equation before Eq. (8) at t = 0, when C = $C_o$, we obtain

$$\left(\frac{dc}{dt}\right)_{t=0} + \frac{D}{\delta_c}\frac{S}{V_o} C_o = 0 \quad .$$

Substituting $k_c = \frac{D}{\delta_c}$ and solving for $k_c$ ,

$$k_c = \frac{V_o}{S}\left[-\left(\frac{d\left(\frac{C}{C_o}\right)}{dt}\right)_{t=0}\right] \quad . \tag{27}$$

We estimate the mass transfer coefficient by using Eq. (27) on experimental data at early times during the experiments.

For the dry cases, the data from the Nuclear Safety Pilot Plant, the Containment Mockup Facility, and the Containment Research Installation are used. Only one run in the CMF has been done in air. The one run in the CRI is also an air run. We will use these data to estimate size effects, but replication is needed to establish confidence. Table 1 shows the dry CMF and CRI results,[1] with the mass transfer coefficient corrected to one atmosphere for comparison. This pressure correction is derived using a model which will be described later. Twenty concentration-time histories obtained in Runs 1-7 in the NSPP[2] by means of paper tape samplers and May packs were evaluated to obtain the mass transfer coefficients.

The NSPP data is scattered, partly due to the unreliability of the paper tape samplers, which have since been replaced, and partly due to natural scatter.

The general time behavior of the concentration in the vessel at various positions indicates that immediately after the iodine injection, while the mixing fan operated, the concentration at a given position showed either a rise, or general scatter. After the fan was shut off, the concentration began to drop as time progressed, and in some cases showed approach to a run-zero asymptote as predicted by this model. This behavior is illustrated by a typical case shown in Fig. 3. In order to evaluate the mass

Table 1. Mass Transfer Coefficients Estimated From CMF and CRI Data in Dry Air[1]

| Facility | Experiment | Conditions | S/V (1/cm) | Pressure Atm. | Observed Mass Transfer Coefficient (cm/sec) | Mass Transfer Coefficient Corrected to One Atmosphere (cm/sec) |
|---|---|---|---|---|---|---|
| CMF | 6-11-64 | $^{131}I$ + carrier I | 0.113 | 2 | $3.0 \times 10^{-3}$ | $4.25 \times 10^{-3}$ |
| CRI | 100 | " | 0.029 | 2 | $3.5 \times 10^{-3}$ | $4.96 \times 10^{-3}$ |

transfer coefficient, a line is drawn tangent to the estimated curve at the time at which maximum concentration is reached, generally shortly after the fan shut-off. (This assumes very small wall surface coverage at this time.) The pertinent conditions and the results are shown in Table 2.

## 2. A Model for Predicting the Mass Transfer Coefficient in a Containment Vessel

We devised a very approximate model of flow patterns from which to predict the mass transfer coefficients, and here show that the values predicted by the model fall within the range of observed values.

The fundamental assumptions on which the model is based are as follows:

1. The mass transfer coefficients can be predicted by film theory, the thickness of the film being determined by the flow structure.

2. The flow is caused primarily by buoyant effects due to very small temperature differences between the bulk of the air in the containment vessel and the vessel walls.

3. The concentration of iodine in the air is so small that we may assume that the buoyancy effects due to concentration differences are negligible compared to those due to temperature differences.

4. Due to the small iodine concentrations the mass flux near the walls is small.

The above assumptions are all reasonable, and could be the foundation for a sound theoretical treatment of the problem. However, to obtain some rough estimates without solving the flow problem exactly, some further assumptions are made. These assumptions cannot be defended on a sound theoretical basis, but are used in the hope that a first order approximation to the problem can be obtained.

5. The velocity structure of the flow near the wall can be approximated by the solution of the problem of an infinite vertical wall in infinite stagnant air of different temperature.

6. Since the containment vessel is not infinite, flow patterns will be set up as shown in Fig. 1. As the

Table 2. Mass Transfer Coefficients Estimated from NSPP Runs 1-7[a]

| Run | Melt Conditions | Sampler Position[b] | Half-Life (hr) | Fan Oper. Time | Time at which Slope is taken | Type[c] of Sampler | Mass Transfer Coefficient, (cm/sec) |
|---|---|---|---|---|---|---|---|
| 3 | $UO_2$ 304 L-SS clad, NaI | A-SW-60 | 8 | 0 | 5 hr | PTS | $1.415 \times 10^{-3}$ |
| 3 | " | B-SW-60 | 2.8 | 0 | 2+ hr | PTS | $4.05 \times 10^{-3}$ |
| 4 | Pyrex $I_2$ | B-SW-60 | 5.8 | 17 min. | 2+ hr | PTS | $1.96 \times 10^{-3}$ |
| 4 | " | B-N-20 | 9.5 | 17 min | 2+ hr | M | $1.19 \times 10^{-3}$ |
| 5 | Pyrex $I_2$ | A-NE-60 | 1 | 2.5 hr | ~0 | PTS | $11.3 \times 10^{-3}$ |
| 5 | " | C-NE-60 | 8 | 2.5 hr | 2.5 hr | PTS | $1.41 \times 10^{-3}$ |
| 5 | " | C-SW-60 | 10 | 2.5 hr | 2.5 hr | PTS | $1.13 \times 10^{-3}$ |
| 5 | " | B-N-70 | 8 | 2.5 hr | 2.5 hr | M | $1.42 \times 10^{-3}$ |
| 5 | " | C-N-20 | 11.3 | 2.5 hr | 2.5 hr | M | $0.983 \times 10^{-3}$ |
| 6 | Pyrex, $I_2$; no plasma torch operation | B-NE-60 | 2 | 5 min | 1.5 hr | PTS | $5.6 \times 10^{-3}$ |
| 6 | " | B-SW-60 | 5 | 5 min | 1.5 hr | PTS | $2.26 \times 10^{-3}$ |
| 6 | " | C-NE-60 | 6 | 5 min | 45 min | PTS | $1.88 \times 10^{-3}$ |
| 6 | " | C-SW-60 | 4.4 | 5 min | 16 hr[e] | PTS | $2.58 \times 10^{-3}$ |
| 6 | " | B-N-20 | 2.3 | 5 min | 0 | M | $4.9 \times 10^{-3}$ |
| 6 | " | C-N-20 | 4.4 | 5 min | 2 hr[f] | M | $2.56 \times 10^{-3}$ |
| 7 | $UO_2$-304L-SS-NaI | A-SW-60 | 10 | 5 min | 30 min | PTS | $1.13 \times 10^{-3}$ |
| 7 | " | A-NE-60 | 6 | 5 min | 2 hr | PTS | $1.88 \times 10^{-3}$ |
| 7 | " | C-NE-60 | 6 | 5 min | 2 hr | PTS | $1.88 \times 10^{-3}$ |
| 7 | " | C-SW-60 | 2.25 | 5 min | 0 | PTS | $5.01 \times 10^{-3}$ |
| 7 | " | B-N-20 | 20 | 5 min | 2 hr | M | $0.565 \times 10^{-3}$ |

Mean $k_c = \bar{k}_c = 2.75 \times 10^{-3}$ $\quad s^2 = 616 \times 10^{-6}$ $\quad \sigma = (s^2)^{\frac{1}{2}} = 2.46 \times 10^{-3}$

a. $T = 30^{\circ}C$, $\Delta\Theta_{max} = 0$ to $1^{\circ}C$, $S/V = 0.017$ 1/cm.

b. Sampler nomenclature, X-YZ-W
X = A,B,C, = vertical levels, A = high, B = middle, C = low.
YZ = azimuthal position, N = North, etc.
W = radius in inches.

c. Type of sampler, M = May pack, PTS ± paper tape sampler.

d. In run 6, the iodine was heated by use of hot water in the furnace cooling jacket. No water was in physical contact with the iodine.

e. There was bad scatter prior to this time.

f. There was bad scatter in this curve. The value given here is a guess.

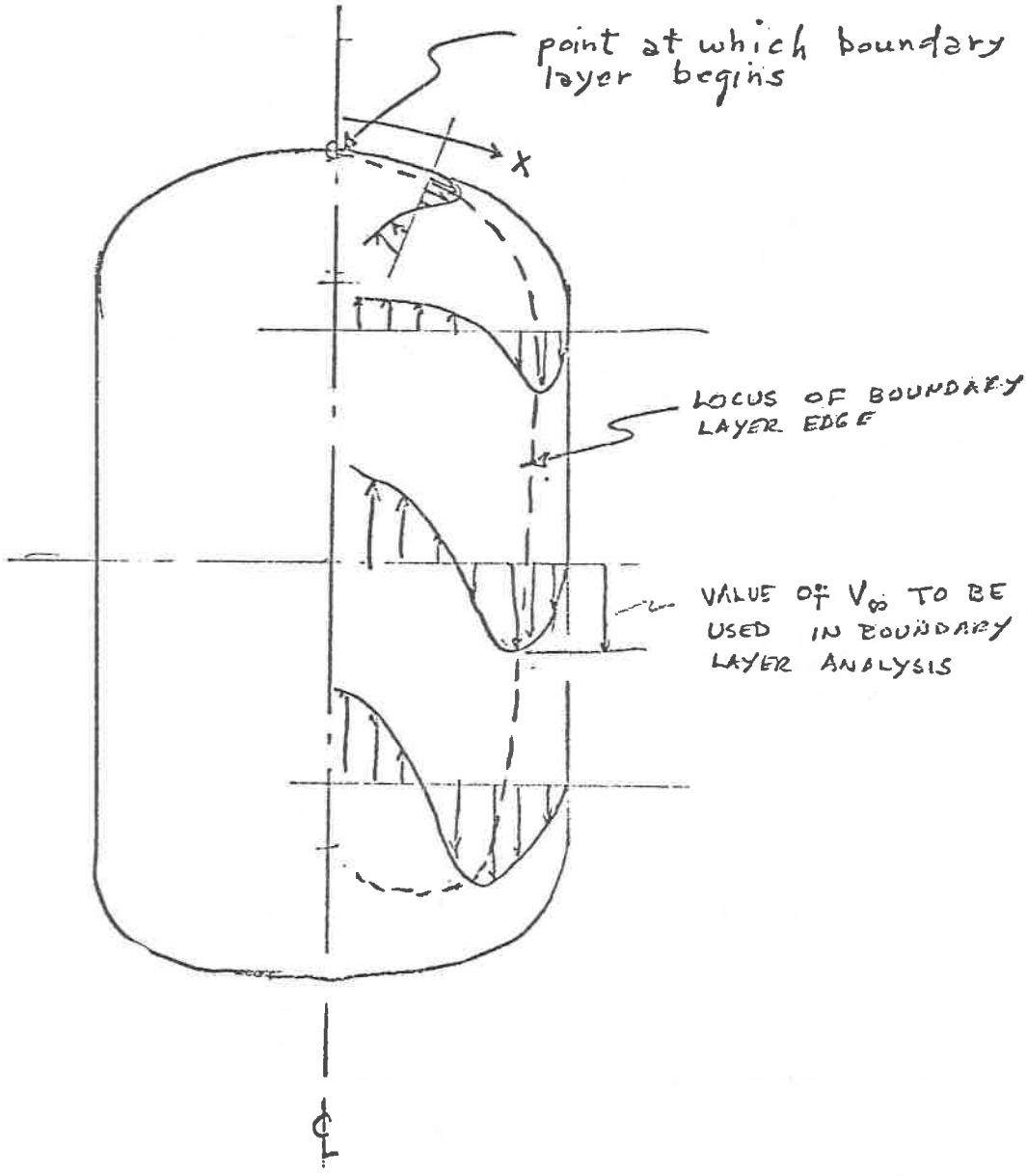


Fig. 1. Assumed Velocity Distribution in Cylindrical Containment Vessel. No central heat source, contained air cooled by wall.

flow in the center of the vessel reaches the top of the vessel and turns, a boundary layer is started. We assume that as far as the wall is concerned, the flow near it is similar to that obtained by a boundary layer analysis where the velocity distant from the plate, $v_\infty$, is taken as the maximum velocity obtained from the free convection analysis of Assumption 5. This depends on the distance, x, travelled along the plate.

7. Since the effect of other assumptions probably override this one and nothing is to be gained by a too sophisticated analysis, we use a boundary layer analysis using the Von Karman integral technique and linear velocity and concentration gradients in the boundary layer.

In the problems of interest to us, i.e., the explanation of NSPP, CMF, and CRI results, no heat source exists within the containment vessel. The temperature differences are caused by the walls of the tank cooling the enclosed air by a small amount. The enclosed air is heated slightly above ambient by the warm air carrying the radioiodine into the vessel.

The solution for the problem of finding velocity distributions in the air near a heated or cooled flat plate has been solved by Schmidt and Beckman[3] and described by Jacob.[4] There is no need to restate the solution; the results are given in Fig. 2, in terms of the dimensionless velocity,

$$\zeta' = \frac{v_x}{4\nu b^2\sqrt{x}} \tag{28}$$

and dimensionless distance from the wall,

$$\xi = \frac{by}{x^{\frac{1}{4}}} \quad . \tag{29}$$

The term b is defined as

$$b = \left(\frac{g\Theta_s}{4\nu^2 T_e}\right)^{\frac{1}{4}} \tag{30}$$

We can see from Fig. 2 that the maximum value of $\zeta' = 2.8$ at a value of $\xi = 1$. This value will be used to determine $v_\infty$ needed for the boundary layer analysis.

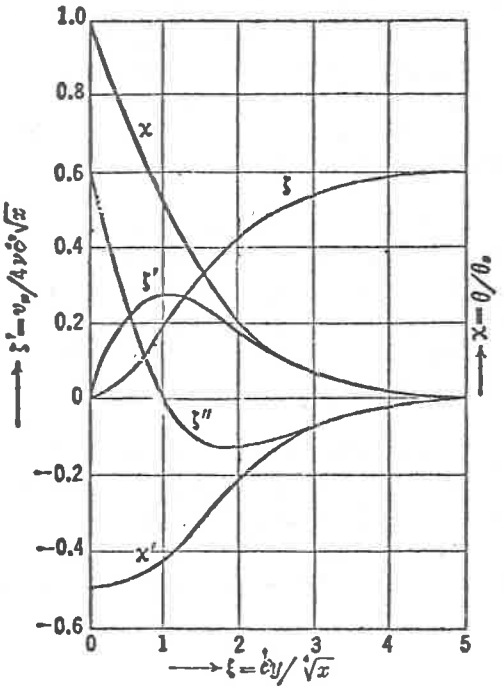


Fig. 2. Dimensionless Representation of the Velocity Field $\xi'$ and Temperatu Field $\chi$ for Air in Free Convection on a Vertical Plate. (11)

Bird, Stewart, and Lightfoot[5] show that for low mass transfer rates, with no chemical reaction, and where the concentration boundary layer $\delta_c$ is amaller than the momentum boundary layer, $\delta_m$, the ratio of the two can be given by:

$$\Delta = \frac{\delta_c}{\delta_m} = N_{Sc}^{-1/3} \quad . \tag{31}$$

Also, with low rates of mass transfer and linear concentration and velocity profiles, the momentum boundary layer thickness can be shown to be:[6]

$$\delta_m(x) = \sqrt{12} \sqrt{\frac{\nu x}{v_\infty}} \quad . \tag{32}$$

We wish to derive an expression for the mass transfer coefficient, $k_c$, which from film theory can be given as

$$k_c = \frac{D}{\delta_c} \quad . \tag{33}$$

We substitute an analytical expression for $\delta_c$ and obtain

$$k_c = \frac{D \sqrt{v_\infty}}{\Delta \sqrt{12 \nu x}} \quad . \tag{34}$$

Since $v_\infty = (0.28)(4) \quad \nu b^2 (x)^{\frac{1}{2}}$ and further substituting the expression for $b^2$, we obtain

$$k_c = \frac{D \, N_{Sc}^{1/3}}{X^{\frac{1}{4}}} \left(\frac{\Theta_s}{T_e}\right)^{\frac{1}{4}} \frac{g^{\frac{1}{4}}}{\nu^{\frac{1}{4}}} \quad (.152) \quad . \tag{35}$$

We are interested in the average value of $k_c$, which is

$$k_c = \int_o^L \frac{k_{c,\,local} \, dx}{L} \quad , \tag{36}$$

yielding

$$k_c = \frac{4}{3} \, (.152) \, \frac{D}{L^{\frac{1}{4}}} \, \frac{N_{Sc}^{1/3}}{\nu^{\frac{1}{2}}} \left(\frac{\Theta_s}{T_e}\right)^{\frac{1}{4}} g^{\frac{1}{4}} \tag{37}$$

Alternatively, substituting for the Schmidt number,

$$k_c = \frac{4}{3}\,(.153)\,\frac{D^{2/3}}{L^{\frac{1}{4}}\,\nu^{\frac{1}{6}}}\left(\frac{\Theta_s}{T_e}\right)^{\frac{1}{4}} g^{\frac{1}{4}} \quad . \tag{38}$$

We see from Eq. (38) that the mass transfer coefficient can be computed without the need for a free constant. However, we shall see that the dependence on the temperature difference, $\Theta_s$, is such that practically immeasurable temperature differences will give the observed mass transfer coefficients.

Substituting values for air at 30°C, and the diffusion coefficient for iodine vapor ($I_2$) in air into Eq. (38) we obtain

$$k_c = .0687\,\frac{\Theta_s^{\frac{1}{4}}}{L^{\frac{1}{4}}} \quad , \tag{39}$$

where $\Theta_s$ must be in °K and L in centimeters, measured from the top of the vessel, along the wall, to the bottom.

## 3. Empirical Estimation of the Mass Transfer Coefficient

Empirical heat transfer correlations for free convection at a short vertical plate in infinite stagnant air are given by McAdams.[7]

For values of $10^9 < N_{Gr}\cdot N_{Kr} < 10^{12}$, the turbulent range of natural convection, the heat transfer Nusselt number is given by

$$\frac{h_c L}{k_f} = 0.13\left[N_{Gr}\cdot N_{Pr}\right]^{1/3} \quad . \tag{40}$$

In the laminar range, $10^4 < N_{Gr}\cdot N_{Kr} < 10^9$, the heat transfer Nusselt number is given by

$$\frac{h_c L}{k_f} = 0.59\left[N_{Gr}\cdot N_{Pr}\right]^{\frac{1}{4}} \quad . \tag{41}$$

We will assume that the concentration of iodine in dry air is so small that mass transfer fluxes are small and concentration gradients are negligible in causing natural convection. Therefore,

in employing the heat-mass transfer analogy, we will continue to use the thermal Grashoff number. Also, since the hydrodynamic forces causing the flow are caused by thermal effects, we will continue to use the $N_{Gr} \cdot N_{Pr}$ modulus to estimate the existence of laminar or turbulent flow.

An indication of the conditions required to induce turbulence in free convection of air from a vertical plate is given in Table 3. Comparison of Table 3 with Table 4, in which temperature differences of 0.001 to 0.002°K may be responsible for the flows giving observed mass transfer coefficients, shows that the flow could well be laminar for all cases. However, the possibility exists that the flow may be completely laminar in the smaller CRI and CMF whereas it may be in transition in the NSPP.

Applying the heat-mass transfer analogy to Eqs. (40 and 41) by replacing the Prandtl number, $N_{Pr}$, by the Schmidt number, $N_{Sc}$, and the Nusselt number for heat transfer, hL/k, by the Nusselt number for mass transfer, $k_c$ L/D, we obtain for turbulent flow:

$$\frac{K_c L}{D} = 0.13 \left[ \frac{L^3 \ \Theta_s \ \rho^2 \ g \ \beta}{\mu^2} \left( \frac{\mu}{\rho D} \right) \right]^{1/3} \tag{42}$$

and for laminar flow

$$\frac{k_c L}{D} = 0.59 \left[ \frac{L^3 \ \Theta_s \ \rho^2 \ g \ \beta}{\mu^2} \left( \frac{\mu}{\rho D} \right) \right]^{1/4} \tag{43}$$

Introducing the values for air and $I_2$ we obtain for turbulent flow (noticing that the L cancels out)

$$k_c = .062 \ \Theta_s^{1/3} \ \text{cm/sec}; \tag{44}$$

for laminar flow

$$k_c = .19 \ \frac{\Theta_s^{\frac{1}{4}}}{L^{\frac{1}{4}}} \ , \tag{45}$$

where $\Theta_s$ is in °K and L in centimeters. Notice that Eq. (45) yields a value of $h_c$ about three times that of Eq. (39) which represents a slightly more realistic model. Both show the same relationship with temperature difference and length.

Table 3. Minimum Differences Required to Induce Turbulent Flow in Free Convection of Air from A Vertical Plate as a Function of Height

| Height | $\theta_s$ (min) ($^{o}$K) |
|---|---|
| 3 | 17 |
| 5 | 3.67 |
| 10 | 0.456 |
| 20 | 0.057 |

## 4. The Effect of Size, Pressure, and Temperature on the Mass Transfer Coefficient

For the purpose of this discussion, we shall use the empirical expression for free convection near a flat plate to approximate the turbulent condition, and the model developed in this paper and summarized by Eq. (38) for the laminar condition.

### a. Effects of Size

For the turbulent case, Eq. (42) shows that $k_c$ should be independent of size. For the laminar case,

$$k_c = f\left(L^{-\frac{1}{4}}\right) \tag{46}$$

### b. Effect of Pressure

The diffusion coefficient, D, is inversely proportional to pressure[8]; the kinematic viscosity $\nu$, being $\mu/\rho$, is inversely proportional to pressure since $\mu$ is fairly insensitive to pressure[9] in the pressure range of interest to us. Substituting these relationships into the model as expressed in Eq. (38) yields

$$k_c = f\left(\frac{1}{p^{\frac{1}{2}}}\right) . \tag{47}$$

The empirical expressions for turbulent flow (Eq. 18) yields

$$k_c = f\left(\frac{1}{p^{1/3}}\right) . \tag{48}$$

For laminar flow

$$k_c = f\left(\frac{1}{p^{\frac{1}{2}}}\right) . \tag{49}$$

We shall see in Section V, the predicted combined effect of pressure and size scaling agrees exactly with theory in scaling from NSPP data to CMF data, but is off when compared to CRI data.

### c. Effect of Temperature Difference

The effect of temperature difference is given for our model and for the laminar empirical case by

$$k_c = f\left(\Theta_s^{\frac{1}{4}}\right) \tag{50}$$

for the turbulent case,

$$k_c = f\left(\theta_s^{1/3}\right) \quad . \tag{51}$$

The effect will be very difficult to check experimentally for the case of interest to us because of the minute temperature differences involved.

d. Effect of Temperature

We see that in the pressures and temperatures of interest to us,[10]

$$D = f\left(T^{3/2}\right) \quad , \tag{52}$$

$$\rho = f\left(\frac{1}{T}\right) \quad , \tag{53}$$

and $$\mu = f\left(T^{\frac{1}{2}}\right) \quad . \tag{54}$$

Using these relations in our model, for constant temperature differences, we obtain

$$k_c = f\left(T^{\frac{1}{2}}\right) \quad . \tag{55}$$

The empirical relations for turbulent flow give, remembering that $\beta = (1/T)$:

$$k_c = f\left(T^{1/6}\right) \quad . \tag{56}$$

For laminar flow

$$k_c = f\left(T^{\frac{1}{2}}\right) \quad . \tag{57}$$

There is no experimental data available at this time that can be used to check the effect of absolute temperature.

## V. TESTS OF THE MODELS

For the dry case, the model has been tested by correlation of experimental data obtained in three containment systems of different sizes and $\left(\frac{S}{V_o}\right)$ ratios. The scaling of the mass-transfer coefficients with size and pressure was attempted by using the data from one facility to predict the observed behavior on the other two. The surface chemistry effects were assumed equal in all three systems and the behavior predicted by our model was compared with experiment.

For the dry cases, there were seven NSPP experiments, but only one CRI and one CMF experiment. Obviously additional replication is needed to improve confidence in the data as well as in the method of comparison.

### 1. Effect of Temperature Difference on the Mass Transfer Coefficient.

Table 4 shows the very small temperature differences required to yield the observed $k_c$ values in the NSPP, CMF, and CRI, and the effect of varying the temperature difference. Also the values of $v_\infty$ are given.

Temperature differences observed in the NSPP are on the order of less than 0.5 °K; within the error ranges of the thermocouples. Table 4 shows the essentially unobservable temperatures could be causing unobservable flow patterns yielding the observed mass transfer coefficients. Flow velocity measurements were attempted in the NSPP with an ALNOR hot wire probe, sensitive to 10 ft/min. No flow was observed. Velocities of the magnitude predicted by the model could not have been seen. We should point out that although the model assumes symmetrical flow, the case of assymmetric flow is very likely due to very small temperature gradients across the vessel, which was uninsulated during these runs.

### 2. Effect of Pressure and Size on the Mass Transfer Coefficient.

Comparing the observed $k_c$ for the NSPP and CMF, corrected to one atmosphere pressure by Eq. (47) we see that

$$\frac{k_{CMF,(1\ atm)}}{k_{NSPP}} = \frac{4.25 \times 10^{-3}}{2.75 \times 10^{-3}} = 1.54 \qquad (58)$$

Table 4. Effect of Temperature Difference on Average Mass Transfer Coefficient and Maximum Velocity at Midplane in NSPP, CMF, and CRI as Predicted by the Model

| $\theta_s$ (°K) | NSPP ($k_{c,obs} = 2.75 \times 10^{-3}$) | | CRI ($k_{c,obs} = 4.96 \times 10^{-3}$)* | | CMF ($k_{c,obs} = 4.25 \times 10^{-3}$)** | |
|---|---|---|---|---|---|---|
| | $k_c$ (cm/sec) | $v_\infty$ (ft/min) | $k_c$ (cm/sec) | $v_\infty$ (ft/min) | $k_c$ (cm/sec) | $v_\infty$ (ft/min) |
| 0.0005 | $1.02 \times 10^{-3}$ | 1.89 | $2.55 \times 10^{-3}$ | 1.07 | $2.99 \times 10^{-3}$ | 0.785 |
| 0.001 | $2.28 \times 10^{-3}$ | 2.24 | $3.03 \times 10^{-3}$ | 1.28 | $3.56 \times 10^{-3}$ | 0.933 |
| 0.002 | $2.73 \times 10^{-3}$ | 2.69 | $3.62 \times 10^{-3}$ | 1.53 | $4.26 \times 10^{-3}$ | 1.12 |
| 0.02 | $4.85 \times 10^{-3}$ | 4.77 | $6.43 \times 10^{-3}$ | 2.72 | $7.56 \times 10^{-3}$ | 1.98 |
| 0.2 | $8.62 \times 10^{-3}$ | 8.49 | $11.42 \times 10^{-3}$ | 4.83 | $13.43 \times 10^{-3}$ | 3.52 |
| 0.5 | $10.85 \times 10^{-3}$ | 10.67 | $14.38 \times 10^{-3}$ | 6.09 | $16.90 \times 10^{-3}$ | 4.43 |
| 1.0 | $12.90 \times 10^{-3}$ | 12.67 | $17.10 \times 10^{-3}$ | 7.24 | $20.1 \times 10^{-3}$ | 5.27 |

* One data point only, corrected to 1 atm pressure.

** One atmosphere value.

We can use this ratio to determine an empirical size behavior for these two tanks,

$$\frac{k_{CMF}}{k_{NSPP}} = \left(\frac{L_{NSPP}}{L_{CMF}}\right)^n \quad . \tag{59}$$

Numerically this is $1.54 = \left(\frac{26}{4.5}\right)^n$ ,

yielding n = 0.246.

This is almost exactly the value of 0.25 predicted by our model. Since this is based on only one run for the CMF, the agreement must at this time be termed fortuitous.

Scaling the CRI similarly, and again using the NSPP data as a reference base because of the larger number of data points available for it, we obtain:

$$\frac{4.96 \times 10^{-3}}{2.75 \times 10^{-3}} = \left(\frac{26}{8.53}\right)^n ,$$

giving n = 0.528. We see here that the size relationship is greater than any theory predicts. To confidently evaluate the effects of size more runs in a dry atmosphere are required in CMF and CRI to establish a statistical basis for the values used in the comparisons. Our judgement at this time would be that the size scaling as expressed by the value of n will fall within O and 0.25.

3. Treatment of NSPP, CRI, and CMF Data Using the Model Developed for the Case of Dry Air with Limited Surface Coverage (Case 2).

Figure 3 shows the typical behavior of the normalized iodine concentration-time curve at a given position of the NSPP; in this case, the horizontal midplane, southwest quadrant, at a 60 inch radius. Three major segments of this time history are: (1) Early time while fans are on and homogenization of the concentration within the tank is taking place, (2) plate-out

period where the concentration decreases with time, (3) asymptotic region when surface coverage has an effect on the gas phase concentration. The time scale has been shifted for purposes of analysis so that zero time is taken as the time at which the maximum concentration is reached and begins to decay.

The initial slope of the experimental curve was used to estimate the mass transfer coefficient, $k_c$, by use of Eq. (27), and the asymptotic region was used to estimate $\alpha$.

The results of Case 2, expressed in Eq. (60),

$$\frac{C}{C_o} = \frac{1}{1+\alpha}\left(e^{-\frac{S}{V_o}k_c(1+\alpha)t} + \alpha\right) , \qquad (60)$$

were used to compute the theoretical curve shown on Fig. 3.

In order to test both the model predicting the mass transfer coefficient, and the overall model of Case 2 we attempted to predict the behavior of the CMF and the CRI entirely by scaling the NSPP results. The mass transfer coefficient was scaled with size and pressure according to Eqs. (46) and (47). For the rough comparison, we assumed that the surfaces of all the tanks were similar.

The surface parameter, $\alpha$, can be split into two components:

$$\alpha = \left(\frac{Ks}{R}\right) \cdot \left(\frac{V_o}{S}\right) . \qquad (61)$$

The first is dependent only on the character of the surface and the adsorbed species, the second on the geometry of the tank. We computed Ks/R from NSPP data, and assumed this remained constant for both the CMF and the CRI. Predicted values of $\alpha$ were then computed for these last two by using the proper surface-to-volume ratios.

The results of this procedure are shown in Figs. 4 and 5. We see that for the CMF, the hydrodynamic model scaling the mass transfer coefficient predicts the observed value almost exactly, as can be seen by the slope of the theoretical curve at zero time. The assumption of similar surfaces, however, leads to a predicted asymptote off by a factor of 1/6. For the CRI the experimental mass transfer coefficient is greater than predicted and the predicted asymptote is approximately 3 times that of the experimental value.

Fig. 3

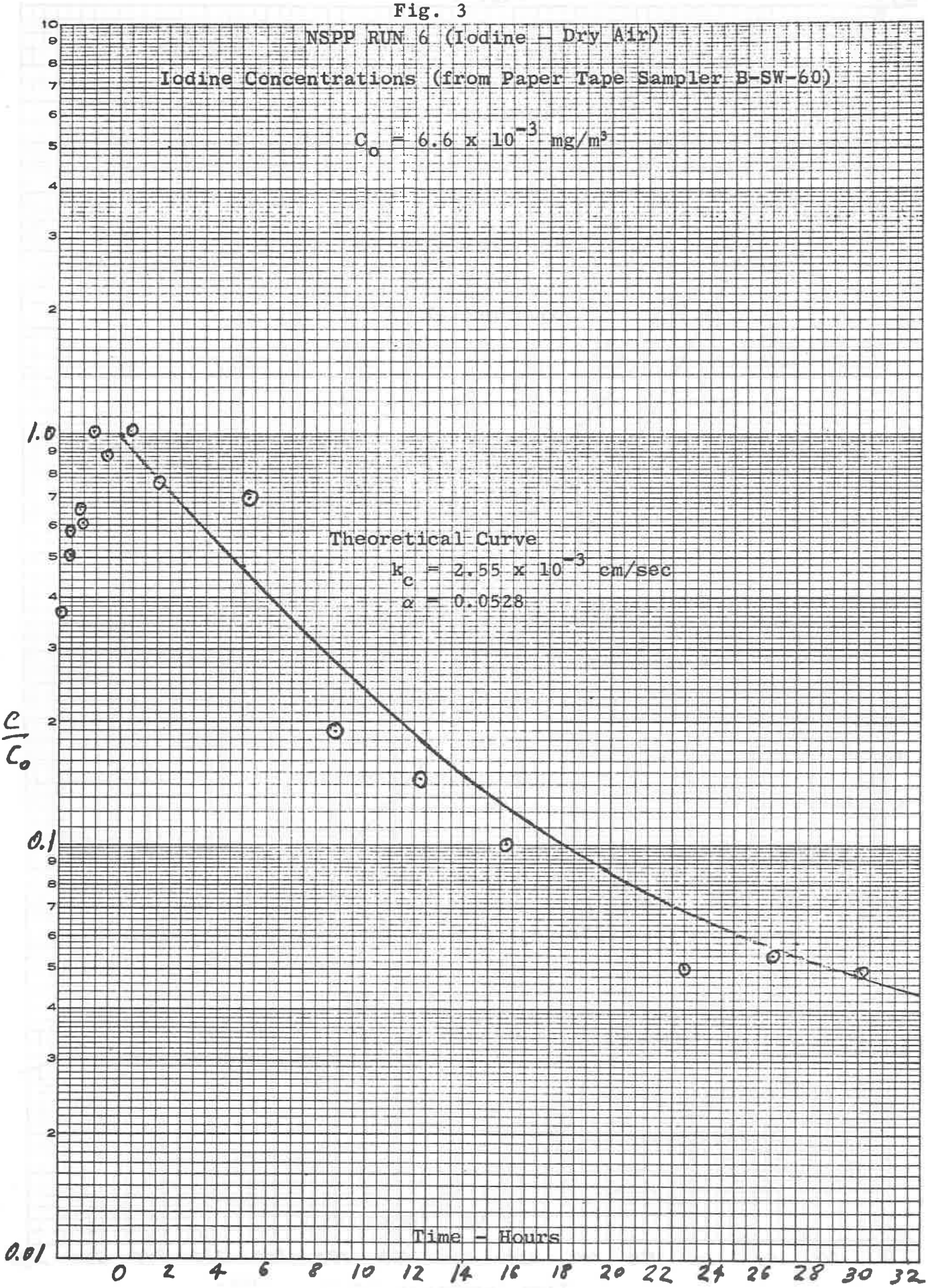
NSPP RUN 6 (Iodine – Dry Air)
Iodine Concentrations (from Paper Tape Sampler B-SW-60)
$C_o$ = 6.6 x $10^{-3}$ mg/m³
Theoretical Curve
$k_c$ = 2.55 x $10^{-3}$ cm/sec
$\alpha$ = 0.0528
C/Co
1.0
0.1
0.01
Time – Hours
0 2 4 6 8 10 12 14 16 18 20 22 24 26 28 30 32

Fig. 4

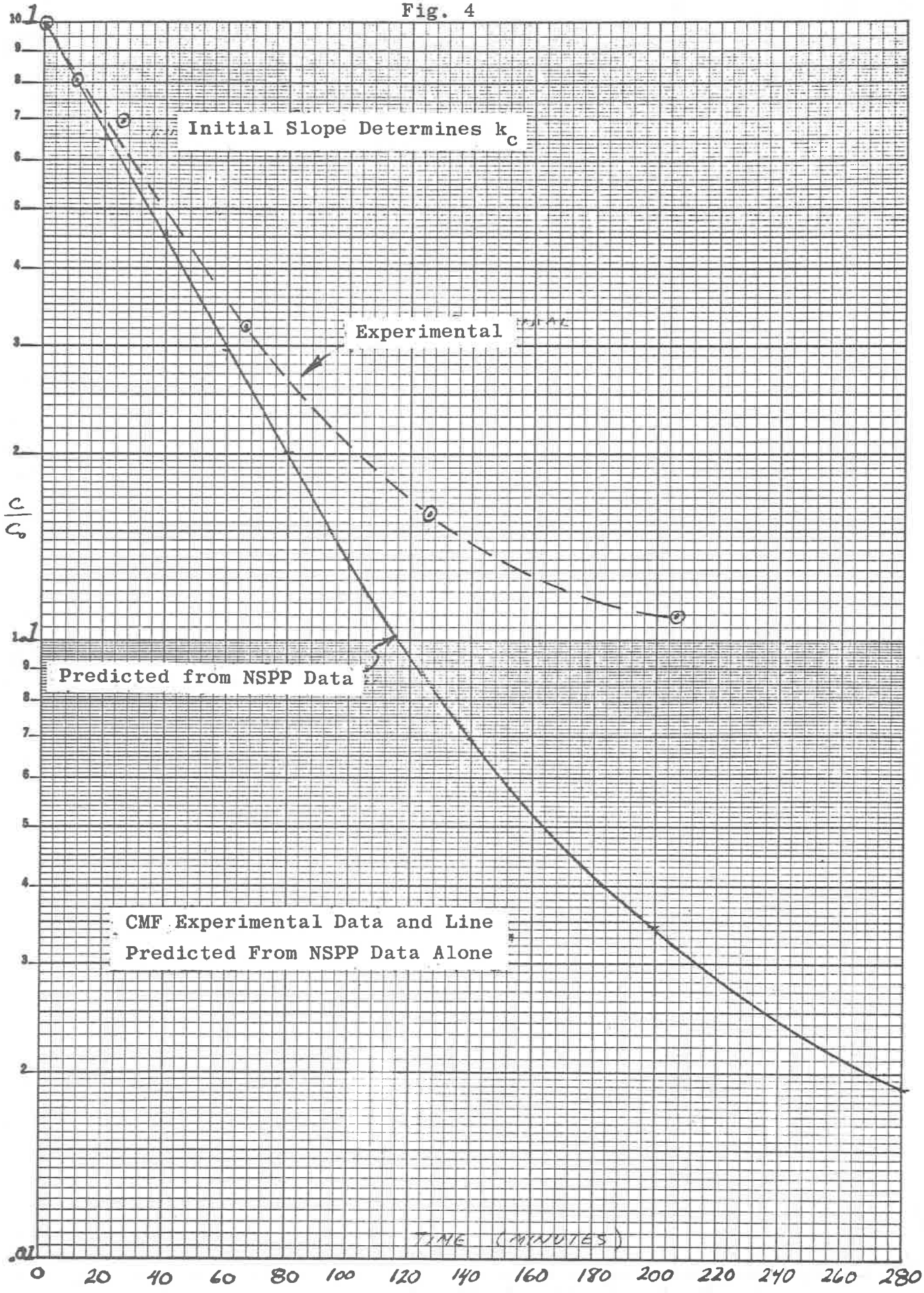
Initial Slope Determines $k_c$
Experimental
Predicted from NSPP Data
CMF Experimental Data and Line
Predicted From NSPP Data Alone
C/Co
TIME (MINUTES)
0
20
40
60
80
100
120
140
160
180
200
220
240
260
280
Time (minutes)

Fig. 5

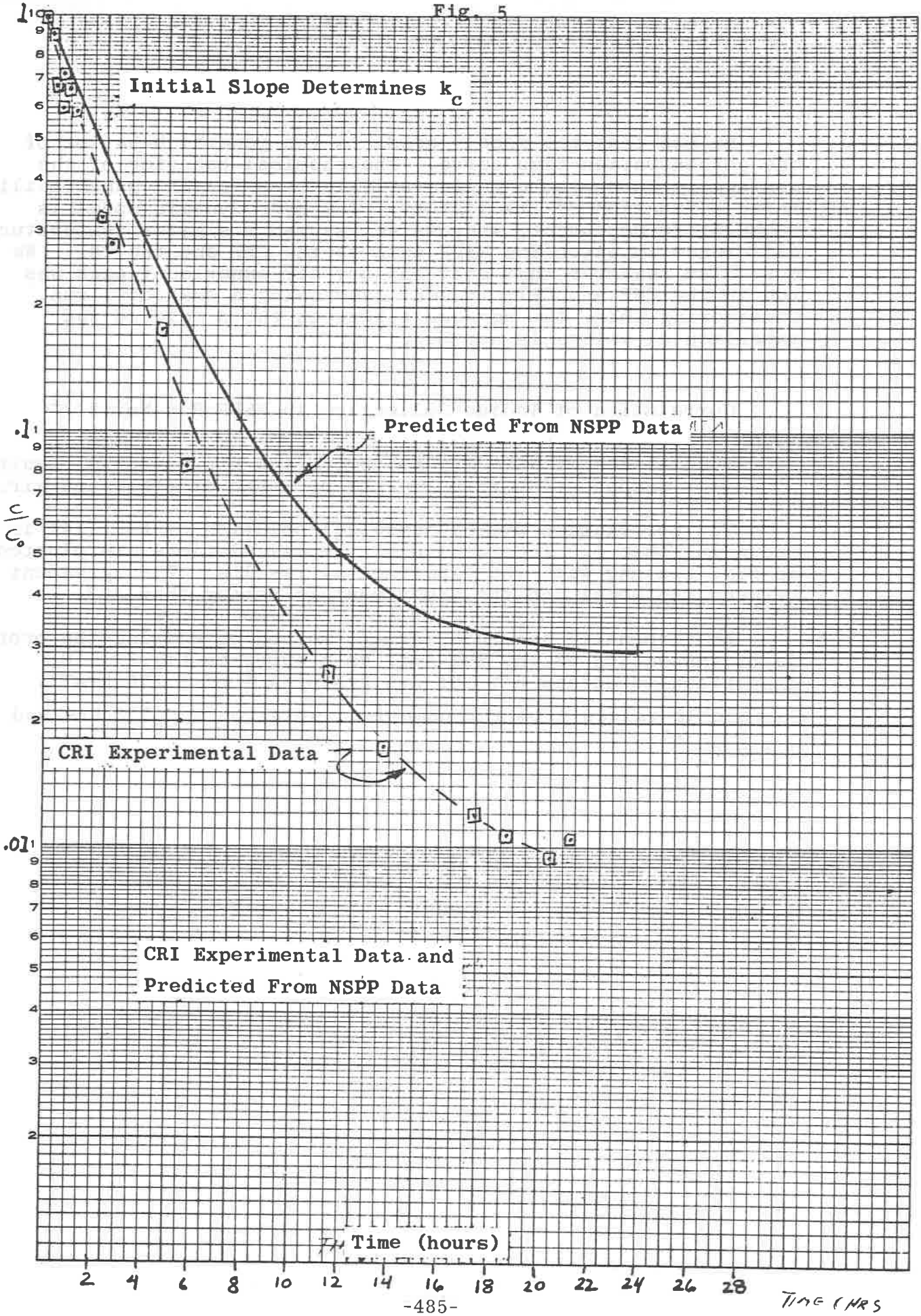
Initial Slope Determines $k_c$
Predicted From NSPP Data
C/C₀
CRI Experimental Data
CRI Experimental Data and
Predicted From NSPP Data
Time (hours)
1
.1
.01
2
4
6
8
10
12
14
16
18
20
22
24
26
28
TIME (HRS

We see that the model predicts the general behavior of the concentration-time curve. The chemical behavior of the surface is known to be quite variable even for the same facility, being a function of its history. The hydrodynamic model is temperature dependent, whereas we assumed a similar temperature difference in extending NSPP data to the CMF and the CRI. We must also remember that only one dry air experiment each was run in the CMF and CRI; the CRI case being a shakedown run. Considering this, the agreement between the predicted and experimental values is not bad.

## Correlation of Iodine Collection in NSPP Run No. 8[11]

The results of NSPP Run No. 8 provide experimental results of iodine condensation rates in the presence of steam and air.

The correlation by the numerical solution of Eq. (14) is shown in Table 5. The results of the calculations are plotted in Fig. 6 along with the experimental results. The agreement between the model and the experiment is better than 20%.

An alternate, and much easier, method of solving the proble is by inspection of the log n(t) vs t curve in Fig. 7. By inspection we obtain a $t_{\frac{1}{2}}$ of 2.5 hrs or a $\frac{1}{\tau}$ of 0.278 $hrs^{-1}$. Comparable values from the numerical solution are 2.2 hrs and 0.315 $hrs^{-1}$.

TABLE 5

CORRELATION OF NSPP RUN #8

Calculation of Rate Constant by Numerical Treatment of Experimental Data

| t hr | $P_{H_2O}$ Psia | T K | $\left(\frac{P}{T}\right)$ | Fraction in Vapor | Condensate Rate | | Rate Constant $\frac{1}{T}$ - $hrs^{-1}$ | $\frac{C}{C_o}$ |
|---|---|---|---|---|---|---|---|---|
| | | | | | Experimental | Smoothed | | |
| 0 | 27.0 | 380.5 | 0.0709 | 1.00 | | | | 1.00 |
| 1 | 18.0 | 370 | 0.0486 | 0.69 | 0.31 | 0.22 | 0.319 | 0.73 |
| 2 | 13.8 | 361 | 0.0381 | 0.54 | 0.15 | 0.15 | 0.278 | 0.57 |
| 3 | 10.5 | 354 | 0.0297 | 0.42 | 0.12 | 0.12 | 0.288 | 0.42 |
| 4 | 8.0 | 349 | 0.0229 | 0.32 | 0.10 | 0.10 | 0.313 | 0.29 |
| 5 | 6.25 | 345 | 0.0181 | 0.26 | 0.06 | 0.081 | 0.312 | 0.21 |
| 6 | 4.75 | 340 | 0.0140 | 0.198 | 0.062 | 0.063 | 0.318 | 0.15 |
| 7 | 3.50 | 336 | 0.0104 | 0.147 | 0.051 | 0.052 | 0.354 | 0.084 |
| 8 | 2.35 | 332 | 0.00708 | 0.100 | 0.047 | 0.058 | 0.380 | 0.048 |
| 9 | 2.00 | 328 | 0.00610 | 0.086 | 0.014 | 0.027 | 0.314 | 0.053 |
| 10 | 1.50 | 325 | 0.00462 | 0.065 | 0.021 | 0.018 | 0.278 | 0.046 |
| | | | | | | | av 0.315 | |

$$\ell n \frac{C}{C_o} = - \int_o^t \frac{\frac{S}{V_o n_o} J(t')\, dt'}{1 - \left(\frac{S}{V_o n_o}\right) \int_o^{t'} J(t'')\, dt''}$$

$t_{\frac{1}{2}} = 2.2$ hrs

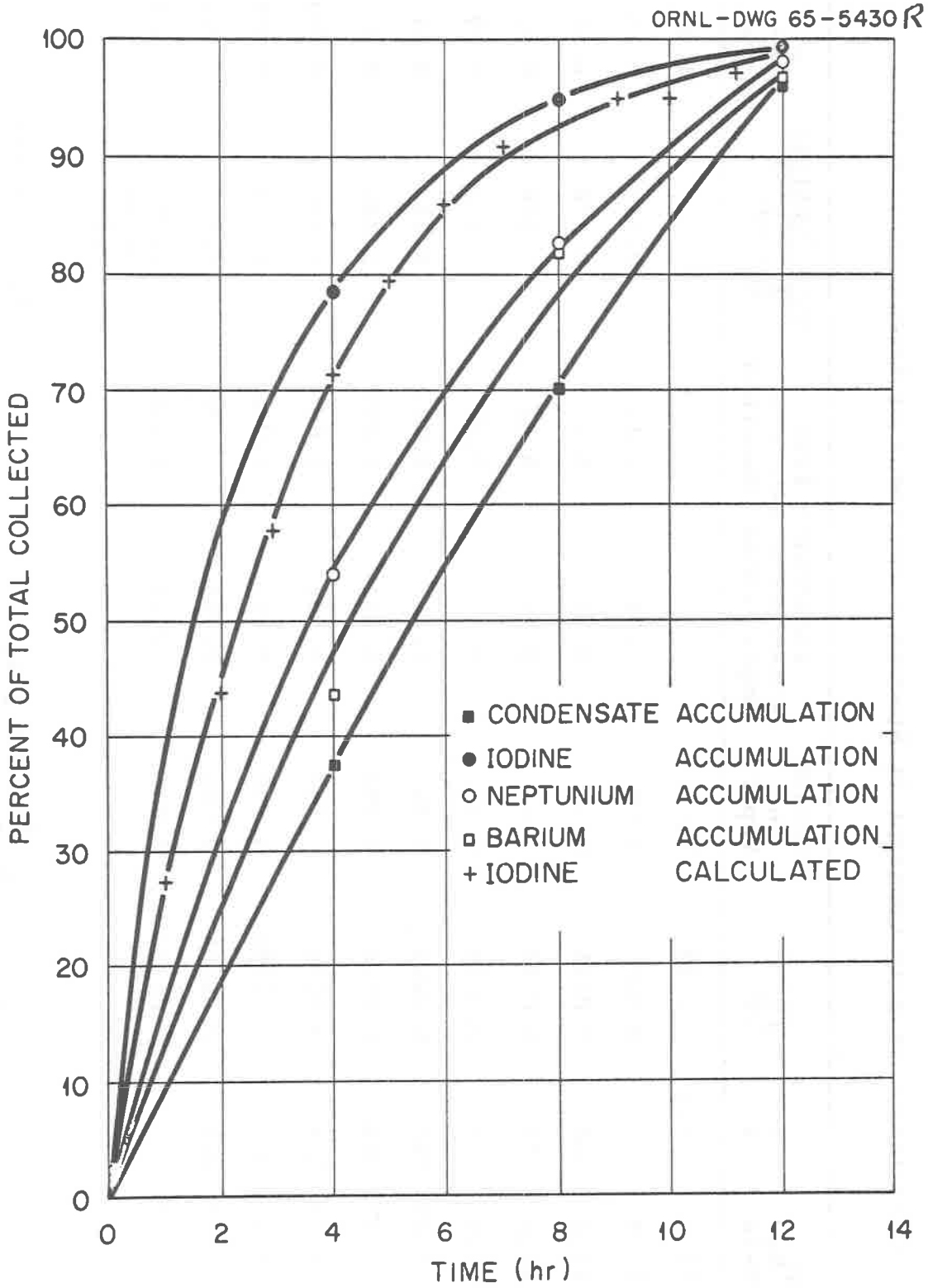


Fig. 6 Accumulation of Condensate and of Fission Products in Condensate vs Time; NSPP Run No. 8.

Fig. 7 NSPP RUN 8

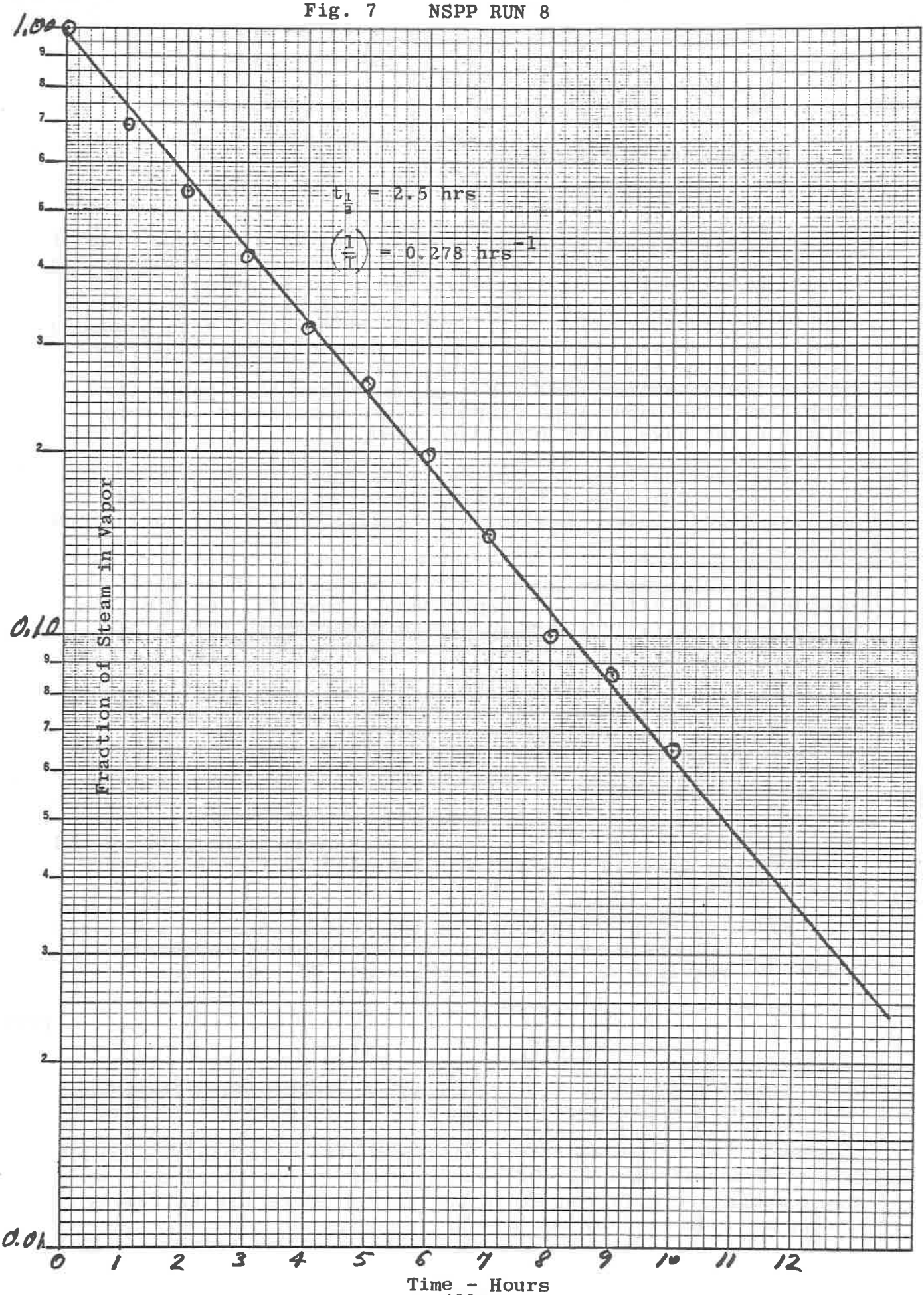

## VI. RECOMMENDED EXPERIMENTS

### 1. Dry Air Experiments.

In order to check the model and possibly elucidate some of the mechanisms involved, further experimental data with dry air conditions in different size vessels are required. The NSPP, CMF, CRI, and CSE are available for out-of-pile tests. The ORNL in-pile experiments will shortly be equipped with a mockup containment vessel approximately the size of CMF. Additional experiments in the NSPP should be re-run with dry air and a common iodine source, using May packs rather than paper tape samplers. The paper tape samplers were considered not very reliable and have since been discarded.

The chemical behavior of surfaces needs to be better understood. There is a laboratory program underway at ORNL to investigate this. Preliminary results show great variations in realistic surfaces.

Since it would be prohibitively expensive to permute completely the effects of temperature, pressure, and size, an incomplete statistical design of the experiments should be planned early in the program.

Differential thermocouples should be installed in the vessels at proper locations (e.g., centerline vs a position near the wall; one wall vs the opposite wall, etc), in an attempt to measure the small temperature differences which may be responsible for the convection currents, if they indeed do exist.

A search for better low flow measurement techniques should be made. At present, velocities less than 10 ft/min are very difficult to measure.

Smoke pattern experiments in transparent models of various sizes may be considered. Since similarity of the Grashoff number is required in scaling experiments of this nature,

$$\left(\frac{L^3 \Theta_s \rho^2 g\beta}{\mu^2}\right)_1 = \left(\frac{L^3 \Theta_s \rho^2 g\beta}{\mu^2}\right)_2 , \qquad (62)$$

we see that a decrease in size allows a greater (and therefore measurable) temperature difference to be used in the smaller scale models. Notice that a factor of 10 in size requires a factor of 1000 in temperature difference to maintain similarity of the Grashoff number. Obviously, this is practical only when the temperature differences in the larger sizes are extremely small, as indicated by our model.

In planning and evaluating the experiments, we should keep in mind that in the larger size tank, the flow may become turbulent with very small temperature differences. If the condition is reached where the large experiments are in turbulent free convection and the small experiments are laminar, comparison of size effects will be difficult because of the non-similarity of the flow regimes.

2. Experiments with Condensing Steam.

Experiments are needed to establish the limits of applicability of our assumption that the ratio of the concentration of iodine to steam throughout the experiment remains constant. If limits of applicability are established, the prediction of the behavior of iodine will be greatly simplified because a great deal is known about steam behavior that would become directly applicable to iodine.

Simple experiments with methyl iodide (or methyl iodide-iodine) in containment systems in the presence of steam should be performed to check deposition rates against those predicted from theory.

Simple experiments should be devised to test the effect of air on the condensation behavior of iodine-steam. Our present guesses predict only a slowing down effect due to the presence of air, but no change in the ratios of the condensation rates of the species. It is quite possible that this prediction is wrong, in which case, the present steam condensation models may be valid only in the cases where air is absent.

The exact coupled differential equations describing the concurrent mass transfer-heat transfer conditions in ideal systems are currently being studied by Dr. N. Ocisik at North Carolina State University. Rather precise studies of flow patterns are being done by J. Wantland at ORNL and Professor Knudsen of Oregon State. When this information becomes available, the boundaries of our treatment should be better delineated.

TABLE OF NOMENCLATURE

$a$ = Langmuir's constant ($cm^3$/mole)

$A_o$ = specific radioactivity of iodine at time = 0 (dpm/sec-$cm^3$)

$A$ = specific radioactivity of iodine at time t (dpm/sec-$cm^3$)

$b$ = group of terms, defined by Eq. (7)

$C$ = concentration

$C_w$ = concentration near the surface

$C_o$ = initial concentration in tank volume

$C_f$ = final concentration in tank

$C_g$ = concentration of methyl iodide in the gas phase (moles/$cm^3$)

$D$ = diffusion coefficient ($cm^2$-sec)

$D_T$ = ternary diffusion coefficient ($cm^2$/sec)

$g$ = gravitational acceleration (cm/$sec^2$)

$h_c$ = convection heat transfer coefficient (cal/$cm^2$-sec-$^oK$)

$J_1$ = net iodine flux (moles/$cm^2$-sec)

$J(t)$ = total net flux of iodine and steam (moles/$cm^2$-sec)

$J_s(t)$ = flux of steam (moles/$cm^2$-sec)

$k_c$ = mass transfer coefficient in terms of concentration (cm/sec)

$k_f$ = thermal conductivity of gas in the film near the surface (cal/cm-sec-$^oK$)

$K$ = constant describing linear portion of adsorption isotherm (moles/$cm^3$)

$L$ = total distance measured parallel to surface (cm)

$N_{Gr}$ = Grashoff number (dimensionless)

$N_{Pr}$ = Prandtl number (dimensionless)

$N_{Sc}$ = Schmidt number (dimensionless)

$\overline{N}$ = Avagadro's number ($6.023 \times 10^{23}$ molecules/mole)

$n$ = total concentration of gas (moles/$cm^3$)

$n_a$ = concentration of air (mole/$cm^3$)

$n_s$ = concentration of steam (moles/$cm^3$)

$n_w$ = concentration of steam due to vapor pressure of water wetting the wall (moles/$cm^3$)

$\bar{n}$ = molecules adsorbed (molecules)

P = total pressure (dyne/$cm^2$) or (atm)

R = roughness factor of surface $\frac{\text{actual surface}}{\text{geometric surface}}$ (dimensionless)

S = tank inner surface area ($cm^2$)

s = area covered by one adsorbed iodine molecule ($cm^2$)

T = temperature, absolute ($^oK$)

$T_e$ = temperature of environment ($^oK$)

$V_o$ = velocity parallel to surface (cm/sec)

$v_\infty$ = "free stream" velocity parallel to surface at distances far from the surface (cm/sec)

x = distance measured parallel to surface (cm)

$x_1$ = mole fraction of iodine in iodine-steam mixtures (dimensionless)

$\bar{x}_1$ = iodine mole fraction in steam-air mixture (dimensionless)

$x_2$ = mole fraction of methyl iodide in water (dimensionless)

z = distance perpendicular to the wall (cm)

$\alpha$ = parameter describing surface conditions (dimensionless)

$\beta$ = coefficient of volume thermal expansion ($^oK^{-1}$)

$\bar{\beta}$ = parameter describing surface condition and properties of adsorbed molecule ($cm^{-3}$)

$\Delta$ = ratio of concentration boundary layer thickness to momentum boundary layer thickness (dimensionless)

$\delta_c$ = concentration boundary layer thickness (cm)

$\delta$ = momentum boundary layer thickness (cm)

$\eta$ = fraction of iodine atoms as molecular iodine

$\theta$ = fraction of surface covered

$\theta_s$ = temperature difference between ambient air and surface ($^oK$)

$\mu$ = "absolute" viscosity (gm/cm-sec)

$\nu$ = kinematic viscosity ($cm^2/sec$)

$\rho$ = density ($gm/cm^3$)

$\rho'$ = dimensionless velocity

$\tau$ = relaxation time of system $(V_o/Sk_s)$(sec)

$\chi$ = dimensionless temperature = $\theta/\theta_x$ (dimensionless)

$\Omega$ = Henry's law constant ($moles/cm^3$)

REFERENCES


1. G. E. Creek and G. W. Parker, personal communication, Sept. 1, 1966.

2. J. L. Wantland and T. H. Row, The Behavior of Iodine in Air Atmospheres - A Resume of the First Seven Runs Conducted at the Nuclear Safety Pilot Plant, to be issued.

3. E. Schmidt and W. Beckman, Techn. Mech. U. Thermodynamik, 1, 341 and 391 (1930).

4. M. Jacob, Heat Transfer, Vol. 1, John Wiley and Sons, New York (1949), p. 443 et. seq.

5. R. Byron Bird, Warren E. Stewart, and Edwin N. Lightefoot, Transport Phenomena, John Wiley and Sons, New York (1960), p. 607.

6. R. B. Bird, et al., op. cit., p. 606.

7. William H. McAdams, Heat Transmission, 3rd Ed., McGraw-Hill, New York, 1954, p. 172

8. W. E. Bird, op. cit., p. 505.

9. W. H. McAdams, op. cit., p. 408

10. W. E. Bird, et al., op. cit., p. 21, 510.

11. G. M. Watson and M. J. Kelly, A Correlation of Iodine Condensation in NSPP Run 8, ORNL-CF-66-9-13, in press, Sept. 1966.

# VENT GAS TREATMENT PLANT

J. Ackerman, R. Bundrick, J. Cowles, V. DuVal, J. Grens,
R. Holzman, C. Hannon, J. Harrar, C. Morris, L. Rigdon,
R. Heckman and D. Snoeberger

Lawrence Radiation Laboratory, University of California
Livermore, California

## INTRODUCTION

As part of the Vela Uniform program, Project Dribble was concerned with the measurement of seismic signals generated by nuclear detonation in a salt dome. The principal objective of the project was a test of the decoupling theory proposed by Latter et al.[1,2]

In September 1962, after resumption of underground nuclear testing, Project Dribble was redefined. Certain technical responsibilities including the detailed design of the experiment, development of the technical program and execution of the on-site portion of the technical program were assigned to the Lawrence Radiation Laboratory through the Atomic Energy Commission.

The planned 5-kiloton detonation occurred October 22, 1964, in the Tatum Salt Dome near Hattiesburg, Mississippi.

Technical objectives of the post-shot program for this event were to:

1) Obtain samples of radioactive debris for yield determination.

---

[1] Latter, A. L., E. LeLevier, E. Martinelli, and W. McMillan, "A Method of Concealing Underground Nuclear Explosions," J. Geophys. Research, 66, 943-946 (1961).

[2] Werth, G., and P. Randolph, "Prepared Statement on the Theory of Decoupling and the Status of Project Dribble, for the Joint Committee on Atomic Energy, Congress of United States," UCRL-7323, March 6, 1963.

2) Sample the gas in the cavity to determine whether radioactive material which might cause a public safety problem had escaped.

3) Examine the feasibility of re-use of the cavity for firing decoupled nuclear shots. Measurements to be made included distribution of radioactivity, temperature, volume, geophysical logging, and television survey.

4) Extract core from a second drill hole passing close to the cavity for property measurements.

To accomplish this post-shot technical program, an assured means of obtaining access to the cavity was required. Based on studies completed in 1961 on the cost and engineering feasibility of the various means of assuring cavity access, it was decided that a vent-gas treatment facility was needed. This facility was to be connected to the post-shot drilling rig at the well head and was to remove radioactive particulates from the cavity effluents and control release rate of gaseous radioactivity to meet public health safety standards.

Process engineering studies resumed in September 1962. The problem was redefined with more stringent performance requirements added. The new requirements included the following points: The facility must remove radioiodine to eliminate any possible public safety problems. The release rate for the noble gas fission products, xenon and krypton, must not exceed limitations set by the limited test ban treaty, i. e., no detectable activity beyond national borders. The plant must be removable before shot time and be quickly reinstalled to prevent damage to the plant components by nuclear seismic shockwave. Absolute reliability and control of plant radioactivity releases was to be accomplished by use of shut-off valves at the well head.

It was recognized that an explosive mixture of gases might be present in the post-shot cavity. To prevent any possibility of catastrophic failure of the plant components with subsequent radioactivity release, an air dilution venturi was added at the plant inlet. The flow rate of cavity gas into the dilution venturi was controlled so that an explosive mixture was never possible beyond the dilution venturi. In addition, all the well head piping upstream of the venturi was designed to contain any gas explosion that might occur.

Since drill back into the cavity might occur as early as D + 7 days, the facility must be capable of handling the following fission product activity mixed with the gas: particulate – $4 \times 10^5$ curies; radioiodine – $8 \times 10^5$ curies; and radioxenon and krypton – $1 \times 10^6$ curies; or a total of $2.2 \times 10^6$ curies.

## GAS TREATMENT PROBLEM

Predictions of the chemical environment of an underground nuclear explosion are very difficult; yet that is the problem with which we were faced in attempting to describe the feed conditions into our vent gas treatment facility. The design of the facility had to be sufficiently flexible to cover any possible situation that could occur in the field. From test hole samples, salt dome composition was estimated to be NaCl 91%, $CaSO_4$ 8%, $CO_2$ 0.015%, $H_2O$ <0.01%, and traces of hydrocarbons. The principal gas-producing reactions were thought to be:

1) $Fe + H_2O \longrightarrow FeO + H_2$

2) $CaSO_4 \rightleftharpoons CaO + SO_3$

or

$CaSO_4 \rightleftharpoons CaO + SO_2 + 1/2\ O_2$

3) $SO_3 + H_2O \longrightarrow H_2SO_4$

$2\ NaCl + H_2SO_4 \longrightarrow 2\ HCl + Na_2SO_4$

4) $H_2 + CO_2 \rightleftharpoons CO + H_2O$

5) $H_2O\ (\ ) \longrightarrow H_2O\ (g)$

The iron was present from the emplacement canister. There was an uncertainty in amount of salt melt to be produced by the nuclear detonation and therefore the amount of $CaSO_4$ available for reaction.

With these great uncertainties in the general chemical environment, we attempted to make predictions of the chemical state of the radioiodine. These predictions indicated the most likely forms to be $I_2$ and HI.

Predictions of the cavity volume produced further uncertainties in expected pressures; cavity collapse would radically affect cavity pressure and temperature at the time of re-entry. With no collapse, the cavity temperature was estimated to be below the melting point of salt. The cavity pressure might range from 10 atm to a partial vacuum, depending on which chemical equilibrium prevailed.

With these considerations as background, we chose the following as design criteria for the facility: The problem was to release at controlled and safe rate approximately $5.6 \times 10^5$ $ft^3$ of gas initially at a pressure of 10 atmospheres or less. Release was to begin one to four weeks after the shot, depending upon time required to drill the postshot well. The vented gas temperature would be at ground ambient temperature because of heat transfer to the earth and well casing during passage up the well. There might be enough hydrogen and oxygen present to constitute an explosive mixture, possibly in a detonation range. The gas was expected to be acidic, corrosive

and saturated with water. It might carry suspended salt particles capable of plugging flow passages. Radioactivity was estimated to be a maximum of 4.0 curie per cubic foot of gas fed to the plant.

Later times of re-entry and bleed down would allow further decay of radioactivity. Radioiodine activity, $I^{133}$, predominates after 10 days, but decreases by a factor of 10 per month. Xenon activity falls off a little faster but krypton 85 activity predominates over those of xenon and iodine after roughly three months, contributing approximately a total of 200 curies.

A controlled release of the cavity gas these further effects were expected: Excess water vapor would condense on the wall or on cold salt, dissolve salt, and return to the cavity. This process might continue by reflux. There may be a net beneficial effect in separation of gases and particulates by this "wetted wall column." There might be problems with salt plugging in the well.

Radioactive particulates and iodine were to be removed from the vented gas; xenon and krypton were to be dispersed in the atmosphere.

The release rate was limited to allowable rates for iodine, xenon and krypton as determined by public safety and limited test ban treaty consideration. It was important to complete bleed down in as short a time as possible to minimize cost and degradation of data for the post shot programs.

Pre-operational tests with radioactive iodine were made in July 1964. The plant was removed to avoid shock damage, then reinstalled after the test detonation. Operational use began in February 1965, and continued intermittently through May 1965. Figure 1 shows the plant piped to the re-entry well late in the operational period. The plant is now in caretaker status pending development of requirements in connection with re-use of the cavity for further experiments.

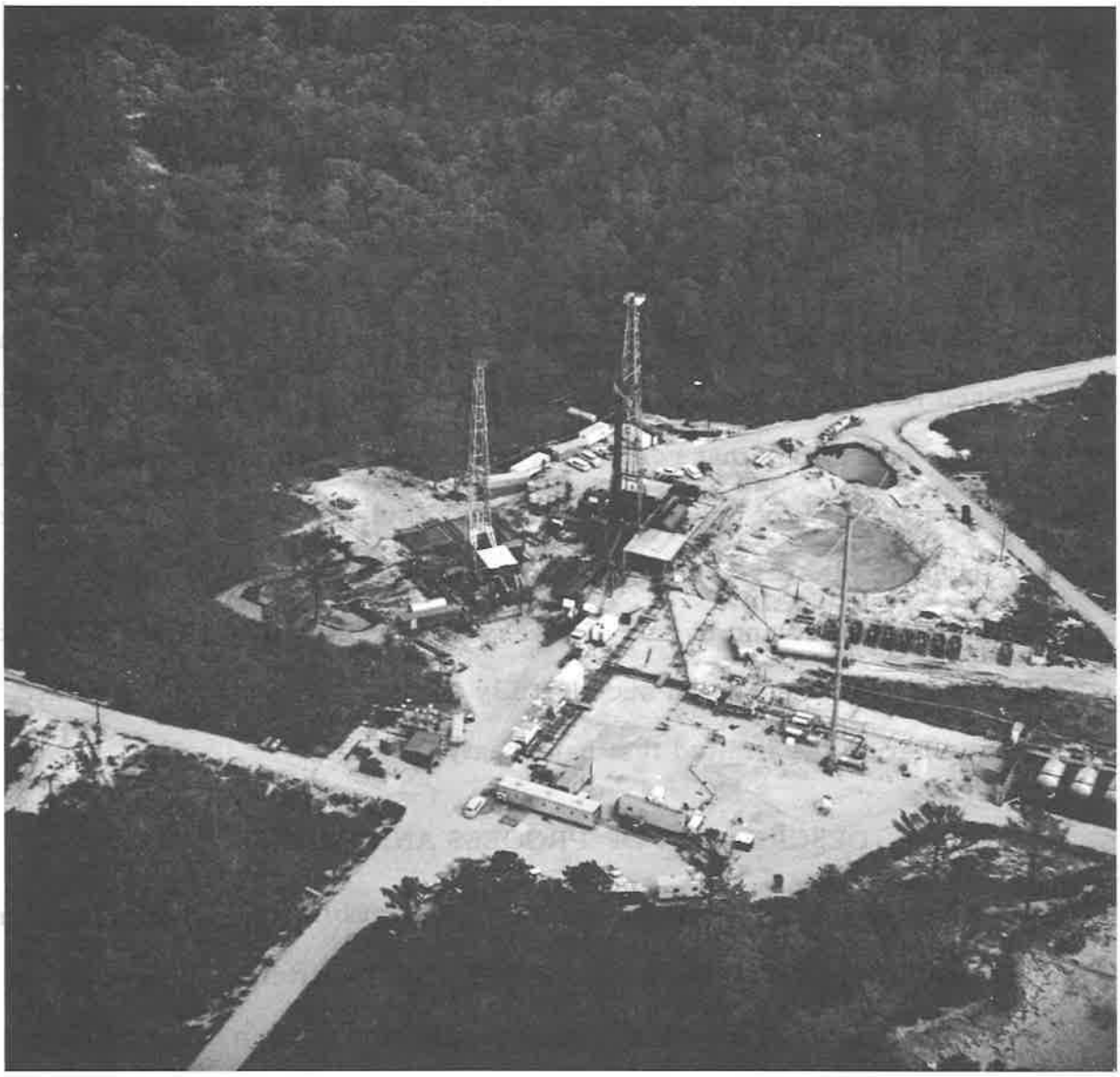

Fig. 1. Aerial view of vent gas treatment plant.

Prior to the actual detonation the decision was made to delay start of post-shot drill back for 60 days to accomplish additional technical requirements for the detection program. Because of this delay a large fraction of radioactivity decayed, and the cavity cooled to 204° C. At the time of cavity penetration, the cavity was found to be under a partial vacuum of 313 millibars.

On the basis of pre-operational performance tests and the actual operating experience, we feel that we successfully designed and built a vent gas treatment facility whose performance exceeded our original design specifications. The desired flexibility was demonstrated by our ability to support a wide variety of down-hole operations that resulted from actual conditions found in the field. However, our ability to predict the chemical environment of an underground nuclear explosion leaves something to be desired. We recognized our ignorance in this area and by use of a very conservative design we did conduct a post-shot technical program successfully without endangering the public safety or violating the limited test ban treaty.

## DESCRIPTION OF PROCESS AND PLANT

The process is a remotely operated gas scrubbing and filtering system with charcoal adsorption units incorporated with the filters. It is sized to take up to 200 $ft^3$/min of cavity gas mixed with 2000 $ft^3$/min of air to dilute hydrogen. Effluent gas is discharged from a 150-foot stack after mixing with 20,000 cfm of additional air. Liquid wastes from the scrubbers are stored in four 25,000-gal tanks for later disposal. Figure 2 shows the sutdown, flow control and main process units.

### Well Head

The well head includes the cavity gas shut-off valves. There are six, two in series plus a sampling valve on each of the two connections to the plant.

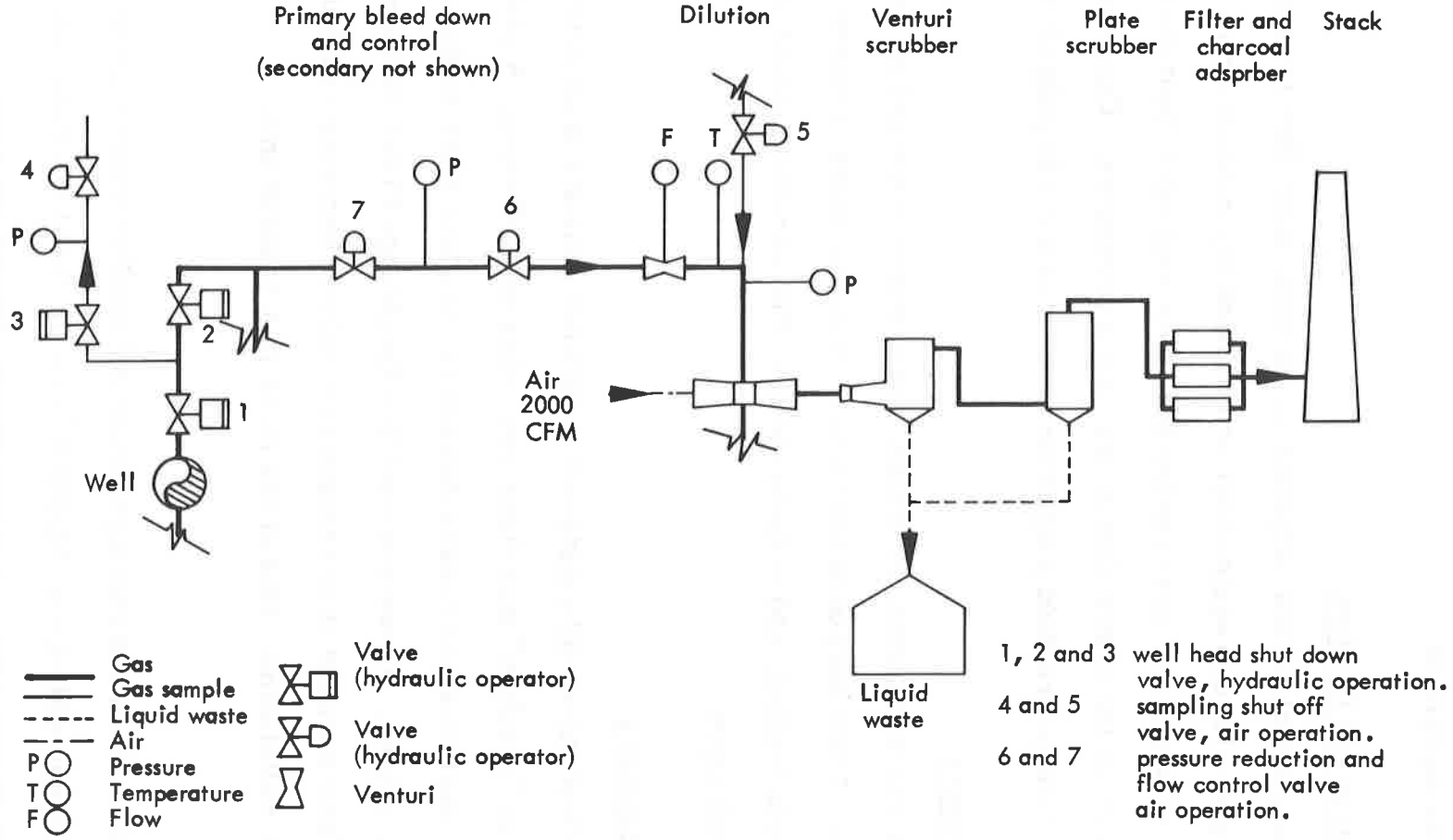


Fig. 2. Project Dribble bleed-down process flow and control schematic.

These valves are remotely operable. They are designed to fail to a closed position and will close automatically on loss of electric power or failure of the process equipment.

Flow Control and Dilution

Flow control valves, adjacent to the well, limit flow to rates based on the hydrogen dilution requirement or radioactivity release limit. The venturi serves to dilute cavity gas to below the lower explosive limit for hydrogen and provide suction for faster flow at low cavity pressures. Equipment working pressure ratings are 3000 psig prior to dilution and 150 psig after dilution.

Gas Scrubbers

The two scrubbers, in series, are a venturi-type and an impingement plate type. Their purposes are to remove particulates, protecting the filters from excess loading, and remove iodine. The scrubbing liquid is aqueous sodium hydroxide.

Filter Adsorbers

Each of three units installed in parallel consists of an activated charcoal bed with an "absolute" type filter preceding and following. A prefilter is used with each to avoid caustic damage to the glass fiber media of the high efficiency filters. These are modified Cambridge Filter Company C. B. R.* units. Their purpose is to remove particulates carrying radioactivity and to adsorb radioiodine. One of the three is a reserve unit.

Stack

The stack is 150 feet high, clearing local trees and hills by 50 to 100 feet. A stack blower adds air at 20,000 $ft^3$/min for local dilution. All effluent and contaminated tank vent gas is discharged through the stack.

*Chemical Biological Radiological.

Laboratory Trailer

A gas chromatograph provides feed gas analysis by sample pipe or bottle. Scrubbing solution analysis is provided by "auto analyzer" and pH and density instruments.

## PREOPERATIONAL TESTS

During the course of the project increasing emphasis was placed on removal of radioactive iodine. Although quantities and the compounds of iodine to be expected in the gas were not predictable, tests with a probable form, $I_2$, were made using I-131 as a gamma tracer. Results were excellent. The removal factor for the combined scrubbers and charcoal beds was $4 \times 10^5$.

## OPERATION OF FACILITY

This period began on February 26, 1965. It can be divided roughly into three phases: 1) a standby period prior to cavity penetration (Feb. 26 to Mar. 3); 2) an operation period during which the greatest part of actual vent gas treatment took place (Mar. 4 to Mar. 13); 3) a continuing period of standby and occasional operation (Mar. 14 onward).

A summary of operational experience follows:

1. Cleaning of air drilling returns

A crossover line was installed from the drill rig "blooie line" into the plant 10-inch process gas line. This system allowed the plant to provide protection against spreading of radioactive salt dust and release of radiogas encountered in the final stages of drilling. Drilling returns were diverted

to the plant for cleaning when radioactivity release limits were approached. This was done on penetration drilling into the cavity and later while drilling for cores below the cavity.

2. Vent gas treatment

The true operating phase began at cavity penetration, early on March 4. A pressure measurement shortly after penetration showed 0.8-inch Hg vacuum, so no immediate attempt was made to bleed off cavity gas.

Gas sample bottles and temperature measuring instruments were lowered into the cavity, and the plant gas chromatography unit analyzed a sample of this gas. This important findings were that the gas was primarily air, with $CO_2$ the primary additional constituent. Both $H_2$ and $SO_2$ were present, but in concentrations too low to be of concern in operations.

The first appreciable quantity of gas vented from the cavity occurred of March 6, following pressurization of the cavity to one-half atmosphere positive pressure with drilling compressors for purposes of cavity volume measurements. This gas was released through the crossover pipe installed for drilling returns, which allowed flows at approximately 1000 cfm. Cyclic flow pulses, with a period of about 30 to 60 seconds, were observed during bleeding off of the gas. These may have been caused by a reflux water leg, which also may have been responsible for closing the hole with a salt plug.

Activity release was very low. The maximum release rate of radioactive rare gas is estimated at less than 200 millicuries/minute. Approximately 30 curies of rare gas, mostly $Kr^{85}$, were released in the initial bleed down of the 300,000 cubic feet of air added for cavity volume measurement. Due to dilution by the stack blower, 5 microcuries per cubic foot was the maximum concentration in effluent gas. $I^{131}$ was so slight as to be detectable only with difficulty.

The second and final major release of cavity gas was from the flushing operation. This was a procedure to reduce the concentration of radioactive gas to such a level that treatment of vent gases would no longer be required. Three cavity volumes of air were pumped into the cavity and bled off, reducing residual gas to 40 microcuries per cubic foot rare gas radioactivity.

Release rate was a maximum of 50 millicuries per minute early in the operation, and declined slightly. Total release was approximately 50 curies, primarily $Kr^{85}$.

3. Downhole operations support

Regulated flows of nitrogen and air and slight suctions were provided to the well on demand to assist in the use of well logging instruments and television cameras. Cavity pressures were decreased to just below atmospheric pressure to establish downdrafts during insertion and removal of drilling equipment and instruments.

Repeated use of plant equipment was made to test by pressurization and pressure decay measurement for communication between well and cavity. The dilution venturi suction was used to speed up final stages of gas pressure bleed down for the time saving benefit.

Suction of gas downward from the well head was used to reduce gas hazards on the rig floor when unsealed insertions or removals were necessary.

## CONCLUSIONS GAINED FROM OPERATIONAL EXPERIENCE

The experience gained from the design and operation of this unique vent gas treatment facility has initiated a number of research and development studies to overcome many of the process engineering problems uncovered.

We are actively studying methods of arresting detonation waves. Solution of this problem would eliminate necessity of air dilution, with a subsequent decrease in size of processing equipment capacity by an order of magnitude.

From the measured performance of the charcoal scrubbers, we believe much of the radioiodine released was present as organic compounds possibly $CH_3I$. We have completed studies on improving the performance of charcoal adsorption beds for the removal of $CH_3I$. We are now studying new analytical techniques which will allow us to determine the chemical state of iodine in future field experiments.

Basic studies of the chemical nature of an undergound nuclear explosion are underway. We plan to use computer calculation tenchiques and laboratory scale experiments, as well as actual field experiments involving underground nuclear detonations.

With the results obtained from these basic studies, we expect to be able to make better predictions of inlet feed streams and to design more compact, higher performance vent gas treatment plants in the future.

# AN ENGINEERING EVALUATION OF A RADIOACTIVE-WASTE INCINERATOR

David G. Lachapelle

US ARMY
NUCLEAR DEFENSE LABORATORY
Edgewood Arsenal, Maryland

## ABSTRACT

A 50 lb/hr incinerator and associated gas-cleaning equipment for the concentration of low-level radioactive waste have been evaluated by use of non-radioactive material. Optimum operating conditions for the incinerator and the gas cleaning equipment have resulted from this investigation. These optimum operating conditions are being employed during the radiological evaluation.

Tests utilizing sawdust charges containing up to 200 μc/kg of charge have been successfully incinerated. Activity concentration of the $Sr^{89}$ discharged to atmosphere were always below MPC limits.

Tests are presently being conducted in which animals injected intravenously with $Sr^{89}$ are being incinerated to determine if this type charge can be safely handled by the facility. The maximum amount of $Sr^{89}$ injected corresponds to 200 μc/kg of weight.

## INTRODUCTION

With the US Army's increased participation in nuclear activities, its requirements for practical and economic disposal of radioactive wastes have necessitated studies in incineration as a means of concentrating and disposing of combustible wastes. The US Army Nuclear Defense Laboratory (USANDL) has been requested to study and recommend disposal methods for these wastes.

As part of this overall effort, the USANDL and the Atomic Energy Commission (AEC) have co-sponsored an evaluation program for a 50-lb/hr incinerator and associated gas-cleaning equipment for the concentration of low-level radioactive combustible waste.[1,2] This experimental facility was designed and fabricated under joint sponsorship of the AEC and USANDL, AEC Agreement 18-62, to develop an economical incineration system to satisfy US Army and AEC requirements.

Two AEC-contracted preliminary studies were conducted. The Bureau of Mines, in an evaluation of their own unit, concluded that uniform combustion rates and maximum combustion efficiency were best achieved by use of

a tangential overfire air supply.[3] The Harvard University Air Cleaning Laboratory (ACL) then conducted an extensive stack-sampling and experimental program on the Bureau of Mines unit. As a result of these two investigations, the Harvard Laboratory developed the ACL II, a 25-lb/hr incinerator, which featured tangential overfire air and a secondary combustion chamber. Design of the 50-lb/hr incinerator was based on the evaluation of the ACL II.[3,4]

Techniques evaluated under the USANDL program included the use of overfire auxiliary air, continuous auxiliary gas fuel, combustion temperatures up to 2000°F, and effluent cleaning by dry methods.

## 1. BACKGROUND

### 1.1 Description of Facility.

1.1.1 Incinerator. The experimental incinerator, Figure 1.1, consists of a primary and secondary combustion chamber constructed of mild steel and lined with 2-1/2-inch-thick insulating-type refractory.[4]

Primary overfire air is admitted tangentially into the primary combustion chamber through two openings approximately 155 degrees apart and 24 inches above the grate. The primary air inlets consist of 3-inch stainless steel pipes into which specially shaped, annular-pipe sections may be inserted so that the effects of velocity variation at constant volumetric flow rate may be studied. Two sets of air inlets, constructed as panel insert sections, are provided. One pair is for tangential horizontal air admission; the other is for directing inlet air tangentially downward at a 30-degree angle relative to the horizontal.

Secondary combustion air is admitted tangentially through a single 2-inch pipe, 6-3/8 inches above the base of the secondary combustion chamber. Annular inserts are again provided to permit velocity variation.

The incinerator utilizes continuous auxiliary gas firing in both combustion chambers to minimize discharge of unburned materials, and to maintain desired operating temperatures up to 2500°F. The auxiliary gas-firing system also serves to preheat the combustion chambers prior to the charging of waste.

Waste material is introduced as packaged charges, 6 to 10 pounds at a time, through a side-loading door (Figure 1.2). A three-pronged sliding fork, inserted through the loading door, permits temporary suspension of wet packaged charges above the grate to facilitate

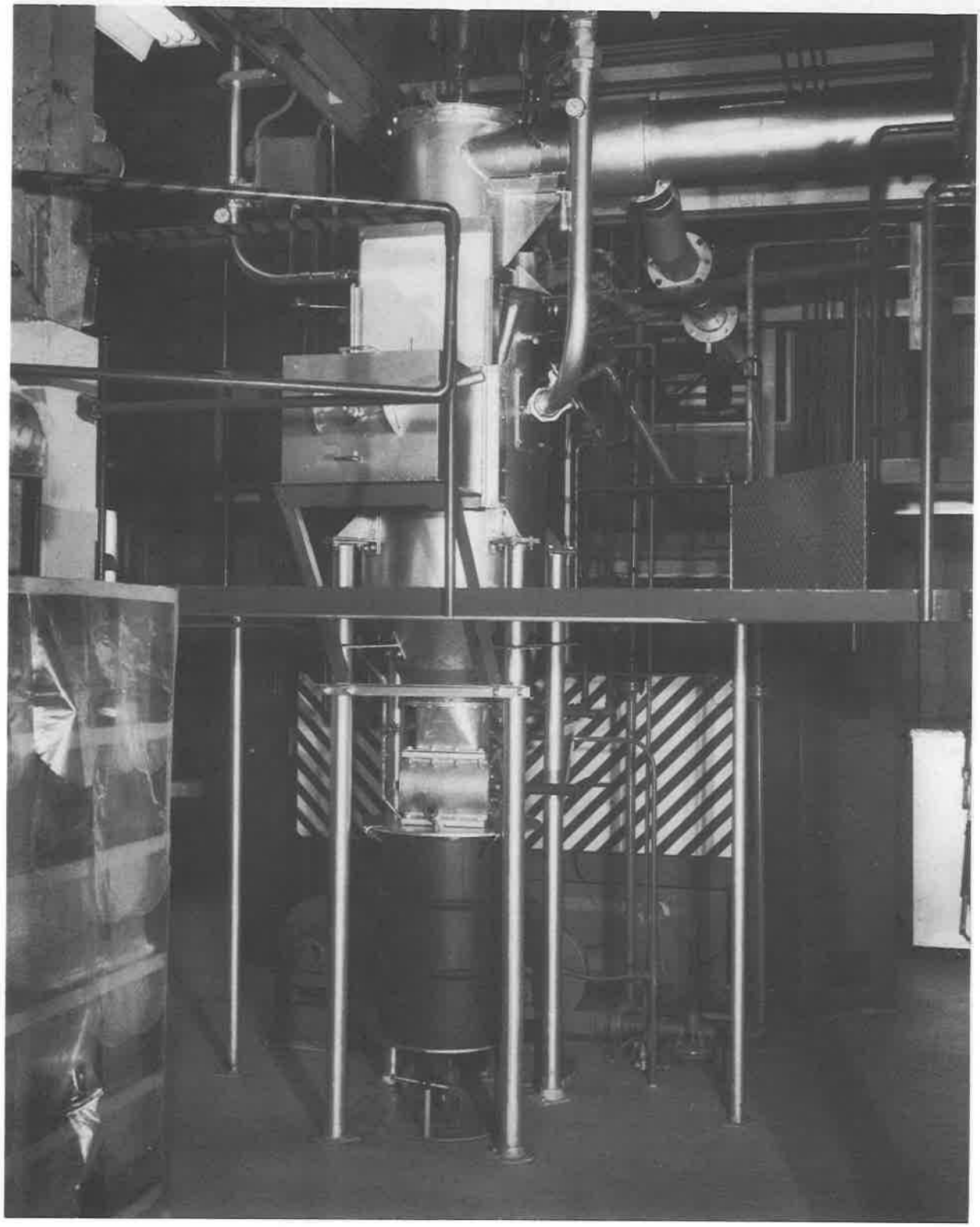

Figure 1.1 Incinerator for disposal of low-level radioactive waste.

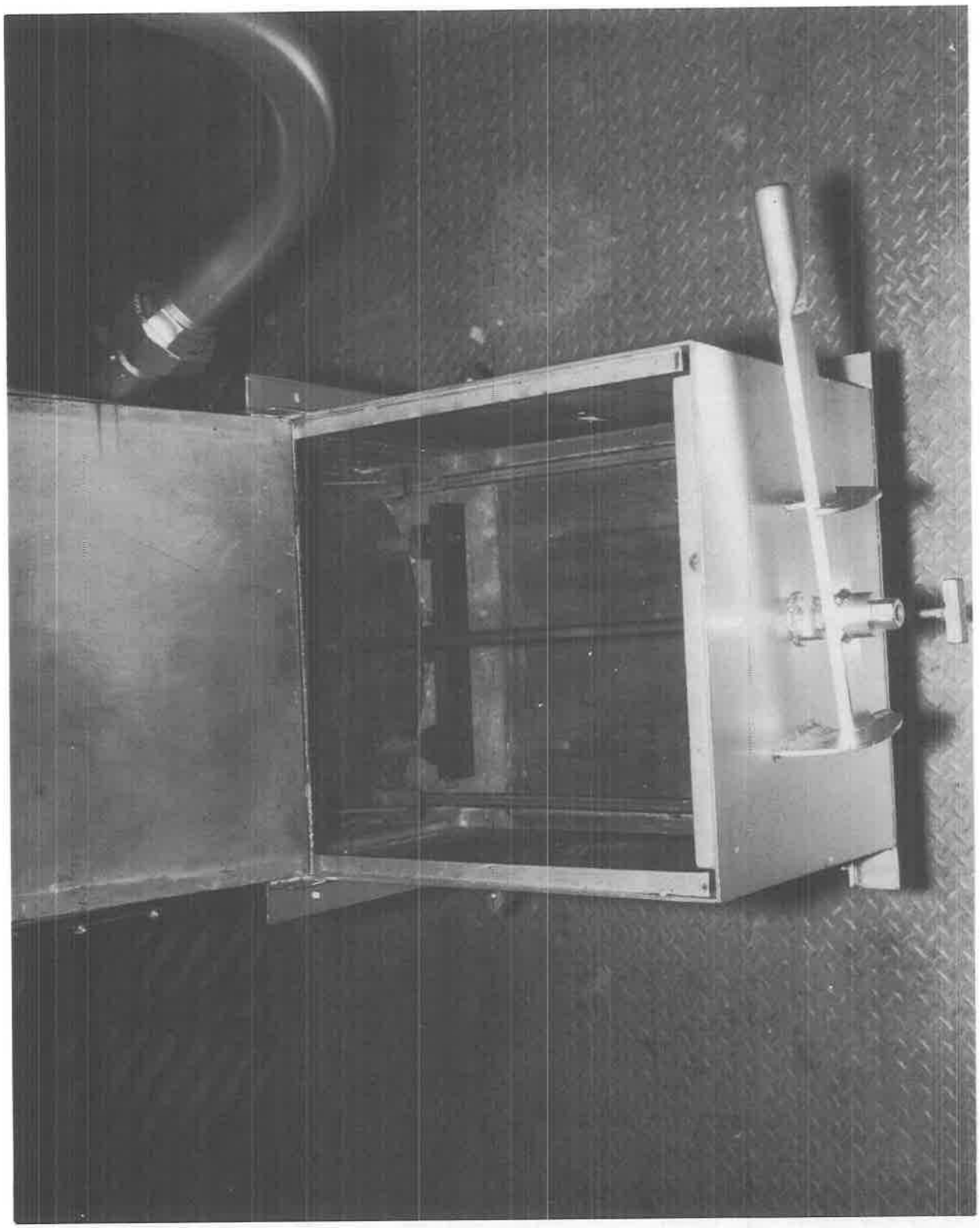

Figure 1.2 Side loading door.

rapid drying. A manually operated protective guillotine door, in conjunction with a totally enclosed charging lock, is provided to eliminate exposure of operating personnel to accidental release of dust or fumes during the charging operation.

Ashes drop through grate openings into a conical ash receiver and are discharged through a rotary valve into a 55-gallon drum for storage. A hydraulic jack maintains a tight air seal between the drum rim and the rotary valve.

Hot combustion gases exit tangentially from the secondary combustion chamber, and are cooled by dilution with ambient air before they enter the gas-cleaning equipment. (Figure 1.3).

1.1.2 Gas-Cleaning Equipment. Cooled combustion gases, after leaving the incinerator and passing through the air-dilution valve, enter a medium-velocity, involute-cyclone separator which removes coarse entrained particulate. The cyclone also provides extended cooling surface for gas-temperature reduction. Collected particulate is discharged through a slide valve into a 55-gallon drum. The slide valve permits continuous operation of the gas-cleaning system while drums are being changed. A hydraulic jack maintains a tight air seal between the drum rim and the cyclone bottom. Screw jacks are employed as a safety measure in the event of hydraulic failure.

Effluent from the cyclone enters a Cottrell-type electrostatic precipitator for removal of fine solid particles, soot, mineral dust, and tar droplets formed by condensation of volatile organic vapors. The precipitator is designed to apply a high negative charge to the gas-borne particles and collect the charged particles on grounded metal plates.

The particles are charged by rows of vertical wires mounted in parallel frames, 4 inches apart. The frames are connected to the negative terminal of a variable 30,000-volt DC power supply. The wires are cleaned by vibrators connected to the frames through nonconductive shafts. Dust shaken from the wires falls into a hopper. The grounded collector plates are parallel to the rows of wires in an alternate array and are cleaned by a rapper mechanism which lightly raps the bottom plate support to release the dust particles; this dust also falls into the hopper. Gas flow is parallel to the wire frames and collector plates. The collected dust is discharged through a slide valve into a 55-gallon drum beneath the hopper. The slide valve allows continuous operation of the precipitator while the drums are being changed. A hydraulic jack maintains a tight air seal between the drum rim and hopper bottom. As with the cyclone, screw jacks are employed as a safety measure. The precipitator is cleaned only when the remainder of the facility is inoperative; otherwise, dust would be carried into the filter bank.

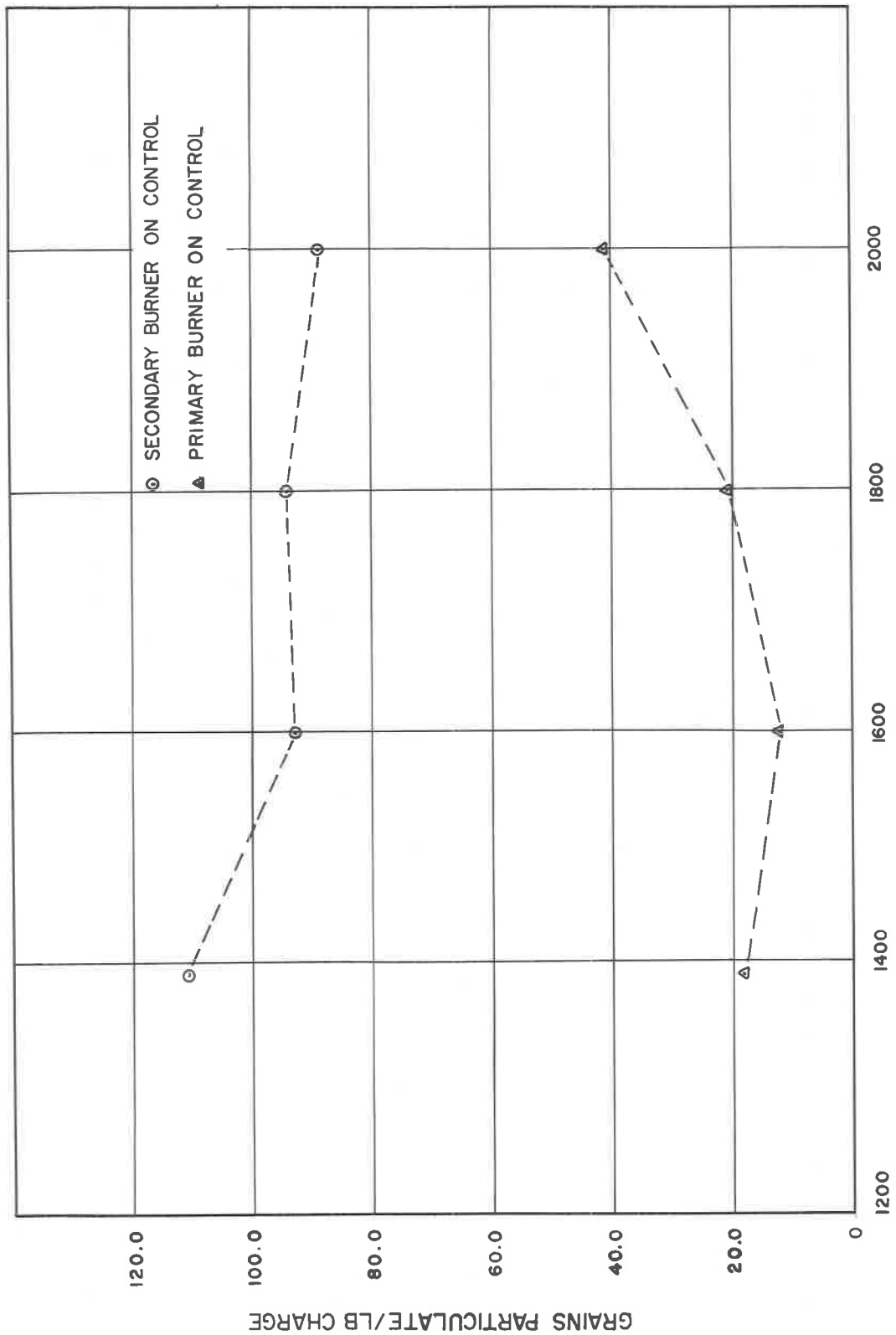


Figure 3.1 Incinerator effluent dust load versus control mode and control temperature.

Charge Composition: Sawdust

Gas leaving the precipitator enters a filter bank of two absolute filters. The unit is designed to collect particulate blow-off from the electrostatic precipitator and to provide limited emergency protection in the event of electrical power failure or precipitator malfunction. The unit accepts filters 24 by 24 inches, up to 12 inches deep.

REFERENCES


1. Dennis, R., Kyritsis, W., and Bloore, E., An Evaluation Program for Radioactive Waste Incineration, NDL-TM-8, March 1963.

2. Lachapelle, D., Tarbox, J., and Goff, D., Evaluation Program for Radioactive Waste Incineration (Supplement), NDL-TM-24, October 1965.

3. Corey, R. C., Spano, L. A., Schwartz, C. H., and Perry, H., Experimental Study of Effects of Tangential Overfire Air on the Incineration of Combustible Waste, Air Repair 3, 1-8, 1953.

4. Bloore, E., and Lachapelle, D., A Radioactive Waste Incinerator, Proceedings of the 8th AEC Air Cleaning Conferences, October 22-25, 1963; TID-7677.


## 2. ENGINEERING EVALUATION

The engineering evaluation was concerned with studying and defining the operating conditions that would result in the most efficient operation of the facility. These tests utilized combustible charges that were radioactively "cold" but similar to the types of waste that the system was designed to handle (waste paper, towels, swab rags, surgical dressings, wood, animal carcasses, human or animal organs, rubber gloves, rubber or plastic tubing, and animal pen debris, such as sawdust, feces, and vegetable matter). To eliminate the charge composition as a process variable, the types of waste incinerated during the engineering evaluation were minimized; they included sawdust of known moisture content and consistency, and frozen animal carcasses. Each experiment outlined in succeeding sections was performed on each of these wastes individually.

The limiting factor in the successful radiological operation of this system is the efficiency of the gas-cleaning system. Therefore, it was imperative that the combustion process be regulated to generate effluent that the gas-cleaning system could most efficiently remove from

the exhaust gases. Variables that were investigated to determine combustion conditions for optimum gas cleaning included: furnace temperature, air-gas ratios and rates of the auxiliary fuel supply, auxiliary combustion air rates, velocities, and angle of entry. These variables affected burning rates, combustion efficiency, and dust loadings into the cyclone, ESP, and absolute filters. Variables that affected the gas-cleaning system were: dust load, cyclone-inlet velocity, flow rate and temperature through the ESP, ESP output voltage, and flow rate through the absolute filters.

Results of the engineering evaluation have defined (1) overall cleaning efficiencies of each gas-cleaning unit and of the entire gas-cleaning system; (2) optimum operating conditions of the incinerator and gas-cleaning system for each type waste; and (3) the overall weight and volume reduction of each type waste, under optimum conditions.

The engineering evaluation was divided into three major sections: (1) temperature experiments, (2) overfire air experiments and (3) gas-cleaning system efficiency experiments.

## 3. TEMPERATURE EXPERIMENTS

### 3.1 Background.

Incinerator effluent gas temperature is controlled by an on-off controller connected to a platinum/platinum-10 percent rhodium (Type-S) thermocouple located in the incinerator exit pipe. Either the primary or secondary burner can be controlled, the controlled burner modulating from a high-fire to low-fire position when required. Temperature modulation during control is $\pm 20^{\circ}$F about the set point. The burner not being controlled can be locked on a high-fire or low-fire position. Approximate burner outputs are as follows:

| | | |
|---|---|---|
| Primary Burner: | High Fire: | 290,000 BTU/h |
| | Low Fire: | 134,500 BTU/h |
| Secondary Burner: | High Fire: | 165,000 BTU/h |
| | Low Fire: | 73,000 BTU/h |

### 3.2 Objectives.

The objectives of these experiments were to establish a correlation of incinerator operating temperature and temperature control mechanism (control on primary combustion-chamber burner or on secondary combustion-

chamber burner) with effluent-dust loadings and gross burning rate. Appropriate temperature-operating conditions for optimum combustion efficiency and gas-cleaning efficiency have resulted from these experiments.

## 3.3 Procedures.

Tests performed during these experiments utilized two fixed composition charges of sawdust and rabbit carcasses. Horizontal auxiliary-air and dilution-air rates were adjusted to yield approximate design capacity and velocities throughout the system. Temperature controller set point was varied from 1400°F to 2000°F during the tests with sawdust. The carcasses were incinerated at 2000°F since trial runs had indicated the impracticability of incinerating carcasses at lower temperatures. Tests were conducted in both instances with primary and secondary burner control. Iso-kinetic sampling on pre-weighed filters was utilized to determine effluent dust loads and weight collection efficiency for the gas-cleaning system.

## 3.4 Results.

Tables 3.1 to 3.6 show the operating data and results pertinent to the specific test conducted.

## 3.5 Discussion.

Incinerator effluent dust loads generated during incineration of the sawdust charges were significantly lower with the primary burner on control than with the secondary burner on control, as shown in Figure 3.1. Additionally, loading periods were substantially shorter while on primary control modes, except at 2000°F (Figures 3.2 through 3.9). An AISI dust sampler with photo-electric cell and readout was used. Burner modulation in the sawdust tests conducted at 1800°F and 2000°F with the primary burner on control caused disturbance of the burning charge, exposed additional surface for combustion, and resulted in an increase in the amount of particulate leaving the incinerator. The AISI and temperature curves for the specific tests indicate the extent to which this effect occurred. Lowest loadings for sawdust charges occurred at 1600°F with the primary burner on control (Figure 3.1).

Figure 3.10 shows the burning rate for sawdust charges at the temperatures and control modes employed. Burning rates with the secondary burner on control are essentially constant since the primary burner is in a locked high-fire position and burner modulation occurs only in the secondary chamber.

TABLE 3.1 TESTS WITH SAWDUST AT 1400°F*

| | Primary on Control | Secondary on Control |
|---|---|---|
| Primary Auxiliary Air No. 1 CFM STP | 44.0 | 43.4 |
| Primary Auxiliary Air No. 2 CFM STP | 42.5 | 42.0 |
| Secondary Auxiliary Air CFM STP | 29.1 | 28.8 |
| Primary Burner Air CFM STP | 25.1 | 53.0 |
| Primary Burner Gas CFM STP | 0.99 | 2.13 |
| Secondary Burner Air CFM STP | 29.5 | 13.0 |
| Secondary Burner Gas CFM STP | 1.23 | 0.54 |
| Dilution Air CFM STP | 984.6 | 976.1 |
| Total Input CFM STP | 1157 | 1159 |
| Time at Load Conditions (min) | 2.59 | 5.53 |
| Burning Rate lb/h | 39.0 | 97.5 |
| Particulate Load: grains/$ft^3$ | $6.06 \times 10^{-2}$ | $1.73 \times 10^{-1}$ |
| Grains Particulate/lb Charge | 18.2 | 110.9 |

*Charge weight 10 lbs.

TABLE 3.2 TESTS WITH SAWDUST AT 1600°F*

| | Primary on Control | Secondary on Control |
|---|---|---|
| Primary Auxiliary Air No. 1 CFM STP | 44.3 | 44.3 |
| Primary Auxiliary Air No. 2 CFM STP | 42.9 | 42.9 |
| Secondary Auxiliary Air CFM STP | 29.8 | 29.8 |
| Primary Burner Air CFM STP | 25.1 | 53.2 |
| Primary Burner Gas CFM STP | 0.99 | 2.13 |
| Secondary Burner Air CFM STP | 29.5 | 13.0 |
| Secondary Burner Gas CFM STP | 1.23 | 0.54 |
| Dilution Air CFM STP | 992.2 | 980.1 |
| Total Input CFM STP | 1166 | 1166 |
| Time at Load Conditions (min) | 2.06 | 5.0 |
| Burning Rate lb/h | 44.6 | 94.3 |
| Particulate Load: grains/$ft^3$ | $5.11 \times 10^{-2}$ | $1.59 \times 10^{-1}$ |
| Grains Particulate/lb Charge | 12.3 | 92.7 |

*Charge weight 10 lbs.

TABLE 3.3 TESTS WITH SAWDUST AT 1800°F*

| | Primary on Control | Secondary on Control |
|---|---|---|
| Primary Auxiliary Air No. 1 CFM STP | 44.0 | 43.4 |
| Primary Auxiliary Air No. 2 CFM STP | 42.5 | 42.0 |
| Secondary Auxiliary Air CFM STP | 29.1 | 28.8 |
| Primary Burner Air CFM STP | 25.1 | 53.0 |
| Primary Burner Gas CFM STP | 0.99 | 2.13 |
| Secondary Burner Air CFM STP | 29.5 | 13.0 |
| Secondary Burner Gas CFM STP | 1.23 | 0.54 |
| Dilution Air CFM STP | 985.6 | 976.1 |
| Total Input CFM STP | 1157 | 1159 |
| Time at Load Conditions (min) | 2.04 | 5.6 |
| Burning Rate lb/h | 54.5 | 97.5 |
| Particulate Load: grains/$ft^3$ | $8.86 \times 10^{-2}$ | $1.45 \times 10^{-1}$ |
| Grains Particulate/lb Charge | 20.9 | 94.1 |

*Charge weight 10 lbs.

TABLE 3.4 TESTS WITH SAWDUST AT 2000°F*

| | Primary on Control | Secondary on Control |
|---|---|---|
| Primary Auxiliary Air No. 1 CFM STP | 44.3 | 44.3 |
| Primary Auxiliary Air No. 2 CFM STP | 42.9 | 42.9 |
| Secondary Auxiliary Air CFM STP | 29.8 | 29.8 |
| Primary Burner Air CFM STP | 25.1 | 53.2 |
| Primary Burner Gas CFM STP | 0.99 | 2.13 |
| Secondary Burner Air CFM STP | 29.5 | 13.0 |
| Secondary Burner Gas CFM STP | 1.23 | 0.54 |
| Dilution Air CFM STP | 992.2 | 980.1 |
| Total Input CFM STP | 1166 | 1166 |
| Time at Load Conditions (min) | 6.47 | 4.75 |
| Burning Rate lb/h | 80.0 | 100.0 |
| Particulate Load: grains/$ft^3$ | $5.48 \times 10^{-2}$ | $1.60 \times 10^{-1}$ |
| Grains Particulate/lb Charge | 41.3 | 88.6 |

*Charge weight 10 lbs.

TABLE 3.5 TESTS WITH CARCASSES AT 2000°F

| | Primary on Control | Secondary on Control |
|---|---|---|
| Primary Auxiliary Air No. 1 CFM STP | 24.4 | 24.4 |
| Primary Auxiliary Air No. 2 CFM STP | 24.7 | 24.7 |
| Secondary Auxiliary Air CFM STP | 19.8 | 19.8 |
| Primary Burner Air CFM STP | 24.7 | 52.3 |
| Primary Burner Gas CFM STP | 1.08 | 2.38 |
| Secondary Burner Air CFM STP | 28.3 | 12.5 |
| Secondary Burner Gas CFM STP | 1.16 | 0.51 |
| Dilution Air CFM STP | 874.9 | 862.4 |
| Total Input CFM STP | 999 | 999 |
| Time at Load Conditions (min) | 1.0 | 1.5 |
| Charge Wt. (lbs) | 5.5 | 5.3 |
| Burning Rate lb/h | 11.4 | 12.5 |
| Particulate Load: grains/$ft^3$ | $1.84 \times 10^{-1}$ | $9.82 \times 10^{-2}$ |
| Grains Particulate/lb Charge | 33.4 | 27.8 |

TABLE 3.6 TESTS WITH CARCASSES AT 2000°F

| | Both Burners High-Fire | Primary on Control* |
|---|---|---|
| Primary Auxiliary Air No. 1 CFM STP | 24.4 | 24.4 |
| Primary Auxiliary Air No. 2 CFM STP | 24.7 | 24.7 |
| Second Auxiliary Air CFM STP | 19.8 | 19.8 |
| Primary Burner Air CFM STP | 52.3 | 24.7 |
| Primary Burner Gas CFM STP | 2.38 | 1.08 |
| Secondary Burner Air CFM STP | 28.3 | 28.3 |
| Secondary Burner Gas CFM STP | 1.16 | 1.16 |
| Dilution Air CFM STP | 846.0 | 874.9 |
| Total Input CFM STP | 999 | 999 |
| Time at Load Conditions (min) | 1.0 | 4.0 |
| Charge Wt. (lbs) | 5.3 | 16.5 |
| Burning Rate lb/h | 12.4 | 37.2 |
| Particulate Load: grains/$ft^3$ | $1.24 \times 10^{-1}$ | $1.0 \times 10^{-1}$ |
| Grains Particulate/lb Charge | 23.4 | 24.2 |

*Special test for gross charging rate.

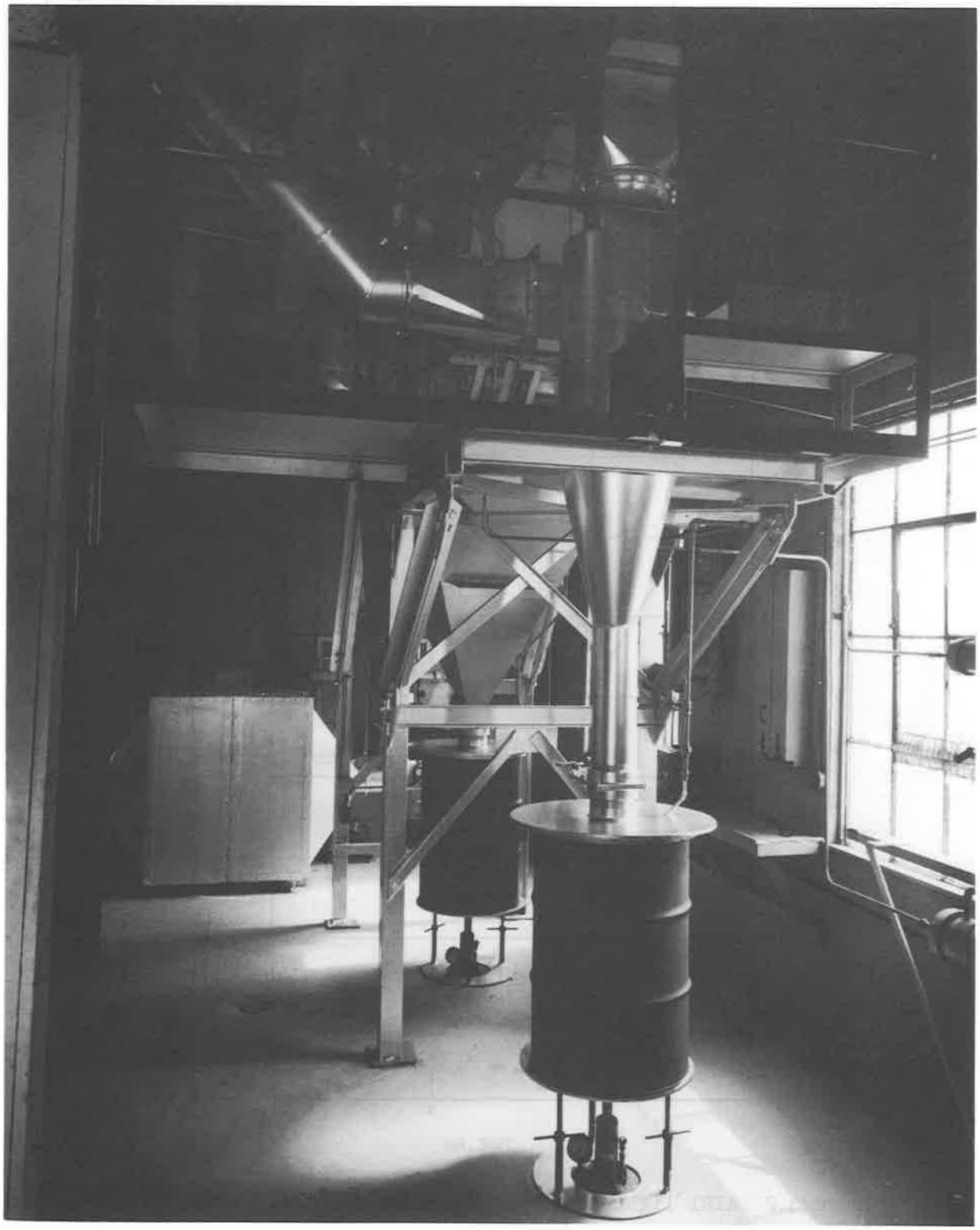

Figure 1.3 Gas-cleaning system.

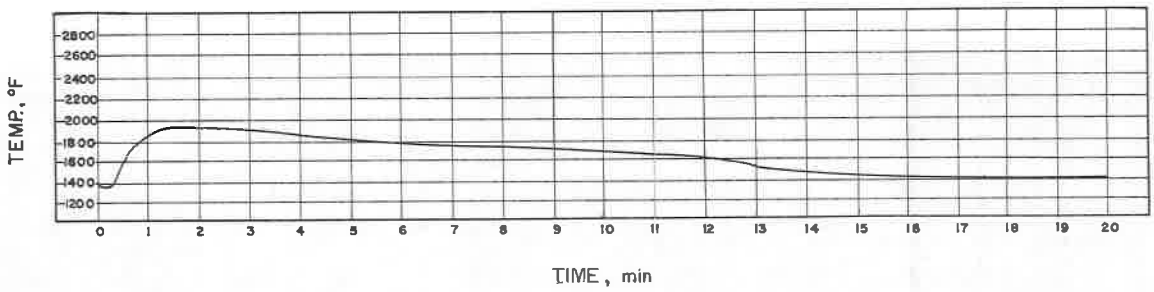


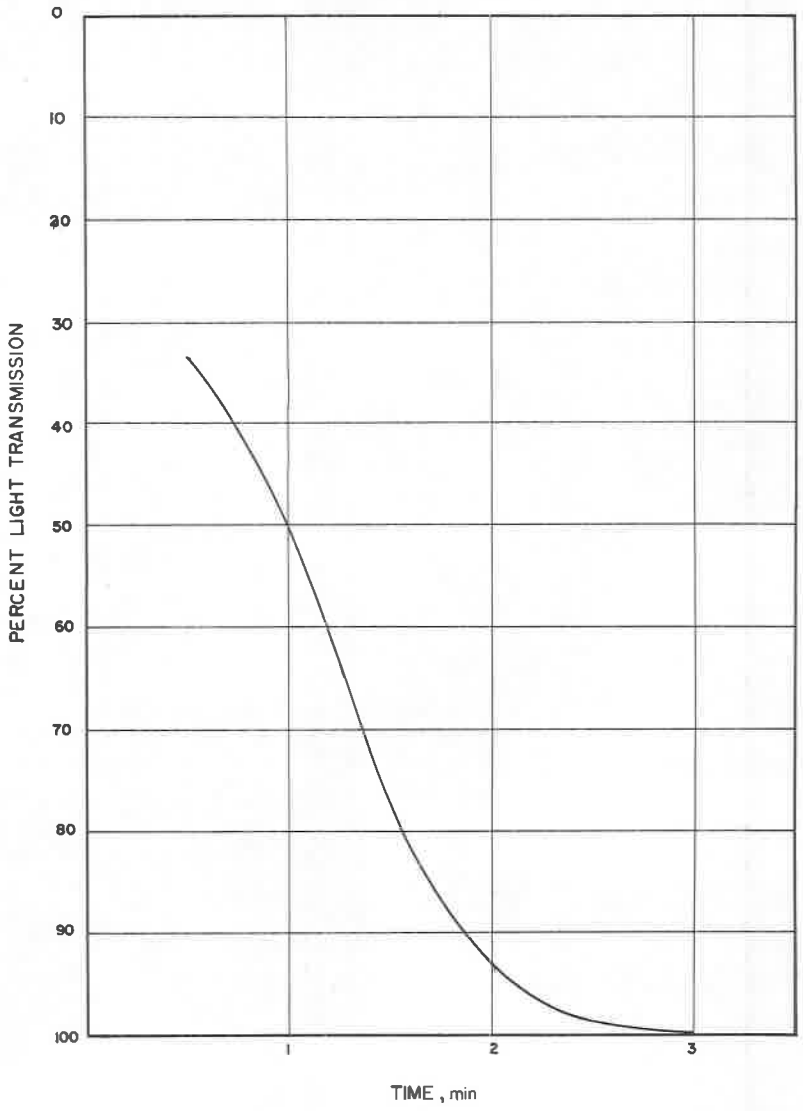


Figure 3.2 AISI light transmission curve and temperature curve.

Control Temperature: 1400°F
Primary Burner on Control
Charge Composition: Sawdust

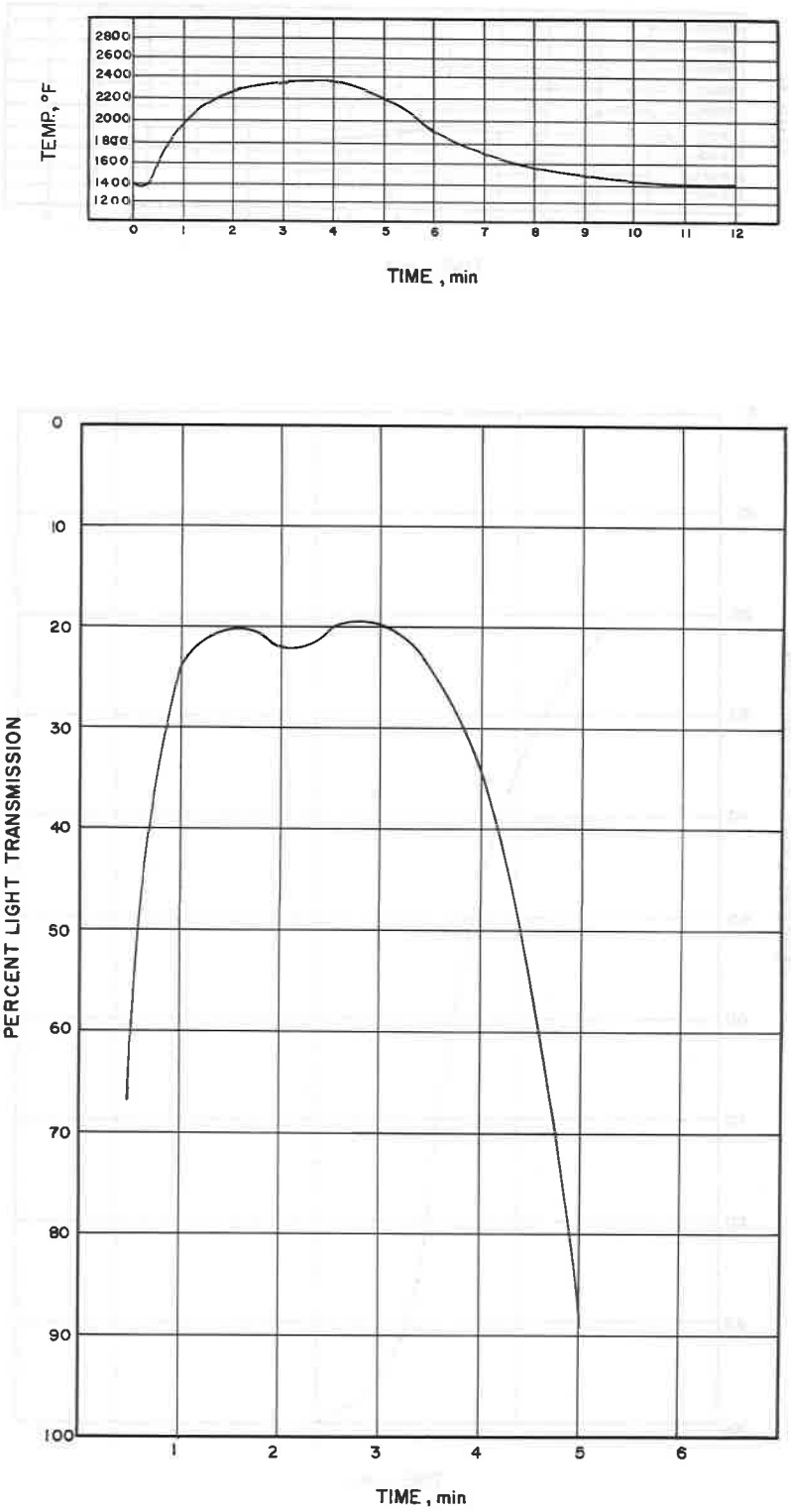


Figure 3.3 AISI light transmission curve and temperature curve.

Control Temperature: 1400°F
Secondary Burner on Control
Charge Composition: Sawdust

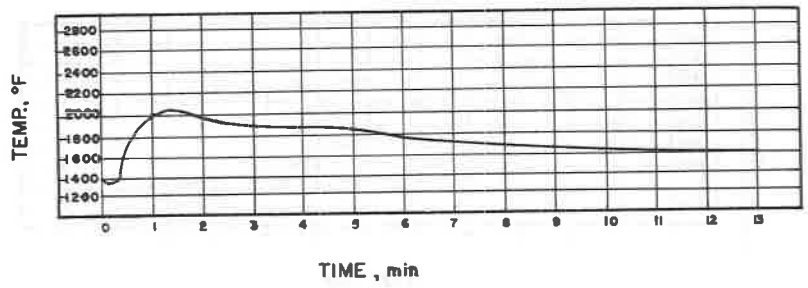


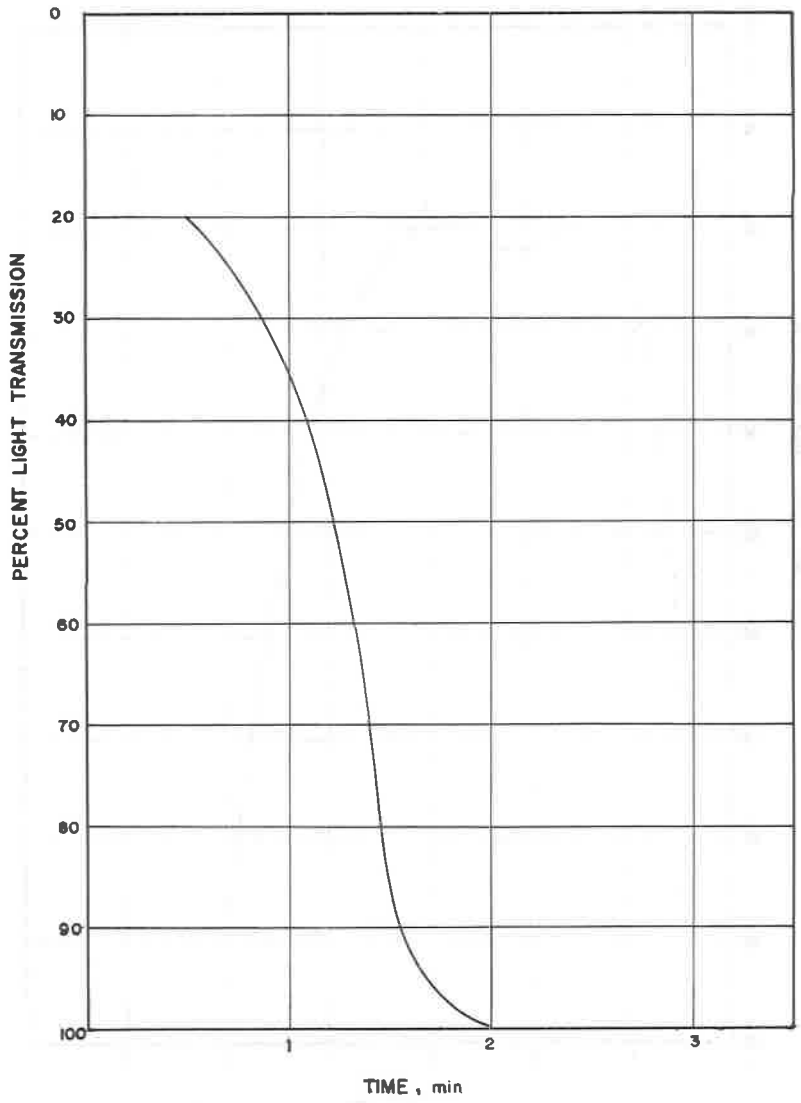


Figure 3.4 AISI light transmission curve and temperature curve.

Control Temperature: 1600°F
Primary Burner on Control
Charge Composition: Sawdust

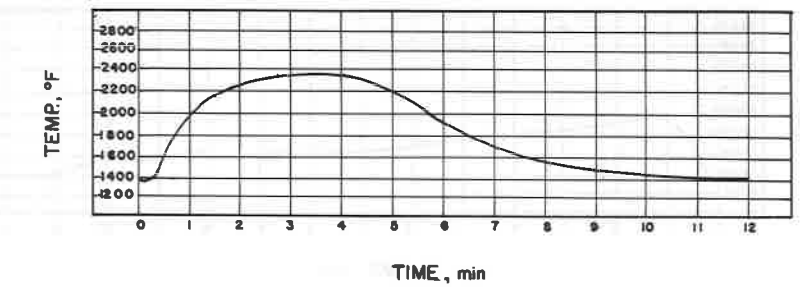


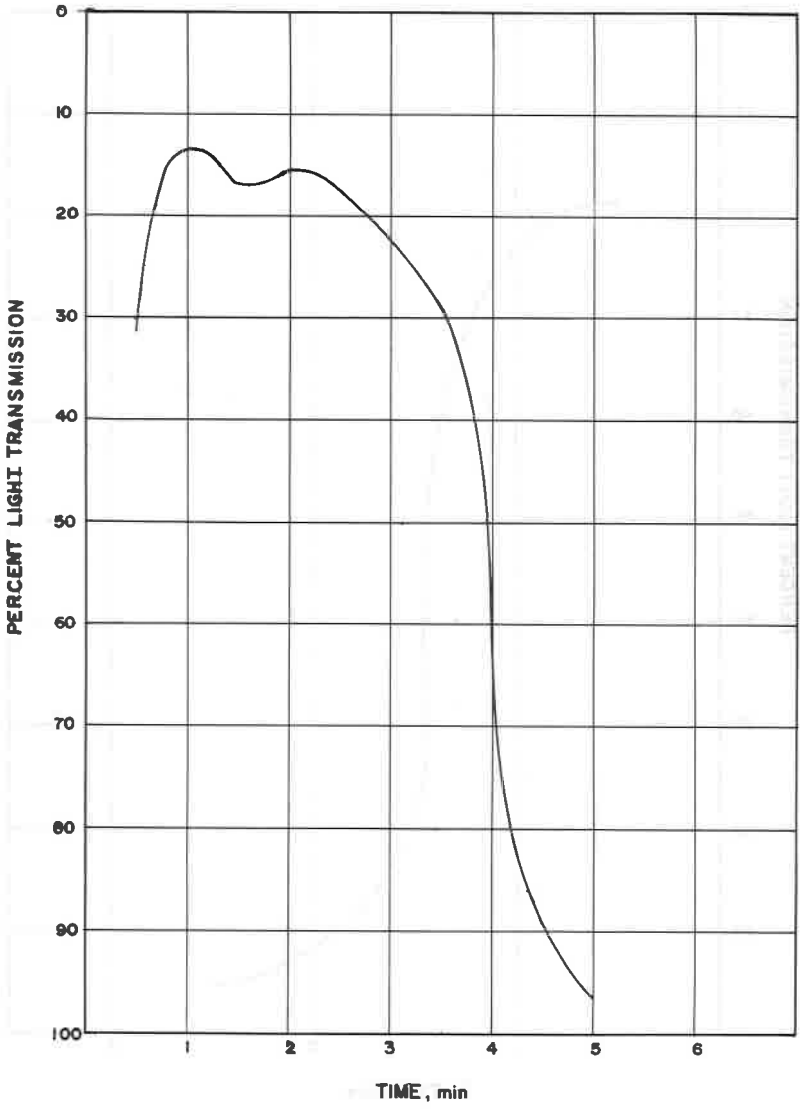


Figure 3.5 AISI light transmission curve and temperature curve.

Control Temperature: 1600°F
Secondary Burner on Control
Charge Composition: Sawdust

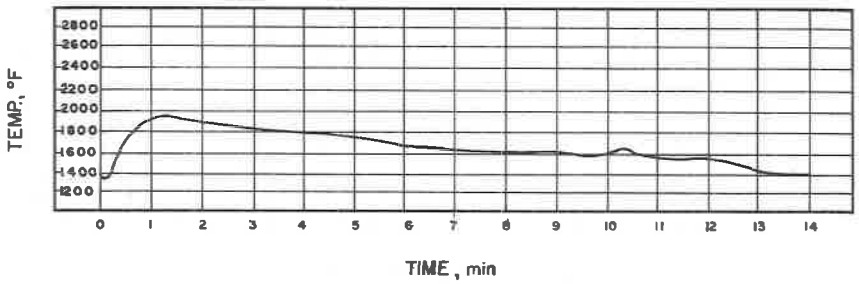


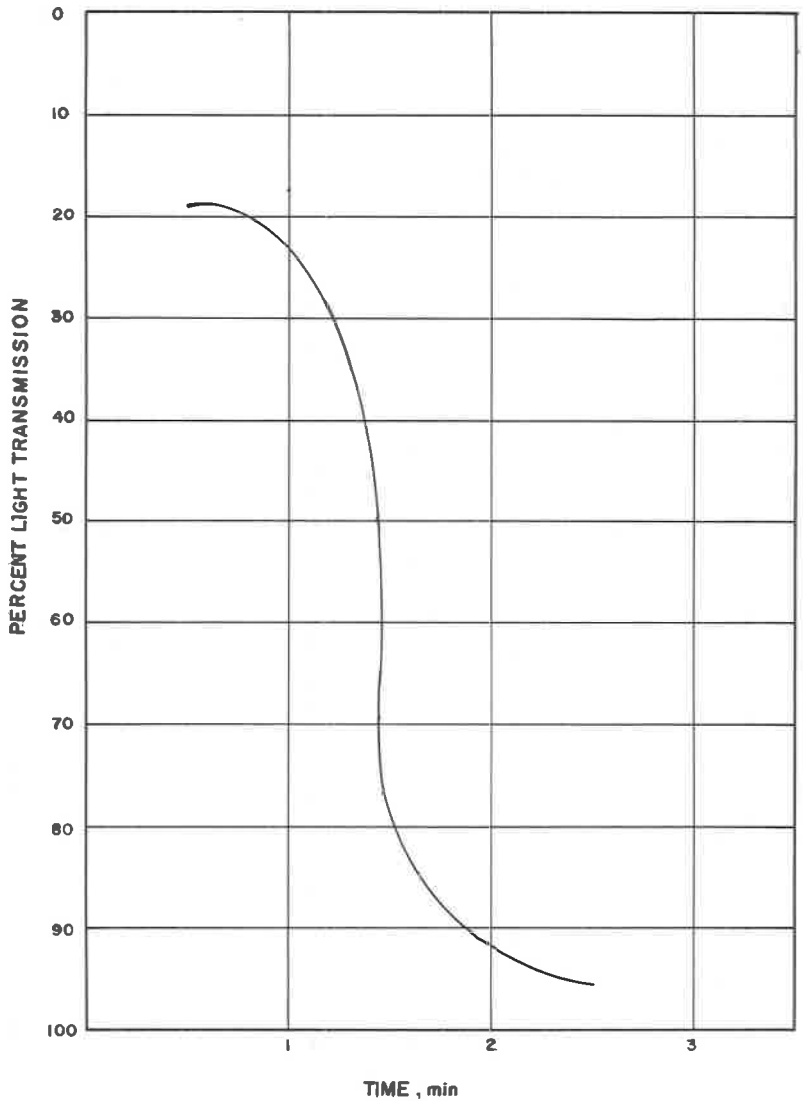


Figure 3.6 AISI light transmission curve and temperature curve.

Control Temperature: 1800°F
Primary Burner on Control
Charge Composition: Sawdust

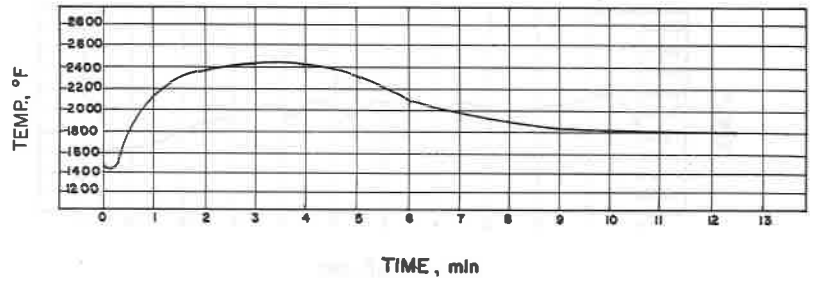


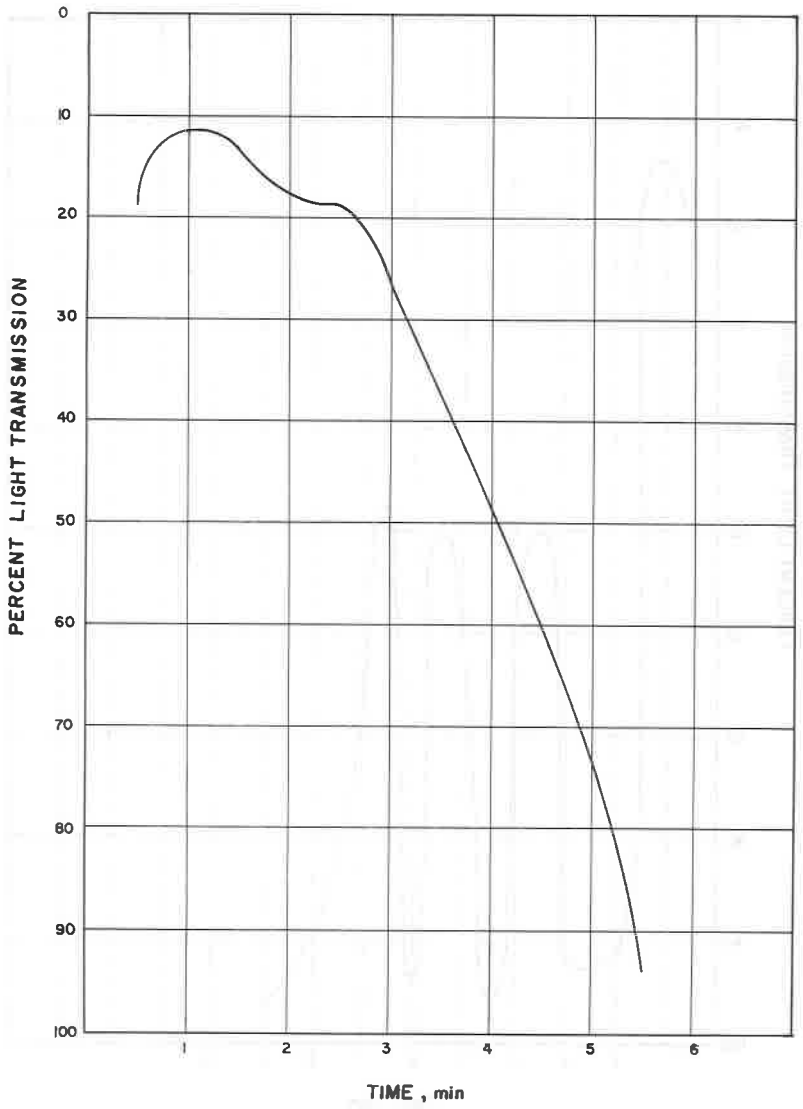


Figure 3.7 AISI light transmission curve and temperature curve.

Control Temperature: 1800°F
Secondary Burner on Control
Charge Composition: Sawdust

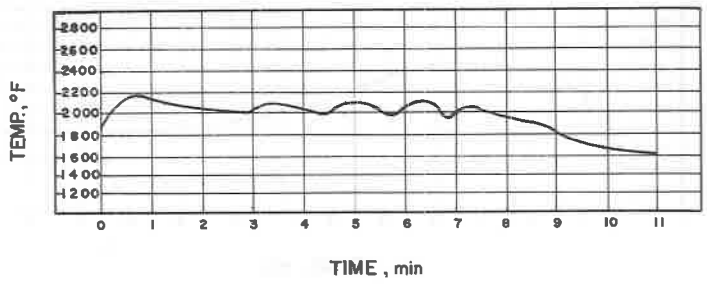


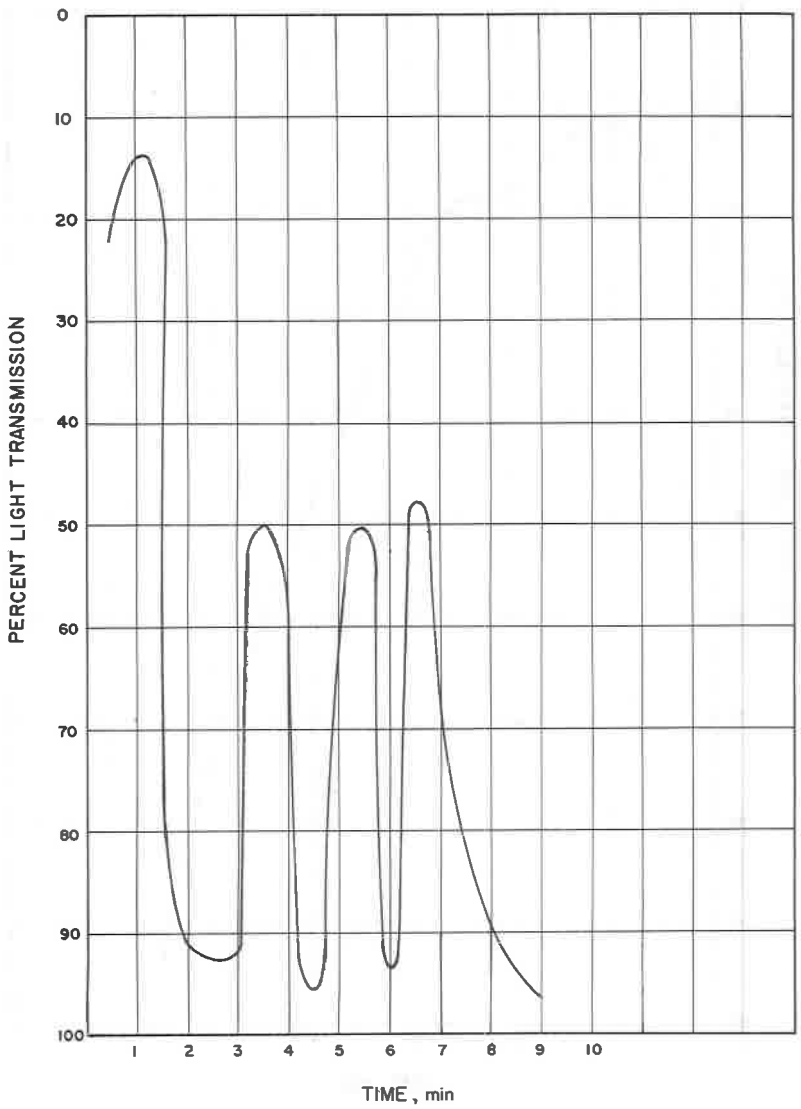


Figure 3.8 AISI light transmission curve and temperature curve.

Control Temperature: 2000°F
Primary Burner on Control
Charge Composition: Sawdust

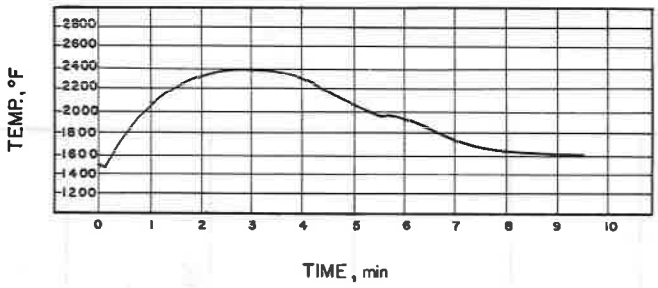


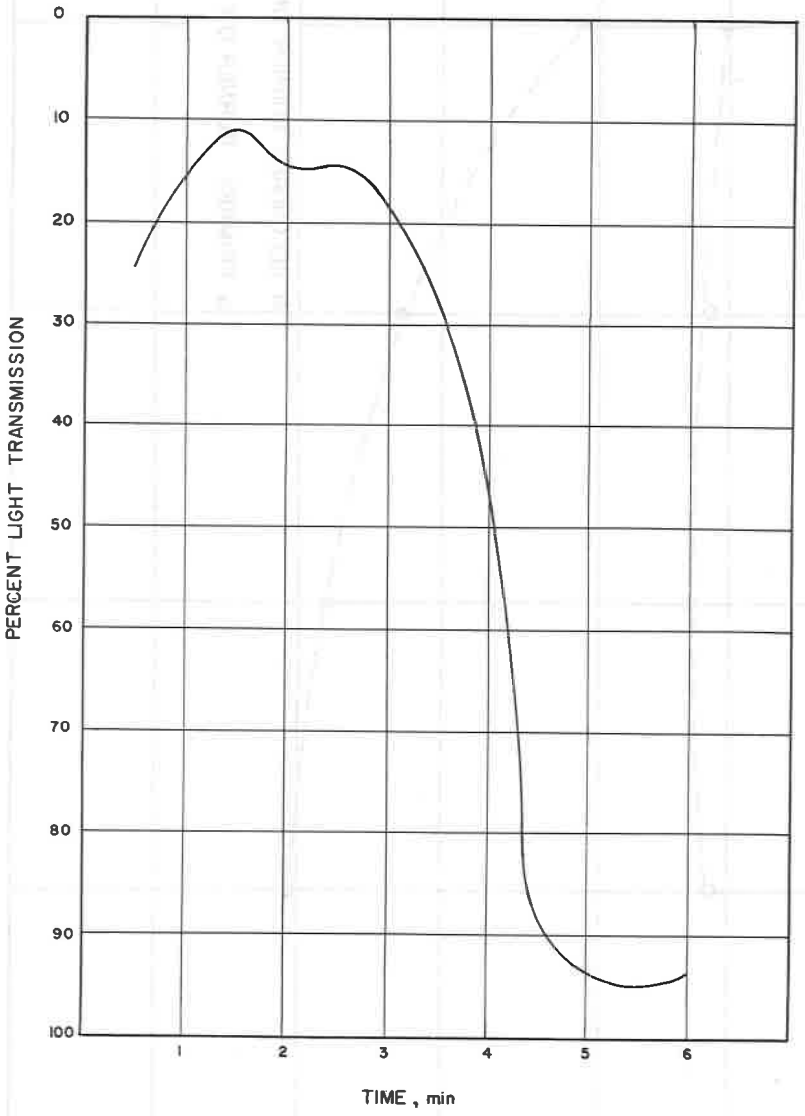


Figure 3.9 AISI light transmission curve and temperature curve.

Control Temperature: 2000°F
Secondary Burner on Control
Charge Composition: Sawdust

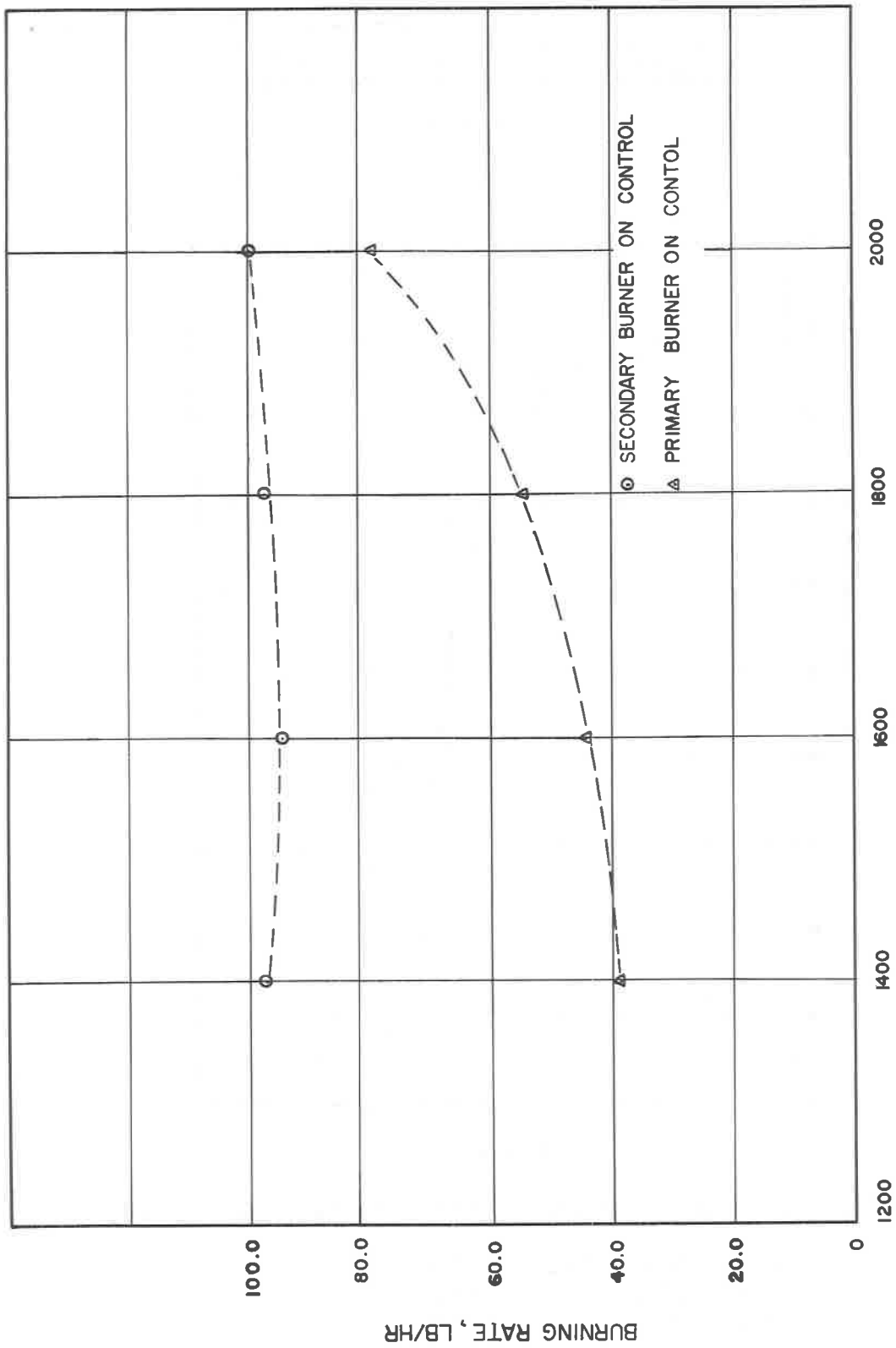


Figure 3.10 Burning rate versus control mode and control temperature.

Charge Composition: Sawdust

However, burning rates varied significantly with the primary burner on control, since burner modulation served to disturb the burning charge and expose more surface for combustion. These higher burning rates were accompanied by higher dust loads at temperatures above 1600°F.

Incinerator effluent dust loads generated during incineration of carcasses were somewhat higher than those obtained at the optimum condition of 1600°F for sawdust. It should be mentioned here that the carcasses were enclosed in a large polyethylene bag which in turn was placed on a cardboard slab for efficient charging purposes. Therefore, the dust load figures shown for carcasses include combustion products from the plastic and cardboard.

It appears that burner control is not as critical for incineration of carcasses as it is for sawdust and other cellulosic type wastes. The difference between dust loads for the two control modes was not nearly as significant as were the results of the sawdust tests.

Although burning rates for carcasses appear to be low, it should be stressed that when these tests were conducted, a single carcass was used for each test. Carcass size was very uniform but because of their size, only about 20 percent of the available grate area was being utilized as opposed to about 40 percent for sawdust charges. Another test conducted with four carcasses in a single bag gave the same burning time (3.3 times the gross burning rate) at no apparent increase in average effluent dust load.

## 3.6 Conclusions.

The secondary burner is a valuable aid in reducing the quantity of unburned material rising from the primary chamber. Consequently, the primary burner should be controlled and the secondary burner locked on a high-fire position.

Control temperatures in excess of 1600°F for sawdust charges result in burner modulation which increases the gross burning rate and the quantity of unburned material leaving the incinerator.

A control temperature of 1600°F with the primary burner on control appears to be the optimum combustion condition at which to incinerate cellulosic wastes, if a minimum amount of particulate is to be discharged into the gas-cleaning system.

Since burner control does not appear to be as critical for incineration of carcasses, primary burner control may also be employed, optimum temperature being 2000°F. If reasonable burning rates are to be achieved for carcasses, maximum utilization should be made of the available grate area.

## 4. OVERFIRE-AIR EXPERIMENTS

### 4.1 Background.

The advantages offered by the design of this facility's combustion chamber attributable to overfire (above grate) tangential-combustion-air entry include:

1. Elimination of gas flow fluctuations caused by passage of underfire air through a diminishing charge mass and variable open grate area.

2. Increased gas stream turbulence, resulting in improved mixing of combustibles with air.

3. Rapid heat transfer from the heated furnance walls to the gas stream.

4. Increased combustible retention time due to vortical or cyclonic gas flow thus minimizing discharge of unburned material.

5. Increased solids retention in the burning chamber resulting from centrifugal forces exerted on entrained particulate in the rotating gas stream.

Additionally, the secondary chamber maintains the cyclonic flow pattern and provides additional combustion air and heat to further minimize discharge of unburned material.

### 4.2 Objectives.

The objectives of these experiments were to establish a correlation of the auxiliary-air-inlet rate, velocity, and angle of entry with incinerator dust loading, combustion efficiency, and gross burning rate. Results of these experiments have defined optimum overfire-air conditions for optimum combustion efficiency and gas-cleaning efficiency.

### 4.3 Procedures.

Tests performed during these experiments utilized the two fixed composition wastes (sawdust and frozen rabbit carcasses). Control temperatures of 1600°F for sawdust and 2000°F for carcasses were employed. Primary burner control was used throughout these tests. Annular inserts in the primary and secondary auxiliary air inlets permitted variation in Reynolds numbers, $N_{Re}$ (11,000 to 70,000) through the inserts. Auxiliary-air flow rates were varied from 20 to 45 cfm for each air inlet during the sawdust experiments. Fixed air rates of 25 cfm in each primary

auxiliary air inlet and 20 cfm in the secondary auxiliary air inlet were used for the tests with carcasses. For ease in the presentation and discussion of results, code letters and subscripts are used. The code letters are: P indicating Primary air inlets and S indicating Secondary air inlet. Subscripts indicate the diameter of the annular insert being used. Subscript "0" indicates that no insert was used. Inside diameters are as follows:

$P_0$: 2.900 inches
$P_1$: 1.875 inches
$P_4$: 1.625 inches
$P_7$: 1.062 inches
$S_0$: 1.939 inches
$S_{11}$: 1.125 inches
$S_{13}$: 0.813 inches

When combinations of inserts are used they will be coded such as $P_1/S_{11}$ indicating that the primary air inlets had inserts of 1.875 inches inside diameter and that the secondary air inlet had an insert of 1.125 inches inside diameter.

## 4.4 Results.

Tables 4.1 to 4.4 show the results of the specific overfire air test conducted.

## 4.5 Discussion.

Figure 4.1 shows the incinerator effluent dust load for sawdust charges as a function of $N_{Re}$ through the horizontal primary auxiliary air inlets. No inserts were used in the secondary air inlet for these tests. $N_{Re}$ in the secondary auxiliary air inlet was essentially constant for the particular air rate involved. $N_{Re}$'s in the secondary auxiliary air inlet were approximately 19,750, 29,600, and 44,000 for 20, 30, and 45 cfm. These tests therefore represent the effects of turbulence in the primary chamber with an essentially constant condition in the secondary chamber.

Minimum dust loads occurred with the $P_4$ annular insert, and 20 and 30 cfm per inlet auxiliary air; the dust load was lower at the higher air rate. Further increase in turbulence at these air rates caused higher dust loads and rapid disturbance of the burning bed. Tests at 45 cfm gave a steady rise in dust load due to increased bed turbulence.

Figure 4.2 shows the incinerator effluent dust load for sawdust charges as a function of $N_{Re}$ through the secondary auxiliary air inlet. No annular inserts were used in the horizontal primary air inlets for these tests. $N_{Re}$'s in the horizontal primary auxiliary air inlets were

TABLE 4.1 OVERFIRE AIR TESTS WITH SAWDUST CHARGES

Note: Flow rate per inlet, 20 cfm STP

| Insert | Grains Particulate Per Pound of Charge | |
|---|---|---|
| | Horizontal Air | 30° Air |
| $P_0/S_0$ | 20.3 | 34.8 |
| $P_1/S_0$ | 39.2 | 37.4 |
| $P_4/S_0$ | 20.7 | 25.2 |
| $P_7/S_0$ | 49.7 | 50.0 |
| $P_0/S_{11}$ | 20.0 | 31.2 |
| $P_0/S_{13}$ | 15.9 | 22.6 |
| $P_1/S_{11}$ | 24.5 | 29.6 |
| $P_4/S_{13}$ | 20.3 | 27.3 |

TABLE 4.2 OVERFIRE AIR TESTS WITH SAWDUST CHARGES

Note: Flow rate per inlet, 30 cfm STP

| Insert | Grains Particulate Per Pound of Charge | |
|---|---|---|
| | Horizontal Air | 30° Air |
| $P_0/S_0$ | 24.5 | 31.0 |
| $P_1/S_0$ | 25.9 | 27.1 |
| $P_4/S_0$ | 13.7 | 22.2 |
| $P_7/S_0$ | 33.6 | 24.7 |
| $P_0/S_{11}$ | 17.2 | 19.3 |
| $P_0/S_{13}$ | 16.4 | 18.7 |
| $P_1/S_{11}$ | 20.7 | 27.7 |
| $P_4/S_{13}$ | 14.5 | 18.0 |

TABLE 4.3 OVERFIRE AIR TESTS WITH SAWDUST CHARGES

Note: Flow rate per inlet, 45 cfm STP

| Insert | Grains Particulate Per Pound of Charge | |
|---|---|---|
| | Horizontal Air | 30° Air |
| $P_0/S_0$ | 13.9 | 13.4 |
| $P_1/S_0$ | 21.0 | 56.0 |
| $P_4/S_0$ | 22.9 | 29.6 |
| $P_7/S_0$ | 36.4 | 27.5 |
| $P_0/S_{11}$ | 17.0 | [a] |
| $P_0/S_{13}$ | [a] | [a] |
| $P_1/S_{11}$ | 14.0 | 9.8 |
| $P_4/S_{13}$ | [a] | [a] |

[a] No data.

TABLE 4.4 OVERFIRE AIR TESTS WITH CARCASS CHARGES

Note: Fixed flow rates of 25 cfm STP per primary air inlet and 20 cfm STP in secondary air inlet

| Insert | Grains Particulate Per Pound of Charge | |
|---|---|---|
| | Horizontal Air | 30° Air |
| $P_0/S_0$ | 25.9 | 23.5 |
| $P_1/S_0$ | 45.6 | 17.8 |
| $P_4/S_0$ | 30.0 | 25.5 |
| $P_7/S_0$ | 45.5 | 19.2 |
| $P_0/S_{11}$ | 18.9 | 29.1 |
| $P_0/S_{13}$ | 11.0 | [a] |
| $P_1/S_{11}$ | 25.9 | 23.0 |
| $P_4/S_{13}$ | 16.8 | 20.3 |

[a] No data.

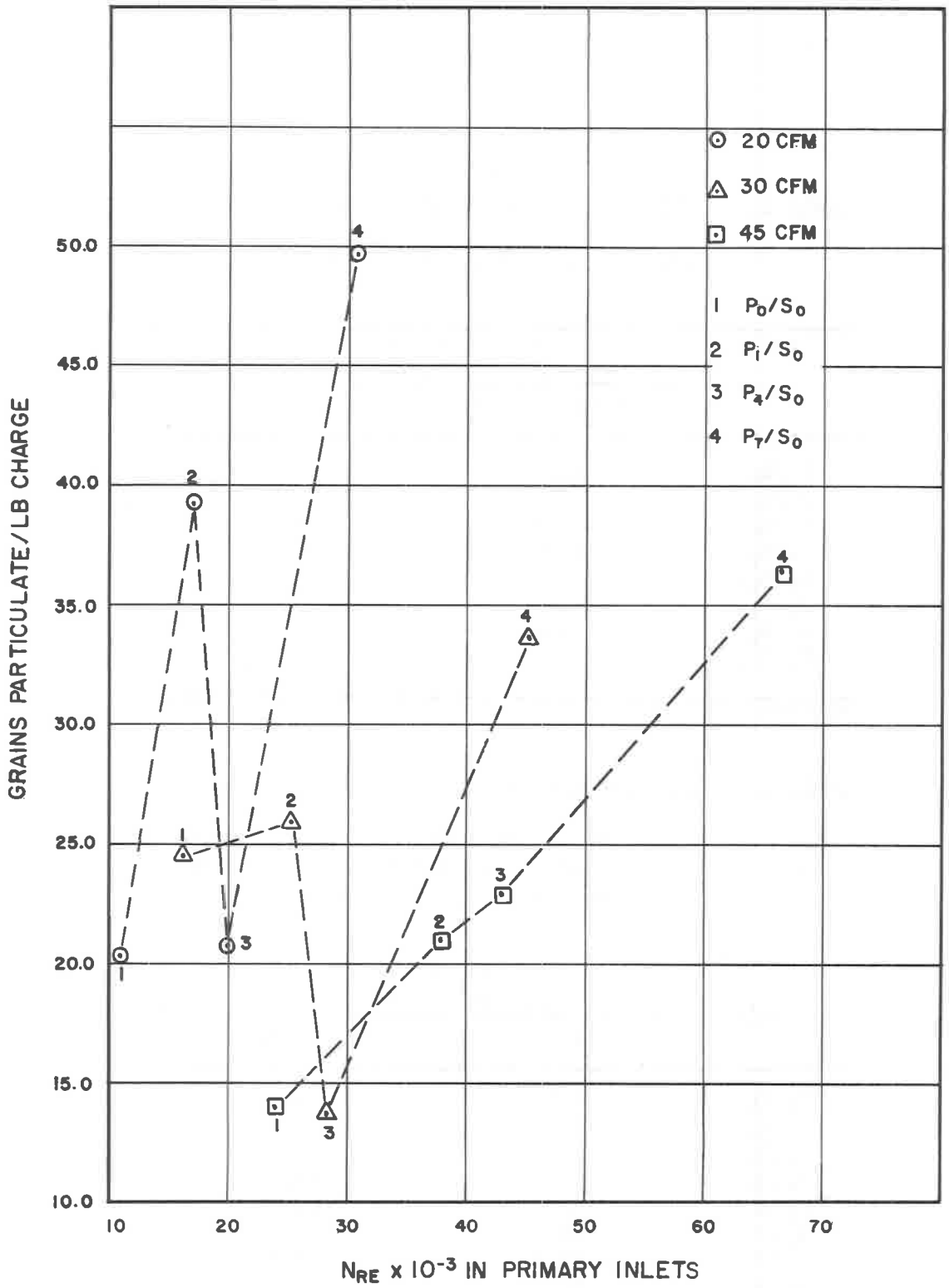


Figure 4.1 Effects of increasing Reynolds number in the horizontal primary auxiliary air inlets with constant Reynolds number in the secondary auxiliary air inlet.

Charge Composition: Sawdust

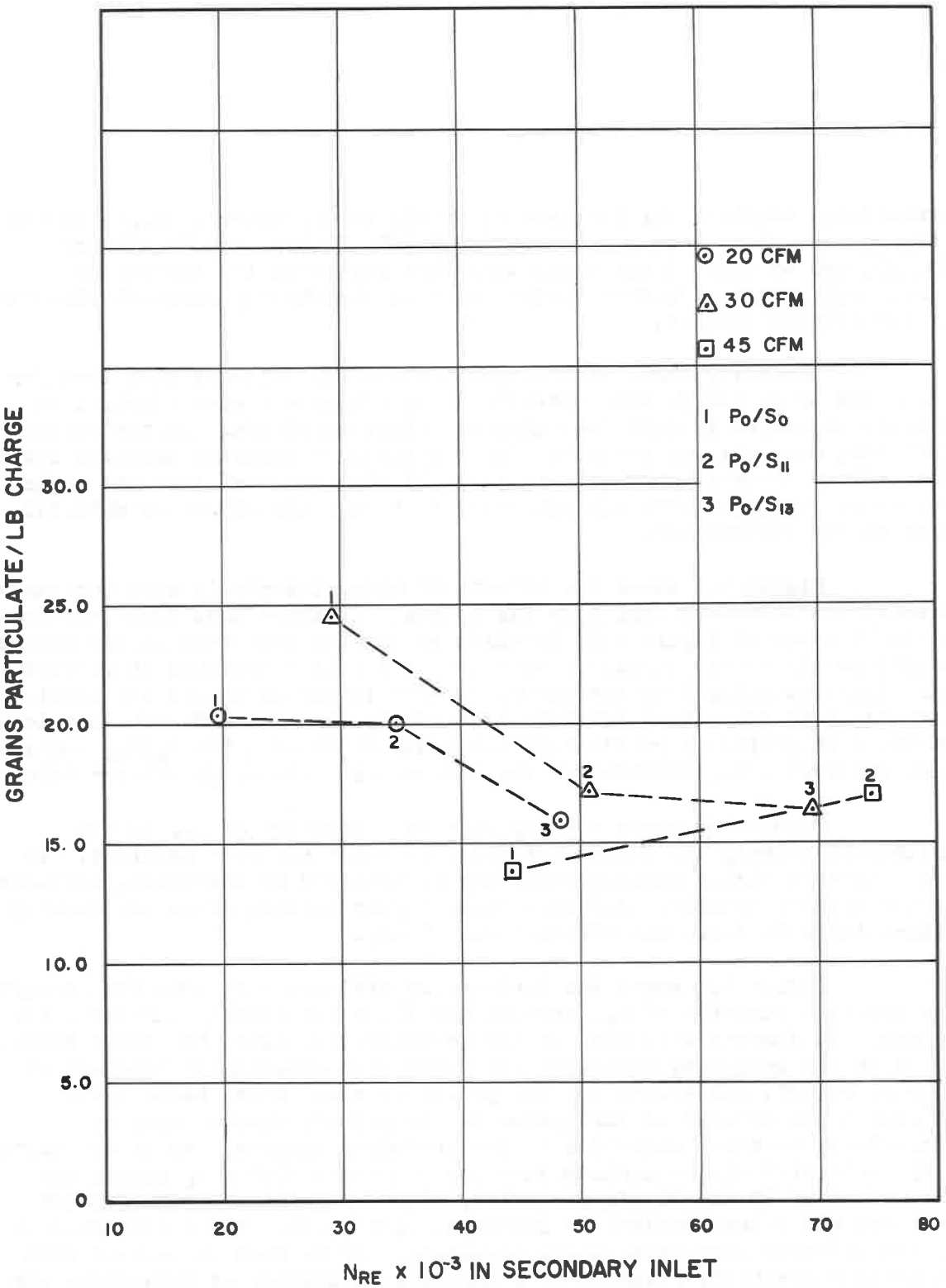


Figure 4.2 Effects of increasing Reynolds number in the secondary auxiliary air inlet with constant Reynolds number in the horizontal primary auxiliary air inlets.

Charge Composition: Sawdust

essentially constant for the particular air rate involved. $N_{Re}$'s in the primary air inlets were approximately 11,100, 16,650, and 24,975 for 20, 30, and 45 cfm. These tests therefore represent the effects of turbulence in the secondary chamber with an essentially constant condition in the primary chamber.

Generally there is a slight decrease in effluent dust load for air rates of 20 and 30 cfm. Results at 30 cfm gave a more significant overall reduction in dust load than did those at 20 cfm. In the former instance, more air was available for oxidation of unburned material leaving the primary chamber. However, tests at 45 cfm indicated that the higher air rates and turbulence did not serve to reduce the amount of material leaving the incinerator.

Figure 4.3 shows the effects of using inserts in both horizontal primary and secondary auxiliary air inlets. If these dust loads are compared to those of Figure 4.1, in which no inserts were used in the secondary auxiliary air inlet, it may be seen that there is a decrease in effluent dust load resulting from the use of inserts in the secondary air inlet. Although both conditions achieved essentially the same effluent dust load of about 14 grains of particulate per pound of charge, the $P_4/S_{13}$ combination achieved this condition at the reduced air rate of 30 cfm per inlet.

Figure 4.4 shows burning rate as a function of $N_{Re}$ in the horizontal primary air inlets for the particular air rate involved. In each instance higher burning rates may be achieved by increasing turbulence in the primary chamber. However, these higher burning rates are usually associated with increased effluent dust loads.

Figure 4.5 shows the incinerator effluent dust load for sawdust charges as a function of $N_{Re}$ through the 30-degree primary auxiliary air inlets. No inserts were used in the secondary air inlet for these tests. $N_{Re}$'s in the secondary auxiliary air inlet were essentially constant at 19,750, 29,600, and 44,000 for 20, 30 and 45 cfm. These tests again represent the effects of turbulence in the primary chamber with an essentially constant condition in the secondary chamber. As in the tests with horizontal air, a minimum dust load occurred with a $P_4$ insert and flow rates of 20 and 30 cfm per inlet. Further increase in turbulence at these air rates resulted in increased dust loads. Tests conducted at 45 cfm differed from those using horizontal air in that an initial peak in loading occurred, followed by a decrease in loading as turbulence was further increased.

Figure 4.6 shows the incinerator effluent dust load as a function of $N_{Re}$ through the secondary air inlet. No inserts were used in the 30-degree primary auxiliary air inlets for these tests. $N_{Re}$'s in the

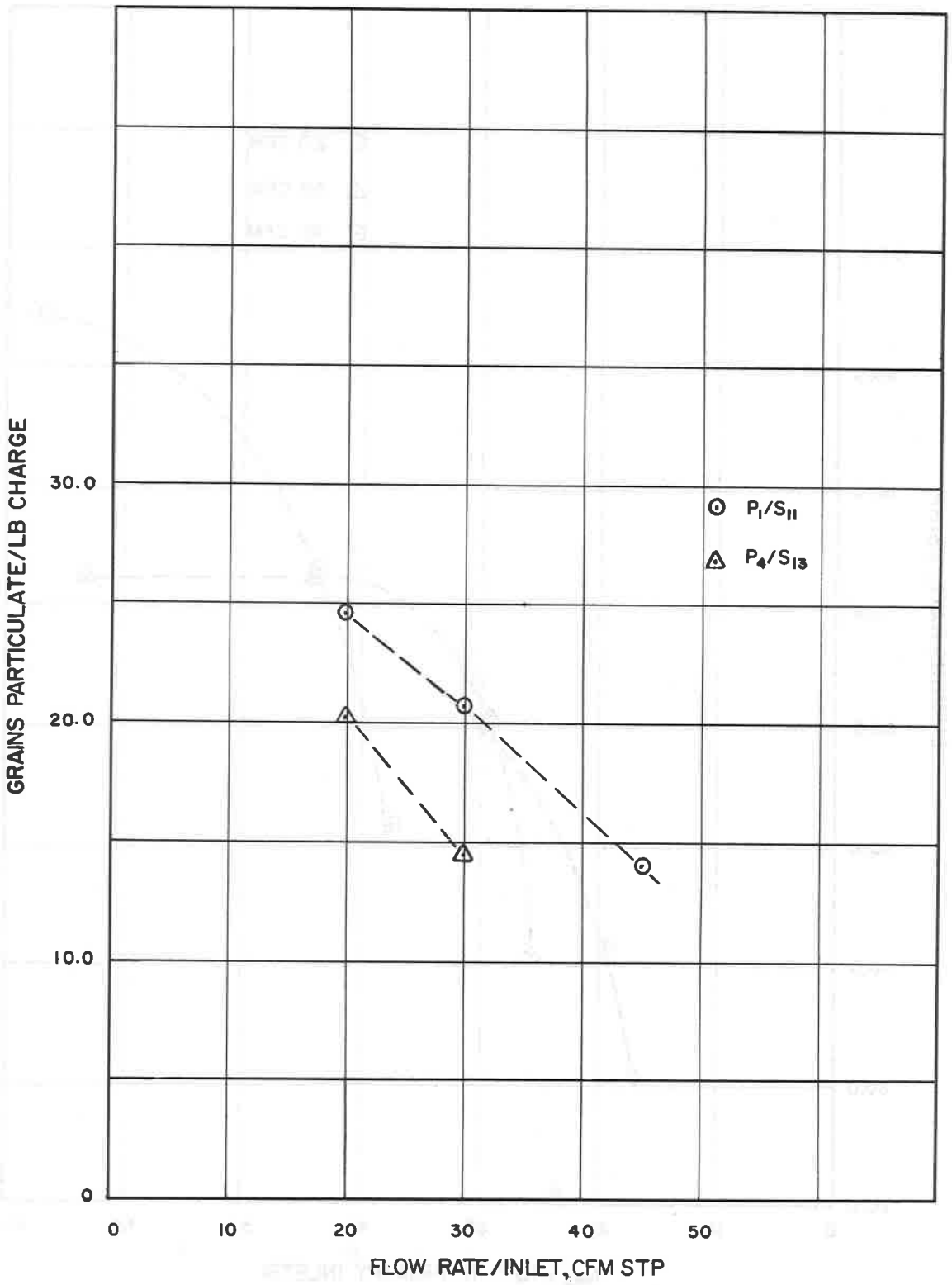


Figure 4.3 Combined effects with horizontal air.

Charge Composition: Sawdust

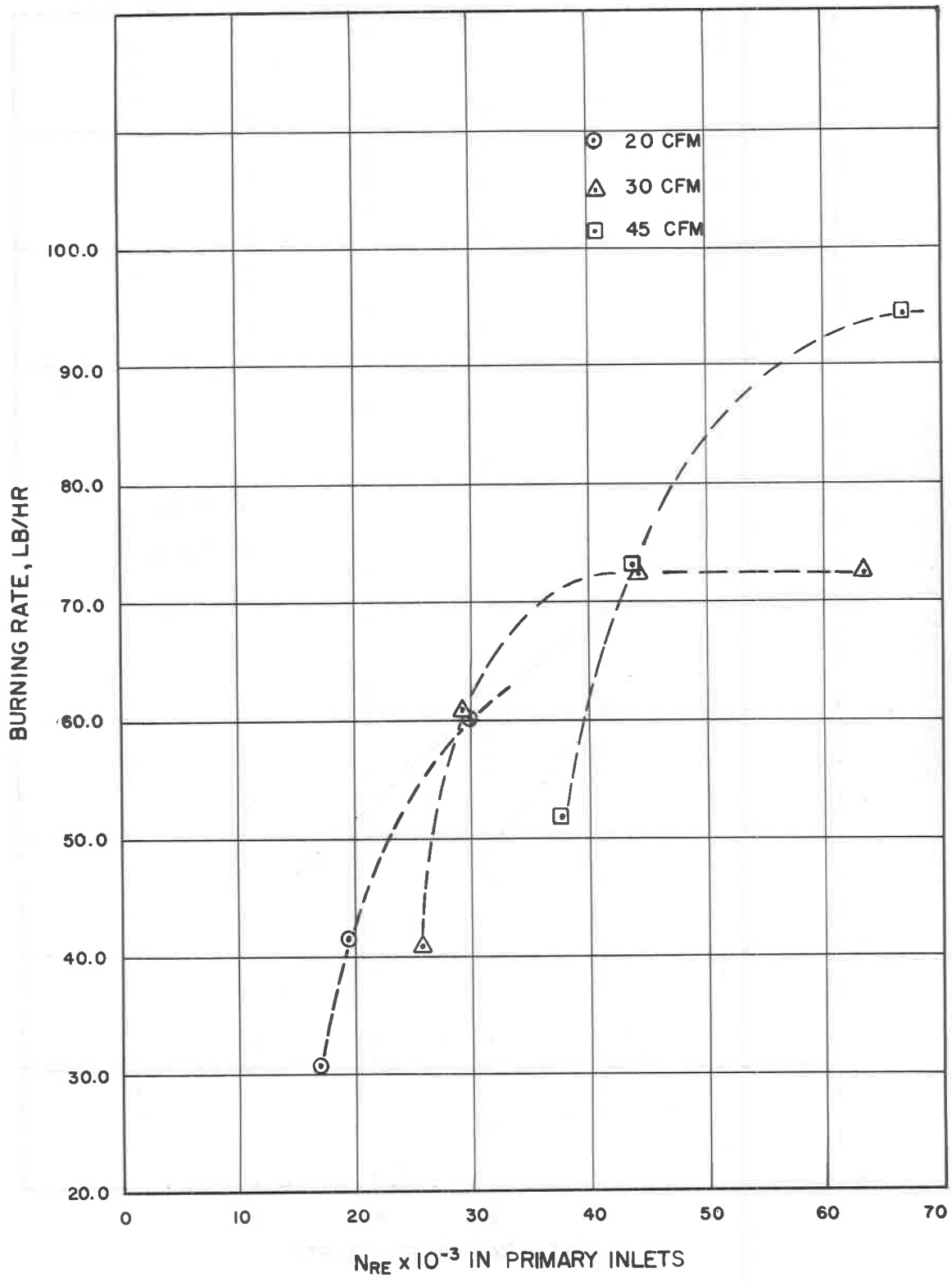


Figure 4.4 Burning rate as a function of Reynolds number in the horizontal primary auxiliary air inlets.

Charge Composition: Sawdust

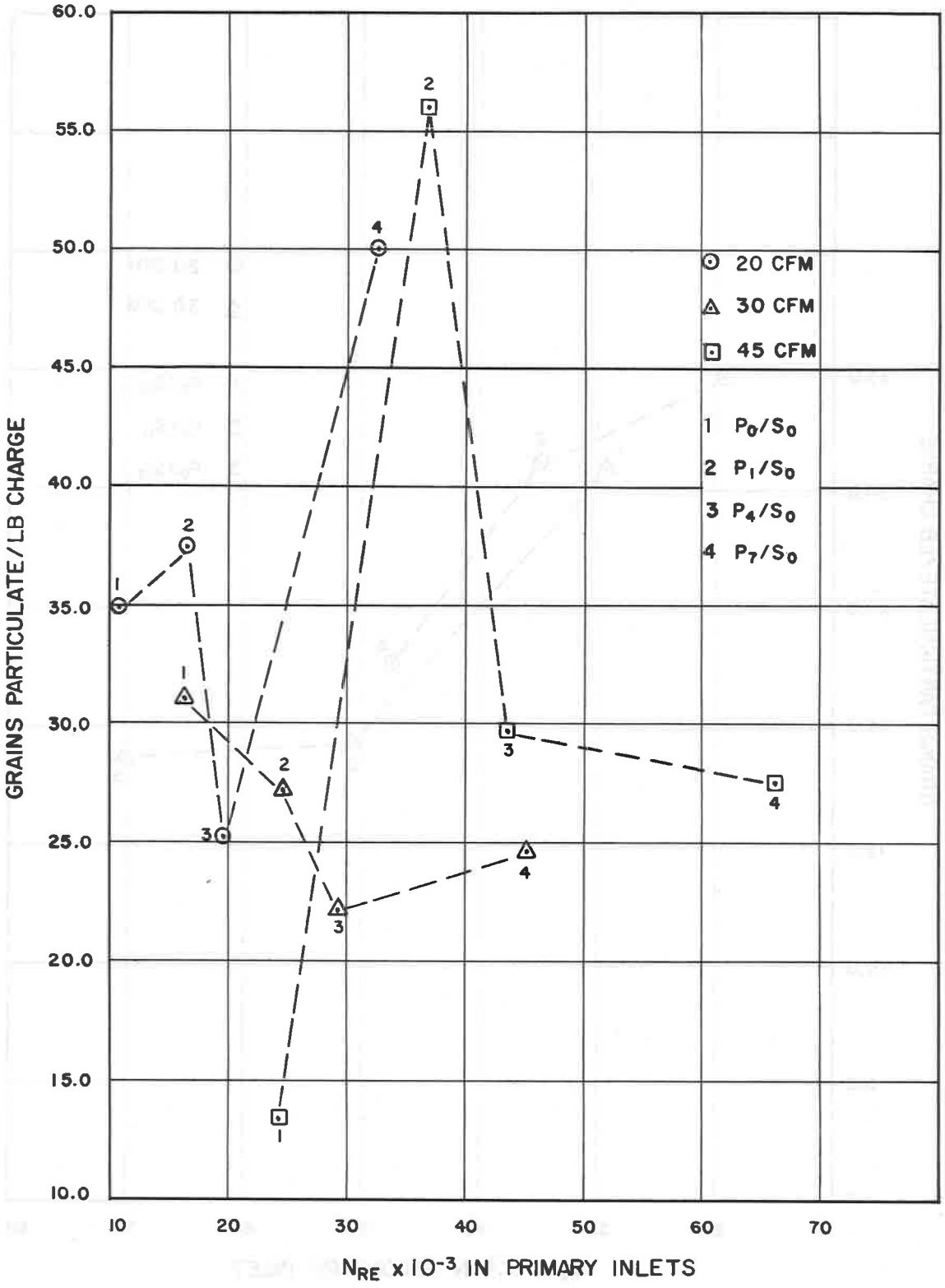


Figure 4.5 Effects of increasing Reynolds number in the 30-degree primary auxiliary air inlets with constant Reynolds number in the secondary auxiliary air inlets.

Charge Composition: Sawdust

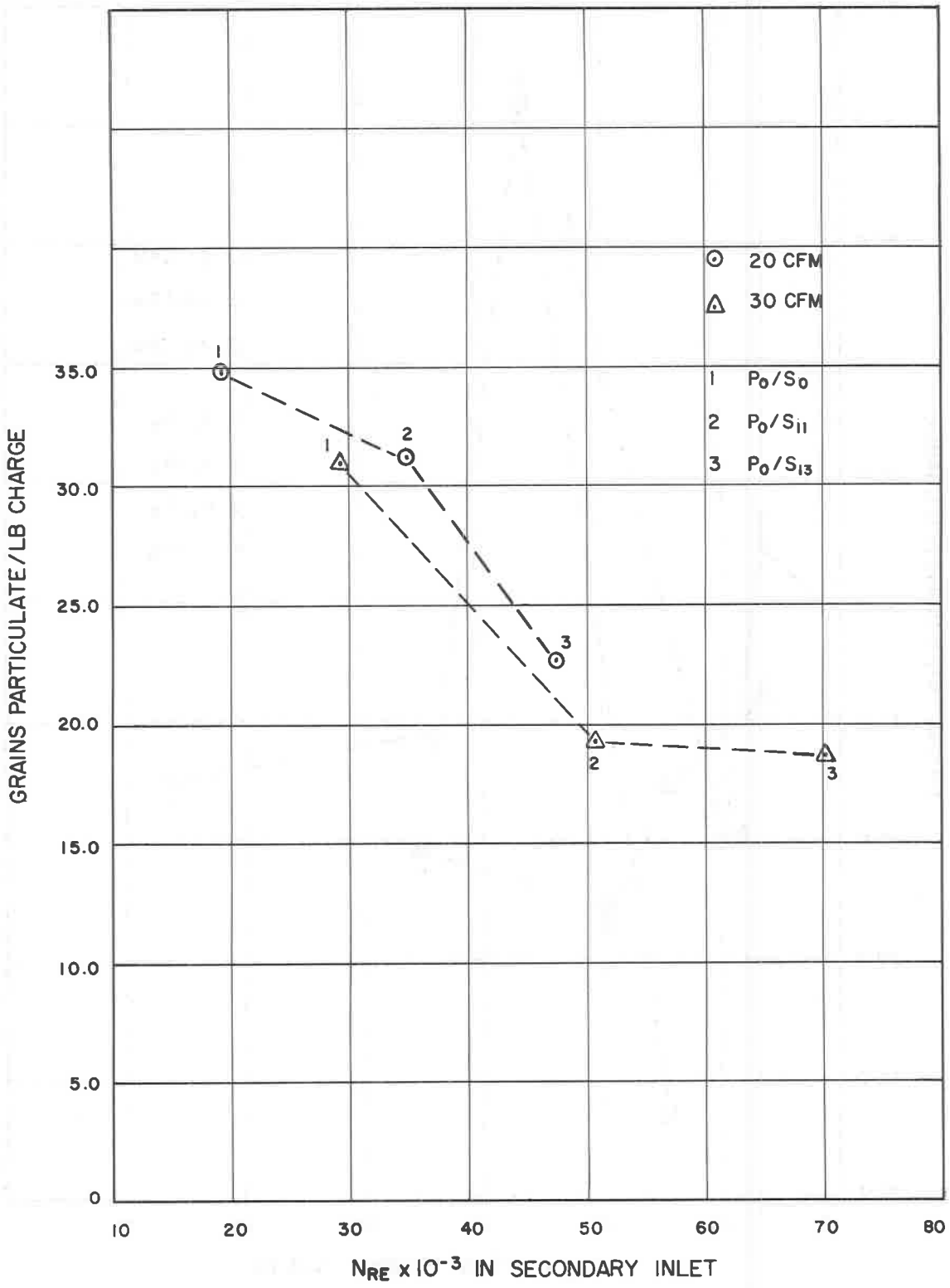


Figure 4.6 Effects of increasing Reynolds number in the secondary auxiliary air inlet with constant Reynolds number in the 30-degree primary auxiliary air inlets.

Charge Composition: Sawdust

primary air inlets were essentially constant at 11,100 and 16,650, for 20 and 30 cfm. (Tests using an air supply of 45 cfm per inlet were not conducted because of operational difficulties.) These tests therefore represent the effects of turbulence in the secondary chamber with an essentially constant condition in the primary chamber. They show a more pronounced reduction in dust load than do the same tests conducted with horizontal air. However, based on the tests conducted to study effects of turbulence in the primary chamber, there was generally more particulate available for oxidation in the tests with 30-degree air.

Figure 4.7 shows the effect of using inserts in both 30-degree primary and secondary auxiliary air inlets. If these dust loads are compared to those of Figure 4.5 in which no inserts were used in the secondary air inlet, it may be seen that there is a decrease in effluent dust load resulting from the use of inserts in the secondary air inlet. Considerably better reduction in dust load was again achieved by using the $P_4/S_{13}$ combination.

Figure 4.8 shows burning rates for sawdust charges as a function of $N_{Re}$ through the 30-degree primary auxiliary air inlets. Burning rates were nearly constant for air rates of 20 and 30 cfm per inlet. At the increased air rate of 45 cfm per inlet, the burning rate rose rapidly to a peak and then decreased.

A comparison of the burning rates and resultant dust loads for horizontal and 30-degree primary auxiliary air at 45 cfm per inlet indicates that in the latter, the decreasing dust loads at $N_{Re}$'s in excess of about 37,000 were associated with decreased burning rates (Figures 4.5 and 4.8), whereas horizontal air yielded increasing burning rates as well as increasing dust loads at $N_{Re}$'s in excess of 37,000 (Figures 4.1 and 4.4).

Observations made through sight glasses in the primary chamber during combustion of the sawdust charges showed a spiral conical flow with material being discharged upward when 30-degree air was used as opposed to spiral cylindrical flow when horizontal air was used. Additionally, burning rates were lower with 30-degree air than with horizontal air. Observations through the sight glasses showed that tangential downward entry of air initially gave rapid combustion. This was then followed by reduced burning rates because the tangential downward air served primarily to scour the outer periphery of the grate; therefore, the center of the grate received less air than it did in the tests utilizing the horizontal air supply.

Figure 4.9 shows the incinerator effluent dust load for carcasses as a function of $N_{Re}$ through the horizontal primary auxiliary air inlets. No inserts were used in the secondary air inlet for these

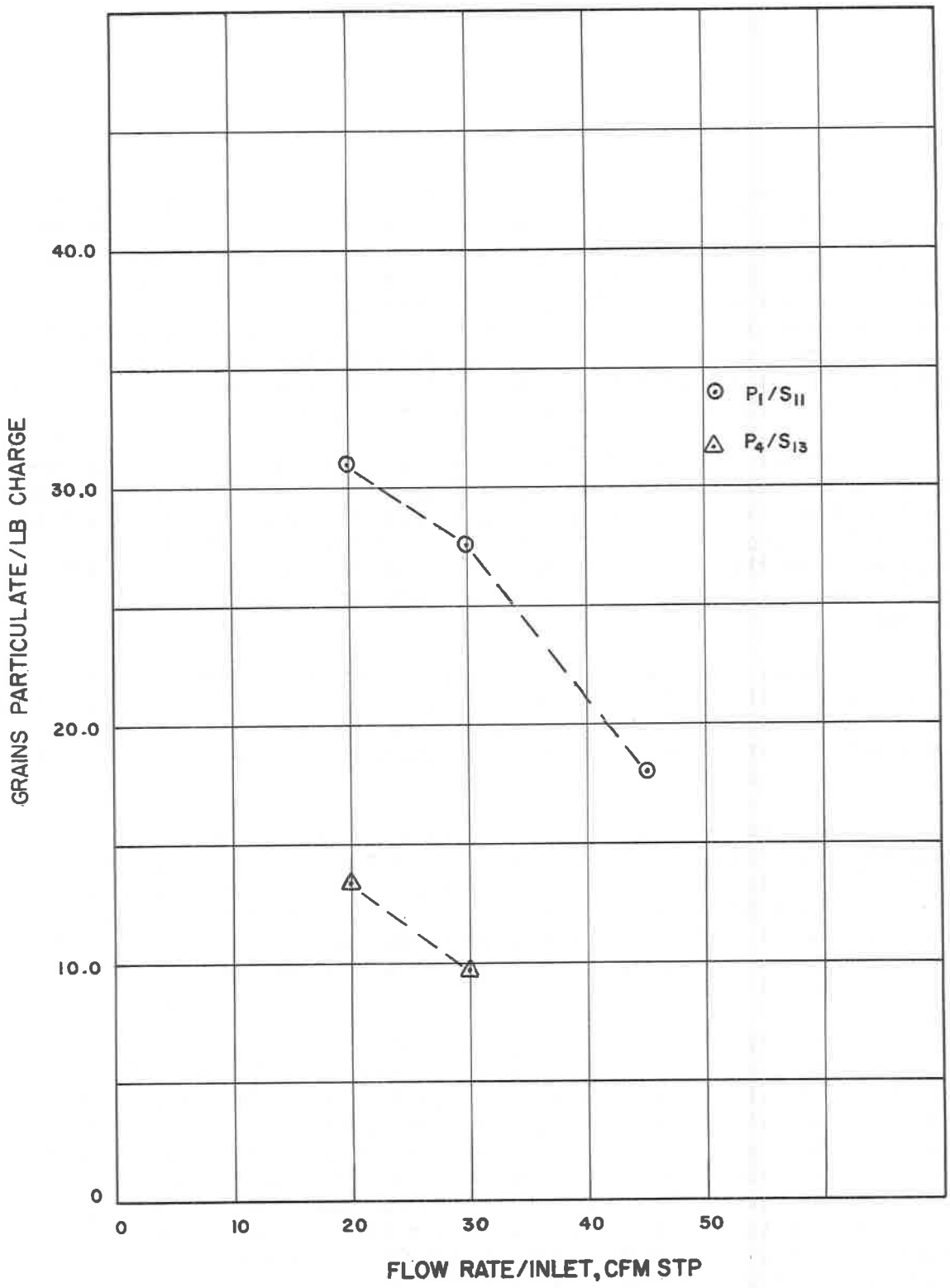


Figure 4.7 Combined effects with 30-degree air.

Charge Composition: Sawdust

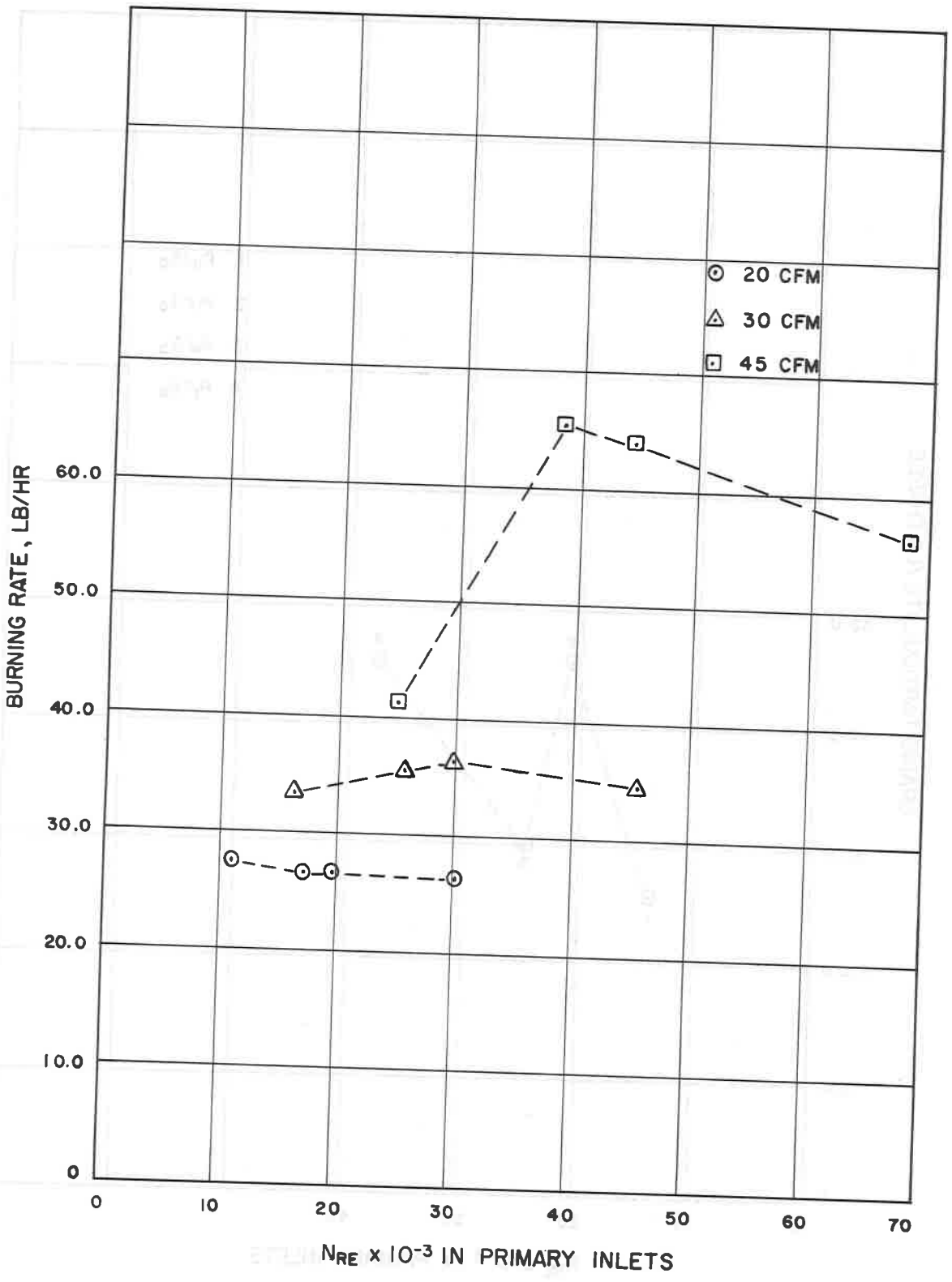


Figure 4.8 Burning rate as a function of Reynolds number in the 30-degree primary auxiliary air inlets.

Charge Composition: Sawdust

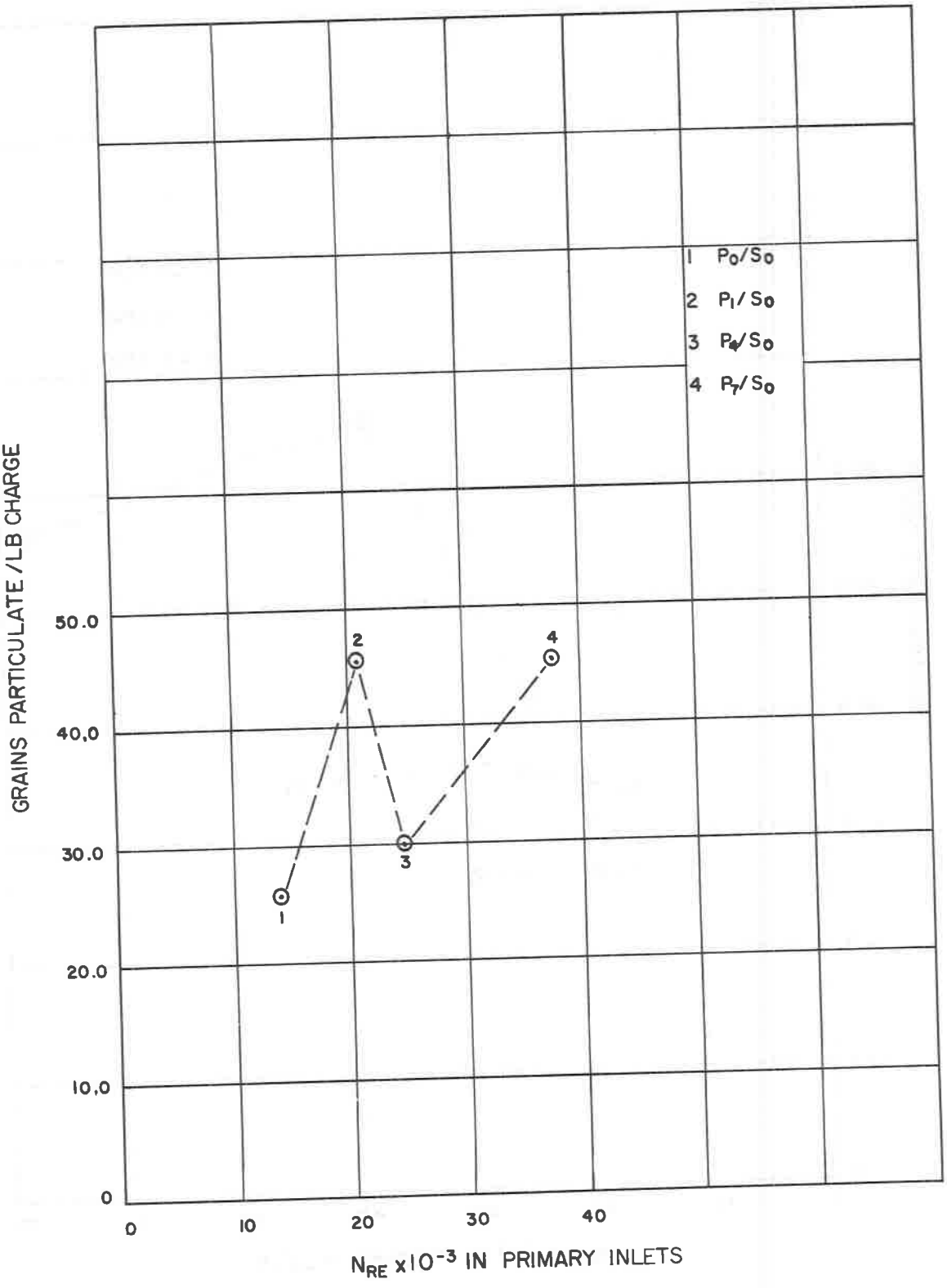


Figure 4.9 Effects of increasing Reynolds number in the horizontal primary auxiliary air inlets with constant Reynolds number in the secondary auxiliary air inlet.

Charge Composition: Carcasses

tests. $N_{Re}$ in the secondary auxiliary air inlet was essentially constant at 19,750. These tests therefore represent the effects of turbulence in the primary chamber with an essentially constant condition in the secondary chamber.

Tests gave essentially the same trend as did the tests using sawdust charges. Although dust loads were at a low point with the $P_4$ insert, slightly lower loads occurred with the $P_0$ insert.

Figure 4.10 shows the incinerator effluent dust load as a function of $N_{Re}$ in the secondary chamber. No inserts were used in the primary inlets for these tests. $N_{Re}$ in the horizontal primary auxiliary air inlets was essentially constant at 14,000. These tests represent the effects of turbulence in the secondary chamber with an essentially constant condition in the primary chamber. A significant reduction in dust load was realized in these tests.

Figure 4.11 shows the incinerator effluent dust load for carcasses as a function of $N_{Re}$ through the 30-degree primary auxiliary air inlets. No inserts were used in the secondary auxiliary air inlet for these tests. $N_{Re}$ in the secondary auxiliary air inlet was essentially constant at 19,750. These tests represent the effects of turbulence in the primary chamber with an essentially constant condition in the secondary chamber. These test results differed from all other test results in the group to study effects of turbulence in the primary chamber; peak loadings occurred using the $P_4$ insert. However, dust loads, during these tests were lower with 30-degree air than with horizontal air.

Tests conducted to study the effects of turbulence in the secondary chamber with an essentially constant $N_{Re}$ of 13,450 through the 30-degree primary auxiliary air inlets (Figure 4.12) indicated that there was no value in increased turbulence in the secondary chamber. Again, the use of a 30-degree primary air supply with carcass charges gave results opposite to those obtained with a horizontal air supply. This condition may be a combined function of the primary air entry angle and the type of waste being incinerated.

## 4.6 Conclusions.

Horizontal primary air at 30 cfm per inlet with a $P_4$ annular insert appears to be an optimum operating condition to be employed for incineration of both sawdust and animal carcasses. Additionally, use of an $S_{13}$ annular insert at 30 cfm can reduce the effluent dust load still further. This optimum condition corresponds to a $N_{Re}$ through the primary inlets of about 29,500 at 30 cfm per inlet and 70,700 through the secondary inlet at 30 cfm.

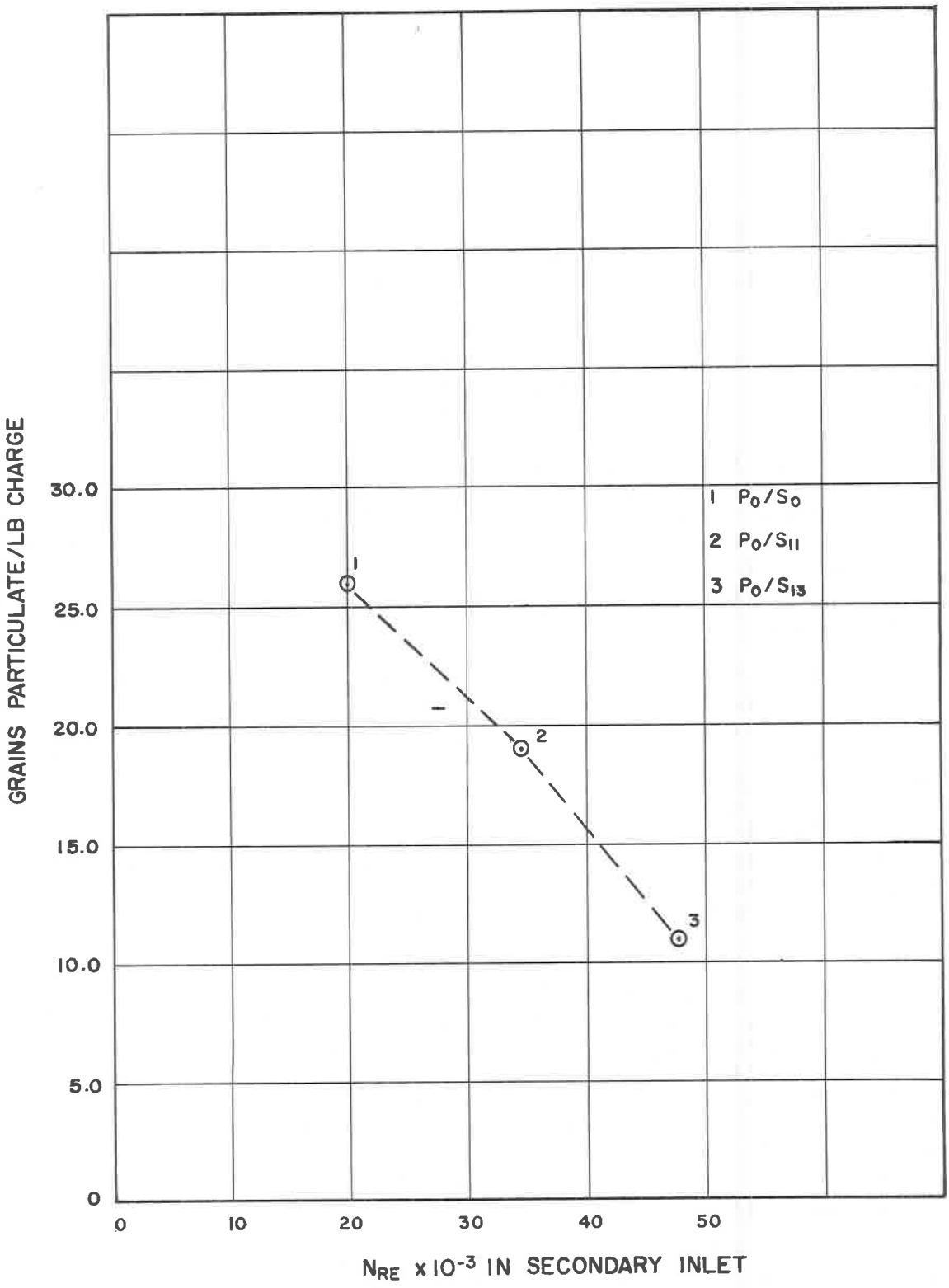


Figure 4.10 Effects of increasing Reynolds number in the secondary auxiliary air inlet with constant Reynolds number in the horizontal primary auxiliary air inlets.

Charge Composition: Carcasses

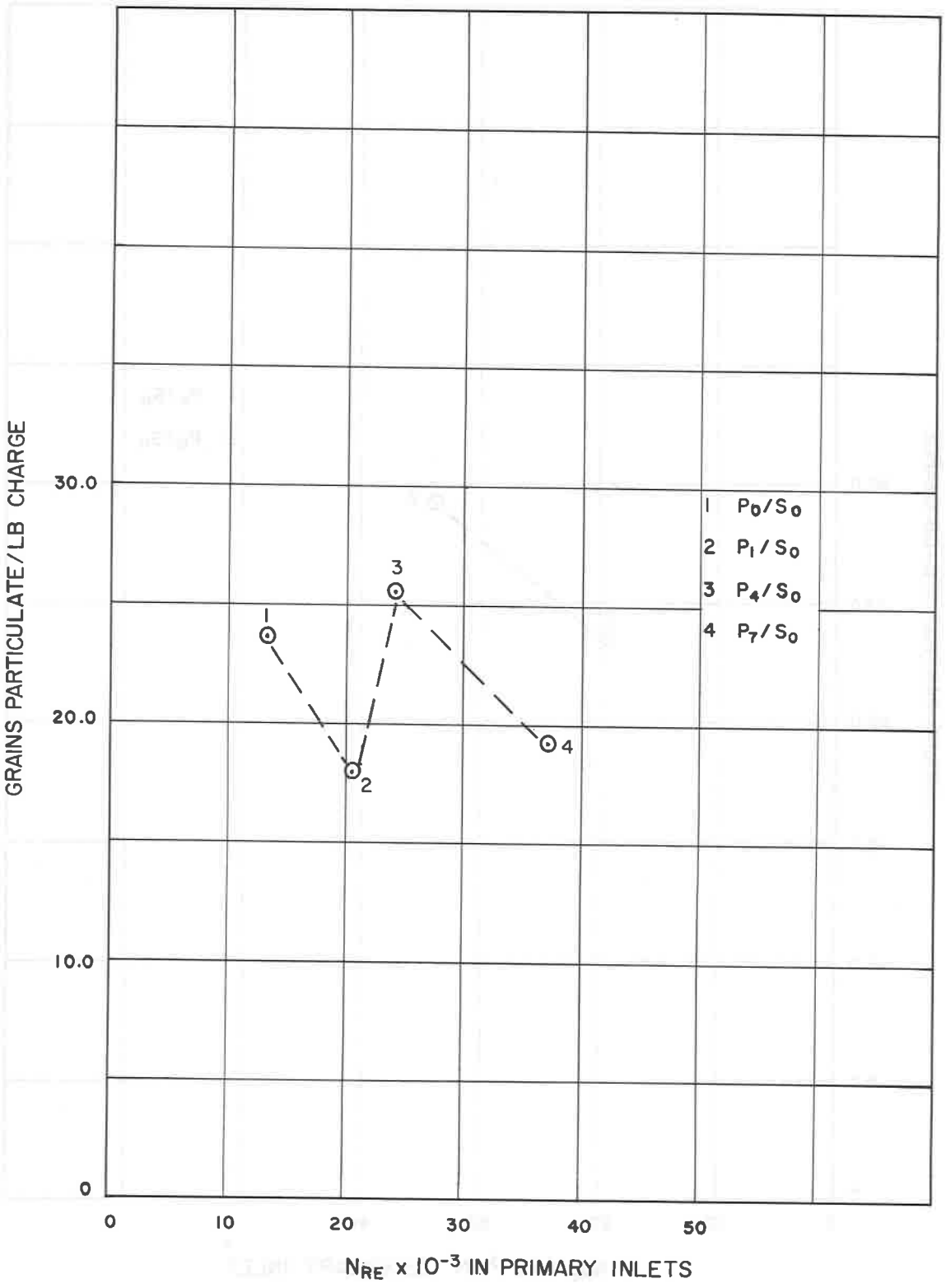


Figure 4.11 Effects of increasing Reynolds number in the 30-degree primary auxiliary air inlets with constant Reynolds number in the secondary auxiliary air inlet.

Charge Composition: Carcasses

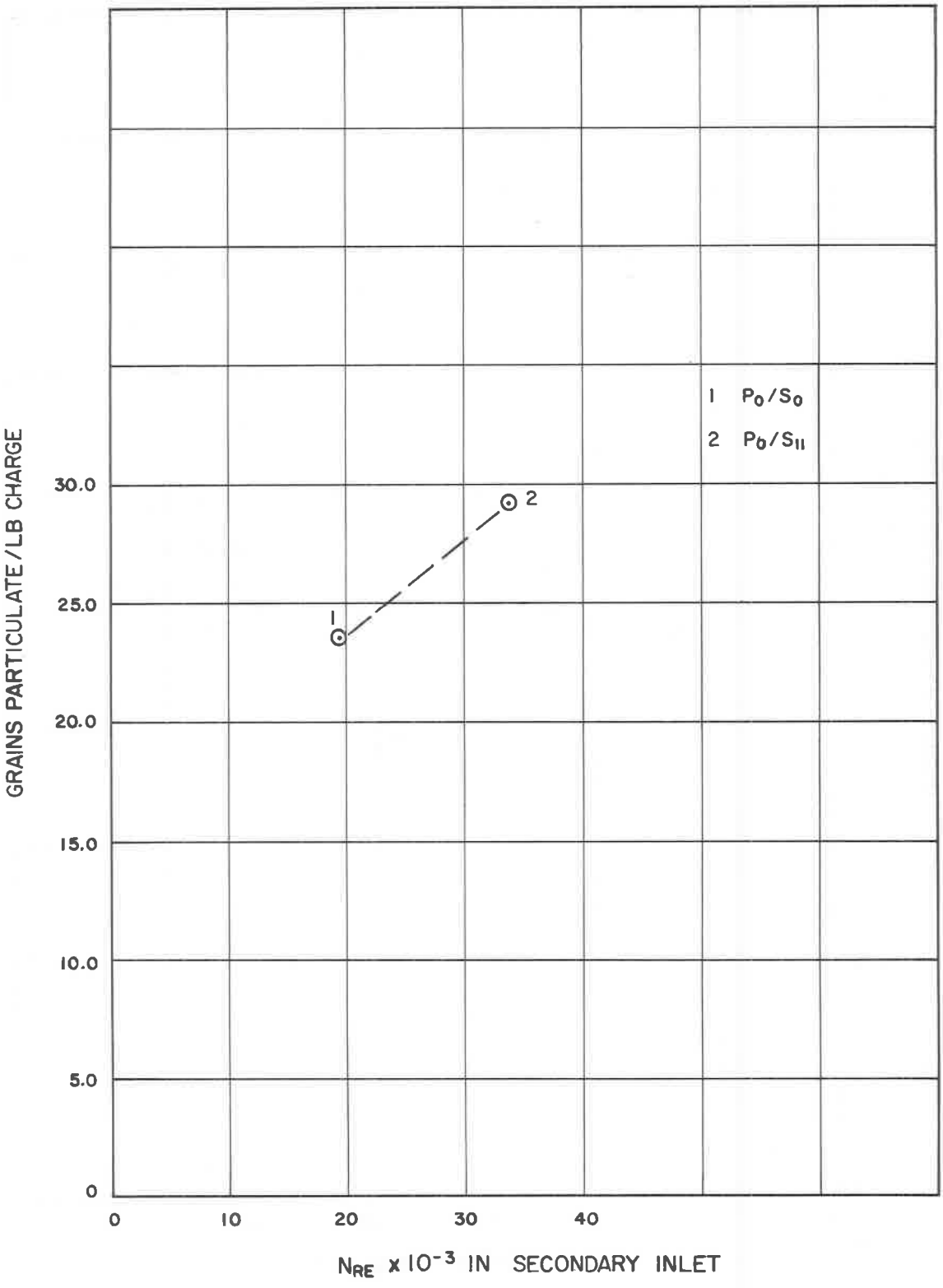


Figure 4.12 Effects of increasing Reynolds number in the secondary auxiliary air inlet with constant Reynolds number in the 30-degree primary auxiliary air inlets.

Charge Composition: Carcasses

Reasonable burning rates of about 60 lb/h for sawdust charges may be achieved at this condition. Burning rates for frozen carcasses are dependent on the utilization of the available grate area and approach 50 lb/h.

## 5. GAS-CLEANING SYSTEM EFFICIENCY EXPERIMENTS

### 5.1 Background.

This facility's gas-cleaning system is designed to remove particulate entrained in the incinerator effluent. As stated previously, the gas-cleaning system consists of a cyclone, electrostatic precipitator, and a bank of absolute filters. During the tests conducted to study gas-cleaning system efficiency, it was decided to evaluate only the cyclone and electrostatic precipitator. It was deemed unnecessary to evaluate the filters since they had already successfully met DOP penetration specifications.

### 5.2 Objectives.

The main objective of these experiments was to define the limitations of the gas-cleaning system in terms of fractional and weight collection efficiency. Additional objectives were to (1) establish a correlation, if any, of fractional-and weight-collection efficiencies with cyclone-inlet velocity and dust loading, and to (2) establish a correlation of ESP fractional and weight collection efficiencies with ESP inlet loadings and ESP output voltages.

### 5.3 Results.

Extensive tests conducted in conjunction with the temperature and overfire air experiments gave considerable data on cyclone and ESP weight collection efficiencies. Attempts were made to obtain samples for size counting of the incinerator effluent and effluent from each gas cleaning unit. Difficulties were encountered in obtaining representative samples suitable for microscopic examination. Sampling periods were found to be quite critical, since short periods of 5 seconds, or less, often did not give sufficient particles for counting; conversely, longer sampling periods usually gave too dense a sample for size counting. Another critical area encountered was the time at which to sample after the charge had begun burning. Samples taken at identical rates, sample periods and time after which the incinerator was charged, gave widely divergent results. It was decided to forego any additional particle size work because of the extensive time that would have been required to obtain dependable data.

Attempts were made to study cyclone weight collection efficiency as a function of dust load and inlet velocity. However, neither incinerator dust load nor velocity could be varied sufficently, without affecting incinerator operating conditions, to show any marked change attributable to dust concentration or velocity.

Table 5.1 summarizes weight collection efficency results obtained during the temperature and overfire air tests. These results represent the complete range of incinerator operating conditions employed during the conduct of the specific tests. The overall efficiency figures apply to the combined cyclone and ESP weight collection efficiencies.

## 5.4 Discussion.

Special tests conducted to show ESP weight percent efficiency as a function of output voltage (Figure 5.1) gave good correlation. ESP weight collection efficiency climbed rapidly as output voltage was increased from 10 kV to 15 kV corresponding to the rapid voltage increase in the 0 to 10 mA range shown on the power curve, Figure 5.2. Weight collection efficiency continued to increase above the 15 kV point but not as rapidly, corresponding to the voltage increase occurring after the 10 mA level was reached.

Figure 5.3 shows ESP weight collection efficiency as a function of inlet dust load. Collection efficiency climbed rapidly at the lower loading and then began to approach a levelling off condition at the higher loads. At the time these tests were conducted, 37.5 mA and 17.6 kV was the normal operating condition for the ESP. Higher voltages resulted in sparking. Since then, a new power supply has been installed and normal operating conditions are 50.0 mA and 18.0 kV without sparking. Additionally, distributor baffles have been installed in the ESP inlet and have markedly improved both gasflow and ESP stability.

## 5.5 Conclusions.

Cyclone weight collection efficiency under a wide range of incinerator operating conditions is usually in excess of 40 percent. ESP weight collection efficiency in normal operation rarely falls below 90 percent. Overall weight collection efficiency for the two units is seldom lower than 95 percent.

Essentially no control is provided for adjusting cyclone collection efficiency. Inlet velocity is usually maintained at about 3600 ft/min. Normal inlet gas temperature is about 550 °F.

TABLE 5.1 AVERAGE WEIGHT COLLECTION EFFICIENCIES FOR CYCLONE AND ESP

| | Cyclone | ESP | Overall |
|---|---|---|---|
| | pct | pct | pct |
| Temperature Tests with Sawdust | 40.3 ±7.1 | 93.5 ±3.8 | 96.1 ±8.0 |
| Temperature Tests with Carcasses | 60.9 ±6.3 | 83.8 ±5.6 | 93.7 ±8.4 |
| Horizontal Air with Sawdust | 44.4 ±9.2 | 92.3 ±4.3 | 95.7 ±10.2 |
| 30-degree Air with Sawdust | 48.4 ±7.2 | 87.2 ±7.3 | 93.4 ±10.2 |
| Horizontal Air with Carcasses | 49.4 ±9.0 | 87.5 ±6.3 | 93.7 ±10.9 |
| 30-degree Air with Carcasses | 41.6 ±7.4 | 92.4 ±3.2 | 95.6 ±8.0 |

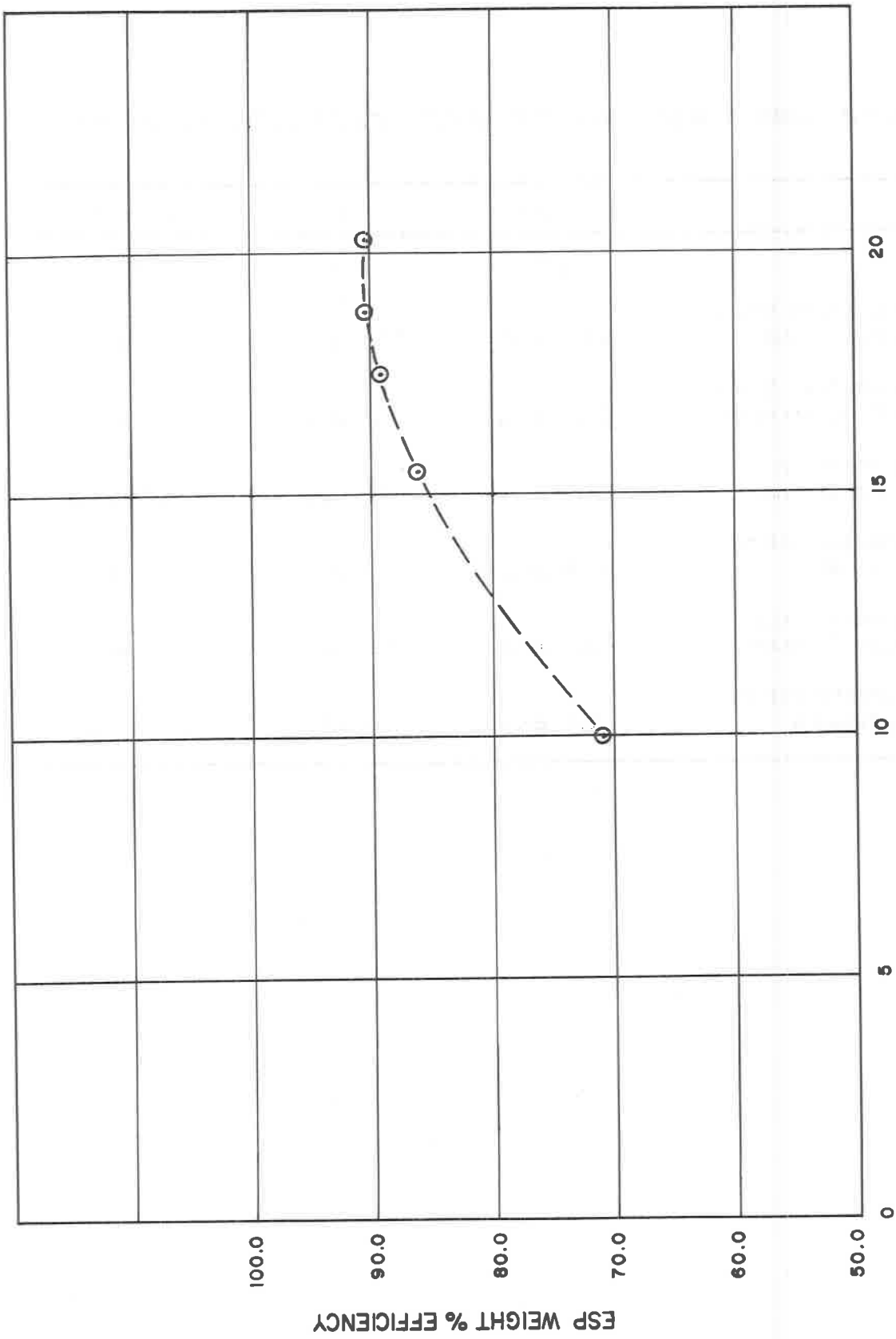


Figure 5.1 ESP weight collection efficiency versus output voltage.

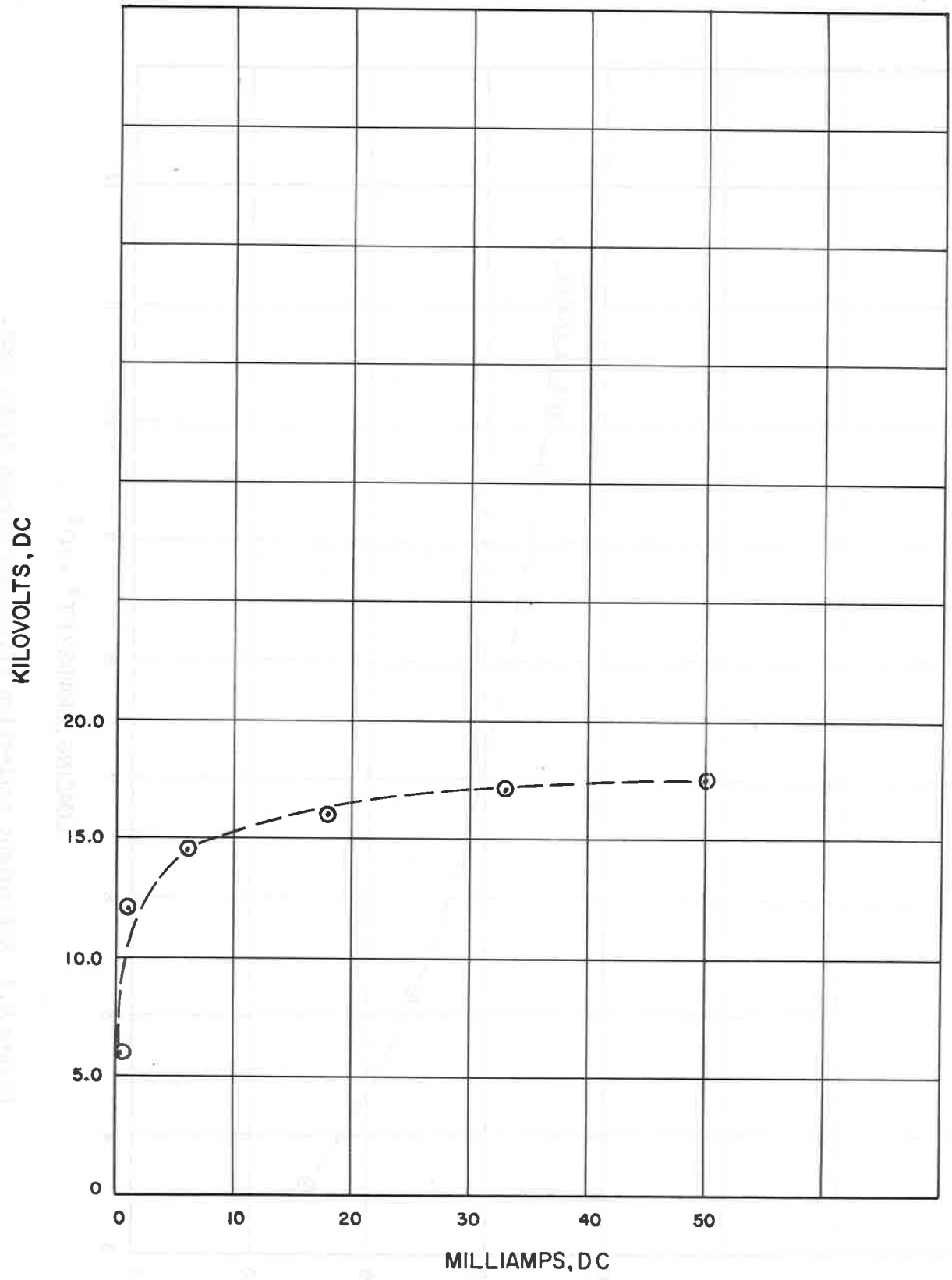


Figure 5.2 Power curve for ESP.

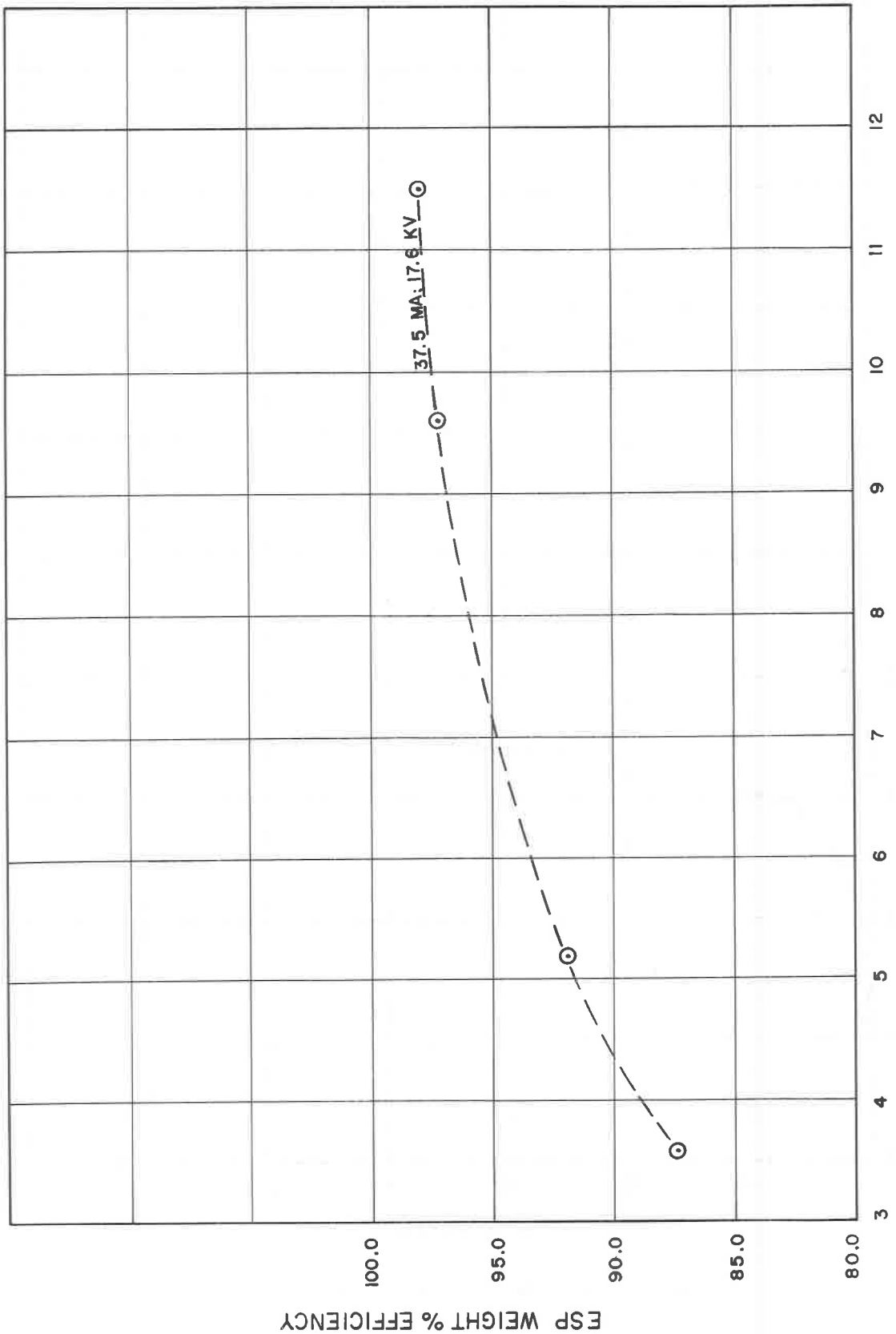


Figure 5.3 ESP weight collection efficiency versus inlet load.

ESP operation is more critical, however, and the unit is always operated at a point slightly below that where sparking may occur. Several factors influence this operating point, such as inlet temperature, dust load, dust buildup on the electrodes and collector plates. Routine cleaning of the ESP intervals with the rapper and vibrators and careful attention to inlet temperatures and incinerator operating conditions ensure stable and dependable operation of the unit.

## 6. RADIOLOGICAL EVALUATION

### 6.1 Background.

Results of the engineering evaluation have defined the optimum operating conditions for the facility. These operating conditions are being employed during the radiological and isotopic evaluation. Specific isotopes are being utilized to determine the efficiency and maximum radioactive charge that can be safely handled by the facility without exceeding maximum permissible concentration (MPC) limits for the particular isotope(s) as set forth in the Federal Register Part 20, "Standards for Protection Against Radiation."

At this writing, the isotopes $Sr^{89}$ and $I^{131}$ have been chosen because of their nature and usage by the Army. Additional isotopes may be used if warranted. The results that follow are for $Sr^{89}$.

### 6.2 Objectives.

During this phase of evaluation, a determination is being made of the maximum radioactive charge that can be safely handled by the facility without exceeding MPC limits for the particular isotope.

Additionally, decontamination factors (DF's)* for the particular isotope being used are being determined for the incinerator, cyclone, electrostatic precipitator, and absolute filters. An overall DF will be determined for the facility.

### 6.3 Procedures.

For the phase utilizing radioactive materials, known quantities of $Sr^{89}$ were dispersed uniformly into pre-weighed packages of sawdust. For carcass charges, live animals were fed intravenously with the isotope.

*Decontamination factor is the ratio of input activity to output activity.

During the tests with sawdust charges, activity concentrations were varied from 10 μc/kg of waste to 200 μc/kg of waste in increments of 10 μc/kg. Tests utilizing carcasses do not undergo the incremental steps employed during the sawdust tests since the tests with sawdust determined the maximum charge concentration that could be safely handled by the facility. Therefore, for the tests utilizing carcasses, the charge concentration was essentially equal to the maximum concentration used with sawdust.

The contaminated charges were incinerated and samples of the effluent particulate were obtained before and after each gas-cleaning unit. Ash samples and filter samples were assayed to permit determination of DF's.

## 6.4 Results and Discussion.

Initial tests with sawdust at the 10 μc/kg level indicated that a significant portion of the $Sr^{89}$ had become "fixed" to the interior refractory walls of the incinerator and to the discharge hopper. Subsequent cold runs removed some of the activity from the walls as a result of the "scrubbing" effects of the swirling particulate, and also removed some activity from the discharge hopper. However, no prediction can be made as to the number of cold runs that would be required to decontaminate the incinerator to background levels. Usually, four cold runs were sufficient to decontaminate the refractory walls to a point where filter samples from the next "hot" run would not be significantly influenced by residual surface activity. Additionally, it does not appear that the refractory is approaching a "saturation" condition. Table 6.1 summarizes the activity fractions as ash, particulate and absorbed. Additionally, the right-hand column lists the amount of activity that did not leave the incinerator as particulate in the effluent.

The absorbed fraction appears to be dependent primarily on the fraction of activity that is associated with the ash that falls through the open grate area (Figure 6.1). The absorbed fraction has been assumed to be that fraction unaccounted for as ash or particulate.

The total amount of ash which fell through the open grate area was recovered after each hot run. The entire sample was weighed and placed in a ball mill and milled for about 3 hours. Weighed portions of the milled ash were mounted on planchets and counted. Results using this milling technique were very reproducible.

TABLE 6.1 ACCOUNTABILITY OF $Sr^{89}$

| Total Input Activity | Released as Ash | Released as Particulate | Absorbed by Refractory | Retained by Incinerator |
|---|---|---|---|---|
| μc | pct | pct | pct | pct |
| 94.2 | 45.2 | 2.4 | 52.4 | 97.6 |
| 186.3 | 33.9 | 1.3 | 64.8 | 98.7 |
| 299.2 | 27.3 | 1.0 | 71.7 | 99.0 |
| 389.6 | 15.9 | 1.4 | 82.7 | 98.6 |
| 483.2 | 40.4 | 1.0 | 58.6 | 99.0 |
| 546.4 | 23.6 | 1.1 | 75.3 | 98.9 |
| 638.0 | 17.4 | 1.8 | 80.8 | 98.2 |
| 726.0 | 30.0 | 1.2 | 68.8 | 98.8 |
| 806.4 | 31.4 | 1.3 | 67.3 | 98.7 |
| 898.6 | 29.7 | 1.5 | 68.8 | 98.5 |
| 985.6 | 37.4 | 1.2 | 61.4 | 98.8 |
| 1100.8 | 29.4 | 1.8 | 69.4 | 98.2 |
| 1188.0 | 29.9 | 1.2 | 68.9 | 98.8 |
| 1272.0 | 21.3 | 2.4 | 76.3 | 97.6 |
| 1360.8 | 22.6 | 3.9 | 73.5 | 96.1 |
| 1466.4 | 36.1 | 3.1 | 60.8 | 96.9 |
| 1552.4 | 28.6 | 2.1 | 69.3 | 97.9 |
| 1624.4 | 29.5 | 1.5 | 69.0 | 98.5 |
| 1732.0 | [a] | 1.7 | [a] | [a] |
| 1820.3 | 30.0 | 1.9 | 68.1 | 98.1 |

[a] No data.

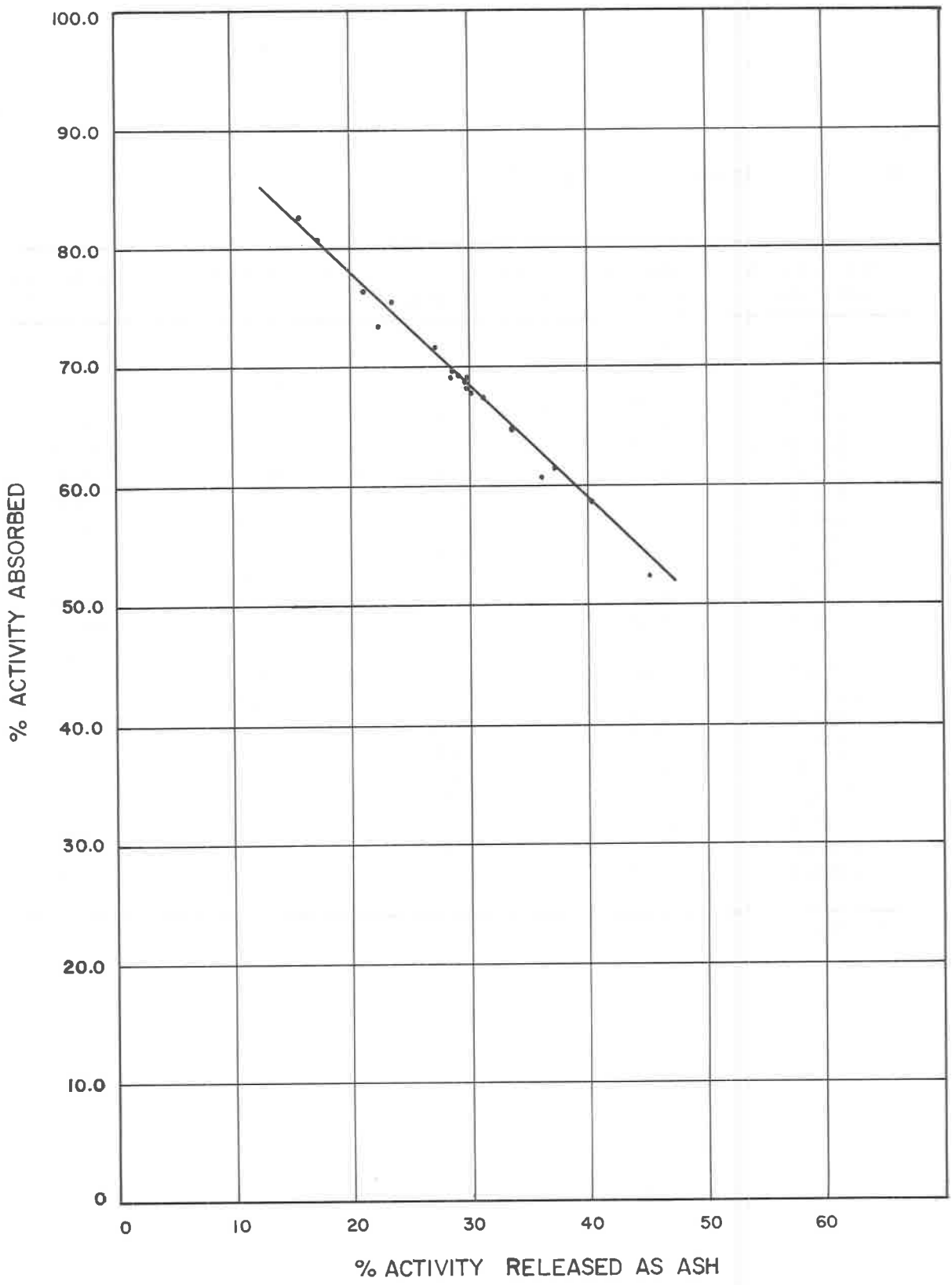


Figure 6.1 Percent activity absorbed versus percent activity released as ash.

Pre-weighed sample filters containing particulate from the effluent gas stream were sectioned and the entire filter was counted. Total activity in the gas stream at each of the four sample points was calculated; the weight of particulate, its activity, dust loading, effluent flow rate, sampling rate and sampling time were considered.

Figure 6.2 and Table 6.2 show the activity of the sampled particulate leaving the incinerator as a function of the total activity leaving the incinerator. Despite some variation in effluent flow rates, dust loads, sample rates and sample times, the data correlated quite well and showed that the total activity released to the cyclone was directly proportional to the measured activity per milligram of sampled particulate.

Figure 6.3 and Table 6.3 show the total activity to the ESP (cyclone outlet) as a function of total activity to the cyclone. The inverse slope of the line is the approximate DF for the cyclone during the radiological tests conducted. The triangulated data points shown on Figure 6.3 were not included in the determination of the slope, since it was later found that the sample probe used to sample particulate leaving the cyclone had begun to plug and was yielding a low weight and activity sample. The condition was remedied by blowing compressed air back through the sample probe.

Figure 6.4 and Table 6.4 show the total activity to the absolute filters (ESP outlet) as a function of total activity to the ESP. The inverse slope approximates the average DF for the ESP. The triangulated points correspond to those cited previously. The data points above the line correspond to a condition where the collecting plates and electrodes of the ESP were in need of cleaning. Operation of this unit is quite critical especially from a radiological aspect. The unit was cleaned twice during the evaluation when DF's began to vary significantly. Normal procedure is to clean the unit only when sparking begins to occur frequently or when discharge loads begin to increase markedly at essentially constant inlet loads. It is not unusual with the unit to experience reduced collection efficiency immediately after cleaning. The unit then stabilizes after several charges have been processed through the facility. Some of the variance occurring above the line results from particulate blow-off from the plates during the initial 30 seconds of combustion of the charge when the gas temperature to the ESP rises sharply. This is sometimes accompanied by a "popping" sound as the ESP internals and shell expand. It is during this period that collected dust is re-entrained; it is immediately noticeable as a drop in differential pressure across the resistance meter connected to the sample system on the discharge side of the ESP. The sample filter at this location will always show a heavy accumulation of particulate with agglomerates on the surface of the filter. Additionally, this filter will always yield a high count-rate.

TABLE 6.2 ACTIVITY TO CYCLONE

| Total Input Activity To Incinerator | Total Activity To Cyclone | Particulate Activity To Cyclone |
|---|---|---|
| μc | μc | $10^{-3}$ μc/mg |
| 94.2 | 2.22 | 0.073 |
| 186.3 | 2.46 | 0.077 |
| 299.2 | 2.96 | 0.097 |
| 389.6 | 5.54 | 0.18 |
| 483.2 | 5.00 | 0.19 |
| 546.4 | 5.98 | 0.21 |
| 638.0 | 11.55 | 0.46 |
| 726.0 | 8.86 | 0.32 |
| 806.4 | 10.60 | 0.45 |
| 898.6 | 13.65 | 0.48 |
| 985.6 | 12.15 | 0.52 |
| 1100.8 | 19.85 | 0.71 |
| 1188.0 | 13.75 | 0.50 |
| 1272.0 | 30.5 | 1.20 |
| 1360.8 | 52.5 | 1.84 |
| 1466.4 | 44.9 | 1.28 |
| 1552.4 | 32.0 | 1.21 |
| 1624.4 | 24.4 | 0.73 |
| 1732.0 | 28.9 | 1.30 |
| 1820.3 | 34.6 | 1.21 |

TABLE 6.3 CYCLONE INLET AND OUTLET ACTIVITIES

| Inlet Activity to Cyclone | Inlet Activity to ESP |
|---|---|
| μc | μc |
| 2.22 | 0.58 |
| 2.46 | 0.71 |
| 2.96 | 1.03 |
| 5.54 | 1.79 |
| 5.00 | 0.91 |
| 5.98 | 2.27 |
| 11.55 | 3.36 |
| 8.86 | 1.96 |
| 10.60 | 2.57 |
| 13.65 | 3.93 |
| 12.15 | 3.58 |
| 19.85 | 5.90 |
| 13.75 | 1.88 |
| 30.5 | 4.43 |
| 52.5 | 5.46 |
| 44.9 | 7.00 |
| 32.0 | 8.27 |
| 24.4 | a |
| 28.9 | a |
| 34.6 | 11.45 |

[a] No data.

TABLE 6.4 ESP INLET AND OUTLET ACTIVITIES

| Inlet Activity to ESP | Inlet Activity to Absolute Filter |
|---|---|
| μc | $10^{-2}$ μc |
| 0.58 | 1.39 |
| 0.71 | 1.34 |
| 1.03 | 1.72 |
| 1.79 | 3.27 |
| 0.91 | 4.68 |
| 2.27 | 4.41 |
| 3.36 | 4.36 |
| 1.96 | 5.62 |
| 2.57 | 7.70 |
| 3.93 | 6.85 |
| 3.58 | 13.3 |
| 5.90 | 10.2 |
| 1.88 | 21.6 |
| 4.43 | 18.5 |
| 5.46 | 7.38 |
| 7.00 | 27.4 |
| 8.27 | 26.3 |
| a | a |
| a | a |
| 11.45 | 40.8 |

[a]No data.

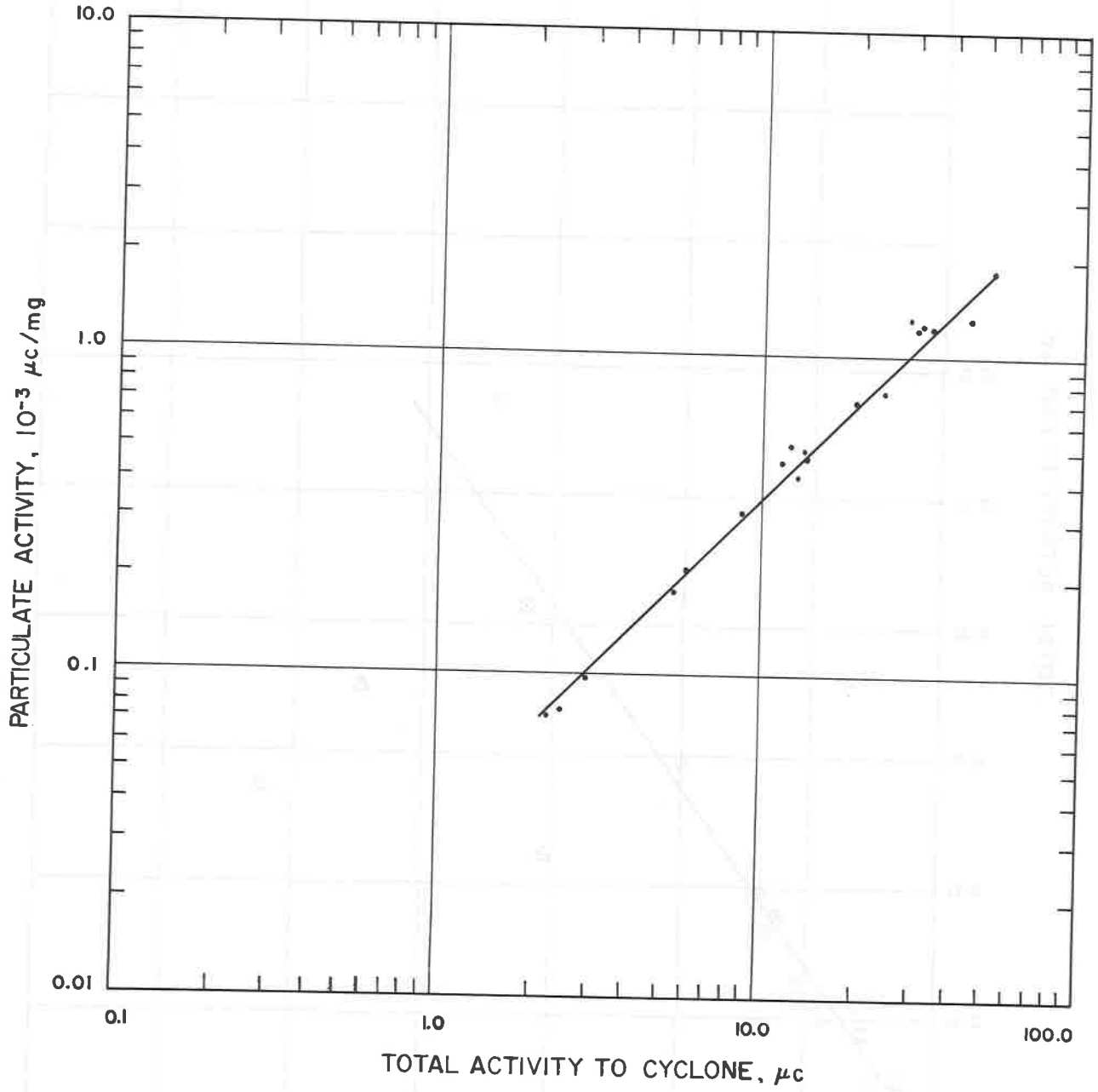


Figure 6.2 Particulate activity to cyclone versus total activity to cyclone.

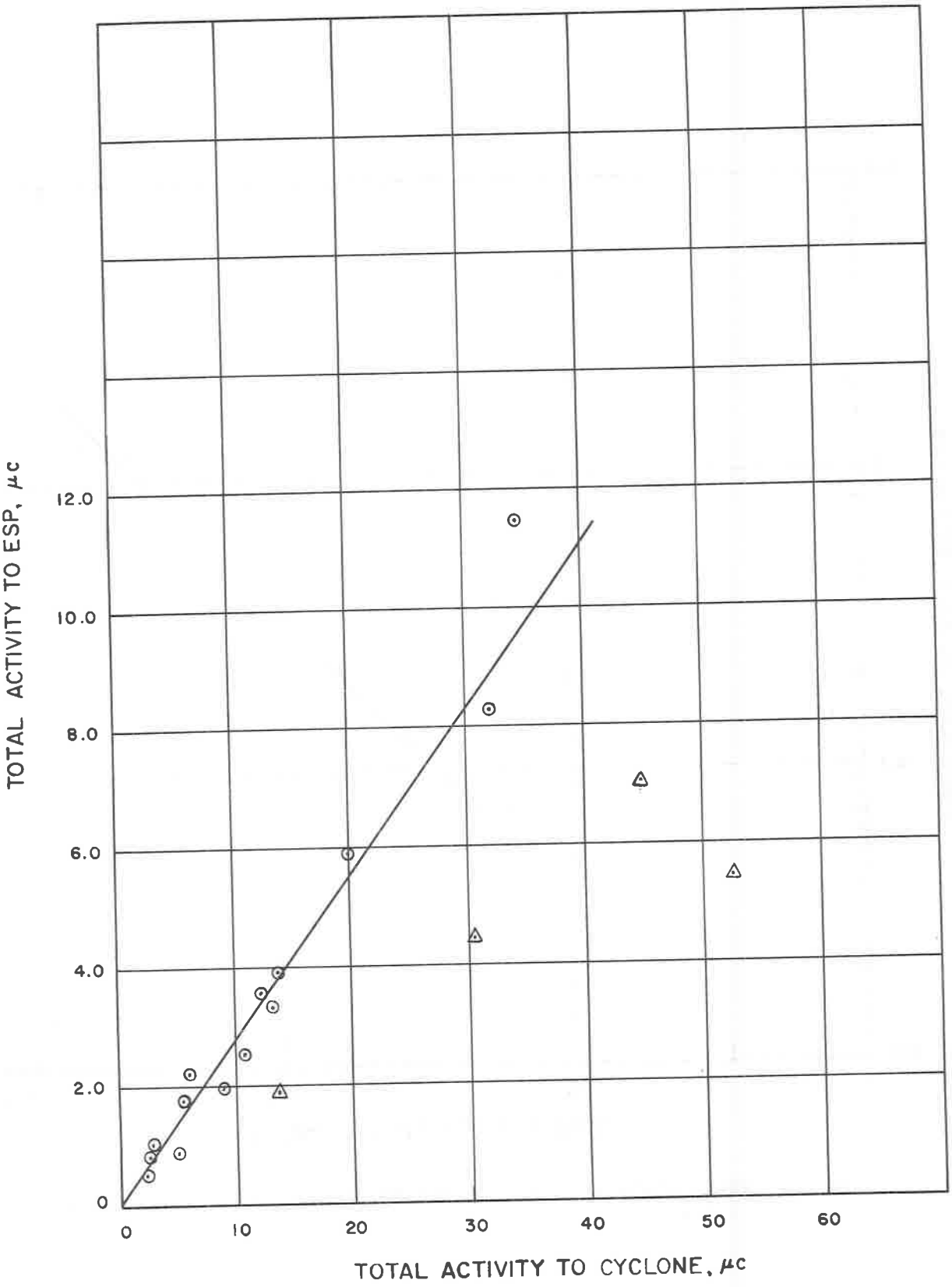


Figure 6.3 Cyclone inlet activity versus ESP inlet activity.

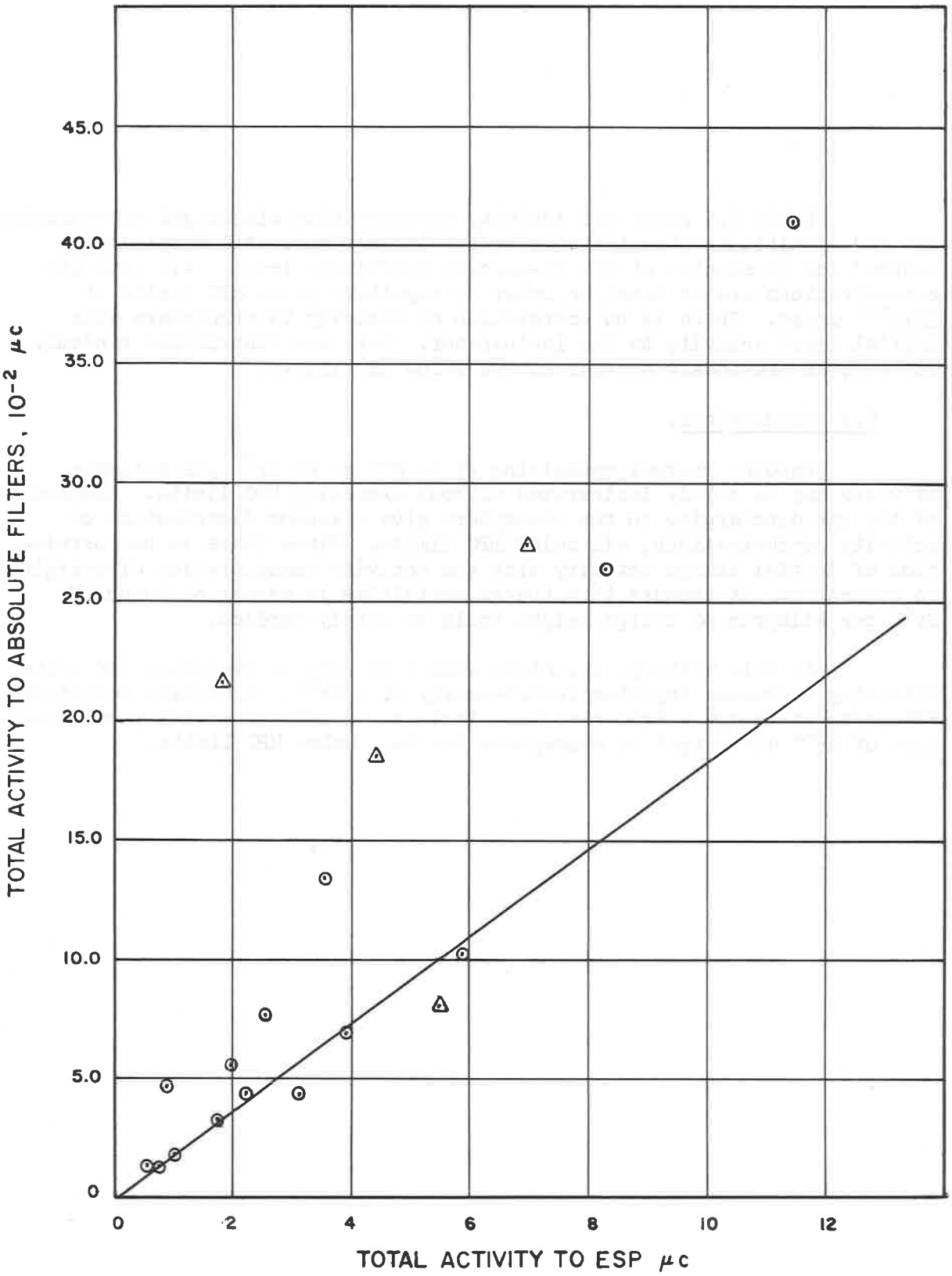


Figure 6.4 ESP inlet activity versus absolute filter inlet activity.

Table 6.5 gives the activity concentration discharged to atmosphere for the specific input activities to the incinerator. All samples were counted for 60 minutes at the 95-percent confidence level. All activity concentrations are at least an order of magnitude below MPC limits of $3 \times 10^{-10}$ μc/cc. There is no correlation of activity to atmosphere with initial input activity to the incinerator. Data was distributed randomly but was, as previously stated, always below MPC limits.

## 6.5 Conclusions.

Sawdust charges containing up to 200 μc of $Sr^{89}$ per kilogram of waste may be safely incinerated without exceeding MPC limits. Samples of the gas discharging to the atmosphere give a random distribution of activity concentrations, all below MPC limits. Since there is no correlation of initial charge activity with the activity concentration discharging to atmosphere, it appears that charge activities in excess of 200μc of $Sr^{89}$ per kilogram of charge weight could be safely handled.

At this writing, a limited amount of data is available for tests utilizing carcasses injected intravenously with $Sr^{89}$. Carcasses containing 200 μc/kg of charge weight have been incinerated and the activity concentration of $Sr^{89}$ discharged to atmosphere has been below MPC limits.

TABLE 6.5 ACTIVITY CONCENTRATION DISCHARGED TO ATMOSPHERE

| Input Activity to to Incinerator | Activity Concentration to Atmosphere[a] |
|---|---|
| μc/kg | μc/cc |
| 10 | ≤ Background |
| 20 | ≤ Background |
| 30 | $(5.8 \pm 5.0) \times 10^{-12}$ |
| 40 | $(9.0 \pm 20.9) \times 10^{-13}$ |
| 50 | ≤ Background |
| 60 | $(7.2 \pm 40.5) \times 10^{-13}$ |
| 70 | $(6.6 \pm 2.4) \times 10^{-12}$ |
| 80 | $(3.8 \pm 2.8) \times 10^{-12}$ |
| 90 | $(7.1 \pm 3.1) \times 10^{-12}$ |
| 100 | $(2.2 \pm 0.6) \times 10^{-11}$ |
| 110 | $(6.2 \pm 4.8) \times 10^{-12}$ |
| 120 | $(3.1 \pm 3.2) \times 10^{-12}$ |
| 130 | $(3.3 \pm 3.7) \times 10^{-12}$ |
| 140 | $(1.3 \pm 0.5) \times 10^{-11}$ |
| 150 | $(4.4 \pm 3.8) \times 10^{-12}$ |
| 160 | $(1.9 \pm 4.1) \times 10^{-12}$ |
| 170 | ≤ Background |
| 180 | [b] |
| 190 | $(2.6 \pm 0.5) \times 10^{-11}$ |
| 200 | $(4.0 \pm 4.7) \times 10^{-12}$ |

[a] Individual samples counted for 60 minutes at 95 percent confidence level.

[b] Sample accidentally contaminated.

# DISPOSAL OF LOW LEVEL RADIOACTIVE WASTE IN COMMERCIAL INCINERATORS

by

M. W. First, P. Zilles, and J. Walkley
Harvard School of Public Health
665 Huntington Avenue
Boston, Massachusetts 02115

---

## ABSTRACT

A comparison was made of the performance of a crematory-type incinerator and a combination steam-boiler incinerator in the combustion of difficult laboratory and hospital wastes such as animals and cage litter. Because of excessive stack emissions of smoke, fly ash, and malodorous gases and vapors, the crematory-type proved unsatisfactory. Under the most favorable operating conditions for avoidance of air pollution and for production of a good quality residue, burning capacity was only 2 to 3 lbs/sq. ft./hr. Higher burning rates produced severe nuisances. The mechanized steam-boiler incinerator, on the other hand, provided a sanitary method for handling and burning such wastes in an efficient and rapid manner. A cyclone dust collector proved superfluous for use with gas or oil fuels and it was found that it could be eliminated without decreasing the overall collection efficiency of an electrostatic precipitator which served as a final cleaning stage.

## I. INTRODUCTION

A great deal of the contaminated solid waste originating from the use of low levels of radioactive material is combustible in nature (e.g. paper wipes, animal bedding, animal carcasses) and incineration is an obvious method of concentration. Volume reductions up to 80 to 1 can be obtained.[1]

It is not practical, for obvious reasons, to dispose of septic, radioactive, pyrophoric and poisonous wastes through usual channels. Therefore, institutions generating these classes of special solid waste materials must, of necessity, dispose of them on their own premises and with their own personnel. Suitable equipment of moderate size, high combustion efficiency, low air pollution potential, and possessing safe and sanitary means for handling unburned wastes and disposing of ash is not available commercially nor are most consulting engineers prepared to design suitable facilities of a special nature.

Although not completely satisfactory in terms of sanitation, completeness of combustion, and odor production, most research institutions and hospitals have installed readily-available commercial burning equipment. The causes for dissatisfaction are two-fold; first, commercial trash burners are used with little or no attempt to modify and adapt them to the special needs of hospitals and laboratories. Second, during routine operations, burning is intermittent and the temperatures needed for the complete destruction of items that burn with difficulty, e.g., large animals, are seldom attained. Recently, institutions of this character have grown greatly in size and number, the volume of work generating troublesome waste disposal problems has multiplied, and urban crowding has decreased the safety factor provided by distance from the source. For all of these reasons, better and safer methods of solid waste decontamination and disposal are sorely needed at the present time.

To overcome these obvious difficulties, a combination heavy oil-burning steam boiler and incinerator facility was constructed for Harvard University and its associated medical institutions which are located in a highly crowded urban medical and teaching center. Flue gas emissions of particulate matter during incineration and soot blowing were controlled with the aid of high efficiency dust collection equipment. As this combination boiler-incinerator has a number of unique features, such as a special burning hearth and automatic waste feeding mechanisms that were designed to assure sanitary waste and residue handling as well as reduced air pollution emissions, it was considered to be a prototype unit and its performance was observed and measured over an extended period. Most hospitals and medical research institutions burn large amounts of liquid or gaseous fuel for steam and hot water, making it possible to use similar combination facilities to solve their special waste disposal problems. Many conventional incinerators are likely to remain in service, however, as modification of existing steam boilers for incineration service appears to be overly costly. Therefore, this investigation included additional studies on a typical institutional type of incinerator (usually called a "crematory" unit) to determine its operating characteristics, gaseous emissions, and methods that may be used to reduce air pollution when burning typical hospital and laboratory wastes containing low level radioactive matter.

## II. DESCRIPTION OF INCINERATORS

### A. Commercial Crematory-type Incinerator.

Figure 1 is a schematic of the conventional incinerator used in this study. It is typical of those supplied for this service by several manufacturers. Material to be burned is placed by hand on the fire-brick hearth of the combustion chamber. Auxiliary heat is provided by means of a single underhearth gas jet which burns 5.5 cfm of 1050 Btu natural gas. After traversing the under-hearth chamber, the gas flame makes a pass through the combustion chamber, sweeping over the material to be burned, and thereby providing auxiliary heating over and under the charge. From the combustion chamber, the gases pass through a settling chamber and then to a 1-ft. square flue. The hearth area is 11 sq. ft. and the combustion chamber volume is 20 cu. ft. The manufacturer's capacity rating for this unit is not known, but the average daily waste load during the test period was 150 lbs. and the peak daily load was only slightly over 500 lbs. The material burned was 45% by weight cage litter (principally sawdust contaminated with urine and feces) and the remainder, eggs and animal carcasses. The incinerator operated approximately 7 hours daily. This is equivalent to an average hearth load of 2 lbs./sq. ft./hr. and a peak load of 6.5 lbs./sq. ft./hr. These are, obviously, very low hearth loadings, and, in fact, the nature of the material to be burned was such that complete destruction, rather than a high burning rate, was the objective.

Normally, incinerator combustion gases discharged to the roof through a 60-ft. natural draft flue. It was observed that dark smoke emissions customarily followed the addition of a charge to the burning hearth, the intensity and duration being more or less proportional to the weight of material in the newly added batch. In addition, white fly ash was emitted when the partially consumed charge on the hearth was stoked, or otherwise disturbed. In an effort to decrease the nuisance and air contamination resulting from the operation of this incinerator, a cyclone dust collector and an electrostatic precipitator were installed and an induced draft fan was added to overcome the resistances of the collectors and the added ducting. This is shown in Figure 2. An adjustable room air opening was provided upstream of the collectors to keep flue gas temperatures within the 500°F maximum limit recommended for the electrostatic precipitator. Total volumetric flow through the collectors and blower was 780 cfm, made up of 185 cfm of room air with the remainder being combustion products from the incinerator. As the temperature of the flue gases increased, following addition of a charge to the hearth, the total weight flow through the blower decreased and the proportion of total gas from the combustion zone decreased, as well. Temperature of the combustion gases from the hearth chamber seldom exceeded 850°F before cooling. These low flue gas temperatures are compatible with the observed poor combustion characteristics of the incinerator and may be accounted for, in part, by the large amounts of excess air, ranging up to 700%, that were involved in the combustion process.

The primary dust collector was a single 10-in. diameter cyclone tube. The final cleaning state, an electrostatic precipitator, contained nine 6-in. diameter vertical tubes 57 ins. long with a total rated capacity of 800 cfm. The high voltage discharge electrodes were rigid, star-shaped probes suspended from insulated supports so as to hang free inside the tubes. Air flow was from the bottom upward. Operating voltages of 28-33 KV negative D.C. were supplied by an electrostatic high voltage power supply unit with manual controls. The precipitator tubes were cleaned manually when the unit was out of operation.

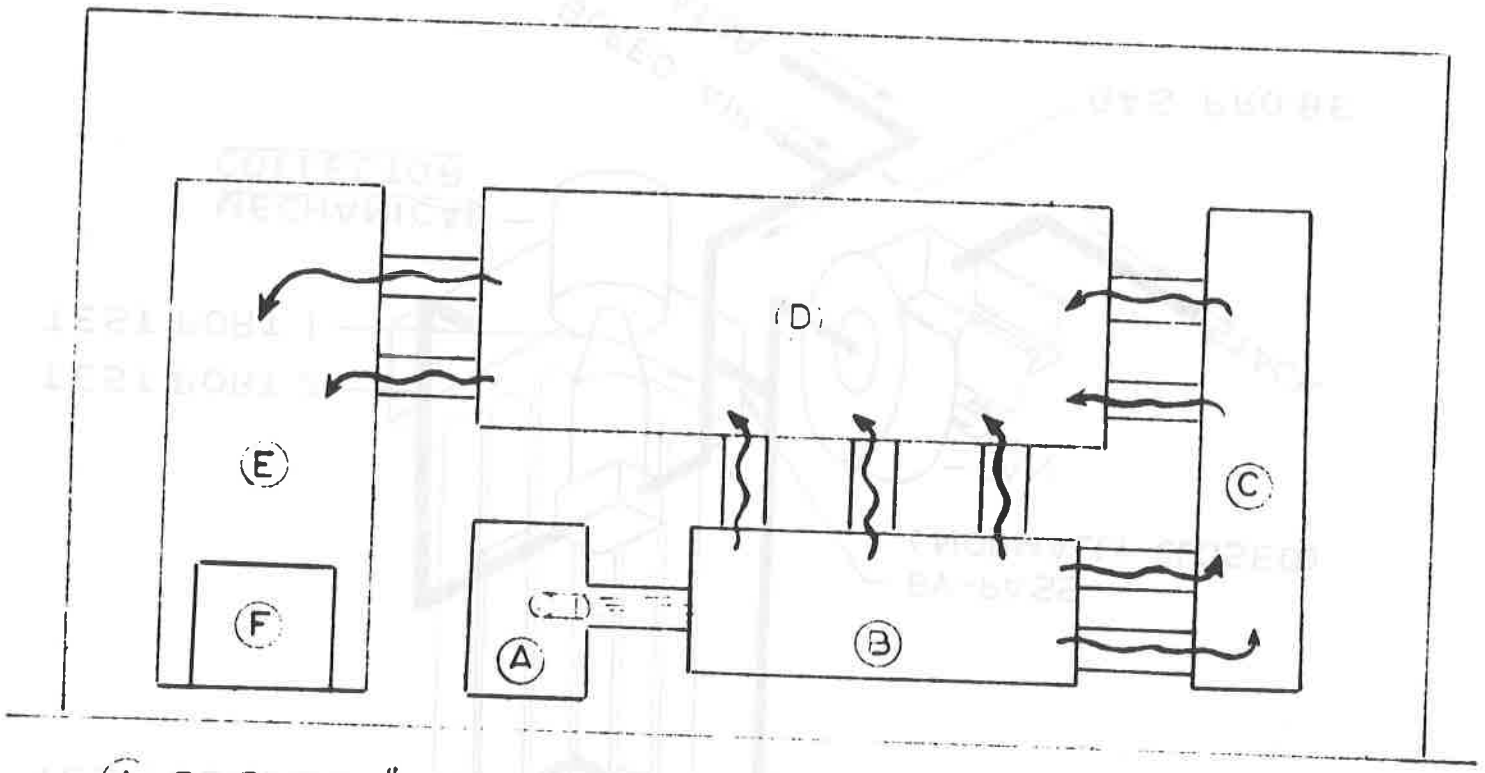


(A) BURNER & AIR INLET
(B) FIREBOX
(C) MIX & TURN
(D) COMBUSTION CHAMBER
(E) SETTLING CHAMBER
(F) FLUE

FIG. 1 SCHEMATIC OF D.I.D. CREMATORY

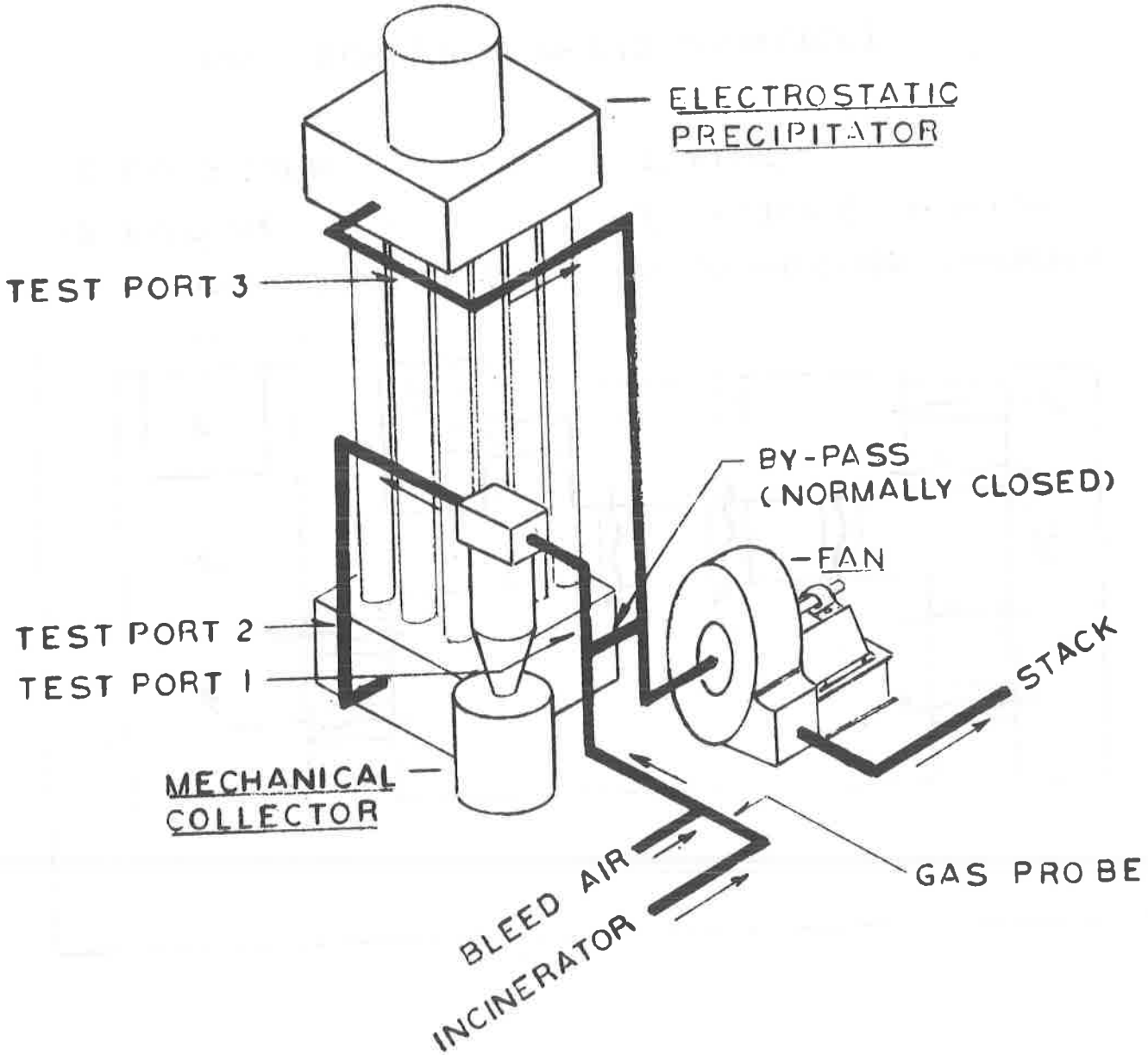


FIG. 2 GAS CLEANER ADDITIONS TO DID. CREMATORY INSTALLATION

Connecting ducts were 1-ft. square and turning vanes were installed in all bends. Sampling ports were located upstream of the collectors (after the cooling air inlet), between the cyclone and the electrostatic precipitator, and after the precipitator. These permitted measurement of the emissions from the incinerator and dust collecting efficiency of the primary and secondary dust collectors. In addition, the system was fitted with thermocouple wells and pressure measuring taps at numerous locations.

B. Combination Steam Boiler-Incinerator.

The steam boiler-incinerator facility is shown diagramatically in Figure 3. It consists of a modern, heavy-oil-fired boiler modified to burn packaged solid materials on a specially constructed hearth. An automatic system was added to receive, store, transport, and charge packages into the combustion chamber. A cyclone dust collector followed by an electrostatic precipitator was installed to reduce particulate emissions from incineration and from oil burning.

Boiler capacity is 40,000 lbs. steam/hr. at 225 psi. The boiler is fired with two internal mix, steam atomizing, conical flame burners which fire across the short dimension of the rectangular combustion chamber. Combustion air is introduced through a wind box in the opposite wall. Fully automatic combustion controls regulate fuel and air in proper relation to the steam load.

Boiler construction is conventional except for the combustion chamber which is considerably taller than normal to accommodate a large volume of waste. Two waste charging locks, approximately 5 ft. above hearth level, are located in one end wall of the combustion chamber. A service opening is located in the opposite end wall and a covered opening in the hearth connects to a vacuum system for the removal of ash. The hearth is specially shaped to slope from the charging doors to the ash removal hatch and packages have a tendency, because of the slope, to tumble away from the point of impact. This prevents piling up of waste in one spot and helps to utilize the full hearth area for burning.

The mechanical dust collector and electrostatic precipitator are matched for a gas volume of 23,600 cfm. The mechanical collector is of the multiple cyclone type, having 27 tubes arranged in 3 rows of 9 each. All assemblies are contained in a single housing with a common inlet, outlet, and dust hopper.

The electrostatic precipitator is a Cottrell type, with vertically suspended collector plates and discharge electrodes. Eleven gas passages, 12 ft. high and 9 ft. deep in the direction of gas flow, are contained in the collector plate arrangement. Collector plates and discharge electrode suspensions are rapped periodically to dislodge dust which falls into the hopper for subsequent removal. High voltage energizing equipment and automatic controls complete the installation.

The power plant ash handling system was designed for pulverized coal before conversion to oil so the coal ash system is available for use in the incinerator-boiler.

Waste charging locks, shown in Figure 4, maintain an air seal on the combustion chamber while a carton of waste is being charged. They consist of air-tight welded steel housings containing a tilt shelf for receiving and dumping

HARVARD UNIVERSITY MEDICAL CENTER

INCINERATOR - BOILER FACILITY

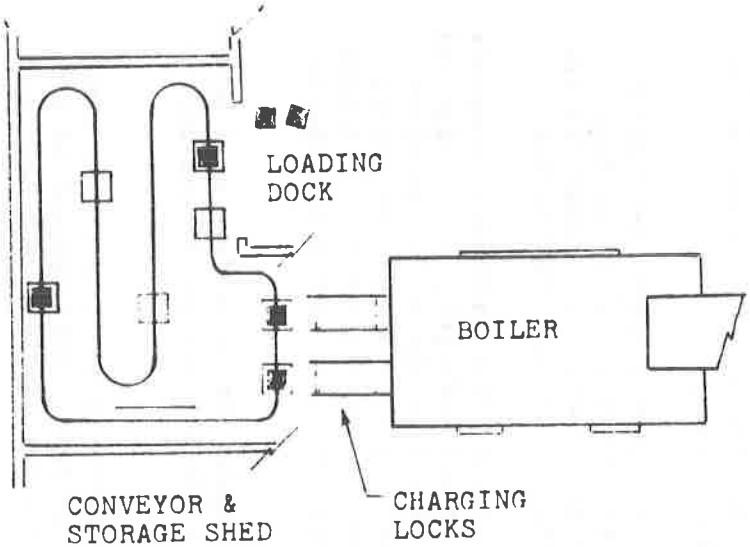


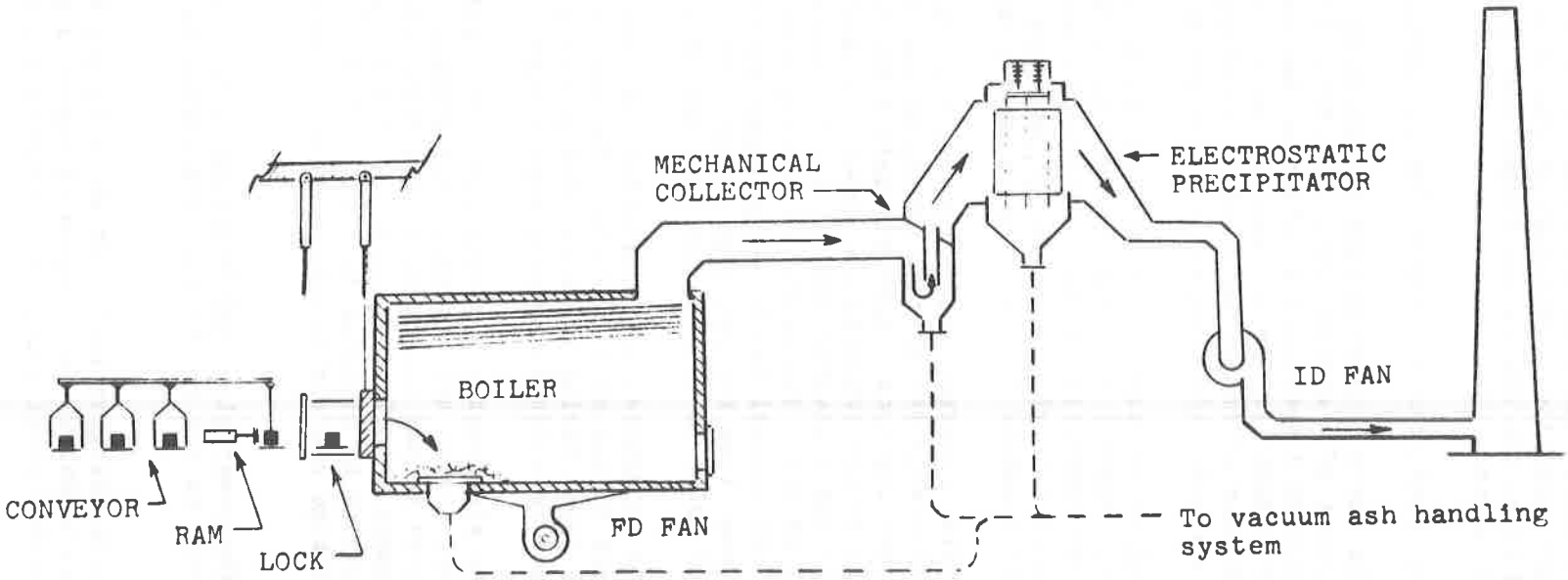


FIG. 3 LAYOUT OF INCINERATOR BOILER SYSTEM

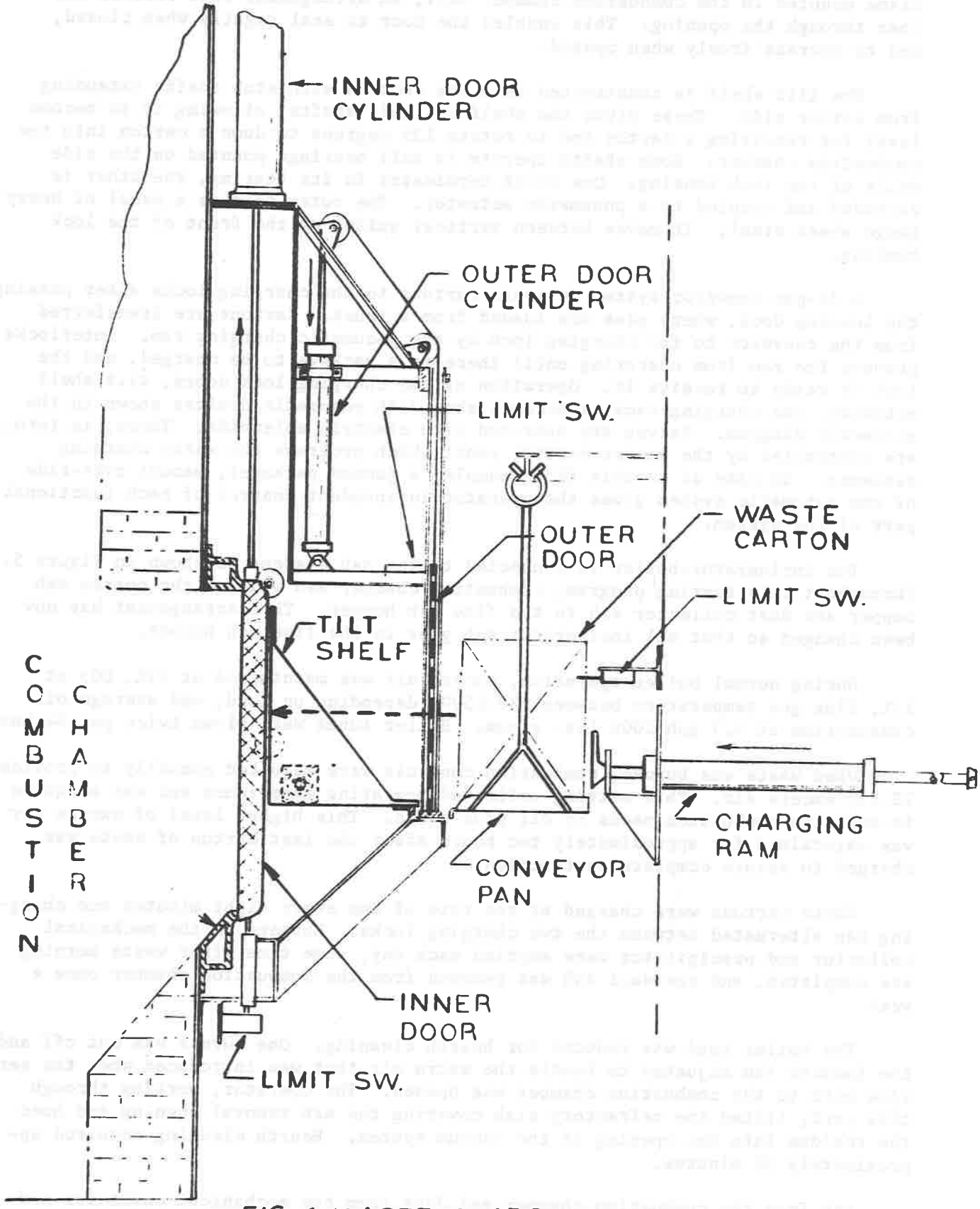


FIG. 4 WASTE CHARGING LOCK

the carton, and guillotine type doors for sealing the openings. The inner door is lined with refractory material. When closed, it rests against a water-cooled frame mounted in the combustion chamber wall, an arrangement that reduces heat loss through the opening. This enables the door to seal tightly when closed, and to operate freely when opened.

The tilt shelf is constructed as a box section with stub shafts extending from either side. These pivot the shelf on their shafts, allowing it to become level for receiving a carton and to rotate 135 degrees to dump a carton into the combustion chamber. Both shafts operate in ball bearings mounted on the side walls of the lock housing. One shaft terminates in its bearing, the other is extended and coupled to a pneumatic actuator. The outer door is a panel of heavy gauge sheet steel. It moves between vertical guides at the front of the lock housing.

A 36-pan conveyor system delivers cartons to the charging locks after passing the loading dock, where pans are loaded from a truck. Cartons are transferred from the conveyor to the charging lock by the pneumatic charging ram. Interlocks prevent the ram from operating until there is a package to be charged, and the lock is ready to receive it. Operation of the charging lock doors, tilt shelf actuator, and charging rams is accomplished with pneumatic devices shown in the schematic diagram. Valves are operated with electric solenoids. These, in turn, are controlled by the master control panel which programs the waste charging sequence. In case of trouble (for example, a jammed package), manual over-ride of the automatic system gives the operator independent control of each functional part of the system.

The incinerator-boiler is connected to the ash systems as shown in Figure 5. Throughout this testing program, combustion chamber ash went to the coarse ash hopper and dust collector ash to the fine ash hopper. This arrangement has now been changed so that all incinerator ash goes to the fine ash hopper.

During normal boiler operation, excess air was maintained at 15%, $CO_2$ at 13%, flue gas temperature between 580-650°F depending on load, and average oil consumption at 9.3 gph/1000 lbs. steam. Boiler tubes were blown twice per 24 hours.

When waste was burned, combustion controls were adjusted manually to provide 22-23% excess air. This setting reflected operating experience and was adequate to meet the combustion needs of oil plus waste. This higher level of excess air was maintained for approximately two hours after the last carton of waste was charged to assure complete destruction.

Waste cartons were charged at the rate of one every eight minutes and charging was alternated between the two charging locks. Hoppers on the mechanical collector and precipitator were emptied each day, some time after waste burning was completed, and residual ash was removed from the combustion chamber once a week.

The boiler load was reduced for hearth cleaning. One burner was cut off and the induced fan adjusted to handle the extra air that was introduced when the service port to the combustion chamber was opened. The operator, working through this port, lifted the refractory slab covering the ash removal opening and hoed the residue into the opening of the vacuum system. Hearth cleaning required approximately 30 minutes.

Ash from the combustion chamber and dust from the mechanical collector and precipitator hoppers was conveyed to storage hoppers for subsequent disposition

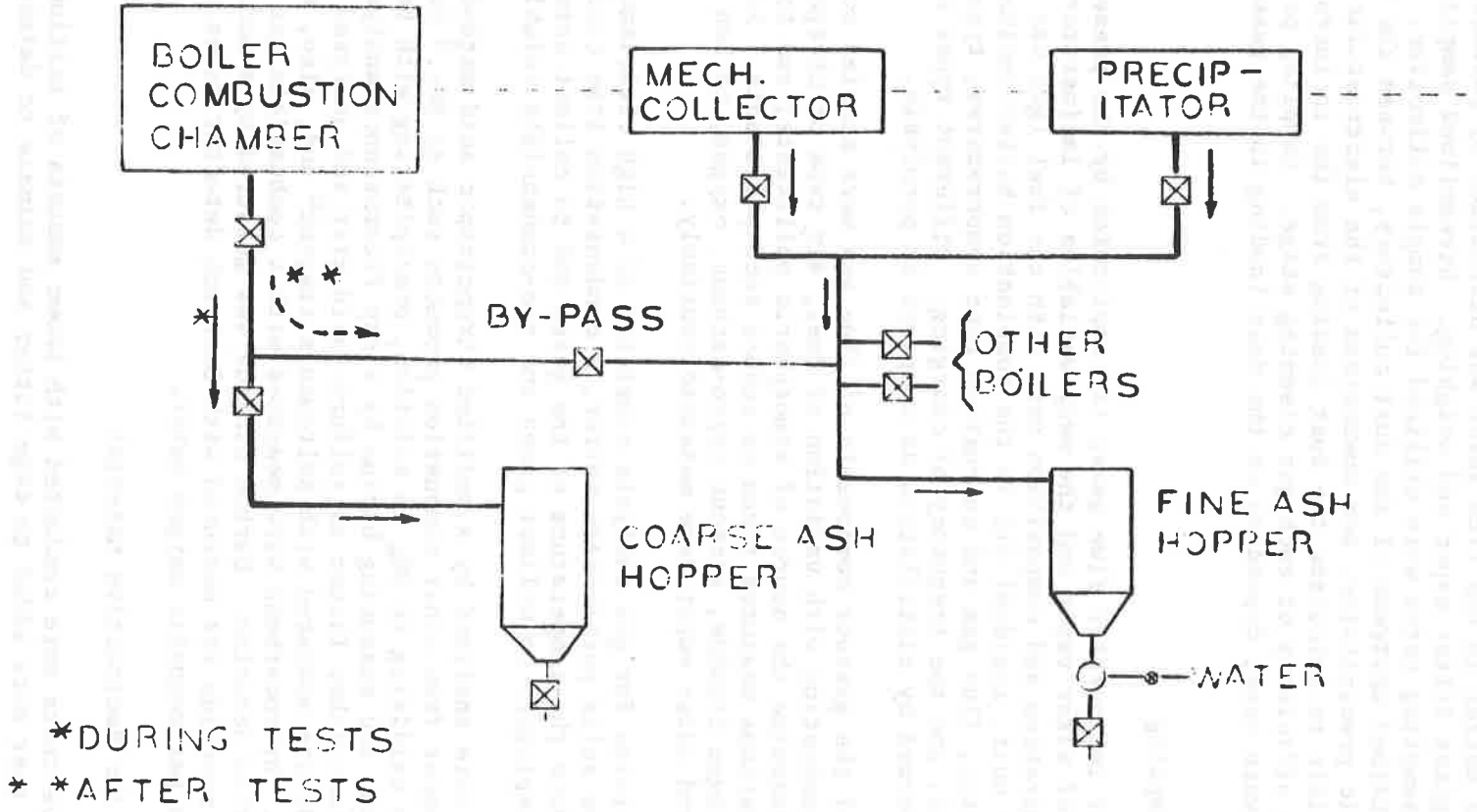


FIG. 5 ASH HANDLING SYSTEM

by truck at 4-6 week intervals.

## III. TEST PROCEDURES

The kinds of tests that were performed and the test procedures utilized were almost identical for the two incinerator installations, permitting a comparison of results as well as an examination of the performance characteristics of each unit.

### A. Determination of Particulate Matter

Particulate matter in the flue gases was determined by collection on high efficiency all-glass filter paper and weighing. Streamlined sampling probes and isokinetic sampling rates were utilized for sample collection. Simultaneous samples were obtained upstream of the dust collectors, between the cyclone and the electrostatic precipitator, and downstream of the electrostatic precipitator to make it possible to calculate the dust loading from the incinerator and the dust collection efficiency of each gas cleaning stage. Sampling periods of one to three hours were used, depending on the dust loading in the gases that were sampled.

### B. Gas Sampling

Sampling of incinerator flue gases is complicated by the presence of high concentrations of water vapor and the many variables of incinerator operation. Effluent concentration and composition vary with the fuel (gas was used in the small crematory unit, residual oil in the combination boiler-incinerator), with the fuel-air ratio, flue gas and combustion zone temperatures, type and amount of waste charged, and the frequency of charging. Different types of organic compounds are formed by distillation as compared to pyrolysis.

Analyses of the gaseous components of flue gas were carried out to determine efficiency of combustion with variation of fuel, air, type of charge, and rate of charging; to determine the source of atmospheric pollutants; and to determine the efficiency of various measures taken to reduce such pollutants. Aldehydes, oxides of sulfur, nitrogen dioxide, gaseous hydro-carbons, oxygen, carbon dioxide, carbon monoxide, and water vapor were measured routinely.

Sampling trains for gas analysis consisted of a high efficiency glass paper filter to remove solid particulate matter, a condensation trap cooled with an ice bath to reduce the temperature of the gases and to collect water vapor, gas scrubbers and impingers to collect gases and non-condensible soluble vapors.

Aldehydes were analyzed by a modified chromotropic acid method that minimized interferences from other combustion products such as $NO_2$.[2] Sulfur dioxide was analyzed by oxidizing to $SO_4$ in solution, precipitating with barium chloride in acid solution, and measuring barium by x-ray fluorescence analysis.[3] $SO_3$ was trapped on a glass fiber filter as sulfuric acid mist and analyzed in the same way. Nitrogen dioxide was measured with Saltzman's reagent[4] and, also, with Drager $NO_2$ detector tubes. Hydrocarbons were measured with a combustible gas detector and a flame ionization detector. Carbon dioxide was measured by a modified Orsat technique. Carbon monoxide was measured with Bachrach detector tubes. Oxygen was measured with a paramagnetic oxygen meter.

### C. Tests for Radioactive Material

Radioactive tests were conducted with known amounts of tritium, carbon-14, and sulfur-35, that were added to cage litter and animals to determine the release

rates of these substances from the charge and the distribution between flue gases, residue, furnace linings, and duct surfaces.

Tritium was collected as tritiated water in a condensing trap followed by two impingers immersed in an ice bath and counted by liquid scintillation.

Carbon-14 was collected from the flue gases as $CO_2$ in fritted glass bubblers containing 6N KOH. The carbonate was precipitated with barium, dried, and weighed. A finely ground aliquot was weighed into a scintillation vial, suspended in a dioxane-based scintillation liquid, and counted.

Sulfur-35 was collected from the flue gases as sulfuric acid mist on a high efficiency all-glass filter paper and as $SO_2$ in two impingers in series containing dilute NaOH. The solids on the filters and the ash were counted using a shielded end-window GM tube. The filters containing sulfuric acid mist were analyzed by leaching with water and counting by liquid scintillation. It was possible to dilute aliquots of impinger solutions from the gas-fired incinerator directly in scintillation liquid for counting. The solutions from the oil-fired incinerator contained excessive amounts of dissolved solids from high $CO_2$ and $SO_2$ concentrations and were not directly soluble. The solutions were (a) stripped of sodium ions by passing them through a strongly acid cation exchange resin (b) concentrated by evaporation and (c) counted in a scintillation liquid.

## IV. RESULTS

### A. Particulate Emissions.

For the batch-fed crematory incinerator, there was no trend of fly ash emissions (when expressed as $mg/M^3$ of flue gas) with type of charge (i.e. litter, frozen animals, unfrozen animals, or a mixture of litter and animals), with size of charge, or whether additions were made to a cold or a hot hearth. It was observed that small animal carcasses were consumed much more rapidly than large ones and that there were large variations in the amount of water contained in the cage litter, and hence the burning time. The burning time of carcasses was found to average 5.5 min./kg. During each test the charge was left to burn on the hearth without agitation although the burning rate would have been more rapid if the partially burned charge had been stoked periodically. However, particulate emissions would have been greater, also. Litter, for example, smokes while it heats (about 1/3 the total burning time), burns briskly until the surface layer is consumed, and then glows for the remainder of the burning cycle.

When the particle emission results were calculated on the basis of total grams emitted per kilogram of charge, a pattern emerged. Frozen animals produced 4 gm/kg and unfrozen animals started on a hot hearth, 1.3 gm/kg. Litter placed on a cold hearth released 5.6 gm/kg, on a hot hearth, the yield was only 2 gm/kg. Mixed litter and carcasses released 5.3 gm/kg from a cold hearth and 3.3 gm/kg from a hot hearth; not much different from the results for litter alone.

Dust collector efficiency was not influenced by the nature of the charge or the burning conditions. The first stage cyclone averaged 9% by wt. and the secondary electrostatic precipitator averaged 76% by wt., for a combined efficiency of 85%.

The residual fuel-oil-burning boiler-incinerator produced a significant particulate loading in the flue gases even when the incinerator was not in service. This soot loading ranged from 117 to 180 $mg/M^3$ of flue gas (corrected to STP) depending on the rate at which fuel oil was being burned. The average

was 149 mg/$M^3$; equivalent to 0.06 gr/SCF, corrected to 12% $CO_2$. This is the higher limit of the normal range cited in the U.S. Public Health Service publication, Atmospheric Emissions from Fuel Oil Combustion.[5]

When oil and waste, consisting principally of animal carcasses, were burned in the fire box, the loading of solids in the flue gas rose to 204 mg/$M^3$. This increase of 55 mg/$M^3$ represented a rise of only one third in dust loading over what was present when oil alone was burned. The comparable figure for the crematory incinerator when handling animal carcasses was 48 mg/$M^3$, a figure that is not greatly different from the added loading of 55 mg/$M^3$ found in the boiler-incinerator.

Considerably higher dust loadings were found during soot blowing. Over periods of approximately 10 minutes, twice a day, soot loadings of 520 mg/$M^3$ were measured.

The collection efficiency of the multi-cyclone on the boiler incinerator was found to be 19% by weight during oil burning, 22% during waste burning, and 41% during soot blowing. Electrostatic precipitator efficiencies were 56% during oil burning, 65% during waste burning, and 60% during soot blowing. This efficiency of the electrostatic precipitator was considered to be unsatisfactory and the manufacturer elected to install air straightening guide vanes before and after the precipitator to even out the flow distribution. After this modification, precipitator efficiency increased from 61% to 72% for oil and oil-plus waste burning and the combined efficiency for primary and secondary dust collectors was 80%. The reasons for the continued poor efficiency of the electrostatic precipitator are not yet known. It is possible that the low resistivity of the oily carbonaceous dust was a factor but in our opinion the poor precipitator efficiency should be attributed to electrical troubles.

B. Gases

Oxides of nitrogen, unburned hydrocarbons, and carbon monoxide were present in the flue gases of both incinerators in concentrations which were detectable during a high percentage of tests but in no case were they present in abnormal amounts. For example, $NO_2$ averaged 200 ppm during burning and 250 ppm during waste burning in the boiler-incinerator and less than 100 ppm in the crematory incinerator. Carbon monoxide was less than 1 ppm during oil burning and rose to 15 ppm during waste burning.

Sulfur dioxide was present in the flue gases of the gas-fired crematory incinerator in concentrations up to 4.7 gm/kg of charge when animal carcasses, and more especially when large numbers of eggs, were incinerated. These values for $SO_2$ were less than 5 ppm in the flue gas. Usual values for litter alone were less than 0.5 gm/kg of charge. Natural gas contributed a negligible fraction to these totals. By contrast, the sulfur content of 2.5% in the residual oil burned in the boiler-incinerator resulted in flue gas concentrations of approximately 1000 ppm $SO_2$ and 5-7 ppm $SO_3$. The contribution from the incinerated material, even using the highest value found in the gas-fired incinerator of 5 gm/kg of animal carcass, would be a negligible addition.

Aldehydes were found at concentrations close to the sensitivity of the analytical method and, in all cases, less than 0.1 ppm in the flue gases

from the boiler-incinerator. By contrast, a maximum of 100 mg aldehyde per kilogram of charge was found in the crematory unit indicating an average concentration of 0.5-0.6 ppm. This difference reflects the high combustion temperatures of the boiler-incinerator and the relatively low temperatures in the crematory unit which permitted distillation and cracking of partially pyrolysed organic materials during part of each burning cycle.

C. Radionuclide Tests

All of the tritium, introduced into animals and cage litter as tritiated water or thymidine, was accounted for in the flue gases as water vapor in both incinerators.

Almost 100% of the carbon-14 added to animals and cage litter as sodium acetate was accounted for in the flue gases in the form of $CO_2$. A negligible quantity was found in the unburned carbon of the ash and airborne particulate matter.

Sulfur-35, added in the form of $Na_2SO_4$, partitioned between the flue gases and residue. A large amount remained behind in the ash and about 55% was accounted for in the flue gases in the form of $SO_2$, with a small fraction of this as $SO_3$.

Even if we assume that a steam-boiler incinerator is used to burn radioactive laboratory wastes and the carcasses of animals used in experiments, there is no likelihood of exceeding the maximum permissible release rates to the atmosphere for these commonly-used radionuclides. This is especially true because of the enormous dilution ratios attainable in a well functioning incinerator of this type. Such factors, however as the radioactive material concentrated in the ash, external exposures of plant personnel, as well as permissible levels for disposal in public dumps, require careful control. Dilution of the residue by burning non-radioactive wastes along with the radioactive is permissible for many low-energy radionuclides but becomes difficult for substances as refractory and as biologically active as radio-calcium, often used for nutrition and bone and teeth growth studies.

V. DISCUSSION

Combustion of solid wastes contaminated with other low level radioactive substances has yielded results differing, quantitatively, from those observed during the present study. For example, measurements of the distribution of radiophosphorus, -iodine, and -strontium after incineration in a crematory type unit were made by Kruse et al.[6] They found that about 90% of the phosphorus and strontium remained in the ash; the rest distributed itself in the furnace linings or was lost to the atmosphere with fly ash emissions. About 80% of the charged radioiodine was emitted with the flue gases, although it was noted that sizable fractions of the radioactivity first deposited on furnace and stack linings and then was eluted slowly by the hot flue gases.

Substances such as volatilized iodine-131, unlike tritium or carbon-14, may not receive sufficient dilution by the flue gases to be considered innocuous when weather is unfavorable for rapid spread from the source and when the chimney

is in an unfavorable location with respect to surrounding buildings and terrain features. This difficulty may be overcome to a considerable extent by selecting only days of favorable weather for burning substances containing this radionuclide. This practice is generally simplified because packages containing radioactive matter are usually identified for inventory purposes and even animal carcasses may be stored under refrigeration for a few days without excessive hardship while waiting for favorable weather. In addition, significant radioactive decay may take place during storage. When the incinerator stack extends well above surrounding buildings and nearby terrain, there is unlikely to be a health problem associated with the discharge of gaseous radioactive material to the atmosphere because of the low-level concentration customarily present in wastes from research and teaching establishments and medical facilities.

The disposal of residues containing radioactive substances is complicated by the very low values permitted by U.S. regulations for land disposal in ordinary dumps. This suggests that, when possible, radionuclides should be in a chemical form that favors formation of a gas or vapor which, when diluted with flue gas, will meet limits for atmospheric release. Failing this, and when dilution with sufficient non-radioactive residue to reduce activity to an acceptable level is impractical, the residue must be packaged in a dust-free manner and shipped to a radioactive storage facility for ultimate disposal.

Kruse et al[6] also noted, as did Megonnell et al[7], that exposure of incinerator personnel to the dust from the hearth residue in a commercial crematory-type incinerator represents an important health hazard when the wastes being burned are contaminated with radioactive and other toxic substances. The automatic ash handling system in use for the Harvard boiler-incinerator eliminates this hazard.

## VI. CONCLUSIONS

On the basis of these studies, it is concluded that a crematory-type incinerator is an unsatisfactory device for burning difficult laboratory and hospital wastes such as animals and cage litter. This is primarily due to the excessive stack emissions of smoke, fly ash, and malodorous gases and vapors. Under the most favorable operating conditions for avoidance of air pollution and for production of a good quality residue (i.e. no organic matter), the burning capacity of such a unit is only 2-3 lbs/sq. ft./hr. Higher burning rates can and do, produce severe nusiances. High efficiency dust collection equipment can reduce particulate emissions, including bacteria and radioactive particles, but can not eliminate offensive gases and vapors.

The Harvard boiler-incinerator, handling packaged wastes in mechanical systems, provided a sanitary method for handling and burning especially troublesome laboratory wastes in an efficient and rapid manner. The enormous heat flux inside the combustion chamber of a base-loaded boiler assures optimum conditions for incineration at all times. A cyclone dust collector proved superfluous for use with gas or oil fuels and it was found that it could be eliminated without decreasing the overall collection efficiency of an electrostatic precipitator which served as a final cleaning stage. The reasons for the poor efficiency of the electrostatic precipitator in this type of service require additional study.

## REFERENCES


1. Collins, J. C. and Fleck, A. Radioactive Wastes. John Wiley. N.Y.C. 1960.

2. Walkley, J. "Reduction of Interference from Oxides of Nitrogen in the Chromotropic Acid Method for Formaldehyde," Paper delivered at Am. Ind. Hyg. Conf., Pittsburgh, Pa. May, 1966.

3. Walkley, J. "The Determination of Sulfur Dioxide and Sulfates by X-Ray Emission Spectrometry, " Paper delivered at Am. Ind. Hyg. Conf., Pittsburgh, Pa. May, 1966.

4. Saltzman, B.E., "Colorimetric Microdetermination of Nitrogen Dioxide in the Atmosphere," Anal. Chem., 26:1949, 1954.

5. Smith, W. S. "Atmospheric Emissions from Fuel Oil Combustion," PHS Pub. No. 999-AP-2. Public Health Service. Division of Air Poll., Cinn., Ohio Nov. 1962.

6. Kruse, C. W., Feese, P. V., Mochis, A., and Behn, V. C. Behavior of Institutional Incinerators when used to Burn Radioactive Wastes, Final Project Report for August 1, 1950-November 1, 1952. (from USAEC-TIS, Oak Ridge, Tenn.)

7. Megonnell, W.H., Ludwig, J. H. and Silverman, L. "Dust exposures during ash removal from incinerators", AMA Arch. Ind. Health. 15:215 (1957).

# RECENT ADVANCES IN MONITORING OF RADIOACTIVE GASEOUS WASTES AT ORNL

J. F. Manneschmidt

Oak Ridge National Laboratory*

## ABSTRACT

Many activities at the Oak Ridge National Laboratory are concerned with the chemical processing of radioactive materials. Gaseous effluents from these operations are treated to remove dangerous contaminants prior to release to the atmosphere. Routine monitoring of such emissions was started in 1956 when manually operated particulate monitors were installed at each of three process stacks. Since that date, coverage has been extended to six stacks, the sample withdrawal system has been rebuilt, and the detection equipment has been added to and modernized. The intensive monitoring has lead to process improvements which have reduced the environmental releases of radioactivity in the Laboratory's gaseous waste effluents by a factor of three since 1962.

## INTRODUCTION

The Oak Ridge National Laboratory, functioning as a research center for the Atomic Energy Commission, is engaged in a wide variety of activities, most of which involve operations that use radioactive materials. Research and development groups are involved in experimental studies that include the chemical processing of many highly active substances, ranging in quantity from millicuries to kilocuries. There are at the Laboratory eight nuclear reactors of different types, three of which operate continuously and provide facilities for numerous experiments. One of these, the High Flux Isotope Reactor, will operate at a power of 100 Mw and generate a flux of $5 \times 10^{15}$ neutrons $cm^{-2}$ $sec^{-1}$. This reactor will be used to irradiate curium targets and produce, over a period of years, gram quantities of $^{252}Cf$. The transplutonics program is already well under way at the Laboratory with gram quantities of the curium and americium isotopes being processed routinely. Such operations as these invariably produce quantities of gaseous waste, usually containing some degree of activity, which must be treated for removal of the dangerous contaminants before discharge to the atmosphere.

---

*Operated by the Union Carbide Corporation for the U. S. Atomic Energy Commission.

The Laboratory's gaseous waste disposal and monitoring systems were described by the author in a report[1] published in 1961. This report presents a brief review of the systems as they are operating at present with new developments which have been added since that time.

## GASEOUS WASTE DISPOSAL SYSTEMS

The greater part of the Laboratory's gaseous waste is discharged to the atmosphere from six stacks. (Some buildings release small quantities of ventilation air from roof exhausts; however, the amounts of radioactivity involved are small and such systems will not be discussed here. It should also be pointed out that any operation at the Laboratory which proposes to release gaseous wastes directly to the atmosphere in this manner is scrutinized very carefully and the safety of the operation must be assured beforehand.)

In the Melton Valley area of the Laboratory (Figure 1) are located the newest research facilities: the High Flux Isotope Reactor (HFIR), the Transuranium Facility (TRU) where the targets from the HFIR will be processed, and the Thorium-Uranium Fuel Cycle Development Facility (TUFCDF). Gaseous wastes from these areas consist mainly of off-gas from reactor coolant degasifiers and chemical processing equipment and ventilation air from cells and containment areas. The off-gas streams, being the most radioactive, are passed first through charcoal beds where adsorbable activities are removed and then through absolute filters before discharge to the stack. Cell-ventilation air is only filtered. A common stack serves all these areas. Initial testing of the HFIR is now being carried out at low power levels, and no targets have yet been irradiated. Likewise, the TRU facility has only recently gone "hot" and at this time only small amounts of activity are present in the cells. Consequently, the discharge of gaseous activity from these areas is negligible at the present.

The Molten Salt Reactor Experiment (MSRE), also located in this valley, has the capability of producing radioactive gaseous waste. Off-gas from the fuel pump and the reactor cell and ventilation air from other cells and containment areas is treated, as at the HFIR, either by filtering alone or by both filtering and exposure to charcoal. This facility is served by its own stack. Activity releases from this area have been found to be very low, consisting mainly of $^{131}I$ and rare gases.

Most of the Laboratory's operations are located in Bethel Valley (Figure 2), and it is from this area that most of the gaseous activity originates. The oldest contributor to the gaseous waste system in this area is the Graphite Reactor, now out of service. The fuel channels are still ventilated and the exhaust air is filtered before it is released through the stack. No significant amount of activity can be detected in the release.

The Pilot Plant stack discharges ventilation air from cells and operating areas where several types of irradiated fuel elements are processed and also from an analytical laboratory in the same building. The gaseous waste from this area passes through absolute filters but is found to contain $^{131}I$ and traces of the thoron daughters when it is discharged to the atmosphere.

A recently completed analytical laboratory, designed and equipped to carry out analytical procedures on very highly active substances, is also considered a

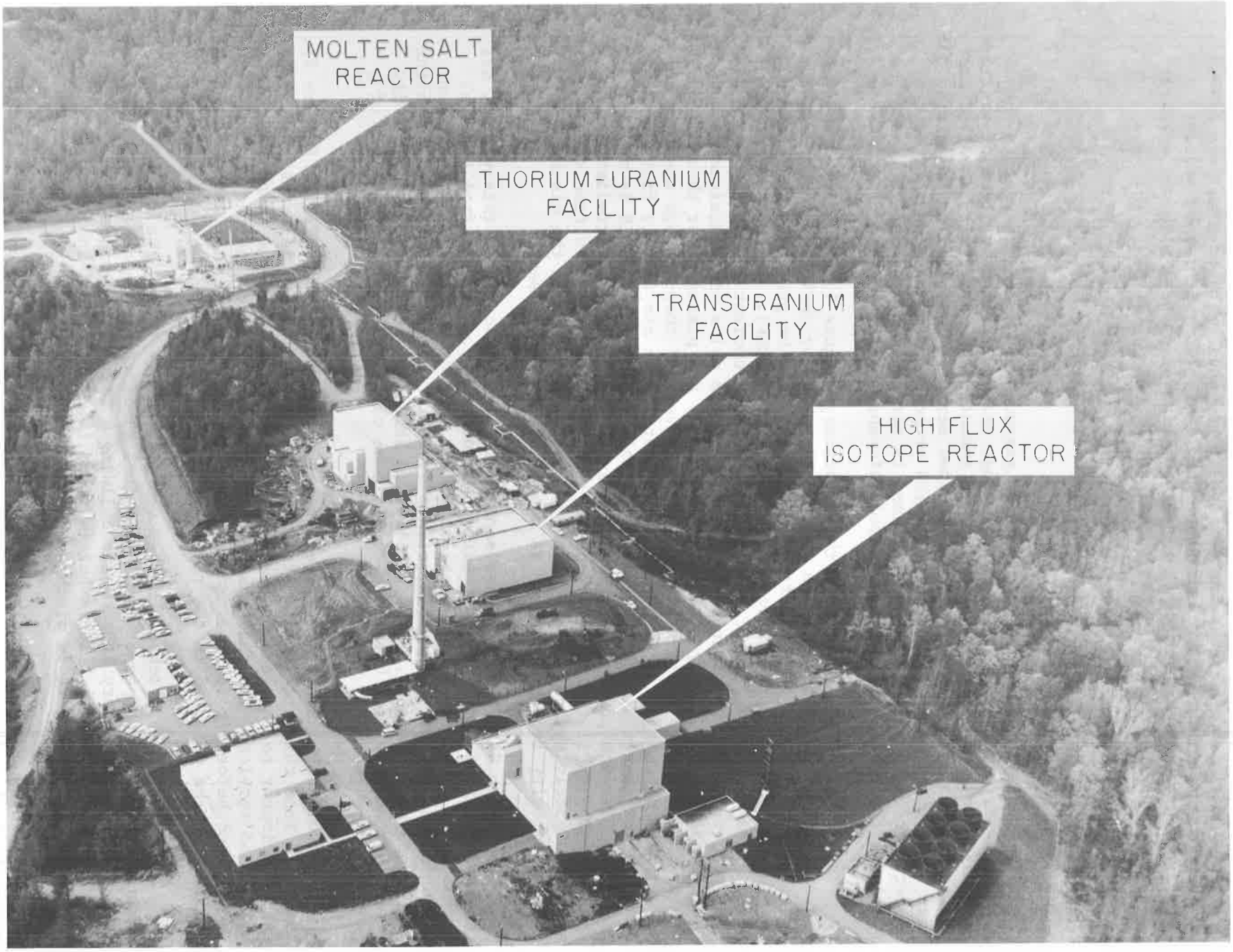


Figure 1. Melton Valley Area of the Oak Ridge National Laboratory

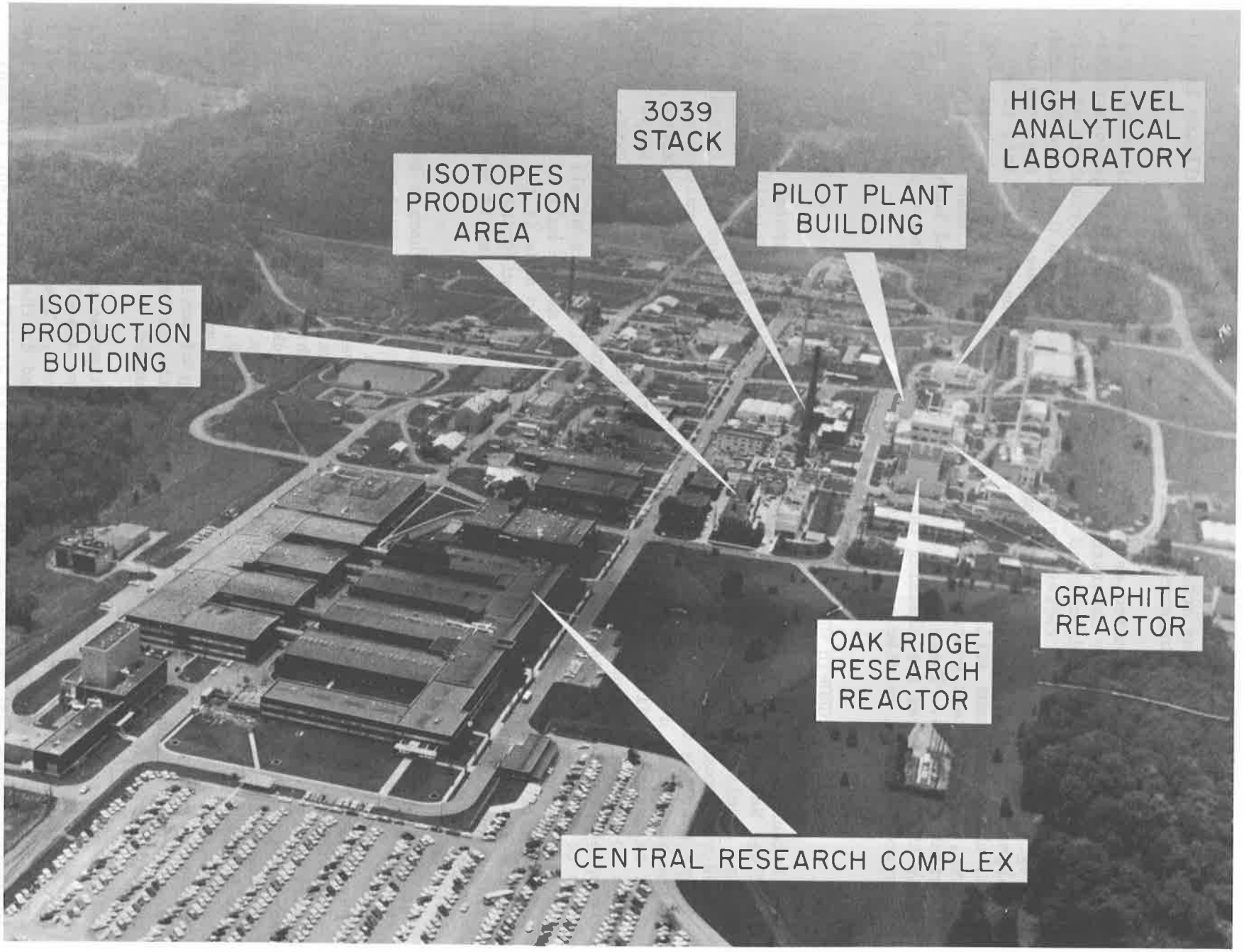


Figure 2. Bethel Valley Area of the Oak Ridge National Laboratory

potential source of gaseous activity. The exhaust air from this building is filtered before release to the environment.

A sixth stack, designated as the 3039 Stack, serves most of the chemical and research facilities of the Laboratory; and about 99% of the total gaseous activity generated at ORNL is discharged through it. Principal contributors of activity to this stack are the radioisotopes processing areas, the Oak Ridge Research Reactor (ORR), and the large complex of buildings which houses the research and development groups. Although a wide variety of operations is tied into this stack, the predominant activity here, as elsewhere, is and has always been $^{131}I$. However, during recent years, at least 24 other nuclides have been identified in the stack emissions. There is a variety of equipment employed both at this stack and in the work areas for cleaning the gaseous discharges; however, that phase of the system will not be discussed at this time.

## GROWTH OF THE MONITORING SYSTEM AT ORNL

Because monitoring is vital to any radioactive waste disposal system, the Oak Ridge National Laboratory has placed much emphasis on developing and maintaining a reliable monitoring system. Gaseous waste monitoring at the Laboratory serves two important functions. First, it enables supervision to maintain better control over the many activities and operations which generate gaseous activity. At the same time, a sensitive monitoring system will alert the Laboratory in the event of a serious discharge into the atmosphere; and the necessary steps can be taken to protect personnel and property from fallout or radiation danger. Second, a complete monitoring system will provide sufficient information on a periodic basis to compute, with reasonable accuracy, the total amounts of all important nuclides being released to the environment. Inasmuch as the bulk of the discharged activity comes from one stack, it was decided to make it the pilot stack for the development of a monitoring system. There are monitoring devices on the five other stacks mentioned earlier; however, they are similar to those on the 3039 Stack and so will not be discussed in detail.

Routine monitoring of the Laboratory gaseous waste discharges was first started by our Health Physics Division in 1956 when a filter tape monitor was installed on the Graphite Reactor Stack. In 1957 a similar device was put into operation at the Pilot Plant Stack, and in 1959 coverage was extended to the 3039 Stack. Prior to these dates, grab sampling was done but not routinely. The first monitor was a very simple affair (Figure 3) which consisted of a 2-in. filter tape through which a measured stream of the stack gas was drawn. A side-window G-M tube was located adjacent to the tape in such a manner as to detect the buildup of activity during the collection period. The tape was changed daily by manually pulling it through the collection block and cutting it off. The deposited activity was then counted. The buildup of activity, as seen by the G-M tube, served as a measure of stack behavior; if the buildup occurred at an abnormal rate and exceeded preset limits, an alarm sounded.

Of interest is the type of sample withdrawal probe used in conjunction with these monitors. This probe (Figure 4) was a 1-in. stainless steel pipe inserted across the diameter of the stack at the 50-ft level. The sample stream was withdrawn through perforations in the pipe and carried to the monitor at ground level. Inspection shows that a system of this design is grossly inefficient for many

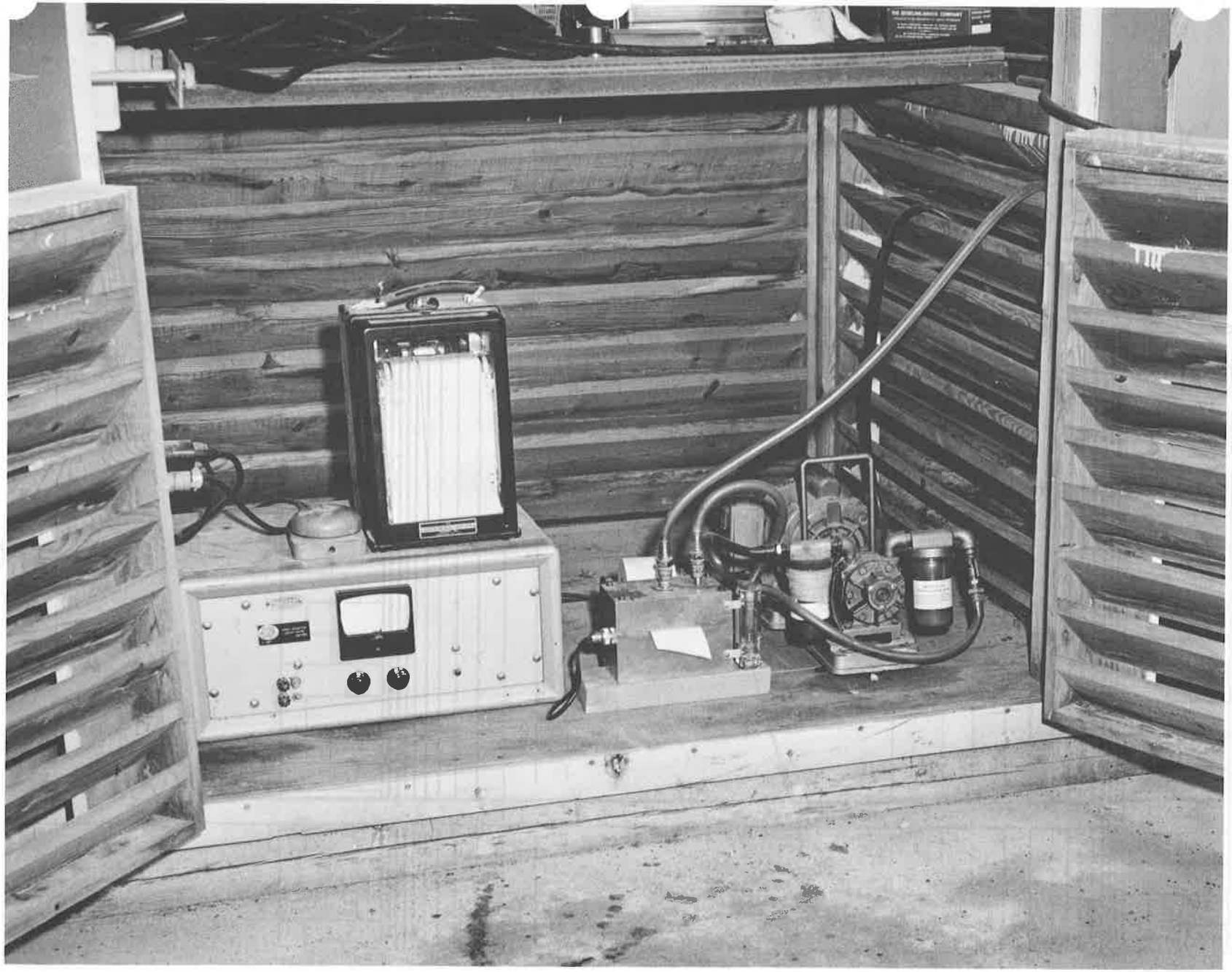

Figure 3. Health Physics Stack Monitor - Early Model

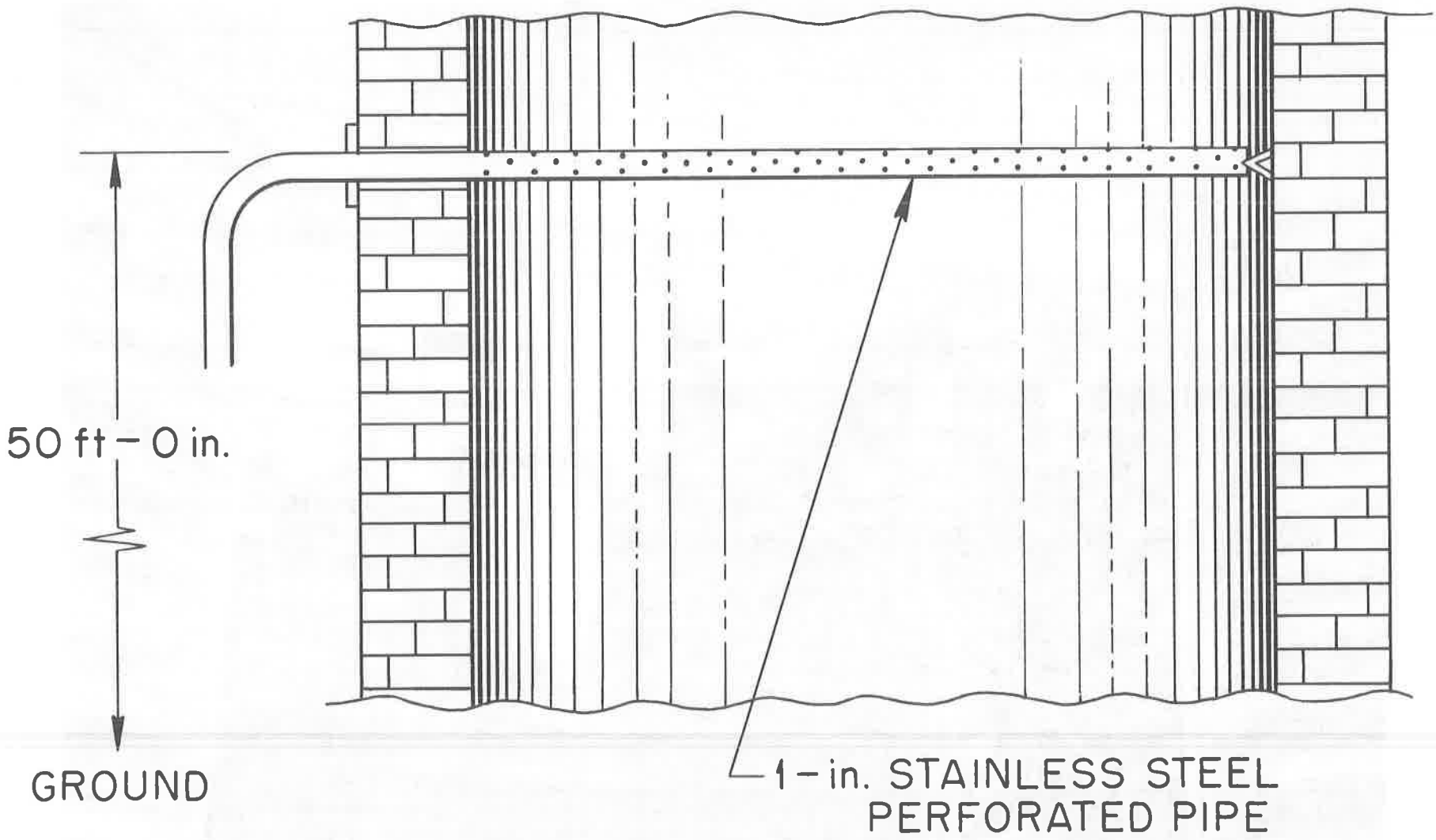


Figure 4. Traverse Type Sampler - 3039 Stack

types of airborne-activity. Centrifugal losses, plate-out (amplified by the great length of connecting tubing), and losses occasioned by horizontal runs all take their toll, particularly in a system where the detection of large particles is of importance. The importance of these factors was not known at the time of installation, however; and it was not until late 1959 that the entire gaseous waste disposal system was examined critically and the first steps were taken to develop a complete, efficient monitoring system.

## IMPROVEMENTS IN THE SAMPLE WITHDRAWAL SYSTEM

The Operations Division of the Laboratory, which is responsible for the operation of the radioactive waste systems, began, in cooperation with the instrumentation and engineering divisions, an extensive program to upgrade and revise the monitoring and sampling systems. A series of experiments was begun to evolve the optimum design for a withdrawal system. The first decision was to relocate all monitoring and sampling devices as near to the point of sample withdrawal as possible. Prior knowledge of the art made it evident that to achieve anywhere near "isokinetic" sampling in the stack the length of the sample duct must be reduced to a minimum. It might be worthwhile to interject at this point that isokinetic sampling under field conditions has proved to be a very idealistic and elusive goal which, for many practical reasons, has not been achieved at ORNL.

In order to gain information about the air-flow pattern within the stack, numerous traverses were made. Some of these were for the purpose of measuring flow rates; others were made simultaneously with the injection of either solids or radioactive gases. In the final phase of testing, three probes were placed in the stack at the 50-ft level; and a tape monitor was attached to each. The activity seen by each probe was then observed for several months. From the information gained a determination was made concerning the arrangement and minimum number of sample nozzles within the stack.

The withdrawal system which finally evolved consisted of a three-probe configuration (Figure 5). Two of the probes are simple withdrawal tubes made of 1-in. stainless steel pipe, to the outside ends of which might be attached monitoring devices. The probes, after insertion, are extended 4 ft from the inner wall of the stack and are curved downward 4 1/2 ft. The third probe accommodates the in-stack sampler which will be described later.

## MODIFICATION AND REVISIONS OF THE PARTICULATE MONITOR

Steps were next taken to provide additional detection instruments and to improve the tape-collection device already in use. The manually operated tape sampler was replaced by a rather crude but entirely functional moving tape monitor (Figure 6). This was the first instrument of this type used at the Laboratory. It employed a 1 1/2-in. tape which moved stepwise on a preset time cycle or which could be advanced by means of a push button. The activity deposited by the stream of gas passing through the tape was then monitored by an end-window G-M tube located in a lead shield. Later models do not use the end-window tube and, therefore, lack the sensitivity inherent in that particular type of tube.

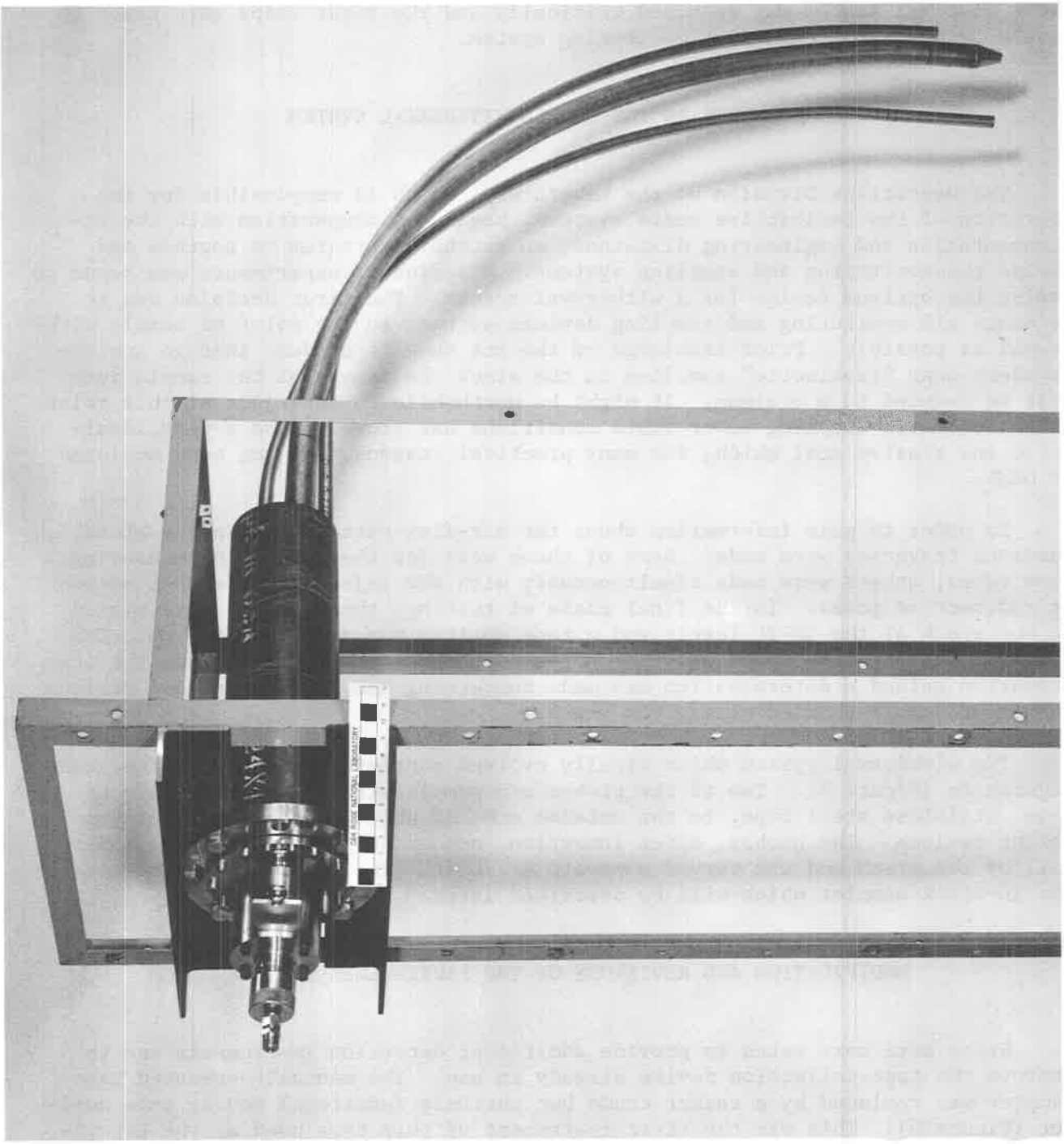

Figure 5. Three-Probe Sampler

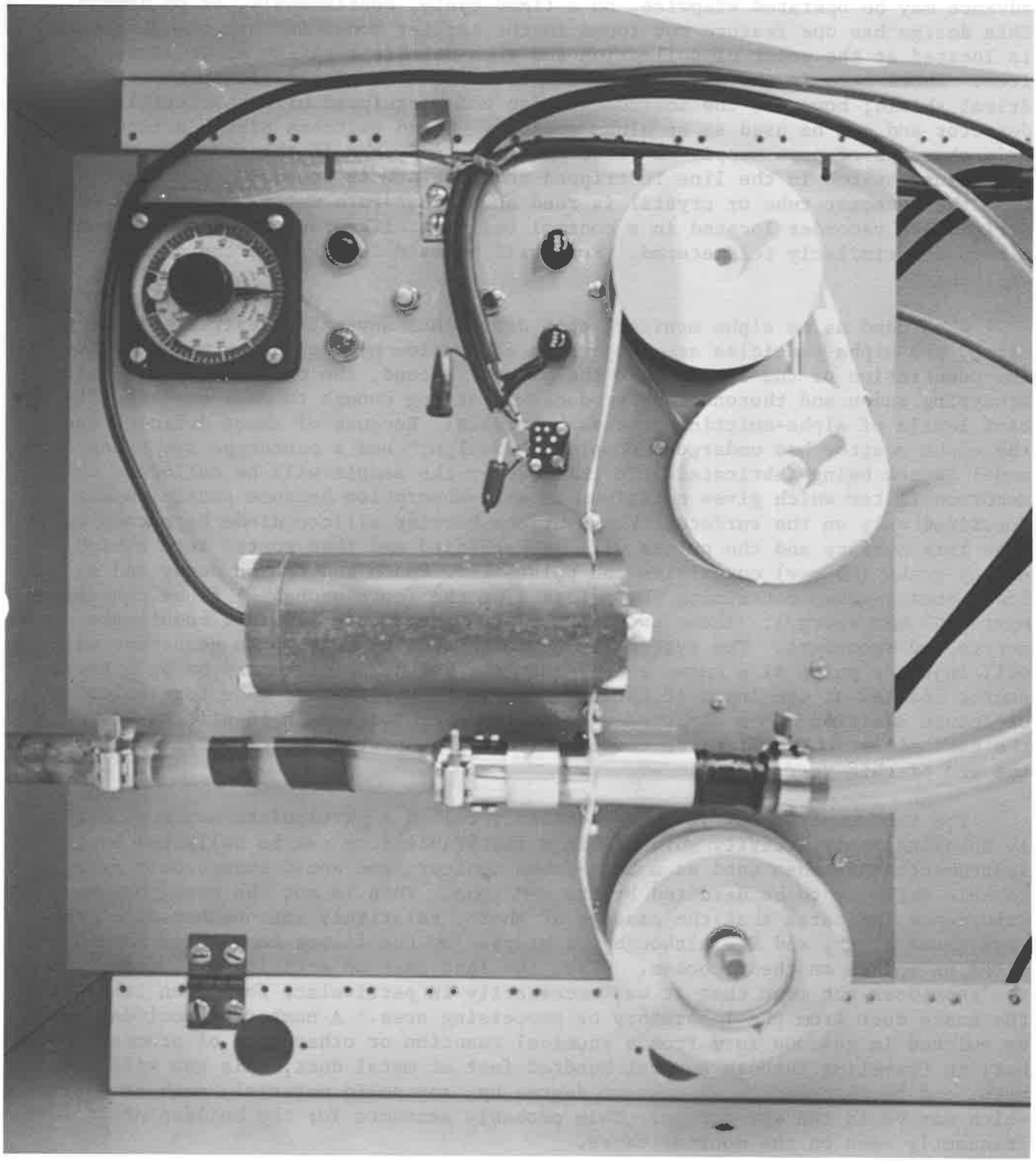

Figure 6. Early Model Moving Tape Monitor

The model which replaced this rather simple design is shown in Figure 7. A 3-in. tape is used here, providing a greater collection area; and the tape advance may be operated stepwise, on a timed cycle, continuously, or on demand. This design has one feature not found in the earlier model in that the detector is located at the point of collection and thus detects activity as it is deposited. Shown here is the side-window G-M tube which is placed within the cylindrical shield; however, the instrument also comes equipped with a scintillation detector and can be used as an alpha monitor. Guard switches signal a tape break or a shortage of tape supply on these monitors; and, should the sample pump stop, a pressure switch in the line is tripped and an alarm is sounded. The signal from the detector tube or crystal is read at a count-rate meter and printed on a strip-chart recorder located in a control building; likewise, the tape and pump alarms are similarly telemetered. More will be said later about the control building.

When used as an alpha monitor, this device has several undesirable features. First, the alpha particles are subject to absorption by the filter media due to the penetration of the sample into the paper. Second, the presence of naturally occurring radon and thoron decay products is strong enough to mask out significant levels of alpha-emitting process materials. Because of these deficiencies, the alpha monitor has undergone complete redesign;[2] and a prototype for a new model is now being fabricated. In this design the sample will be collected on a membrane filter which gives a minimum of self-absorption because particles are deposited only on the surface. Four surface-barrier silicon-diode detectors will view this surface and the pulses will be amplified and then sorted into a high-energy group (>5 mev) containing the pulses from radon and thoron decay and a lower-energy group containing the pulses from the (more probable) alpha contaminants (<5 mev energy). These two signals are then fed to separate count-rate meters and recorders. The system may be calibrated by means of a generator which will inject a pulse of a known energy into the detection circuitry or by a thoron source located at the input of the tape deck. Provisions are made for inclusion or future addition of an alpha energy spectrometer for use in identification of the contaminant. The first of these monitors is expected to be operational by the end of this year.

The tape monitor may be more accurately called a particulate monitor. Strictly speaking, only activity which is in a filterable form can be collected by this instrument; and, when used as a beta-gamma monitor, one would expect only filterable activity to be detected by the G-M tube. This is not the case, however. Experience indicates that the passage of short, relatively intense bursts of the rare gases A, Kr, and Xe, although not stopped by the filter tape, will be indicated as spikes on the recorder. Also, the fact that an activity will deposit on the tape does not mean that it was necessarily in particulate form when it entered the waste duct from the laboratory or processing area. A number of nuclides may be emitted in gaseous form from a chemical reaction or other type of process; but, in traveling through several hundred feet of metal duct, this gas will mix with, and be absorbed to an unknown degree by, any solid material, such as dust, which may be in the air stream. This probably accounts for the buildup of $^{131}I$ frequently seen on the monitor tapes.

No attempt has been made to calibrate this instrument for general use, partly because of the factors just described. The Health Physics Division at the Laboratory has made a study, however, in which an attempt was made to calculate the response of this monitor to certain specific particulate-associated beta-gamma emitting isotopes.[3] For example, the calculated count-rate response for

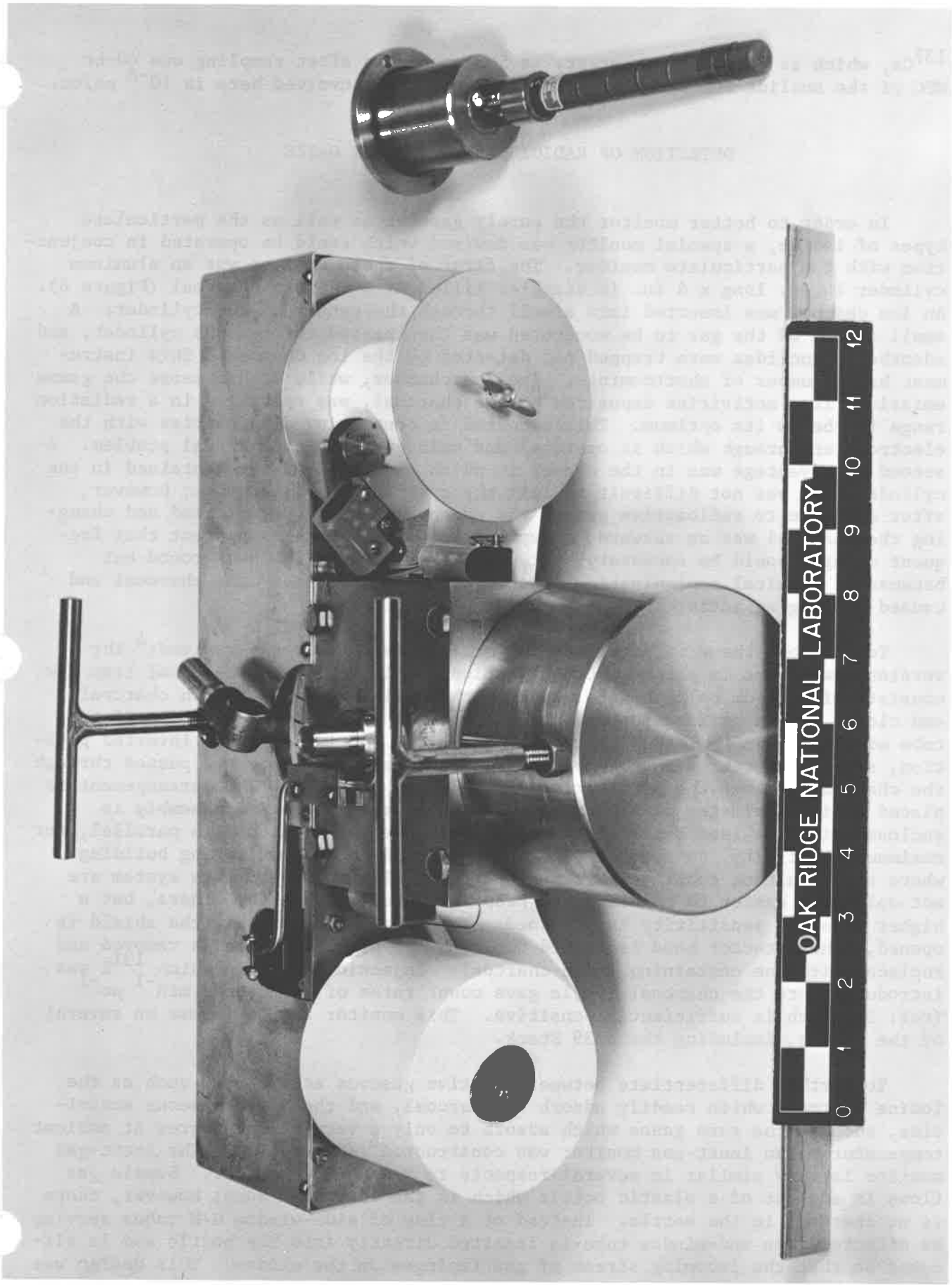


Figure 7. Particulate Monitor - 1961 Model

$^{137}Cs$, which is always of interest, is 590 count/min after sampling one 40-hr MPC of the nuclide for one hour. The concentration involved here is $10^{-8}$ μc/cc.

## DETECTION OF RADIOIODINE AND INERT GASES

In order to better monitor the purely gaseous as well as the particulate types of iodine, a special monitor was devised which could be operated in conjunction with the particulate monitor. The first of these devices was an aluminum cylinder 14 in. long x 4 in. in diameter filled with 14-mesh charcoal (Figure 8). An ion chamber was inserted into a well through the center of the cylinder. A small stream of the gas to be monitored was then passed through the cylinder, and adsorbable nuclides were trapped and detected by the ion chamber. This instrument had a number of shortcomings. The ion chamber, while it did sense the gamma emissions from activities deposited on the charcoal, was operating in a radiation range far below its optimum. This resulted in continuing difficulties with the electrometer through which it operated and maintenance became a real problem. A second disadvantage was in the manner in which the charcoal was contained in the cylinder. It was not difficult to fill the cylinder the first time; however, after exposure to radioactive gases, the charcoal became contaminated and changing the charcoal was an awkward, messy operation. It became apparent that frequent changes would be necessary, not only to maintain a low background but because of chemical contamination which eventually "poisoned" the charcoal and caused a plugging action which resulted in channeling.

To overcome these difficulties the monitor was completely revised;[4] the version now in use is shown in cross section in Figure 9. The charcoal trap now consists of an 8-oz polyethylene, wide-mouth bottle half-filled with charcoal and closed with a perforated cap; attached to the cap is a plastic centrifuge tube with holes in the end (Figure 10). When the bottle is in the inverted position, sample gas can be introduced through the centrifuge tube and passed through the charcoal and out the perforations in the cap, as shown. This arrangement is placed inside a cluster of side-window G-M tubes and the entire assembly is enclosed within a lead shield. The detector tubes are connected in parallel, for maximum sensitivity, to a count-rate meter located in the monitoring building where the resultant count rate is printed. The electronics of this system are not only much easier to maintain and keep in operation than the others, but a higher level of sensitivity is attained. To change the charcoal, the shield is opened, the detector head is lifted out, and the plastic bottle is removed and replaced with one containing fresh charcoal. Injection tests in which $^{131}I$ was introduced into the charcoal bottle gave count rates of 340 counts $min^{-1}$ $\mu c^{-1}$ (ref. 5) which is sufficiently sensitive. This monitor is now in use on several of the stacks, including the 3039 Stack.

To further differentiate between reactive gaseous activities, such as the iodine isotopes which readily adsorb on charcoal, and the inert gaseous activities, such as the rare gases which adsorb to only a very slight degree at ambient temperatures, an inert-gas monitor was constructed[6] (Figure 11). The inert-gas monitor is very similar in several respects to the iodine monitor. Sample gas flows in and out of a plastic bottle which is the detection zone; however, there is no charcoal in the bottle. Instead of a ring of side-window G-M tubes serving as detectors, an end-window tube is inserted directly into the bottle and is situated so that the incoming stream of gas impinges on the window. This design was

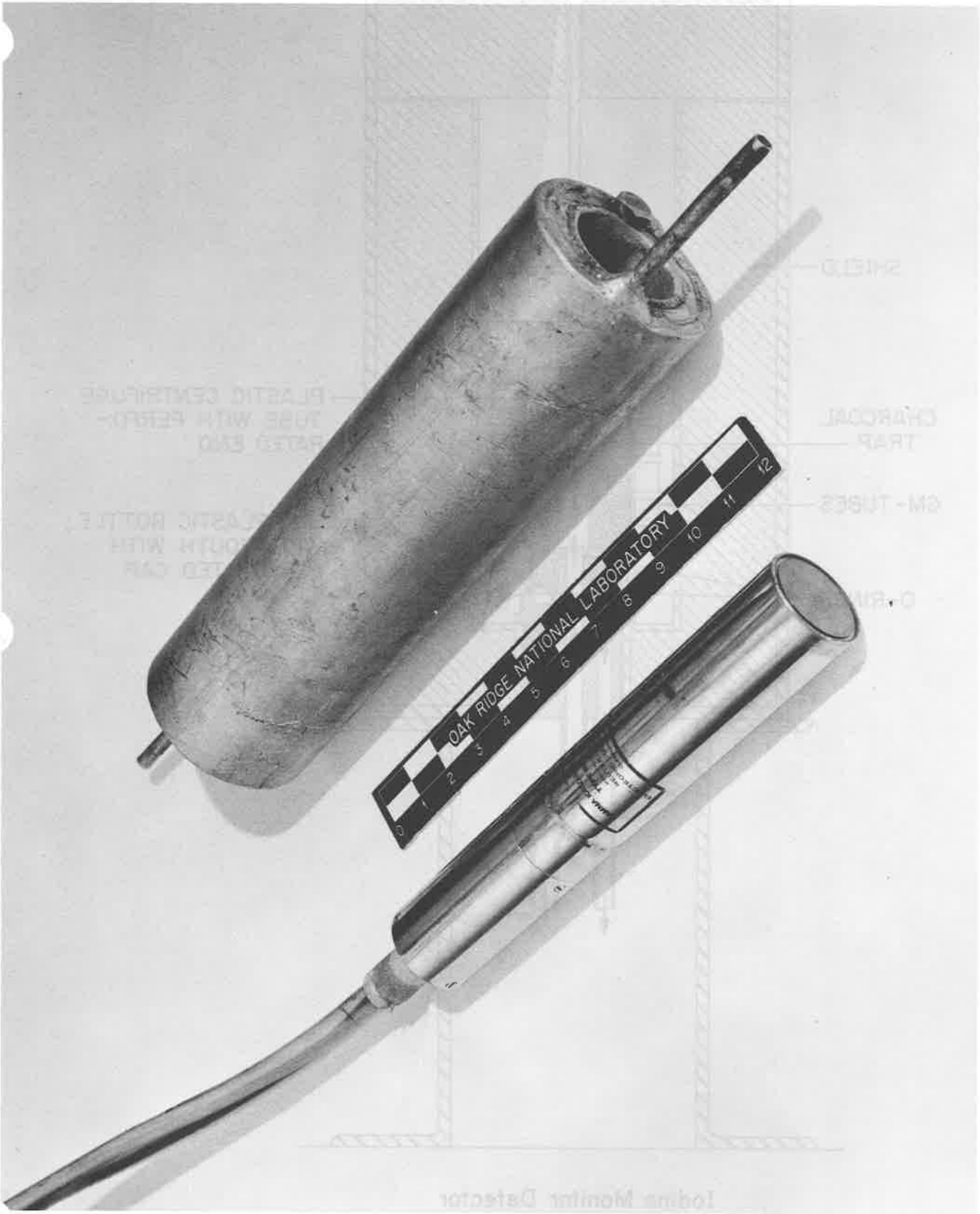


Figure 8. Early Model Iodine Monitor with Ion Chamber

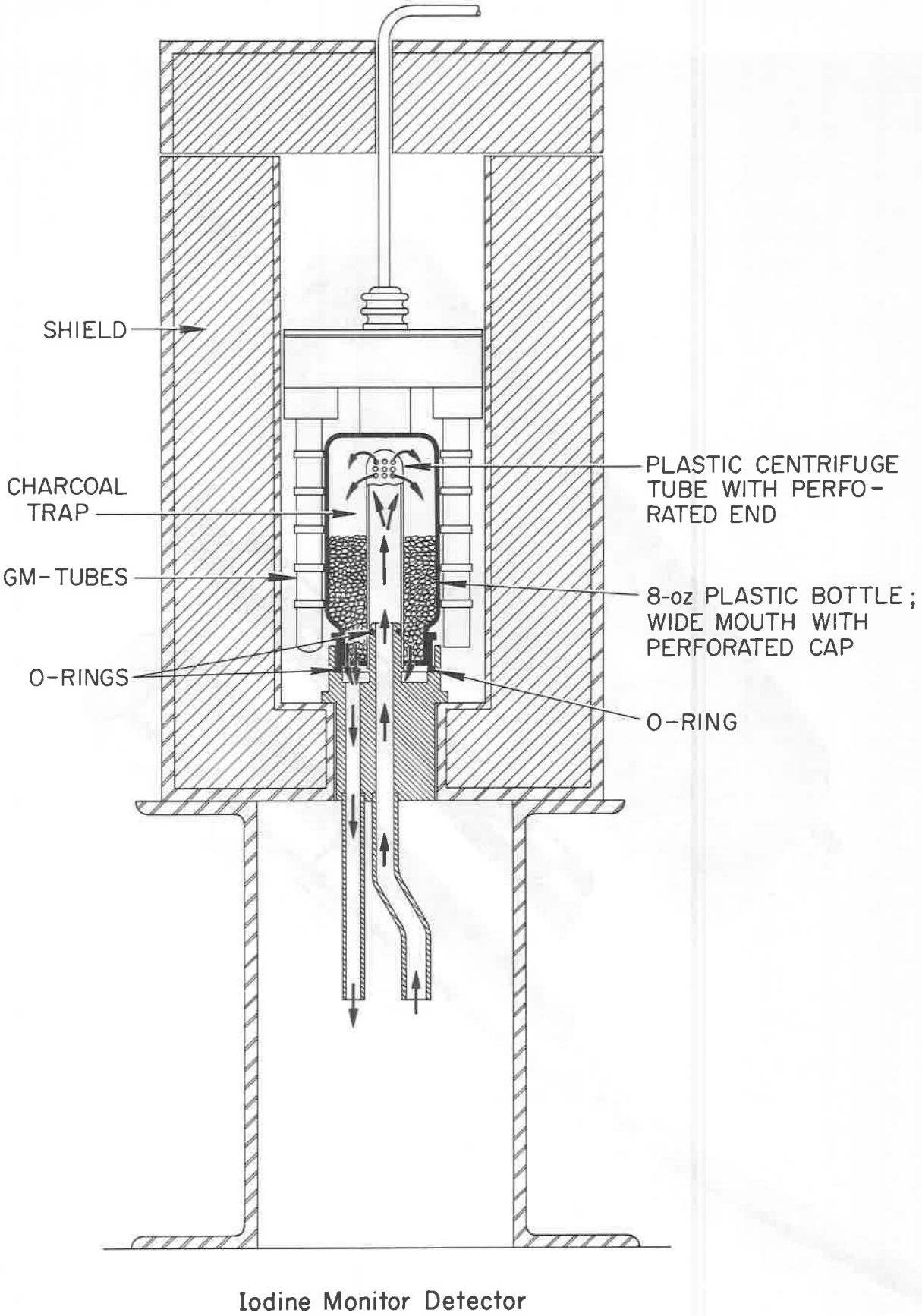


Figure 9. Cross Section of Iodine Monitor - Revised Model

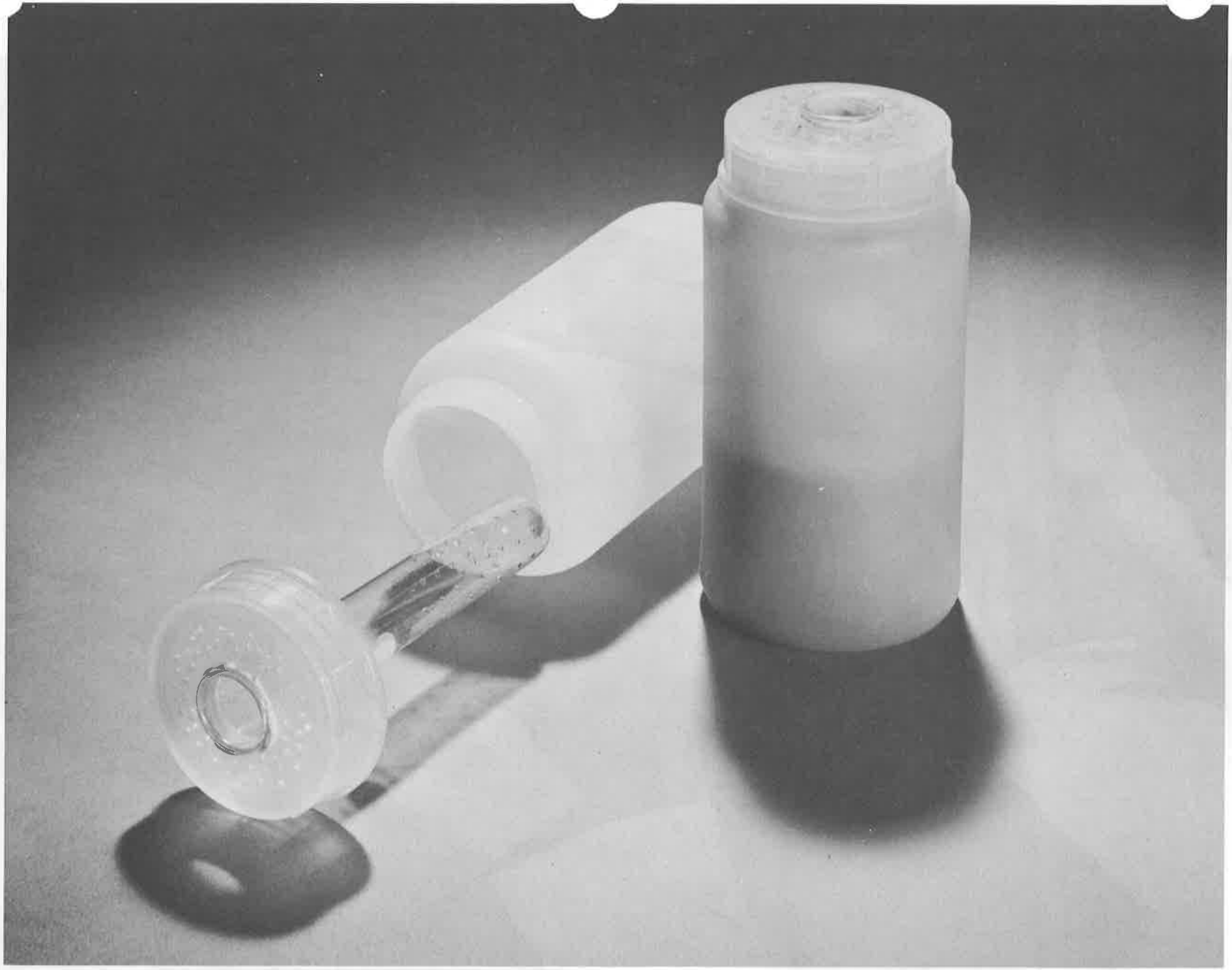

Figure 10. Charcoal Container for Iodine Monitor

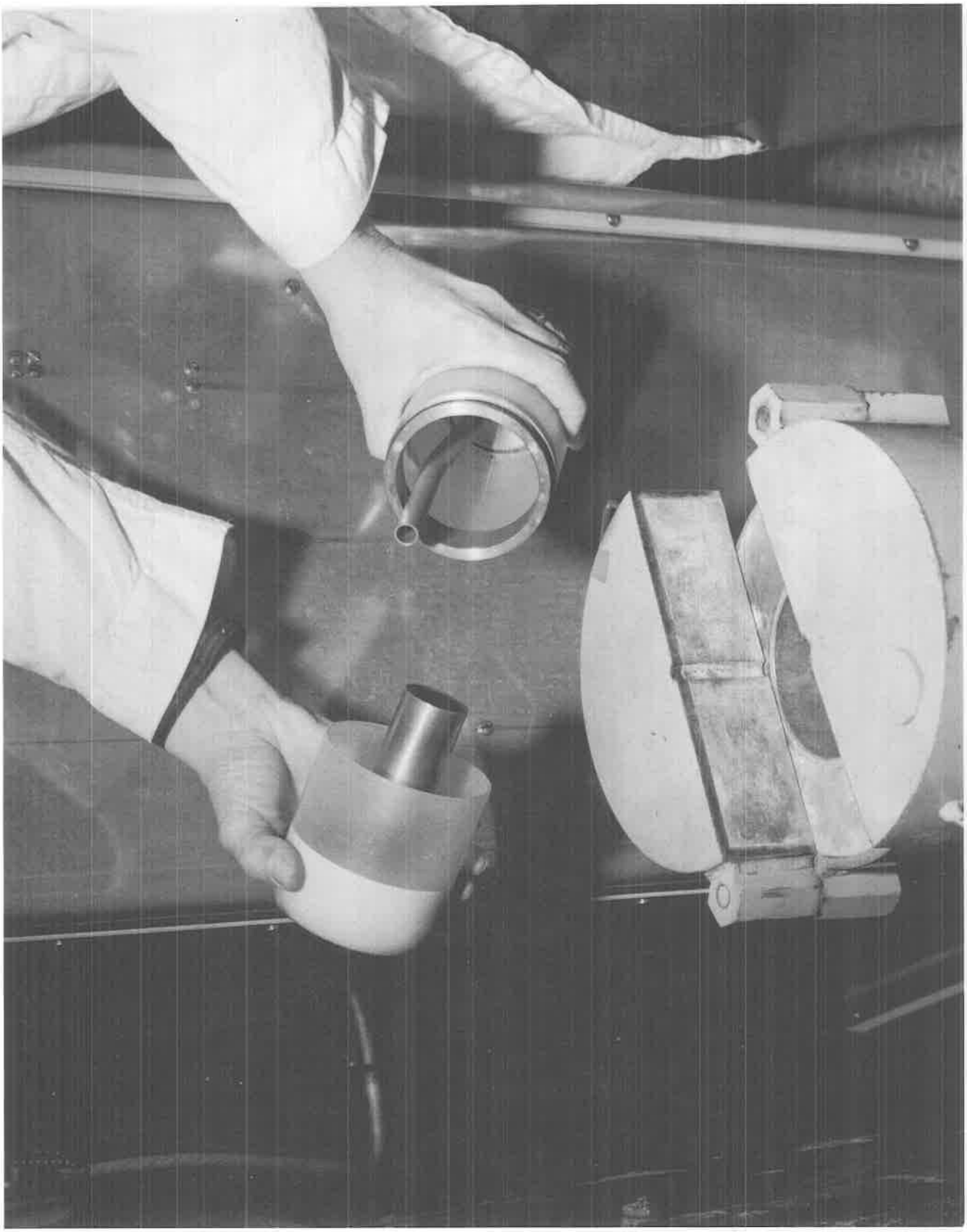

Figure 11. [illegible]rt Gas Monitor

patterned after a Kanne or flow-through ionization chamber. Estimates of the expected count rates for the most probable radioactive gases ($^{41}A$, $^{55}Kr$, $^{133}Xe$, and $^{135}Xe$), based on work done with the Kanne chamber, indicated that an end-window G-M tube would have adequate sensitivity for stack monitoring, Although an actual calibration has not been made on the instrument since it was installed, it has indicated the passage of activity on many occasions; and based on knowledge of the operations being carried out on those occasions one could readily assume that the activities were among those listed above.

## TOP-OF-STACK MONITOR

A last type of monitor which will be described is a gross-gamma detector located at the top of the 3039 Stack. Barely in the design stage five years ago, the top-of-stack monitor is now operational and serves as a useful second line of defense to the other instruments. Figure 12 shows the supporting pole which was erected at the top of the stack, 250 ft above the surrounding countryside. A G-M tube safely encased in styrofoam is securely fastened to an endless nylon rope which passes through the two pulleys. When the package is raised as high as it will go, it is in the correct position to "see" the stack plume without being either in the plume, where it would become contaminated, or above the top of the stack, where it would be exposed to "shine" from the stack walls.

An experimental program is now being carried out by the Instrumentation and Controls Division in which a scintillation detector is used in addition to the G-M tube. A multichannel gamma spectrometer gives a complete, continuous, analysis of the stack emission. Such a system may one day become operational if it can be made simple and uncomplicated. This requires that, first, the data generated by such a machine should be kept to that minimum which can be considered useful for control or inventory purposes; second, the equipment must be simple enough so that nontechnical personnel can operate it and to a large degree interpret what it says; and third, the electronic complexity of the device must not be such as to cause excessive downtime or extensive maintenance.

## MONITORING COMPLEX AT THE 3039 STACK

The 3039 Stack complex gives an example of how the various types of continuous monitors are fitted together to form a system and how the information generated by such a system is processed. Figure 13 is a flowsheet of the 3039 Stack area showing the stack and the ducts which discharge into it. Cell-ventilation air coming from four general areas in the Laboratory is released here after filtering. On the duct from each of those areas is located a particulate tape monitor. Off-gas from those areas is brought here and passed through a caustic scrubber in addition to a filter. The discharge duct from this facility to the stack is likewise monitored by a particulate tape monitor. Included at each of these monitor stations is a collection sampler. This consists of a polyethylene holder into which is placed a cartridge containing charcoal. The filter, which is usually a part of the cartridge assembly, is not used here since the cartridge is located in series with, and downstream from, the collection tape. Occasionally, during special operations it is desirable to sample a duct continuously, perhaps for inventory purposes; or, if an increase should be seen in the activity detected by the tape monitor, it may be necessary to sample with

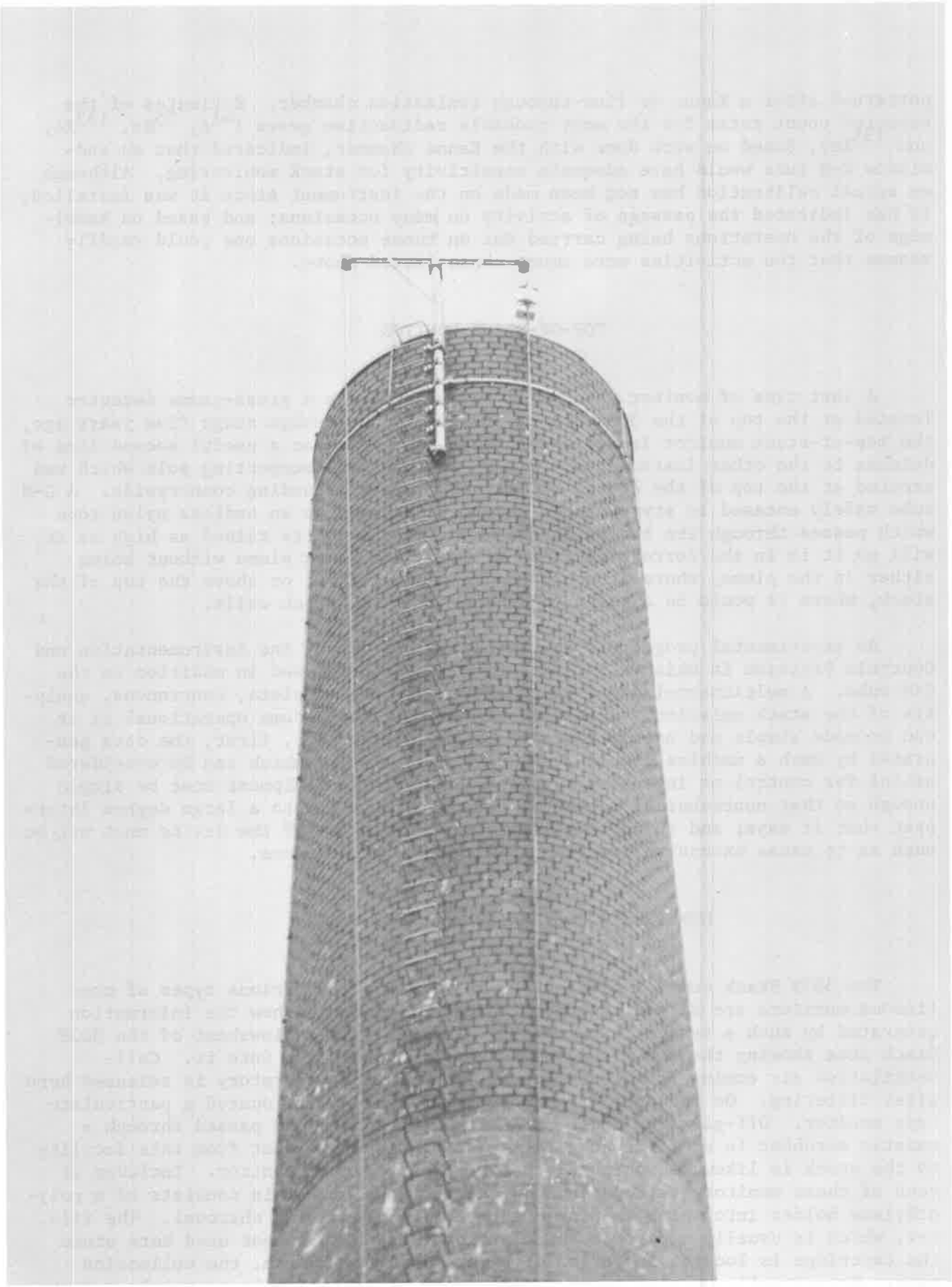

Figure 12. Top-of-Stack Monitor - 3039 Stack

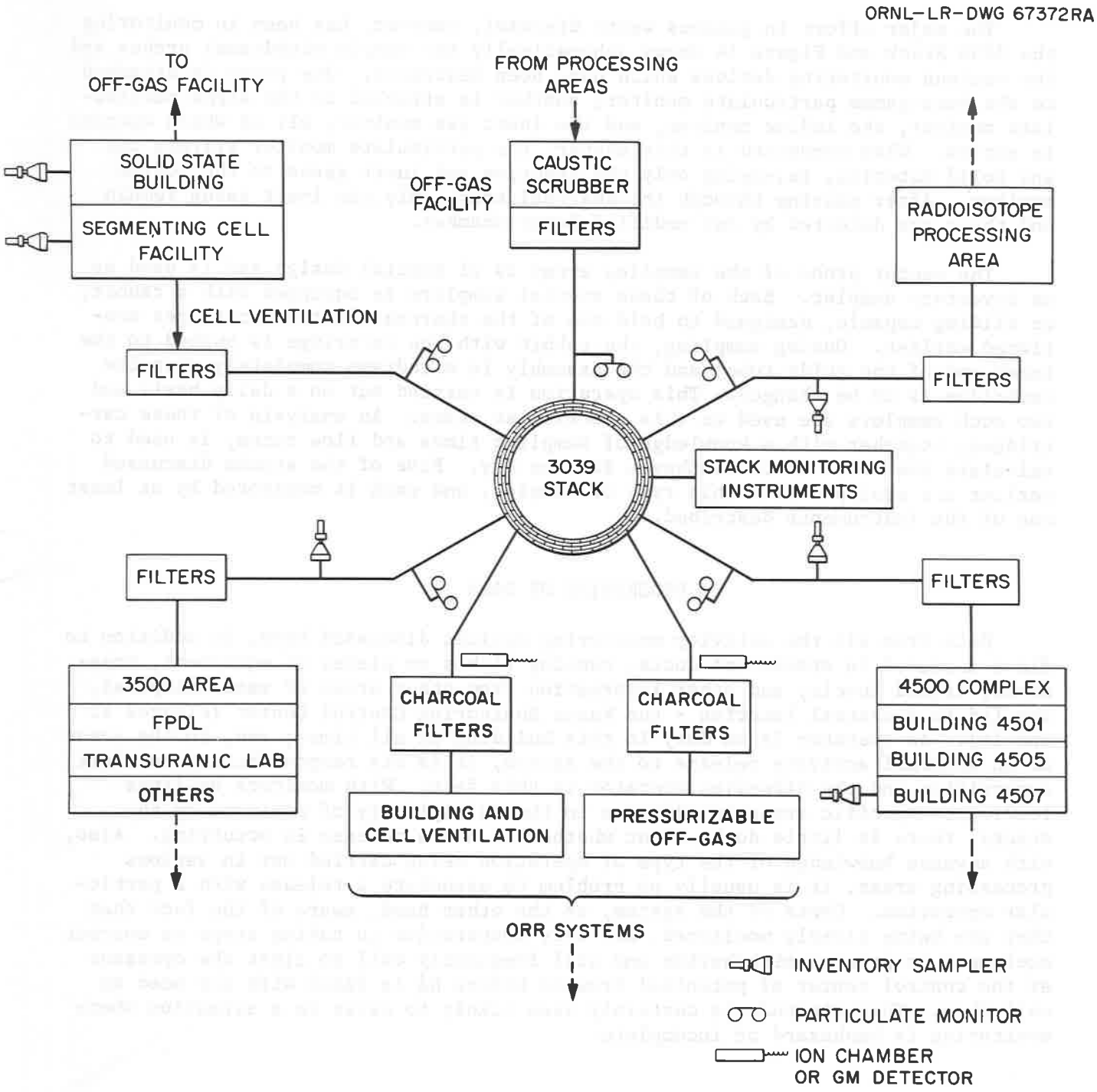


Figure 13. Gaseous Waste Flow Sheet - 3039 Stack Area

a cartridge in order to pinpoint the source of the activity. The ORR is served by two special systems which employ charcoal in addition to filters to remove radioactivity. These systems are monitored by ion-chamber detectors attached to the ductwork.

The major effort in gaseous waste disposal, however, has been in monitoring the 3039 Stack and Figure 14 shows schematically the sample withdrawal probes and the various monitoring devices which have been described. One probe is attached to the beta-gamma particulate monitor; another is attached to the alpha particulate monitor, the iodine monitor, and the inert gas monitor, all of which operate in series. When connected in this manner, the particulate monitor filters out any solid material, releasing only the reactive and inert gases to the iodine monitor. After passing through the charcoal trap, only the inert gases remain and these are detected by our modified Kanne chamber.

The center probe of the sampling array is of special design and is used as an inventory sampler. Each of these special samplers is equipped with a rabbit, or sliding capsule, designed to hold one of the charcoal-filter cartridges mentioned earlier. During sampling, the rabbit with the cartridge is pushed to the inner end of the guide tube; and the assembly is withdrawn completely when the cartridge is to be changed. This operation is carried out on a daily basis and two such samplers are used on this particular stack. An analysis of these cartridges, together with a knowledge of sampling times and flow rates, is used to calculate the total stack discharge for the day. Five of the stacks discussed earlier are equipped with this type of sampler, and each is monitored by at least one of the instruments described.

## PROCESSING OF DATA

Data from all the activity monitoring devices discussed here, in addition to flows measured in stacks and ducts, running lights on pieces of equipment, pressures, liquid levels, and other information from other areas of waste disposal, are fed to a central location - the Waste Monitoring Control Center (Figures 15 and 16). An operator is on duty in this building at all times; and, in the event of an abnormal activity release to the system, it is his responsibility to alert supervision and the offending operator to this fact. With monitors on lines leading to specific areas in addition to the multiplicity of monitors on the stacks, there is little doubt about whether or not a release is occurring. Also, with advance knowledge of the type of operation being carried out in various processing areas, it is usually no problem to associate a release with a particular operation. Users of the system, on the other hand, aware of the fact that they are being closely monitored, are very cooperative in taking steps to correct equipment or process misbehavior and will frequently call to alert the operator at the control center of potential trouble before he is faced with the need to call them. This attitude is certainly less likely to exist in a situation where monitoring is haphazard or incomplete.

## BENEFITS ATTRIBUTABLE TO MONITORING

How has the Laboratory benefitted from its investment in a rather elaborate and expensive monitoring system? The bar chart shown in Figure 17 displays the progress which has been made in cutting back the magnitude of the releases to the environment. The average monthly releases for the years 1962 through 1964 are

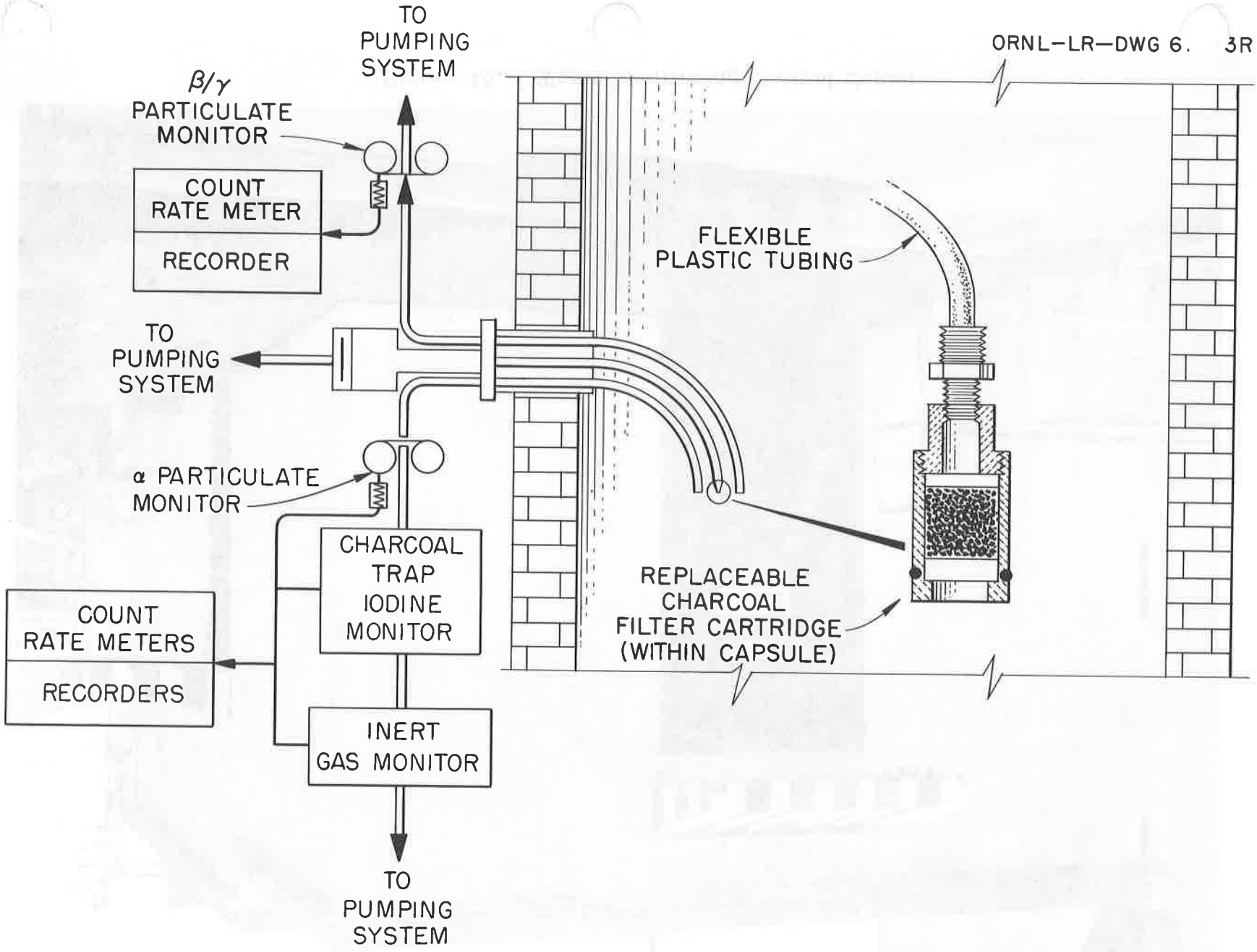


Model II Design of Instack Sampler—3039 Stack.

Figure 14. Schematic of the In-Stack Sampler and Monitoring Devices - 3039 Stack

Figure 15. Waste Monitoring Control Center

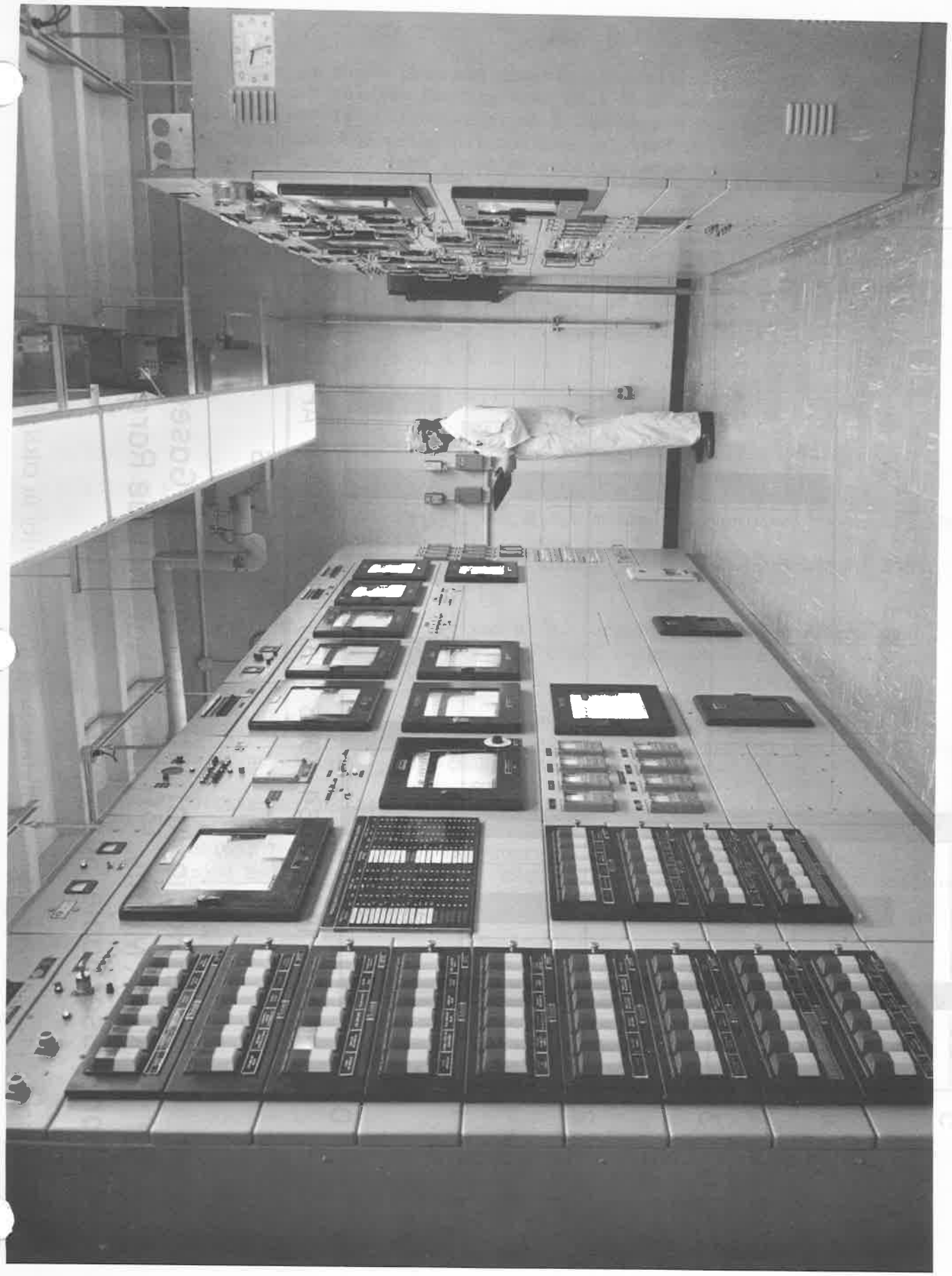

Figure 16. Interior of Waste Monitoring Control Center